A Curiosity Driven Exploration of Hypervalent Iodine(III) Reagents

by

Avery Joseph To

A thesis

presented to the University of Waterloo

in fulfilment of the

thesis requirement for the degree of

Doctor of Philosophy

in

Chemistry

Waterloo, Ontario, Canada, 2024

© Avery Joseph To 2024

Examining Committee Membership

The following served on the Examining Committee for this thesis. The decision of the Examining Committee is by majority vote.

External Examiner	Dr. Chi Zhang, PhD Professor College of Chemistry Nankai University, Tianjin, China
Supervisor	Dr. Graham Murphy, PhD Associate Professor Department of Chemistry University of Waterloo, Waterloo, ON, Canada
Internal Member	Dr. J. Michael Chong, PhD Professor Department of Chemistry University of Waterloo, Waterloo, ON, Canada
Internal Member	Dr. Mónica Barra, PhD Associate Professor Department of Chemistry University of Waterloo, Waterloo, ON, Canada
Internal Member	Dr. Scott Taylor, PhD Professor Department of Chemistry University of Waterloo, Waterloo, ON, Canada
Internal-External Member	Dr. Dale Martin, PhD Assistant Professor Department of Biology University of Waterloo, Waterloo, ON, Canada

Author's Declaration

This thesis consists of material all of which I authored or co-authored: see Statement of Contributions included in the thesis. This is a true copy of the thesis, including any required final revisions, as accepted by my examiners.

I understand that my thesis may be made electronically available to the public.

Statement of Contributions

Avery Joseph To was the sole author of Chapters 1, 3, and 4 which were written under the supervision of Dr. Graham Murphy and were not written for publication. Avery Joseph To conducted all the experimental work for Chapter 2. The resulting manuscript was written by both Avery Joseph To and Dr. Graham Murphy. Additional contribution details are provided in the preface of Chapter 2.

Abstract

Hypervalent iodine (HVI) reagents have established themselves in the literature as reagents with diverse reactivity and utility in many different transformations. Their unique bonding structure often leads to divergent reactivity when compared to common oxidants, making them attractive reagents for study. They are typically easy-to-handle solids and require mild reaction conditions for activation. The field of hypervalent iodine is very active with many new transformations and even new reagents being reported annually.

In Chapter 2 the use of diaryliodonium salts as catalysts for the Nazarov cyclization is discussed. In this study, the structure of the diaryliodonium salt catalyst was optimized for solubility and activity in the Nazarov reaction. Univariate optimization of the reaction for solvent, reaction temperature, and catalyst loading was completed. Using the optimized conditions a series of substrates were explored. Notably, many of the yields obtained were lower than those reported in the literature for the comparable Lewis and Brønsted acid-catalyzed reactions. A ^{1}H-NMR study revealed a possible substrate degradation pathway to account for the lower yields. Control reactions were used to establish the necessity of oxygen in the reaction for catalyst activation and turnover. Overall, reaction conditions were developed for the use of a diaryliodonium salt in the Nazarov cyclization.

In Chapter 3 we investigated the reactions of $TolIF_2$ with styrenyl substrates containing a strained ring. This investigation uses the knowledge gained from previous reactions developed with $TolIF_2$ in the Murphy group. Three different reactions were explored, each giving a unique product, not obtained with classical fluorination methods. The first reaction, the reaction of $TolIF_2$ with methylenecyclopropanes, produced a surprising product which incorporated the iodotoluene from $TolIF_2$ into it, albeit in low yield. The second reaction was the ring expansion of a cyclobutanol to a fluorinated cyclopentanone. This reaction was optimized for Lewis acid activator, reaction solvent, temperature, as well as equivalents of reagent, but unfortunately still only gave the product in 61% yield with substantial side product. The final reaction explored was the *gem*-difluorination of alpha-cyclopropyl styrenes. Again, the conditions were optimized (Lewis acid, reaction temperature, reaction solvent, etc.) to produce the product in 51% yield. In this reaction, a persistent ketone byproduct was always observed.

In Chapter 4 attention was turned to the design of new fluoroiodane derivatives. A survey of the hypervalent iodine literature revealed addition of steric bulk ortho to the iodine atom in HVI reagents led to improvements in reaction outcome. The key structural feature assessed was the torsion angle of the hypervalent bond. X-ray crystal structures of new derivatives were obtained and the torsion angle of the hypervalent bond of five fluoroiodanes and three chloroiodanes were compared. As expected, the torsion angle was larger in newly prepared derivatives (~8° vs. ~20°). A much larger torsion angle of ~55° was achieved with the homologated six-membered fluoroiodane. Unfortunately, preliminary investigations of the reactivity indicate that this series is less reactive compared to the parent reagent.

Acknowledgements

First and foremost, thank you Dr. Graham Murphy for accepting me into your research group, without that none of this would have been possible. The time you took to chat about chemistry and the countless hours we spent at the whiteboard discussing ideas for new reactions will always be deeply appreciated. It allowed me to develop into the chemist I am today and gave me the skills and confidence necessary to identify gaps in the literature and pursue my own ideas in the lab. Thank you for your constant encouragement and support in applying for scholarships/awards and attending conferences.

Thank you to my committee members Profs. Chong, Taylor, and Barra for your support and guidance. In particular, thank you Prof. Chong for sharing chemicals over the years. I will truly miss borrowing chemicals from Prof. Chong's lab and learning about their chemistry from him. A non-trivial amount of my chemical knowledge has originated in these discussions. Thank you Prof. Taylor for your support during my BSc thesis. The skills gained in your laboratory were the foundation on which I built my synthetic organic chemistry abilities. To Prof. Barra, I will never forget first learning about NMR in your CHEM 265 course or working through physical organic problems in CHEM 400. I will always remember your enthusiasm for teaching and diligence in ensuring that I truly understood a concept. A special thank you to Prof. Schwan for opening my eyes to all the possible heteroatom chemistry.

To all Murphy group members with whom I had the pleasure of overlapping with in the lab, thank you for keeping our time together enjoyable. From serious chemistry discussions to ridiculous antics there never was a dull moment. Thank you to all the undergraduate students who patiently worked under my guidance and allowed me to develop my teaching abilities. Thank you to all the technical support staff without whom much of this work would not have been possible. Thank you to Jan Venne and Dr. Blossom Yan in the NMR facility, Dr. Richard Smith for his expertise in mass spectrometry, Val Goodfellow for all things chromatography related, and Dr. Jalil Assoud for his expertise in X-ray crystallography.

Last, but not least, thank you to my family for the constant love and support you have given me throughout my life, I would not be here without it. To my fiancée, Parisa, thank you for your never-ending stream of support, encouragement, patience, and love.

Table of Contents

Examining Committee Membership ii

Author's Declaration iii

Statement of Contributions iv

Abstract v

Acknowledgements vii

List of Figures xi

List of Tables xvii

List of Schemes xviii

List of Abbreviations xxii

List of Symbols xxiv

Chapter 1 Introduction 1

1.1 Preface 1

1.2 Iodine 1

1.3 Hypervalent Iodine 1

1.3.1 General Reactivity 5

1.3.2 Synthesis 6

1.4 Scope of Thesis 8

Chapter 2 Cyclic Diaryliodonium Salts as Lewis Acidic Catalysts 10

2.1 Preface 10

2.2 Introduction 10

2.2.1 The Nazarov Cyclization 10

2.2.2 Diaryliodonium Salts as a Source of Electrophilic Arene 16

2.2.3 Diaryliodonium salts as Halogen Bond Donors 18

2.2.4 Halogen Bonding and the Nazarov Cyclization 22
2.2.5 Research Objectives 23
2.3 Results 23
2.3.1 Optimization 23
2.3.2 Substrate Scope 28
2.3.3 Control Reactions 31
2.4 Concluding Remarks and Future Work 37
2.5 Experimental Details 38
Chapter 3 Interrupting the Known Reactivity of *p*-(Difluoroiodo)toluene and Styrenyl Motifs 39
3.1 Introduction 39
3.1.1 Synthesis of *p*-(Difluoroiodo)toluene 39
3.1.2 Reactivity of (Difluoroiodo)arenes 43
3.1.3 Research Objectives 53
3.2 Reaction Development 55
3.2.1 The Reaction of Methylenecyclopropanes or Methylenecyclobutanes with *p*-(Difluoroiodo)toluene 55
3.2.2 The Reaction of Alpha Cyclobutanols and *p*-(Difluoroiodo)toluene 61
3.2.3 The Reaction of Alpha Cyclopropyl Styrene and *p*-(Difluoroiodo)toluene 67
3.3 Concluding Remarks and Future Work 71
3.4 Experimental Details 73
Chapter 4 Ortho-Substituted Fluoro- and Chloro-iodanes 80
4.1 Introduction 80
4.1.1 Review of the Fluoroiodane 80
4.1.2 Review of the Chloroiodane 92

4.1.3 Review of ortho-Substitution with Monocyclic and Pseudo-monocyclic Hypervalent Iodanes 98
4.1.4 Research Objectives 105
4.2 Synthesis 106
4.2.1 Synthesis of the Iodoalcohol Precursors to the Hypervalent Iodine Reagents 106
4.2.2 Oxidation of the Iodoalcohols to Hypervalent Iodine Species 120
4.3 Analysis of Single Crystal X-ray Structures and Preliminary Reactivity 130
4.4 Concluding Remarks and Future Work 140
4.5 Experimental Details 141
4.5.1 Preparation of Iodoarene Precursors 142
4.5.2 Preparation of Hypervalent Iodine Compounds 163
References 171
Appendices 196
Appendix A Chapter 3: NMR Spectra 196
Appendix B Chapter 4: NMR Spectra 204
Appendix C Chapter 4: X-ray Crystallography Data 275

List of Figures

Figure 1-1. Examples of λ^3- and λ^5-iodanes and their respective names. 2
Figure 1-2. Description of the molecular orbitals of the 3c-4e bond found in hypervalent iodine(III) and (V) compounds. 3
Figure 1-3. HVI compounds with their respective Martin-Arduengo designations. 4
Figure 2-1. The influence of alpha- and beta-substituents on the Nazarov cyclization. 12
Figure 2-2. Illustration of torquoselectivity in a Nazarov cyclization. 12
Figure 2-3. Examples of the two types of diaryliodonium salts. 16
Figure 2-4. Interaction of a Lewis basic lone pair on the oxygen of a ketone with a diaryliodonium salt. 18
Figure 2-5. Examples of the synthetic utility of cyclic diaryliodonium salts as reaction initiators. 20
Figure 2-6. Structurally varied iodonium salts **2.43**-**2.46**. 21
Figure 2-7. ^{1}H NMR study of the conversion of **2.60n** to **2.61n** with catalyst **2.69**. 36
Figure 3-1. Synthesis of $TolIF_2$. 41
Figure 3-2. Methylenecyclopropane substrates **3.69** and **3.70**. 55
Figure 3-3. Major peak in the ^{19}F-NMR overlaid with a potential fluorinated motif. 59
Figure 3-4. Potential substrates to be investigated in the *gem*-difluorination of alpha cyclopropyl styrenes. 72
Figure 4-1. ORTEP representation with a displacement ellipsoid probability of 50%. Crystal structure of the fluoroiodane obtained by Legault and coworkers. A) Illustration of the I•••O interaction of the two independent molecules. B) Envelope of five-membered ring. C) Top-down view of one molecule illustrating the small torsion angle. D) Side on view of one molecule. Note: the second molecule was omitted from C) and D) for clarity. 81
Figure 4-2. Modes of theoretical fluoroiodane activation. 89
Figure 4-3. The chlorobenzoiodoxole **4.3** and the chlorobenzoiodoxolone **4.34**. 93
Figure 4-4. Examples of the chlorination products which can be obtained using the chloroiodane **4.34**. 95
Figure 4-5. Examples of hypervalent iodine reagents accessible through the chloroiodanes. 97
Figure 4-6. Two different energy diagrams of methanol oxidation by IBX. A) The energy diagram calculated by Su and Goddard shows the hypervalent twist to be rate limiting. B) The energy diagram calculated at a higher level of theory shows elimination to be rate limiting. 99

Figure 4-7. Chemical structures of IBX, CH_3-IBX, and Tet-IBX.....100
Figure 4-8. Calculated BDEs of chloroiodanes.....105
Figure 4-9. De-iodinated side-products from the methyl Grignard addition and proposed side-products.....112
Figure 4-10. Summary of iodoalcohol precursors synthesized.....120
Figure 4-11. X-ray crystal structure of the ortho-isopropyl dimer **4.151**.....125
Figure 4-12. Alkyl aryl iodonium salts.....127
Figure 4-13. Side-on and top-down views of the crystal structure of the fluoroiodane **4.143** (R = CH_3).....131
Figure 4-14. Side-on and top-down views of the crystal structure of the fluoroiodane **4.148** (R = OCH_3).....131
Figure 4-15. Side-on and top-down views of the crystal structure of the fluoroiodane **4.149** (R = O*i*-Pr).....132
Figure 4-16. Side-on and top-down views of the crystal structure of the fluoroiodane **4.147** (R = Br).....132
Figure 4-17. Side-on and top-down views of the crystal structure of the fluoroiodane **4.168** (R = CH_3).....132
Figure 4-18. Side-on and top-down views of the crystal structure of the chloroiodane **4.145** (R = CH_3).....133
Figure 4-19. Side-on and top-down views of the crystal structure of the fluoroiodane **4.163** (R = *t*-Bu).....133
Figure 4-20. Side-on and top-down views of the crystal structure of the fluoroiodane **4.169** (R = CH_3).....133
Figure 4-21. Example of the packing in fluoroiodane **4.2**.....134
Figure 4-22. Fluoroiodanes with the fluorine pointing “down” or “up”. The angle is exaggerated for illustrative purposes.....135
Figure 4-23. Short contacts in the crystal structure packing of the tert-butyl chloroiodane **4.163**.....136
Figure 4-24. Variable temperature ^{1}H-NMR of chloroiodane **4.169** from 12.5 °C to 50 °C in 2.5 °C increments.....138
Figure A-1. ^{1}H-NMR (300 MHz, $CDCl_3$) of 2-(2-((4-bromophenyl)fluoromethyl)allyl)-1-iodo-4-methylbenzene (**3.71**):.....198

Figure A-2. ^{13}C-NMR (75 MHz, $CDCl_3$) of 2-(2-((4-bromophenyl)fluoromethyl)allyl)-1-iodo-4-methylbenzene (**3.71**):.....199
Figure A-3. ^{19}F-NMR (282 MHz, $CDCl_3$) of 2-(2-((4-bromophenyl)fluoromethyl)allyl)-1-iodo-4-methylbenzene (**3.71**):.....200
Figure A-4. ^{13}C-DEPT 135 (75 MHz, $CDCl_3$) of 2-(2-((4-bromophenyl)fluoromethyl)allyl)-1-iodo-4-methylbenzene (**3.71**):.....201
Figure A-5. ^{1}H, ^{13}C-HMQC (300 MHz, 75 MHz, $CDCl_3$) of 2-(2-((4-bromophenyl)fluoromethyl)allyl)-1-iodo-4-methylbenzene (**3.71**): 202
Figure A-6. ^{1}H, ^{13}C-HMBC (300 MHz, 75 MHz, $CDCl_3$) of 2-(2-((4-bromophenyl)fluoromethyl)allyl)-1-iodo-4-methylbenzene (**3.71**): 203
Figure B-1. ^{1}H-NMR (300 MHz, $CDCl_3$) of 2-(2-iodo-3-methylphenyl)propan-2-ol (**4.93**): 205
Figure B-2. ^{13}C-NMR (75 MHz, $CDCl_3$) of 2-(2-iodo-3-methylphenyl)propan-2-ol (**4.93**): 206
Figure B-3. ^{1}H-NMR (300 MHz, $CDCl_3$) of 2-amino-3-bromobenzoic acid (**4.94**):.....207
Figure B-4. ^{13}C-NMR (75 MHz, $CDCl_3$) of 2-amino-3-bromobenzoic acid (**4.94**):.....208
Figure B-5. ^{1}H-NMR (300 MHz, $CDCl_3$) of 2-(2-amino-3-bromophenyl)propan-2-ol (**4.96**): 209
Figure B-6. ^{13}C-NMR (75 MHz, $CDCl_3$) of 2-(2-amino-3-bromophenyl)propan-2-ol (**4.96**): 210
Figure B-7. ^{1}H-NMR (300 MHz, $CDCl_3$) of 2-(3-bromo-2-iodophenyl)propan-2-ol (**4.97**): 211
Figure B-8. ^{13}C-NMR (75 MHz, $CDCl_3$) of 2-(3-bromo-2-iodophenyl)propan-2-ol (**4.97**):.....212
Figure B-9. ^{1}H-NMR (300 MHz, $CDCl_3$) of 2-(3-isopropoxyphenyl)propan-2-ol (**4.106**): 213
Figure B-10. ^{13}C-NMR (75 MHz, $CDCl_3$) of 2-(3-isopropoxyphenyl)propan-2-ol (**4.106**): 214
Figure B-11. ^{1}H-NMR (300 MHz, $CDCl_3$) of 2-(2-iodo-3-methoxyphenyl)propan-2-ol (**4.107**): 215
Figure B-12. ^{13}C-NMR (75 MHz, $CDCl_3$) of 2-(2-iodo-3-methoxyphenyl)propan-2-ol (**4.107**): 216
Figure B-13. ^{1}H-NMR (300 MHz, $CDCl_3$) of 2-(2-iodo-3-isopropoxyphenyl)propan-2-ol (**4.108**): .217
Figure B-14. ^{13}C-NMR (75 MHz, $CDCl_3$) of 2-(2-iodo-3-isopropoxyphenyl)propan-2-ol (**4.108**): ..218
Figure B-15. ^{1}H-NMR (300 MHz, $CDCl_3$) of 2-iodo-3-isopropylbenzoic acid (**B1**): 219
Figure B-16. ^{13}C-NMR (75 MHz, $CDCl_3$) of 2-iodo-3-isopropylbenzoic acid (**B1**): 220
Figure B-17. ^{1}H-NMR (300 MHz, $CDCl_3$) of methyl 2-iodo-3-isopropylbenzoate (**4.111**):.....221
Figure B-18. ^{13}C-NMR (75 MHz, $CDCl_3$) of methyl 2-iodo-3-isopropylbenzoate (**4.111**):.....222
Figure B-19. ^{1}H-NMR (300 MHz, $CDCl_3$) of 2-(2-iodo-3-isopropylphenyl)propan-2-ol (**4.112**): 223
Figure B-20. ^{13}C-NMR (75 MHz, $CDCl_3$) of 2-(2-iodo-3-isopropylphenyl)propan-2-ol (**4.112**): 224

Figure B-21. ^{1}H-NMR (300 MHz, $CDCl_3$) of 1-(2-amino-3-(*tert*-butyl)phenyl)ethan-1-one (**4.127**): 225
Figure B-22. ^{13}C-NMR (75 MHz, $CDCl_3$) of 1-(2-amino-3-(*tert*-butyl)phenyl)ethan-1-one (**4.127**): 226
Figure B-23. ^{1}H-NMR (300 MHz, $CDCl_3$) of 1-(2,5-dibromo-3-(*tert*-butyl)phenyl)ethan-1-one (**4.131**): 227
Figure B-24. ^{13}C-NMR (75 MHz, $CDCl_3$) of 1-(2,5-dibromo-3-(*tert*-butyl)phenyl)ethan-1-one (**4.131**): 228
Figure B-25. ^{1}H-NMR (300 MHz, $CDCl_3$) of 2-(2,5-dibromo-3-(*tert*-butyl)phenyl)propan-2-ol (**4.132**): 229
Figure B-26. ^{13}C-NMR (75 MHz, $CDCl_3$) of 2-(2,5-dibromo-3-(*tert*-butyl)phenyl)propan-2-ol (**4.132**): 230
Figure B-27. ^{1}H-NMR (300 MHz, $CDCl_3$) of 2-(5-bromo-3-(*tert*-butyl)-2-iodophenyl)propan-2-ol (**4.133**): 231
Figure B-28. ^{13}C-NMR (75 MHz, $CDCl_3$) of 2-(5-bromo-3-(*tert*-butyl)-2-iodophenyl)propan-2-ol (**4.133**): 232
Figure B-29. ^{1}H-NMR (300 MHz, $CDCl_3$) of 2-(2-iodo-3-methylphenyl)acetic acid (**B2**): 233
Figure B-30. ^{13}C-NMR (75 MHz, $CDCl_3$) of 2-(2-iodo-3-methylphenyl)acetic acid (**B2**): 234
Figure B-31. ^{1}H-NMR (300 MHz, $CDCl_3$) of methyl 2-(2-iodo-3-methylphenyl)acetate (**4.137**): 235
Figure B-32. ^{13}C-NMR (75 MHz, $CDCl_3$) of methyl 2-(2-iodo-3-methylphenyl)acetate (**4.137**): 236
Figure B-33. ^{1}H-NMR (300 MHz, $CDCl_3$) of 1-(2-iodo-3-methylphenyl)-2-methylpropan-2-ol (**4.138**): 237
Figure B-34. ^{13}C-NMR (75 MHz, $CDCl_3$) of 1-(2-iodo-3-methylphenyl)-2-methylpropan-2-ol (**4.138**): 238
Figure B-35. ^{1}H-NMR (300 MHz, $CDCl_3$) of 1-(2-iodophenyl)-2-methylpropan-2-ol (**4.140**): 239
Figure B-36. ^{13}C-NMR (75 MHz, $CDCl_3$) of 1-(2-iodophenyl)-2-methylpropan-2-ol (**4.140**): 240
Figure B-37. ^{1}H-NMR (300 MHz, $CDCl_3$) of 1-fluoro-3,3,7-trimethyl-1,3-dihydro-1λ^3-benzo[*d*][1,2]iodaoxole (**4.143**): 241
Figure B-38. ^{13}C-NMR (75 MHz, $CDCl_3$) of 1-fluoro-3,3,7-trimethyl-1,3-dihydro-1λ^3-benzo[*d*][1,2]iodaoxole (**4.143**): 242
Figure B-39. ^{19}F-NMR (282 MHz, $CDCl_3$) of 1-fluoro-3,3,7-trimethyl-1,3-dihydro-1λ^3-benzo[*d*][1,2]iodaoxole (**4.143**): 243

Figure B-40. ^{1}H-NMR (300 MHz, $CDCl_3$) of 3,3,7-trimethyl-1λ^3-benzo[*d*][1,2]iodaoxol-1(3*H*)-yl 4-methylbenzenesulfonate (**4.144**): 244
Figure B-41. ^{13}C-NMR (75 MHz, $CDCl_3$) of 3,3,7-trimethyl-1λ^3-benzo[*d*][1,2]iodaoxol-1(3*H*)-yl 4-methylbenzenesulfonate (**4.144**): 245
Figure B-42. ^{1}H-NMR (300 MHz, $CDCl_3$) of 1-chloro-3,3,7-trimethyl-1,3-dihydro-1λ^3-benzo[*d*][1,2]iodaoxole (**4.145**): 246
Figure B-43. ^{13}C-NMR (75 MHz, $CDCl_3$) of 1-chloro-3,3,7-trimethyl-1,3-dihydro-1λ^3-benzo[*d*][1,2]iodaoxole (**4.145**): 247
Figure B-44. ^{1}H-NMR (300 MHz, $CDCl_3$) of 7-bromo-1-fluoro-3,3-dimethyl-1,3-dihydro-1λ^3-benzo[*d*][1,2]iodaoxole (**4.147**): 248
Figure B-45. ^{19}F-NMR (282 MHz, $CDCl_3$) of 7-bromo-1-fluoro-3,3-dimethyl-1,3-dihydro-1λ^3-benzo[*d*][1,2]iodaoxole (**4.147**): 249
Figure B-46. ^{1}H-NMR (300 MHz, $CDCl_3$) of 1-fluoro-7-methoxy-3,3-dimethyl-1,3-dihydro-1λ^3-benzo[*d*][1,2]iodaoxole (**4.148**): 250
Figure B-47. ^{19}F-NMR (282 MHz, $CDCl_3$) of 1-fluoro-7-methoxy-3,3-dimethyl-1,3-dihydro-1λ^3-benzo[*d*][1,2]iodaoxole (**4.148**): 251
Figure B-48. ^{1}H-NMR (300 MHz, $CDCl_3$) of 1-fluoro-7-isopropoxy-3,3-dimethyl-1,3-dihydro-1λ^3-benzo[*d*][1,2]iodaoxole (**4.149**): 252
Figure B-49. ^{19}F-NMR (282 MHz, $CDCl_3$) of 1-fluoro-7-isopropoxy-3,3-dimethyl-1,3-dihydro-1λ^3-benzo[*d*][1,2]iodaoxole (**4.149**): 253
Figure B-50. ^{1}H-NMR (300 MHz, $CDCl_3$) of 7-isopropyl-3,3-dimethyl-1λ^3-benzo[*d*][1,2]iodaoxol-1(3*H*)-yl 4-methylbenzenesulfonate (**4.150**): 254
Figure B-51. ^{13}C-NMR (75 MHz, $CDCl_3$) of 7-isopropyl-3,3-dimethyl-1λ^3-benzo[*d*][1,2]iodaoxol-1(3*H*)-yl 4-methylbenzenesulfonate (**4.150**): 255
Figure B-52. ^{1}H-NMR (300 MHz, $CDCl_3$) of 1,1'-oxybis(7-isopropyl-3,3-dimethyl-1,3-dihydro-1λ^3-benzo[*d*][1,2]iodaoxole) (**4.151**) or 1-fluoro-7-isopropyl-3,3-dimethyl-1,3-dihydro-1λ^3-benzo[*d*][1,2]iodaoxole (**4.152**), likely **4.152** based on Figure B-53: 256
Figure B-53. Presumed ^{19}F-NMR (282 MHz, $CDCl_3$) of 1-fluoro-7-isopropyl-3,3-dimethyl-1,3-dihydro-1λ^3-benzo[*d*][1,2]iodaoxole (**4.152**): 257
Figure B-54. ^{1}H-NMR (300 MHz, $CDCl_3$) of 5-bromo-7-(2-hydroxypropan-2-yl)-3,3-dimethyl-2,3-dihydrobenzo[*b*]iodol-1-ium 4-methylbenzenesulfonate (**4.155**): 258

Figure B-55. ^{13}C-NMR (75 MHz, CD_3OD) of 5-bromo-7-(2-hydroxypropan-2-yl)-3,3-dimethyl-2,3-dihydrobenzo[*b*]iodol-1-ium 4-methylbenzenesulfonate (**4.155**): 259
Figure B-56. ^{1}H, ^{13}C- HMQC (300 MHz, 75 MHz, CD_3OD) of 5-bromo-7-(2-hydroxypropan-2-yl)-3,3-dimethyl-2,3-dihydrobenzo[*b*]iodol-1-ium 4-methylbenzenesulfonate (**4.155**): 260
Figure B-57. ^{1}H, ^{13}C- HMBC (300 MHz, 75 MHz, CD_3OD) of 5-bromo-7-(2-hydroxypropan-2-yl)-3,3-dimethyl-2,3-dihydrobenzo[*b*]iodol-1-ium 4-methylbenzenesulfonate (**4.155**): 261
Figure B-58. ^{1}H-NMR (300 MHz, $CDCl_3$) of 5-bromo-7-(*tert*-butyl)-1-chloro-3,3-dimethyl-1,3-dihydro-1λ^3-benzo[*d*][1,2]iodaoxole (**4.163**): 262
Figure B-59. ^{13}C-NMR (75 MHz, $CDCl_3$) of 5-bromo-7-(*tert*-butyl)-1-chloro-3,3-dimethyl-1,3-dihydro-1λ^3-benzo[*d*][1,2]iodaoxole (**4.163**): 263
Figure B-60. ^{1}H-NMR (300 MHz, $CDCl_3$) of 1-(fluoromethyl)-2-iodo-3-methylbenzene (**4.166**):... 264
Figure B-61. ^{19}F-NMR (282 MHz, $CDCl_3$) of 1-(fluoromethyl)-2-iodo-3-methylbenzene (**4.166**): .. 265
Figure B-62. Proton coupled ^{19}F-NMR (282 MHz, $CDCl_3$) of 1-(fluoromethyl)-2-iodo-3-methylbenzene (**4.166**): 266
Figure B-63. ^{1}H-NMR (300 MHz, $CDCl_3$) of 3,3,8-trimethyl-3,4-dihydro-1*H*-1λ^3-benzo[*e*][1,2]iodaoxin-1-yl 4-methylbenzenesulfonate (**4.167**): 267
Figure B-64. ^{13}C-NMR (300 MHz, $CDCl_3$) of 3,3,8-trimethyl-3,4-dihydro-1*H*-1λ^3-benzo[*e*][1,2]iodaoxin-1-yl 4-methylbenzenesulfonate (**4.167**): 268
Figure B-65. ^{1}H-NMR (300 MHz, $CDCl_3$) of 1-fluoro-3,3,8-trimethyl-3,4-dihydro-1*H*-1λ^3-benzo[*e*][1,2]iodaoxine (**4.168**): 269
Figure B-66. ^{19}F-NMR (282 MHz, $CDCl_3$) of 1-fluoro-3,3,8-trimethyl-3,4-dihydro-1*H*-1λ^3-benzo[*e*][1,2]iodaoxine (**4.168**): 270
Figure B-67. ^{1}H-NMR (300 MHz, $CDCl_3$) of 1-chloro-3,3,8-trimethyl-3,4-dihydro-1*H*-1λ^3-benzo[*e*][1,2]iodaoxine (**4.169**): 271
Figure B-68. ^{13}C-NMR (75 MHz, $CDCl_3$) of 1-chloro-3,3,8-trimethyl-3,4-dihydro-1*H*-1λ^3-benzo[*e*][1,2]iodaoxine (**4.169**): 272
Figure B-69. ^{1}H-NMR (300 MHz, $CDCl_3$) of 1-chloro-3,3-dimethyl-3,4-dihydro-1*H*-1λ^3-benzo[*e*][1,2]iodaoxine (**4.170**): 273
Figure B-70. ^{13}C-NMR (75 MHz, $CDCl_3$) of 1-chloro-3,3-dimethyl-3,4-dihydro-1*H*-1λ^3-benzo[*e*][1,2]iodaoxine (**4.170**): 274

List of Tables

Table 2-1. Preliminary test of the Nazarov cyclization initiated by iodolium salts. 25
Table 2-2. Catalyst and reaction conditions optimization. 26
Table 3-1. Attempted optimization of the reaction between methylcyclobutane **3.76** and $TolIF_2$. 60
Table 3-2. Optimization of BF_3•OEt_2 equivalents. 62
Table 3-3. Optimization of Lewis acid. 63
Table 3-4. Exploring the equivalents of $TolIF_2$, solvent, and order of addition. 64
Table 3-5. Reaction optimization with titanium Lewis acids. 65
Table 3-6. Optimization of *gem*-difluorination of alpha cyclopropyl styrenes. 68
Table 3-7. Additional modification of the optimized conditions. 70
Table 4-1. Optimization of deprotonation and lithiation of **4.106**. 110
Table 4-2. Methyl Grignard addition into ester **4.111**. 113
Table 4-3. Optimization of acetylation 116
Table 4-4. Optimization of ligand exchange synthesis of the fluoroiodane. 123
Table 4-5. Torsion angles (°) from the crystal structures of fluoro- and chloroiodanes. 130
Table 4-6. Bond lengths and angles about the hypervalent bond of the various fluoroiodanes. 135
Table 4-7. Bond lengths and angles about the hypervalent bond of the various chloroiodanes. 136

List of Schemes

Scheme 1-1. Isomerization by pseudorotation. *Differentiates the two acetate ligands in the figure. ...5
Scheme 1-2. General description of the proposed reaction mechanism of HVI reagents. ...6
Scheme 1-3. Solvolysis of vinyl iodonium salt **1.15**. ...6
Scheme 1-4. Synthetic methods for the preparation of the diacetate **1.1** and derivatives. ...7
Scheme 1-5. Synthesis of diaryliodonium salts. ...8
Scheme 1-6. Synthesis of IBX and DMP. ...8
Scheme 2-1. The Nazarov cyclization. ...11
Scheme 2-2. A diastereoselective Nazarov cyclization reaction by Tius et al. (2002). ...13
Scheme 2-3. A Lewis acid complex initiated enantioselective Nazarov cyclization. L* is shown in the transition state (copper bound). ...14
Scheme 2-4. Leveraging the beta-silicon effect to stabilize the oxyallyl cation and direct the regioselectivity alkene formation in a Nazarov cyclization. ...14
Scheme 2-5. An interrupted Nazarov cyclization which results in a product with six new stereocenters. ...15
Scheme 2-6. Arylation of methoxide with diphenyliodonium bromide **2.25**.[46] ...16
Scheme 2-7. Radiofluorination of benzene with fluoride from diaryliodonium salt **2.27**. ...17
Scheme 2-8. The preparation of carbazoles from cyclic diaryliodonium salts. ...17
Scheme 2-9. Enantioselective ring opening of cyclic diaryliodonium salts. ...18
Scheme 2-10. Iodonium salt catalyzed Michael addition. ...21
Scheme 2-11. Enantioselective thioaminal formation with a chiral iodonium salt. ...21
Scheme 2-12. Iodine catalyzed Nazarov cyclization. ...22
Scheme 2-13. Nazarov cyclization with an iodine(I) halogen bonding catalyst. ...22
Scheme 2-14. The first series of substrates that were explored. ...28
Scheme 2-15. The series of unsuccessful heteroaromatic substrates. ...29
Scheme 2-16. Substrate scope continued. ...30
Scheme 2-17. Substrate scope continued. ...31
Scheme 2-18. Degradation of substrate **2.60u**. ...35
Scheme 3-1. Synthesis of difluoride **3.8** with xenon difluoride. ...41
Scheme 3-2. Synthesis of $TolIF_2$ by Hara et al. ...42

Scheme 3-3. Synthesis of $TolIF_2$ by Tao and Murphy. 42
Scheme 3-4. *gem*-Difluorination of dithioketals. 44
Scheme 3-5. Preparation of glycosyl fluorides with $TolIF_2$. 44
Scheme 3-6. Fluorination of 1,3-dicarbonyls with $TolIF_2$. 45
Scheme 3-7. The preparation of fluorovinyl iodoniums and (*E*)-iodo-fluoroalkenes. 45
Scheme 3-8. Difluorination of phenyl diazo acetates with $TolIF_2$ by Murphy et al. 46
Scheme 3-9. A) Difluorination of trifluoromethyl diazo compounds. B) Difluorination of diazo phosphonates. 47
Scheme 3-10. Fluorination of silyl enol ethers with $TolIF_2$. 48
Scheme 3-11. Fluorination of a dienamine with (difluoroiodo)benzene. 48
Scheme 3-12. A) Vicinal difluorination of aliphatic alkenes with $TolIF_2$. B) Proposed mechanism of the vicinal difluorination. 49
Scheme 3-13. The fluorocyclization of alcohols and carboxylic acids. 49
Scheme 3-14. *gem*-Difluorination of styrenes with a mechanistic proposal by Carpenter. 50
Scheme 3-15. Ring contraction of aliphatic cyclic alkenes with $TolIF_2$. 51
Scheme 3-16. Ring contraction of endocyclic styrene **3.53** with $TolIF_2$. 51
Scheme 3-17. Fluorinative ring expansions of exocyclic alkenes and allenes with $TolIF_2$. 52
Scheme 3-18. The preparation of allylic geminal fluorides from phenyl allenes with $TolIF_2$. 52
Scheme 3-19. Preparation of difluorocyclobutanes from methylenecyclopropanes. 53
Scheme 3-20. Chlorination and fluorination combined with ring expansion. $(DHQD)_2PHAL$ = Dihydroquinidine 1,4-phthalazinediyl diether, NBLP = *N*-Boc-L-phenylglycine 54
Scheme 3-21. Fluorination of alpha-cyclopropyl styrenes. 55
Scheme 3-22. Initial reaction development. 56
Scheme 3-23. Blue light for the mild activation of $TolIF_2$ and reaction with methylenecyclopropane **3.70**. 57
Scheme 3-24. The transformation reported by Li et al. 58
Scheme 3-25. The mechanism proposed by Li et. al. 58
Scheme 3-26. Reaction of $TolIF_2$ with **3.76**. 59
Scheme 3-27. Initial discovery of the transformation of **3.77** to **3.78**. 61
Scheme 3-28. Reaction conditions developed by Gulder et al. 66
Scheme 3-29. Proposed mechanism for the formation of **3.78** and **3.79**. 66

Scheme 3-30. *gem*-Difluorination with **3.80**. 67
Scheme 3-31. Initial *gem*-difluorination of **3.88**. 67
Scheme 3-32. Potential further synthetic studies with undesired enone **3.79**. 72
Scheme 4-1. Legault's synthesis of the fluoroiodane. 80
Scheme 4-2. Synthetic methods of the fluoroiodane **4.2**. 83
Scheme 4-3. Mono- and difluorination of 1,3-dicarbonyls. 84
Scheme 4-4. *gem*-difluorination of styrenes with **4.2**. 85
Scheme 4-5. Vicinal iodofluorination with **4.2**. 85
Scheme 4-6. Fluorocyclization with fluoroiodane **4.2**. 86
Scheme 4-7. Fluorocyclization of 5-arylpentenoic acids. 87
Scheme 4-8. Various transformations of styrene **4.22** with fluoroiodane **4.2**. 88
Scheme 4-9. Generic illustration of fluorine vs. iodine attack in a reaction between an alkene and **4.2**. 88
Scheme 4-10. Oxyfluorination of diazocarbonyls. 90
Scheme 4-11. Pyridine-directed alpha-functionalization of ketones. 91
Scheme 4-12. alpha-Functionalization of allylic alcohols. 91
Scheme 4-13. Synthesis of chloroiodane with *t*-BuOCl or TCICA. 93
Scheme 4-14. Alkyne difunctionalization with **4.3**. 93
Scheme 4-15. Cyclization of **4.38** with chloroiodane **4.3**. 94
Scheme 4-16. alpha-Chlorination of 1,3-dicarbonyls. 94
Scheme 4-17. 1,2-difunctionalization of alkenes with chloroiodane **4.34**. 95
Scheme 4-18. Chlorination of allenes with the chloroiodane. 96
Scheme 4-19. Diastereoselective chlorocyclization of geranyl acetate with **4.56**. 97
Scheme 4-20. IBX oxidation of methanol. 98
Scheme 4-21. alpha-Tosylation with ortho-substituted iodoarene catalysts by Wirth et al. and Legault et al. 101
Scheme 4-22. Spirolactonization with ortho-substituted N-heterocycle stabilized iodanes. [a] Solvent: $CH_2Cl_2/CHCl_3$ + 6.0 eq. EtOH, -10 °C. 102
Scheme 4-23. Additional transformations with Nachtsheim's ortho-substituted catalyst. 103
Scheme 4-24. Gold catalyzed alkynylation. 104
Scheme 4-25. Hetero-cleavage of Togni reagent and **4.87**. 104

Scheme 4-26. Generic synthesis of the iodoalcohol and the hypervalent iodine reagents. 106
Scheme 4-27. Synthesis of ortho-CH_3-iodoalcohol **4.93**. 107
Scheme 4-28. Synthesis of the ortho-bromo iodoalcohol **4.97**. 107
Scheme 4-29. Synthetic strategy to access the ortho-ether derivatives. 108
Scheme 4-30. The preparation of the ortho-methoxy and isopropoxy iodoalcohols. 109
Scheme 4-31. Preparation of the *ortho*-isopropyl iodoalcohol. 111
Scheme 4-32. Addition of organocerium reagent to **4.111**. 112
Scheme 4-33. Failed additions into iodoacetophenone **4.117a**. 114
Scheme 4-34. The synthesis of **4.122**. 115
Scheme 4-35. Attempted synthesis of *t*-butyl anthranilic acid. 116
Scheme 4-36. Unsuccessful synthetic routes to the ortho-*tert*-butyl iodoalcohol **4.129**. 117
Scheme 4-37. Synthesis of *ortho*-*t*-butyl iodoalcohol **4.133**. 118
Scheme 4-38. The synthesis of the ortho-methyl iodoalcohol precursor to the six-membered fluoro- and chloro-iodanes. 119
Scheme 4-39. Attempted preparation of bromoiodane **4.142**. 121
Scheme 4-40. The successful synthesis of ortho-methyl fluoroiodane **4.143**. 121
Scheme 4-41. An alternative synthetic route to the fluoroiodane **4.143** without silver. 122
Scheme 4-42. Preparation of the chloroiodane **4.145**. 123
Scheme 4-43. Preparation of the ortho-bromo, -methoxy, and -isopropoxy fluoroiodanes. 124
Scheme 4-44. Attempted synthesis of the isopropyl fluoroiodane **4.152**. 125
Scheme 4-45. Attempted synthesis of fluoroiodane **4.153** and discovery of interesting alkyl aryl iodonium **4.155**. 126
Scheme 4-46. An ionic mechanism for the formation of **4.155**. 127
Scheme 4-47. Additional synthetic routes to **4.153** which were explored. 128
Scheme 4-48. Proposed decomposition of **4.138** when treated with AgF_2. 129
Scheme 4-49. Synthesis of the six-membered ortho-methyl fluoroiodane and chloroiodane. 129
Scheme 4-50. Dynamic exchange proposed to occur at higher temperatures with chloroiodane **4.169**. 137
Scheme 4-51. Fluorocyclization of **4.22** with ortho-methyl fluoroiodane **4.143**. 139

List of Abbreviations

$(DHQD)_2PHAL$	dihydroquinidine 1,4-phthalazinediyl diether
1,1-DPE	1,1-diphenylethene
1,2-DCE	1,2-dichloroethane
3c-4e	three-center-four-electron
Ac	acetyl
$BAr^F{}_4$	tetrakis(3,5-bis(trifluoromethyl)phenyl)borate
BDE	bond dissociation energy
BHT	butylated hydroxytoluene
Boc	tert-butyloxycarbonyl
br	broad
brsm	based on recovered starting material
Bu	butyl
C	Celcius
Cp*	Pentamethylcyclopentadienyl anion
CSA	camphorsulfonic acid
d	doublet
DAST	diethylaminosulfur trifluoride
DIB	(diacetoxyiodo)benzene
DMF	*N,N*-dimethylformamide
DMP	Dess-Martin Periodinane
DoM	directed ortho metallation
DPI	diphenyliodonium chloride
EAS	Electrophilic aromatic substitution
eq	equivalents
GC	gas chromatography
gem	geminal
GP	general procedure
h	hour
HMDSO	hexamethyldisiloxane
HFIP	hexafluoroisopropanol
HTIB	Koser's reagent (also known as hydroxy(tosyloxy)iodobenzene)
HVI	hypervalent iodine
i	iso
IBX	2-iodoxybenzoic acid
LED	light emitting diode

m	multiplet
*m*CPBA	*m*-chloroperoxybenzoic acid
MS	mass spectrometry
MO	molecular orbital
NBLP	*N*-Boc-L-phenylglycine
NBS	N-bromosuccinimide
NMR	nuclear magnetic resonance
NR	no reaction
Nu	nucleophile
Oct	octyl
OTf	trifluoromethanesulfonate
OTs	*p*-toluenesulfonate
PFA	perfluoroalkoxy
Ph	phenyl
PIDA	(diacetoxyiodo)benzene (also known as phenyliodo(III)diacetate)
Piv	pivaloyl
Pr	propyl
prod	product
PyBox-Bn	2,6-Bis((R)-4-benzyl-4,5-dihydrooxazol-2-yl)pyridine
q	quartet
qu	quintet
rt	room temperature
s	singlet
sex	sextet
sm	starting material
t	triplet
TBAF	tetra-butylammonium fluoride
TCICA	trichloroisocyanuric acid
TFA	trifluoroacetyl
TFE	2,2,2-trifluoroethanol
TIPS	triisopropylsilyl
TLC	thin layer chromatography
TMEDA	tetramethylethylenediamine
TMS	trimethylsilyl
Tol	tolyl
$TolIF_2$	*p*-(difluoroiodo)toluene
vs.	versus

List of Symbols

°	degree
™	trademark
λ	lambda

Chapter 1
Introduction

1.1 Preface

In this chapter a general introduction to hypervalent iodine (HVI) is provided, along with a description of the structure and reactivity patterns of the reagents. It will conclude with a description of the scope of this thesis. Chapters 2, 3, and 4 will each begin with an introductory section specific to the topic presented in that chapter.

1.2 Iodine

Iodine is a nonmetallic element found in group 17 of the periodic table, which is known to exist in oxidation states ranging from -1 to +7. It is essential for human life and deficiency can lead to serious medical conditions, as it is incorporated into hormones produced by the thyroid gland. Physically, it is a purple-to-black solid which melts at 113.7 °C and boils at 184 °C. The purification of iodine is accomplished by sublimation under vacuum. Iodine production in Chile and Japan accounts for roughly 90% of the global supply.[1] About two-thirds of this 90% is extracted from the Chilean caliche deposits found in the Atacama Desert, while the remainder is obtained from the oil and gas fields of Japan.[2-4] The United States is also a relatively large producer of iodine, where it is extracted from iodine-rich brine wells in Oklahoma.[3, 4] Scientists have found a wide range of applications for iodine. For example, iodine has been incorporated into multiple molecules for use as X-ray contrast agents for imaging specific organs.[5] Industrially, its reactivity has been exploited in polymer synthesis and in the design of dye-sensitized solar cells.[6] Our interests revolve around iodine in the context of synthetic organic chemistry. In particular, this thesis will focus on the application of hypervalent iodine(III) compounds in the field of synthetic organic chemistry.

1.3 Hypervalent Iodine

To have a proper discussion about hypervalent iodine, hypervalency must first be defined. Musher classified molecules or ions formed by elements in Groups 15-18 of the periodic table as hypervalent if they had valences beyond their lowest stable chemical state.[7] A hypervalent atom is referred to as such if it is surrounded by more electron pairs than dictated by the Lewis-Langmuir theory. When

hypervalent, the iodine atom is typically found in the +3, +5, or +7 oxidation states. Both inorganic, as well as organic hypervalent iodine (HVI) compounds exist. For example, sodium periodate ($NaIO_4$), an inorganic iodine(VII) oxidant, is hypervalent as it contains seven bonds to oxygen, three more than dictated by Lewis-Langmuir theory for a full octet. Hypervalent organoiodanes are widely known and are utilized as oxidants and group transfer reagents. Iodine(III) reagents typically transfer one or both ligands during the oxidation reaction (e.g., difunctionalization of an alkene), while iodine(V) reagents are typically used as oxidants (e.g., oxidation of an alcohol to a ketone). These compounds can be classified as acyclic and cyclic HVI reagents (Figure 1-1). In the acyclic variants, the iodine has two ligands which are unbound to the aromatic ring (e.g., **1.1**), while in the cyclic variants, one ligand is tethered to the aromatic ring (e.g., **1.4**), lending significant stability to the reagent. According to IUPAC, hypervalent compounds should be named according to the lambda notation.[8] Lambda, λ^n, is used to denote a formally neutral heteroatom in a nonstandard valence state (n). This naming convention is not used for many common hypervalent iodine compounds such as $PhI(OAc)_2$, and $TolIF_2$. Figure 1-1 lists the common name and abbreviation, if applicable, for a series of hypervalent iodine reagents.

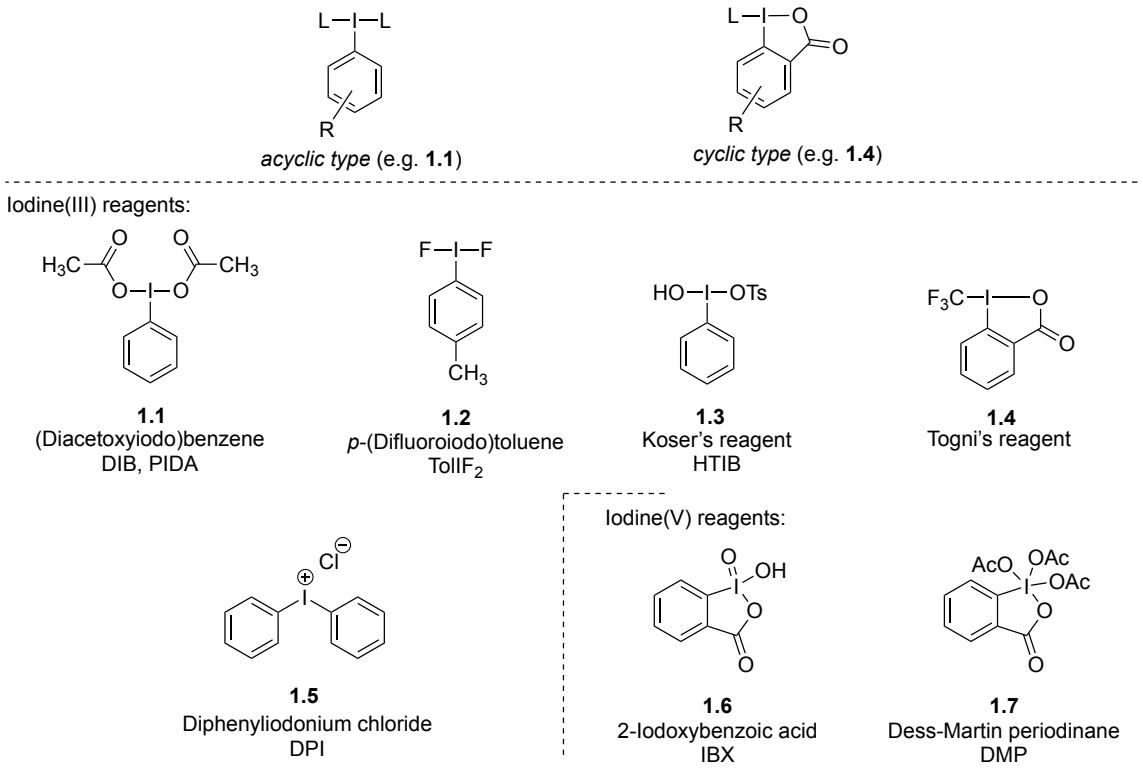


Figure 1-1. Examples of λ^3- and λ^5-iodanes and their respective names.

The hypervalent bonding in molecules **1.1**-**1.7** is best described with molecular orbital (MO) theory and a three-center-four-electron bond (3c-4e). This model was proposed simultaneously by Pimentel and Rundle et al. in 1951.[9, 10] In molecules with the generic structure RIL_2, the collinear atoms L-I-L form the 3c-4e bond (Figure 1-2). In this model, one lone pair is distributed between each ligand, which results in a charge of approximately -0.5 on each ligand, and a charge of +1 on the central iodine. The molecular orbitals are formed from the 5p orbital of the iodine and the half-filled orbitals of the ligands (Figure 1-2). The three atomic orbitals combine to form bonding, non-bonding, and antibonding molecular orbitals. The highest occupied molecular orbital is a non-bonding orbital with a node situated at the iodine, and as such there is more electron density residing on the ligands (L). This bonding results in the three atoms (L-I-L) in the hypervalent bond being collinear. The iodine takes on a distorted trigonal bipyramidal geometry with the two ligands in the apical positions and the aryl ring and two lone pairs in the equatorial positions. The more electronegative atoms (L) tend to occupy the apical positions. This geometry is supported by the solid-state crystal structure of $PhI(OAc)_2$, as well as other HVI reagents.[11] The remaining carbon-iodine bond in organoiodanes is a normal covalent bond. Iodine(V) compounds contain two orthogonal 3c-4e bonds which account for the bonding to both pairs of ligands (Figure 1-2). These compounds take a square bipyramidal shape which places the R-I bond and single lone pair in the apical positions, while the ligands occupy the four equatorial positions. Based on this model the electron density is mostly distributed on the ligands, and as such one can expect hypervalent iodine reagents to be electrophilic at the iodine center, not at the apical ligands. The observed reactivity of HVI reagents can be explained using these principles.

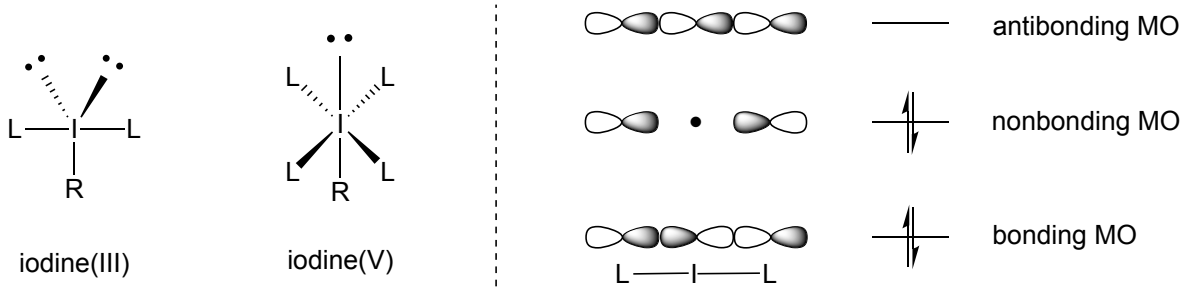
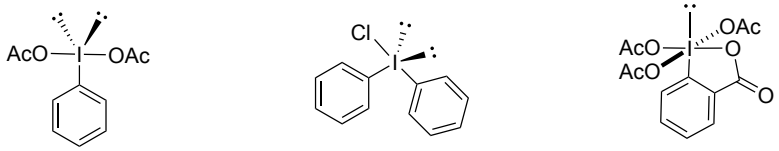


Figure 1-2. Description of the molecular orbitals of the 3c-4e bond found in hypervalent iodine(III) and (V) compounds.

The orientation of the ligands and lone pairs around the hypervalent iodine can be described with the Martin-Arduengo designation.[12, 13] This notation is represented with the following three letters: *N*-*X*-*L*.

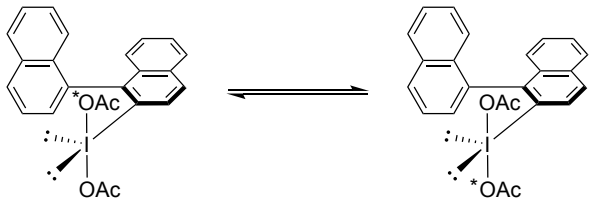
The letter *X* is the central atom around which, *I*, the number of valence electrons (unpaired or bonding), and *L*, the ligands are situated. For example, a generic hypervalent species designated as *12-I-5* indicates a hypervalent iodine atom which is surrounded by *five* ligands and one electron lone pair, for a total of *12* valence electrons. Specific examples are listed in Figure 1-3. The diacetate **1.1** is classified as a *10-I-3* species as the central iodine atom is surrounded by two acetate ligands plus a phenyl ring (total of three ligands), and two lone pairs for a total of 10 valence electrons. Analogously, DMP (**1.7**) can be designated as a *12-I-5* compound. The diphenyliodonium salt **1.5** is more interesting, as formally the iodonium cation is not hypervalent with a total of eight valence electrons. However, it is usually considered to be represented by the structure shown in Figure 1-3 where the weakly coordinating electrons from the counterion (in this case, chloride) are considered to be bonding, making it a *10-I-3* complex.



1.1 *10-I-3* **1.5** *10-I-3* **1.7** *12-I-5*

Figure 1-3. HVI compounds with their respective Martin-Arduengo designations.

Zhdankin lists several general structural features which can be expected in most HVI reagents.[14] RIL_2 compounds, λ^3-iodanes, as previously discussed have a distorted trigonal pyramidal shape. The two most electronegative substituents (L) reside in the apical positions with the lone pairs and the least electronegative C-ligand in the equatorial positions. The C-I bond lengths in these types of compounds are usually the sum of the carbon and iodine covalent radii (2.00-2.10 Å). The I-L bonds are longer than the sum of their covalent radii but shorter than the corresponding ionic bonds. The apical and equatorial ligands are not locked in space, but rather can positionally isomerize rapidly through Berry pseudorotation. This was demonstrated experimentally by Ochiai et al. in 1990.[15] They prepared the optically active binaphthyl diacetate **1.8** which showed two peaks corresponding to the acetoxy groups by ^{1}H-NMR at -10 °C (Scheme 1-1). Warming the sample to 34 °C caused the peaks to coalesce into one singlet with a free energy of activation of 15.1 kcal/mol. They attributed this observation to the degenerate isomerization of the acetate groups in **1.8a** and **1.8b**. The pseudorotation of ligands around iodine is used in the description of HVI reagents' general reactivity.



1.8a **1.8b**

Scheme 1-1. Isomerization by pseudorotation. *Differentiates the two acetate ligands in the figure.

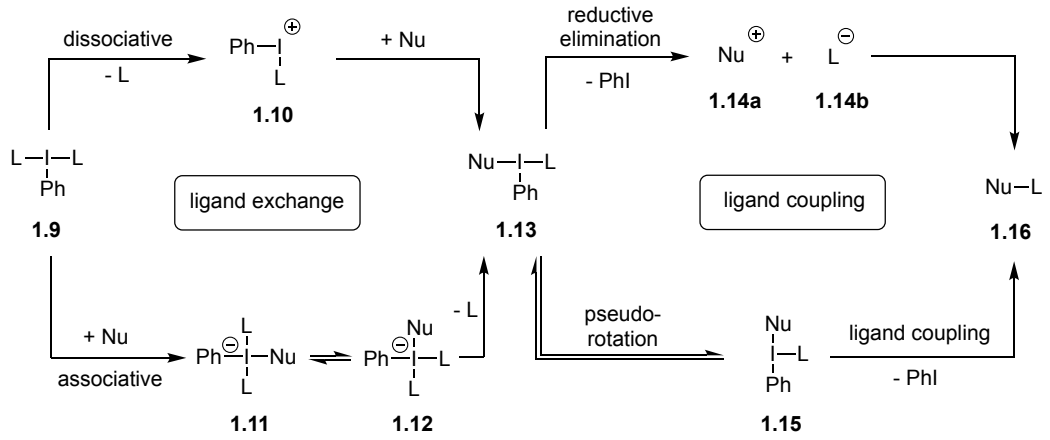
1.3.1 General Reactivity

The general reactivity of HVI reagents has been described with terms that are typically used to describe transition metal chemistry. Typically, the reactivity of HVI reagents is driven by the electrophilic character of the iodine, and its tendency to revert to its natural iodine(I) state through a reductive process. Although no precise mechanism for the individual proposed steps has been elucidated, the sequence shown in Scheme 1-2 is generally accepted to be representative. Outlined in the Scheme is a reaction with an λ^3-iodane; however, this mechanism is equally applicable to λ^5-iodanes.

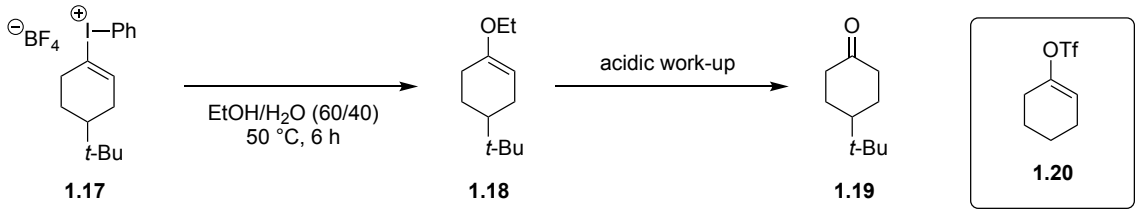
The conversion of **1.9**, through **1.13**, to **1.16** can be described in two steps: (1) the ligand exchange and (2) the ligand coupling (Scheme 1-2).[14] In the first step, the process could in theory be dissociative, where **1.9** loses a ligand to form the *8-I-2* species **1.10**. The addition of the nucleophile would reform a *10-I-3* species **1.13** with two different ligands and the phenyl ring. Although possible, the mechanism is seemingly unlikely to proceed via this route due to the instability of the *8-I-2* species, such as **1.10**.[14] More likely is an associative mechanism where the nucleophile first coordinates the iodine to form the *trans 12-I-4* species **1.11**. Isomerization to the *cis 12-I-4* species (**1.12**), and loss of a ligand gives the intermediate **1.13**. The stability of the *12-I-4* species has been validated by the isolation and X-ray characterization of the ICl_4 anion, lending experimental evidence to this mechanistic route.[16]

The ligand coupling step can also theoretically happen by two different mechanisms.[14] First, direct reductive elimination of iodobenzene would give **1.14a/b**, which after recombination gives the desired product **1.16.** It should be noted that over the course of the reaction, the nucleophile (Nu) **1.14a** has been converted from Nu^- to Nu^+ (i.e., taking on umpolung reactivity). Alternatively, species **1.13** can undergo pseudorotation to convert the Nu/L apical-apical species (**1.13**) to an apical-equatorial species (**1.15**) which can favourably couple the Nu and L while reductively eliminating iodobenzene. In either

pathway, the reductive elimination of iodobenzene is extremely favourable. Ochiai et al. quantified the leaving group ability of PhI^+ and determined it to be almost 10^6 times more favourable than a triflate.[17] This was experimentally determined by a comparison between the solvolysis of **1.17** and the analogous triflate **1.20** (Scheme 1-3).[17, 18] With an understanding that HVI reagents are electrophilic at iodine, the reduction of iodine is favourable, and the ligands can be coupled to the nucleophile, much of the HVI reactivity reported in the literature can be rationalized.



Scheme 1-2. General description of the proposed reaction mechanism of HVI reagents.



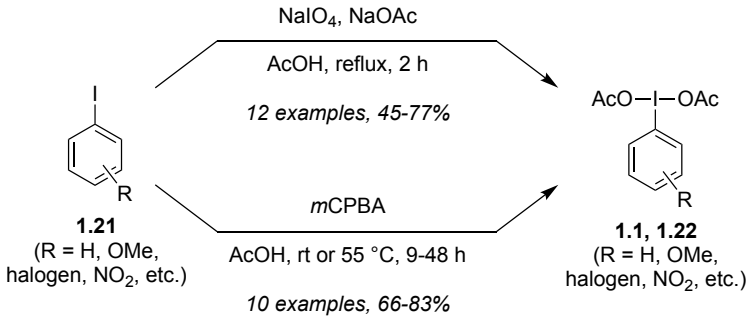
Scheme 1-3. Solvolysis of vinyl iodonium salt **1.15**.

1.3.2 Synthesis

In this section methods to prepare a selection of HVI reagents from Figure 1-1 will be outlined. In general, the syntheses of most HVI reagents begin with an iodoarene precursor which is oxidized to the desired I(III) or I(V) species. The isolation and purification of HVI compounds is usually accomplished by simply filtration, recrystallization, or trituration. Given the extremely polar nature of HVI compounds, they are rarely purified by flash column chromatography. The synthesis of $TolIF_2$ (**1.2**) is

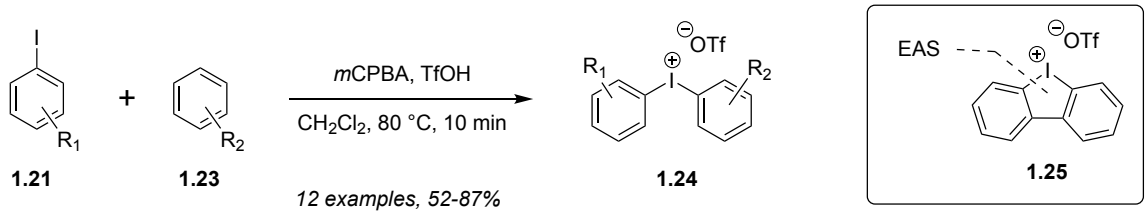
thoroughly discussed in Chapter 3. Reagents similar to Koser's and Togni's reagents are discussed in Chapter 4 and their synthesis is outlined therein.

Although it is commercially available, a myriad of methods were developed to access PIDA (**1.1**) and its derivatives (**1.22**). Two examples are provided below in Scheme 1-4.[19, 20] Common among all methods is the treatment of an iodobenzene **1.21** with an oxidant (inorganic or organic) in the presence of an acetate source to yield the desired hypervalent compound **1.1** or **1.22**. Specifically, when **1.21** was treated with sodium periodate and sodium acetate in refluxing acetic acid, a series of PIDA derivatives were obtained in 45-77% yield. Alternatively, the treatment of **1.21** with *m*-chloroperbenzoic acid (*m*CPBA) in acetic acid gave a separate series with yields between 66-83%.



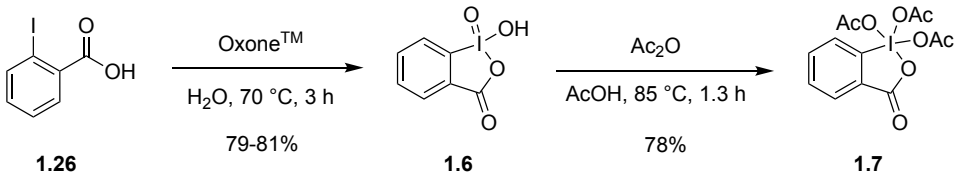
Scheme 1-4. Synthetic methods for the preparation of the diacetate **1.1** and derivatives.

Diaryliodonium salts can easily be accessed by a variety of methods. The method of choice is typically dictated by the desired substitution on the aromatic rings (electron withdrawing vs. donating) and symmetry, or lack thereof.[21] For example, when iodoarenes **1.21** and arenes **1.23** were exposed to *m*CPBA and triflic acid the diaryliodonium salts **1.24** were obtained (Scheme 1-5).[22] This reaction proceeds through oxidation of the aryl iodide to a λ^3-iodane species followed by electrophilic aromatic substitution with the arene **1.23**. In much the same manner, cyclic diaryliodonium salts (e.g., **1.25**) are prepared from the biaryl species where **1.21** and **1.23** are connected by a C-C bond.[23]



Scheme 1-5. Synthesis of diaryliodonium salts.

The λ^5-iodane reagents, IBX (**1.6**) and DMP (**1.7**) are prepared sequentially from 2-iodobenzoic acid (**1.26)**. Santagostino et al. reported that treatment of 2-iodobenzoic acid with Oxone™ in water consistently produced IBX in 79-81% on a 45-50 g scale (Scheme 1-6).[24] This method produced very pure IBX in good yield without the need for any difficult purification, a marked improvement over previous reports. IBX was converted to DMP on a ~20 g scale in 78% yield by acetylation of the oxygen ligands on IBX with a mixture of acetic anhydride and acetic acid.[25]



Scheme 1-6. Synthesis of IBX and DMP.

Overall, HVI reagents are relatively easy to prepare, they offer diverse utility across a range of oxidative transformations, and they are often touted for their non-toxic nature. The last three decades have seen a resurgence in interest in HVI and there is a rapidly growing body of literature. This thesis aims to build and add to the ever-growing collective knowledge about HVI reagents.

1.4 Scope of Thesis

The purpose of this thesis was to gain a deeper understanding of three unique classes of hypervalent iodine reagents. This was accomplished through studies of their reactivity and the design of new reagents. Firstly, diaryliodonium salts, historically used as aryl transfer reagents, were investigated for their mild Lewis acidic properties. Secondly, the reactivity of $TolIF_2$ with new styrenyl substrates was explored. And lastly, synthetic derivatives of a relatively new monofluoroiodane reagent were prepared.

In Chapter 2 the study of diaryliodonium salts as Lewis acidic or halogen bonding catalysts in the Nazarov cyclization is described. Diaryliodonium salts have been exploited in the literature as a source of "electrophilic" arene. More recently, the Lewis acidic character of the central iodine in the diaryliodonium salts has become the focus of intensive study. The potential of these salts in Lewis acid-based transformations is tremendous. Theoretically, they are mild Lewis acids and compatible with many functional groups, their Lewis acidity is tunable by introducing substitution on the aromatic rings, and their general stability allows for recovery after the reaction. A diaryliodonium salt catalyst was successfully applied to the Nazarov cyclization and a unique oxygen-mediate mode of catalyst activation was discovered.

The reactivity of $TolIF_2$ with styrenyl substrates is explored in Chapter 3. This investigation builds on previous reactions with $TolIF_2$ developed in the Murphy group and leverages our reliable method for the gram-scale preparation of $TolIF_2$. $TolIF_2$ has inherently different reactivity from classical electrophilic fluorination reagents and this allows for the synthesis of unique organofluorine structural motifs. Specifically, substrates with the potential to undergo favourable ring strain release and interrupt the classical *gem*-difluorination reaction pathway were explored. This led to the development of reactions between $TolIF_2$ and three unique substrates to provide various fluorinated products.

In Chapter 4 the design of novel monofluoroiodane derivatives with steric bulk ortho to the hypervalent iodine atom was investigated. The parent reagent was initially reported in 2012, and like $TolIF_2$, it exhibits distinct reactivity patterns when compared to classical electrophilic fluorinating reagents. The design of the new derivatives was inspired by reports in the literature indicating that ortho substitution was a powerful design feature for tuning the reactivity of various other HVI reagents. The solid-state torsion angle was presumed to be a key physical feature to be compared between all the derivatives. A series of monofluoroiodane derivatives were successfully prepared and the torsion angles were characterized by X-ray crystallography.

Chapter 2
Cyclic Diaryliodonium Salts as Lewis Acidic Catalysts

2.1 Preface

Reproduced from Ref. 26 with permission from the Centre National de la Recherche Scientifique (CNRS) and the Royal Society of Chemistry.

This chapter is based on the manuscript published in the *New Journal of Chemistry* (To, A. J.; Murphy, G. K., Iodolium salts as halogen-bond donor catalysts in the Nazarov cyclization: the molecular oxygen enigma. *New J. Chem.* **2022,** *46* (32), 15313-15320). I wrote the first draft of the manuscript which was edited in conjunction with Professor Graham Murphy before publication. Additional supporting information can be found on the Royal Society of Chemistry's website for the New Journal of Chemistry.

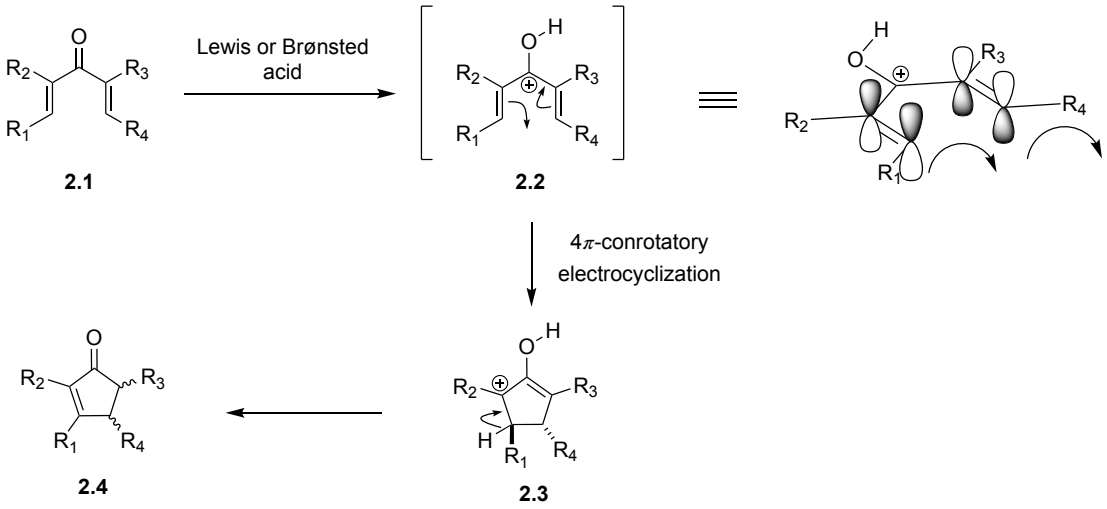
2.2 Introduction

The goal of this project was to demonstrate the viability of diaryliodonium salts as Lewis acidic halogen bonding catalysts for the Nazarov cyclization. The Nazarov cyclization is introduced in Section 2.2.1, followed by a discussion of diaryliodonium salts and their known reactivity in Sections 2.2.2 and 2.2.3. The optimization of the reaction and the breadth of the substrate scope is discussed in Section 2.3, while the control reactions completed to support the overall conclusions of the study are found in Section 2.4.

2.2.1 The Nazarov Cyclization

The Nazarov cyclization is a powerful synthetic tool which provides efficient access to a diverse set of cyclopentenones (e.g., **2.4**). This Lewis or Brønsted acid-mediated electrocyclization converts a planar divinyl ketone to a cyclic pentenone with a minimum of two stereocenters.[27-30] Recent work has seen it modified to include other alkene equivalents (e.g., allenes),[31, 32] interruptions through intermediate capture,[33] and even induction of torquoselectivity to introduce more molecule complexity or control of the selectivity.[34] The typical mechanism of the Nazarov cyclization is illustrated with a Brønsted acid in Scheme 2-1. Activation of the divinyl ketone **2.1** with an appropriate acid will generate the cation **2.2**, which undergoes a 4π-conrotatory electrocyclization to form a cyclic oxyallyl cation, such as **2.3**. Subsequent elimination and keto-enol tautomerization yields the final cyclopentenone **2.4**. Eight possible isomers are obtainable from **2.3** depending on the final position of the alkene as well as the

absolute stereochemistry of the R groups. The stereo- and regioselectivities are typically substrate-controlled; however, in some instances, they have been Lewis acid-controlled with careful optimization of the reaction conditions.[35] Designing a reaction with selectivity for a single stereoisomer remains a challenge in Nazarov cyclization chemistry.[35]



Scheme 2-1. The Nazarov cyclization.

For a Nazarov cyclization to occur the alkenes must be able to adopt an *s*-trans conformation, **2.5b**/**2.6b**, to promote cyclization (Figure 2-1). The addition of substituents at the alpha-position of the carbonyl makes **2.5b** the more energetically favourable conformation (favouring cyclization), while substituents placed at the beta-position makes the conformation **2.6b** favourable (disfavouring cyclization) (Figure 2-1).[35] The difference in conformer stability, and ultimately proportion in the equilibrium, is based on the amount of allylic strain experienced by the molecule. In the **2.5a**/**2.5b** pair, greater allylic strain is present in **2.5a**, so **2.5b** is the favoured conformer. While in the **2.6a**/**2.6b** pair, there is greater allylic strain in **2.6b,** favouring conformer **2.6a** which is not predisposed for a Nazarov cyclization. Substitution of oxygen at the alpha-position (e.g., compound **2.7**) proved to be particularly beneficial, and substrates of this design underwent Nazarov cyclizations with mild reaction conditions and catalytic amounts of Lewis acid.[35, 36] This was likely due to the stabilization of the electrocyclization transition state through the donation of electron density by oxygen (e.g., **2.7-TS**). If total control of the product stereo- and regioselectivity is desired, three aspects of the reaction must be controlled: (1)

torquoselectivity, or the direction of *conrotatory* cyclization (2) the regioselectivity of the double bond formation, and (3) the protonation of the enol.[35]

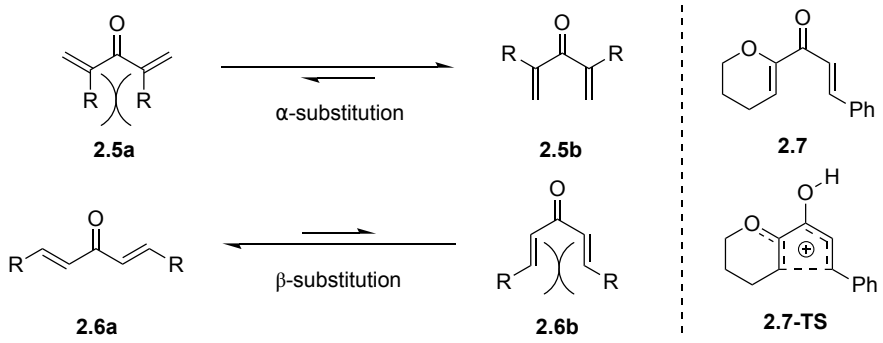


Figure 2-1. The influence of alpha- and beta-substituents on the Nazarov cyclization.

To achieve a completely enantioselective Nazarov cyclization one must, first, control the direction of the *conrotatory* cyclization (Figure 2-2). That is to say, its torquoselectivity (i.e., the direction of the electrocyclization), which can occur in a clockwise or counterclockwise fashion, must be controlled. In the example below, the direction of the rotation determines the absolute stereochemistry at the R_4 or R_1 carbons (Figure 2-2). If compound **2.2** were to rotate clockwise, the R_1 substituent would be up, while the R_4 is down (e.g., **2.3a**). If the rotation was counterclockwise, R_1 and R_4 would have the opposite configuration (e.g., **2.3b**).

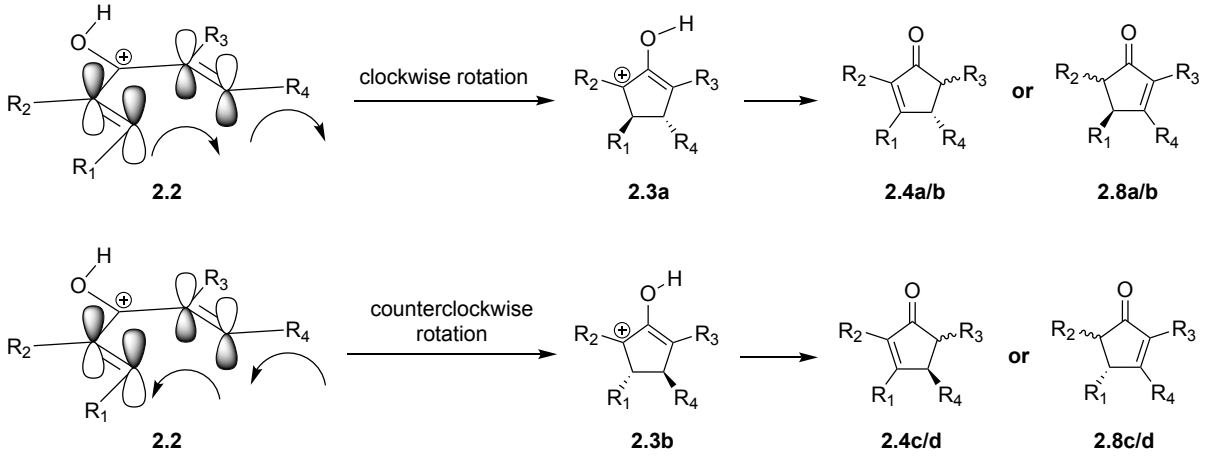
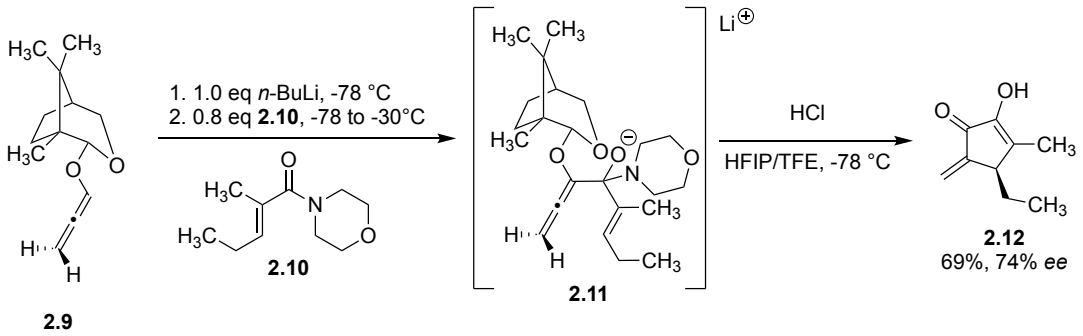


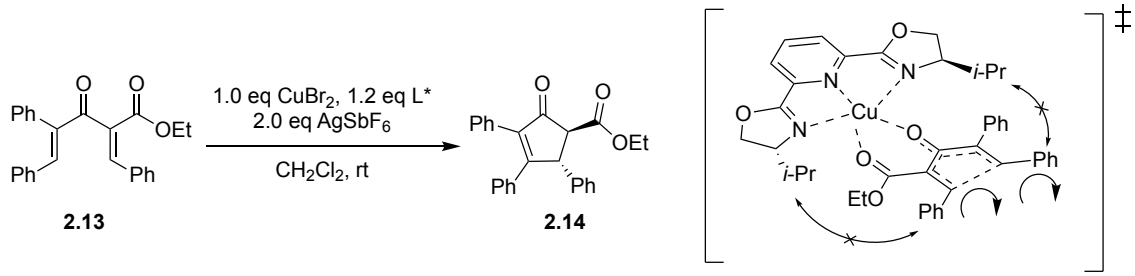
Figure 2-2. Illustration of torquoselectivity in a Nazarov cyclization.

The torquoselectivity of a reaction can be either substrate or initiator (Brønsted or Lewis acid) controlled. In 2002, Tius et al. published a successful diastereoselective Nazarov cyclization where camphor-derived auxiliaries linked to the substrate were utilized to achieve products with high enantiomeric purity (Scheme 2-2).[37] The divinyl ketone was prepared *in situ* from the allene **2.9**, which was lithiated and trapped with morpholine amide **2.10**. This intermediate **2.11** was quenched via addition into a solution of hydrochloric acid in HFIP and TFE to give the product in 69% and 74% *ee*.[37] This is an example of substrate-controlled diastereoselectivity which leads to a single enantiomer. The torquoselectivity arises from the preference of the alkene to rotate counterclockwise away from the steric bulk of the camphor-derived auxiliary. The utility of this method was demonstrated on seventeen substrates giving yields up to 84% and up to 87% enantiomeric excess.



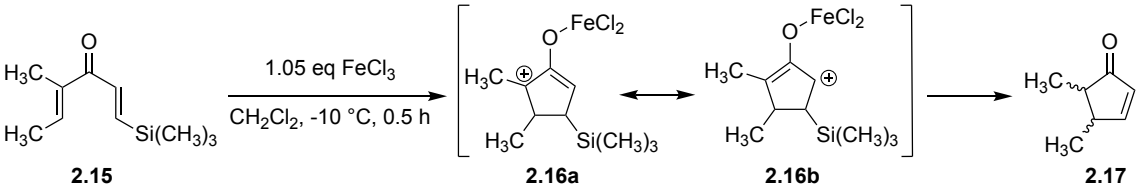
Scheme 2-2. A diastereoselective Nazarov cyclization reaction by Tius et al. (2002).

Enantiocontrol can be achieved using a chiral initiator, such as a chiral Lewis acid, to induce stereochemistry in the final product. The first successful use of a chiral Lewis acid catalyst in the Nazarov cyclization was published by Aggarwal and Belfield in 2003.[38] They developed and optimized an enantioselective Nazarov cyclization reaction with copper bisoxazoline-based Lewis acid complexes (Scheme 2-3). They envisioned a transition state where the ligand/copper complex interacted with the 1,3-dicarbonyl **2.13** and as a result, the steric hindrance of the isopropyl groups forced a clockwise *conrotatory* cyclization (as shown in the transition state in Scheme 2-3).[38] The substrate with the highest yield (98%) and enantiomeric excess (86%) is presented, along with the optimal bisoxazoline ligand.[38] This methodology also set the stereochemistry at the alpha-carbon, producing the single thermodynamically favoured trans-diastereomer **2.14**, where the steric strain between the neighbouring groups is minimized.[38]



Scheme 2-3. A Lewis acid complex initiated enantioselective Nazarov cyclization. L* is shown in the transition state (copper bound).

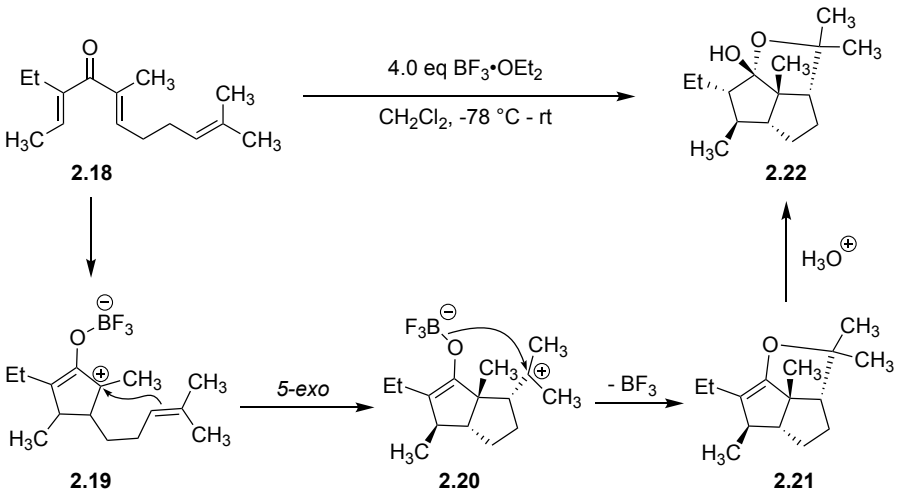
An important contribution to the development of the Nazarov cyclization came from the work of Professor S. E. Denmark. These seminal works utilized the beta-silicon effect to stabilize the oxyallyl cation intermediate (e.g., **2.16**) and direct the regioselectivity of the alkene formation after cyclization (Scheme 2-4).[39] Treatment of the divinyl ketone **2.15** with $FeCl_3$ gave the expected cyclic oxyallyl cation **2.16a**/**2.16b**. Once the intermediate **2.16** is generated, the silyl group will preferentially stabilize the positive charge on the beta-carbon (e.g., **2.16b**) through hyperconjugation. Elimination of the silyl group gives the desired cyclopentenone **2.17** in 95% yield as a mixture of diastereomers (59:41, cis:trans). The methodology was explored with six other substrates and yields between 27-84% were obtained for the desired products.



Scheme 2-4. Leveraging the beta-silicon effect to stabilize the oxyallyl cation and direct the regioselectivity alkene formation in a Nazarov cyclization.

A major contribution to the effectiveness of the Nazarov cyclization for building complex molecules was made by the research group of Professor F. G. West, and their development of the "Interrupted Nazarov", which involves trapping the oxyallyl cation with a nucleophile.[33] The interrupted Nazarov sequence reported by Bender et al. is illustrated in Scheme 2-5.[33] Beginning from triene **2.18**, a compound with no stereocenters at any of the sp^3-carbons, the tricyclic product **2.22** with six stereocenters was synthesized.[33] The reaction began as a typical Nazarov cyclization with the activation

of the ketone and conrotatory cyclization of **2.18**. The resulting oxyallyl cation **2.19**, which normally terminates via proton elimination, was trapped by a pendant alkene in a 5-exo cyclization to form bicycle **2.20**. The resulting tertiary cation was captured with the boron-coordinated alkoxide to form tricycle **2.21** which upon hydration gave the final product **2.22** in 73% yield as a racemic mixture of a single diastereomer. A total of five substrates were successfully cyclized in this manner and obtained in 42% to 89% yield. Over the years, the interrupted Nazarov has been further developed and the oxyallyl cation has been trapped (1) intermolecularly with arenes or alkenes; (2) in [3+4] cycloadditions, and (3) with N-, O-, or halogen-based nucleophiles to produce a wide range of complex products.[40] Proper design of the Nazarov substrate and/or the initiator can be leveraged to transform relatively simple starting materials into complex stereo-defined products making it a particularly useful reaction in the total synthesis of natural products.[41-45]



Scheme 2-5. An interrupted Nazarov cyclization which results in a product with six new stereocenters.

2.2.2 Diaryliodonium Salts as a Source of Electrophilic Arene

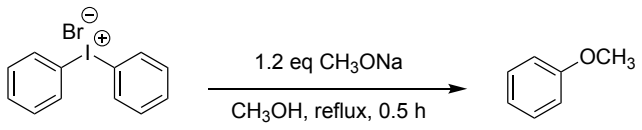


2.23, X = OTf
cyclic diaryliodonium salt

2.24, X = OTf
acyclic diaryliodonium salt

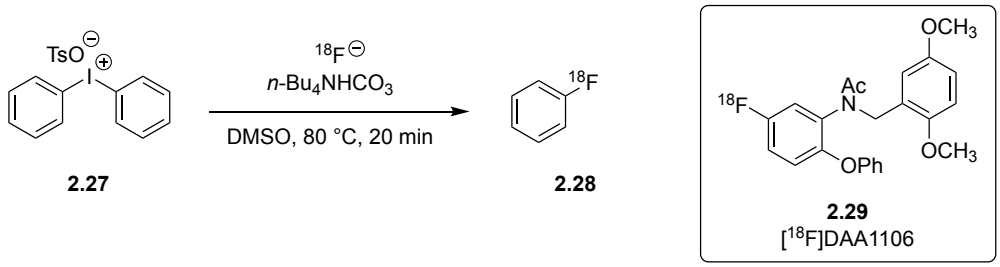
Figure 2-3. Examples of the two types of diaryliodonium salts.

There are two types of diaryliodonium salts, the cyclic variant (e.g., **2.23**) and the acyclic type (e.g., **2.24**) without a bond between the aromatic rings (Figure 2-3). Both of these are hypervalent iodine(III) compounds that contain an iodine atom between two aromatic rings. The iodine is positively charged and therefore has a counter anion (e.g., X). The counter anion can be another halogen, a tosylate, a tetrafluoroborate, or as shown in the example above, a triflate anion. Given the oxidation state and the charge on the iodine, these reagents are powerful yet versatile electrophiles that serve as arene-transfer agents when reacted with nucleophiles.[46-60] For example, in 1953 Beringer et al. demonstrated that methoxide could be arylated with diphenyliodonium bromide **2.25** in 67% yield (Scheme 2-6). There have since been many further developments in the synthetic methodology which allows for more complex ether synthesis, as well as the functionalization of nitrogen and sulfur nucleophiles. Diaryliodonium salts are also competent electrophiles for the alpha-arylation of carbonyls or C-H arylation of electron-rich heteroaromatic systems.[61, 62] Notably, diaryliodonium salts have been used as precursors to radiofluorinated compounds. The treatment of diaryliodonium salt **2.27** with fluoride and the phase transfer catalyst tetrabutylammonium carbonate provided fluorobenzene **2.28** in 90% yield (Scheme 2-7).[63] This methodology was used to produce a radiofluorinated PET ligand **2.29** for the imaging of a peripheral benzodiazepine receptor.



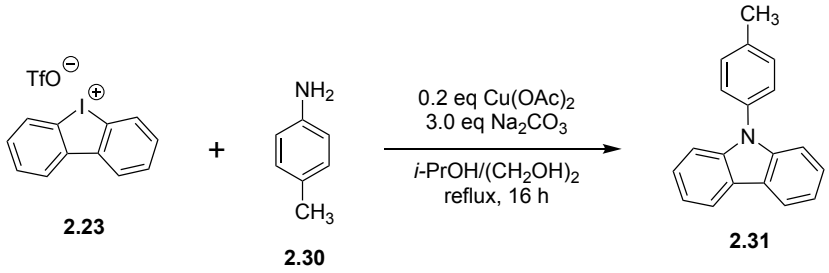
2.25 **2.26**

Scheme 2-6. Arylation of methoxide with diphenyliodonium bromide **2.25**.[46]

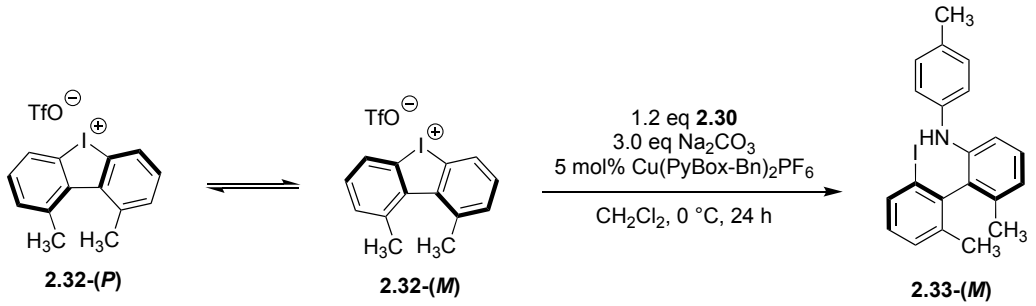


Scheme 2-7. Radiofluorination of benzene with fluoride from diaryliodonium salt **2.27**.

The related biphenyl-derived cyclic diaryliodonium salts (e.g., **2.23**) also reacted with nucleophiles but instead afforded substituted biphenyl derivatives, [64, 65] and underwent dual arene transfer in metal-catalyzed cross-coupling reactions.[66-70] For example, under copper catalysis, the cyclic diaryliodonium salt **2.23** was aminated twice to form the carbazole **2.31** in 71% yield (Scheme 2-8).[71] This type of reactivity was not exclusive to nitrogen-based nucleophiles, but could also be achieved with O- and S-based nucleophiles to prepare the corresponding heterocycles.[67, 72] The enantioselective mono-functionalization of diaryliodonium salts with chiral copper catalysts was possible with substitution on the aryl rings that limited bond rotation (e.g., **2.32**). The equilibrating mixture of the *P* and *M* stereoisomers of **2.32**, when treated with the copper-PyBox complex, led to a major enantiomer of the product **2.33** in 99% yield and 98% *ee* (Scheme 2-9).[64] This was highlighted with 44 examples varying both the diaryliodonium salt and the amine. Both the yields and the enantiomeric excess were typically greater than 95%. Overall, both cyclic and acyclic diaryliodonium salts have found extensive use as reagents in the preparation of functionalized aromatic molecules.



Scheme 2-8. The preparation of carbazoles from cyclic diaryliodonium salts.



Scheme 2-9. Enantioselective ring opening of cyclic diaryliodonium salts.

2.2.3 Diaryliodonium salts as Halogen Bond Donors

In all the above processes, the reactions were driven by the reduction of iodine from a hypervalent to a standard oxidation state. Another entirely different synthetic application recently emerged for diaryliodonium salts, which does not involve the reduction of iodine(III) to iodine(I). This application is homogeneous halogen-bond catalysis, where the electropositive region of an iodine atom from an organoiodine motif activates a Lewis basic functional group through a non-covalent interaction (Figure 2-4).[73]

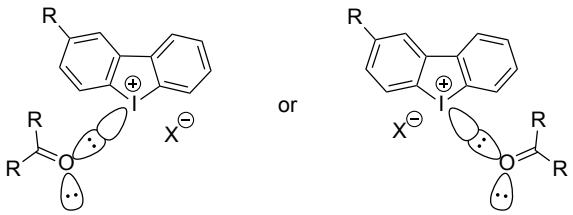


Figure 2-4. Interaction of a Lewis basic lone pair on the oxygen of a ketone with a diaryliodonium salt.

Recently, Legault and Mayr investigated the Lewis acidity of both cyclic and acyclic diaryliodonium salts and quantified these against various Lewis bases.[74, 75] They investigated seventeen different diaryliodonium salts against halide, oxygen, nitrogen, and phosphorus-based Lewis bases by NMR titration, photometric or conductometric methods, and isothermal calorimetry. This study showed that cyclic diaryliodonium salts (e.g., **2.23)** were more Lewis acidic than their acyclic counterparts (e.g., **2.24**),[75] but more importantly, it confirmed these ions as possible Lewis acidic catalysts.[76] The biaxial Lewis acidic nature of cyclic diaryliodonium salts was also demonstrated through both spectroscopic

and isothermal calorimetric methods (Figure 2-4, e.g., the carbonyl could interact with the "left" or "right" side of a non-symmetric iodonium salt). The majority of the examples demonstrating the catalytic reactivity of diaryliodonium salts found in the literature concern halide abstraction, such as cyclic diaryliodonium salts catalyzing the solvolysis of benzhydryl chlorides (Figure 2-5a),[77] activation of metal-halogen bonds[78] or catalyzing cationic living polymerizations.[79] A series of diaryliodonium salts were screened using NMR for reaction analysis in the chloride abstraction and solvolysis of **2.34**, with the reaction proceeding in ~80% yield with salt **2.23**. While diaryliodonium salts have also been used as versatile catalysts in symmetric and asymmetric Mannich reactions,[80] there also exist examples of selective carbonyl activation, such as the diaryliodonium salt-catalyzed Diels-Alder reaction between cyclopentadiene and methyl vinyl ketone (Figure 2-5b)[77] or Knorr pyrazole synthesis (Figure 2-5c).[81] In the example of the Diels-Alder reaction a catalytic amount of the diaryliodonium salt **2.38** was proposed to accelerate the reaction by activating the methyl vinyl ketone **2.36** through coordination with the carbonyl. With this catalytic system, greater than 95% ^{1}H-NMR yield is achieved. In the case of the Knorr pyrazole synthesis, the desired product **2.42** was isolated in 99% yield with 10 mol% of the catalyst (15 examples, 46-90% yields). Similar investigations revealed both **2.23** and **2.24** to be competent catalysts in a Groebke-Blackbrun-Bienaymé reaction.[82] Notably, the cyclic diaryliodonium salt **2.23** was more active than its acyclic counterpart **2.24**.

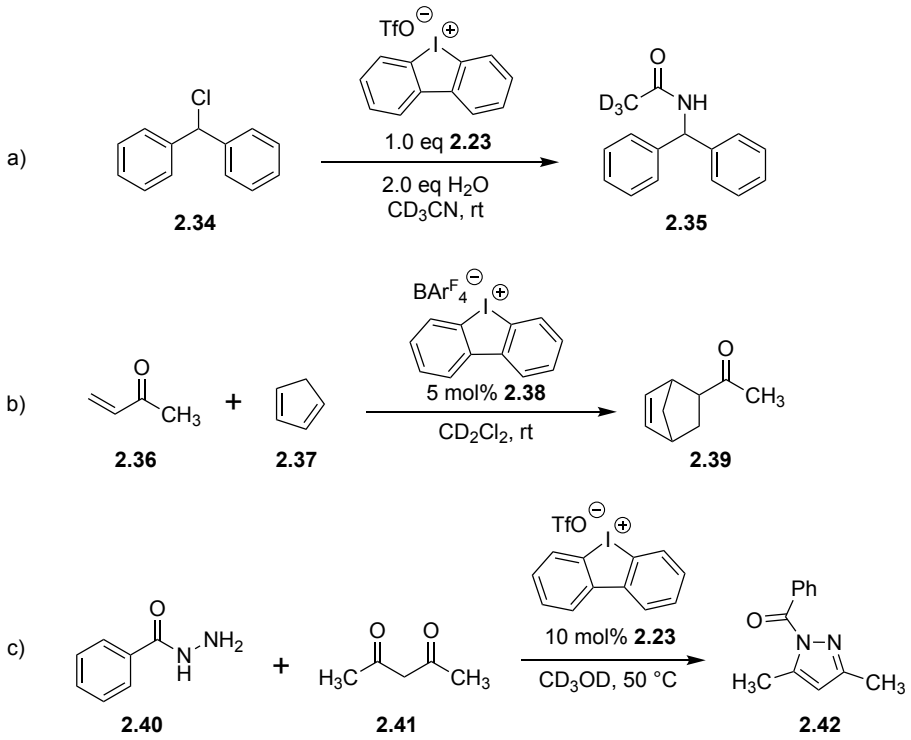


Figure 2-5. Examples of the synthetic utility of cyclic diaryliodonium salts as reaction initiators.

The research groups of Huber and Nachtsheim have further investigated the structural design of the diaryliodonium salt catalysts/initiators. Nachtsheim reported the heterocyclic iodopyrazolium salt **2.43**, which demonstrated improved reactivity in the halide abstraction and solvolysis of substrate **2.34**.[83] Huber prepared three alternative iodonium salts **2.44**-**2.46** (Figure 2-6) and tested them in the solvolysis reaction (Figure 2-5a).[84] The iodonium salt **2.44**, with a larger central ring, had significantly diminished reactivity. The addition of the electronegative fluorine atoms on one aromatic ring in **2.45** drastically improved the reactivity compared to **2.23**, while iodonium salt **2.46** showed mild improvements. Huber et al. have also investigated the bidentate iodonium salt **2.49** in the significantly more challenging Michael addition of indole **2.47** into enone **2.48** (Scheme 2-10).[85] This catalyst is considered to be bidentate as each lone pair of the carbonyl oxygen could interact simultaneously with separate iodine atoms, therefore binding more strongly to the substrate. While this catalyst showed near quantitative ^{1}H-NMR yields in the reaction, the monodentate catalyst **2.38** showed no activity, clearly illustrating the greater halogen-bonding strength or Lewis acidity of the bidentate iodonium salt **2.49**. These studies demonstrate the tunability of the iodonium salts by structural modifications and how they can be modified to achieve superior halogen-bonding activity.

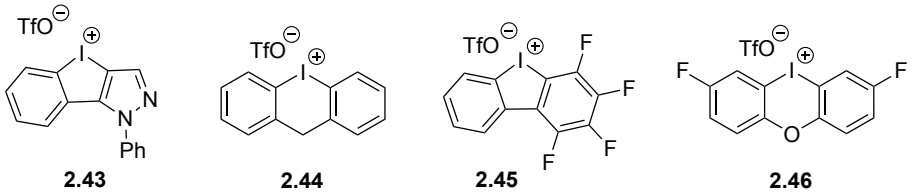
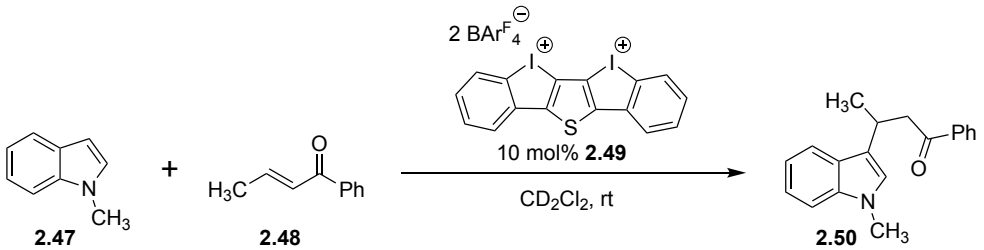
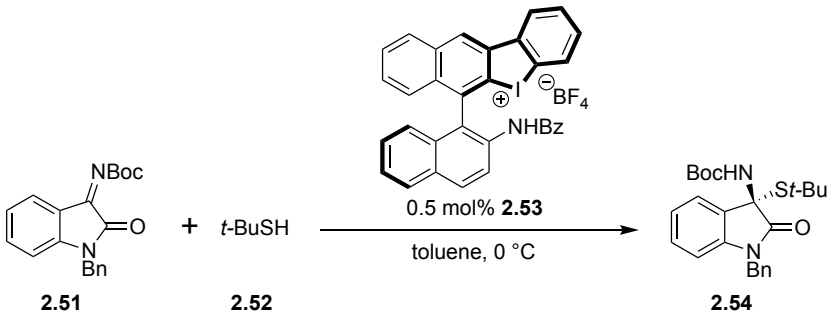


Figure 2-6. Structurally varied iodonium salts **2.43**-**2.46**.



Scheme 2-10. Iodonium salt catalyzed Michael addition.

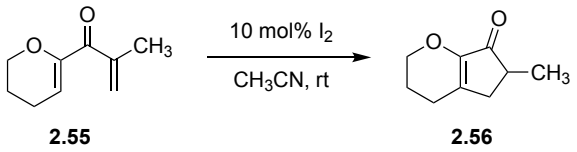
In addition to the development of the Lewis acidity or halogen bonding strength of the iodonium salts, Yoshida et al. exploited the possibility of enantioselective induction.[86] The iodonium catalyst they designed (**2.53**) has an axially chiral naphthyl group adjacent to the iodine. Using only 0.5 mol% of the catalyst, the formation of thioaminal **2.54** was accomplished in >99% yield and 95% *ee* from the ketimine **2.51** and thiol **2.52** (Scheme 2-11). Over the 19 examples presented, the yields and enantioselectivities were generally high (>90%); however, low enantioselectivities were obtained with thiophenols instead of aliphatic thiols. The extremely low catalytic loading and high enantioselectivities achieved in this report demonstrate the potential of these iodonium salts as organo-catalysts.



Scheme 2-11. Enantioselective thioaminal formation with a chiral iodonium salt.

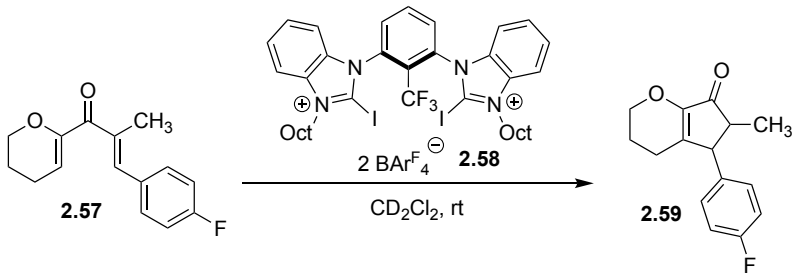
2.2.4 Halogen Bonding and the Nazarov Cyclization

In addition to the typical use of Brønsted- or Lewis acids as Nazarov reaction initiators, two instances of iodine(I)-based halogen-bond donor catalysis were reported in 2019. In the first report, Breugst et al. showed an elemental iodine initiated Nazarov cyclization (Scheme 2-12).[87] When the divinyl ketone **2.55** was treated with molecular iodine it induced a 4π conrotatory cyclization to give the Nazarov product **2.56** in 80% yield. An additional eighteen substrates were successfully cyclized with this methodology (56-98% yield). Theoretical studies indicated that the reactions proceeded upon coordination of the halogen-bond donor (iodine) to the carbonyl of the divinyl ketone starting material. This lowered the transition state energy for the transformation of **2.55** to **2.56** by 6.7 kcal/mol. Huber reported an organocatalyzed Nazarov cyclization initiated by a bidentate bis(2-iodobenzimidazolium) salt **2.58** (Scheme 2-13).[88] The iodine(I) atoms bonded to the electron-deficient aromatic rings interacted strongly with the lone pairs of the carbonyl to initiate the reaction. Overall, halogen bonding is an effective mode of carbonyl activation and was effectively demonstrated in these two Nazarov cyclization examples.



2.55 **2.56**

Scheme 2-12. Iodine catalyzed Nazarov cyclization.



2.57 **2.59**

Scheme 2-13. Nazarov cyclization with an iodine(I) halogen bonding catalyst.

2.2.5 Research Objectives

Considering the successful use of both iodine(I) and (III) species in catalyzing transformations based on the activation of a carbonyl, this project explored the viability of diaryliodonium salts (iodine(III) compounds) as catalysts for the Nazarov cyclization. As the halogen-bond donor in a diaryliodonium salt is iodine(III) as opposed to iodine(I) (e.g., **2.58**), they might serve as stronger halogen-bond donors for initiating the Nazarov cyclization. Further, given that such catalysts are recyclable, their electrophilicity and solubility can be tuned through counterion exchange or functional group substitution, and that chiral variants of these salts are known,[86] they hold tremendous potential as Nazarov cyclization catalysts. In the following Sections the results of this investigation are discussed and show that while diaryliodonium salts are indeed effective Nazarov cyclization catalysts, the actual catalytic cycle is rather complex.

2.3 Results

2.3.1 Optimization

Our investigation began with an activated divinyl ketone known to readily undergo the Nazarov cyclization,[36] and the unsubstituted iodolium triflate salt **2.23**, which possessed a weakly coordinating triflate salt. The initial substrate and catalyst to be studied were chosen with purpose. The initial substrate was known to readily undergo a Nazarov cyclization and would allow us to quickly determine if this reaction was at all viable. For example, if a diaryliodonium salt could not initiate or catalyze the reaction with even the most active substrate, it was likely significant structural modification of the catalyst would be necessary. The iodonium triflate salt **2.23** was chosen for its simplicity and lack of additional substitution on the aromatic ring. Ideally, the reaction could proceed with the simplest diaryliodonium salt catalyst and in an excellent yield.

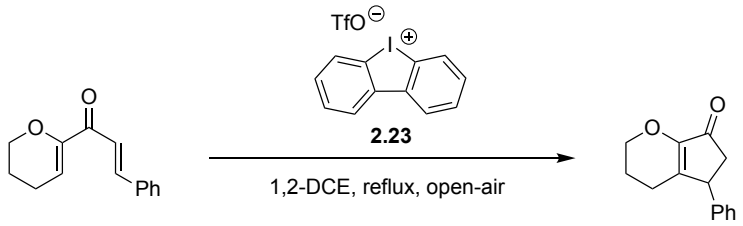
We first wanted to determine if **2.23** was at all active in the desired transformation. Combining **2.60a** and **2.23** in a 1:1 ratio in 1,2-DCE under ambient atmosphere and heating at reflux for 0.5 h consumed **2.60a** and provided **2.61a** in 56% ^{1}H NMR yield (Table 2-1, entry 1). This initial result showed that **2.23** was indeed sufficiently electrophilic to initiate the Nazarov reaction. Although this result was interesting, the use of stoichiometric diaryliodonium salt is inefficient if only catalytic quantities are necessary for the reaction. Therefore, we decreased the loading of **2.23** to 20 mol% and performed the

reaction again. This required a longer time for **2.60a** to be consumed (0.5 vs. 1 hour) and gave **2.61a** in an increased 78% yield, suggesting that the reaction was superior when conducted as a catalytic process (Table 2-1, entry 2). Difficulties in further reaction development were soon encountered. The time required to consume **2.60a** under seemingly identical conditions began fluctuating inconsistently, and as we continued to investigate this phenomenon, the reaction eventually stopped producing **2.61a** entirely. In these instances, complete consumption of **2.60a** was observed without any observable product formation (Table 2-1, entry 3). We hypothesized that seasonal changes were causing the ambient humidity in the air to dramatically increase, which led to atmospheric moisture deactivating the iodolium salt **2.23** and reducing its catalytic activity. Based on this assumption, we anticipated that a return to the original level of catalytic activity (e.g., 1 hour, 78% yield; Table 2-1, entry 2) would be achieved if we instead conducted the reaction under a nitrogen atmosphere and excluded atmospheric moisture. Unfortunately, none of the desired product **2.61a** was observed upon heating at reflux, and ^{1}H NMR analysis of the crude reaction mixture showed only minimal decomposition of **2.60a** (Table 2-1, entry 4). Evidently, critical reaction parameters were not understood or accounted for and inadvertently being overlooked.

Given the failure of the reaction under a nitrogen atmosphere, the first hypothesis explored was the possibility that another component of the ambient atmosphere was crucial for the success of the reaction. Reproducibility and improved yields were re-established when the reaction was conducted using a balloon of compressed air, or when equipped with a Drierite-packed drying tube (Table 2-1, entries 5 and 6). These conditions allowed for the moisture-free exchange of the reaction mixture with an air atmosphere, and while they both required 2 hours for **2.60a** to be consumed, **2.61a** was observed in improved 90% and 95% yields, respectively. This result suggested that indeed another component of the ambient atmosphere, such as oxygen, plays an important role in the reaction. This idea will be explored further with control reactions in Section 2.3.3. As an initial control to confirm whether the catalyst was necessary, the reaction was conducted without catalyst **2.23**, which resulted in no conversion of substrate **2.60a** being observed (Table 2-1, entry 7). From these initial studies, we were pleased to find that iodolium salts were viable initiators of the Nazarov cyclization; however, there appeared to be a competing decomposition pathway that could consume **2.23** unproductively (compare entries 1 and 2, and see entry 3), and the data also suggested that the reaction required exposure to the

atmosphere to proceed. Both of these phenomena were the subject of various control experiments described in equations 2-1 to 2-6.

Table 2-1. Preliminary test of the Nazarov cyclization initiated by iodolium salts.



2.60a **2.61a**

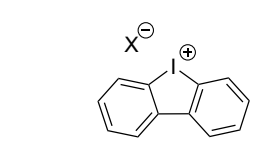
Entry	X mol% of **2.23**	Time[a] (h)	Yield of **2.61a**[b] (%)
1	100	0.5	56
2	20	1	78
3	20	>36	0[c]
4	20	1	0[d]
5	20	2	90[e]
6	20	2	95[f]
7	0	2	0[fg]

[a]Time required for consumption for **2.60a**. [b]Yield determined by ^{1}H NMR with hexamethyldisiloxane (HMDSO) as the internal standard. [c]Increased atmospheric humidity. 100% conversion of **2.60a** without observable product formation. [d]Reaction performed under N_2 gas. Minimal conversion of **2.60a**. [e] Under compressed air balloon. [f] Reflux condenser fitted with a drying tube packed with Drierite. [g]No conversion of **2.60a**.

Further reaction optimization was achieved upon testing various other iodolium catalysts. First, we tested the counterion of the catalyst, since its coordinating ability should have a significant impact on the catalytic activity.[89] Unsurprisingly, using chloride (**2.62**) and tosylate (**2.63**) counterions, which are known to bind strongly with diaryliodonium cations, resulted in diminished yields and longer reaction times, presumably due to both diminished Lewis acidity and poor catalyst solubility (Table 2-2, entries 2 and 3). An iodolium salt possessing the weakly coordinating hexafluorophosphate counterion (**2.64**) displayed better solubility and consumed **2.60a** approximately twice as fast as compared to catalysts **2.62** and **2.63**; however, the yield was comparably low (Table 2-2, entry 4). Salt **2.65**, which possessed the weakly coordinating tetrafluoroborate counterion, showed improved reactivity over **2.62** – **2.64**, converting **2.60a** to **2.61a** in 73% yield over 5 hours (Table 2-2, entry 5). We also tested the $BAr^F{}_4$

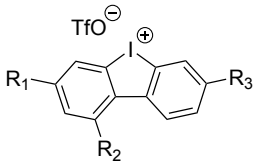
counterion-containing catalyst **2.66** (Table 2-2, entry 6), which consumed **2.60a** in only 2 hours (same as catalyst **2.23**); however, it produced **2a** in 83% yield, which was significantly lower than that achieved with **2.23**. Overall, no increase in yield or reaction rate was observed by solely changing the diaryliodonium salt counterion. We therefore employed triflate salts in all subsequent catalyst optimization efforts, which included the preparation and evaluation of three CF_3-substituted diaryliodonium salt derivatives (**2.67**, **2.68**, **2.69**). We hoped to induce greater catalytic activity by increasing the catalyst's electrophilicity by appending additional electron-withdrawing groups.[80, 84] The reactions of each salt with **2.60a** were complete in 2-2.5 hours, with only catalyst **2.69** giving yields comparable to **2.23** (Table 2-2, entries 7-9). As catalyst **2.69** displayed significantly improved solubility compared with **2.23**, we elected to carry out all further investigations with it.

Table 2-2. Catalyst and reaction conditions optimization.

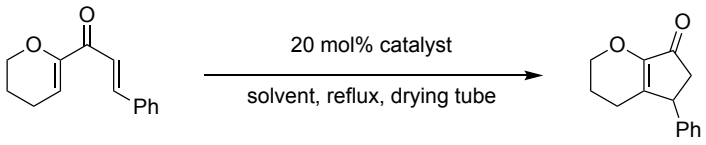


2.23, X = OTf
2.62, X = Cl
2.63, X = OTs

2.64, X = PF_6
2.65, X = BF_4
2.66, X = BAr^F_4



2.67, R_1 = CF_3, R_2, R_3 = H
2.68, R_1, R_3 = CF_3, R_2 = H
2.69, R_1, R_2 = CF_3, R_3 = H



2.60a **2.61a**

Entry	Solvent	Catalyst	Counterion	Time[a] (h)	Yield of **2.61a**[b] (%)
1	1,2-DCE	**2.23**	OTf	2	95
2	1,2-DCE	**2.62**	Cl	20	34
3	1,2-DCE	**2.63**	OTs	20	32
4	1,2-DCE	**2.64**	PF_6	11	36
5	1,2-DCE	**2.65**	BF_4	5	73
6	1,2-DCE	**2.66**	BAr^F_4	2	83
7	1,2-DCE	**2.67**	OTf	2.5	58
8	1,2-DCE	**2.68**	OTf	2	85

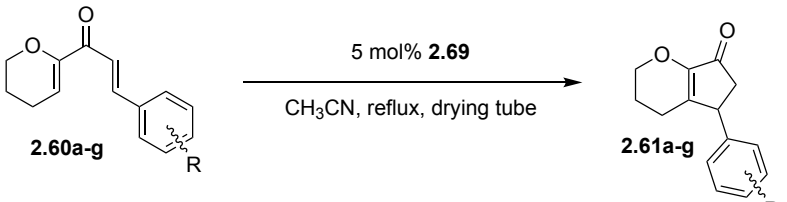
Entry	Solvent	Catalyst	Counterion	Time[a] (h)	Yield of **2.61a**[b] (%)
9	1,2-DCE	**2.69**	OTf	2	94
10	CH_3CN	**2.69**	OTf	7.5	>95
11	$CHCl_3$	**2.69**	OTf	8	87
12	Acetone	**2.69**	OTf	10.5	75
13	CH_2Cl_2	**2.69**	OTf	10.5	18
14	CH_3CN	**2.69**	OTf	25	75[c]
15	CH_3CN	**2.69**	OTf	10	95[d]

[a]Time required for consumption for **2.60a**. [b]Yield determined by ^{1}H NMR with hexamethyldisiloxane (HMDSO) as internal standard. [c]Reaction conducted at 65 °C. [d]Reaction conducted with 5 mol% **2.69**. $BAr^F{}_4$ = tetrakis(3,5-bis(trifluoromethyl)-phenyl)borate.

We next tested the reaction solvent as it would be expected to have a significant impact on the resulting catalytic activity.[90] Presumably, fully solubilizing the diaryliodonium salts was crucial for optimal catalyst activity. These salts are typically most soluble in relatively polar solvents. Unfortunately, most common polar (protic or aprotic) solvents also contain a Lewis basic lone pair, and as such the solvents could compete with the substrate for the active sites on the diaryliodonium salt catalyst. Nonetheless, these solvent studies were performed and revealed that reactions performed in CH_3CN were cleaner by ^{1}H NMR than those performed in 1,2-DCE, while the consumption of **2.60a** took significantly longer, the yields were comparable. Weak coordination of acetonitrile to the Lewis acidic sites on the diaryliodonium might explain the longer reaction time. Other solvents such as chloroform, acetone and methylene chloride offered no advantage in terms of either reaction rate or yield of **2.61a** (Table 2-2, entries 10-13). Reducing the reaction temperature was counterproductive as the reaction time in CH_3CN increased to 25 hours, and the yield of **2.61a** decreased to 75% (Table 2-2, entry 14). Fortunately, we could reduce the loading of **2.69** to 5 mol% and still achieve a 95% yield of **2.61a** in only 10 hours (Table 2-2, entry 15). These counterion optimization studies indicated that halogen-bond catalysis is dependent on both catalyst solubility and the strength of the counterion coordination, and while solvents of widely differing polarities (and donor abilities) were compatible in the reaction, strong donors and those with lower boiling points were less effective. From this, the optimal conditions were determined to be heating the substrate at reflux in acetonitrile with 5 mol% of catalyst **2.69**, in a flask equipped with a Drierite-packed drying tube. Having these optimized conditions in hand we explored the scope of this iodonium salt catalyzed Nazarov reaction.

2.3.2 Substrate Scope

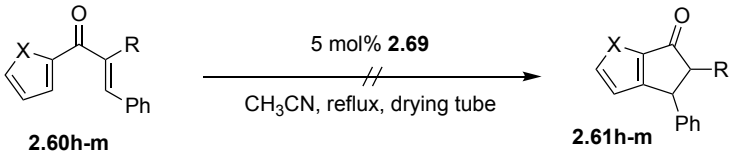
We next investigated the substrate scope of this reaction, first through the impact of aryl ring substitution (Scheme 2-14, **2.61a-g**). The unsubstituted substrate **2.60a** underwent cyclization in 70% isolated yield, which is well within the 56-99% yields reported in the literature using either protic or Lewis acid activation.[36, 87, 91-94] The addition of strongly (**2.60b**) or moderately (**2.60c**) electron-donating groups reduced the yields to 62% and 56%, respectively, and halogenation of the aryl ring (4-F, **2.60d**; 2-Br, **2.60e**) also negatively impacted the yields, giving products in 55% and 42% yield, respectively. Methoxy group substitution at the 3-position of the aryl ring resulted in partial consumption of starting material; however, none of product **2.61f** was observed and starting material **2.60f** could only be recovered in 34% yield. Similarly, complete decomposition of the *p*-CF_3 derivative **2.60g** was also observed under the standard conditions; however, in this instance neither the product **2.61g** nor starting material **2.60g** were recoverable. Given the generation of positive charge in both the transition states and intermediates it is not surprising that electron-withdrawing groups were detrimental to the yield.



2.61a, R = H, 7.5 h, 70%
2.61b, R = 4-OCH_3, 5 h, 62%
2.61c, R = 4-CH_3, 7 h, 56%
2.61d, R = 4-F, 26 h, 55%
2.61e, R = 2-Br, 9 h, 42%
2.61f, R = 3-OCH_3, 24 h, 0%
2.61g, R = 4-CF_3, 24 h, 0%

Scheme 2-14. The first series of substrates that were explored.

The related substrates containing five-membered heteroaromatics (Scheme 2-15, **2.60h-2.60m**) in place of the activating dihydropyran moiety exhibited no reactivity and produced none of the products **2.61h-2.61m**. Even the doubly-activated pyrrole-derived substrate **2.61m**, whose carbonyls might have been activated by both of the catalyst's halogen-bond donor sites, was unreactive under these conditions. Curiously, reacting Boc-protected **2.60l** with 5 mol% **2.69** resulted in none of the desired reaction, but instead gave **2.60j** in 48% yield, presumably via a halogen-bond-initiated Boc cleavage.

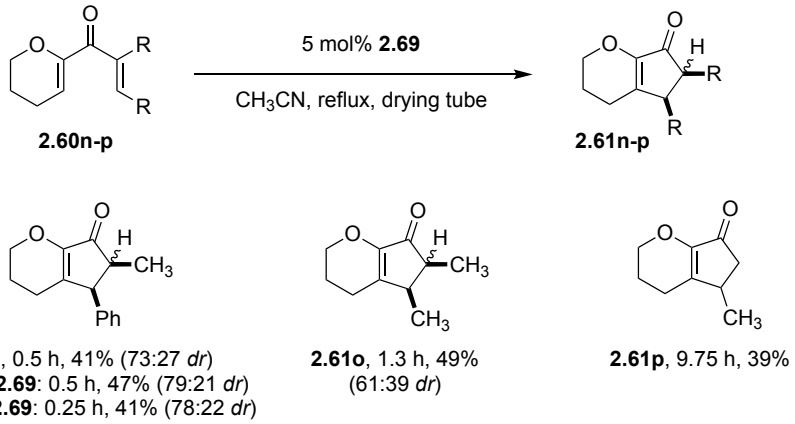


2.60h-m **2.61h-m**

2.61h, R = H, X = O
2.61i, R = H, X = S
2.61j, R = H, X = NH
2.61k, R = H, X = NBn
2.61l, R = H, X = NBoc
2.61m, R = CO_2CH_3, X = NH

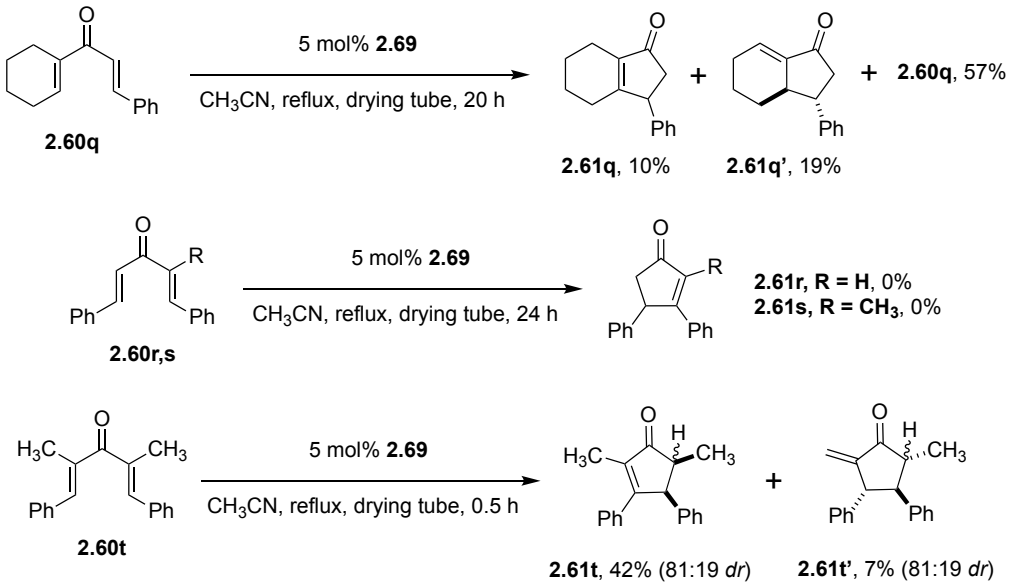
Scheme 2-15. The series of unsuccessful heteroaromatic substrates.

We next tested the alpha-methyl derivative **2.60n**, which reacted to give **2.61n** in 41% yield, favouring the *syn* stereoisomer (*dr* = 73:27). To demonstrate the reusability of the catalyst, **2.69** was recovered and reused in this experiment, from which **2.61n** was again recovered in a similar yield and *dr* (47%, 79:21 by ^{1}H NMR). Increasing the catalyst loading to 20 mol% accelerated the reaction but neither improved the yield nor changed the *dr* of product **2.61n**. This result is a significant departure from the 88% yield and 100% *syn*-selectivity reported by Trauner et al. under traditional Lewis acid catalysis with $AlCl_3$.[36] Cyclization of the alpha,beta-dimethyl substrate **2.60o** occurred in 49% yield (vs. >80% in the literature)[70, 72, 73] with 61:39 *dr* favoring the *syn*- stereoisomer.[36, 91, 93, 94] The β-methyl derivative **2.60p** reacted to give **2.61p** in 39% yield, which is again low in comparison to other literature reports (84-95%).[87, 91, 92, 94] While these results are unsatisfactory when compared with typical acid-catalyzed cyclizations, collectively these deviations strongly suggest that the reactivity observed herein is not a result of hidden acid-catalysis.[95] Hidden acid-catalysis describes the idea that Brønsted acid, deliberately or accidentally, generated in situ by the reaction conditions is the true catalyst, and not the initially added metal or organic catalyst. For example in our reaction, if the diaryliodonium salt catalyst was decomposing into hydroiodic acid (i.e., the hidden acid), the hydroiodic acid and not the diaryliodonium salt would likely catalyze the reaction. This was unlikely to be operative in our reaction due to the aforementioned comparison of our yields to the literature reports. Likewise, the differences in reaction rate and product yield observed for these substrates under iodolium ion catalysis and under molecular iodine catalysis were strongly indicative that the catalyst is not decomposing into molecular iodine in situ.[87] Again, if iodine catalysis was operative one would expect identical or near identical yields and reaction times.



Scheme 2-16. Substrate scope continued.

Moving away from the activated dihydropyran-derived motif, we first reacted **2.60q** with catalyst **2.69** and obtained two cyclized alkene isomers **2.61q** and **2.61q'** in 10% and 19% yield, respectively. This unpolarized substrate did exhibit significantly higher stability under the current reaction conditions, as 57% of **2.60q** was recovered from the reaction even after 20 hours of heating. Additional unpolarized systems **2.60r** and **2.60s** were also tested, but these failed to cyclize after 24 hours and the starting materials were recovered. The lower reactivity of these substrates was explained by considering the population of the conformers. With less substitution at the alpha-positions, the population of the *s*-trans conformer will be lower and cyclization disfavoured. The more reactive Nazarov substrate **2.60t** was fully consumed after 0.5 hours of heating, and produced diastereomeric mixtures of alkene isomers **2.61t** and **2.61t'** in 42% and 7% yield, respectively. These final results showed that iodolium ion catalysis was poorly suited for unpolarized Nazarov substrates; however, the background degradation process that unproductively consumed polarized substrates (e.g., **2.60f**, **2.60g**) was less problematic with these, as recovery of unreacted starting materials was possible.



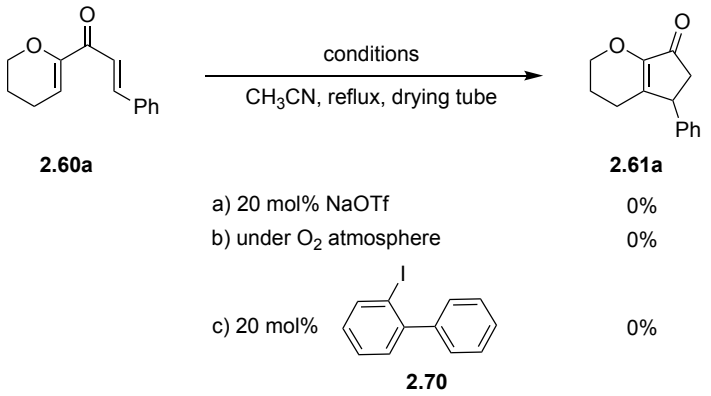
Scheme 2-17. Substrate scope continued.

Overall, we showed that a variety of diaryliodonium salts were effective catalysts in the Nazarov cyclization of pre-activated divinyl ketones. The reactions were tolerant to various substituents and substitution patterns and gave the desired products in moderate to good yields. As the product yields widely differed from those achieved under either Brønsted or Lewis acid catalysis, hidden acid catalysis was unlikely to be operative here.

2.3.3 Control Reactions

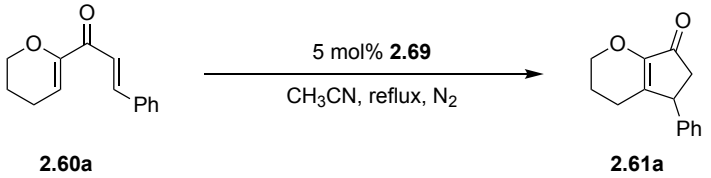
To determine the origin of the specific reaction conditions required, (i.e., the need for a drying tube) a series of control experiments were performed. First investigating the observed catalyst (de)activation phenomena described earlier (see Table 2-1). We were able to rule out any impact of triflate ions or molecular oxygen on their own, as **2.60a** was unchanged and no product was produced in a reaction between **2.60a** and NaOTf, or when stirring **2.60a** under an atmosphere of oxygen in the absence of catalyst **2.69** (equations 2-1a and 2-1b). To rule out a hidden background reaction catalyzed by an iodine(I) species, we reacted **2.60a** with 2-iodo-1,1'-biphenyl (the iodoarene precursor to **2.23**), from which no product was again observed (equation 2-1c). Additionally, different batches of catalyst **2.69** could be used in reactions of **2.60a**, with no discernable difference in reaction rate or product yield

observed. Collectively, these results implied that triflate ions, molecular oxygen and organoiodine(I) catalysts were not responsible for the observed reactivity.



(2-1)

A stringent analysis of the water content in the reaction was conducted to probe whether water was activating the catalyst instead of oxygen. Karl–Fischer titrations allowed us to quantify the water in the acetonitrile (39 ppm) and in a solution of catalyst **2.69** in CH_3CN (0.005 M, 700 ppm). We degassed the CH_3CN using a freeze-pump-thaw sequence to ensure no residual dissolved oxygen remained, then reacted **2.60a** and **2.69** under an atmosphere of nitrogen, where the reactions contained specifically 46, 92 and 141 mol% of total water content. As quantified by ^1H NMR analysis, yields of only 2%, 6% and 3% of **2a** were observed along with recovery of approximately 95% of **2.60a** in all cases (equation 2-2). From these trials, we concluded that water, in the absence of oxygen, was deactivating the catalyst and was not responsible for the catalytic activity observed.

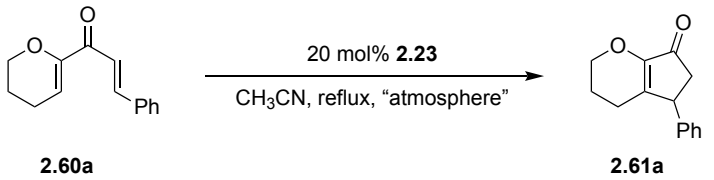


(2-2)

a) using 46 mol% H_2O — 2% (95% of **2.60a**)
b) using 92 mol% H_2O — 6% (94% of **2.60a**)
c) using 141 mol% H_2O — 3% (95% of **2.60a**)

We next investigated the apparent need for oxygen activation of the catalyst. The reaction previously failed to proceed under a nitrogen atmosphere (Table 2-1, entry 4), so to rule out the possibility that contaminants were being introduced from the nitrogen source, we repeated the experiment under argon.

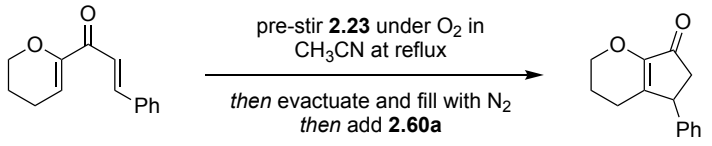
Substrate **2.60a** was stirred with 20 mol% of **2.23** in acetonitrile at reflux under argon for 1 h, after which no product was observed. Upon temporarily removing the condenser and exposing the reaction to the air, consumption of **2.60a** and formation of **2.61a** began immediately, with a 77% ^{1}H NMR yield of **2.61a** achieved after 1 h (equation 2-3).



2.60a **2.61a** (2-3)

a) under argon, 1 h, 0% **2.61a**;
b) then exposure to ambient atmosphere, 1 h, 77% **2.61a**

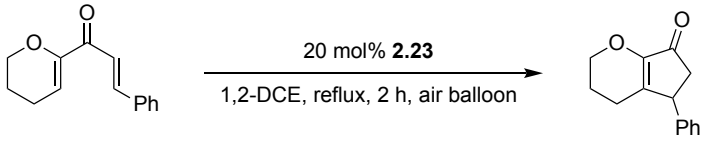
Though it was (to the best of our knowledge) unprecedented in the literature, we continued with the premise that oxygen was required to activate the catalyst. We next carried out several experiments to support and possibly quantify this effect. First, we pre-stirred 20 and 40 mol% of catalyst **2.23** in CH_3CN at reflux under an oxygen atmosphere, seeking to activate **2.23** in the absence of substrate. We then evacuated the flasks, refilled them with nitrogen and added **2.60a** (equation 2-4), from which we observed **2.61a** in 25% and 47% ^{1}H NMR yield, respectively. These results indicated that the pre-activated catalyst was viable in the absence of oxygen, but more importantly, that oxygen was necessary for achieving catalyst turnover. In an attempt to spectroscopically observe a structural change in the catalyst upon its activation by oxygen, catalyst **2.69** was stirred at reflux in CH_3CN under either an atmosphere controlled with a calcium chloride packed drying tube or an oxygen balloon. Subjecting these activated catalyst mixtures to both ^{1}H NMR and quantitative ^{19}F NMR analysis (comparing against the triflate counterion ^{19}F NMR signal) showed little to no change or degradation of the diaryliodonium motif. These results, in conjunction with the fact that iodolium salts are typically air stable and do not readily oxidize to higher valent species, suggested that the catalyst's activation and turnover perhaps involved coordination with molecular oxygen, rather than a formal oxidative chemical event.



2.60a **2.61a** (2-4)

a) 20 mol% **2.23**, 25% **2.61a**
b) 40 mol% **2.23**, 47% **2.61a**

To assess whether radical reactivity was occurring under either the air or oxygen atmospheres we conducted another series of quantitative ^{1}H NMR experiments. Using the result from Table 2-1, entry 5 as the parent reaction (see equation 2-5a), we repeated the reaction in the dark and obtained 68% of **2.61a** along with 13% of **2.60a**. Conducting the reaction in the presence of the radical trap 1,1-diphenylethylene (1,1-DPE) had minimal impact, as **2.61a** was generated in 85% yield. Repeating the reaction with butylated hydroxytoluene (BHT) produced no product. As both **2.60a** and BHT were observed in 86% and 100% ^{1}H NMR yield, respectively, we inferred that catalyst deactivation through a Lewis acid/base interaction was impeding the reaction, rather than radical trapping of a Nazarov cyclization intermediate. From these trials we concluded that a radical cyclization was unlikely to be operative. The exact nature of the interaction between molecular oxygen and the catalyst remained unknown.

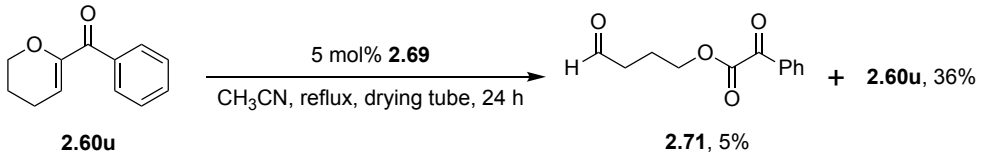


2.60a **2.61a** (2-5)

a) 90% **2.61a** (Table 2-1, entry 5)
b) in the dark: 68% **2.61a** (13% **2.60a**)
c) with 1.0 equiv 1,1-DPE: 85% **2.61a** (8% **2.60a**)
d) with 1.0 equiv BHT: 0% **2.61a** (86% **2.60a** and 100% BHT)

Finally, we conducted a series of experiments to elucidate which degradation pathways were operative with these substrates. First, we subjected substrate **2.60u** to the reaction conditions, as the arene would prevent it from cyclizing, making it ideal for probing which degradation pathways were available to the dihydropyran unit. In this reaction, **2.60u** underwent significant decomposition over 24 hours, from which we isolated **2.71** in 5% yield and **2.60u** in 36% yield (Scheme 2-18). As there were

no other products easily isolable from this experiment, and as structures **2.60u** and **2.71** differed only by the addition of two oxygen atoms, we could only deduce that at least one degradation pathway appeared to exploit both the catalyst (perhaps through pyran activation) and molecular oxygen, leading to cleavage of the pyran double bond. This type of reactivity is not known with diaryliodonium salts; however, HVI reagents such as $PhIO_2$ have been used to facilitate ozonolysis-like reactivity.[96]



2.60u **2.71**, 5%

Scheme 2-18. Degradation of substrate **2.60u**.

Following these control experiments, we conducted a ^{1}H NMR study with substrate **2.60n** to spectroscopically identify either unknown side-products or, possibly, Nazarov intermediates in situ (Figure 2-7). This substrate was chosen because it easily undergoes the Nazarov cyclization at room temperature, better accommodating a time-lapse NMR experiment and because the occurrence of new methyl peaks in the ensuing spectrum would be easily observable indicators of any new species. Although no intermediates were revealed, we did observe the formation of alcohol **2.72**, which is known to arise from the hydrolytic ring opening of **2.61n**.[91, 97, 98] The conversion of **2.60n** to **2.72** is documented in both a palladium[97] and Amberlyst-15[91] catalyzed Nazarov cyclization of this substrate. This rapidly accumulated to 50% yield (by ^{1}H NMR, using hexamethyldisiloxane, HMDSO, as internal standard), far eclipsing the observed yields of the initial Nazarov products *cis*- and *trans*-**2.61n**. While the yields of isomers **2n** observed here were entirely consistent with our earlier isolated yields (41% combined, see Scheme 2-16), only 13% of **2.72** was isolable from this reaction. This is in stark contrast with the >90% yields reported for **2.72** by others, and it suggests that **2.72** is further degrading under the reaction conditions or during the purification. Even though side products analogous to **2.72** were not isolated from the reactions of the other polarized substrates, given the easy formation and subsequent degradation of **2.72** at room temperature, we believed that this decomposition pathway may have been partially responsible for the diminished yields observed throughout this study.

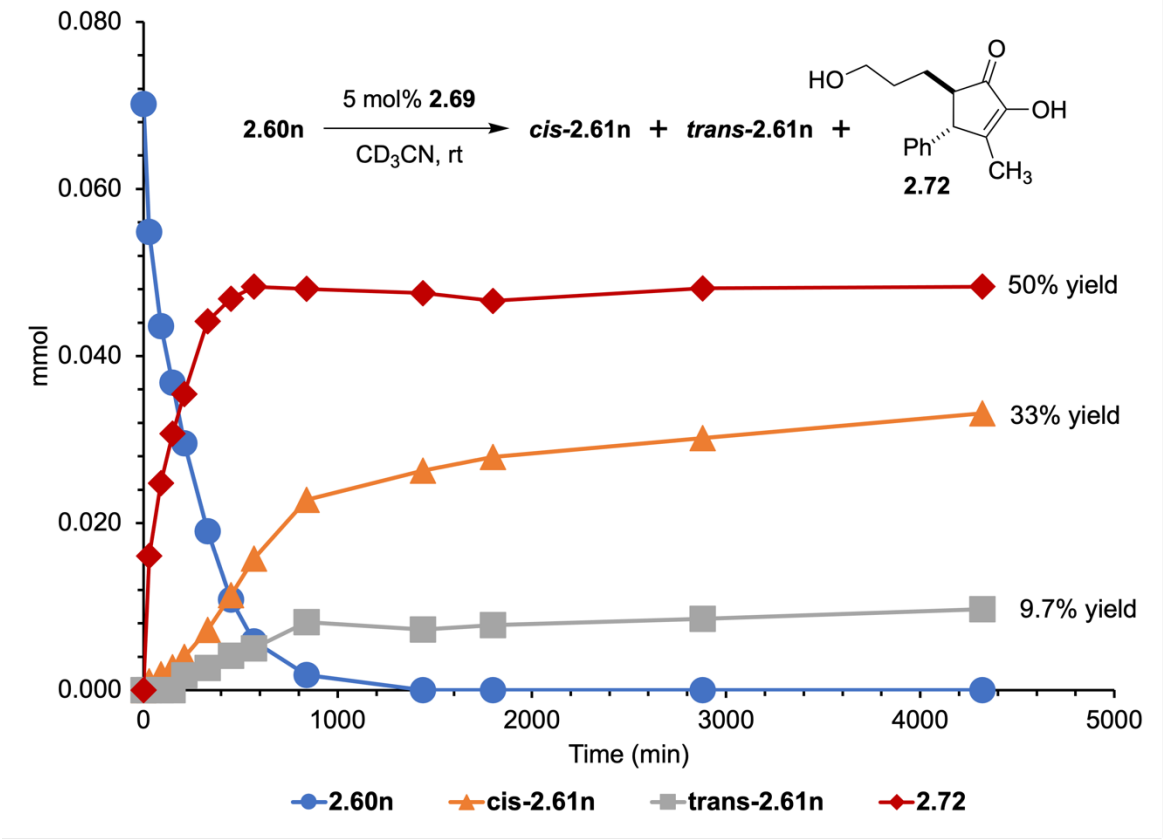
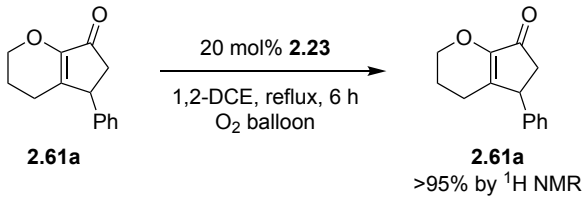


Figure 2-7. ^{1}H NMR study of the conversion of **2.60n** to **2.61n** with catalyst **2.69**.

To confirm that the Nazarov products, once formed, were not degrading under the reaction conditions, we subjected product **2.61a** to catalyst **2.23** at reflux under an oxygen atmosphere (equation 2-6). Analysis of this reaction mixture by quantitative ^{1}H NMR resulted in a spectrum lacking impurities, from which **2.61a** was measured in >95% retention. These NMR results are strongly indicative that a reaction intermediate is unproductively diverted.



(2-6)

2.4 Concluding Remarks and Future Work

Overall, iodonium salts were shown to be effective catalysts for the Nazarov cyclization. A substrate scope was explored and the reaction was found to be successful mostly with the most activated divinyl ketone systems. The moderate to good yields obtained were typically lower than what was observed in the literature with classical Brønsted or Lewis acid-based catalysts. The most interesting result from this study is the necessity of an oxygen-containing reaction atmosphere for iodonium catalysis to be functional. Critical control experiments showed that water deactivated the catalyst, whereas atmospheric oxygen was necessary for in situ catalyst activation and subsequent turnover. It is important to highlight that as the product yields widely differed from those achieved under either Brønsted or Lewis acid catalysis, hidden acid catalysis was unlikely to be operative. Further control experiments suggested that the lower yields arose from the decomposition of a reaction intermediate, rather than due to a deficiency in the catalyst or due to decomposition of the product under the reaction conditions. While this investigation has added to the growing body of work on iodolium ions serving as halogen bond donor catalysts, their apparent in situ activation by oxygen is a novel concept in iodolium ion catalysis that surely warrants further attention. Future work should be directed at uncovering the unusual need for oxygen in iodonium salt activation and turnover. This would involve a series of experiments probing the mechanism and true identity of the iodonium salt catalyst. Firstly, given it appears that the activated catalytic species only exists in situ, characterization of the reaction mixture by in situ IR spectroscopy may further our understanding of the reaction. In particular, observation of I-O stretches would be indicative of the formation of a new bond. Secondly, reaction kinetics relative to oxygen could be explored. Performing a series of reactions with variable concentrations of oxygen (e.g., 10%, 20%, 30% etc.) in a nitrogen atmosphere could help determine the order of the reaction relative to the concentration of oxygen. Lastly, although only present in trace quantities in the atmosphere, the influence of carbon dioxide or carbon monoxide on the reaction should be explored. The carbon monoxide or carbon dioxide may interact as a ligand with the iodine(III) of the diaryliodonium salt. The influence of these gases on the reaction could be explored by conducting the reaction under atmospheres of both gases individually. The results of these mechanistic investigations would guide further mechanistic inquiry into this unusual observation.

2.5 Experimental Details

Standard Reaction Protocol:

To an oven-dried 10 mL round bottom flask equipped with a stir bar, a water-cooled condenser and a drying tube packed with Drierite, was added divinyl ketone **2.60** (0.25 mmol, 1.0 equiv.), catalyst (**2.69**) (7.1 mg, 5 mol%, 0.0125 mmol) and acetonitrile (0.1 M, 2.5 mL). The reaction mixture was lowered into a preheated oil bath and heated at reflux until the disappearance of **2.60** was observed by TLC analysis. The reaction was cooled to room temperature and concentrated under reduced pressure. The residue was then either subject to flash chromatography with silica gel, or HMDSO was added and the mixture was analyzed by quantitative ^{1}H NMR.

Chapter 3
Interrupting the Known Reactivity of *p*-(Difluoroiodo)toluene and Styrenyl Motifs

3.1 Introduction

p-(Difluoroiodo)toluene **3.1** ($TolIF_2$) is a fluorine gas surrogate and as such is simultaneously a source of both electrophilic and nucleophilic fluorine. Given the ambiphilic nature of $TolIF_2$, many of the transformations with it involve the difunctionalization of a corresponding ambiphilic substrate, such as an alkene. In this Chapter, the reactivity will continue to be explored with a focus directed at increasing the molecular complexity of the obtained products through carbo-skeletal rearrangements of the substrates. In essence, the goal is to interrupt the known difunctionalization of the alkene with a rearrangement before the final termination event. The topic and the project goals will be introduced in Section 3.1 over three subsections. A discussion of the synthesis of $TolIF_2$ as well as its origin in the literature is found in Section 3.1.1. The general reactivity of $TolIF_2$ is discussed in Section 3.1.2 and will focus on select examples to showcase the possible synthetic transformations. The project will be outlined in Section 3.1.3. This will be followed by Section 3.2 which contains a discussion of our results to date. Finally, concluding remarks for all three transformations are provided in Section 3.3, as well as the proposed future direction of this project.

3.1.1 Synthesis of *p*-(Difluoroiodo)toluene

$TolIF_2$ was first prepared more than a century ago. Over the years there have been several different methods developed to access $TolIF_2$ in synthetically useful quantities. Fundamentally, they all involve an oxidation to convert an iodine(I) species to an iodine(III) species with the addition of two fluorine ligands to the iodine atom. The methods discussed are summarized in Figure 3-1; however, the yield of $TolIF_2$ is not discussed in all the syntheses as it was not provided in the original literature.

$TolIF_2$ was first prepared by Weinland and Stille in 1903 by treating *p*-iodosotoluene **3.2** with 48% aqueous hydrogen fluoride in acetic acid at 40 °C (Figure 3-1).[99] Procedurally, this involved dissolving the *p*-iodosotoluene **3.2** in hot acetic acid, likely resulting in the formation of the *p*-(diacetoxyiodo)toluene **3.3**. After cooling the solution to 40 °C the 48% aqueous hydrogen fluoride was

added and the desired product **3.1** precipitated out of the solution. Precipitation of the final product is a common means of isolation across most synthetic procedures. The research groups of Wirth and Gouverneur disclosed a similar method for the preparation of $TolIF_2$. They began their syntheses with *p*-iodotoluene and oxidized to *p*-(diacetoxyiodo)toluene **3.3** with sodium perborate which was followed by hydrolysis with sodium hydroxide to obtain iodosotoluene **3.2**. Treatment of the crude iodosotoluene **3.2** with aqueous hydrogen fluoride gave **3.1** (~60%, 0.72 -2.1 g).[100, 101]

p-Iodotoluene can also be oxidized with SelectFluor™ in acetonitrile at room temperature to produce **3.1** directly.[102] Isolation of **3.1** from this reaction mixture required the addition of minimal Et_3N•3HF which was hypothesized to stabilize the product. This method was expanded upon by the research group of Gilmour where they discovered a system of SelectFluor™ and CsF would cleanly furnish the desired product **3.1**.[103] The preparation of $TolIF_2$ **3.1** can also be accomplished via the direct oxidation of iodotoluene **3.4** with $F_{2(g)}$.[104, 105] This was done by bubbling a steady stream of $F_{2(g)}$, diluted in $N_{2(g)}$, through a solution of **3.4** in a perhalogenated solvent (CCl_3F) at low temperature. The need for specialized equipment to handle the $F_{2(g)}$, as well as the low temperature, makes this procedure unattractive for the routine preparation of this reagent in the laboratory. The reagent was also successfully prepared from *p*-(dichloroiodo)toluene **3.5** with mercuric oxide and hydrogen fluoride in 60-90% yield.[106] The significant downside to this preparation is the need for stoichiometric mercuric oxide and the generation of the mercuric chloride byproduct. Alternatively, the bis(trifluoroacetoxyiodo)toluene **3.6** can be treated with $SF_{4(g)}$ at -20 °C in dichloromethane to provide **3.1**.[107] A compound of the same class, (difluoroiodo)benzene **3.8**, was prepared by treating the iodobenzene with xenon difluoride and anhydrous hydrogen fluorine in a solution of dichloromethane at room temperature (Scheme 3-1).[108, 109]

Although all the above methods successfully prepared the desired product **3.1**, not all are practical in a research laboratory or desirable for the larger scale preparation of **3.1**. In addition to $F_{2(g)}$, SF_4 is also gaseous and toxic, especially if it comes into contact with moisture as it releases both $SO_{2(g)}$ and $HF_{(g)}$ making it an undesirable reagent for laboratory use. SelectFluor™ is an easy-to-handle commercial solid; however, the cost is high for the transfer of a single fluorine atom. While aqueous hydrogen fluoride is an extremely toxic reagent, the synthetic routes converting **3.2** to **3.1** (i.e., Figure 3-1, the

original method outlined by Weinland and Stille in 1903) were most amenable to scale-up and the development of a practical and reproducible synthetic method.

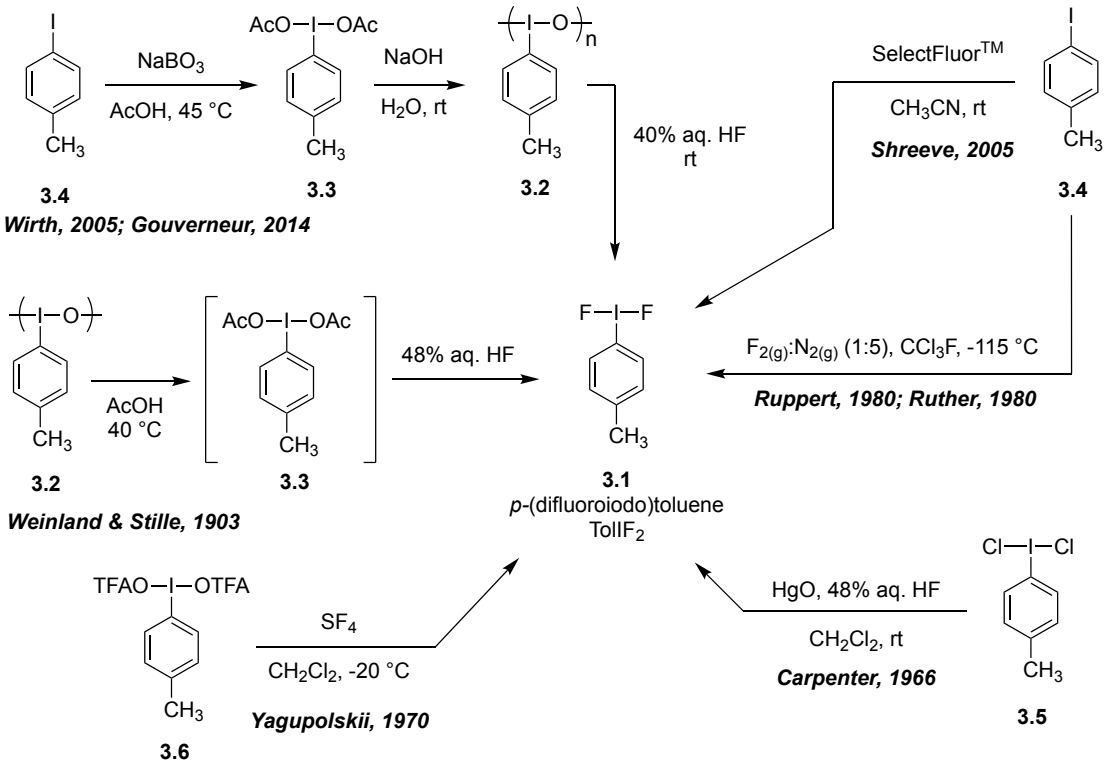
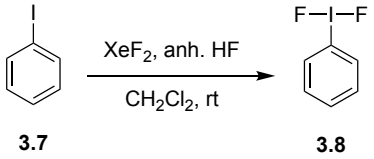


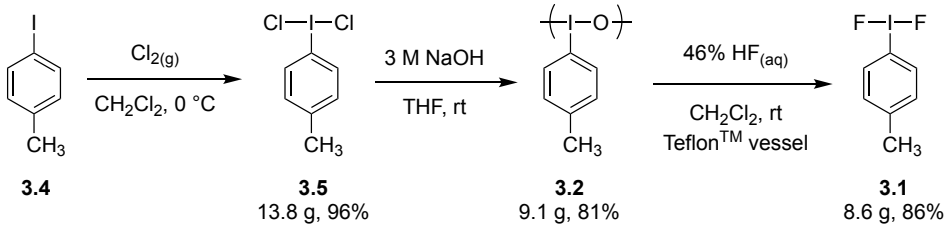
Figure 3-1. Synthesis of $TolIF_2$.



Scheme 3-1. Synthesis of difluoride **3.8** with xenon difluoride.

There have been two publications outlining the synthesis of $TolIF_2$ on a preparative scale for the research laboratory (~8 g).[110, 111] Both syntheses use the same general three-step strategy but employ slightly different reaction conditions. In the first synthesis disclosed by Hara et al., they converted iodotoluene **3.4** to the dichloride **3.5** in 96% yield with chlorine gas generated ex situ with manganese dioxide and concentrated hydrochloric acid (Scheme 3-2).[110] The dichloride was subsequently hydrolyzed with sodium hydroxide to the iodosotoluene **3.2** in 81% yield. The iodosotoluene **3.2** was

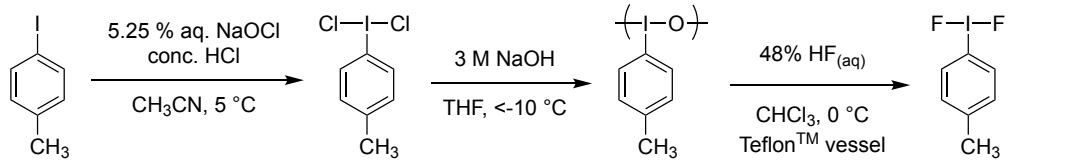
suspended in dichloromethane in a Teflon™ perfluoroalkoxy (PFA) vessel. To this suspension was added 46% aqueous hydrogen fluoride to give a clear solution from which the desired product **3.1** was isolated in 86% yield (67% over three steps).



3.4 | **3.5** 13.8 g, 96% | **3.2** 9.1 g, 81% | **3.1** 8.6 g, 86%

Scheme 3-2. Synthesis of $TolIF_2$ by Hara et al.

The second synthesis, published by our research group, featured significantly more experimental details to ensure reproducibility across the synthetic organic community.[111] Our synthesis began with the treatment of iodotoluene **3.4** with commercial household bleach (specifically hydroxide-free bleach) and concentrated hydrochloric acid to form dichloride **3.5** (Scheme 3-3). Hydrolysis of the dichloride **3.5** with sodium hydroxide gave **3.2** which was isolated as a wet filter cake and used directly in the next step. Suspension of this crude material in chloroform and treatment with 48% hydrogen fluoride gave the desired product **3.1** in 64-72% yields over the three steps. Of note, this procedure uses cheap and easily accessible reagents and can easily be completed in one working day to efficiently provide **3.1**. The product is stored in a PFA vial in the freezer for long-term use. Storage in a regular glass vessel leads to faster decomposition of $TolIF_2$.



3.4 10.9 g | **3.5** 15-16 g | **3.2** *used without purification or weighing* | **3.1** 8.2-9.2 g 64-72% over 3 steps

Scheme 3-3. Synthesis of $TolIF_2$ by Tao and Murphy.

Overall, there are multiple different synthetic methods to synthesize $TolIF_2$. Some are significantly more convenient and procedurally safer than others (e.g., use of HgO or F_2 vs. the procedures by Tao

and Murphy or Hara et al.). There is also an entry for $TolIF_2$ in the Encyclopedia of Reagents for Organic Synthesis.[112] The methodology developed by our research group was used to prepare the $TolIF_2$ used in all of the experiments found in this Chapter. Not covered in this section, or elsewhere in this Chapter, is the generation of catalytic (chiral[113, 114] or achiral[115]) $ArIF_2$ species or in or ex situ electrochemical synthesis of $TolIF_2$ or $ArIF_2$.[116-120]

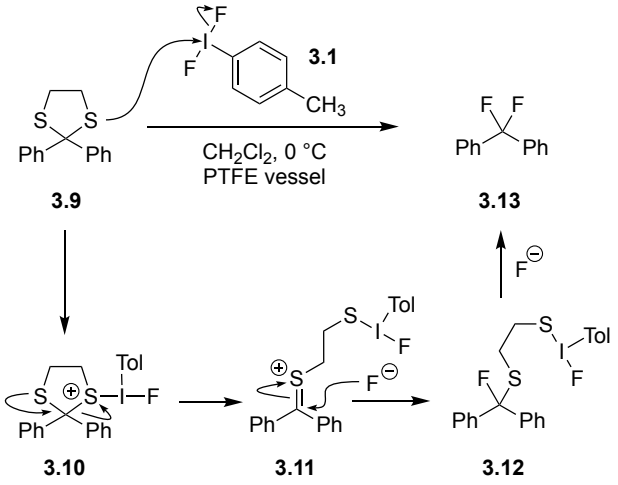
3.1.2 Reactivity of (Difluoroiodo)arenes

The introduction to the reactivity of (difluoroiodo)arenes will be separated into two subsections. In the first subsection 3.1.2.1 its general reactivity with several different reactive functional groups will be demonstrated. In subsection 3.1.2.2 the reactivity between a (difluoroiodo)arene and an alkene will be discussed. This discussion is directly pertinent to the reaction development completed in this Chapter. The Sections are specifically titled (difluoroiodo)arene and not (difluoroiodo)toluene as researchers have employed various aryl derivatives while exploring the reactivity of these difluoroiodides. It is not unusual for reactions with $TolIF_2$ to be carried out in vessels made of perfluorinated polymer materials. This ensures $TolIF_2$ is reacting exclusively with the substrate and not degrading on the surface of the glass. Additionally, these vessels are compatible with any hydrogen fluoride which might be generated throughout the reaction.

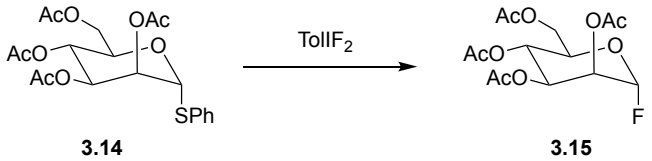
3.1.2.1 Miscellaneous Reactivity of (Difluoroiodo)arenes

(Difluoroiodo)arene reagents have been used to mono- and/or difluorinate a variety of functional groups. In 1991, Motherwell et al. demonstrated the dethiolation and fluorination of dithioketals with $TolIF_2$.[121] Beginning with dithioketal **3.9** treatment with $TolIF_2$ in a PTFE vessel gave the *gem*-difluoro product **3.10** in 65% yield (6 examples, 65-90% yield) (Scheme 3-4). Mechanistically, they proposed that a sulfur atom first attacked the $TolIF_2$ at the iodine atom to give **3.10**. Ring opening and substitution with fluoride could give **3.12**. Finally, substitution with a second fluoride gave the desired *gem*-difluoro product **3.13**. The reactivity between sulfur and $TolIF_2$ was further exploited by Motherwell et al. to prepare glucosyl fluorides (Scheme 3-5).[122, 123] For example, mannose derivative **3.14** was fluorinated in 56% yields exclusively as the alpha-isomer **3.15**. An additional six sugar derivatives were successfully fluorinated in yields ranging from 55-80% with varying alpha/beta selectivity. These studies show that $TolIF_2$ can effectively activate thioethers as leaving groups and replace them with

fluoride. An additional four studies by Motherwell et al. used the same reactivity pattern between sulfur and $TolIF_2$ to achieve fluorination of xanthate esters,[124] alpha-phenylsulfanyl esters,[125] alpha-phenylsulfanyl acetamides,[126] and alpha-phenylsulfanyl lactams.[127] The reactivity patterns observed in these reactions were not unique to $TolIF_2$ when compared to aza-fluorinating reagents (e.g., SelectFluor^{TM}); however, they did demonstrate the utility of the reagent.[128]



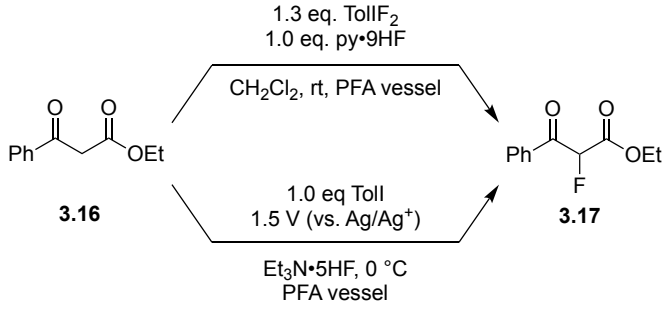
Scheme 3-4. *gem*-Difluorination of dithioketals.



Scheme 3-5. Preparation of glycosyl fluorides with $TolIF_2$.

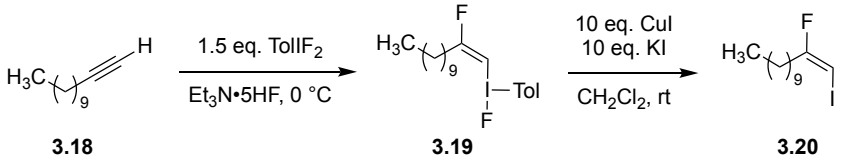
The fluorination of 1,3-dicarbonyls was accomplished in two ways by Hara et al., first with the stoichiometric addition of $TolIF_2$ and second with in situ electrochemically generated $TolIF_2$.[117, 129] Again, this reactivity was also achieved with Selectfluor^{TM} under basic reaction conditions.[130, 131] Hara et al. explored a series of six beta-ketoesters that were fluorinated with $TolIF_2$ in yields ranging from 50-80% (Scheme 3-6).[129] For example, **3.16** was fluorinated with $TolIF_2$ in the presence of pyridine•9HF in 73% yield. The pyridine•9HF additive was crucial to the success of the reaction as without it the reaction did not produce any of the desired product **3.17**. The hydrogen fluoride complex is likely both increasing the enol content in the keto-enol equilibrium of the substrate and activating the $TolIF_2$. Activation of $TolIF_2$ is likely occurring by hydrogen bonding between a fluorine ligand of

$TolIF_2$ and HF, increasing the electrophilicity of the reactive hypervalent iodine center. Hara et al. later found that if the HF complex is omitted and the reaction is instead heated to 40 °C, **3.17** could be obtained under neutral conditions in 72% yield.[132] The same substrate can be electrochemically fluorinated with iodotoluene as the mediator.[117] Treatment of **3.16** and iodotoluene in a solution of Et_3N•5HF at 0 °C with 1.5 V gave the product **3.17** in 72% yield. Mechanistically, they proposed that $TolIF_2$ is electrochemically generated, which in turn reacts with **3.16** as it did in the non-electrochemical reaction.



Scheme 3-6. Fluorination of 1,3-dicarbonyls with $TolIF_2$.

An interesting series of compounds were prepared from alkynes and $TolIF_2$. Hara et al. treated a series of seven alkynes with $TolIF_2$ in the presence of Et_3N•5HF to give fluorovinyl iodoniums (e.g., **3.19**), which were immediately iodinated with copper iodide and potassium iodide in 55-80% yield (Scheme 3-7).[133] Specifically, beginning with alkyne **3.18** it can be transformed into fluorovinyl iodonium **3.19** in 80% yield with $TolIF_2$ in the presence of Et_3N•5HF. No matter the substituent on the alkyne, the stereochemistry of the alkene product (e.g., **3.19** and **3.20**) was always obtained in the (*E*) configuration.

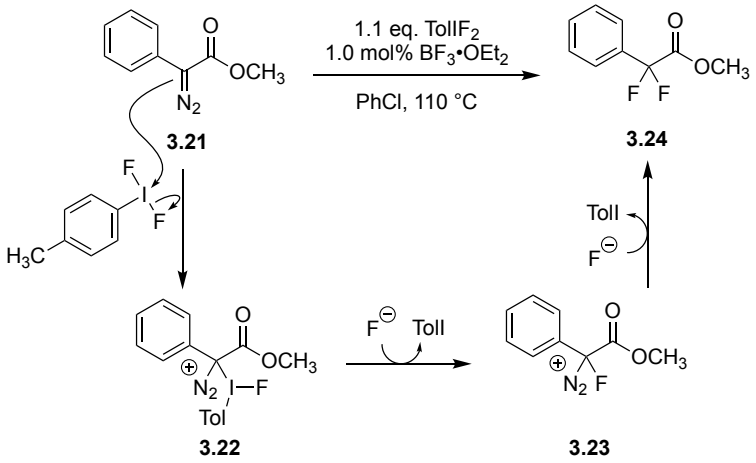


3.18 **3.19** **3.20**

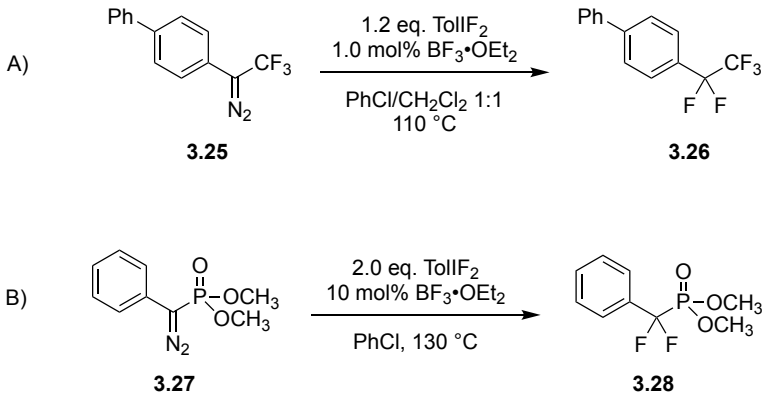
Scheme 3-7. The preparation of fluorovinyl iodoniums and (*E*)-iodo-fluoroalkenes.

Being a fluorine (F_2) surrogate, $TolIF_2$ has one "electrophilic" and one "nucleophilic" fluorine atom, and as such ambiphilic diazo-containing substrates were attractive targets for difluorination. Murphy et

al. first demonstrated this reactivity with the successful difluorination of phenyl diazoacetates, such as **3.21**, in yields of 17-79% (Scheme 3-8).[134] They proposed that the reaction occurs through the nucleophilic attack of the diazo on $TolIF_2$ to give **3.22**. Displacement of the diazonium and iodonium leaving groups yielded the final difluorinated product **3.24** in 66% yield. Further investigation revealed that the borosilicate glass of the reaction vessel was able to activate $TolIF_2$ for the reaction.[135] Using more pure $TolIF_2$, **3.21** was converted to **3.24** in 81% yield without any BF_3•OEt_2 additive. When an analogous substrate was submitted to the reaction conditions in a PFA or Nalgene vessel it failed to produce any of the difluoro product (e.g., **3.24**). The addition of 5 weight percent of ground borosilicate glass recovered the yield in those vessels. Gouverneur et al. applied this methodology to the difluorination of trifluoromethyl diazo compounds (Scheme 3-9, A).[101] Four examples were explored and the products were obtained in yields between 37-80%, which included the conversion of **3.25** into **3.26** in 52% yield. Diazophosphonates were equally difluorinated with similar methodology (Scheme 3-9, B; 8 examples, 49-73%).[136] For example, phosphonate **3.27** was fluorinated in 67% yield. The fluorination of diazo compounds by $TolIF_2$ was a marked improvement over previous methods which required CF_3OF or F_2.[137, 138] Overall, the reactivity between $TolIF_2$ and various nucleophilic functional groups has been developed into synthetically useful methodologies.



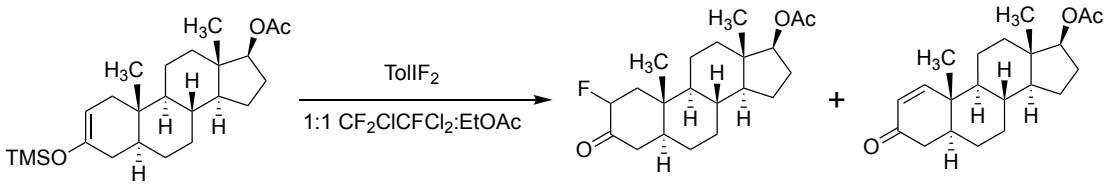
Scheme 3-8. Difluorination of phenyl diazo acetates with $TolIF_2$ by Murphy et al.



Scheme 3-9. A) Difluorination of trifluoromethyl diazo compounds. B) Difluorination of diazo phosphonates.

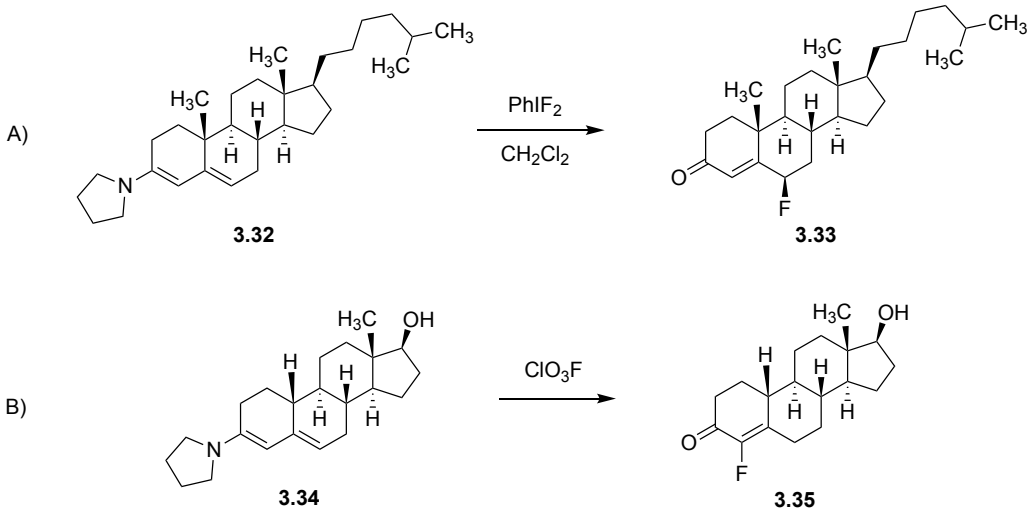
3.1.2.2 Reactivity of (Difluoroiodo)arenes with Alkenes

The reactivity between $TolIF_2$ and alkenes is well explored and continues to be an active topic of research. One of the early examples of the synthetic utility of $TolIF_2$ as a source of electrophilic fluorine was disclosed by Tsushima et al. in the fluorination of silyl enol ethers (Scheme 3-10).[139] They successfully fluorinated steroid-based silyl enol ethers in 23-67% yield. In their example shown below, by treating **3.29** with $TolIF_2$ produced a 4:1 mixture of **3.30** in 38% yield, along with 17% of the unsaturated ketone **3.31**. Motherwell et al. explored a similar substrate **3.32** with a series of (difluoroiodo)arenes, including (difluoroiodo)benzene ($PhIF_2$) (Scheme 3-11, A).[140] In the specific example below, one of the three substrates studied by Motherwell et al., the desired product **3.33** was obtained in an 18% yield. It should be noted that this product is the thermodynamically less stable axial fluoride product. Additionally, treatment of a dienamine with perchloryl fluoride, not a hypervalent iodine reagent, divergent reactivity was observed and the alpha-fluoro product **3.35** was obtained (Scheme 3-11, B).[141] $TolIF_2$ is not simply an addition to the litany of electrophilic fluorine reagents available, but a reagent with divergent reactivity in many cases, as compared to non-hypervalent iodine-based fluorination reagents.



3.29 **3.30a/b**, 4:1 **3.31**

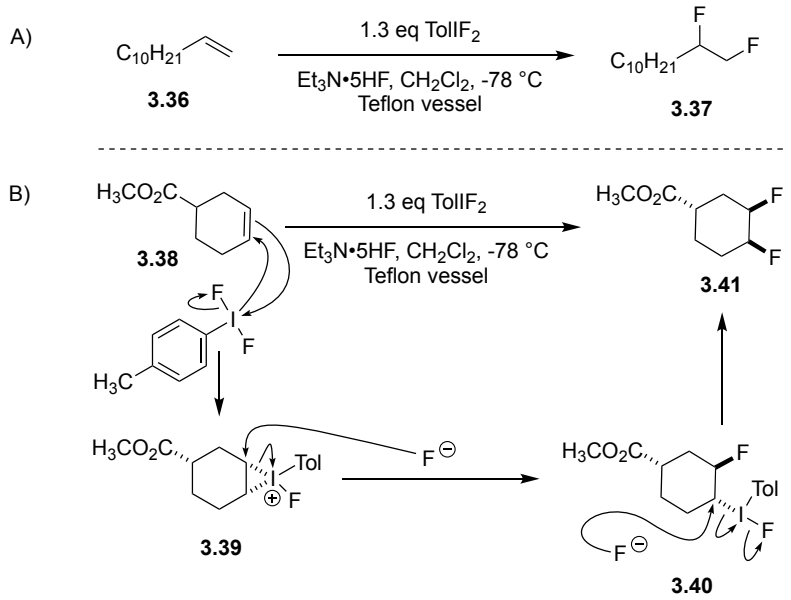
Scheme 3-10. Fluorination of silyl enol ethers with $TolIF_2$.



3.32 **3.33** **3.34** **3.35**

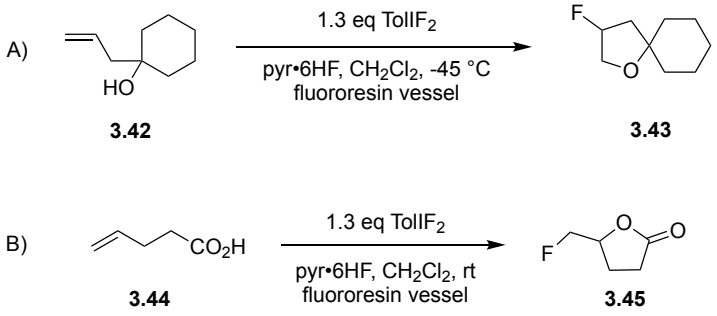
Scheme 3-11. Fluorination of a dienamine with (difluoroiodo)benzene.

The vicinal difluorination of terminal aliphatic alkenes was demonstrated by Hara et al. in 1998.[142] The nine substrates investigated gave yields between 53-70% of the difluoro products (e.g., Scheme 3-12). The treatment of 1-dodecene **3.36** with $TolIF_2$ gave the difluoride **3.37** in 65% after 2.5 hours (Scheme 3-12, A). The same reaction with internal alkenes was sluggish and gave complex mixtures of products, however, the reaction was viable with cyclic alkenes, such as **3.38**. As the *cis*-1,2-difluoro product **3.41** was obtained exclusively it informed their mechanistic proposal. To obtain the correct stereochemical orientation in **3.41**, they postulated that the alkene and $TolIF_2$ first react to produce the iodonium **3.39**. This cyclic hypervalent iodine species is opened by fluoride attack to give **3.40** which reacts with an additional fluoride to produce the *cis*-vicinal difluoride **3.41**. The vicinal difluorination of alkenes with $TolIF_2$ is not particularly noteworthy as this transformation has been achieved with multiple other fluorination reagents in comparable yields.[143]



Scheme 3-12. A) Vicinal difluorination of aliphatic alkenes with $TolIF_2$. B) Proposed mechanism of the vicinal difluorination.

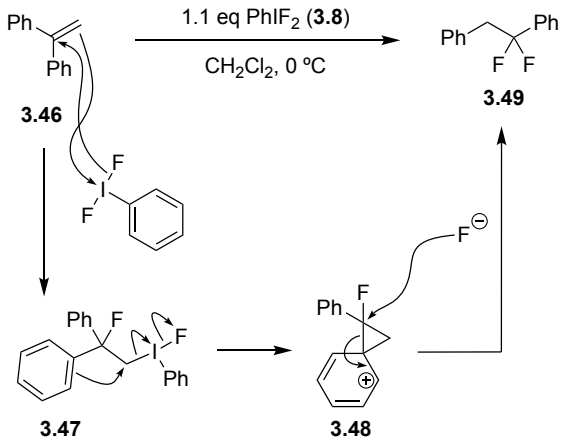
In the difluorination reaction described above, both nucleophiles are fluorine atoms. The second nucleophilic attack could theoretically be replaced with an intramolecular nucleophile. This was demonstrated by Hara et al. with pendant alcohols and carboxylic acids (Scheme 3-13).[144] The alcohol **3.42** was cyclized in 40% yield to provide **3.43** (total of 4 examples, 40-60%) (Scheme 3-13, A). Analogously, the carboxylic acid **3.44** was cyclized to the desired lactone **3.45** in 40% yield (total of 3 examples, 40-50) (Scheme 3-13, B).



Scheme 3-13. The fluorocyclization of alcohols and carboxylic acids.

In 1966, Carpenter confirmed interesting reactivity between $TolIF_2$ and styrenyl alkenes (Scheme 3-14).[106] At face value, one would expect the same vicinal difluorination observed with aliphatic

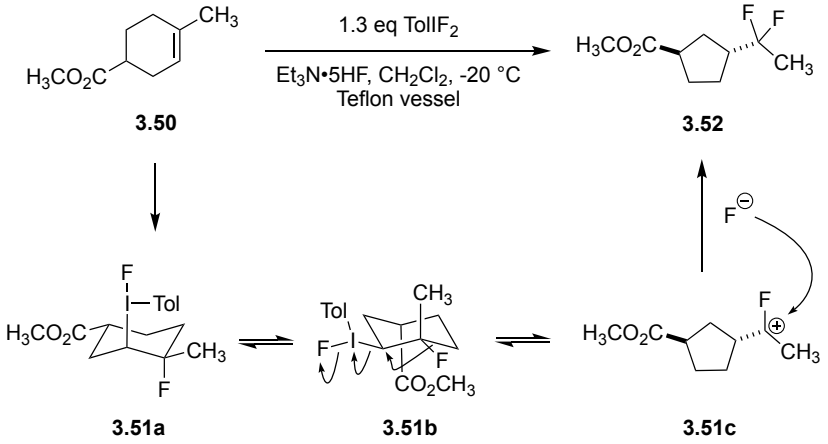
alkenes to occur (see Scheme 3-12). However, instead what is observed is the geminal difluorination of styrene. For example, when alkene **3.46** is treated with the hypervalent iodine difluoride **3.8** ($PhIF_2$) the geminal product **3.49** is obtained. This unexpected product is proposed to arise from a 1,2-phenyl shift. Mechanistically, this can be described as follows: first, the alkene and **3.8** react to give intermediate **3.47**. Of note, the addition of $TolIF_2$ occurs specifically in this orientation with the fluoride making a new bond at the most substituted carbon with the most partial positive charge, and with the large iodine atom bonding at the least sterically hindered terminal position. Given the hypernucleofugality of the iodobenzene moiety, the adjacent phenyl ring expels the iodobenzene and forms a spirocyclic phenonium ion **3.48**. Finally, the attack of another fluoride at the most partial positive carbon affords the final geminal product **3.49**. The relative migratory aptitude of various substituted phenyl rings was explored by Patrick et al. in 1980.[145] As expected, they found that the electron-donating substituents had a higher propensity to migrate. This was in line with the substituent's ability to stabilize a phenonium ion (e.g., **3.48**). Ultimately, they determined the relative migratory aptitude to be (in decreasing order) *p*-OCH_3 > *p*-CH_3 > H > *p*-Cl > *m*-Cl. The 1,2-phenyl shift leading to the *gem*-difluoro products is arguably the most unique and synthetically powerful reactivity pattern of $TolIF_2$. Without $TolIF_2$, isolated *gem*-difluorides are most commonly prepared through either the deoxy-fluorination of carbonyl groups and its derivatives (e.g., DAST) or the dihydrofluorination of alkynes.[146, 147]



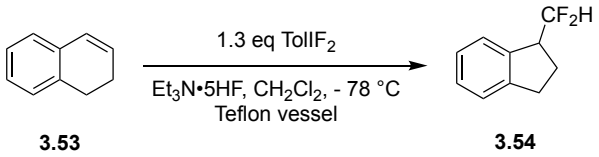
Scheme 3-14. *gem*-Difluorination of styrenes with a mechanistic proposal by Carpenter.

Rearrangements of carbo-skeletons were further exploited by Hara et al. who demonstrated cyclic internal alkenes, such as **3.50** and **3.54**, could be difluorinated and ring contracted with $TolIF_2$ (Scheme

3-15, Scheme 3-16).[148] They showed that this transformation was possible with a series of nine aliphatic and styrenyl alkenes in 50-82% yield. The six-membered endocyclic alkene **3.50** when treated with $TolIF_2$ contracts to the cyclopentane **3.52** in 66% yield (Scheme 3-15). The contraction and stereochemical outcome were rationalized mechanistically. If $TolIF_2$ reacts axially with **3.50** (fluoride bonded to the most partially positive carbon; iodoarene bond to the least sterically hindered carbon) then the chair **3.51a/b** is obtained. A 1,2-carbon bond migration and elimination of iodotoluene gave the carbocation **3.51c**, which was subsequently trapped with fluoride to afford the final product **3.52**. The ring contraction of endocyclic styrene **3.53** was equally successful obtaining **3.54** in 50% yield (Scheme 3-16). This ring contraction was due to the 1,2-phenyl shift previously demonstrated above in Scheme 3-14.



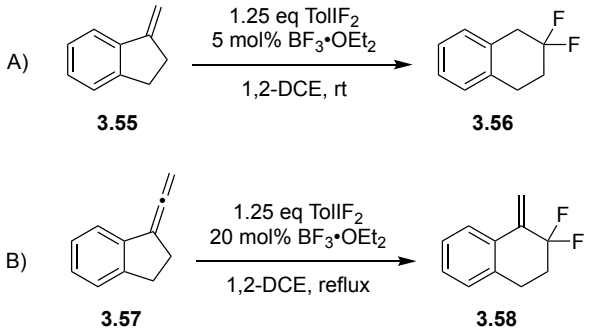
Scheme 3-15. Ring contraction of aliphatic cyclic alkenes with $TolIF_2$.



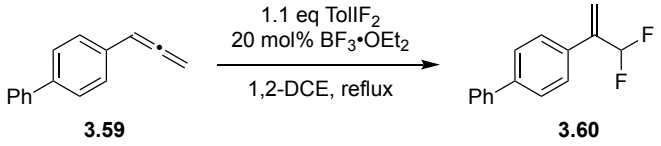
Scheme 3-16. Ring contraction of endocyclic styrene **3.53** with $TolIF_2$.

Conceptually applying the same ideas to exocyclic styrenyl alkenes, Murphy et al. accomplished a ring expansion and difluorination (Scheme 3-17).[149] This methodology was successfully applied to 20 substrates with yields between 49-89%. In the example below, alkene **3.55** is treated with $TolIF_2$ (activated with a catalytic amount of the Lewis acid BF_3•OEt_2) to give the ring-expanded product **3.56** in 63% (Scheme 3-17, A). Interestingly, when this method was applied to the analogous allenes (e.g.,

3.57) the corresponding allylic geminal difluorides (e.g., **3.58**, 74% yield) were obtained. A small series of substrates illustrated the scope of this transformation (8 examples, 29-78%). A second fluorination and ring expansion of **3.58** likely does not occur due to the electron-deficient nature of the allylic geminal difluoride products. The fluorinative ring expansion of the allenes was ultimately inspired by earlier work disclosed by Murphy et al. in 2017 (Scheme 3-18, 25 examples, 10-70% yield),[150] where the product **3.60** arises from the regioselective reaction of $TolIF_2$ with the internal alkene, 1,2-phenyl shift, and difluorination to obtain **3.60**.



Scheme 3-17. Fluorinative ring expansions of exocyclic alkenes and allenes with $TolIF_2$.



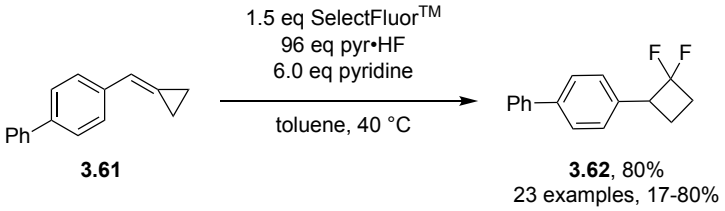
Scheme 3-18. The preparation of allylic geminal fluorides from phenyl allenes with $TolIF_2$.

This body of work has formed the basis for the development of catalytic variations, as well as catalytic enantioselective variations of this class of chemical transformation. Initial contributions to the catalytic variation of this chemistry were made by Kitamura et al.,[151] Gilmour et al.,[103, 114, 115, 152] and Jacobsen et al.[113, 153] Generally, this research topic remains very research active and new transformations and advancements are regularly disclosed.

3.1.3 Research Objectives

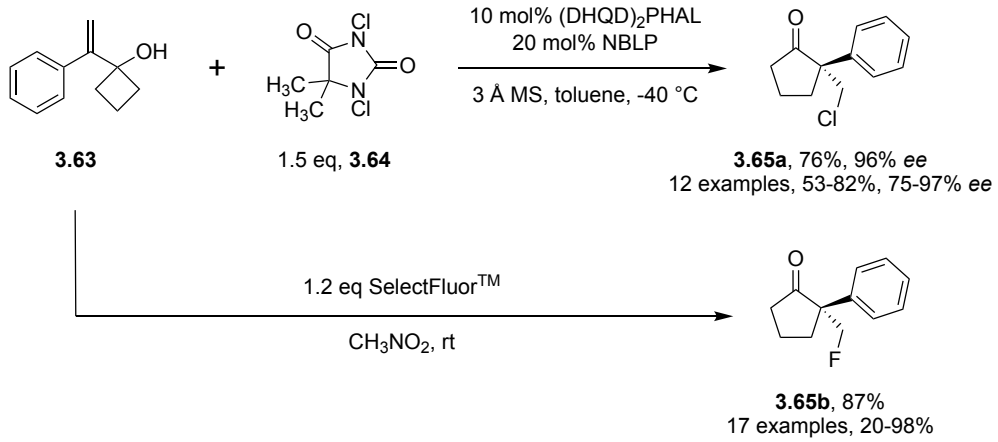
The goals of this project were to further develop the reactivity of $TolIF_2$ to obtain fluorinated motifs which are not accessible or otherwise difficult to access. A series of substrates were designed to encourage additional carbo-skeleton rearrangements prior to the final fluoride trap and termination of the reaction (e.g., Scheme 3-14 to Scheme 3-18). Specifically, we were interested in leveraging the strain in small rings to guide reactivity and potentially obtain more complex fluorinated molecules. This was accomplished by exploring four unique substrates which contained both a small ring and an alkene. We were inspired by reports in the literature which showed interesting reactivity in various halogenation reactions with three different classes of substrates.

The first example was the ring expansion and fluorination of methylene cyclopropanes (e.g., **3.61**) to difluorocyclobutanes (e.g., **3.62**) (Scheme 3-19).[154] Interestingly, the two functional groups in this substrate, the olefin and the cyclopropane, are both known to react with $TolIF_2$. Additionally, this substrate was previously explored in the direct functionalization of the olefin through cycloaddition,[155] ring-opening reactions,[156, 157] and other oxidative ring expansions.[158] The two reactive centers of the substrate in combination with the diverse reactivity previously reported make this a curious substrate to explore with $TolIF_2$.



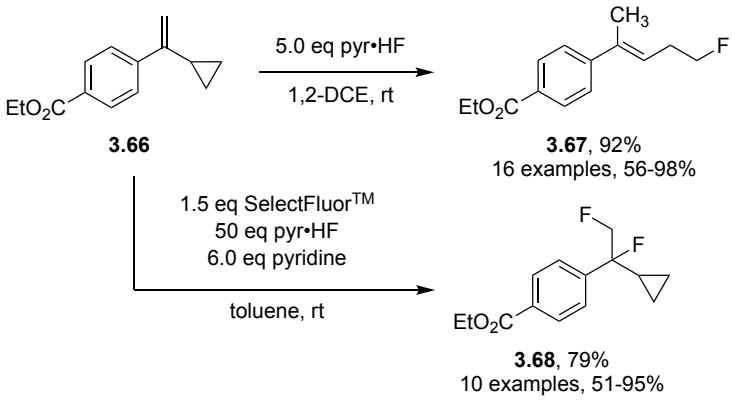
Scheme 3-19. Preparation of difluorocyclobutanes from methylenecyclopropanes.

The second was the enantioselective chlorination of styrenyl cyclobutanols (e.g., **3.63**) to alpha-chlorocyclopentanones (e.g., **3.65a**) (Scheme 3-20).[159] The fluorination of **3.63** was also achieved with SelectFluor™, albeit not enantioselectively, and gave **3.65b** in 87% yield (Scheme 3-20).[160] The same ideas were also applied to achieve amination, arylation, and azidation with other HVI reagents.[161-163] The successful development of the halogenation reactions and transformations with HVI reagents boded well for the exploration of $TolIF_2$ with this substrate class.



Scheme 3-20. Chlorination and fluorination combined with ring expansion. $(DHQD)_2PHAL$ = Dihydroquinidine 1,4-phthalazinediyl diether, NBLP = *N*-Boc-L-phenylglycine.

Lastly, fluorinative reactions with alpha-cyclopropyl styrenes (e.g., **3.66**) were reported in the literature (Scheme 3-21).[164] The first was the ring-opening reaction of alpha-cyclopropyl styrenes with pyridine•HF to obtain fluorinated products such as **3.67**. Alternatively, under reaction conditions for electrophilic fluorination, the difluorination of **3.66** was achieved with a mixture of SelectFluor™/pyridine•HF to obtain vicinal difluorination products (e.g., **3.68**) (Scheme 3-21). The potential for multiple different products to form from a single substrate made this an attractive substrate to investigate. Further supporting the diverse reactivity of this substrate is its utilization as a radical clock for probing the mechanism of HVI-based reactions and various other transformations.[165-167]Additionally, treatment of this substrate with strong fluorinating reagents, such as XeF_2 or an *N*-fluoropyridinium salt, led to complex reaction mixtures.[168] Treatment of alpha-cyclopropyl styrene with Koser's reagent gave two products, one of which was a ring-expanded cyclobutane.[169] Given that $TolIF_2$ often demonstrates complementary reactivity to other fluorination methods and the previously demonstrated diverse reactivity of alpha-cyclopropyl styrenes, the exploration of this substrate presented an opportunity for new reaction development.



Scheme 3-21. Fluorination of alpha-cyclopropyl styrenes.

3.2 Reaction Development

3.2.1 The Reaction of Methylenecyclopropanes or Methylenecyclobutanes with *p*-(Difluoroiodo)toluene

3.2.1.1 Methylenecyclopropanes

The first substrate to be investigated was the methylenecyclopropane **3.69** (Figure 3-2). The 4-methyl substituted substrate was chosen for the initial investigation to aid in the identification of new products based on the pair of doublets in the ^{1}H-NMR. Due to concerns about potential product volatility, attention was turned to the heavier 4-bromomethylenecyclopropane **3.70** and as such the majority of the reaction exploration and development was completed on this substrate.

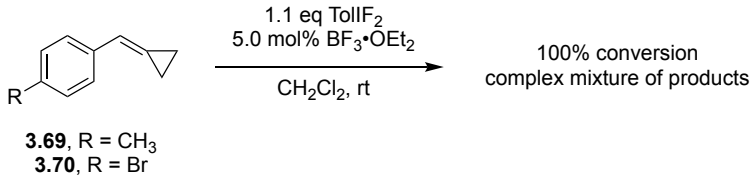


3.69 **3.70**

Figure 3-2. Methylenecyclopropane substrates **3.69** and **3.70**.

Initial reaction development began with the treatment of **3.69** or **3.70** with 1.1 equivalents of $TolIF_2$ and 5.0 mol% of BF_3•OEt_2 as an activator. These reaction conditions were chosen as they are often successfully employed at the onset of new projects in the Murphy group involving reactions with $TolIF_2$. Unfortunately, analysis of the crude reaction mixtures by both ^{1}H and ^{19}F-NMR revealed only minor products. Notably, the ^{19}F-NMR spectrum had signals between -150 ppm and -220 ppm, signals

indicative of aromatic C-F fluorine atoms or monofluoroalkyl species arising from the ring opening of the cyclopropane. Although the products were minor, there were potentially new products forming during the reactions and a thorough optimization was attempted. Of note, there was no peak in the ^{19}F-NMR at approximately -88 ppm indicative of a difluorocyclobutane (e.g., **3.62**). A significant component of the crude reaction mixture was iodotoluene, a byproduct of productive or unproductive $TolIF_2$ reduction.

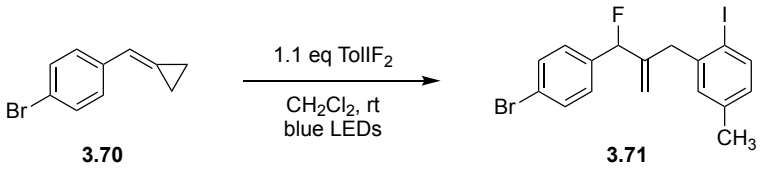


Scheme 3-22. Initial reaction development.

The next step was to try and mitigate the unproductive reaction pathways by controlling the reaction temperature. Repeating the reaction at 0 °C showed no improvement and the same crude reaction mixture was obtained by NMR spectroscopy. Further cooling to -20 °C or -40 °C completely stopped any reaction from occurring. Beginning the reaction at -20 °C and slowly warming the reaction mixture gave the same result, by thin layer chromatography (TLC) and NMR spectroscopy, as beginning at room temperature. As soon as a reaction temperature of approximately -10 °C was reached, **3.70** was consumed and multiple products appeared by TLC. Using low temperature to control the reactivity was unsuccessful as it appears the reactivity was "on" or "off" around -10 °C. Reducing the reactivity of $TolIF_2$ by omitting the BF_3•OEt_2 was equally unsuccessful. Performing the reaction at room temperature without BF_3•OEt_2 led to the recovery of the starting material **3.70** while heating to reflux (in CH_2Cl_2 or 1,2-DCE) led to full consumption of **3.70** and the same reaction profile as described above. To ensure that the Lewis acid was not degrading the substrate in a background reaction, **3.70** was exposed to BF_3•OEt_2 at room temperature. No significant decomposition was observed and as such it was concluded that the combination of $TolIF_2$ and the Lewis acidic BF_3•OEt_2 were causing substrate degradation. Although no additional Lewis acids were screened in this investigation, other previously developed $TolIF_2$-mediated reactions were successfully catalyzed with various Lewis acidic metal fluorides in the Murphy group.[149, 150, 170] Screening a full panel of metal fluorides might reveal the optimal Lewis acidic for this reaction. Given that the decomposition of starting material is consistently

observed with BF_3•OEt_2, screening milder Lewis acids, such as copper or zinc fluoride, was a logical next step.

In a search for a mild way to activate $TolIF_2$, we took inspiration from a recent Murphy group publication which used blue LEDs to activate iodonium ylides.[171] Stirring compound **3.70** with 1.1 equivalents of $TolIF_2$ in dichloromethane at room temperature under blue light gave **3.71** (Scheme 3-23). This product was isolated in 16% yield, however, with some unidentified minor impurities. The structure was unambiguously assigned by 1D and 2D NMR spectroscopy, and low-resolution mass spectrometry. As mentioned above, the control reaction without any activator or blue light led to the recovery of starting material. The exact mechanism of blue light activation was not further investigated. Hypothetically, reaction initiation could occur by two methods, either homolytic cleavage of an I-F bond initiating a radical chain reaction, or degradation of $TolIF_2$ by blue light and adventitious water creating trace hydrogen fluoride to activate $TolIF_2$. Further optimization failed to improve the yield of the product. The yield was not improved by reducing the reaction temperature to 0 °C or increasing the equivalents of $TolIF_2$. Based on previous work exploring this substrate (**3.70**) in unrelated radical reactions, several additives were explored. The addition of a catalytic amount (10 mol%) of silver nitrate or copper(I) bromide diminished the product yield.[172, 173] Interestingly, the addition of 1.2 equivalents of NaH_2PO_4 stopped the reaction and starting material **3.70** was recovered. This result lends evidence to the possibility of HF or acid generation being important in the reaction.

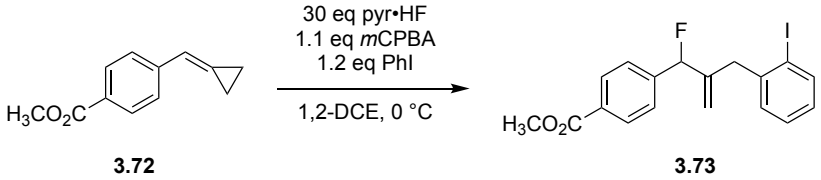


3.70 **3.71**

Scheme 3-23. Blue light for the mild activation of $TolIF_2$ and reaction with methylenecyclopropane **3.70**.

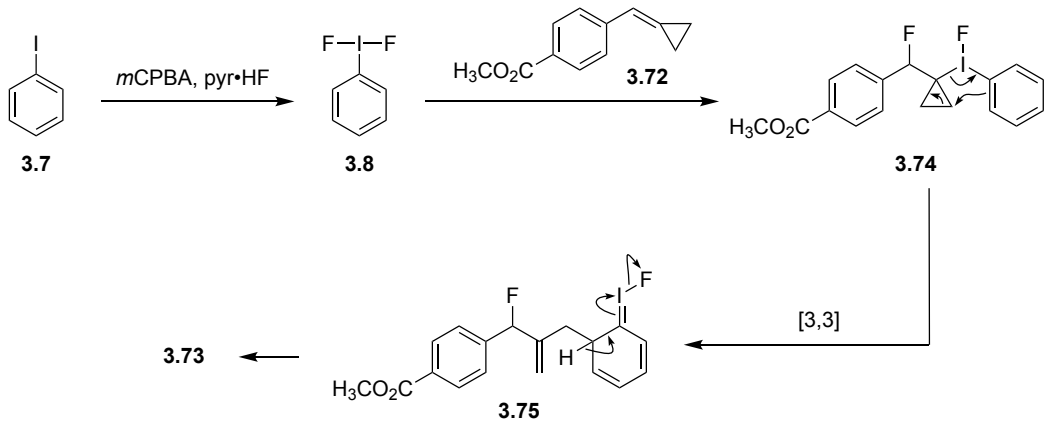
Ultimately, this project was stopped as during the investigation Li et al. disclosed an identical transformation under very similar reaction conditions (Scheme 3-24).[174] Similar to our result, they also found that Lewis acids, such as TMSOTf or BF_3•OEt_2 were detrimental to the reaction outcome. In their report the transformation was demonstrated on 40 examples with up to 86% yield; however, many yields were below 50%. Mechanistically, they proposed that the hypervalent difluoride species **3.8**,

formed in situ, adds across the alkene to give **3.74**. This intermediate is proposed to undergo a [3,3]-rearrangement to form a new carbon-carbon bond and give intermediate **3.75**, which rearomatizes to the final product **3.73**.



3.72 **3.73**

Scheme 3-24. The transformation reported by Li et al.



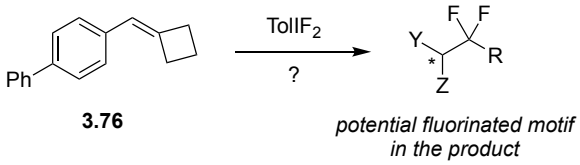
Scheme 3-25. The mechanism proposed by Li et. al.

Overall, we realized a unique transformation which included the formation of a new carbon-carbon. Further, our results indicate that blue light from LEDs may be a viable way to activate $TolIF_2$. The origin or mechanism of this activation is currently unknown; however; this development could be applied to future reaction development where the substrate has extreme Lewis or Brønsted acid sensitivity.

3.2.1.2 Methylenecyclobutanes

The reaction of methylenecyclobutane **3.76** and $TolIF_2$ was concurrently explored (Scheme 3-26). Difficulties were immediately encountered in the reaction development. Initially, **3.76** was treated with $TolIF_2$ in the presence or absence of BF_3•OEt_2 as the Lewis acid activator (Table 3-1, entries 1 and 2). The unidentified major product of the reaction was obtained in a very low yield and only determined to have a fluorine based on ^{19}F-NMR spectroscopy. Determination of the structure by ^{1}H-NMR was

inconclusive. Isolation of the product from the complex reaction mixture and full characterization proved difficult and was not achieved. However, information could be gathered from the crude ^{19}F-NMR spectrum as the signal appeared to be a set of diastereotopic fluorine atoms. Based on the chemical shift (~ -100 ppm) and the J-value (225 Hz) the product likely contained a -CF_2- group with a nearby stereocenter (Figure 3-3).



Scheme 3-26. Reaction of $TolIF_2$ with **3.76**.

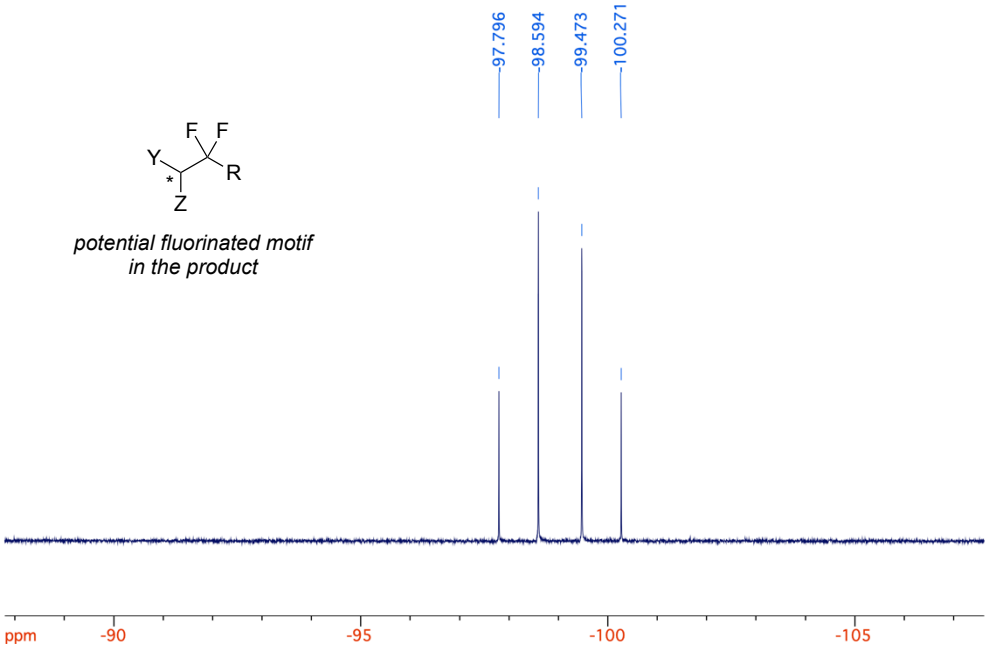
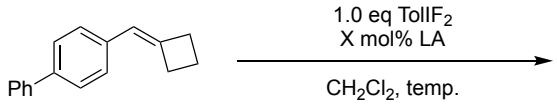


Figure 3-3. Major peak in the ^{19}F-NMR overlaid with a potential fluorinated motif.

Optimization of the reaction conditions was undertaken to gain more information about the identity of the product as well as to develop functional reaction conditions. The first reaction parameter to be manipulated was the loading of the Lewis acid. Increasing the amount of BF_3•OEt_2 from 0 to 10 mol% did not improve the yield nor the reaction profile (Table 3-1, entries 1-4). Reducing the temperature of the reaction, with or without BF_3•OEt_2, proved equally unsuccessful (Table 3-1, entries 5-7). Exploring

other Lewis acidic metal fluorides has proven fruitful in other reaction development campaigns in the Murphy group.[149, 150] As such, a series of six different Lewis acids (TiF_3, SnF_2, GaF_3, AlF_3, BiF_3, InF_3) were explored, but again, none improved the reaction outcome (Table 3-1, entries 8-13). The loading of the solid Lewis acid in these entries was higher compared to BF_3•OEt_2 (25 mol% vs. 0-10 mol%) to ensure accurate quantities of the solids were weighed and added to the reactions. Finally, based on successful reaction development in the literature, two protic activators were used, Et_3N•3HF and pyridine•HF.[115] The reaction with 100 mol% of Et_3N•3HF did not convert the substrate (Table 3-1, entry 14). This was surprising as the Et_3N•3HF complex appeared to be inhibiting the reaction instead of activating and accelerating the reaction. A simple comparison between entry 1 and 14 (Table 3-1) shows that the reaction proceeds without the addition of any activator. The use of the pyridine•HF complex as the activator provided only trace amounts of the product by ^{19}F-NMR (Table 3-1, entry 15). Overall, the optimization and development of this reaction was unsuccessful. Increasing the yield and/or decreasing the complexity of the reaction mixture was not achieved. Without any clear product identity or decomposition pathways, logical next steps for reaction optimization were not apparent and further reaction development was abandoned.

Table 3-1. Attempted optimization of the reaction between methylcyclobutane **3.76** and $TolIF_2$.



3.76

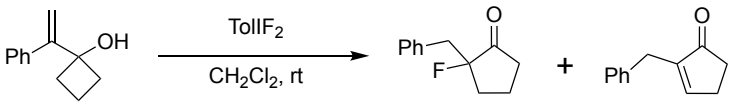
Entry	X mol%	LA	Temperature (°C)	Yield (%)[a]
1	0	-	rt	<5%
2	1	BF_3•OEt_2	rt	<5%
3	5	BF_3•OEt_2	rt	<5%
4	10	BF_3•OEt_2	rt	<5%
5	5	BF_3•OEt_2	0	<5%
6	0	-	0	<5%
7	0	-	-15 to 0	<5%
8	25	TiF_3	rt	<5%
9	25	SnF_2	rt	<5%
10	25	GaF_3	rt	<5%

Entry	X mol%	LA	Temperature (°C)	Yield (%)[a]
11	25	AlF_3	rt	<5%
12	25	BiF_3	rt	<5%
13	25	InF_3	rt	<5%
14	100	Et_3N•3HF	rt	NR
15	100	pyr•HF	rt	trace

[a]Yield obtained by quantitative ^{19}F-NMR with 3.0 μL of trifluorotoluene. NR = no reaction.

3.2.2 The Reaction of Alpha Cyclobutanols and *p*-(Difluoroiodo)toluene

Initial results showed that $TolIF_2$ reacted quite cleanly with styrenyl cyclobutanol **3.77** to give both the fluorinated cyclopentanone **3.78** (20% yield) and the enone **3.79** (12% yield), along with the recovery of 8% of the starting material **3.77** (Scheme 3-27). Beginning from this result a reaction optimization for the fluorocyclopentanone **3.78** was undertaken.



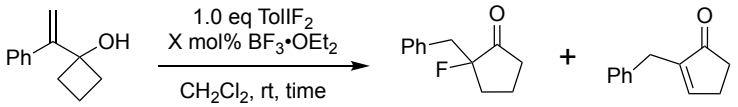
3.77 **3.78** **3.79**

Scheme 3-27. Initial discovery of the transformation of **3.77** to **3.78**.

The development of the reaction between cyclobutanol **3.77** and $TolIF_2$ began with a screen for the amount of BF_3•OEt_2 additive (Table 3-2). As mentioned above, without any BF_3•OEt_2 the reaction proceeded in 20% yield after a reaction time of 30 minutes (Table 3-2, entry 1). Increasing the loading of BF_3•OEt_2 from 0 to 5 mol% saw marginal improvements in yield, but the addition of 10 mol% saw an increase to 28% yield (Table 3-2, entries 2-5). Further increasing the loading to 25 mol% was detrimental to the yield of the desired fluorinated product, however, a large increase in enone product **3.79** was observed (Table 3-2, entry 6). The addition of BF_3•OEt_2 consistently reduces the reaction time from 30 to 10 minutes, as determined by a 100% conversion of **3.77** through TLC analysis. Although, the yield of the desired product **3.78** was increased with the addition of BF_3•OEt_2, so was the yield of the undesired enone **3.77**. Hypothetically, the BF_3•OEt_2 either promotes an additional reaction pathway from **3.77** to **3.79** or catalyzes the decomposition of **3.78** into **3.79**. Nonetheless, the BF_3•OEt_2 reduced

the non-specific decomposition of the starting material **3.77** as more material was recovered overall with BF_3•OEt_2 as an additive.

Table 3-2. Optimization of BF_3•OEt_2 equivalents.



3.77 **3.78** **3.79**

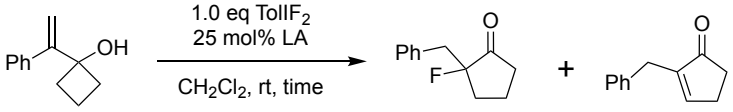
Entry	X mol%	Time (min)	Yield of **3.78** (%)[a]	Yield of **3.79** (%)[b]
1	0	30	20	12
2	0.2	10	20	12
3	1	10	22	16
4	5	10	21	33
5	10	10	28	30
6	25	10	25	48

[a]Yield obtained by quantitative ^{19}F-NMR with 3.0 µL of trifluorotoluene. [b]Yield determined by comparison to **3.78** in ^{1}H-NMR.

The next reaction parameter to be investigated was the Lewis acid. A series of fluoride Lewis acids were explored, along with a few others. Again, a catalyst loading of 25 mol% was used to ensure consistency and accuracy in the weighing and addition of the solid on the small (0.1 mmol) reaction scale. First, three more Lewis acids from group 13 were explored which gave slightly lower yields compared to BF_3•OEt_2 and longer reaction times (Table 3-3, entries 1-3). The enone side product **3.79** was again observed but to a lesser degree. The use of tin or bismuth fluoride provided similar results to the group 13 Lewis acids and did not improve the yield of **3.78** (Table 3-3, entries 4 and 5). The use of either titanium(III) or titanium(IV) fluoride showed a marked increase in yield to 39% (Table 3-3, entries 6 and 8). This increase in yield was accompanied by a corresponding increase in the yield of the enone **3.79**. Additionally, the use of TiF_3 provided a slightly cleaner ^{1}H-NMR profile than typically achieved with other Lewis acids. Increasing the loading to 100 mol% of TiF_3 improved the yield slightly; however, the ^{1}H-NMR spectrum contained an increased number of unidentified impurities (Table 3-3, entry 7). Evidently, the Lewis acidic properties, such as strength, of titanium were well suited for this transformation. Neither of the silicon-based Lewis acids were effective (Table 3-3, entries 9 and 10). The reaction with TMSCl gave the chlorinated product **3.65**, while the reaction with TMSOTf

caused non-specific decomposition of the substrate. In the reaction with TMSCl, $TolIF_2$ likely oxidized free chloride ions to "Cl^+" which reacted in a manner similar to the chlorination and semi-pinacol rearrangement listed in Scheme 3-20. The protic Et_3N•3HF complex was ineffective at catalyzing the desired transformation (Table 3-3, entry 11). The use of *p*-TsOH as the activator resulted in 100% conversion of **3.77**, however, **3.79** was the sole product (Table 3-3, entry 12). With this information, 25 mol% of TiF_3 was chosen as the Lewis acid activator to be carried forward into further optimization studies.

Table 3-3. Optimization of Lewis acid.



3.77 **3.78** **3.79**

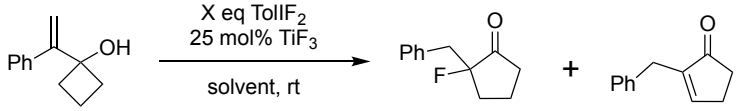
Entry	Lewis acid (LA)	Time (min)	Conversion (%)	Yield of **3.78** (%)[a]	Yield of **3.79** (%)[b]
1	AlF_3	60	94	20	11
2	GaF_3	30	95	17	9
3	InF_3	30	82	21	11
4	SnF_2	15	91	25	15
5	BiF_3	30	94	15	10
6	TiF_3	25	96	39	24
7	TiF_3[c]	10	100	43	28
8	TiF_4	25	ND	39	ND
9	TMSCl	60	100	-	-
10	TMSOTf	15	100	-	-
11	Et_3N•3HF	60	71	24	14
12	*p*-TsOH	10	100	0	ND

[a]Yield obtained by quantitative ^{19}F-NMR with 3.0 μL of trifluorotoluene. [b]Yield determined by comparison to **3.78** in ^{1}H-NMR. [c]100 mol% of TiF_3. TMSCl = trimethylsilyl chloride; TMSOTf = trimethylsilyl triflate. ND = not determined.

A comparison of chlorinated solvents when using 1.2 equivalents of $TolIF_2$ did not show any significant improvement in the yield of product or enone (Table 3-4, entries 1-3). Further increasing the equivalents of $TolIF_2$ was beneficial up to 1.5 before giving marginal returns on yield with 2.0 and

2.5 equivalents (Table 3-4, entries 3-6). However, the amount of enone **3.79** was reduced with increasing equivalents of $TolIF_2$. Next, we were curious if the order of reagent addition could influence the yield. The reaction was typically carried out by adding starting material **3.77**, $TolIF_2$, and then the Lewis acid, quickly in sequential order. Reversing the order of TiF_3 and $TolIF_2$ addition moderately reduced the yield, while the dropwise addition of $TolIF_2$ more than halved the yield of the product (Table 3-4, entries 7 and 8). To this point in the optimization, an initial yield of 20% had been improved to 49%.

Table 3-4. Exploring the equivalents of $TolIF_2$, solvent, and order of addition.



3.77 **3.78** **3.79**

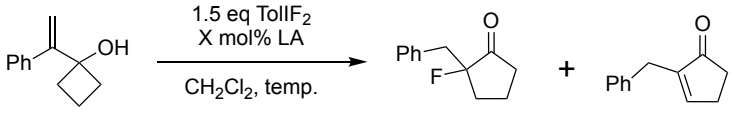
Entry	Equivalents of $TolIF_2$	Solvent	Yield of **3.78** (%)[a,b]	Yield of **3.79** (%)[c]
1	1.2	1,2-DCE	38	30
2	1.2	$CHCl_3$	44	30
3	1.2	CH_2Cl_2	42	32
4	1.5	CH_2Cl_2	49	31
5	2.0	CH_2Cl_2	51	20
6	2.5	CH_2Cl_2	46	20
7	1.2	CH_2Cl_2[d]	35	32
8	1.2	CH_2Cl_2[e]	23	17

[a]Yield obtained by quantitative ^{19}F-NMR with 3.0 µL of trifluorotoluene. [b]100% conversion of **3.77**. [c]Yield determined by comparison to **3.78** in ^{1}H-NMR.[d]Order of addition: **3.77**, TiF_3, $TolIF_2$. [e]Order of addition: $TolIF_2$, TiF_3, **3.77 (**dropwise in CH_2Cl_2).

As the titanium-based Lewis acids TiF_3 and TiF_4 were the most successful for catalyzing the reaction, we were interested in exploring the possibility of using $TiCl_4$ or Ti(O*i*-Pr)$_4$. Unfortunately, the use of $TiCl_4$ gave the undesired chlorinated product **3.65**, likely by the same mechanism which TMSCl gave **3.65**. Gratifyingly, the yield increased with 25 mol% of Ti(O*i*-Pr)$_4$ (Table 3-5, entry 1). Reduction of the Ti(O*i*-Pr)$_4$ loading to 1 mol% gave an identical yield but with a favourable reduction in the enone side product (Table 3-5, entry 2). Hoping to increase the favourability of the desired reaction pathway the reaction temperature was reduced. Running the reaction at 0 °C or -10 °C was beneficial (Table 3-5,

entries 3 and 4). A comparison of TiF_3 and Ti(O*i*-Pr)$_4$ at 0 °C gave the same results (Table 3-5, entry 3 vs. 5). Two additional hypotheses were explored to combat the low yield of the desired product. One, adventitious water might be inactivating the Lewis acid or aiding in the decomposition of unknown reaction intermediate. To test this hypothesis powdered molecule sieves were added to sequester water, but unfortunately, that did not improve the yield of **3.78** or the ratio of the enone produced (Table 3-5, entries 6). Adventitious water, if present, was not causing any issues in the reaction. Two, as the substrate contains an allylic tertiary alcohol it could theoretically decompose under the acidic reaction conditions via the formation of a carbocation; however, it was shown that this proposed decomposition was not an issue. Firstly, substrate **3.77** was found to be stable to 1 mol% Ti(O*i*-Pr)$_4$ over the reaction time. Second, beginning the reaction from the silylated alcohol did not improve the yield of **3.78** or the ratio of enone produced (Table 3-5, entries 7).

Table 3-5. Reaction optimization with titanium Lewis acids.



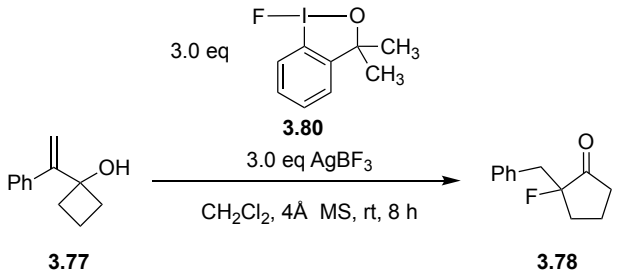
3.77 **3.78** **3.79**

Entry	X, LA	Temperature (°C)	Yield of **3.78** (%)[a,b]	Yield of **3.79** (%)[c]
1	25, Ti(O*i*-Pr)$_4$	rt	57	32
2	1, Ti(O*i*-Pr)$_4$	rt	56	25
3	1, Ti(O*i*-Pr)$_4$	0	58	21
4	1, Ti(O*i*-Pr)$_4$	-10	61	27
5	25, TiF_3	0	57	23
6[d]	1, Ti(O*i*-Pr)$_4$	0	51	20
7[e]	1, Ti(O*i*-Pr)$_4$	0	53	24

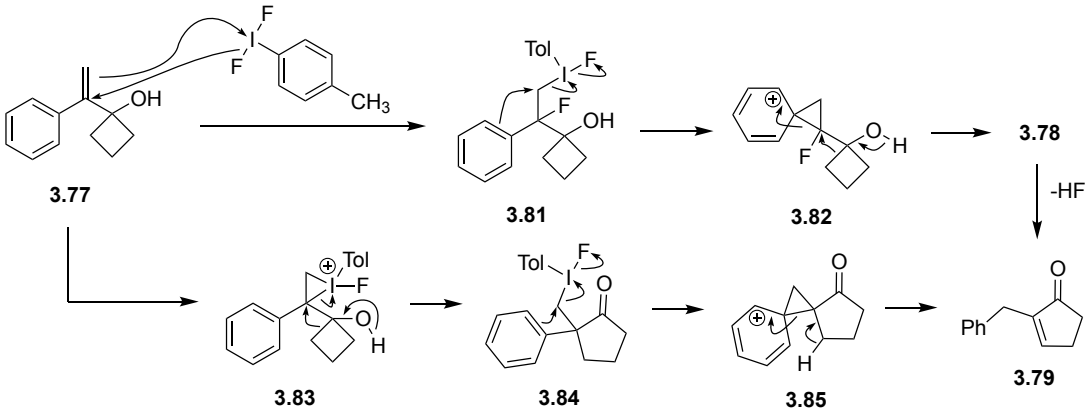
[a]Yield obtained by quantitative ^{19}F-NMR with 3.0 µL of trifluorotoluene. [b]100% conversion of **3.77**. [c]Yield determined by comparison to **3.78** in ^{1}H-NMR. [d]4Å molecule sieves added. [e]Trimethylsilyl alcohol starting material instead of free alcohol **3.77**.

Gulder et al. developed the same transformation with a different HVI reagent **3.80**.[175] Their optimized condition required 3 equivalents of **3.80** and $AgBF_4$ with 4Å molecular sieves in CH_2Cl_2 (Scheme 3-28, 18 examples, 70-96% yield). They did not mention any observation of the side product enone which was found in all of our reactions. Our optimal conditions to date involve reacting 1.5 equivalent of

$TolIF_2$, 1 mol% of Ti(O*i*-Pr)$_4$ with **3.77** at -10 °C. Based on their mechanism, we propose that the titanium-activated $TolIF_2$ reacts with the alkene to provide intermediate **3.81**. Formation of the phenonium ion, as described in Scheme 3-14, provides the spirocyclic intermediate **3.82**. Finally, ring expansion of the cyclobutanol and rearomatization of the phenyl ring provides the final product **3.78**. The elimination of HF from this product could give the enone **3.79**. Alternatively, **3.77** may react with $TolIF_2$ to provide iranium ion **3.83**. Ring expansion at this point in the mechanism would provide the cyclopentanone **3.84**. A 1,2-phenyl shift terminated by the elimination of a proton from the cyclopentanone ring would equally provide enone **3.79**.



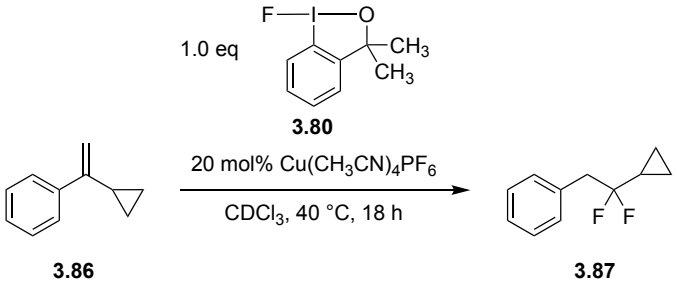
Scheme 3-28. Reaction conditions developed by Gulder et al.



Scheme 3-29. Proposed mechanism for the formation of **3.78** and **3.79**.

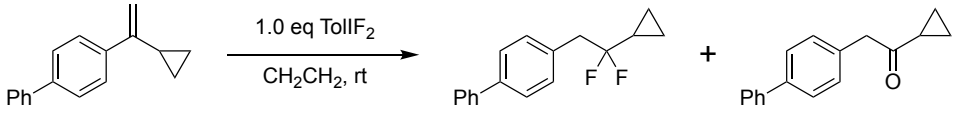
3.2.3 The Reaction of Alpha Cyclopropyl Styrene and *p*-(Difluoroiodo)toluene

The final substrate to be explored was the alpha cyclopropyl styrene **3.88**. Early reactivity between this type of substrate and **3.80** had been observed by Szabo et al. (Scheme 3-30).[176] They treated **3.86** with 1 equivalent of **3.80** and 20 mol% of the copper(I) catalyst in deutero-chloroform and obtained **3.87** in 58% yield. This is the sole example in the literature.



Scheme 3-30. *gem*-Difluorination with **3.80**.

We were curious to determine if carboskeleton rearrangements could occur with the more reactive HVI reagent, $TolIF_2$. Unfortunately, the same reactivity was observed with $TolIF_2$ (Scheme 3-31). Initial reaction discovery and reaction optimization were performed with **3.88** instead of **3.86**, as the product **3.87** was volatile. Treatment of **3.88** with 1.0 equivalents of $TolIF_2$ in CH_2Cl_2 produced **3.89** (15% yield) and **3.90** (8% yield) in 10 minutes at room temperature. The *gem*-difluoride **3.89** arises from the fluorination and 1,2-phenyl shift, the mechanism for which is outlined in Scheme 3-14. The undesired side product **3.90** presumably appears when an oxygen nucleophile captures a reaction intermediate. The oxygenated side product is known to occur in reactions with $TolIF_2$.[134] The origin of the oxygen was determined to be the borosilicate glass from the reaction vessel and not adventitious water.[135]

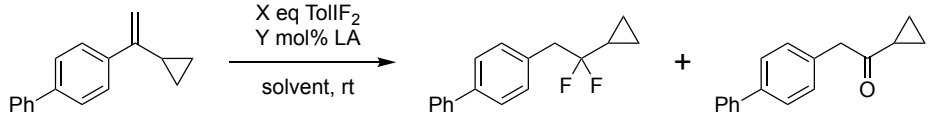


Scheme 3-31. Initial *gem*-difluorination of **3.88**.

Again, optimization began with a screen for loading of the Lewis acid, $BF_3{\bullet}OEt_2$. The use of 0.1, 5, or 10 mol% of $BF_3{\bullet}OEt_2$ gave similarly poor results to 0 mol% $BF_3{\bullet}OEt_2$; however, 1 mol% gave a

three-fold increase in yield (Table 3-6, entries 2-5). Screening common reaction solvents revealed that higher yields were generally obtained with the chlorinated solvents, but none were superior to CH_2Cl_2 (Table 3-6, entries 6-12). Increasing the equivalents of $TolIF_2$ to 1.2 equivalents was beneficial, but a further increase returned an identical result (Table 3-6, entries 13 and 14). Given the success of titanium-based Lewis acids in the previous section, the same three were tested in this transformation. Unfortunately, none improved the yield of the desired transformation (Table 3-6, 15-17). An additional five Lewis acids were screened, but no discernable reactivity pattern or yield increase was observed (Table 3-6, entries 19-25). It should be noted that the solid Lewis acids were screened at 10 mol% in the reaction. As such a large difference was seen between 1 vs. 10 mol% of BF_3•OEt_2, the reaction should be scaled and tested with AlF_3, the best-performing alternative Lewis acid. A control reaction of simply BF_3•OEt_2 and the starting material **3.88** indicated that they reacted unproductively under the typical reaction conditions. This might be one reason for the poor yield obtained in the reaction. Unfortunately, without any activator, the reaction does not proceed. Overall, varying reaction solvent, Lewis acid, or equivalents of $TolIF_2$ showed no dramatic increase in yield. As such the optimal conditions were 1 mol% BF_3•OEt_2 and 1.2 equivalents of $TolIF_2$ in CH_2Cl_2 which converted **3.88** in to the desired *gem*-difluoride **3.89** in 51% yield and 12% yield of the undesired ketone **3.90**.

Table 3-6. Optimization of *gem*-difluorination of alpha cyclopropyl styrenes.



3.88 **3.89** **3.90**

Entry	X, equivalents of $TolIF_2$	Y, mol% of Lewis acid, Lewis acid	Solvent	Yield of **3.89** (%)[a]	Yield of **3.90** (%)[b]
1	1.0	0.0, BF_3•OEt_2	CH_2Cl_2	15	8
2	1.0	0.1, BF_3•OEt_2	CH_2Cl_2	8	ND
3	1.0	1, BF_3•OEt_2	CH_2Cl_2	46	12
4	1.0	5, BF_3•OEt_2	CH_2Cl_2	9	2
5	1.0	10, BF_3•OEt_2	CH_2Cl_2	7	2
6	1.0	1, BF_3•OEt_2	$CHCl_3$	26	6
7	1.0	1, BF_3•OEt_2	1,2-DCE	39	12
8	1.0	1, BF_3•OEt_2	PhCl	8	ND

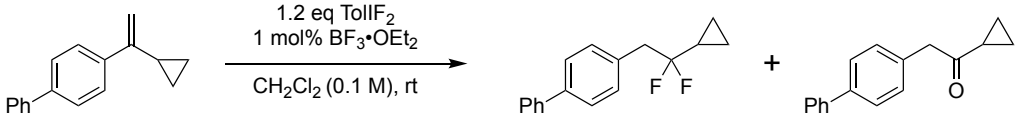
Entry	X, equivalents of $TolIF_2$	Y, mol% of Lewis acid, Lewis acid	Solvent	Yield of **3.89** (%)[a]	Yield of **3.90** (%)[b]
9	1.0	1, BF_3•OEt_2	Tol	6	ND
10	1.0	1, BF_3•OEt_2	CH_3CN	8	ND
11	1.0	1, BF_3•OEt_2	THF	3	ND
12	1.0	1, BF_3•OEt_2	HFIP	0	-
13	1.2	1, BF_3•OEt_2	CH_2Cl_2	51	12
14	1.5	1, BF_3•OEt_2	CH_2Cl_2	46	9
15	1.2	1, Ti(O*i*-Pr)$_4$	CH_2Cl_2	26	12
16	1.2	10, Ti(O*i*-Pr)$_4$	CH_2Cl_2	12	ND[c]
17	1.2	10, TiF_3	CH_2Cl_2	38	15
18	1.2	10, TiF_4	CH_2Cl_2	38	10
19	1.2	10, InF_3	CH_2Cl_2	36	13
20	1.2	10, SnF_2	CH_2Cl_2	42	9
21	1.2	10, BiF_3	CH_2Cl_2	35	12
22	1.2	10, GaF_3	CH_2Cl_2	35	13
23	1.2	10, AlF_3	CH_2Cl_2	46	11
24	1.2	1, $Cu(BF_4)_2$	CH_2Cl_2	41	12
25	1.2	1, $AgBF_4$	CH_2Cl_2	48	10

[a]Yield obtained by quantitative ^{19}F-NMR with 3.0 μL of trifluorotoluene. [b]Yield determined by comparison to **3.89** in ^{1}H-NMR. [c]Yield not determined due to peak overlap with impurity. ND = not determined.

Further conditions were explored, but again the changes resulted in diminished or equivalent yields. No improvements to the yield were made. Adjusting the concentration of the reaction to 0.2 M reduced the yield by a factor of two while decreasing the concentration 2-fold gave roughly the same result (Table 3-7, entries 2 and 3). As hexafluoroisopropanol (HFIP) has been shown to activate HVI reagents, it was added as the activator to this reaction, but unfortunately, only 8% yield was achieved with an equivalent amount of ketone **3.90** (Table 3-7, entry 4).[177] The material of the reaction vessel was also explored. Identical results were obtained with a silanized vial, while a Teflon vial showed diminished yields (Table 3-7, entries 5 and 6). Finally, the order of reagent addition was modified. Typically, the starting material **3.88** was dissolved in CH_2Cl_2, followed by $TolIF_2$ before the Lewis acid was added to

initiate the reaction. The order of addition was modified in two different ways. First, the starting material **3.88** was added dropwise to a solution of $TolIF_2$ and BF_3•OEt_2, which again returned the same yield (Table 3-7, entry 1 vs. 7). Although unlikely to succeed, because of the reactivity between **3.88** and BF_3•OEt_2, $TolIF_2$ was added to a mixture of **3.88** and BF_3•OEt_2. As expected, the yield was lower (Table 3-7, entry 1 vs. 8). Lastly, the use of a protic acid activator, such as *p*-TsOH, also made no improvements to the yield (Table 3-7, entry 9). After screening 33 different reaction conditions the optimal conditions only gave a 51% yield of the desired product **3.89** with 12% of the undesired ketone **3.90**.

Table 3-7. Additional modification of the optimized conditions.



3.88 **3.89** **3.90**

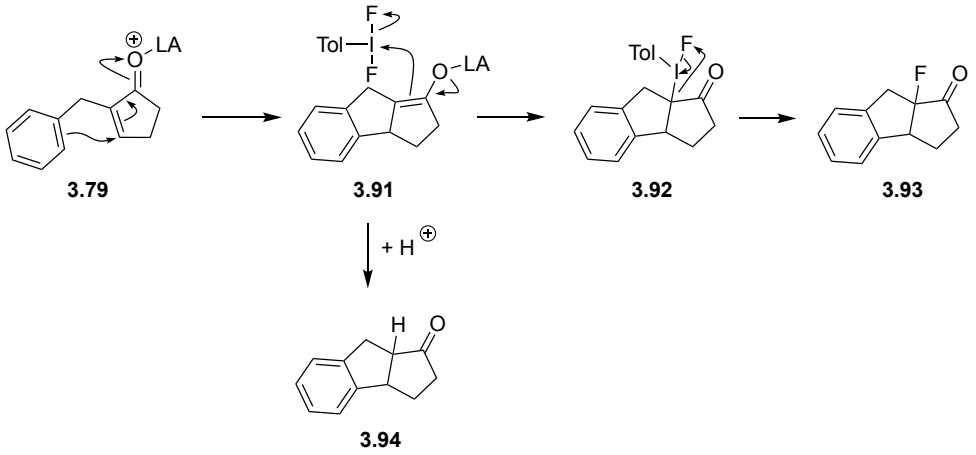
Entry	Modification	Yield of **3.89** (%)[a]	Yield of **3.90** (%)[b]
1	-	51	12
2	concentration = 0.2 M	25	5
3	concentration = 0.05 M	48	11
4	HFIP instead of BF_3•OEt_2	8	9
5	Silanized glass vessel	49	10
6	Teflon vessel	31	9
7	**3.88** to $TolIF_2$ + BF_2•OEt_2	49	12
8	$TolIF_2$ to **3.88** +BF_3•OEt_2	19	4
9	*p*-TsOH instead of BF_3•OEt_2	22	12

[a]Yield obtained by quantitative ^{19}F-NMR with 3.0 μL of trifluorotoluene. [b]Yield determined by comparison to **3.89** in ^{1}H-NMR.

3.3 Concluding Remarks and Future Work

The first project involving methylenecyclopropanes resulted in the discovery of a unique transformation which incorporated the iodotoluene from the $TolIF_2$ into the final product (Section 3.2.1). This product was unambiguously identified by 1D and 2D NMR spectroscopy and low-resolution mass spectrometry. Blue LED activation was observed as opposed to classical Lewis acid activation of $TolIF_2$. Future work could explore this mode of activation in a series of known transformations with $TolIF_2$ to determine if it is a general mode of activation or exclusive to this transformation.

For the second project, the fluorination and expansion of the styrenyl cyclobutanol, the reaction conditions were optimized to deliver the desired product in a 61% yield, with 27% of an enone side product, for a mass recovery of 88% (Section 3.2.2). Future work should be focused on reducing the amount of enone side product produced during the reaction to obtain exclusively the desired product. Further decreasing the reaction temperature and the equivalents of $Ti(O\textit{i}\text{-}OPr)_4$ are reasonable reaction conditions to explore in future experiments. Determining the origin of the enone would be ideal for reaction development. As a control, pure product **3.78** should be reacted under the optimized condition to determine if the product is stable under these conditions. If the product is stable under the reaction conditions, then the reaction work-up could be explored. For example, upon reaction completion, the reaction mixture could be immediately filtered through basic alumina, silica, or celite. The enone **3.79** could also be the focus of further synthetic studies (Scheme 3-32). For example, optimizing the reaction for enone instead of **3.78**. Based on the trends of the data collected to date, it is likely increasing the catalyst loading would favour a greater enone product yield. Hypothetically, the enone could be transformed in situ to more complex products. Nucleophilic cyclization of the aromatic ring onto the enone could give a tricyclic product such as **3.91**. The resulting enolate might be captured by a proton (e.g., **3.94**) or an additional equivalent of hypervalent iodine reagent to fluorinate the carbon (e.g., **3.93**).



Scheme 3-32. Potential further synthetic studies with undesired enone **3.79**.

For the third project, the reaction between $TolIF_2$ and alpha-cyclopropyl styrenes was explored. The reaction conditions were optimized to give the desired product **3.89** in 51% yield with a significant amount of the ketone side product **3.90** (12% yield) (Section 3.2.3). Remarkably no other significant side products were identified even with reaction cyclopropane ring. Extensive optimization was not successful in finding improved reaction conditions. Future work should be directed at expanding the scope of the transformation. This could include examples such as **3.95**, **3.96**, and **3.97** to test the reaction compatibility with electron-rich or poor heteroaromatic and aliphatic chains. A suite of different groups could be placed on the aromatic ring to explore functional group compatibility (e.g., **3.98**).

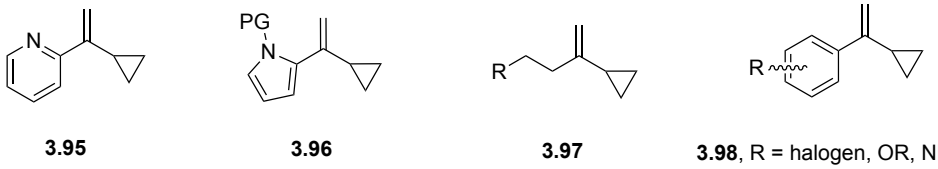


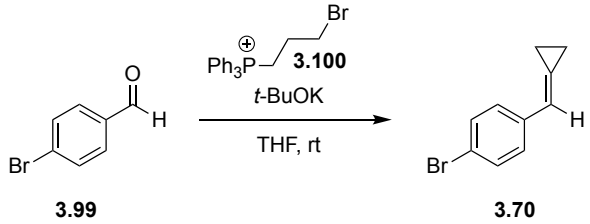
Figure 3-4. Potential substrates to be investigated in the *gem*-difluorination of alpha cyclopropyl styrenes.

Broadly, these three projects explored the reactivity of $TolIF_2$ and demonstrated its reactivity in complex systems where additional rearrangements were possible. The observation that $TolIF_2$ is most effectively activated by group 13 and titanium-based Lewis acids was further reinforced in these studies.

3.4 Experimental Details

Solvents were dried and purified using a JC Meyer solvent purification system and were used without further purification (exceptions listed below). CH_3CN was stirred with flame-dried K_2CO_3 overnight before sequential drying with 4Å molecular sieves (2x), and $CHCl_3$ was washed with water before sequential drying with 4Å molecular sieves (2x). Transfer of anhydrous solvents and reagents was accomplished with oven-dried needles. Thin layer chromatography was performed on glass plates pre-coated with 0.25 mm Kieselgel 60 F254 (Silicycle). Flash chromatography columns were packed with 230-400 mesh silica gel (Silicycle). Proton NMR spectra (^{1}H NMR) were recorded at 300 MHz and are reported (ppm) relative to the residual solvent peak. Carbon NMR spectra (^{13}C NMR) were recorded at 75 MHz and are reported (ppm) relative to the center line of the residual solvent peak. Fluorine NMR spectra (^{19}F NMR) were recorded at 282 MHz and are reported (ppm) relative to the peak of trifluoroacetic acid at -76.55 ppm. All coupling constants (J) are reported in hertz (Hz). Singlet = s, broad singlet = br. s, doublet = d, triplet = t, quartet = q, quintet = qu., sextet = sex, multiplet = m. All literature known compounds matched the spectral data found in the literature. Spectral data of new compounds are provided in Appendix A.

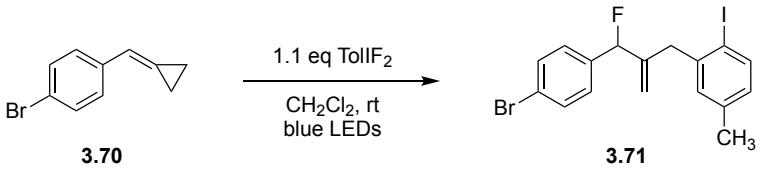
Preparation of 1-bromo-4-(cyclopropylidenemethyl)benzene (3.70):



3.99 **3.70**

To a flame-dried round bottom flask under nitrogen was added Wittig reagent **3.100** (1.40 g, 3.00 mmol, 1.5 eq), 12 mL of THF, and *t*-BuOK (673 mg, 6.00 mmol, 3.0 eq). The mixture was refluxed for 90 minutes before cooling back to room temperature. Aldehyde **3.99** (370 mg, 2.00 mmol, 1.0 eq) was added and the reaction was stirred for 22 hours at room temperature, then refluxed for 2 hours. The reaction was cooled to room temperature and poured into hexanes (40 mL), filtered, and concentrated under reduced pressure. Flash column chromatography with 100% hexanes afforded **3.70** (358 mg, 1.7 mmol, 86%) as a white solid. R_f = 0.53 (100% hexanes). ^{1}H-NMR (300 MHz; $CDCl_3$): δ 7.45-7.42 (m, 2H), 7.40-7.37 (m, 2H), 6.69 (tt, *J* = 2.0, 2.0 Hz, 1H), 1.43-1.37 (m, 2H), 1.20-1.14 (m, 2H).[178]

Preparation of 2-(2-((4-bromophenyl)fluoromethyl)allyl)-1-iodo-4-methylbenzene (3.71):



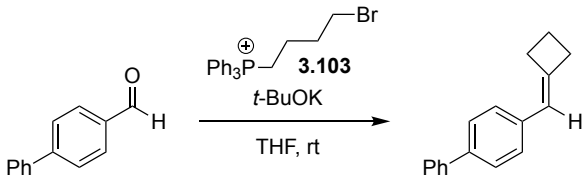
3.70 **3.71**

Example procedure with blue LEDs: The blue LED experimental setup was adopted from a previous publication from the Murphy research group.[171] To a one dram oven-dried scintillation vial was added **3.70** (10 mg, 0.05 mmol, 1.0 eq), $TolIF_2$ (13 mg, 0.055 mmol, 1.1 eq), and CH_2Cl_2 (1.0 mL). A stir bar was added and the vial was purged with nitrogen. The vial was placed directly over a single blue LED light and stirred for 15 minutes. The reaction mixture was concentrated under reduced pressure, $PhCF_3$ (3.0 µL, 0.024 mmol) was added, dissolved in $CDCl_3$ and a quantitative ^{19}F-NMR was obtained. Flash column chromatography with 5% ethyl acetate in hexanes afforded **3.71** as a solid. R_f = 0.28 (5% ethyl acetate in hexanes). Spectra were analogous to products reported by Li et al.[174] ^{1}H-NMR (300 MHz; $CDCl_3$): δ 7.69 (d, *J* = 8.0 Hz, 1H), 7.57-7.53 (m, 2H), 7.32-7.28 (m, 2H), 6.98 (d, *J* = 2.0 Hz, 1H), 6.76 (dd, *J* = 8.0, 1.7 Hz, 1H), 5.87 (d, *J* = 46.8 Hz, 1H), 5.33-5.31 (m, 1H), 4.76-4.74 (m, 1H), 3.41 (d, *J* = 16.7 Hz, 1H), 3.29 (d, *J* = 16.4 Hz, 1H), 2.29 (s, 3H). ^{13}C-NMR (75 MHz; $CDCl_3$): δ 145.0 (d,

J = 19.2 Hz), 140.8, 139.5, 138.4, 137.1 (d, *J* = 21.8), 131.7, 131.6, 129.5, 128.3 (d, *J* = 6.8 Hz), 122.7, 115.5 (d, *J* = 9.3 Hz), 97.4, 95.0 (d, 175.3 Hz), 42.2 (d, 2.7 Hz), 21.0. LRMS-EI $C_{17}H_{15}{}^{79/81}BrFI$ $[M]^{\bullet+}$ 445.85, 443.78, $[M\text{-}I]^+$ 319.01, 316.98.

Example procedure with $BF_3{\bullet}OEt_2$: To a 10 mL round bottom flask with a stir bar under nitrogen was added **3.70** (21 mg, 0.10 mmol, 1.0 eq), $TolIF_2$ (27 mg, 0.11 mmol, 1.1 eq), and CH_2Cl_2 (0.50 mL). Once all the material was dissolved, $BF_3{\bullet}OEt_2$ (12.5 µL, 0.005 mmol, 5 mol%, 0.4 M in CH_2Cl_2) was added to initiate the reaction and it was stirred at room temperature for 10 minutes. The reaction mixture was concentrated under reduced pressure, $PhCF_3$ (3.0 µL, 0.024 mmol) was added, dissolved in $CDCl_3$ and a quantitative ^{19}F-NMR spectrum was obtained.

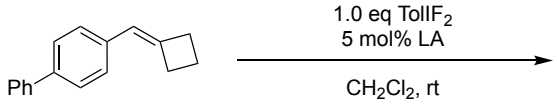
Preparation of 4-(cyclobutylidenemethyl)-1,1'-biphenyl (3.76):



3.102 **3.76**

To a flame-dried round bottom flask under nitrogen was added Wittig reagent **3.103** (3.65 g, 7.5 mmol, 1.5 eq), 25 mL of THF, and *t*-BuOK (1.85 mg, 16.5 mmol, 3.0 eq). The mixture was refluxed for 90 minutes before cooling back to room temperature. Aldehyde **3.102** (911 mg, 5.00 mmol, 1.0 eq) was added and the reaction was stirred for 22 hours at room temperature, then refluxed for 2 hours. The reaction was cooled to room temperature and poured into hexanes (100 mL), filtered, and concentrated under reduced pressure. Flash column chromatography with 100% hexanes afforded **3.76** as a white solid. ^{1}H-NMR (300 MHz; $CDCl_3$): δ 7.61-7.58 (m, 2H), 7.56-7.52 (m, 2H), 7.46-7.40 (m, 2H), 7.35-7.26 (m, 3H), 6.12 (tt, *J* = 2.4, 2.4 Hz 1H), 3.13-3.06 (m, 2H), 2.95-2.88 (m, 2H), 2.19-2.08 (m, 2H).[174]

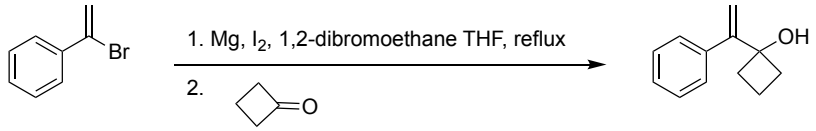
Procedure for the reaction of $TolIF_2$ with 3.76:



3.76

To a 10 mL round bottom flask with a stir bar under nitrogen was added **3.76** (21 mg, 0.10 mmol, 1.0 eq), $TolIF_2$ (24 mg, 0.10 mmol, 1.0 eq), and CH_2Cl_2 (1.0 mL). Once all the material was dissolved, BF_3•OEt_2 (12.5 µL, 0.005 mmol, 5 mol%, 0.4 M in CH_2Cl_2) was added to initiate the reaction and it was stirred at room temperature for 10 minutes. The reaction mixture was concentrated under reduced pressure, $PhCF_3$ (3.0 µL, 0.024 mmol) was added, dissolved in $CDCl_3$ and a quantitative ^{19}F-NMR spectrum was obtained.

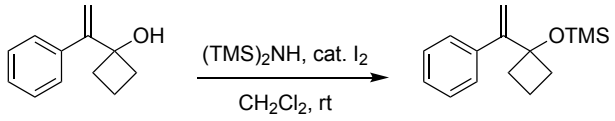
Preparation of 1-(1-phenylvinyl)cyclobutan-1-ol (3.77):



3.104 **3.77**

To a flame-dried 100 mL two-neck round bottom flask fitted with a reflux condenser with a stir bar was added magnesium (288 mg, 12.0 mmol, 4.0 eq), THF (2 mL) and dibromoethane (135 µL, 1.6 mmol, 0.4 eq). A few crystals of iodine were added. After stirring at room temperature for 5 minutes, alpha-bromostyrene (714 mg, 3.90 mmol, 1.0 eq) in THF (20 mL) was added dropwise with an addition funnel over 30 minutes (significant exotherm observed). The reaction was then heated at reflux for two hours. After cooling to room temperature, cyclobutanone (287 µL, 3.90 mmol, 1.0 eq) was added and the reaction was stirred for an additional 2 hours. The reaction was quenched with sat. NH_4Cl and extracted with ethyl acetate (3x). The combined organic layers were washed with water, brine, dried over $MgSO_4$, filtered and concentrated under reduced pressure. Flash column chromatography with a gradient (100% hexanes to 2.5% ethyl acetate in hexanes to 5% ethyl acetate in hexanes) afforded **3.77** (451 mg, 2.56 mmol, 66%) as a clear oil. ^{1}H-NMR (300 MHz; $CDCl_3$): δ 7.52-7.46 (m, 2H), 7.37-7.26 (m, 3H), 5.38 (d, J = 0.9 Hz, 1H), 5.37 (d, J = 0.9 Hz, 1H), 2.54-2.43 (m, 2H), 2.31-2.20 (m, 2H), 2.17-2.08 (m, 1H), 2.08-1.92 (m, 1H), 1.64 (dtt, J = 10.9, 8.9, 6.9 Hz, 1H).[159]

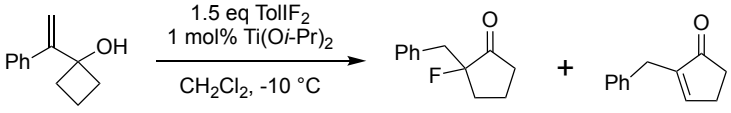
Preparation of trimethyl(1-(1-phenylvinyl)cyclobutoxy)silane (3.105):[179]



3.77 **3.105**

To a flame-dried 25 mL round bottom flask with a stir bar was added **3.77** (261 mg, 1.50 mmol, 1.0 eq), CH_2Cl_2 (6.0 mL), and iodine (3.8 mg, 0.015 mmol, 1 mol%). After stirring at room temperature for a minute $(TMS)_2NH$ (248 µL, 1.20 mmol, 0.8 eq in 1.5 mL CH_2Cl_2) was added dropwise. After 30 minutes $Na_2S_2O_3$ (~500 mg) was added portion wise and stirred for an additional 30 minutes. The mixture was filtered through a pad of celite and washed with CH_2Cl_2. The solvent was removed under reduced pressure to afford **3.105** (356 mg, 1.44 mmol, 96%). ^{1}H-NMR (300 MHz; $CDCl_3$): δ 7.60-7.51 (m, 2H), 7.37-7.24 (m, 3H), 5.47 (d, J = 0.8 Hz, 1H), 5.41 (d, J = 0.7 Hz, 1H), 2.52-2.29 (m, 4H), 1.91-1.79 (m, 1H), 1.64-1.48 (m, 1H), 0.06-0.02 (m, 9H).[163]

Procedure for the reaction of $TolIF_2$ with (3.77):



3.77 **3.78** **3.79**

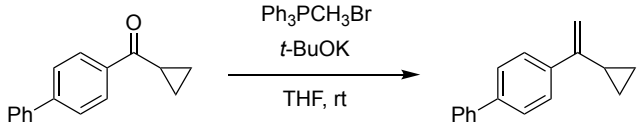
To a 10 mL round bottom flask with a stir bar under nitrogen was added **3.77** (017 mg, 0.10 mmol, 1.0 eq), $TolIF_2$ (36 mg, 0.15 mmol, 1.0 eq), and CH_2Cl_2 (1.0 mL). Once all the material was dissolved the reaction was cooled to -10 °C in an ice:acetone bath (1:1). $Ti(O\textit{i}\text{-}Pr)_4$ (5 µL, 0.001 mmol, 1 mol% in 0.207 M in CH_2Cl_2) was added to initiate the reaction and it was stirred for 10 minutes at the same temperature. After which the reaction was filtered through ~1 cm layer of celite in a small Pasteur pipette and rinsed with CH_2Cl_2 (3x, 1 mL). The reaction mixture was concentrated under reduced pressure, $PhCF_3$ (3 µL, 0.024 mmol) was added, dissolved in $CDCl_3$ and a quantitative ^{19}F-NMR was obtained.

The two products (**3.78** and **3.79**) were isolated from an experiment at a 0.5 mmol scale with TiF_3 (25 mol%) as the initiator. Flash column chromatography was run with a gradient (5% to 10% ether in hexanes) to afford **3.78** and **3.79**.

2-benzyl-2-fluorocyclopentan-1-one (**3.78**): ^{1}H-NMR (300 MHz; $CDCl_3$): δ 7.35-7.28 (m, 3H), 7.27-7.22 (m, 2H), 3.18 (dd, *J* = 14.1, 14.1 Hz, 1H), 2.92 (dd, *J* = 27.9, 14.1 Hz, 1H), 2.52-2.41 (m, 1H), 2.27-2.14 (m, 1H), 2.10-1.95 (m, 3H), 1.80-1.70 (m, 1H). ^{13}C-NMR (75 MHz; $CDCl_3$): δ 213.0 (d, *J* = 16.5 Hz), 134.8 (d, *J* = 5.0 Hz), 130.4, 128.6, 127.2, 97.6 (d, *J* = 184.3 Hz), 38.8 (d, *J* = 24.6 Hz), 35.8, 33.0 (d, *J* = 21.7 Hz), 17.5 (d, *J* = 3.8 Hz). ^{19}F-NMR (282 MHz; $CDCl_3$): δ -153.4.[175]

2-benzylcyclopent-2-en-1-one (**3.79**): ^{1}H-NMR (300 MHz; $CDCl_3$): δ 7.45-7.15 (m, 7H), 3.51 (d, *J* = 1.6 Hz, 2H), 2.59-2.53 (m, 2H), 2.47-2.44 (m, 2H).[180]

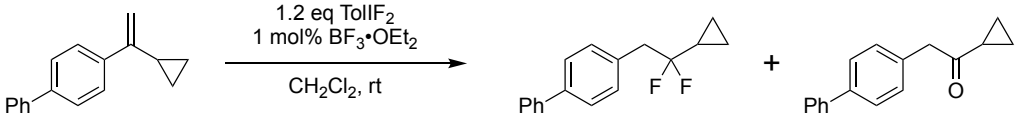
Preparation of 4-(1-cyclopropylvinyl)-1,1'-biphenyl (3.88):



3.106 **3.88**

To a flame-dried round bottom flask with a stir bar under nitrogen was added methyltriphenylphosphonium bromide (1.85 g, 5.18 mmol, 1.2 eq), 10 mL of THF, and *t*-BuOK (582 mg, 5.18 mmol, 1.2 eq) at 0 °C. The mixture was stirred for 45 minutes before warming back to room temperature. Ketone **3.106** (960 mg, 4.32 mmol, 1.0 eq) was added and the reaction was stirred overnight at room temperature. The reaction was diluted with diethyl ether and washed with water (3x), and brine. The solution was dried with $MgSO_4$, filtered, and concentrated under reduced pressure. Flash column chromatography with 100% hexanes afforded **3.88** (750 mg, 3.41 mmol, 79%) as a white solid. R_f = 0.24 (100% hexanes). ^{1}H-NMR (300 MHz; $CDCl_3$): δ 7.72-7.69 (m, 2H), 7.64-7.58 (m, 4H), 7.48-7.43 (m, 2H), 7.38-7.33 (m, 1H), 5.36 (s, 1H), 4.99 (s, 1H), 1.75-1.66 (m, 1H), 0.91-0.85 (m, 2H), 0.66-0.61 (m, 2H).[181]

Procedure for the reaction of $TolIF_2$ with 3.88:



3.88 **3.89** **3.90**

To a 10 mL round bottom flask with a stir bar under nitrogen was added **3.88** (22 mg, 0.10 mmol, 1.0 eq), $TolIF_2$ (29 mg, 0.12 mmol, 1.0 eq), and CH_2Cl_2 (1.0 mL). Once all the material was dissolved, BF_3•OEt_2 (2.5 μL, 0.001 mmol, 1 mol%, 0.4 M in CH_2Cl_2) was added to initiate the reaction and it was stirred at room temperature for 10 minutes. The reaction was filtered through ~1 cm layer of celite in a small Pasteur pipette and rinsed with CH_2Cl_2 (3x, 1 mL). The reaction mixture was concentrated under reduced pressure, $PhCF_3$ (3.0 μL, 0.024 mmol) was added, dissolved in $CDCl_3$ and a quantitative ^{19}F-NMR was obtained.

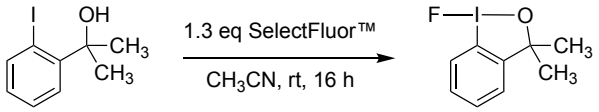
Chapter 4
Ortho-Substituted Fluoro- and Chloro-iodanes

4.1 Introduction

Formally, both the fluoroiodanes and chloroiodanes are pseudo-electrophilic sources of their respective halogens. General methods for their syntheses have been reported in the literature and several derivatives of each have been synthesized.[182-185] The fluoroiodane **4.2** has been used as a source of electrophilic fluorine ("cold" and "hot"), and as an intermediate hypervalent iodine species to be further transformed into perfluoroalkyl hypervalent iodine compounds or diaryliodonium salts.[182, 186-188] The chloroiodane **4.3** has found less use as a chlorinating reagent but is often used as a precursor to other hypervalent iodine species.[187] Broadly, the goal of this project was to synthesize a series of ortho-substituted fluoro- and chloro-iodanes, characterize them by X-ray crystallography and determine their reactivity. Overall, this project aims contribute knowledge to our fundamental understanding of HVI-based fluorinating and chlorinating reagents. In Section 4.1 the overall topic was introduced, the inception of the reagents, their synthesis and demonstrated reactivity, and the research objectives of this project. The synthetic results are described in Section 4.2, while a discussion of the crystal structures and preliminary reactivity observations are provided in Section 4.3. Concluding remarks, as well as future work is found in Section 4.4, and full experimental details are specified in Section 4.5.

4.1.1 Review of the Fluoroiodane

The fluoroiodane **4.2** was first synthesized and crystallized by Professor Claude Legault and coworkers at the University of Sherbrooke.[189] Their synthesis used SelectFluor™ as both the oxidant and the fluorine source to convert iodoalcohol **4.1** directly to fluoroiodane **4.2** (Scheme 4-1). It should be noted that during the isolation of the crude product, $MgSO_4$ cannot be used as a drying agent as the sulfate ion will swap with the fluorine. Crystals suitable for structure determination by single crystal X-ray crystallography were obtained by slow diffusion of pentane into a solution of **4.2** in dichloromethane.



4.1 **4.2**

Scheme 4-1. Legault's synthesis of the fluoroiodane.

The crystal structure of **4.2** (Figure 4-1, A) contains two independent molecules which interact weakly in the crystal lattice through their respective iodine and the bridging oxygen atoms, forming a trapezoidal shape. The five-membered ring comprised of the bridging sidearm and the hypervalent iodine atom resides in an envelope conformation, with the oxygen pointed out of plane compared to the iodine and three carbon atoms (Figure 4-1, B). The torsion angles of F-I-C1-C2 are 8.8°/8.2° on the two asymmetric molecules of the crystal (Figure 4-1, C) (all subsequent torsion angles discussed throughout this chapter are considering the same atoms unless otherwise specified). Further, careful examination of the structure reveals that the O-I-F triad is not perfectly 180° from all angles. From the top-down a straight line is formed between the atoms; however upon viewing side-on it becomes apparent that the fluorine is pointed downwards towards the aryl ring. Measuring the angle of O-I-F bonds reveals an angle of 166.4° (Figure 4-1, D). The correlation of these structural observations to reactivity, stability, or physical properties of the fluoroiodane has not been hypothesized or disclosed in the literature.

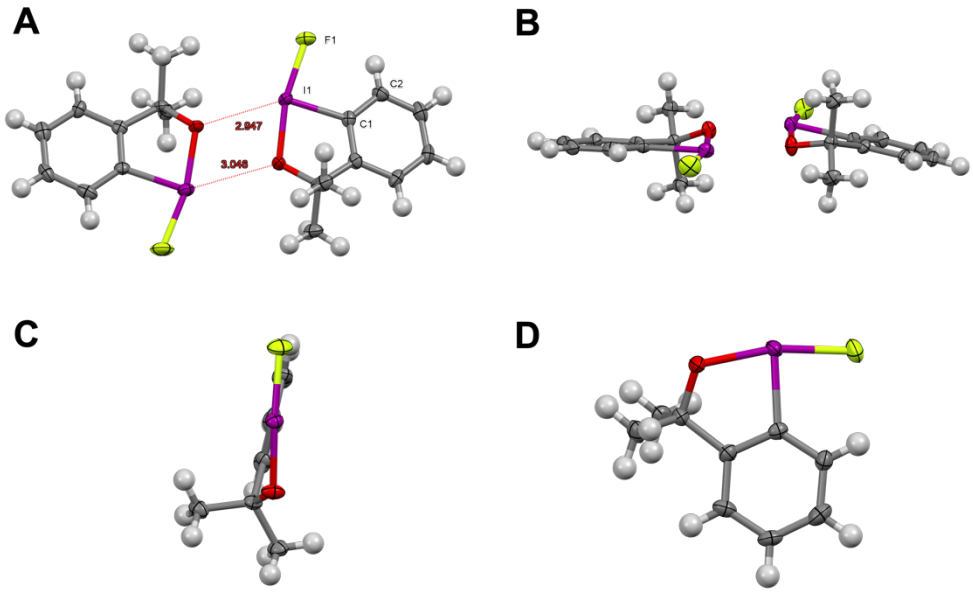
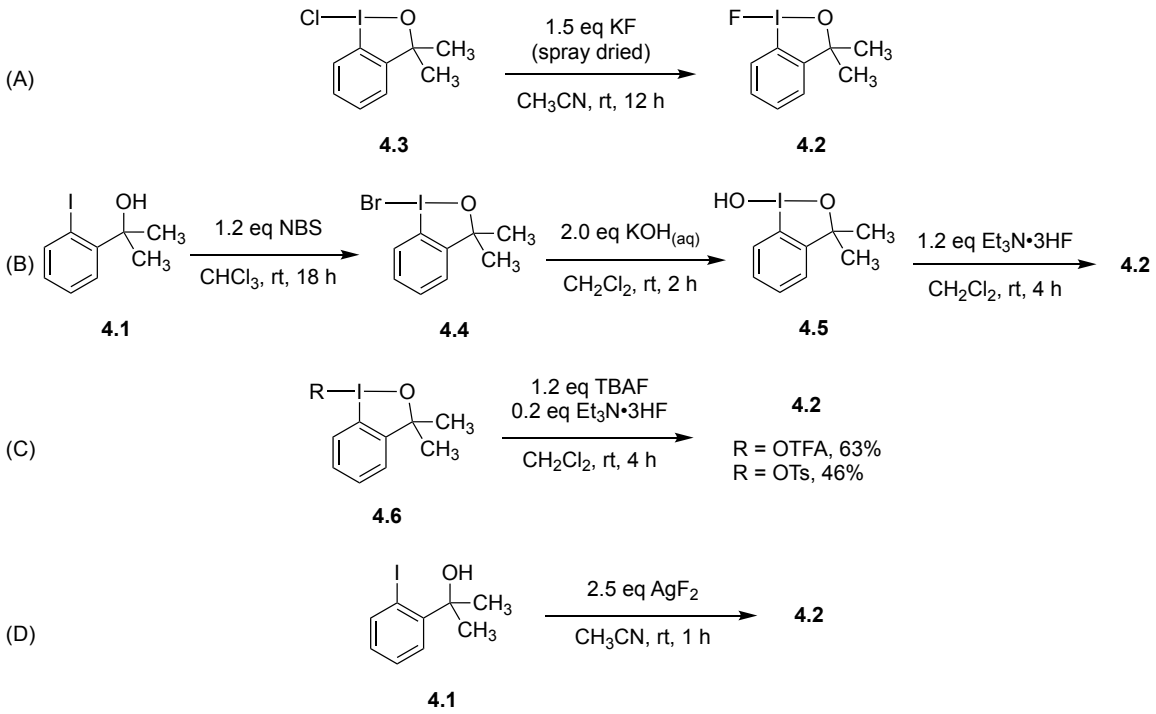


Figure 4-1. ORTEP representation with a displacement ellipsoid probability of 50%. Crystal structure of the fluoroiodane obtained by Legault and coworkers. A) Illustration of the I•••O interaction of the two independent molecules. B) Envelope of five-membered ring. C) Top-down view of one molecule illustrating the small torsion angle. D) Side on view of one molecule. Note: the second molecule was omitted from C) and D) for clarity.

4.1.1.1 Synthesis of the Fluoroiodane

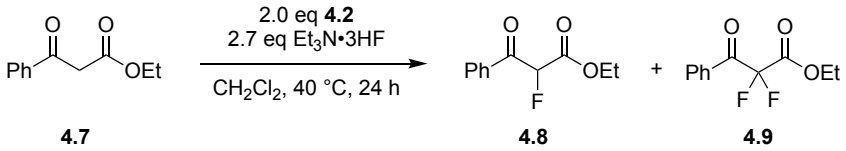
Several synthetic routes to the fluoroiodane **4.2** have been reported. The first is the oxidation of the iodoalcohol **4.1** to **4.2** with SelectFluor™ as shown above (Scheme 4-1). Togni et al. reported the conversion of chloroiodane **4.3** (synthesis discussed in Section 4.1.2) to fluoroiodane **4.2** with spray-dried potassium fluoride under inert conditions in 94% yield (Scheme 4-2, A).[190] The use of spray-dried potassium fluoride is critical to the success of the reaction. Any hydration of the fluoride likely stabilizes the anion and renders it non-nucleophilic in the reaction. In the same year, Stuart et al. disclosed a convenient three-step procedure from the iodoalcohol **4.1** which did not necessitate inert or anhydrous reaction conditions (Scheme 4-2, B).[182] They first oxidized **4.1** with *N*-bromosuccinimide (NBS) to obtain the bromoiodane **4.4** (79% yield), hydrolysis of **4.4** with aqueous potassium hydroxide gave **4.5** (76% yield), which upon treatment with triethylamine trihydrofluoride gave the fluoroiodane **4.2** in 94% yield. This sequence was easily carried out on a gram scale without any chromatographic purification, allowing for convenient access to large quantities of the fluoroiodane to be used in further reactivity studies. In the same publication, they disclosed a method using tetra-butylammonium fluoride (TBAF) and triethylamine trihydrofluoride to displace an appropriate leaving group (**4.6**, R = OTFA or OTs). This procedure was developed as it is theoretically amendable to radiofluorination which utilizes fluoride ions in conjunction with a non-coordinating counterion to improve nucleophilicity (Scheme 4-2, C).[191] Murphy et al. outlined a similar strategy for the preparation of radiolabeled fluoroiodane **4.2**, where polystyrene-bound or perfluorous-tagged sulfonyloxy iodanes were used as precursors to enable quick purification of the radiolabelled fluoroiodane.[192] Finally, Zhang et al. employed silver(II) difluoride to oxidize and fluorinate a series of iodoalcohols to the corresponding fluoroiodanes (e.g., Scheme 4-2, D).[183] While the other synthetic methods listed (Scheme 4-2, A-C) use a ligand exchange strategy to install the fluorine, Zhang et al. used a reaction pathway consisting of two single-electron oxidations with AgF_2. The original unsubstituted iodoalcohol **4.1** can be converted to the fluoroiodane in 94% yield on a 1.4 g scale using silver(II) difluoride. In summary, there are multiple synthetic methods to access the fluoroiodanes, some more practical than others for the preparation of the fluoroiodane on a gram-scale.



Scheme 4-2. Synthetic methods of the fluoroiodane **4.2**.

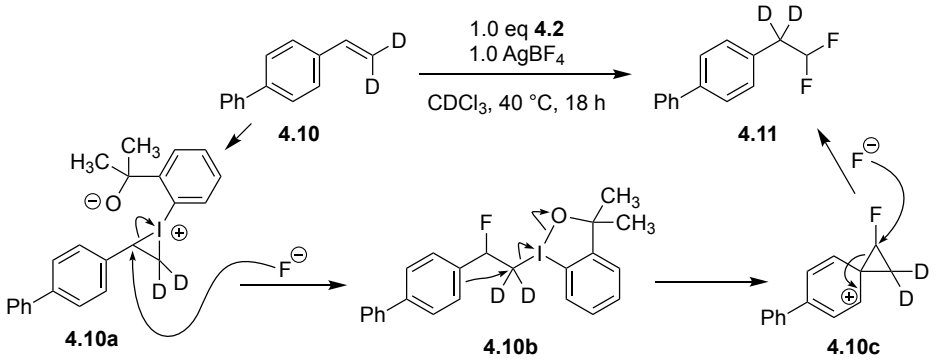
4.1.1.2 Reactivity of the Fluoroiodane

The reactivity of fluoroiodane **4.2** was first explored in the fluorination of 1,3-dicarbonyls where both mono and difluorination were achieved (Scheme 4-3).[182] The ease of fluorination was related directly to the keto-enol tautomeric equilibrium of the substrate. The amount of enol tautomer at equilibrium correlated directly with an increase in difluoride **4.9** produced. The monofluoride product **4.8** could be obtained in 63% yield at 40 °C with 2.0 equivalent of the fluoroiodane **4.2** and 2.7 equivalents of Et_3N•3HF. Reducing the reaction concentration or the equivalents of Et_3N•3HF reduced the yield. Increasing the temperature to 80 °C increased the fraction of the difluorinated product. Stuart et al. monofluorinated four 1,3-dicarbonyls with yields spanning 55-67% and difluorinated two 1,3-dicarbonyls at 60 °C in 45-71% yield (analogous to **4.8** and **4.9**). Although not synthetically more attractive than the state-of-the-art, this reaction provides insight into the reactivity and proof of concept for further reagent development as an electrophilic source of fluorine.[193]



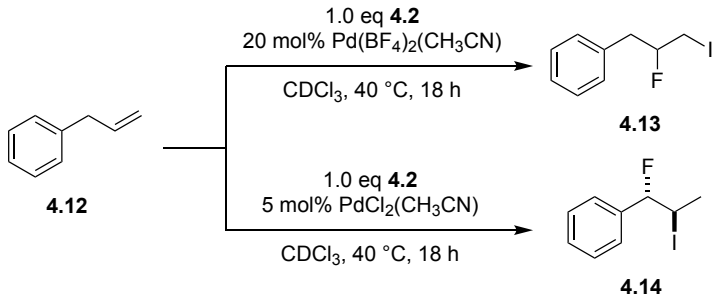
Scheme 4-3. Mono- and difluorination of 1,3-dicarbonyls.

In a similar fashion to *p*-(difluoroiodo)toluene, the fluoroiodane **4.2** can react with olefins to achieve either vicinal or geminal 1,2-difunctionalization. The simplest example of this chemistry is the *gem*-difluorination of styrene. Treatment of styrene **4.10** with an equivalent of **4.2** and $AgBF_4$ in $CDCl_3$ at 40 °C afforded *gem*-difluoride **4.11** in 74% yield (Scheme 4-4).[194] The silver tetrafluoroborate salt effectively provided an equivalent of fluoride to furnish the *gem*-difluoro product while other tetrafluoroborate salts proved less effective. The $AgBF_4$ salt was likely the most effective as the silver(I) acts as a Lewis acid to activate **4.2**. A series of twelve styrenes was explored and the desired products were isolated in 52-88% yield. The exact phenonium shift seen when $TolIF_2$ reacts with styrenes (Scheme 3-14) is observed in the reaction of fluoroiodane **4.2** with styrenes. Experimentally this was tracked *via* deuteration of the terminal position of the alkene. Upon treatment of **4.10** with **4.2** the phenyl ring migrated to the deuterated carbon *via* a 1,2-phenyl shift. This result was mechanistically explained in four steps. First, coordination of the alkene to the hypervalent iodine center gives the iodonium **4.10a**. Fluoride addition at the position with more partial positive charge yielded an intermediate **4.10b**. This was followed by aromatic displacement of the iodonium driven by the energetically favourable reduction of I(III) to I(I) and produced the highly reactive spirocyclic intermediate **4.10c**. This phenonium ion was quickly trapped with another fluoride ion, again at the carbon center with a more partial positive charge, to yield the final *gem*-difluoride **4.11**. Further reaction scope investigations with 1,1-diarylalkenes revealed that the more electronically rich aromatic ring migrates in this *gem*-difluorination reaction. This was consistent with expectation, as in the third step of the mechanism the aromatic ring must act as a nucleophile. With 1-alkyl-1-arylalkenes, the aromatic group migrated preferentially compared to the alkyl group.[176] This reactivity pattern is observed consistently between styrenes and **4.2**.



Scheme 4-4. *gem*-difluorination of styrenes with **4.2**.

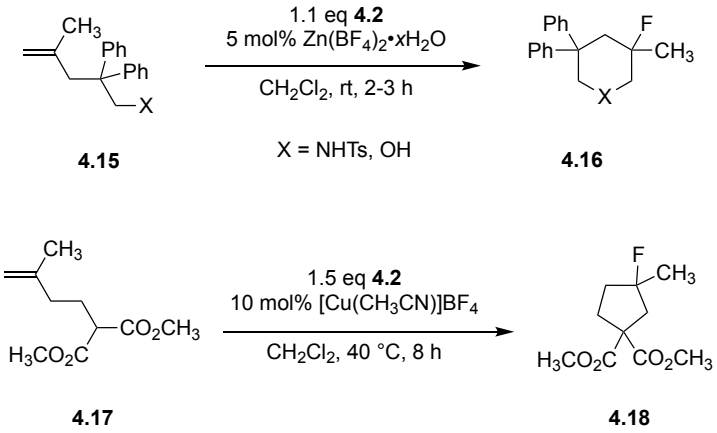
Interestingly, Szabo et al. observed divergent reactivity when they employed $PdCl_2(CH_3CN)_2$ or $Pd(BF_4)_2(CH_3CN)_2$ as the fluoroiodane activator. The palladium tetrafluoroborate salt gave the expected products; however, the chloride salt gave vicinal iodofluoro-functionalization of the alkene in 43% yield (not shown).[194] This finding was further optimized to efficiently iodofluorinated allyl benzene derivatives (Scheme 4-5).[195] Allylbenzene (**4.12**) can be converted to **4.13** with the palladium tetrafluoroborate salt in 76% yield. This methodology was demonstrated on an additional seventeen examples and produced the analogous products in 40-86% yield. Alternatively, treating allylbenzene (**4.12**) with the palladium chloride salt first facilitates an isomerization to the conjugate alkene and subsequent iodofluorination leads to **4.14** in 71%.



Scheme 4-5. Vicinal iodofluorination with **4.2**.

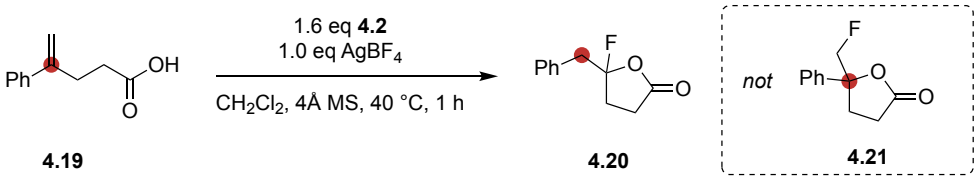
The fluoroiodane was also used to facilitate fluorocyclizations. Szabo et al. demonstrated that alkenyl substrates with pendant nucleophiles could cyclize to provide hetero- and carbocycles (Scheme 4-6).[196] Instead of a second fluoride capturing an intermediate to produce difluorinated products (as seen in Scheme 4-2), an internal nucleophile, strategically included in the substrate, could capture the

intermediate to provide fluorinated hetero- and carbocyclic products such as **4.16** (X = NHTs, 73%, X = OH, 62%) and **4.18** (55% yield).[196] Across seventeen examples, aminofluorination and oxyfluorination products were obtained in yields of 60-84%. A small series of carbofluorination substrates yielded products analogous to **4.18** in 55-76% yield.



Scheme 4-6. Fluorocyclization with fluoroiodane **4.2**.

Both Stuart et al. and Gulder et al. published fluorocyclizations which incorporated an aryl migration (conceptually the same as the geminal difluorination of styrene, Scheme 4-2).[197, 198] Stuart et al. developed conditions to cyclize 5-arylpentenoic acids into fluorinated lactones **4.20** (Scheme 4-7). Notably, this product **4.20** is different from the corresponding reaction product **4.21** obtained with classical aza-fluorination reagents. Cyclization of **4.19** in 81% yield was achieved with 1.6 equivalents of the fluoroiodane **4.2** in the presence of both molecular sieves and silver tetrafluoroborate. They demonstrated this transformation on twelve examples and obtained the fluorocyclized products in 38-81% isolated yields. Keeping in line with the possibility of using the fluoroiodane as a [^{18}F]fluorination reagent, they developed completely metal-free conditions with the fluoroiodane being the only possible source of fluorine. Treatment of **4.19** in acetonitrile with fluoroiodane **4.2** and molecular sieves as the activator achieved the same transformation, albeit in 54% yield. In a subsequent publication, they disclosed activation of the fluoroiodane by hexafluoroisopropanol (HFIP) avoiding the use of any Lewis acids. Repeating the cyclization shown in Scheme 4-7 with HFIP as the solvent and activator (i.e., no $AgBF_4$, CH_2Cl_2 replaced with HFIP) gave the fluorocyclized product in a comparable yield of 84%.[199]

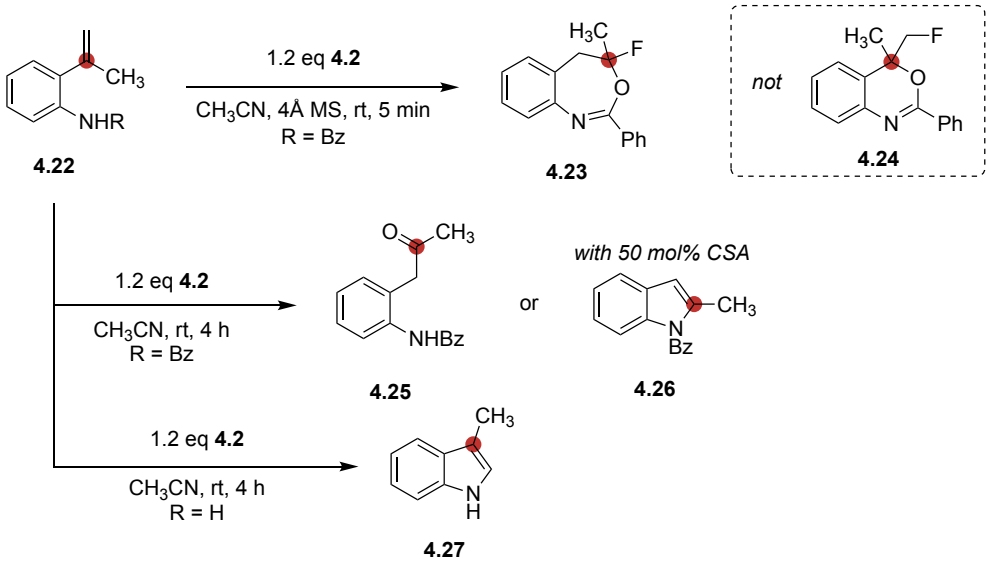


Scheme 4-7. Fluorocyclization of 5-arylpentenoic acids.

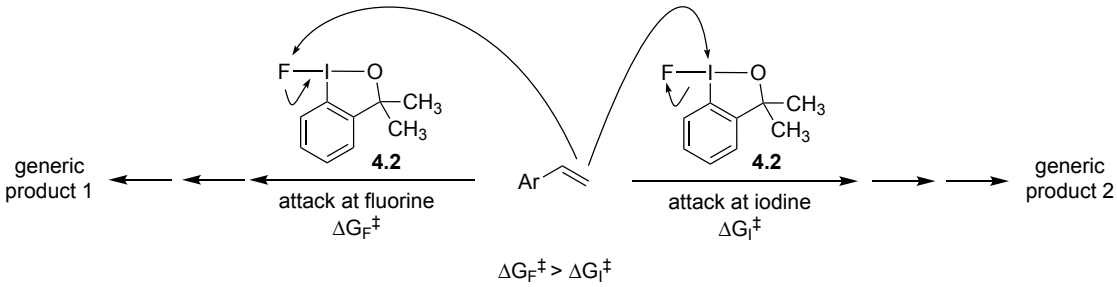
Gulder et al. produced fluorobenzoxazepines by a similar mechanism. Reacting the fluoroiodane **4.2** in the presence of molecular sieves smoothly converted styrene **4.22** to the seven-membered fluorobenzoxazepine **4.23** in 77% yield (Scheme 4-8). The product **4.23**, resulting from a 1,2-phenyl shift, was isolated exclusively without any of the theoretical six-membered product **4.24**. This transformation can also be carried out "hot" with [^{18}F]radiofluoroiodane to give uniquely radiofluorinated benzoxazepines.[186] Further, this transformation was broadly applicable, in good yield (66-85%), to a variety of aryl and vinyl substituents. Carefully tracking the carbon atoms reveals the 1,2-phenyl shift to be crucial in providing the seven-membered ring products. In-depth side product analysis unveiled the tunability of the reaction conditions to control the ultimate product outcome.[200] Performing the reaction without molecular sieves yielded a benzyl ketone **4.25** (12 examples, 71% to quantitative yield), where adventitious water is believed to trap an intermediate to produce the oxygenated product, outcompeting the typical intramolecular cyclization reaction pathway leading to **4.23** (Scheme 4-8). The addition of 50 mol% camphorsulfonic acid (CSA) to these conditions converted the styrene **4.22** to the C2-substituted indole **4.26** in one pot via the intermediate ketone (27 examples, 61-96% yield). Changing the substituent on the nitrogen also controlled the reaction outcome. For example, when **4.22** (R = H) was treated with the same reaction conditions it gave indole **4.26** in quantitative yields (Scheme 4-8). Additional examples with variation on the nitrogen, aromatic ring, or alkene gave the desired products in yields between 55% and 89%.

The selectivity of the transformations developed by Stuart et al. and Gulder et al. are unique as they afford products which are distinct when compared to the products obtained using traditional electrophilic *N*-fluoro reagents. The treatment of **4.19** with *N*-fluoropyridinium triflate under basic conditions produced exclusively lactone **4.21** in 74% yield with an exocyclic fluorine.[201] Similarly, styrene **4.22**, when cyclized with SelectFluor^{TM}, gave the six-membered **4.24** instead of **4.23**.[198, 202] This selectivity was further supported by a computational study that showed attack by the olefin **4.22** at the

fluorine vs. the iodine resulted in a transition state which was roughly 20 kcal/mol higher in energy.[203] A generic illustration of this concept is shown in Scheme 4-9. Following the reaction arrow to the left, the alkene attacks the fluorine directly, leading to a higher transition state energy when compared to attack at the iodine (arrow to the right). The electrophilicity of the iodine in the fluoroiodane reagent allows for these distinct reactivity pathways to be accessed. When the fluoroiodane reacts with a nucleophile it reacts with the iodine first, not the fluorine. Therefore, the iodonium intermediate formed can react by several different pathways not accessible by electrophilic *N*-fluoro reagents.



Scheme 4-8. Various transformations of styrene **4.22** with fluoroiodane **4.2**.



Scheme 4-9. Generic illustration of fluorine vs. iodine attack in a reaction between an alkene and **4.2**.

It is apparent from these examples that fluoroiodane **4.2** must be activated in the reaction mixture to deliver the desired products. This is accomplished with protic (Scheme 4-3) or Lewis acids (Scheme

4-6). How exactly that activation occurs was the subject of multiple computational investigations. They sought to determine whether activation occurred by coordination of the Lewis acid to the fluorine atom or the endocyclic oxygen.[204, 205] The studies focused on the electrophilic addition of three distinct alkene-containing substrates to the activated fluoroiodane. First, comparing F vs O coordination in the ground state they determined that silver tetrafluoroborate preferentially coordinates the oxygen, while zinc tetrafluoroborate preferentially coordinates the fluorine. They rationalized that this was likely due to zinc's higher affinity to fluorine compared to silver. However, in all cases, the energy barrier for the addition of the alkene to the "oxygen-activated complex" was significantly higher than addition to the "fluorine-activated complex". In the case of styrene, the addition to the "oxygen activated" fluoroiodane had a barrier of 30.2 kcal/mol (-3.9 to 26.3 kcal/mol), while the addition to the "fluorine activated" fluoroiodane was only 20.0 kcal/mol (-3.0 to 17.0 kcal/mol), a difference of 9.3 kcal/mol at the transition state. Ultimately, they concluded that coordination to the fluorine, and not oxygen, may be the general mode of Lewis acid activation for the fluoroiodane. This result differed from the related Togni reagent where activation is achieved by coordination of the Lewis acid to the oxygen.[206] In further computation studies, Himo et al. deduced that after activation at the fluorine by a zinc Lewis acid, the complex rearranged to have the F-I bond parallel to the phenyl-iodine bond (Figure 4-2).[207] This higher energy complex reacts with the alkene in a metathesis-like fashion, proceeding through a four-membered transition state where the alkene pi bond and F-I bond are breaking, while the C-F and C-I bonds are forming. They found that any reaction pathway which included the formation of a three-membered iodonium species had higher energy intermediates (e.g., **4.10a**).

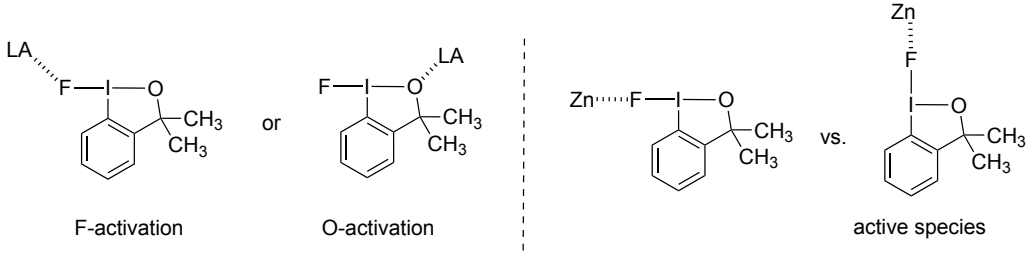
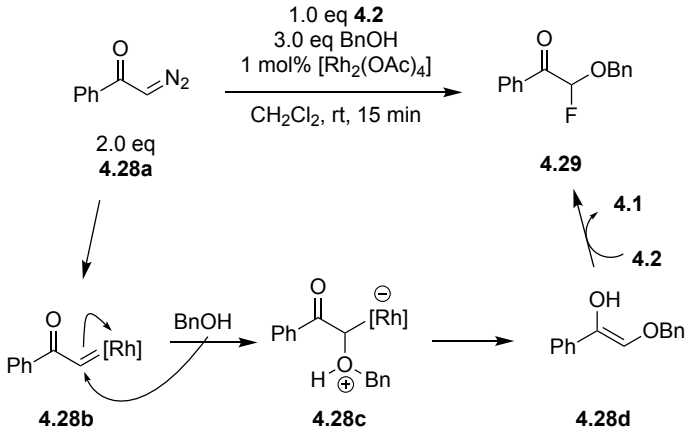


Figure 4-2. Modes of theoretical fluoroiodane activation.

The success of the transformations discussed above led to a multitude of similar fluoroiodane-mediated fluorocyclizations with olefins. This reactivity was used to produce fluorinated and radiofluorinated oxazolidine-2-ones;[208] azabenzoxazepines and azaindole;[209] tetrahydroxpyridazines

and dihydrooxazines;[210] oxazepanes;[211] and cyclic *N*-methoxyimidates.[212] The fluoroiodane **4.2** has also mediated cyclizations without the inclusion of fluorine in the final products, such as oxazoles,[213] imidazoles,[213] isoxazoles,[214] and 6H-1,2-oxazines.[214] Interestingly, the synthesis of the imidazoles by this method was the first reported instance of intermolecular trapping in this type of reaction with nitriles to afford Ritter adducts which ultimately cyclized to the desired imidazoles.[213]

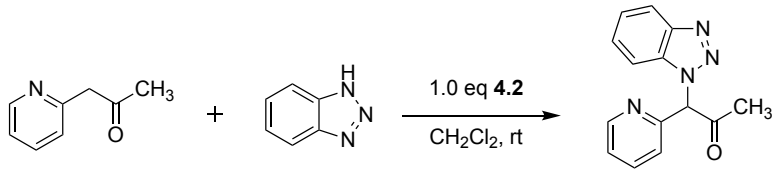
The reactivity of the fluoroiodane **4.2** is not limited to olefinic systems. Rhodium carbenes derived from diazocarbonyl compounds can be oxyfluorinated with the fluoroiodane **4.2** and an appropriate alcohol (e.g., Scheme 4-10).[215] When the diazo compound **4.28a** was treated with catalytic rhodium, benzyl alcohol, and the fluoroiodane, it gave the desired product **4.29** in 62% yield (11 examples, 35-62% yield). Computational analysis of the reaction mechanism revealed that the reaction proceeds through initial rhodium carbene formation (**4.28b**) followed by the addition of the alcohol to furnish an oxonium ylide (**4.28c**). Proton transfer from the oxonium ylide to the carbonyl and dissociation of the rhodium catalyst forms an enol (**4.28d**). This enol species reacts with the electrophilic fluoroiodane **4.2** to produce the oxyfluoride **4.29**.[216]



Scheme 4-10. Oxyfluorination of diazocarbonyls.

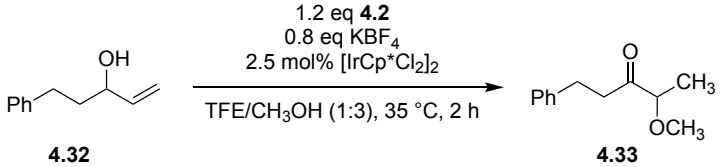
Gulder et al. discovered the importance of non-covalent interactions while exploring the reactivity of the fluoroiodane **4.2**. To highlight the non-covalent interactions they tried to alpha-functionalize various ketones with BTA (Scheme 4-11).[217] This reactivity was only observed with 2-pyridyl systems, such as **4.30**. They proposed the reaction began by coordination of the fluoroiodane to the pyridine nitrogen *via* non-covalent I-N interactions. This was followed by the addition of the hypervalent iodine

to the alpha-position of the ketone and finally displacement of the I(III) species by BTA to give the functionalized product **4.31** in 66% yield (16 examples, 28-81% yield). NMR studies were used to quantify the proposed non-covalent interactions observed. An electrophilic "BTA-hypervalent iodine" species was considered; however, it was discounted by ^{1}H-NMR studies which showed no generation of a new species when BTA and **4.2** were mixed in the absence of **4.30**. Control studies solidified the need for the nitrogen atom at the 2-position as the benzyl-, 3-pyridyl, and 4-pyridyl ketones were unreactive under identical reaction conditions.



Scheme 4-11. Pyridine-directed alpha-functionalization of ketones.

Matute et al. exploited the umpolung reactivity of the fluoroiodane **4.2** in combination with their expertise in iridium catalysis to convert allylic alcohols to alpha-functionalized ketones (Scheme 4-12).[218] The reaction proceeded through the iridium-catalyzed isomerization of the allylic alcohol to an iridium enol, which upon reaction with the fluoroiodane produced an electrophilic alpha-carbon. Displacement of the hypervalent iodine was achieved with several simple alcohols (CH_3OH, 78% yield; EtOH, 32% yield; *i*-PrOH, 18% yield). In the example shown below the catalytically generated iridium enolate from allylic alcohol **4.32** was functionalized with methanol to give **4.33** in 78% yield (Scheme 4-12). Functionalization with methanol was generalized with 24 substrates in yields ranging from 45% to 90%.



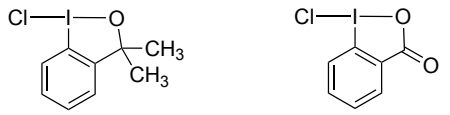
Scheme 4-12. alpha-Functionalization of allylic alcohols.

Beyond using the fluoroiodane as an electrophilic source of fluorine, it has also been used as a precursor to other electrophilic perfluoroalkyl reagents. Most notably, Togni et al. accessed the Togni reagent through the in situ formation of the fluoroiodane and then subsequent conversion into the desired reagent with $TMSCF_3$.[190] This was extended to the preparation of hypervalent iodine reagents with longer perfluoroalkyl chains. The utility of these reagents was demonstrated with the tetrafluoroalkyl variant, which was used to perfluoroalkyl label cysteine residues of proteins.[219]

This summary is certainly not comprehensive in its discussion of the reactions which have been published with fluoroiodane **4.2**, but it provides an overview of its reactivity demonstrated to date. Briefly, one should be aware that the fluoroiodane holds potential for use as an electrophilic no-carrier added [^{18}F]fluorinating agent. Second, the fluoroiodane is a convenient precursor to other electrophilic perfluoroalkyl hypervalent iodine reagents – again, largely difficult to access without this chemistry. Lastly, and importantly, the reagent can be used for reactivity entirely divergent compared to the classical *N*-fluoro reagents. Given the utility of the fluoroiodane reagent **4.2** in its first 10 years of life, the synthesis of new analogues and exploration of their reactivity is warranted.

4.1.2 Review of the Chloroiodane

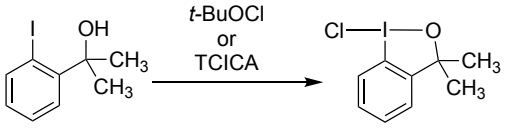
Analogous to the fluoroiodane **4.2**, the chloroiodanes are a source of pseudo-electrophilic chlorine. However, compared to fluorine there are more easily accessible sources of electrophilic chlorine with similar reactivity (e.g., *N*-chlorosuccinimide). The two general monochloro-hypervalent iodanes which exist are the acid (benzoiodoxolone **4.34**) and the alcohol (benzoiodoxole **4.3**) analogues (Figure 4-3). The acid analogue is significantly more reactive and has been used as an electrophilic source of chlorine. The alcohol variant on the other hand has been primarily used as a precursor to access further functionalized hypervalent iodine reagents. For example, treatment with spray-dried KF converts chloroiodane **4.3** to fluoroiodane **4.2** (Scheme 4-2 A). Further, when generated in situ the fluoroiodane is converted to Togni's reagent with $TMSCF_3$,[190] or to other hypervalent reagents with electrophilic perfluoroalkyl chains.[187] The chloroiodanes are used as precursors as they are generally easily accessible from the corresponding iodine(I) compound (e.g., Scheme 4-13).



4.3 **4.34**

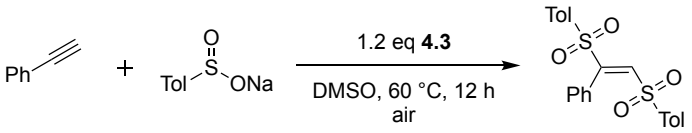
Figure 4-3. The chlorobenzoiodoxole **4.3** and the chlorobenzoiodoxolone **4.34**.

The chlorobenzoiodoxole **4.3** can be directly prepared from the corresponding iodoalcohol **4.1** by treatment with either TCICA or *tert*-butyl hypochlorite (Scheme 4-13).[190, 220] Due to its stability, it is not often used in chlorination reactions, and the more reactive **4.34**, or a derivative, is used. Nonetheless, **4.3** is a competent oxidant and has been used in a handful of reactions which do not result in the transfer of the chlorine atom. For example, alkynes were 1,2-difunctionalized with sulfonates in the presence of **4.3** by way of a radical mechanism (Scheme 4-14; 48 examples, 42-90% yield).[221] In this reaction the typically more reactive **4.34** was ineffective and the alkyne was fully recovered. The proposed reaction mechanism consisted of an exchange of the $TolSO_2Na$ with the Cl in **4.3** to afford a new hypervalent iodine species. Radical decomposition of this proposed hypervalent intermediate produced $TolSO_2$ radicals which were trapped at both carbons of the alkyne to furnish the final product **4.37**.



4.1 **4.3**

Scheme 4-13. Synthesis of chloroiodane with *t*-BuOCl or TCICA.

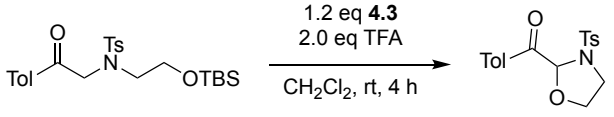


4.35 **4.36** **4.37**

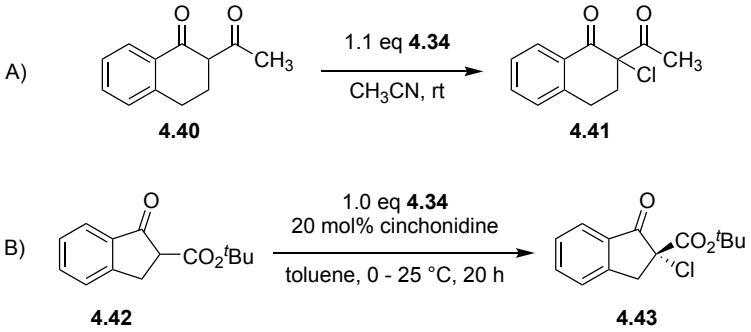
Scheme 4-14. Alkyne difunctionalization with **4.3**.

The chloroiodane **4.3** also worked particularly well in the umpolung activation of ketone **4.38** for an intramolecular cyclization with a pendant alcohol to furnish oxazolidine **4.39** (Scheme 4-15).[222] This transformation was demonstrated on twenty different substrates with variations of the aromatic ring as

well as the ethylene unit to obtain the desired products in yields between 67% and 99%. Generally, chloroiodane **4.34** has been employed as a chlorinating agent for carbonyls (e.g., **4.40**), aromatic rings (e.g., **4.44**), and alkenes (e.g., **4.47**). In the example below the 1,3-dicarbonyl **4.40** could be directly chlorinated with **4.34** by attack of the corresponding enol on the hypervalent iodine and subsequent displacement by a free chloride ion to deliver the racemic product **4.41** in 85% yield (Scheme 4-16, A; 17 examples, 75-97% yield).[223] Waser et al. demonstrated that the addition of a cinchonidine catalyst could interrupt the process and render it enantioselective with portionwise addition of **4.34** (Scheme 4-16, B).[224] They successfully chlorinated **4.42** in 74% yield and 80% *ee* with this method. Depending on the substrate, enantioselectivities up to 88% *ee* were achieved. In their mechanistic proposal, the cinchonidine catalyst was first chlorinated to give an Cl-N electrophilic chloride compound which acted as the active chlorinating reagent.



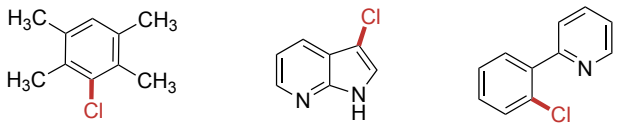
Scheme 4-15. Cyclization of **4.38** with chloroiodane **4.3**.



Scheme 4-16. alpha-Chlorination of 1,3-dicarbonyls.

The chloroiodane was also shown to be a competent aromatic chlorinating reagent. In a very early study of the chloroiodane **4.34**, it chlorinated durene in the presence of acetic acid and trace HCl via the liberation of $Cl_{2(g)}$.[225] It is also a competent chlorinating reagent in neutral conditions. For example, various heterocycles (e.g., **4.45**, 77% and **4.46**, 81%) could be selectively chlorinated in good yield at

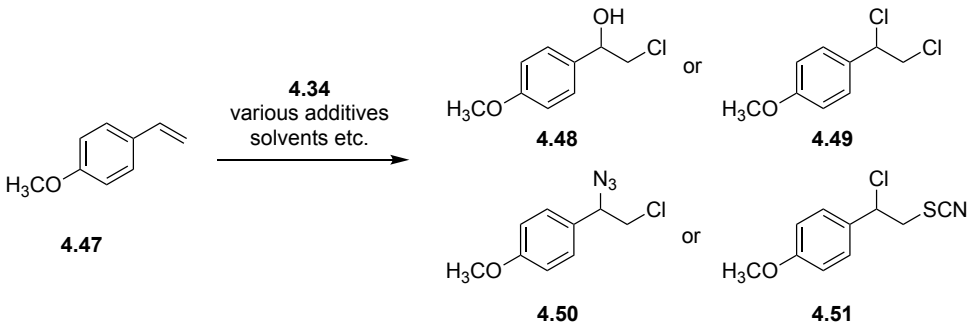
room temperature in DMF.[226] It can also serve as a source of chlorine in a copper catalyzed aromatic chlorination.[227]



4.44 | **4.45** *28 examples 50-99% yield* | **4.46** *16 examples 28-81% yield*

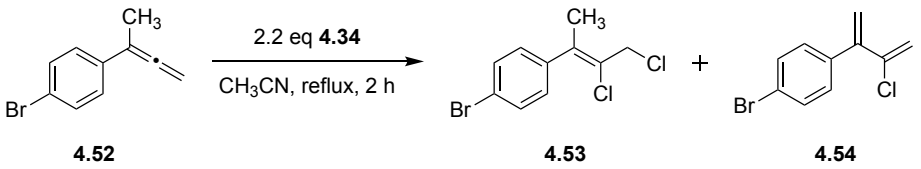
Figure 4-4. Examples of the chlorination products which can be obtained using the chloroiodane **4.34**.

Like many other hypervalent iodine reagents, the chloroiodane **4.34** reacts with alkenes and has even been demonstrated to chlorinate allenes.[228, 229] By varying the reaction conditions a variety of alkenes can be 1,2-difunctionalized (Scheme 4-17).[228] For example, treatment of styrene **4.47** with chloroiodane **4.34** in a solvent mixture of acetone and water at 40 °C gives the chlorohydrin product **4.48** in 76% yield. If instead the equivalents of the chloroiodane are doubled and a 4-phenylpyridine *N*-oxide is included, the dichloride **4.49** is obtained in an 80% yield. To achieve azidochlorination, $TMSN_3$ was included as the source of azide and CsF was used as an activating agent to convert **4.47** to **4.50** in quantitative yield. Finally, reacting the chloroiodane **4.34** with TMSNCS gives **4.51** in 88% yield. It should be noted that the chlorine atom is added at the benzylic position, as opposed to the terminal position as seen with the other transformations (Scheme 4-17, **4.51** vs. **4.48** or **4.50**). The 1,2-phenyl shift observed when treating styrenes with fluoroiodane **4.2** is never observed with chloroiodane **4.3** or **4.34**.



Scheme 4-17. 1,2-difunctionalization of alkenes with chloroiodane **4.34**.

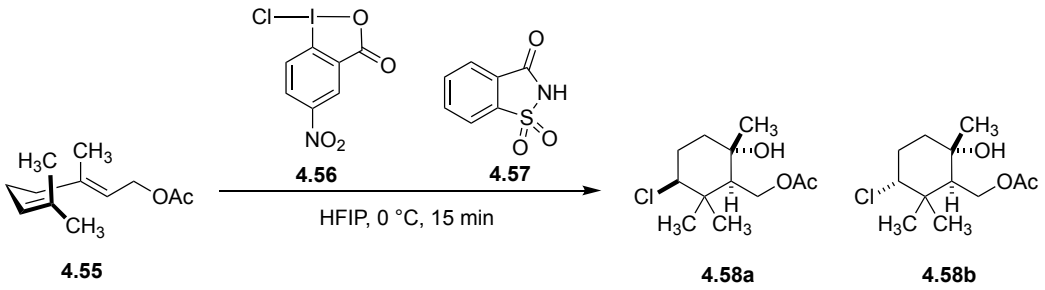
Under conditions of refluxing acetonitrile, allenes were found to react with the chloroiodane **4.34** (Scheme 4-18).[229] Mechanistically, it was proposed that the elevated temperature homolyzed the chloroiodane to release a Cl radical. This radical subsequently reacted with the central carbon of the allene and placed a carbon-centered radical at the benzylic position. In the absence of any alpha-hydrogens, terminal 1,2-dichlorination products were observed exclusively (e.g., **4.53**) from the addition of a second chlorine radical to the terminal position. When an alpha-hydrogen was available an elimination reaction would at times compete with the second chlorination event and give either the 1,2-dichlorinated products, a mixture (e.g., **4.53** and **4.54**), or solely the elimination product (e.g., **4.54**). For example, when **4.52** was treated with **4.34**, the 1,2-dichlorinated product **4.53** was observed in 23% yield, along with the monochlorinated elimination product **4.54** in 31% yield. A range of substrates diversified on the aromatic ring or at the alpha-position of the allene gave the corresponding products in total yields ranging from 20-94%.



4.52 **4.53** **4.54**

Scheme 4-18. Chlorination of allenes with the chloroiodane **4.34**.

A more reactive nitrated derivative of the carbonyl chloroiodane (**4.56**) was recently used to induce a chlorocyclization of terpenes in HFIP.[230] Achieving a chlorocyclization, as opposed to an iodo- or bromocyclization, with good diastereoselectivity was a long-standing challenge in this type of halocyclization. Treatment of geranyl acetate in HFIP at 0 °C with chloroiodane **4.56** and 20 mol% of **4.57** as an additive gave the desired product as a mixture of separable diastereomers (83:17, **4.58a:4.58b**) in 30% overall yield (Scheme 4-19). This methodology was used to cyclize seventeen different polyenes in 26-78% yield.



Scheme 4-19. Diastereoselective chlorocyclization of geranyl acetate with **4.56**.

Both chloroiodanes **4.3**/**4.34** have been used to access other hypervalent iodine reagents which are not accessible by direct oxidation of the precursor. The ease of oxidation to the chloroiodane and their stability make them convenient and reliable precursors to more complex hypervalent iodine reagents. As previously mentioned, the chloride can be exchanged for a trifluoromethyl group to give the commonly known Togni reagent **4.59** (R = CF_3).[184] Although not exhaustive, Figure 4-5 provides an overview of the reagents accessible from the respective chloroiodanes. Perfluoroalkyl hypervalent iodine reagents, such as the pentafluoroethyl **4.60**,[231] (phenylsulfonyl)difluoromethyl **4.61**,[232] or tetrafluoroimidazole hypervalent iodine reagents **4.63**,[233] can be comparably accessed *via* exchange with the chloride. Preparation of the reagents containing an electrophilic phthalimide,[234] indole,[235] or nitrile,[236] is also possible by this exchange mechanism giving **4.62**, **4.64**, and **4.65**, respectively.

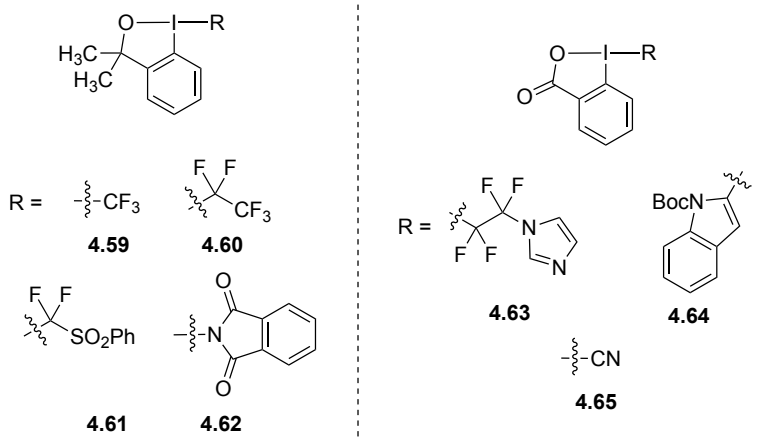


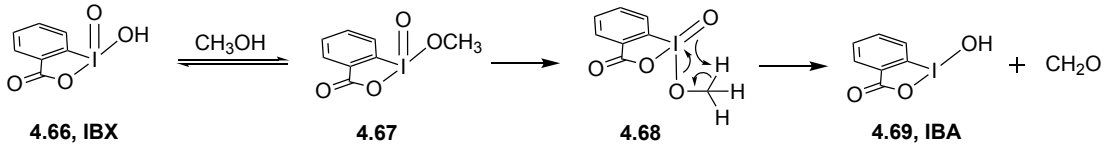
Figure 4-5. Examples of hypervalent iodine reagents accessible through the chloroiodanes.

Overall, chloroiodanes are useful sources of electrophilic chlorine as demonstrated through alpha-functionalization of ketones, selective aromatic chlorination, various alkene functionalizations, or even

in biomimetic cyclizations of terpenes. The synthesis and evaluation of new structural derivatives may prove useful in tuning their reactivity to find the exact profile needed to complete or achieve currently inaccessible transformations in this active field of study. Further, their use as precursors to other hypervalent iodine reagents (e.g., Figure 4-5) could hold tremendous potential, especially if new reactivity is observed.

4.1.3 Review of ortho-Substitution with Monocyclic and Pseudo-monocyclic Hypervalent Iodanes

Hypervalent iodine reagents with substitution ortho to the iodine atom on the aromatic ring have, at times, shown markedly different reactivity compared to the unsubstituted reagent. In this Section the origins of the idea will be reviewed, beginning with a discussion of 2-iodoxybenzoic acid (IBX). The mechanism of alcohol oxidation by IBX was proposed to begin with a rapid equilibration between IBX and the alcohol to form **4.67** (Scheme 4-20). This proposal was supported by kinetic data obtained using ^{1}H-NMR spectroscopy.[237] The IBX-alcohol complex is then thought to undergo rotation about the iodine to situate the alcohol in the equatorial position (**4.68**). Elimination by disproportionation results in the oxidized alcohol and 2-iodosobenzoic acid (**4.69**, IBA). Oxidation does not occur directly from **4.67** as it would result in an IBA with the hydroxy and acid functional groups at an angle of 90°, a highly unfavourable species.



4.66, IBX **4.67** **4.68** **4.69, IBA**

Scheme 4-20. IBX oxidation of methanol.

To further the understanding of this proposed mechanism, in 2005 Su and Goddard computationally studied the oxidation of simple alcohols to carbonyls with IBX. From their studies, they concluded that the hypervalent twist, the exchange of the apical and equatorial ligands (alcohol and oxo group, **4.67** → **4.68**), was the rate-determining step in the oxidation mechanism, with an energy barrier of 12.1 kcal/mol for methanol (Figure 4-6, A). As such, based on their conclusions, increasing the rate of the apical-equatorial exchange should increase the overall rate of the reaction. They theorized that the addition of steric bulk at the position ortho to the iodine would increase the oxidizing power of the

hypervalent iodine reagent relative to IBX (e.g., **4.66** vs. **4.70** in Figure 4-7) by reducing the transition state energy barrier of the hypervalent twist. Repeating the calculations with **4.70** they determined that the rate-determining step hypervalent twist did have a lower energy barrier. For example, in the oxidation of methanol the rate-determining step had a barrier of 9.7 kcal/mol with CH_3-IBX versus 12.1 kcal/mol for IBX.

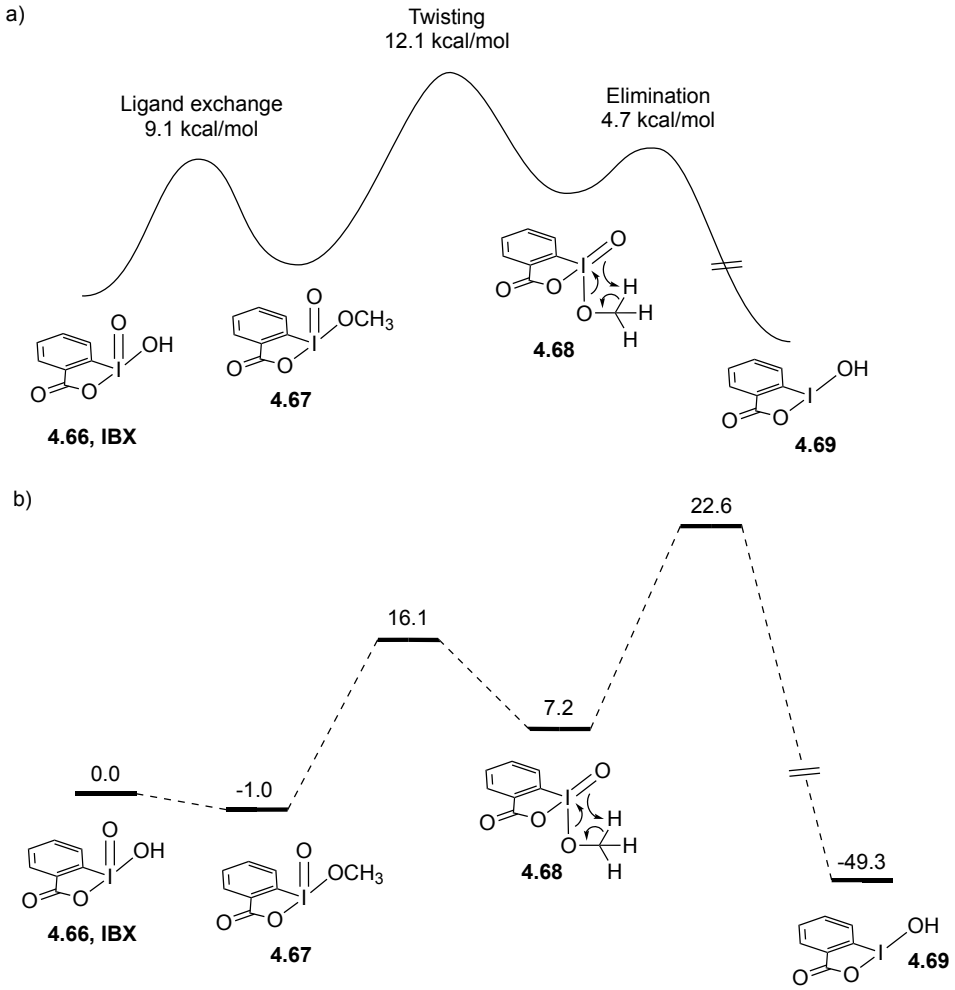


Figure 4-6. Two different energy diagrams of methanol oxidation by IBX. A) The energy diagram calculated by Su and Goddard shows the hypervalent twist to be rate limiting. B) The energy diagram calculated at a higher level of theory shows elimination to be rate limiting.

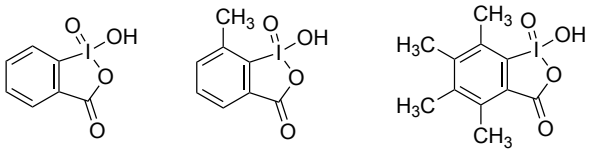
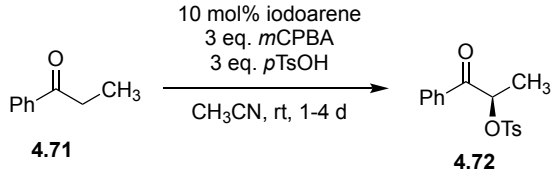


Figure 4-7. Chemical structures of IBX, CH_3-IBX, and Tet-IBX.

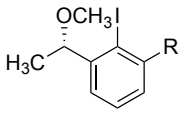
Though interesting computational results, the conclusion that the hypervalent twist was the rate-determining step did not match the experimental results from the KIE experiments reported by both Corey et al. and Moorthy et al.[238, 239] Corey determined the kinetic isotope effect to be 6.3 when comparing the oxidation of $C_6H_5CH_2CH_2OH/C_6H_5CH_2CD_2OH$, a number indicative of a primary kinetic isotope effect leading to the conclusion that the breaking of the C-H bond is part of the rate-determining step.[238] Moorthy reported a KIE ratio of 3.3 for the oxidation of methanol and methanol-d_4 with Tet-IBX (**4.71**, Figure 4-7).[239] Their computational results also indicated the hypervalent twist to be the rate-limiting step, and as such they proposed that the twist and disproportion/elimination steps occurred concertedly in one step.

Due to this discrepancy in the computational and experimental results, the reaction mechanism was reinvestigated computationally with four different density functional theory quantum chemical methods and seven different basis sets.[240] Using more advanced theory and a larger basis set than what was used in the original Su & Goddard investigation revealed the disproportionation/elimination to be the rate-limiting step (Figure 4-6, B). This result was consistent with the previous experimental results. They attributed the difference in results to the consideration of the iodine *f* orbitals in the larger basis sets and ultimately the improper consideration of the I-O and I-OCH_3 interactions in the original calculations. As such, the barrier to the I-OCH_3 bond breaking is underestimated relative to the barrier of the hypervalent twist. Further computational studies corroborated these results and concluded that the *f*-functions (used to consider the *f* orbitals of iodine) in the larger basis sets were required for correct predictions of the rate-determining step.[241] Although not rate limiting, the hypervalent twist was found to be a crucial step in the mechanism of both alcohol and amine oxidation by IBX.[242] All of these calculations were completed on IBX and not the substituted variants. Despite the varying experimental and computational results, over time a variety of IBX derivatives have been synthesized and used successfully in oxidative transformations.[243]

Although the idea of introducing steric bulk ortho to the iodine atom was proposed for the λ^5-hypervalent iodine compounds, this idea has been explored with λ^3-hypervalent iodine reagents as well. In 2008, Wirth et al. designed multiple iodoarene catalysts with ortho groups (Scheme 4-21).[244] The addition of an ethyl or benzyloxy group ortho to the iodine roughly doubled the enantioselectivity. Legault et al. also studied the alpha-tosylation of ketones and observed a similar pattern, but again, there was an upper limit of steric bulk tolerated before the reaction failed. With catalysts **4.74**, the addition of a methyl or ethyl group greatly improved the yield, but with the much larger isopropyl group the reactivity was equivalent to the catalyst with R = H.[245] They also saw improvement with a chiral oxazoline-based catalyst **4.75**.[245, 246] Although the enantiomeric excess did not increase significantly (24% vs ~30%), the yield increased six-fold when using either the methyl or ethyl substituted derivative. It appears that once the group is too large the benefits are outweighed by the additional steric interactions that likely occur during the reaction (e.g., **4.73** R = H vs O*t*-Bu or **4.74** R = CH_3 vs *i*-Pr).



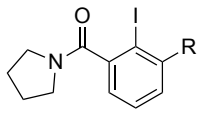
4.71 **4.72**



4.73

Wirth, 2008

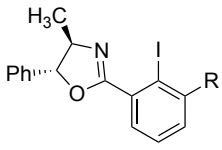
R =	% *ee*	% yield
H	12	68
Et	27	59
OBn	25	48
O*t*-Bu	3	-



4.74

Legault, 2012

R =	% yield
H	<1
CH_3	50
Et	61
i-Pr	1



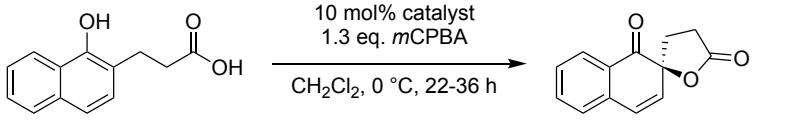
4.75

Legault, 2012

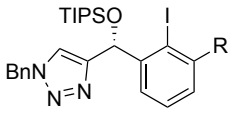
R =	% *ee*	% yield
H	24	9
CH_3	33	60
Et	30	59

Scheme 4-21. alpha-Tosylation with ortho-substituted iodoarene catalysts by Wirth et al. and Legault et al.

In their exploration of *N*-heterocycle-stabilized iodanes as competent iodoarene catalysts (**4.78**) for oxidations, Nachtsheim explored a series with substitution beside the iodine atom.[247] When the known spirolactonization of **4.76** was carried out with catalyst **4.78** (R = H) the product **4.77** was obtained in only 36% yield (64% *ee*). Improvement of the yield was seen with ortho-substitution of Cl, Me, and OCH_3 substitution (54, 62, and 81%, respectively). The highest enantiomeric excess was achieved with the OCH_3 group and further optimization of the solvent gave the product **4.77** in 85% and 99% *ee*. They were unable to crystallize any of the active hypervalent iodine species for characterization; however computational studies reveal a larger dihedral angle between the hypervalent bond and arene ring when sterics (e.g., OCH_3) are imposed ortho to the iodine. From this preliminary analysis, and based on Legault's previous work, they concluded that the OCH_3 group caused a "hypervalent twist" in the active reagent, which efficiently mediated the spirolactonization. Further analysis of the proposed reactive species with vibrational circular dichroism revealed a cationic hydroxy-iodane **4.78-active** to be the hypervalent iodine species.[248]

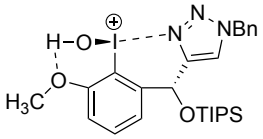


4.76 **4.77**



4.78

R =	% *ee*	% yield
H	64	36
Cl	60	54
CH_3	78	62
OCH_3	82/99[a]	81/85[a]

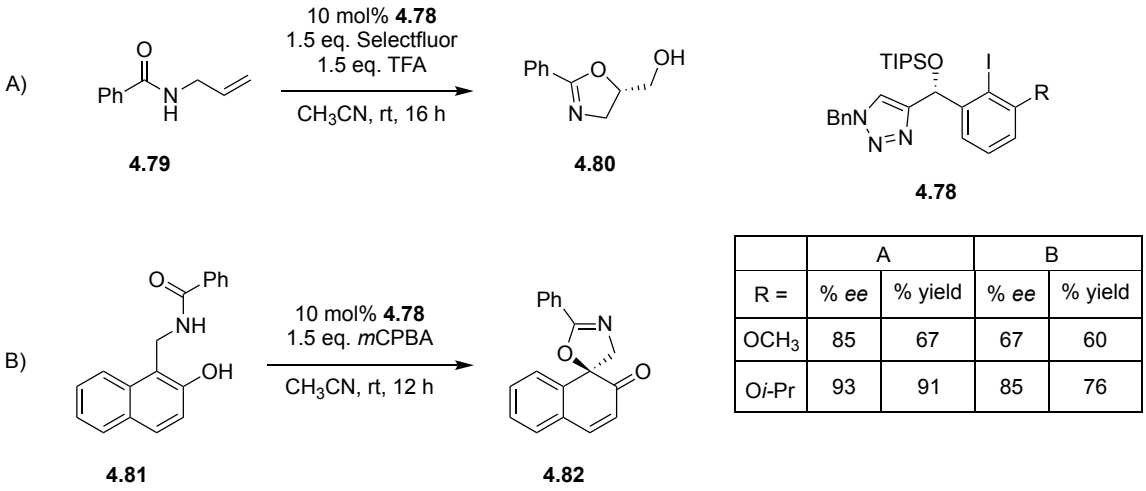


4.78-active

Scheme 4-22. Spirolactonization with ortho-substituted N-heterocycle stabilized iodanes. [a] Solvent: $CH_2Cl_2/CHCl_3$ + 6.0 eq. EtOH, -10 °C.

They utilized this family of catalysts in two additional transformations. Replacement of the OCH_3 group with an O*i*-Pr saw improvements in both the yield and the enantiomeric excess. This was first demonstrated in the cyclization of *N*-allyl benzamide **4.79** to the chiral oxazoline **4.80** (Scheme 4-23).[249] When catalyst **4.78** (R = OCH_3) was used a yield of 67% with 85% *ee* was obtained, and improvement to 85% yield and 91% *ee* was achieved with **4.78** (R = O*i*-Pr). A similar increase in both yield and

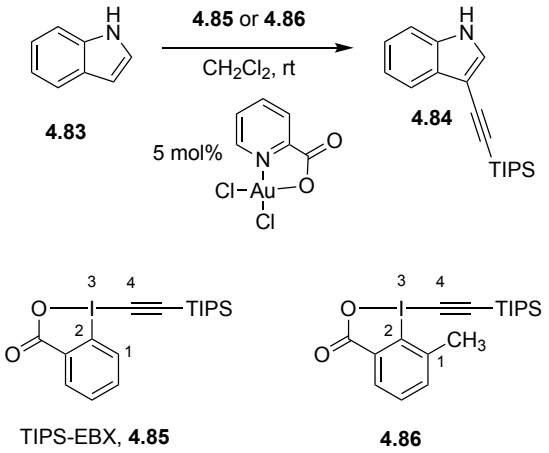
enantiomeric excess was seen in the formation of spirooxazolines **4.82** when the OCH_3 group was changed to an O*i*-Pr group.[250]



	A		B	
R =	% *ee*	% yield	% *ee*	% yield
OCH_3	85	67	67	60
O*i*-Pr	93	91	85	76

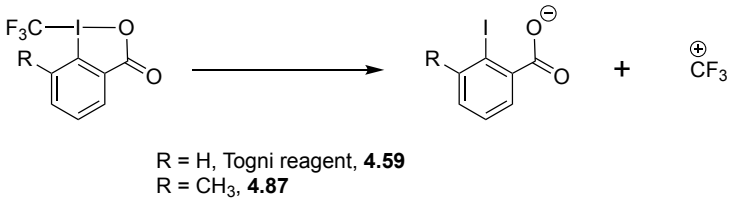
Scheme 4-23. Additional transformations with Nachtsheim's ortho-substituted catalyst.

Waser et al. synthesized an ortho-methyl substituted TIPS-EBX reagent (**4.86**) and compared it to the reactivity of the unsubstituted parent (TIPS-EBX, **4.85**) by X-ray crystallography and NMR.[251] Crystallography showed that the torsion angle (C1-C2-I3-C4) was 8.33° in TIPS-EBX vs 34.6° in **4.86**, the I-C(alkyne) bond was slightly shorter (2.043 Å vs 2.0539 Å) and the I-O bond was slightly longer (2.385 Å vs 2.3379 Å). NMR studies of the gold-catalyzed alkynylation of indole revealed a higher rate of reaction with **4.86** vs. **4.85**; however the final yield was similar (Scheme 4-24). Modification of the reagent with the methyl group certainly changes the structure and ultimately the reactivity of the reagent, however, a broader synthetic utility was not demonstrated. The higher reactivity of **4.86** was rationalized by invoking the previously mentioned studies of Su and Goddard, Moorthy et al., and Legault et al., and presumed that the out-of-the-plane twist reduced the strength of the 3c-4e hypervalent bond and therefore increased the reactivity of the reagent.



Scheme 4-24. Gold catalyzed alkynylation.

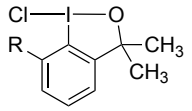
The computational design of new Togni reagents explored both the steric hindrance (substitution ortho to the iodine atom) and linking sidearm.[252] They quantified the reactivity of the newly designed reagents by determining the reaction free energy of the hetero-cleavage of the hypervalent bond (Scheme 4-25). The lower the reaction free energy, the more reactive the reagent. Although the influence of the methyl group steric hindrance was not as strong as the variance in the sidearm (only -CO_2- is shown) it did increase the reactivity of **4.87** (39.3 kcal/mol) vs. **4.59** (32.8 kcal/mol) based on the reaction free energy calculation.



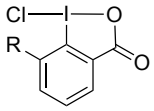
Scheme 4-25. Hetero-cleavage of Togni reagent and **4.87**.

Two separate computational studies noted a decrease in calculated bond dissociation energy when introducing steric bulk ortho to the iodine. Firstly, TIPS-EBX derivatives with ortho methyl, *tert*-butyl, methoxy, or halo substitution decreased the bond dissociation energy (BDE) from 72.7 kcal/mol to 62.2 – 65.3 kcal/mol. Broad conclusions cannot be drawn as the correlation of the BDE with experimental reactivity was not determined for the whole series of reagents. If only **4.86** and **4.85** are compared the correlation is positive (i.e., more steric hindrance = more reactive reagent). More experimental data

would be needed to determine if the correlation is general, and whether it holds true over a larger set of reagents. The second report described the BDEs of the chloroiodanes (**4.3**, **4.34**, **4.88**, **4.89**). Again, the same pattern is seen, when the ortho methyl group is introduced the BDE decreases, therefore making a more homolytically reactive species.[253] Experimentally, **4.34** is generally more reactive than **4.3**, which is counter to the BDE data, albeit the difference in BDE is minimal. However, once the methyl group is added, according to the BDE data, chloroiodane **4.88** (vs. **4.89**) is the more reactive reagent. The corresponding experimental reactivity data is not presently available to determine if this prediction is correct. Overall, the use of BDEs to predict reactivity may or may not be accurate as these reagents do not typically react in a homolytic manner.



4.3, 4.88



4.34, 4.89

Compound	R =	BDE (kcal/mol)
4.3	H	46.4
4.88	CH_3	41.2
4.34	H	47.7
4.89	CH_3	40.3

Figure 4-8. Calculated BDEs of chloroiodanes.

Although ortho substitution of the aromatic ring is not a guaranteed method to achieve higher yields and better enantioselectivity, it does modify the reagent in such a way that the hypervalent bond is affected and maybe even weakened. Given that the hypervalent bond is the reactive center of the molecule, it is not unreasonable to assume modifications to this bond could alter the reactivity and selectivity of these and other related reagents.

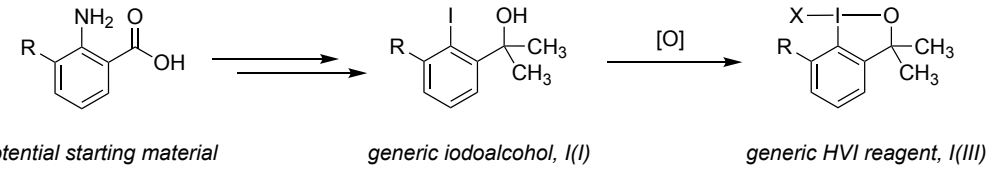
4.1.4 Research Objectives

The goal of this project was to explore a series of ortho-substituted fluoro- and chloroiodanes. This will be accomplished through the synthesis of the series and obtaining their crystal structures. The hypervalent iodine bond and the aryl ring in reagents such as **4.2** or **4.3** are nearly co-planar. We hypothesized that the addition of steric hindrance (through ortho substitution) would force the

hypervalent bond out of co-planarity. Additionally, to minimize steric clash, the iodine-halogen (fluorine or chlorine) bond may also lengthen. Ultimately, the goal was to relate the magnitude of the torsion angle between the hypervalent iodine bond and the arene ring to the reactivity of the reagents in known reactions. Furthermore, we hoped to relate any other unexpected solid-state structural differences to the reactivity of the reagents.

4.2 Synthesis

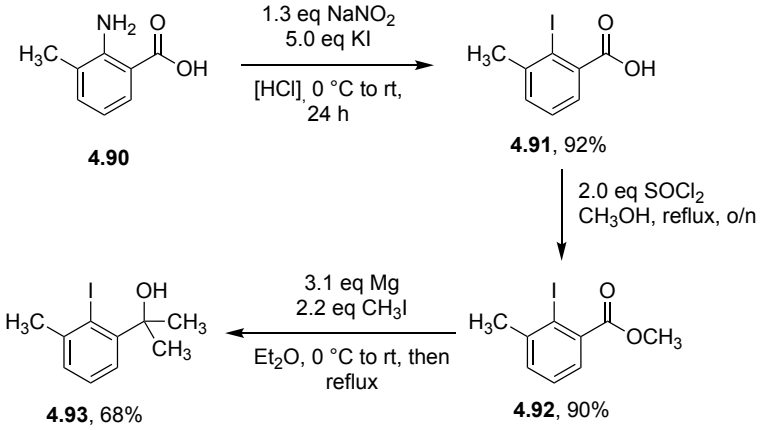
The synthesis of the fluoro- and chloroiodanes can be conceptually separated into two sections: (1) the synthesis of the iodoalcohol precursors and (2) their oxidation to a hypervalent species (Scheme 4-26). The synthesis and any challenges encountered in the synthesis of the iodoalcohols will be discussed in Section 4.2.1, while Section 4.2.2 contains a discussion of the reaction conditions, both successful and unsuccessful, explored to convert the synthesized iodoalcohols from the I(I) to I(III) oxidation states.



Scheme 4-26. Generic synthesis of the iodoalcohol and the hypervalent iodine reagents.

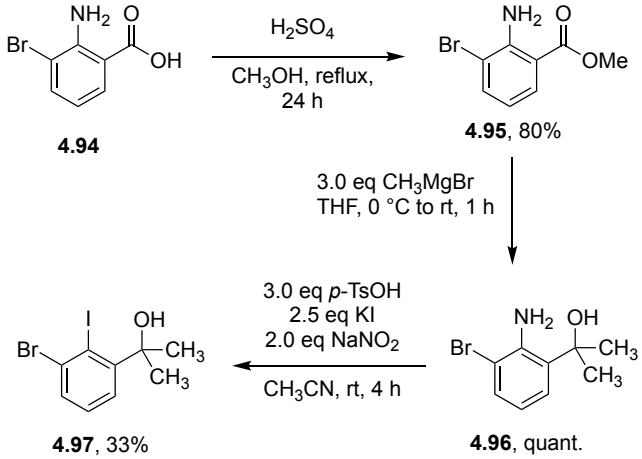
4.2.1 Synthesis of the Iodoalcohol Precursors to the Hypervalent Iodine Reagents

The first iodoalcohol to be targeted was the ortho-methyl derivative **4.93** (Scheme 4-27). Retrosynthetically, it can be synthesized in the same manner as the already published fluoroiodane from 3-methylanthranilic acid (as opposed to anthranilic acid). The commercially available 3-methyl anthranilic acid **4.90** was converted in three steps to the iodoalcohol (Scheme 4-27), beginning with the treatment of **4.90** with previously reported Sandmeyer reaction conditions to give **4.91** in 92% yield on a 5-gram scale. Esterification of **4.91** with thionyl chloride in methanol smoothly provided the corresponding ester **4.92** in 90% yield. Gram-scale reaction conditions for the double methyl Grignard addition were developed by the research group of Togni to obtain the Togni reagent efficiently.[220] These conditions were replicated to obtain the desired alcohol **4.93** in 68% yield (56% over three steps).



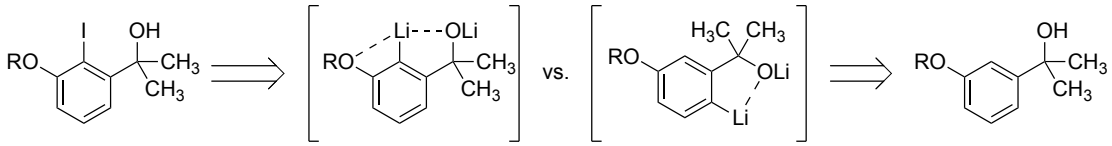
Scheme 4-27. Synthesis of ortho-CH_3-iodoalcohol **4.93**.

The ortho-bromo alcohol **4.97** was similarly synthesized from the 3-bromoanthranilic acid **4.94** which was ultimately prepared from 2-bromoaniline (Scheme 4-28). Treatment of the 2-bromoaniline with choral hydrate, Na_2SO_4, and $HCl_{(aq)}$ gave an oxime intermediate which was cyclized in concentrated H_2SO_4 to the isatin, oxidation and hydrolysis with basic hydrogen peroxide afforded 3-bromoanthranilic acid **4.94** as a tan powder in 64% on a 25-gram scale (not shown). Esterification was achieved with sulfuric acid in methanol to provide **4.95** in 80% yield. Methyl Grignard addition into ester **4.95** provided aminoalcohol **4.96** quantitatively. Sandmeyer iodination in non-aqueous conditions provided the desired iodoalcohol, albeit in only 33% yield.



Scheme 4-28. Synthesis of the ortho-bromo iodoalcohol **4.97**.

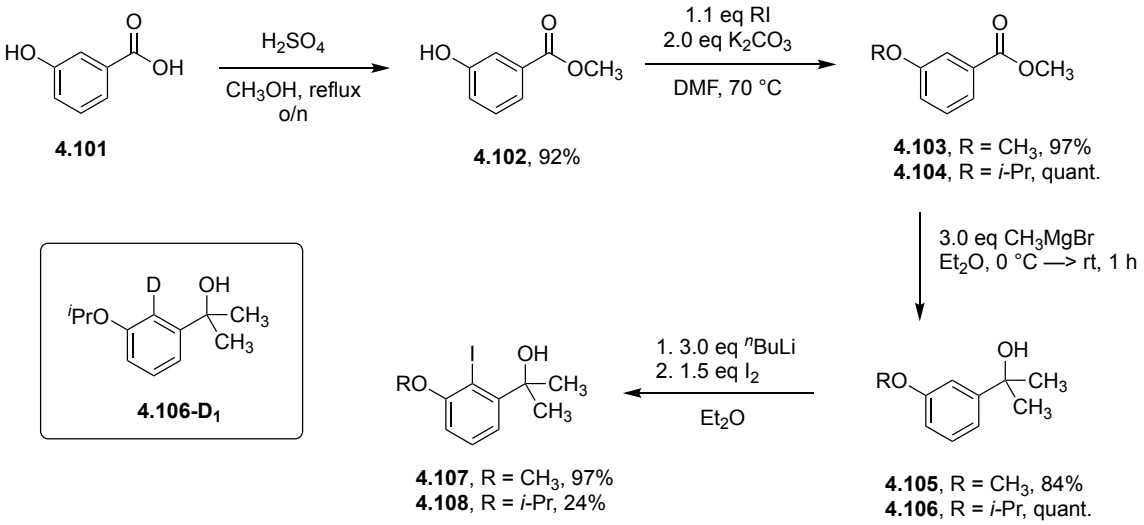
The ortho-ether derivatives (**4.107** and **4.108**) were synthesized from the readily available 3-hydroxybenzoic acid **4.101** using a directed ortho-metalation (DoM) approach to install the iodine (Scheme 4-29). Retrosynthetically, the iodine could be disconnected from iodoarene **4.98** to give an aryllithium species which could be accessed from the 1,3-substituted tertiary alcohol **4.100**. It was rationalized that the lithiation would occur between the ether and the alkoxide to give the desired 1,2,3-trisubstituted product **4.99a** due to the coordination of the two oxygen atoms to the lithium atom. The less stable aryllithium species **4.99b**, with single oxygen coordination, giving rise to the 1,2,4-trisubstituted product would not occur. As such, the tertiary alcohol **4.98** would be prepared by this synthetic route.



4.98 **4.99a** *favoured* **4.99b** *unfavoured* **4.100**

Scheme 4-29. Synthetic strategy to access the ortho-ether derivatives.

The synthesis began with the esterification of 3-hydroxybenzoic acid **4.101** in refluxing methanol to obtain phenolic ester **4.102** (Scheme 4-30). The phenolic oxygen was then alkylated with the appropriate alkyl iodide under basic reaction conditions to provide the methyl ether **4.103** or isopropyl ether **4.104**. Double methyl Grignard addition to the esters smoothly furnished the corresponding tertiary alcohols (**4.105** and **4.106**) in quantitative yield and set the stage for optimization of the DoM reaction to install the iodine.

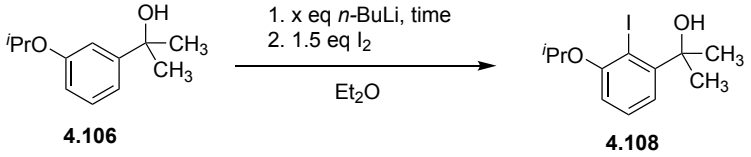


Scheme 4-30. The preparation of the ortho-methoxy and isopropoxy iodoalcohols.

Optimization of the DoM and iodination conditions began with treatment of the isopropoxy alcohol **4.106** with 2.3 equivalents of *n*-BuLi (2.1 M in hexanes) for two hours in anhydrous diethyl ether to achieve lithiation. This species was quenched with a solution of molecular iodine in diethyl ether at 0 °C. By crude ^{1}H-NMR, we obtained approximately a 1:1 mixture of starting material **4.106** to desired product **4.108** (Table 4-1, Entry 1). Therefore, either complete deprotonation of **4.106** did not occur or the iodination of the aryllithium failed. Considering the nucleophilicity of the aryllithium and the electrophilicity of iodine, it is likely that the reaction failed at the initial deprotonation step. To test this hypothesis the deprotonation time was extended and a quench with deutero-methanol was performed. If lithiation was successful and the iodination was failing, 4.106-D_1 would be recovered instead of **4.106**. As such, increasing the lithiation time to 3 hours and quenching with 1.5 equivalents of iodine was followed by the addition of D_4-methanol which gave an improved ratio of 13:1 (**4.108**:**4.106**) and after isolation afforded pure **4.108** in 72% yield (Table 4-1, Entry 2). As no deuterated products were detected by GC-MS the iodination was likely high yielding and incomplete deprotonation was the culprit for the poor product yield. Increasing the lithiation time to 5 hours saw no improvement in the reaction outcome (4.6:1, **4.108**:**4.106**) (Table 4-1, Entry 3). The decrease in ratio could point to a degradation of the lithiated product over the longer reaction time. As the increase in reaction time did not improve yield the next logical experiment was to increase the equivalents of the base. With 3.0 equivalents of *n*-BuLi, the arene was deprotonated in 3 hours and quenched with 1.5 equivalents molecular iodine and gave a crude product with 20:1 (**4.108**:**4.106**) selectivity from which **4.108** was

isolated in 80% yield (Table 4-1, Entry 4). Scaling the reaction to 10 mmol was unsuccessful and only proceeded in 24% yield (765 mg, isolated); however, this was likely due to unidentified operator error. For example, the use *n*-BuLi with an inaccurate titer could result in the incomplete formation of the aryllithium species. As the 765 mg of product **4.108** was enough material to continue the study a proper assessment of the reproducibility on scale was not completed. The ortho-methoxy iodoalcohol was prepared with the same strategy and reaction conditions. The phenol was first methylated with methyl iodide, followed by double methyl Grignard addition into the ester, and finally directed *ortho*-lithiation to install the iodine in 79% yield over 3 steps (Scheme 4-30). Of note, the iodination of **4.105** proceeded in 97% yield on a 3.8 mmol scale. Overall, both ortho-alkoxy iodoalcohols were successfully prepared.

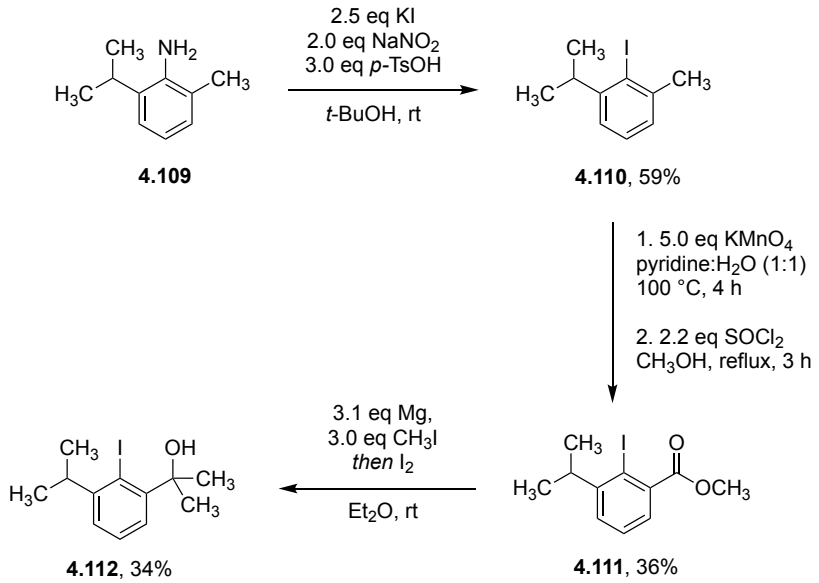
Table 4-1. Optimization of deprotonation and lithiation of **4.106**.



4.106 **4.108**

Entry	Equivalents of *n*-BuLi	Time (h)	Ratio (**4.108**:**4.106**)	Isolated yield (%)
1	2.3	2	1:1	-
2	2.3	3	13:1	72
3	2.3	5	4.6:1	-
4	3.0	3	20:1	80

Preparation of the ortho-isopropyl and ortho-*tert*-butyl iodoalcohol derivatives was more challenging than expected. The synthetic strategy to access the ortho-isopropyl alcohol was analogous to Steps 2 and 3 of Scheme 4-27 (**4.91** to **4.93**), and while successful, the desired material was recovered in very low overall yield. 2-Isopropyl-6-methylaniline **4.109** was converted to the aryl iodide **4.110** under Sandmeyer conditions in 59% yield (Scheme 4-31). Selective oxidation of the benzylic methyl group with $KMnO_4$ in hot pyridine afforded the benzoic acid which was smoothly converted into the ester **4.111** in 36% yield over the two steps and set the stage for the double methyl Grignard addition.



Scheme 4-31. Preparation of the *ortho*-isopropyl iodoalcohol.

Unfortunately, the proposed double methyl Grignard addition was not trivial, and numerous attempts were made to increase the yield of this reaction. Reaction conditions similar to those of Scheme 4-27 were first explored. The addition of 2.2 equivalents of commercial methyl magnesium bromide into a solution of **4.111** and stirring in THF at either 0 °C, room temperature or reflux did not consume the starting material. While increasing the amount of methyl Grignard to 5.0 equivalents consumed more starting material, no desired product **4.112** was formed. To mitigate error due to quality of the reagent, the Grignard was freshly prepared going forward. The ester **4.111** was stirred with freshly prepared methyl magnesium iodide at room temperature for 15 hours and as expected, based on the previous experiments, consumption of the starting material was not complete. Consumption of the starting material was still not complete even after refluxing the same mixture for an additional 5 hours, however, new products did appear. ^{1}H-NMR and GC-MS analysis of the crude reaction mixture revealed the starting material to be the major component of the reaction mixture along with three minor products, one being the de-iodinated tertiary alcohol **4.109** (Figure 4-9). Ultimately, using fresh methyl Grignard did not improve the reaction outcome. To develop a better understanding of the reaction profile ester **4.111** was treated with 3.0 equivalents of commercial Grignard overnight at room temperature. Careful analysis of the crude reaction mixture by GC-MS revealed five products. Analysis of the fragmentation patterns of the corresponding mass spectra showed the peaks to correspond with de-iodoalcohol (**4.113**):de-iodoester (**4.114**):unknown:starting material (**4.111**):product (**4.112**) in a ratio of

14:24:7:37:19 based on the peak area. The structure of the most minor product was inconclusive by MS and its exact identity was not pursued further. The corresponding methylated products (**4.115** and **4.116**) were considered; however, the experimental data did not match the expected fragmentation patterns arising from cleavage about the ether or carbonyl functional groups. (Figure 4-9). The methylated products could theoretically arise from alkylation with methyl iodide generated in the metal-halogen exchange process.

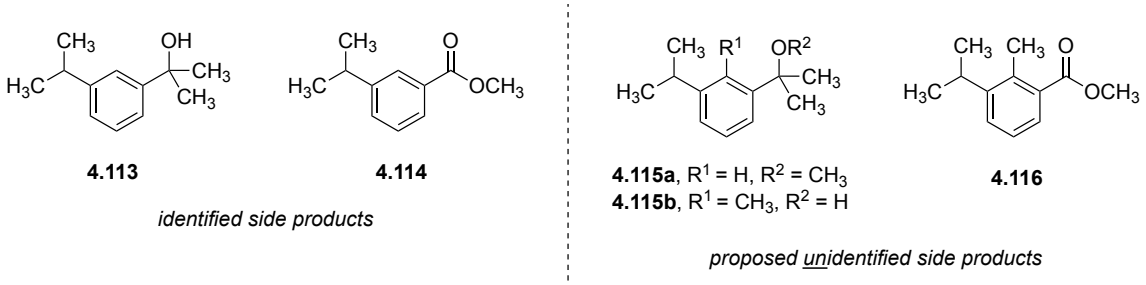
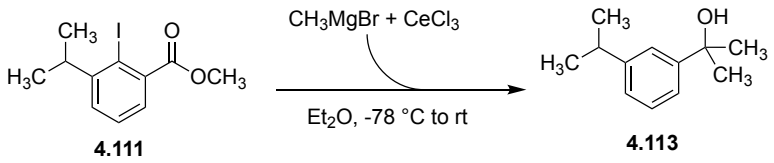


Figure 4-9. De-iodinated side-products from the methyl Grignard addition and proposed side-products.

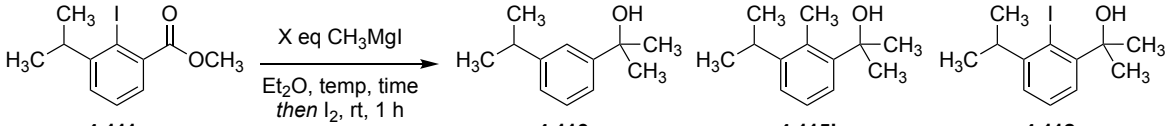
Ideally, any modification to the reaction conditions would reduce the propensity of the methyl Grignard to undergo metal-halogen exchange while simultaneously increasing the electrophilicity of the ester. Organocerium reagents are known to improve both selectivity for 1,2-addition to enolizable ketones and decrease metal-halogen exchange.[254, 255] This would in theory eliminate undesired side-products and increase conversion of the starting material, and ultimately the yield of the desired product. Therefore, to test this hypothesis, commercial CH_3MgBr was transmetallated to the organocerium reagent with anhydrous $CeCl_3$ at -78 °C (Scheme 4-32). Slow addition of the ester **4.111** to this solution, followed by warming to room temperature produced a single major product. Although nucleophilic addition to the ester appeared to occur smoothly, the isolated product was not the desired tertiary alcohol **4.112**, but the deiodinated tertiary alcohol **4.113**, which was isolated in 41%.



Scheme 4-32. Addition of organocerium reagent to **4.111**.

Given the apparent ease by which the iodine was lost from the molecule by metal-halogen exchange, the elimination of this undesired reaction pathway is likely extremely difficult. Focus was instead put on increasing the productive consumption of the starting material, with the goal of quenching any aryl-metal species with iodine at the end of the reaction. Treatment of the ester with freshly prepared CH_3MgI (3.0 eq) for 3 hours and quenching with iodine (3.0 eq) gave a crude product distribution of ~2:1 (**4.111**:**4.112**, sm:prod) by GC-MS (Table 4-2, Entry 1). Gratifyingly, only minor amounts of de-iodinated products were obtained compared to the previous experiments. Increasing the reaction time to 16 hours increased the proportion of the desired product in the mixture; however, the material recovery was significantly reduced (Table 4-2, Entry 2). Refluxing the reaction for 3 hours further reduced the amount of the desired product (Table 4-2, Entry 3). Increasing the reaction temperature also led to a marked increase in the alkylated side-product **4.115b**, and further increasing the equivalents of CH_3MgI (to push the consumption of all starting material), was similarly unsuccessful. Although the product ratio was 1:2.4 (sm:prod) the material recovery was low (Table 4-2, Entry 4). Ultimately, the conditions listed in Table 4-2, Entry 1 were chosen as this led to the cleanest crude reaction mixture with the desired product and the opportunity to recover ester for recycling. Given the success of the earlier experiment with the organocerium reagent and the iodine quench, future experiments exploring equivalents of said reagent with an iodine quench should be completed. If the intermediate aryl cerium reagent can be generated quantitatively, perhaps the iodination would also be successful and lead to higher conversion of the ester and yield of the desired product.

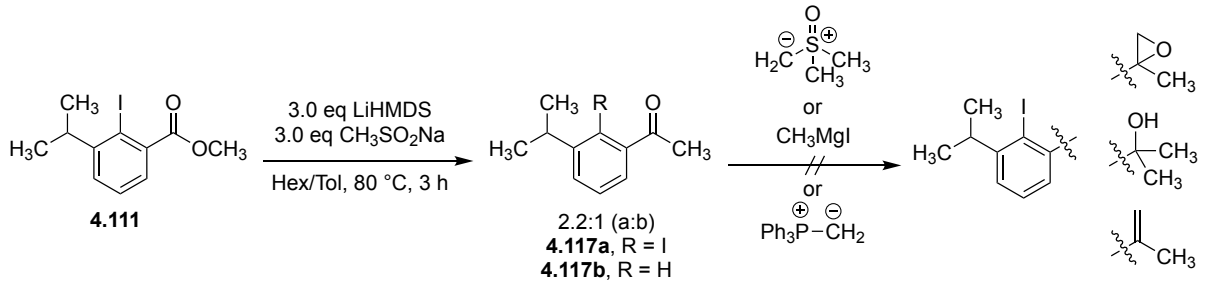
Table 4-2. Methyl Grignard addition into ester **4.111**.



4.111 **4.113** **4.115b** **4.112**

Entry	Equivalents of CH_3MgI	Time (h)	Temp.	Crude yield (%)	Ratio (**4.111**:**4.113**:**4.115b**:**4.112**)
1	3.0	3	rt	89	65:3:3:29
2	3.0	16	rt	53	19:12:13:50
3	3.0	3	reflux	71	20:18:34:26
4	10	3	rt	47	26:0:0:62

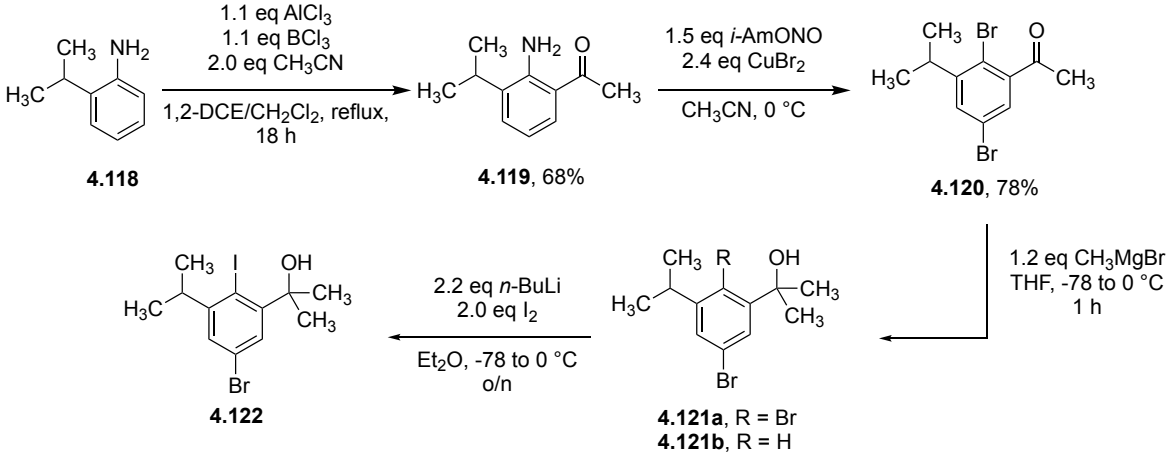
Alternative synthetic routes were explored concurrently. Hypothetically, the ester could be converted into a more electrophilic carbonyl to increase the addition rate of the nucleophile while minimizing the de-iodination by metal-halogen exchange. The methodology published by Fier et al. was used to convert ester **4.111** into ketones **4.117a/b** as an inseparable mixture with LiHMDS and sodium methanesulfinate in 55% yield (Scheme 4-33).[256] Treatment of this mixture with three different nucleophiles resulted in the addition of the nucleophile to **4.117b** (the de-iodinated compound) with full recovery of **4.117a**. Attempted Corey-Chaykovsky epoxidation at room temperature, 80 °C and 120 °C provide none of the desired epoxide. In the Grignard reaction, **4.117b** was smoothly converted to the corresponding tertiary alcohol while the iodoacetophenone **4.117a** was recovered. Transmetallation of the Grignard to the organocerium reagent (to reduce any potential enolization), did not improve the addition to the ketone. Again, **4.117b** was fully converted to the tertiary alcohol, and the iodoacetophenone **4.117a** was recovered. The alkene was targeted with methyl phosphonium ylide and unsurprisingly, the same reactivity pattern was observed.



Scheme 4-33. Failed additions into iodoacetophenone **4.117a**.

Given the ease at which the nucleophiles could add into **4.117b** and the significantly reduced reactivity of **4.117a** (and **4.111**), it raised a question of how much steric bulk could be tolerated at the 2-position of the arene with a large group at the 3-position (e.g., an isopropyl group). Based on the recovery of the starting material in the above reactions, the steric effects imposed by these contiguous groups seemingly reduces the electrophilicity of the ester. To explore this idea the bromo derivative **4.121** was prepared, and a final lithium-halogen exchange reaction could be used to install the iodine atom. The synthesis began with the acetylation of 2-isopropylaniline **4.118** with acetonitrile under Lewis acidic conditions (Scheme 4-34). Dibromination of the aminoacetophenone **4.119** with *i*-AmONO and $CuBr_2$ gave the desired product **4.120** in 78% yield.

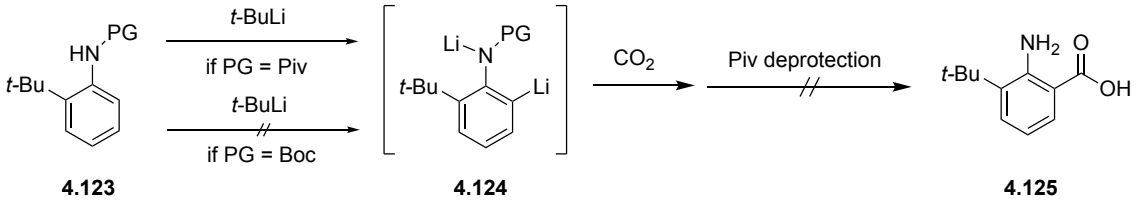
The preliminary investigation into the methyl Grignard addition (**4.120** → **4.121**) gave an inseparable mixture of the mono and dibromo tertiary alcohols. To determine the viability of this route, lithium-halogen exchange with *n*-BuLi and quenching with iodine was done with a mixture of **4.121a/b**, and fortunately, the desired alcohol **4.122** was obtained in a mixture with **4.121a/b**. As neither **4.121** or **4.122** were isolated in pure form a yield was not reported. The iodination was confirmed by the presence of ^{13}C-NMR signal at 99.8 ppm, indicative of an aromatic C-I bond. As the initial route (**4.109** to **4.112**, Scheme 4-31) was eventually successful further development of this route was halted. Future optimization of the route will include using the organocerium reagent to suppress the metal-halogen exchange reaction and obtain exclusively the desired dibromo tertiary alcohol **4.121a**. Simply reducing the size of the halogen from iodine to bromide completely alleviated the difficulties with the nucleophilic addition into the carbonyl. Two possible explanations exist for this increased rate of addition. Firstly, the bromine as a more electronegative substituent might increase the reactivity of the carbonyl, reducing the energy barrier for the Grignard addition. Alternatively, the sterically smaller bromine atom reduces the steric interactions experienced in the transition state (vs. iodine), therefore increasing the rate of addition to the carbonyl. Overall, two viable synthetic routes were developed to access the desired ortho-isopropyl alcohols (**4.112** and **4.122**).



Scheme 4-34. The synthesis of **4.122**.

Similar unsuccessful and successful synthetic strategies were used to target the ortho-*tert*-butyl iodoalcohol **4.129**. The initial strategy involved targeting the anthranilic acid through a DoM of *N*-protected 2-*tert*-butylaniline **4.123** (Scheme 4-35). Lithiation and trapping with CO_2 of the pivaloyl

protected *tert*-butylaniline **4.123** was successful. Unfortunately, all attempts to remove the pivaloyl (Piv) protecting group were unsuccessful. Alternatively, when the aniline was protected with a Boc group the first lithiation step was unsuccessful. Attempted lithiation with *t*-BuLi, *n*-BuLi, or *n*-BuLi with TMEDA were all unsuccessful. The lithiation step, and not the electrophilic trapping with CO_2 was confirmed to be the problematic step as quenching with D_2O did not yield any deuterated product.

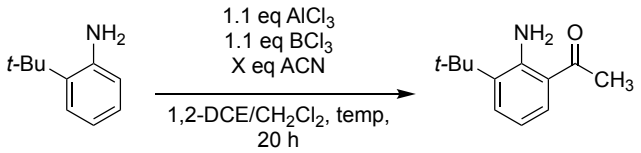


4.123 **4.124** **4.125**

Scheme 4-35. Attempted synthesis of *t*-butyl anthranilic acid.

The second synthetic strategy was to use the acetylation methodology applied to the isopropylaniline in Scheme 4-34. Due to the very similar R_f values and inseparable nature of the starting aniline and the desired acetylated product, a short optimization was carried out to improve the reaction outcome. In a sealed vessel, experiments with univariate increases of the CH_3CN equivalents and temperature were performed (Table 4-3). Increasing the reaction temperature (Table 4-3, Entry 1 vs 5) and the equivalents of CH_3CN improved the conversion and yield of the reaction. The reaction was successfully scaled at atmospheric pressure using conditions similar to Entry 5 (Table 4-3) and afforded **4.127** in 80% yield.

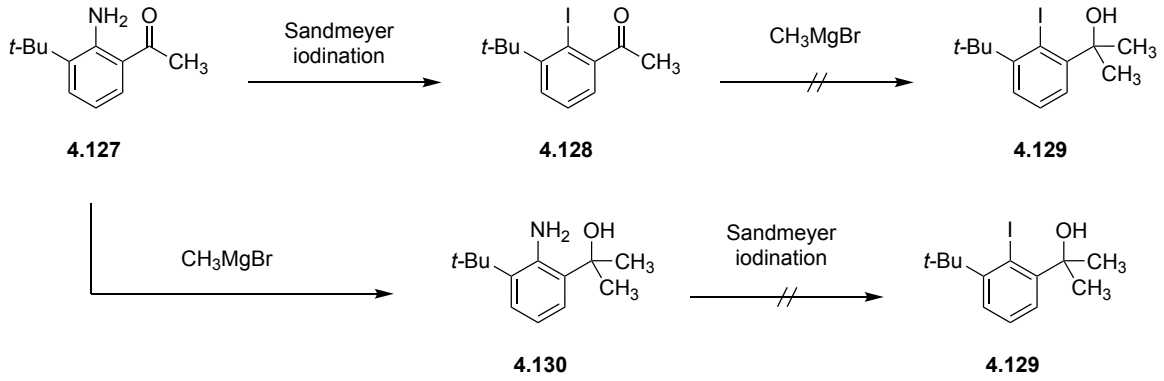
Table 4-3. Optimization of acetylation



4.126 **4.127**

Entry	Equivalents of CH_3CN	Temperature (°C)	Crude yield (%)	Ratio (**4.126**:**4.127**)
1	1	80	55	1:1
2	2	80	43	1:4
3	5	80	46	1:5.6
4	10	80	47	1:6.1
5	2	100	62	1:14

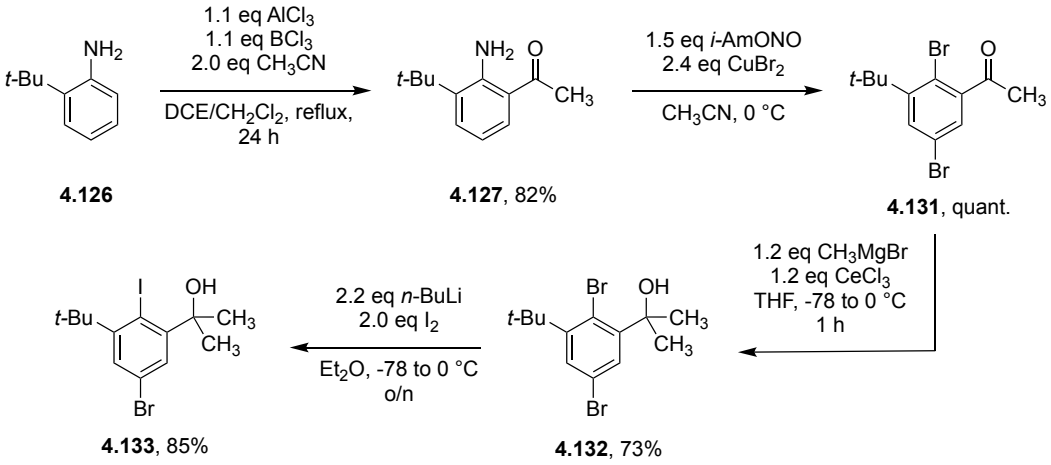
After Sandmeyer iodination of the 2-aminoacetophenone **4.127** (albeit in poor yield) addition of a nucleophilic source of a methyl group was attempted (Scheme 4-36). Stirring the acetophenone **4.128** with 1.0 equivalents of CH_3MgBr in THF, initially at 0 °C and warmed to room temperature overnight, only gave starting material by GC-MS and ^{1}H-NMR. Preparation of fresh CH_3MgI made no difference in yield or conversion, nor did the addition of $CeCl_3$. These results were expected as Grignard addition into the less sterically hindered isopropyl variant was equally as difficult. As adding the Grignard into the iodoacetophenone **4.128** was not successful, in theory, the order of the synthetic steps can be reversed. Methyl Grignard addition into the amino acetophenone **4.127** proceeded smoothly to give the amino alcohol **4.130** (Scheme 4-36). To obtain the desired iodoalcohol **4.129** the amino group had to be converted into an iodine while being mindful of the potentially sensitive benzylic tertiary alcohol. The amino alcohol **4.130** was stable to *p*-TsOH in CH_2Cl_2 and ACN on the time scale of hours. However, treatment of the amino alcohol **4.130** with the Sandmeyer iodination conditions of *p*-TsOH/$NaNO_2$/KI in CH_3CN led to a complex mixture containing multiple alkenes. Either the product or an intermediate is likely unstable to the reaction conditions and the tertiary alcohol is eliminated to provide the alkene. Treatment with the alternative Sandmeyer conditions of CH_2I_2/$NaNO_2$/AcOH in a biphasic solvent mixture provided an intractable mixture of products. This was not necessarily an unexpected result as exposure of **4.130** to acetic acid in a CH_2Cl_2/H_2O mixture led to partial decomposition of the material. Overall, these routes proved unsuccessful.



Scheme 4-36. Unsuccessful synthetic routes to the ortho-*tert*-butyl iodoalcohol **4.129**.

The sequence of Sandmeyer bromination, Grignard addition and lithium-halogen exchange might be a viable route to the desired iodoalcohol **4.133**, as it was successfully outlined above with the isopropyl variant. The same sequence of synthetic steps was applied to 2-*tert*-butylaniline **4.126**. It was cleanly

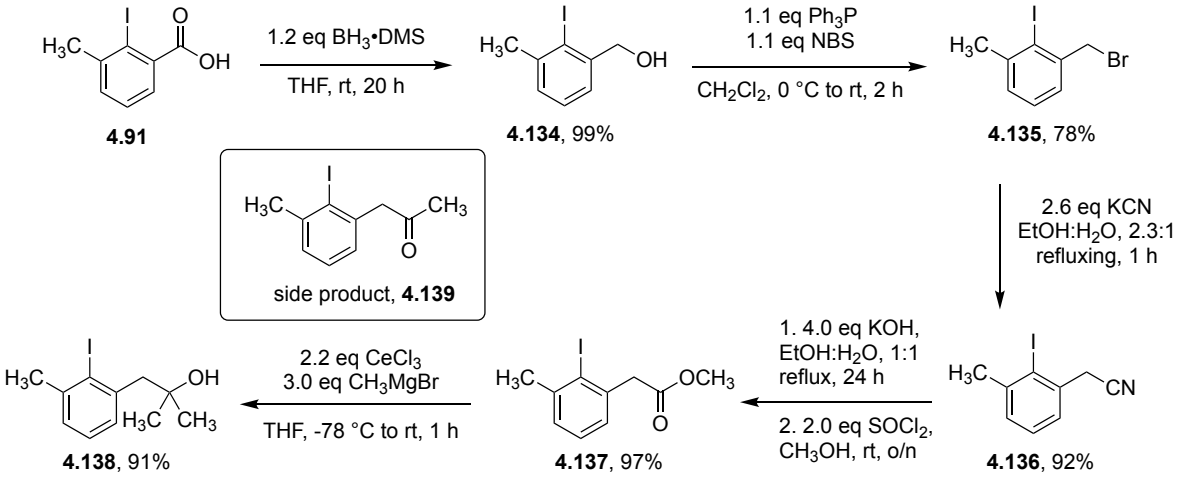
acetylated over 24 h to provide the aminoacetophenone **4.127** in 82% isolated yield (Scheme 4-37). Dibromination using *i*-AmONO and $CuBr_2$ cleanly provided **4.131** in quantitative yield. Various conditions targeting monobromination were tried, however, none were successful in obtaining the desired product. The addition of methyl Grignard quickly consumed the material at 0 °C giving a mixture of products. Alternatively, preformation of the organocerium reagent, to limit side products derived from magnesium-halogen exchange, gave the desired tertiary alcohol **4.132** cleanly in 73% yield without any of the monobrominated product (e.g., analogous to **4.121b** encountered in Scheme 4-34). Again, just as was observed with the isopropyl variant, the methyl Grignard added with ease to the ketone of **4.131** (the bromoacetophenone) compared to **4.128** (the iodoacetophenone). The steric demand of the adjacent iodine is clearly attenuating the reactivity of the carbonyl. To finish the synthetic sequence, alcohol **4.132** was treated with *n*-BuLi and quenched with iodine to furnish the desired material **4.133** in 85% yield. Overall, this sequence was simple and high yielding.



Scheme 4-37. Synthesis of *ortho*-*t*-butyl iodoalcohol **4.133**.

The iodoalcohol **4.138** was synthesized from **4.91** in seven steps (Scheme 4-38). 2-Iodobenzoic acid was obtained from a Sandmeyer reaction of the corresponding anthranilic acid, as discussed previously in Scheme 4-27. Acid **4.91** was reduced to benzylic alcohol **4.134** with BH_3•$S(CH_3)_2$ in 99% yield. Halogenation of the alcohol with triphenylphosphine and NBS gave the benzylic bromide **4.135** in 78% yield. The use of phosphorus tribromide in this transformation consistently resulted in a yield of no more than 50%, despite full conversion of the starting material. As the reaction was also relatively free of impurities following a simple aqueous work-up, it is likely the side-products were water soluble,

although they were not characterized or further investigated. Nucleophilic substitution of the bromide with cyanide, hydrolysis and esterification provided the phenylacetate **4.137**. Grignard addition into ester **4.137** gave tertiary iodoalcohol **4.138** in 60% (74% brsm) yield along with minor amounts of ketone **4.139**. To prevent enolization of the ester **4.137** or intermediate **4.139**, the organocerium reagent was prepared in situ before the addition of the ester. Using 3.0 equivalents of CH_3MgBr and 2.2 equivalents of $CeCl_3$ gave the desired product **4.138** in 91% yield. The same synthetic sequence was used to prepare the analogous iodoalcohol **4.140** without the ortho methyl group.



Scheme 4-38. The synthesis of the ortho-methyl iodoalcohol precursor to the six-membered fluoro- and chloro-iodanes.

In summary, various synthetic strategies and routes were used to prepare nine iodoalcohol precursors (Figure 4-10). The size of the ortho group was varied (methyl, **4.93** vs. isopropyl, **4.112** vs. *tert*-butyl, **4.133**) while maintaining similar electronic properties, and with differing electronic properties (methyl, **4.93** vs. bromine, **4.97** vs. methoxy, **4.107**). Additionally, the length of the linking arm was homologated by one carbon (**4.93** vs **4.138**).

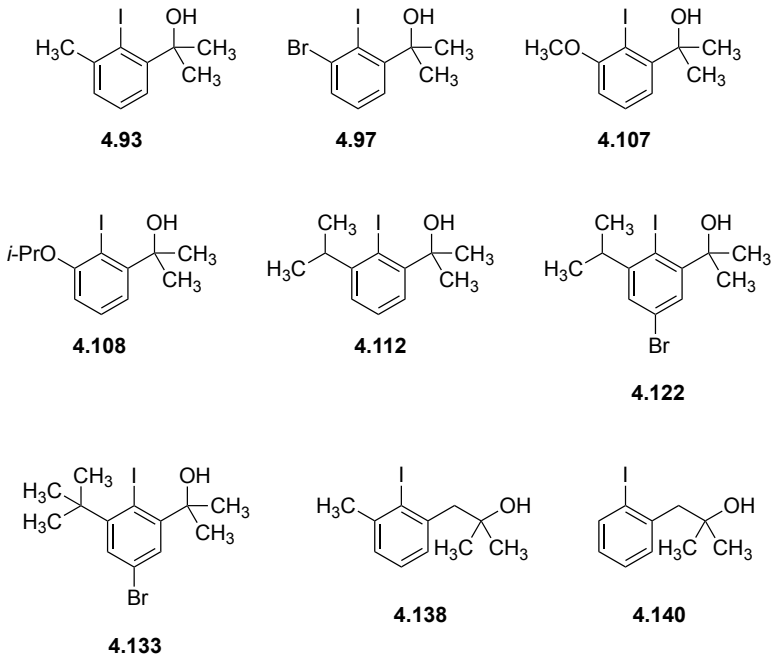


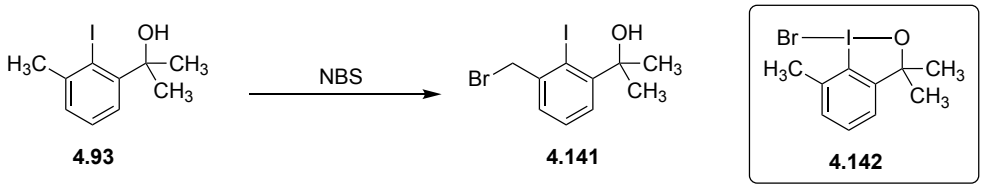
Figure 4-10. Summary of iodoalcohol precursors synthesized.

4.2.2 Oxidation of the Iodoalcohols to Hypervalent Iodine Species

The fluoro- and chloroiodanes were prepared by multiple different methods, chosen for their expediency, and in most cases remain unoptimized for product yield. As such, synthetic methods from the literature were explored and modified as required. The goal of the project was to compare the torsion angle with the size of the ortho substituent, and eventually relate both to the reactivity of the reagent. Therefore, the synthetic goal was to simply obtain enough material to grow a crystal of high enough quality for structure determination by single crystal X-ray diffraction.

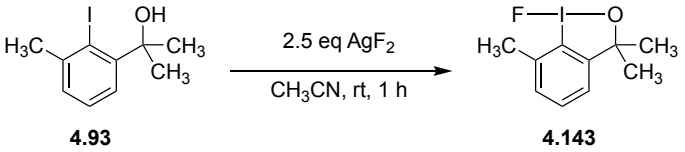
The conversion of the ortho-methyl iodoalcohol **4.93** to the ortho-methyl fluoroiodane **4.143** was first attempted *via* the route used by Stuart (Scheme 4-2, B).[182] Unfortunately, instead of isolating the desired bromoiodane **4.142** from the first step – likely an orange crystalline solid – a dark oil was obtained (Scheme 4-39). Analysis of the crude ^{1}H-NMR revealed a peak at ~4.4 ppm which is characteristic of a benzyl bromide such as **4.141**. Although this was not investigated further, one possible explanation for this product would be the in situ generation of the bromoiodane **4.142** and immediate reaction with either the tolyl group of another bromoiodane **4.142** molecule or the tolyl group of the starting material **4.93**. Direct bromination of the tolyl group by NBS is unlikely as the

conversion of toluene to benzyl bromide with NBS typically requires irradiation, heat or a chemical radical generator.[257]



Scheme 4-39. Attempted preparation of bromoiodane **4.142**.

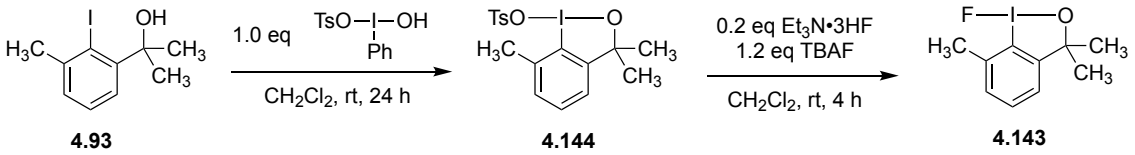
The method of Zhang et al. with AgF_2 was employed and gave the desired ortho-methyl fluoroiodane **4.143** (Scheme 4-40). Both the ^{1}H-NMR and ^{13}C-NMR spectra were consistent with expectation, but the ^{19}F-NMR was significantly different than the ^{19}F-NMR of the fluoroiodane **4.2**. The fluorine in **4.2** is represented by a sharp peak in the ^{19}F-NMR spectrum with a chemical shift of -142 ppm. The ortho-methyl fluoroiodane **4.143** on the other hand – synthesized by this method – has a weak broad peak at -105 ppm. The difference in chemical shift might be explained by the position of the fluorine in **4.143** (discussed further in Section 4.3). The fluorine in **4.143** is above (or below) the plane of the aromatic ring, compared to in the plane with **4.2**, and therefore experiences different ring anisotropic effects. The peak broadening is hypothesized to be due to remaining silver ions which were not entirely removed in the purification by filtration. Consequently, the exchange of the silver ions between molecules of **4.143** on an NMR timescale would lead to broad peaks.



Scheme 4-40. The successful synthesis of ortho-methyl fluoroiodane **4.143**.

To determine whether peak broadening was characteristic of ortho-substituted fluoroiodanes or due to residual silver, a second synthetic route to the fluoroiodane was attempted (Scheme 4-41). Treatment of the iodoalcohol with an equimolar amount of Koser's reagent gave the tosyl iodane **4.144**. Hypothetically, the mixture of the iodoalcohol and Koser's reagent slowly equilibrates to the cyclic and

thermodynamically more stable species **4.144**, a tosyl iodane. The tosyl iodane was then treated with TBAF and Et_3N•3HF to facilitate a ligand swap to afford the desired fluoroiodane **4.143**.



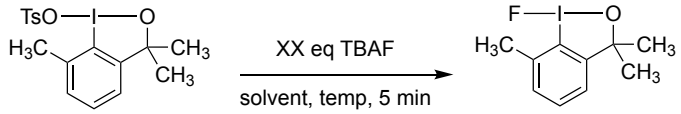
4.93 **4.144** **4.143**

Scheme 4-41. An alternative synthetic route to the fluoroiodane **4.143** without silver.

The ^{1}H-NMR spectrum of the fluoroiodane synthesized by this two-step method matched that of the fluoroiodane synthesized by AgF_2. The ^{19}F-NMR spectrum had an identical chemical shift value however the peak was sharp. This observation is consistent with the conclusion that residual silver remained in the first sample. A crystal of X-ray crystallography quality was grown from the product of the AgF_2 method by slow diffusion and evaporation of layered hexanes and dichloromethane. The second method, in our hands, gave a reagent with higher purity by NMR, free of silver ions. Silver was employed as a catalyst in multiple different transformations with **4.2** (e.g., Scheme 4-4 and Scheme 4-7). Therefore, ensuring the reagent is free of silver ions is crucial when comparing the reactivity of the different derivatives or synthetic batches.

The reaction conditions of alternative synthesis, using TBAF and tosyl iodane, were further explored in Table 4-4. As previously shown the iodoalcohol can be converted to the tosylate by treatment with Koser's reagent for 24 hours at room temperature. Ligand exchange with a source of anionic fluorine provided the fluoroiodane **4.143**. This type of ligand exchange reactivity had previously been demonstrated by both Murphy and Stuart.[182, 192] The addition of 0.95 and 1.2 equivalents of TBAF (1 M in THF) to the tosylate **4.144** gave the fluoroiodane cleanly in 54 and 69% yield, respectively (Table 4-4, Entry 1 and 2). Further increasing the equivalents to 2.5 did not improve the yield and instead gave a complex crude reaction mixture, which included the fluoroiodane (Table 4-4, Entry 3). Reducing the reaction temperature to 0 °C decreased the yield to 65% (Table 4-4, Entry 4). Changing the solvent to either toluene (68%) or ether (63%) did not improve the yield (Table 4-4, Entry 5 and 6). Overall, treatment of **4.144** with 1.2 equivalents of TBAF in hexanes at room temperature gave the highest yield, although changing the reaction temperature to 0 °C or solvent to toluene provided comparable yields.

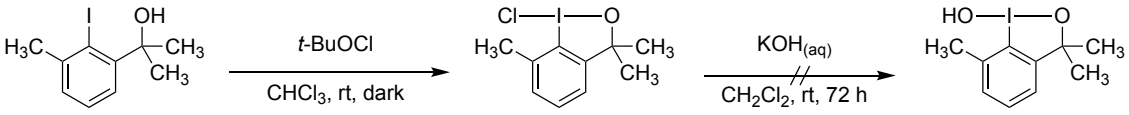
Table 4-4. Optimization of ligand exchange synthesis of the fluoroiodane.



4.144 **4.143**

Entry	Equivalents of TBAF	Solvent	Temperature	Crude yield (%)
1	0.95	hexanes	rt	54
2	1.2	hexanes	rt	69
3	2.5	hexanes	rt	58
4	1.2	hexanes	0 °C	65
5	1.2	Et_2O	rt	63
6	1.2	toluene	rt	68

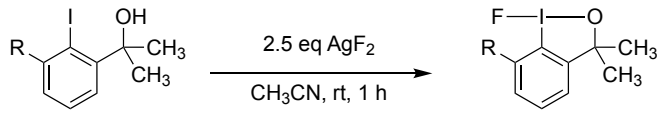
The chloroiodane **4.145** was synthesized by treating **4.93** in the absence of light with freshly prepared *t*-BuOCl. The reaction progressed from clear, to yellow and finally to orange. Removal of the solvent revealed a yellow solid which was recrystallized from acetonitrile to provide crystals of high enough quality for structure determination by single crystal X-ray diffraction. Oxidation of **4.93** with TCICA using the method of Togni was unsuccessful on a small scale (< 1 mmol) and significantly lower yielding on a large scale (compared to the preparation of the unsubstituted version **4.3**).[190] The parent chloroiodane **4.3** can be easily hydrolyzed with $KOH_{(aq)}/CH_2Cl_2$ in 59% yield in only 3 hours.[258] Monitoring the reaction by visual inspection is normally possible as the yellow colour (chloroiodane) dissipates and eventually disappears when the reaction is complete, as pure hydroxy iodane (e.g., **4.146**) is typically white. Chloroiodane **4.145** was stable under identical reaction conditions for 72 hours after which it was recovered by way of aqueous work-up. Chloroiodane **4.145** is seemingly more stable (vs. **4.3**), contrary to the initial hypothesis of increasing reactivity by introducing ortho-substitution.



4.93 **4.145** **4.146**

Scheme 4-42. Preparation of the chloroiodane **4.145**.

The ortho-bromo, -methoxy, and -isopropoxy derivatives of the fluoroiodane were all successfully synthesized with AgF_2 (Scheme 4-43). Again, the ^{19}F-NMR of all three fluoroiodanes exhibited various degrees of peak broadening. The second synthetic method using TBAF was not attempted on these iodoalcohols. Crystals of each fluoroiodane were grown by slow evaporation and the structure was determined by single crystal X-ray crystallography. Preparation of the corresponding chloroiodanes with *tert*-butyl hypochlorite was also attempted. However, instead of obtaining the desired solid products, a complex mixture of unidentified products was obtained as yellow oils. Purification of the desired chloroiodanes from these mixtures was unsuccessful. The preparation of potentially reactive hypervalent iodine species, such as chloroiodanes, always introduces the pitfall of self-reactions. Theoretically, the generation of a reactive chloroiodane may chlorinate the remaining starting material (e.g., via electrophilic aromatic substitution) or otherwise lead down undesired reaction pathways. This is hypothetically most problematic when preparing chloroiodanes with electronically rich aromatic systems (e.g., **4.107**, **4.108**).



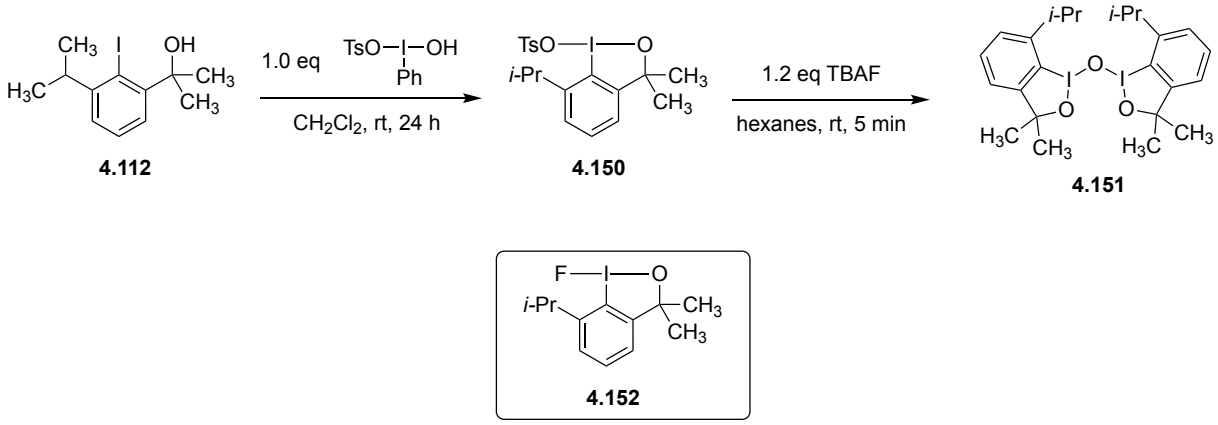
4.97, R = Br
4.107, R = OCH_3
4.108, R = O*i*-Pr

4.147, R = Br
4.148, R = OCH_3
4.149, R = O*i*-Pr

Scheme 4-43. Preparation of the ortho-bromo, -methoxy, and -isopropoxy fluoroiodanes.

Application of the AgF_2 method to the oxidation and fluorination of the ortho-isopropyl derivative **4.112** was unsuccessful and only the starting material was recovered, as opposed to the desired fluoroiodane **4.152**. Instead, oxidation and tosylation were carried out with Koser's reagent to provide **4.150** in 71% yield (Scheme 4-44). Attempted displacement of the tosyl group with reaction conditions established in Table 4-4 appeared by ^{19}F-NMR to provide the desired product **4.152**. However, the compound which was crystallized from the crude reaction was not the desired fluoroiodane **4.152**, but instead an oxo-bridged dimer **4.151**. This structure was confirmed by single crystal X-ray crystallography (Figure 4-11). This type of oxo-bridged hypervalent iodine dimer was previously reported in the literature, where the source of the oxygen in the dimer was determined to be water.[259] In our experiments, it appeared the fluoroiodane was initially formed, and as such there are two possible origins for dimer **4.151**. One possibility is that it was formed during the reaction, as no precautions for

the exclusion of moisture were taken, and it was preferentially crystallized from the crude mixture. Alternatively, during the recrystallization process, the fluoroiodane **4.152** degraded into the dimer **4.151**. Ultimately, the desired fluoroiodane **4.152** was not crystallized.



Scheme 4-44. Attempted synthesis of the isopropyl fluoroiodane **4.152**.

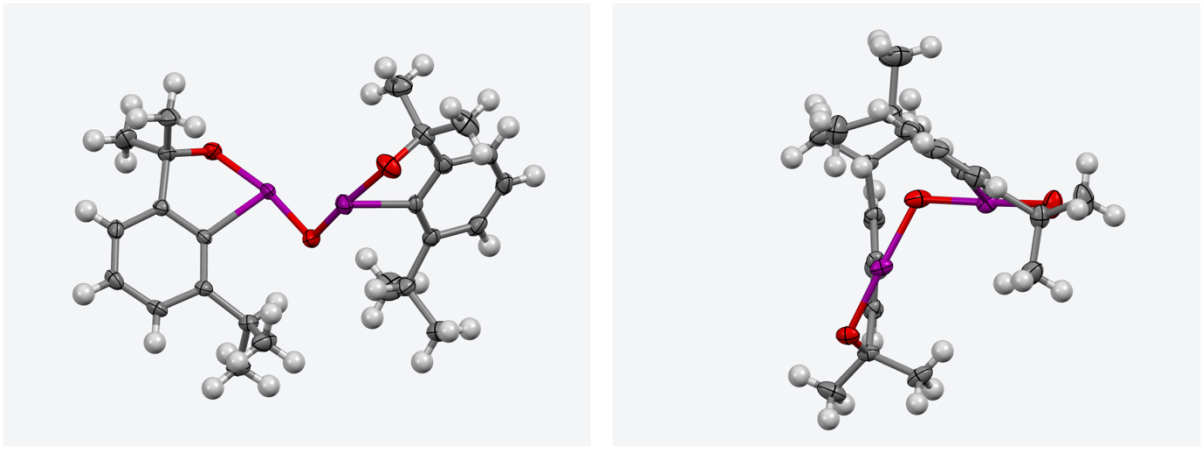
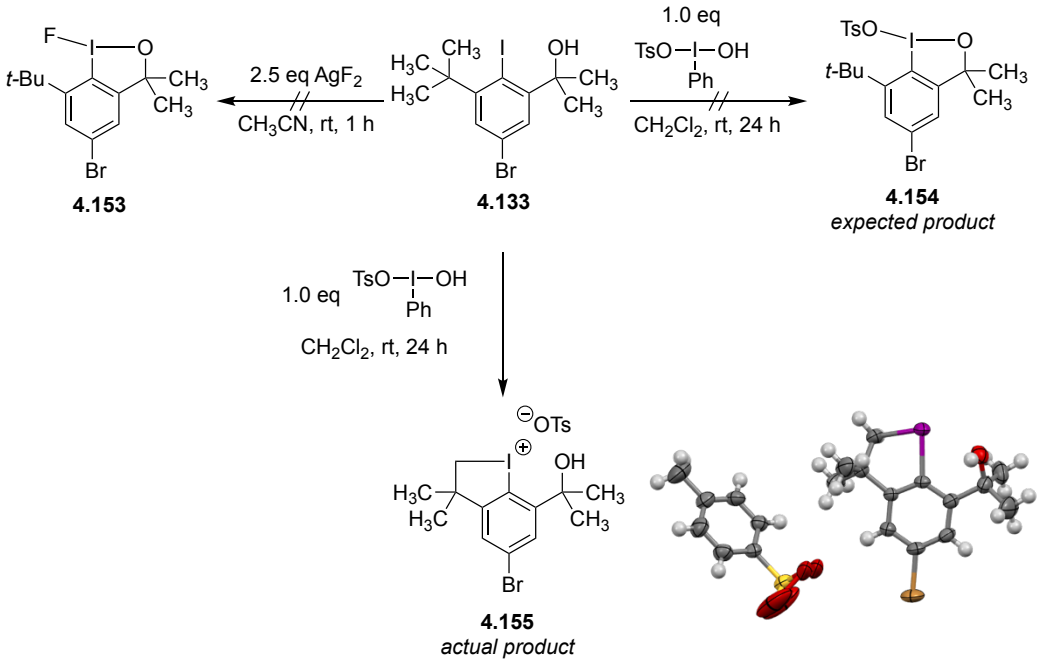


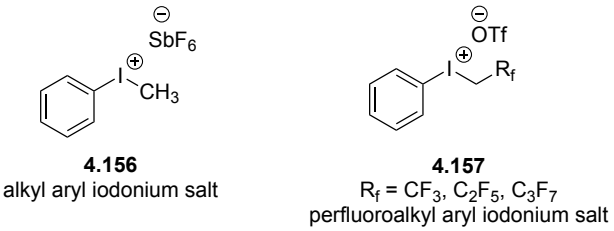
Figure 4-11. X-ray crystal structure of the ortho-isopropyl dimer **4.151**.

Similar synthetic difficulties were encountered when trying to prepare the more sterically hindered tert-butyl fluoroiodane **4.153**. Again, AgF_2 didn't successfully oxidize the iodoalcohol **4.133** to the desired fluoroiodane (Scheme 4-45). A single one-hour reaction produced traces of the desired product, which was detected by ^{19}F-NMR. However, this result was not reproducible, and the same result was never achieved a second time. Increasing the reaction time to five hours gave no product and only unreacted starting material. Instead, the tosylation/fluorination sequence was explored. Oxidation of

4.133 with Koser's reagent cleanly afforded a white solid as expected; however, unexpectedly, the ^{1}H-NMR spectra did not have three aliphatic singlets in a 3:6:9 ratio (expected product **4.154**, Scheme 4-45), but instead in a ratio of 3:6:6. This observation suggested an unexpected reaction had occurred at one of the methyl groups of the *tert*-butyl group. Further corroborating this structure was an additional singlet at 4.42 ppm with an integral of 2. The structure of the compound was assigned to be **4.155** by 1D and 2D NMR experiments and confirmed by single crystal X-ray crystallography. The tosylate salt was represented as having four oxygens bonded to the central sulfur atom. This was due to one oxygen atom occupying a different position amongst alternating unit cells. To our knowledge, this constitutes the first synthesis of an alkyl aryl iodonium salt which is stable at room temperature. Previously, acyclic alkyl aryl iodonium species were characterized at -80 °C and determined to be stable up to -20 °C (e.g., **4.156**, Figure 4-12).[260] If the alkyl chain is perfluorinated the compounds are stable at room temperature and useful synthetic reagents (e.g., **4.157**, Figure 4-12).[261]



Scheme 4-45. Attempted synthesis of fluoroiodane **4.153** and discovery of interesting alkyl aryl iodonium **4.155**.

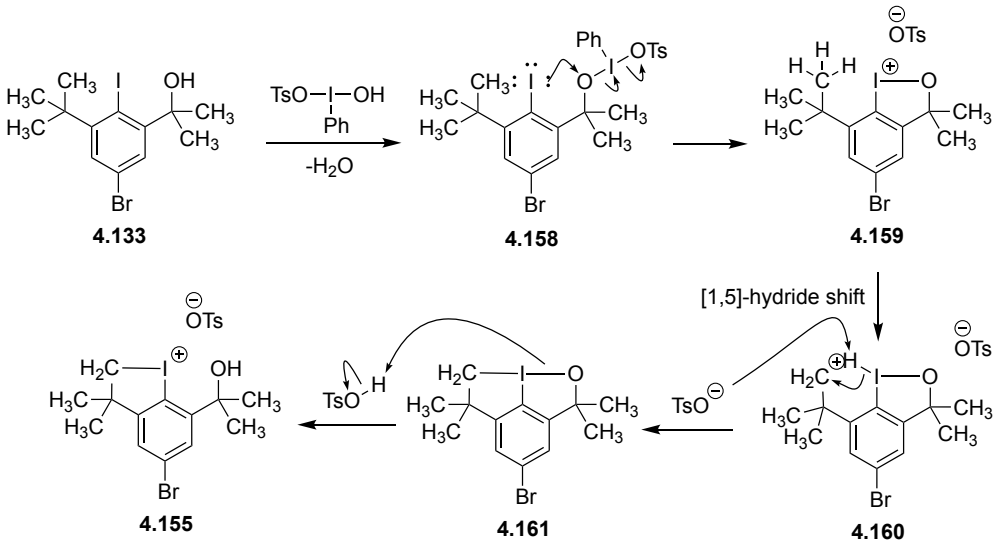


4.156
alkyl aryl iodonium salt

4.157
R_f = CF_3, C_2F_5, C_3F_7
perfluoroalkyl aryl iodonium salt

Figure 4-12. Alkyl aryl iodonium salts.

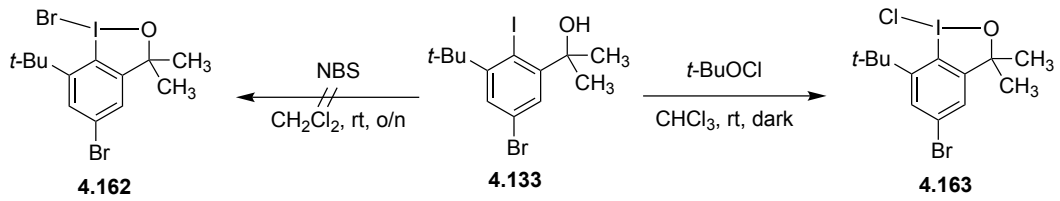
The mechanism for the formation of this product is likely a radical process as a C-H abstraction must theoretically occur to furnish the observed product **4.155**. Typically, direct oxidation of methyl groups by Koser's reagent is not observed. Ultimately, it was difficult to propose a mechanism which did not involve the generation of a primary carbocation or primary carbon-centred radical. Either mechanism likely begins with the generation of **4.158** from **4.133** and Koser's reagent by exchange of the alcohol and the hydroxyl group (Scheme 4-46). Perhaps iodine then attacks the oxygen to eliminate iodobenzene and tosylate to generate **4.159**. A 1,5-hydride shift could furnish **4.160**, and after a series of proton exchanges, the final product **4.155**. A radical mechanism could be drawn in much the same manner, where **4.158** is converted through to the product with a series of single-headed arrows. Experimental evidence would be needed to support either mechanism. Nonetheless, this unexpected reactivity precludes this synthetic pathway from being a viable route to the desired fluoroiodane product **4.153**.



4.133 **4.158** **4.159** **4.160** **4.161** **4.155**

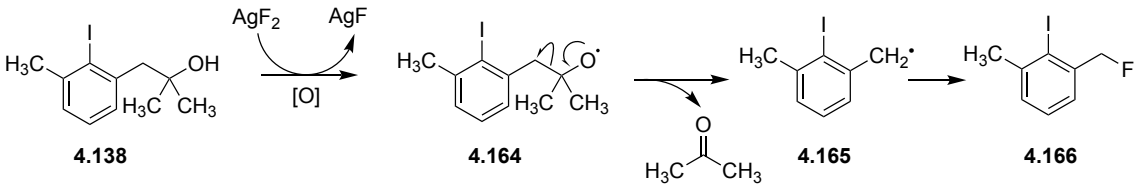
Scheme 4-46. An ionic mechanism for the formation of **4.155**.

Two additional synthetic routes were explored. Firstly, the route originally proposed by Stuart (Scheme 4-2, B) was investigated. However, the synthesis of the fluoroiodane **4.153** via the bromoiodane **4.162** was abandoned as treatment of the iodoalcohol **4.133** with NBS returned only the starting material after stirring overnight (Scheme 4-47). A fourth method was to first chlorinate and then attempt a ligand exchange with fluorine (Scheme 4-47). Chlorination was successful. Treatment of **4.133** with *t*-BuOCl gave a yellow solid which was recrystallized from CH_2Cl_2/hexane to give high-quality crystals of **4.163** with which an X-ray crystal structure was obtained. Although some crystals were successfully collected for analysis there was significant decomposition over time at room temperature. The crystals slowly liquidified under ambient conditions. The compound may not be stable under ambient conditions and was likely decomposing to byproducts which were liquid at room temperature. The investigation of the final ligand exchange with fluoride is in progress, and as such the synthesis of fluoroiodane **4.153** is yet to be completed.



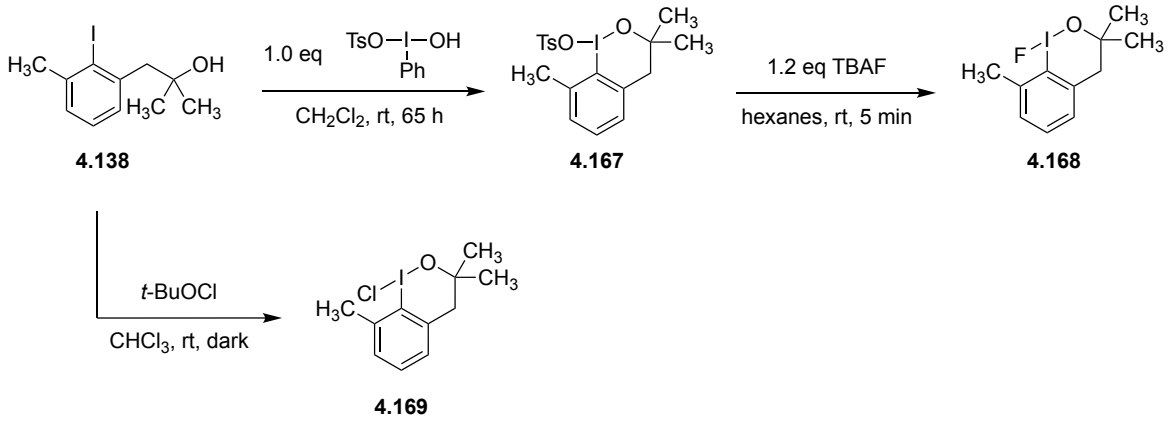
Scheme 4-47. Additional synthetic routes to **4.153** which were explored.

Oxidation of **4.138** with AgF_2 did not produce the desired product **4.168** but instead gave **4.166** (Scheme 4-48). According to the authors in the original publication of this AgF_2 method, the mechanism by which this reaction functions is first the oxidation of the alcohol to the alkoxy radical (e.g., **4.164**), followed by the formation of the 3c-4e bond with a fluorine atom. With **4.138** the first step is presumably the same; however, acetone is likely eliminated to give the benzyl radical **4.165** (Scheme 4-48). This radical can subsequently be trapped by fluorine to give the benzyl fluoride **4.166**. Treatment of alcohol **4.138** with SelectFluor™, according to the procedure of Legault, was equally unsuccessful.[189]



Scheme 4-48. Proposed decomposition of **4.138** when treated with AgF_2.

Given this decomposition pathway and the successful application of the tosylation-ligand exchange sequence to the above derivatives, this method was explored with **4.138**. Oxidation of the iodoalcohol **4.138** with Koser's reagent for 65 hours then treatment with TBAF provided the six-membered fluoroiodane **4.168** (Scheme 4-49). The five-membered variants (especially the parent fluoroiodane) are soluble in hexanes (dilute or hot) and will precipitate on cooling to room temperature or 0 °C. The six-membered variant **4.168** was much more soluble in hexanes at room temperature and any attempt to recrystallize the crude mixture resulted in an oil without any solid crystals present. The fluoroiodane **4.168** was successfully recrystallized from the crude reaction mixture by slow evaporation of CH_2Cl_2/pentanes at room temperature. The corresponding chloroiodane **4.169** was uneventfully prepared by the same method used previously (*tert*-butyl hypochlorite).



Scheme 4-49. Synthesis of the six-membered ortho-methyl fluoroiodane and chloroiodane.

Overall, a variety of synthetic methods to prepare the fluoroiodanes were explored. The ortho-methyl, -bromo, -methoxy, -isopropoxy derivatives, as well as the six-membered fluoroiodane were all successfully prepared. The tosylation-ligand exchange synthetic method is scalable, yields the purest final product, and is applicable across most of the derivatives explored. Difficulties in preparing the

fluoroiodanes were encountered with the most sterically hindered derivatives (e.g., isopropyl and tert-butyl) and as such this synthetic work is ongoing. Three of the desired chloroiodanes were prepared (ortho-methyl, -tert-butyl, and six-membered). The successful synthesis of these above-mentioned compounds allowed for further analysis of the structures by X-ray crystallography.

4.3 Analysis of Single Crystal X-ray Structures and Preliminary Reactivity

As expected, all synthesized fluoroiodanes had larger torsion angles than the parent fluoroiodane **4.2**. When substituted with a methyl, methoxy, isopropoxy, or bromide the torsion angles were 18.2°, 22.6°, 19.6°, and 26.6°/28.2°, respectively (Table 4-5, Entries 1-5). As the fluoroiodanes **4.152** and **4.153** were not prepared no torsion angle is reported. When the sidearm tether (Table 4-5, Entry 8) was extended by a single methylene group the torsion angle was significantly larger at 54.9°. A similar result is observed for the chloroiodane series, although fewer chloroiodanes were prepared, comparison of the parent compound **4.3** to the ortho-methyl substituted chloroiodane saw an increase in torsion angle to 30.1° (Table 4-5, Entry 1 vs. 2). Comparing the ortho-methyl fluoro- and chloroiodanes one can see that the chloro derivative (larger halogen) has a larger angle. This is a result consistent with what one might expect from an analysis based on steric hindrance. The crystal structures are visualized in Figure 4-13 to Figure 4-20. Comparing A-values with the obtained torsion angles, it is clear no positive correlation exists (i.e., larger A-value = larger torsion angle). Instead, a negative correlation exists; counterintuitively, as the A-value increases, the torsion angle decreases. For example, in the chloroiodane series, when R = *t*-Bu (A-value = 4.7 kcal/mol) the torsion was 14.7°, while it was 30.1° when R = CH_3 (A-value = 1.74 kcal/mol) (Table 4-5, entry 7 vs. 2). Based on this data, the A-value of the substituent is not a reliable predictor for the magnitude of the torsion angle.

Table 4-5. Torsion angles (°) from the crystal structures of fluoro- and chloroiodanes.

Entry	Substitution (R =)	A-value (kcal/mol)[b, 262]	Torsion angle (XICC) (°)	
			X = F	X = Cl
1	H, reported in the literature[185, 189]	-	8.8, 8.2	6.1
2	CH_3	1.74	18.2	30.1
3	OCH_3	0.63	22.6	-
4	O*i*-Pr	-	19.6	-

Entry	Substitution (R =)	A-value (kcal/mol)[b, 262]	Torsion angle (XICC) (°)	
			X = F	X = Cl
5	Br	0.48-0.67	26.6, 28.2	-
6	*i*-Pr	2.21	-	-
7	*t*-Bu	4.7	-	14.7
8	CH_3[a]	1.74	54.9	59.3

[a]Six-membered side arm ring. Compounds **4.168** and **4.169**. [b]- = not available or not determined.

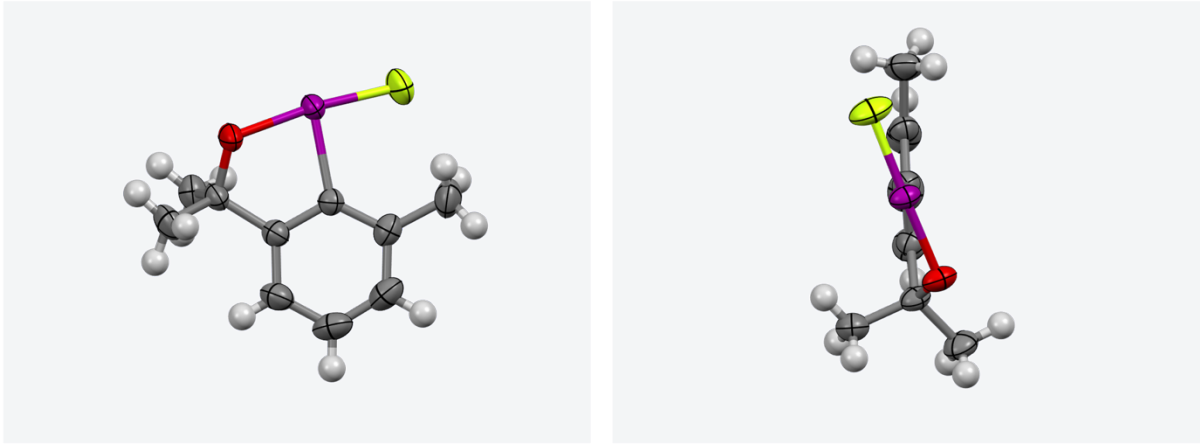


Figure 4-13. Side-on and top-down views of the crystal structure of the fluoroiodane **4.143** (R = CH_3).

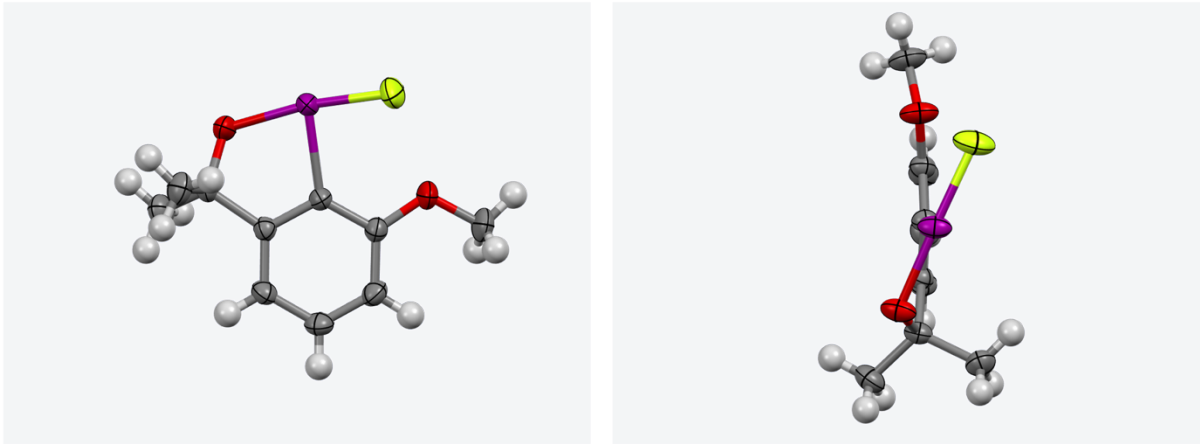


Figure 4-14. Side-on and top-down views of the crystal structure of the fluoroiodane **4.148** (R = OCH_3).

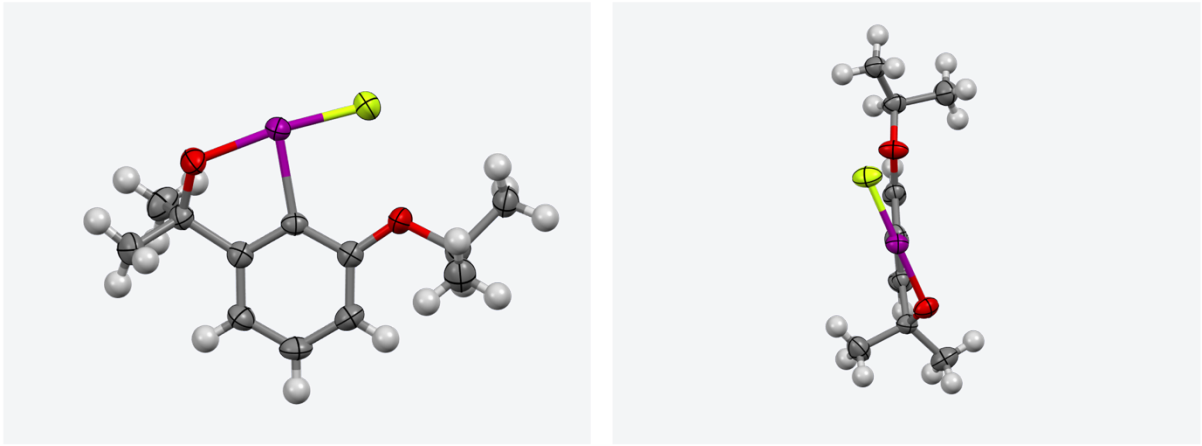


Figure 4-15. Side-on and top-down views of the crystal structure of the fluoroiodane **4.149** (R = O*i*-Pr).

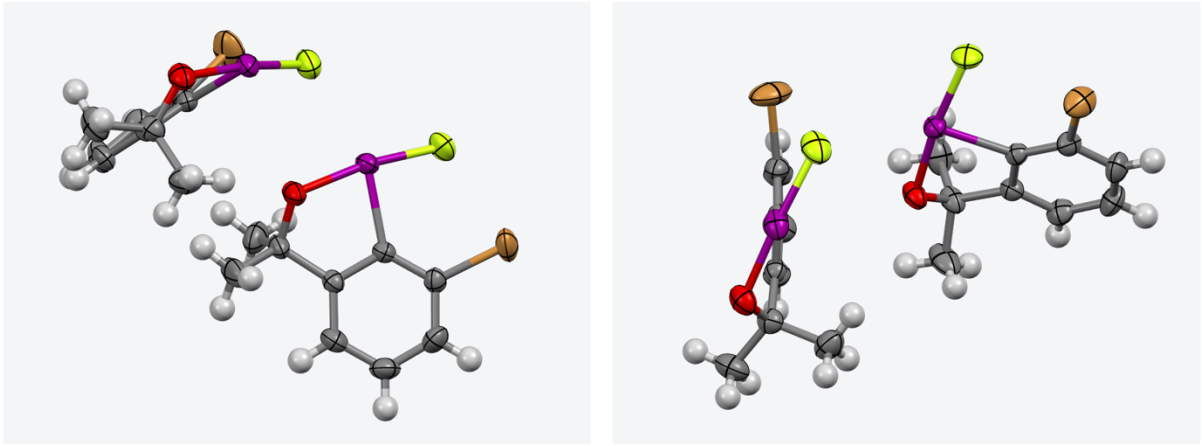


Figure 4-16. Side-on and top-down views of the crystal structure of the fluoroiodane **4.147** (R = Br).

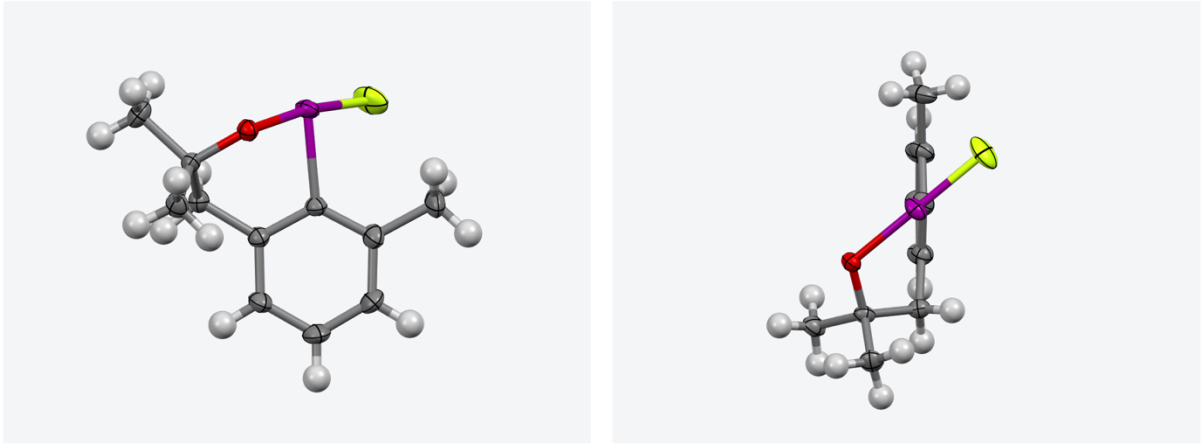


Figure 4-17. Side-on and top-down views of the crystal structure of the fluoroiodane **4.168** (R = CH_3).

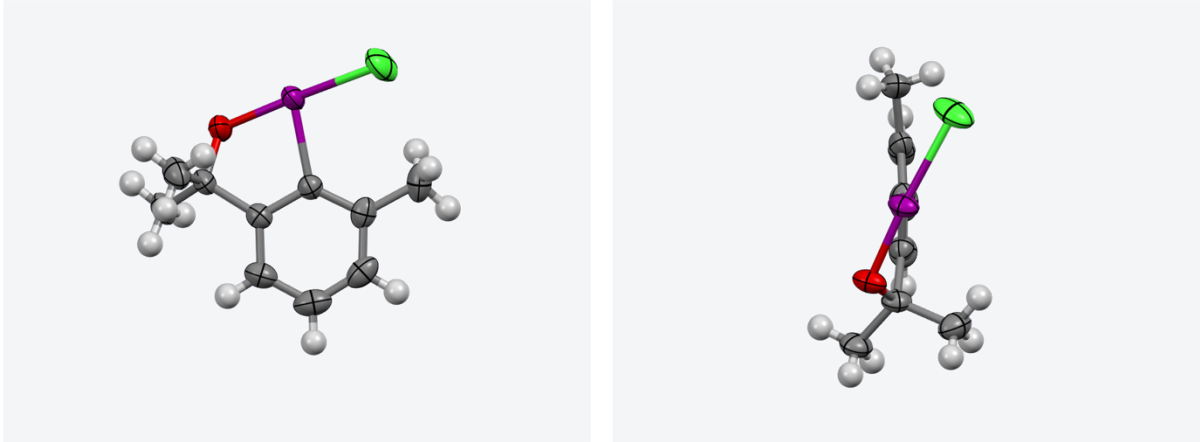


Figure 4-18. Side-on and top-down views of the crystal structure of the chloroiodane **4.145** (R = CH_3).

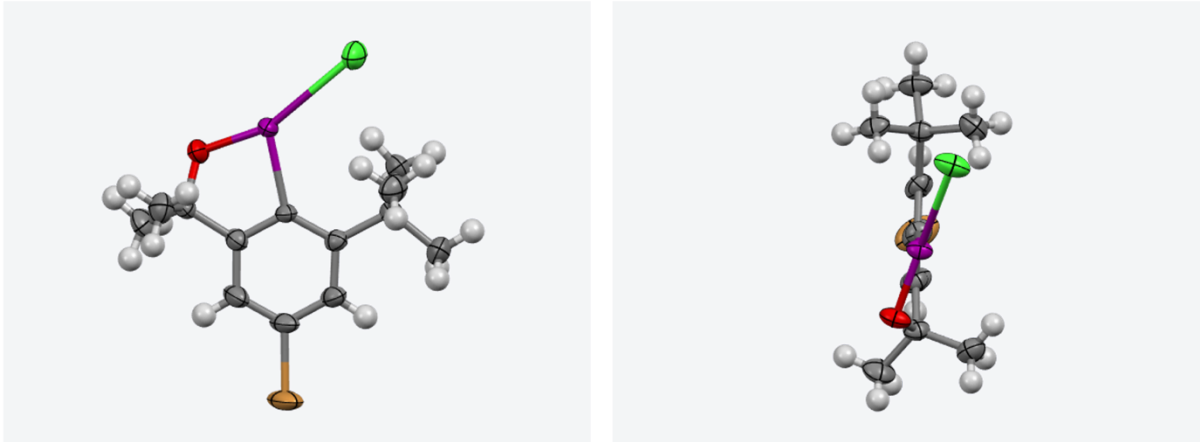


Figure 4-19. Side-on and top-down views of the crystal structure of the fluoroiodane **4.163** (R = *t*-Bu).

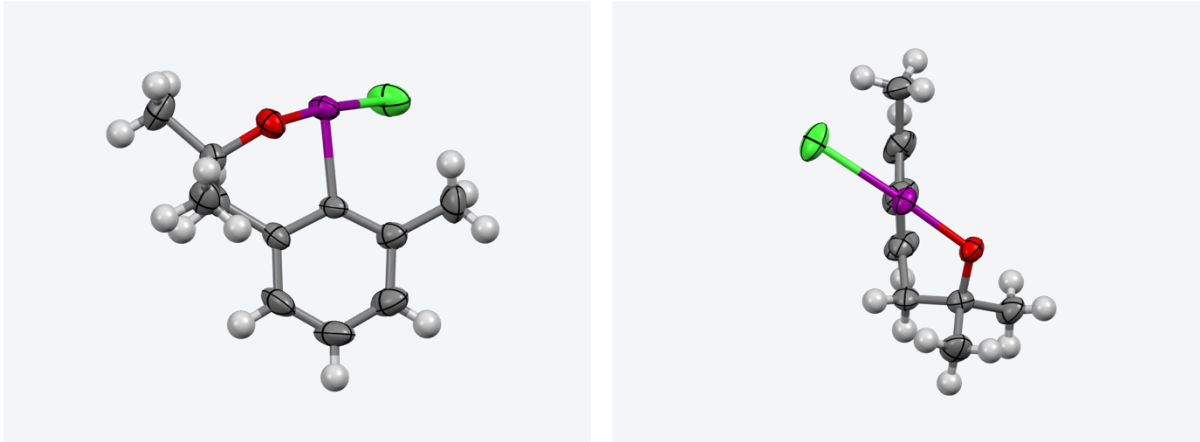


Figure 4-20. Side-on and top-down views of the crystal structure of the fluoroiodane **4.169** (R = CH_3).

The packing structures are similar in fluoroiodanes **4.2** (R = H), **4.143** (R = CH_3), **4.148** (R = OCH_3), and chloroiodane **4.3**, where there are short contacts between the I-O of one molecule with the O-I bond of another (Figure 4-21). The isopropoxy derivative has secondary F-I interactions, as opposed to the I-O interactions, possibly to minimize the steric hindrance between nearby isopropoxy substituents and the isopropoxy sidearm. This is again observed with the ortho-bromo derivative **4.147**. The six-membered fluoro-derivative also forms contacts between the I-F and the corresponding F-I of another molecule, as does the six-membered chloroiodane compound.

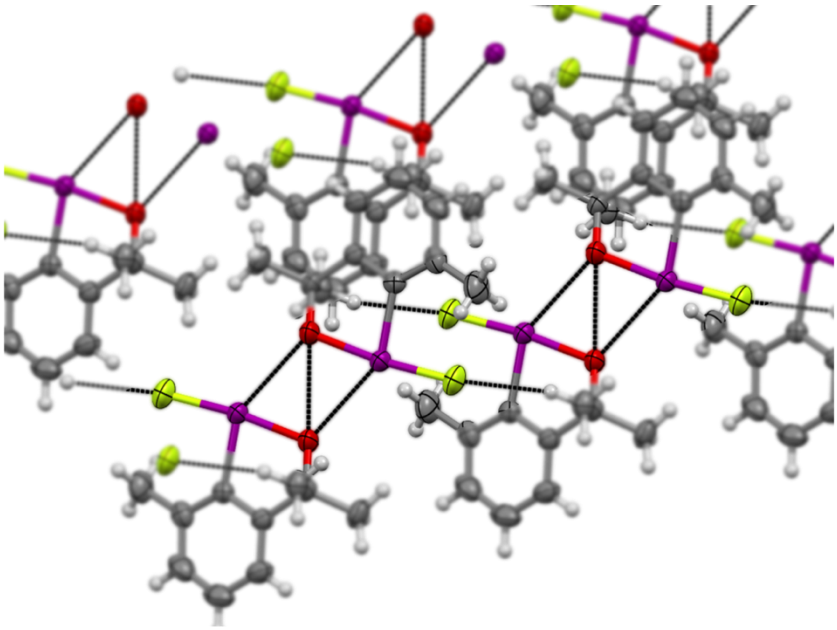


Figure 4-21. Example of the packing in fluoroiodane **4.2**.

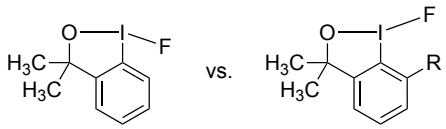
When compared to the parent fluoroiodane **4.2,** the F-I, I-C, and I-O bond lengths of the ortho-substituted fluoroiodanes are all nearly identical (Table 4-6). The percent difference is never more than 3% and on average only 0.7%. Although still minimal, slightly larger differences are seen in the F-I-O and F-I-C angles (Table 4-6). Generally, these differences in the crystal structure can be visualized as the fluorine pointing "down" (R = H) or pointing "up" (R = CH_3, OCH_3, O*i*-Pr, Br) (Figure 4-22). "Down" should be understood as the I-F bond being angled towards the aromatic ring (e.g., **4.2-down**), while "up", understood as the I-F bond pointing away from the aromatic ring (e.g., **4.2-up**). To relieve the steric interactions between the fluoride (or chloride) and the ortho substituent, it appears it was more

energetically favourable to orient the fluoride (or chloride) "up", as opposed to increasing the magnitude of the torsion angle. The isopropyl and tert-butyl fluoroiodanes are not included in the table as they were not successfully prepared. The six-membered derivative did not have any significant deviations beyond the already mentioned torsion angle.

Table 4-6. Bond lengths and angles about the hypervalent bond of the various fluoroiodanes.

Compound #	R =	F-I	I-C	I-O	F-I-O (°)	F-I-C (°)	O-I-C (°)
4.2	H[a]	2.05	2.09	2.02	166.8	87.2	80.3
4.143	CH_3	2.05	2.12	2.03	173.2	93.2	80.1
4.148	OCH_3	2.05	2.11	2.04	172.3	93.4	79.3
4.149	O*i*-Pr	2.06	2.11	2.03	173.7	93.9	79.8
4.147	Br	2.05	2.11	2.01	170.5	92.0	79.7
4.168	CH_3	2.09	2.10	2.02	172.4	88.0	84.3

[a]Literature values.[189]
[b]Percent difference: green = greater than 1%, blue = greater than 5%



4.2-down **4.2-up**

Figure 4-22. Fluoroiodanes with the fluorine pointing "down" or "up". The angle is exaggerated for illustrative purposes.

In the chloroiodane series, the *ortho*-methyl derivative had very similar bond lengths and angles when compared to **4.3** with the largest difference being in the Cl-I-C angle (Table 4-7). The chlorine was pointing "up" to a larger degree with methyl substituent (See Figure 4-22 for an example of "up"). Of all the compounds prepared the *tert*-butyl chloroiodane had the largest structure differences from the parent compound. The Cl-I bond was significantly longer (2.55 vs. 2.99; 17%), and the Cl-I-C angle was significantly larger (91.5° vs. 118.3°; 29%). Visually, these differences can be seen in Figure 4-19. When visually comparing to all the other structures, the chlorine atom is much further from the iodine atom and it is pointed upwards. Further, when analyzing the packing structure there is a second chlorine atom in the vicinity of the iodine which is closer in space (Figure 4-23). Based on traditional

hypervalent iodine bonding the three atoms (Cl, I, O) which are approximately linear are assumed to belong to one molecule. Given that the Cl-I bond is longer than usual it is likely the iodine atom is more electropositive than a typical iodine(III) atom, and as such a second chlorine atom from another molecule interacts strongly in the solid state (Figure 4-23). Of all the fluoro and chloroiodanes compounds prepared, the ortho *tert*-butyl derivative is the most strikingly different. Again, with the six-membered derivative the bond lengths and angles were very similar and, in this case, never greater than 5% different. Generally, between both the fluoroiodanes and chloroiodanes, the most pronounced difference between the parent compound and the ortho-substituted derivative is the torsion angle.

Table 4-7. Bond lengths and angles about the hypervalent bond of the various chloroiodanes.

Compound #	R =	Cl-I	I-C	I-O	Cl-I-O (°)	Cl-I-C (°)	O-I-C (°)
4.3	H[a]	2.55	2.10	2.04	171.1	91.5	80.6
4.145	CH_3	2.55	2.13	2.05	175.3	99.0	79.0
4.163	*t*-Bu	2.99	2.17	1.97	160.7	118.3	81.0
4.169	CH_3	2.60	2.11	2.03	174.1	90.5	84.3

[a]Literature values.[185]
[b]Percent difference: green = greater than 1%, blue = greater than 5%.

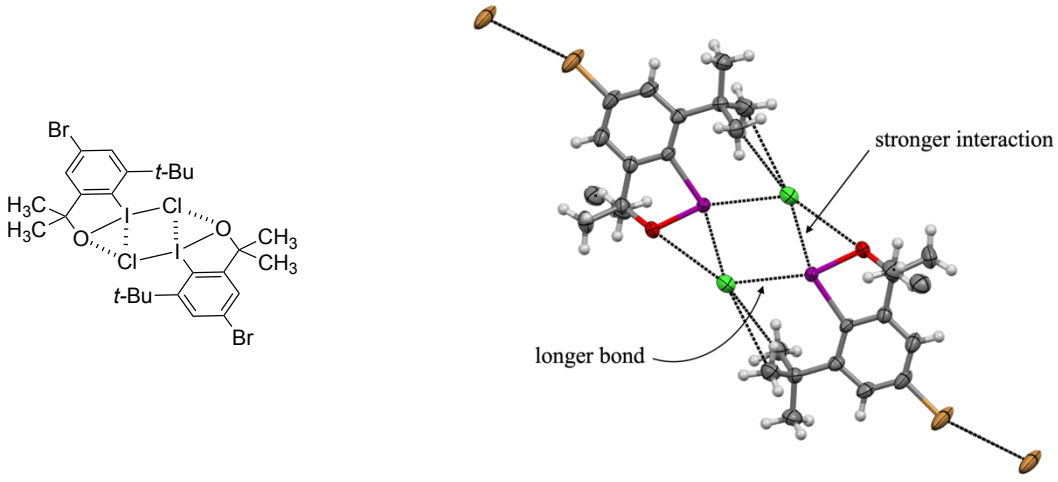
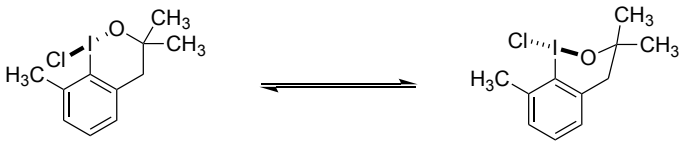


Figure 4-23. Short contacts in the crystal structure packing of the tert-butyl chloroiodane **4.163**.

Comparing the impact of the side arm length (e.g., **4.2** vs. **4.168**) and the ortho steric hindrance it is clear that side arm length has a larger impact. Again, increasing the steric bulk with a *tert*-butyl group (A-value, *t*-Bu = 4.7 kcal/mol vs. CH_3 = 1.74 kcal/mol) compared to a methyl group did not increase the torsion angle in the chloroiodane as originally proposed. Instead, the torsion angle was only 14.7° versus 30.1° in the ortho methyl chloroiodane. The addition of the extra methylene group to the sidearm had a larger effect than adding the additional steric bulk and increased the torsion angle to 59.3° (Table 4-5, Entry 8). Given that all the five-membered fluoroiodanes have roughly the same torsion angle, the torsion angle is likely near the limit based on the flexibility of the five-membered ring. The increased ring flexibility from the additional methylene unit in the six-membered derivatives, in combination with the steric hindrance imposed by the ortho methyl group, accounts for the much larger torsion angle observed. Further lengthening the tether may have a more profound effect on the torsion angle.

Interestingly, the ^{1}H-NMR spectrum of six-membered chloroiodane is temperature dependent and displays the coalescence of signals corresponding to the methylene and the *gem*-dimethyl groups with increasing temperature (12.5 °C to 50 °C) (Figure 4-24). This observation can be attributed to an equilibrium observable on an ^{1}H-NMR time scale. The exchange observed is likely the conformational "chair" flip of the six-membered ring (Scheme 4-50). The process to convert between **4.169a** and **4.169b** requires enough energy to overcome the steric interactions between the ortho-methyl group and the chlorine atom.



4.169a **4.169b**

Scheme 4-50. Dynamic exchange proposed to occur at higher temperatures with chloroiodane **4.169**.

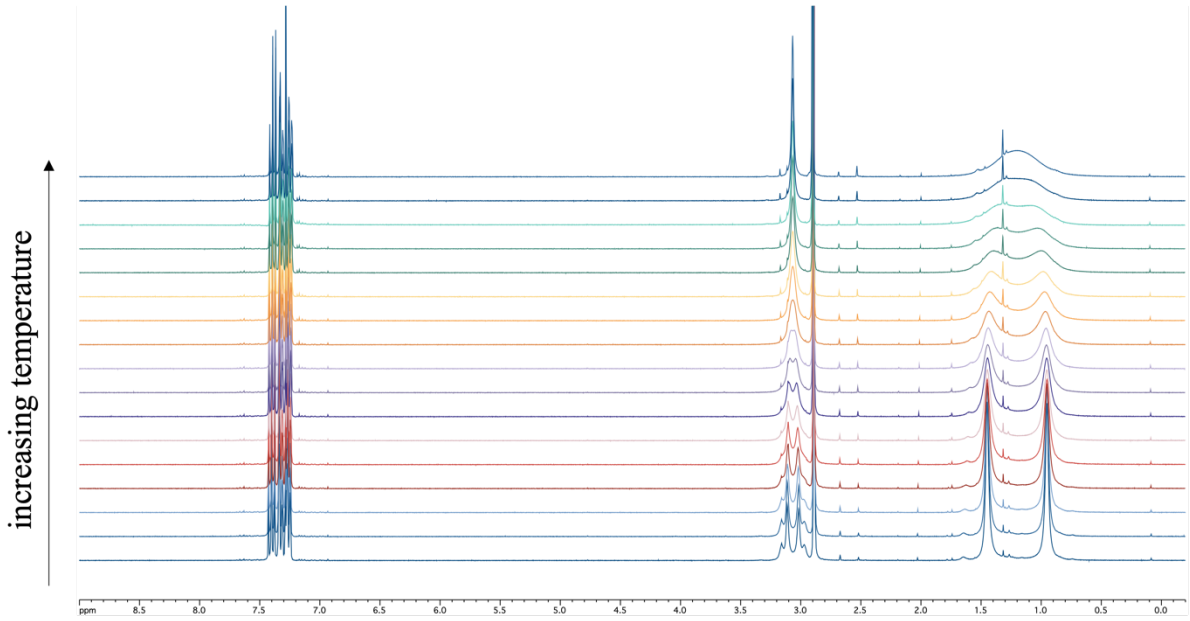


Figure 4-24. Variable temperature ^{1}H-NMR of chloroiodane **4.169** from 12.5 °C to 50 °C in 2.5 °C increments.

If the assumption of a dynamic process is taken to be true one can calculate the energy barrier for this exchange using the following equations:

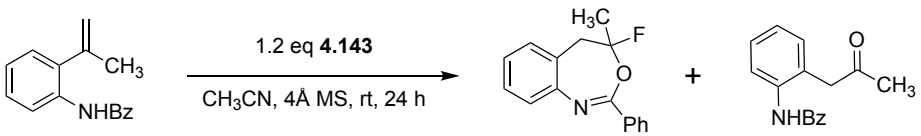
$$k_{exch} = \frac{k_b \bullet T_c}{h} e^{\frac{-\Delta G^{\ddagger}}{RT_c}} \qquad \text{Eq. (1)}$$

$$k_{exch} = \frac{\pi \bullet \Delta\nu}{\sqrt{2}} \qquad \text{Eq. (2)}$$

Where, k_{exch} is the rate of exchange; k_b is the Boltzmann constant; T_c is the coalescence temperature; $\Delta G^{\ddagger}$ is the Gibbs free energy of the exchange barrier; R is the gas constant; $\Delta\nu$ is the difference in chemical shift in Hertz. Extracting the data from this series of spectra and using Equations 1 and 2 the energy barrier is calculated to be 15.0 kcal/mol for the methyl groups and 16.1 kcal/mol for the benzylic methylene (Figure 4-24). Given that both groups are part of the same process one would expect the energy barrier to be identical. The difference in the values is likely due to the resolution of the data collected. This result is slightly larger than the 10.8 kcal/mol necessary for a cyclohexane chair flip.[263] The larger energy barrier is expected and reasonable given that as each chair flip occurs in **4.169** the

chlorine atom and methyl group must eclipse and pass each other. Although, this is likely not a result which could be used to build a structure-reactivity relationship, it is nonetheless an interesting observation which shows that the hypervalent iodine bonding system may rotate about the iodine.

The reactivity of the synthesized reagents has not been explored extensively. The ortho-methyl fluoroiodane **4.143** was tested in the fluorobenzoxazepine cyclization previously discussed in Scheme 4-8. When alkene **4.22** was treated with the parent fluoroiodane **4.2** the product **4.23** was obtained in 77% yield with only a five-minute reaction time. When the same substrate, alkene **4.22**, was treated with ortho-methyl fluoroiodane **4.143** for 24 hours only 5% (^{19}F-NMR yield) of the product **4.23** was obtained (Scheme 4-51). The remaining mass balance of the reaction consisted of unreacted alkene **4.22**, as well as ketone **4.25**, a product previously reported and resulting from the presence of adventitious water.



4.22 **4.23** **4.25**

Scheme 4-51. Fluorocyclization of **4.22** with ortho-methyl fluoroiodane **4.143**.

This result directly opposes our initial hypothesis, where we expected **4.143** to be more reactive. From this result, two possible conclusions could be drawn. One, as opposed to the originally proposed hypothesis, a large torsion angle attenuates the reactivity of the fluoroiodanes. Two, with the methyl group at the position ortho to the iodine, the addition of the fluoroiodane to an alkene is now sterically encumbered and occurs at a much slower rate. It is also possible that a combination of these factors dictates the reactivity of the reagent. A more extensive study of the reactivity of the complete series of derivatives is needed to generate compelling evidence and guide the design of future reagents. These future experiments should include testing the fluoroiodanes in different types of known reactions, such as with olefins (e.g., Scheme 4-4), diazo compounds (Scheme 4-10), and in reactions with non-covalent interactions (e.g., Scheme 4-11). Further, exploring reactions in which the fluoroiodane **4.2** is unreactive (e.g., the fluorination of anisole) would provide insight into the potential utility of our newly reported derivatives. These additional experiments would allow for general reactivity trends to be deduced about the ortho-fluoroiodane series in its entirety.

4.4 Concluding Remarks and Future Work

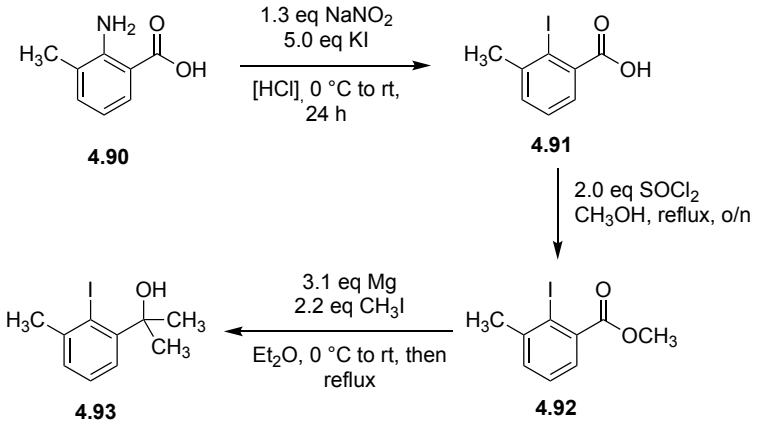
A series of fluoro- and chloroiodanes were synthesized and solid-state structural data was obtained via single crystal X-ray crystallography. The challenges encountered in the synthesis of the more sterically hindered iodoalcohols (R = *i*-Pr, *t*-Bu) were overcome by reaction optimization or changes to the synthetic strategy. This work demonstrated that it was possible to synthesize and isolate these sterically hindered hypervalent iodine compounds. Additionally, the introduction of steric bulk at the position ortho to the iodine does increase the torsion angle of the hypervalent bond in both fluoro- and chloroiodanes. Otherwise, the solid-state bond lengths and angles were largely the same as the previously reported unsubstituted compounds (**4.2** and **4.3**). There were two notable results which were especially different from the parent compounds: (1) the torsion angles of six-membered fluoro- and chloroiodanes were much larger and (2) the bond lengths and angles of the *tert*-butyl chloroiodane deviated significantly from the parent compound. From the *tert*-butyl iodoalcohol precursor, a new room temperature stable alkyl aryl iodonium salt was synthesized. Future experiments should be directed at exploring the reactivity of this compound to a series of nucleophiles to determine if it is reactive at the methylene or aromatic ring. Additional structural studies could explore the necessity of the bromine and/or the hydroxyl group for the formation of the obtained product **4.155**. One preliminary experiment concluded that the reactivity of the ortho-methyl fluoroiodane is less reactive compared to its previously known counterpart **4.2**. A comprehensive study of their reactivity in multiple different synthetic transformations will help establish a complete structure-reactivity profile. To aid in this endeavour, the series of both fluoro- and chloroiodanes should be completed.

4.5 Experimental Details

Reactions were carried out in oven-dried or flame-dried glassware and cooled under a nitrogen atmosphere. Solvents were dried and purified using a JC Meyer solvent purification system and were used without further purification (exceptions listed below). DMF was stirred over 5% wt CaH_2 at room temperature overnight and then stored over 4Å molecular sieves overnight before distillation onto fresh sieves, CH_3CN was stirred with flame-dried K_2CO_3 overnight before sequential drying with 4Å molecular sieves (2x), and $CHCl_3$ was washed with water before sequential drying with 4Å molecular sieves (2x). Transfer of anhydrous solvents and reagents was accomplished with oven-dried needles. *m*CPBA was dried under vacuum before use. Organolithiums were titrated prior to use with benzylbenzamide.[264] When necessary Grignard reagents were titrated with iodine in tetrahydrofuran saturated with LiCl.[265] Thin layer chromatography was performed on glass plates pre-coated with 0.25 mm Kieselgel 60 F254 (Silicycle). Flash chromatography columns were packed with 230-400 mesh silica gel (Silicycle). Proton NMR spectra (^{1}H NMR) were recorded at 300 MHz and are reported (ppm) relative to the residual solvent peak. Carbon NMR spectra (^{13}C NMR) were recorded at 75 MHz and are reported (ppm) relative to the center line of the residual solvent peak. Fluorine NMR spectra (^{19}F NMR) were recorded at 282 MHz and are reported (ppm) relative to the peak of trifluoroacetic acid at 76.55 ppm. All coupling constants (J) are reported in hertz (Hz). Singlet = s, broad singlet = br. s, doublet = d, triplet = t, quartet = q, quintet = qu., sextet = sex, multiplet = m. All literature known compounds matched the spectral data found in the literature. High resolution mass spectroscopy was performed on a Thermo Fisher Scientific Q-Exactive hybrid mass spectrometer. Accurate mass determinations were performed at a mass resolution of 70,000. Samples were infused at 10 μL/min in 1:1 CH_3OH/H_2O + 0.1% formic acid.

4.5.1 Preparation of Iodoarene Precursors

Synthesis of 2-(2-iodo-3-methylphenyl)propan-2-ol (4.93):



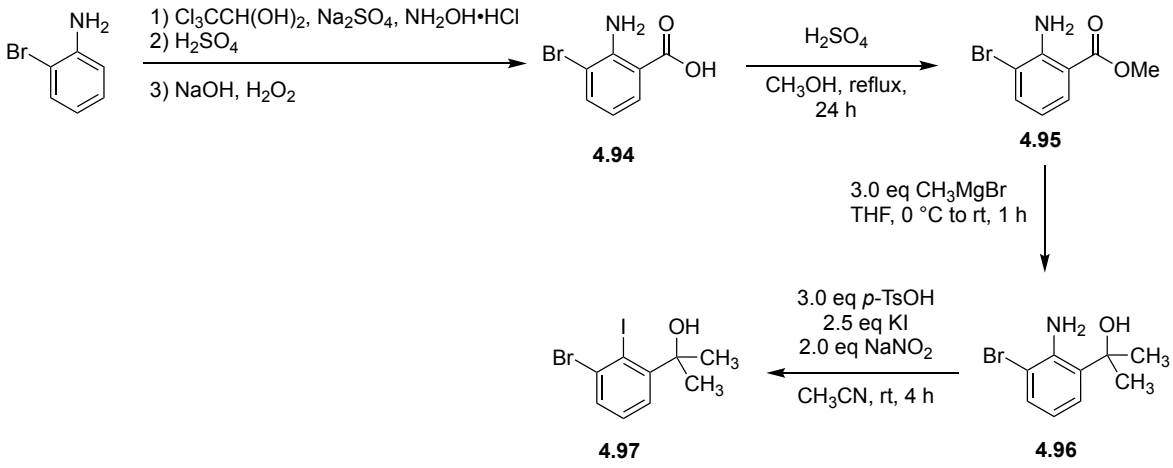
2-iodo-3-methylbenzoic acid (4.91): Prepared according to the literature.[83] 2-Amino-3-methylbenzoic acid (5.0 g, 33 mmol, 1.0 eq) was suspended in conc. HCl (25 mL) and stirred at 0 °C for 5 minutes. Sodium nitrite (2.97 g, 43 mmol, 1.3 eq, in 6 mL of DI water) was added dropwise over 15 minutes. The solution was stirred for 1.5 hours at 0 °C before potassium iodide (27 g, 165 mmol, 5.0 eq, in 31 mL of DI water) was added dropwise. The reaction was stirred at room temperature for 24 hours. EtOAc (50 mL) and DI water (50 mL) were added and the aqueous layer was extracted with EtOAc (3x), the combined organic layers were washed with sat. Na_2SO_3 (until the colour of the organic layer stopped changing), DI water, brine, and dried with $MgSO_4$. A faintly orange solid was isolated by rotary evaporation and used without further purification (7.95 g, 30 mmol, 92%). ^{1}H-NMR (300 MHz; $CDCl_3$): δ 7.63 (dd, J = 7.5, 1.4 Hz, 1H), 7.41 (dd, J = 7.5, 1.3 Hz, 1H), 7.31 (dd, J = 7.6, 7.6 Hz, 1H), 2.56 (s, 3H).[239]

Methyl 2-iodo-3-methylbenzoate (4.92): 2-iodo-3-methylbenzoic acid **4.91** (6.0 g, 23 mmol, 1.0 eq) was dissolved in methanol (80 mL) and cooled in an ice-water bath. $SOCl_2$ (3.3 mL, 46 mmol, 2.0 eq) was added dropwise and the mixture was heated to reflux for 3 hours. The reaction was cooled to room temperature and the solvent was removed under reduced pressure. The crude was redissolved in 50 mL of diethyl ether and washed sequentially with water, sat. $NaHCO_3$, water, and brine; dried with magnesium sulfate, and isolated under reduced pressure. The red crude oil was purified by flash

chromatography (5% ethyl acetate in hexanes) to afford the ester **4.92** (5.7 g, 21 mmol, 90%) as a yellow oil. R_f = 0.28 (5% ethyl acetate in hexanes). ^{1}H-NMR (300 MHz; $CDCl_3$): δ 7.40-7.26 (m, 3H), 3.96 (s, 3H), 2.54 (s, 3H). ^{13}C-NMR (75 MHz, $CDCl_3$): δ 168.9, 143.5, 138.5, 131.9, 127.9, 127.1, 100.1, 52.7, 29.8.[266]

2-(2-iodo-3-methylphenyl)propan-2-ol (4.93): Procedure based on a literature procedure.[184] In a round bottom flask with a condenser, magnesium (1.5 g, 62 mmol, 3.1 eq) was flame-dried under vacuum. Anhydrous diethyl ether (4 mL) was added followed by the dropwise addition of CH_3I (2.7 mL, 44 mmol, 2.2 eq in 4 mL diethyl ether). As soon as the solution began to boil an additional 6.0 mL of diethyl ether was added. Once the addition of CH_3I was complete the reaction was stirred until it cooled to room temperature and the excess magnesium was allowed to settle. The supernatant was transferred with a cannula to a new round bottom flask. The remaining magnesium was rinsed with 4 mL of diethyl ether transferred as well. The solution was cooled to 0 °C and methyl 2-iodo-3-methylbenzoate **4.92** (5.5 g, 20 mmol, 1.0 eq in 4.0 mL of diethyl ether) was added to the solution dropwise. The solution was warmed to room temperature overnight, then refluxed for 1.5 hours. The reaction was cooled to 0°C again, then quenched with sat. NH_4Cl and diluted with water to dissolve the precipitate. The mixture was filtered through celite. The aqueous layer was separated and extracted with diethyl ether (3x). The organic layer was washed with water, brine, dried with $MgSO_4$ and isolated as a thick oil. Flash column chromatography with 10% ethyl acetate in hexanes afforded **4.93** (4.1 g, 15 mmol, 68%) as a thick light-yellow oil. R_f = 0.18 (10% ethyl acetate in hexanes). ^{1}H-NMR (300 MHz; $CDCl_3$): δ 7.41 (dd, *J* = 7.2, 2.3 Hz, 1H), 7.23-7.15 (m, 2H), 2.92 (br. s, 1H), 2.53 (s, 3H), 1.81 (s, 6H). ^{13}C-NMR (75 MHz; $CDCl_3$): δ 149.1, 143.6, 128.8, 128.0, 124.5, 101.6, 74.5, 31.7, 30.2. HRMS-ESI calcd for $C_{10}H_{12}I$ $[M+H-H_2O]^+$ 258.9978, found 258.9974.

Synthesis of 2-(3-bromo-2-iodophenyl)propan-2-ol (4.97):



2-Amino-3-bromobenzoic acid (4.94):

Step 1: In a 1 L beaker was added chloral hydrate (27.0 g, 164 mmol, 1.09 eq), Na_2SO_4 (190 g, 1.3 mol, 8.9 eq), water (370 mL) and heated to 35 °C internally on a hot plate. Once fully dissolved a warm suspension of 2-bromoaniline (25.8 g, 150 mmol, 1.0 eq) in water (105 mL) and concentrated HCl (16 mL) was added. NH_2OH•HCl (33.4 g, 480 mmol, 3.2 eq) in water (150 mL) was added and the solution was heated to 85 °C. After 3 hours at 85 °C the solution was cooled to 25 °C and filtered. The solid product was washed with water (3x, 100 mL) and dried under high vacuum at 55 °C until a constant weight was achieved to afford isonitrosoacetanilide (30.4 g) as a brown solid which was used without further purification.

Step 2: Concentrated sulfuric acid (150 mL) in a 500 mL beaker was heated to 60 °C with a water bath. The crude isonitrosoacetanilide (30.4 g) was added portion wise ensuring to never exceed an internal reaction temperature of 70 °C (~30 minutes). The solution was heated to 85-90 °C and stirred for 15 minutes. The reaction was cooled to room temperature and poured onto ice. The red solid was filtered with a water aspirator and washed with water (500 mL). The red paste was dried under high vacuum for 48 hours to afford isatin (30 g) as a fine red solid which was used without further purification.

Step 3: In a 1 L round bottom flask was added crude isatin (30 g) and NaOH (5%, 500 mL) then heated to 50 °C internally with a water bath. Once at 50 °C hydrogen peroxide (33 mL of 30%, 2.5 eq) was

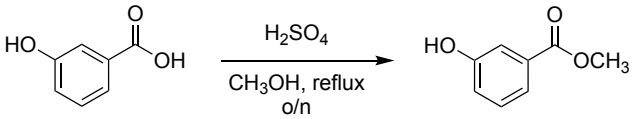
added dropwise and the reaction was stirred for 1 hour. The reaction was cooled to room temperature, filtered through a sintered glass frit, transferred to a round bottom flask (minimal methanol was used to quantitatively transfer), rotary evaporated the methanol, dried under high vacuum at 50 °C to afford the anthranilic acid **4.94** (20.6 g, 95 mmol, 64% over 3 steps) as a brown solid. ^{1}H-NMR (300 MHz; DMSO-d_6): δ 7.77 (dd, *J* = 8.0, 1.5 Hz, 1H), 7.63 (dd, *J* = 7.8, 1.5 Hz, 1H), 6.76 (br. s, 2H), 6.52 (t, *J* = 7.8 Hz, 1H). ^{13}C-NMR (75 MHz; DMSO-d_6): δ 169.1, 147.8, 137.2, 131.1, 115.9, 111.9, 109.6. HRMS-ESI calcd for $C_7H_7{}^{79}BrNO_2$ $[M+H]^+$ 215.9655, found 215.9655. HRMS-ESI calcd for $C_7H_7{}^{81}BrNO_2$ $[M+H]^+$ 217.9634, found 217.9634.

Methyl 2-amino-3-bromobenzoate (4.95): To a round bottom flask open to the atmosphere with a stir bar and a condenser was added 2-amino-3-bromobenzoic acid **4.94** (10 g, 46 mmol, 1.0 eq), methanol (100 mL, 0.5 M) and concentrated sulfuric acid (10 mL). The reaction was refluxed for 24 hours, cooled to room temperature and the volatiles were removed by vacuum. Water (500 mL) was added and was extracted with ethyl acetate (3x). The combined organic layers were washed with water, sat. $NaHCO_3$, water, brine, dried with $MgSO_4$ and concentrated under reduced pressure to afford **4.95** (8.5 g, 37 mmol, 80%) as an orange oil. ^{1}H-NMR (300 MHz; $CDCl_3$): δ 7.85 (dd, *J* = 8.0, 1.5 Hz, 1H), 7.57 (dd, *J* = 7.8, 1.6 Hz, 1H), 6.52 (dd, *J* = 7.9, 7.9 Hz, 1H), 6.33 (br. s, 2H), 3.88 (s, 3H).[267] ^{13}C-NMR (75 MHz; $CDCl_3$): δ 168.1, 147.6, 137.4, 130.8, 116.5, 111.9, 110.8, 52.0.

2-(2-amino-3-bromophenyl)propan-2-ol (4.96): To a flame-dried round bottom flask under N_2 was added methyl 2-amino-3-bromobenzoate **4.95** (571 mg, 2.5 mmol, 1.0 eq) and anhydrous THF (15 mL, 0.17 M) and cooled to 0 °C. CH_3MgBr (2.5 mL, 7.5 mmol, 3.0 M in diethyl ether, 3.0 eq) was added dropwise, the reaction mixture was warmed to room temperature and stirred for 1 hour. The reaction was cooled to 0°C again, quenched with sat. NH_4Cl and diluted with water. The aqueous layer was extracted with diethyl ether (3x). The organic layer was washed with water, brine, dried with $MgSO_4$ and concentrated to an oil which slowly solidified into a yellow/orange solid **4.96** (571 mg, 2.5 mmol, quant.). R_f = 0.32 (20% ethyl acetate in hexanes). ^{1}H-NMR (300 MHz; $CDCl_3$): δ 7.35 (dd, *J* = 7.9, 1.4 Hz, 1H), 7.05 (dd, *J* = 7.8, 1.4 Hz, 1H), 6.53 (dd, *J* = 7.9, 7.9 Hz, 1H), 4.34 (s, 3H), 1.63 (s, 6H). ^{13}C NMR (75 MHz; $CDCl_3$): δ 142.9, 131.91, 131.78, 125.0, 117.9, 112.1, 74.4, 29.2.

2-(3-bromo-2-iodophenyl)propan-2-ol (4.97): At room temperature acetonitrile (9.6 mL, 0.25 M), 2-(2-amino-3-bromophenyl)propan-2-ol **4.96** (550 mg, 2.4 mmol, 1.0 eq), and *p*-toluenesulfonic acid (1.4 g, 7.2 mmol, 3.0 eq) were added to a round bottom flask with a stir bar. The mixture was stirred until complete dissolution was observed. A solution of potassium iodide (993 mg, 6.0 mmol, 2.5 eq) and sodium nitrite (330 mg, 4.8 mmol, 2.0 eq) in water (1.4 mL) was added dropwise. After 4 hours the reaction was diluted with 40 mL of water, adjusted to pH = 9 with $NaHCO_3$, and reduced with 5 mL of sat. $Na_2S_2O_3$. The reaction mixture was extracted with diethyl ether (3x) and the combined organic layers were washed with water, brine, dried with $MgSO_4$, and concentrated under vacuum. Purification by flash column chromatography with 15% ethyl acetate in hexanes afforded **4.97** (270 mg, 0.79 mmol, 33%) as a white solid. R_f = 0.25 (15% ethyl acetate in hexanes). ^{1}H-NMR (300 MHz; $CDCl_3$): δ 7.60 (dd, *J* = 7.8, 1.6 Hz, 1H), 7.53 (dd, *J* = 8.0, 1.6 Hz, 1H), 7.17 (dd, *J* = 7.9, 7.9 Hz, 1H), 2.85 (s, 1H), 1.79 (s, 7H). ^{13}C-NMR (75 MHz; $CDCl_3$): δ 152.5, 134.1, 131.7, 129.4, 125.3, 101.4, 74.6, 30.0. HRMS-ESI calcd for $C_9H_9{}^{79}BrI$ $[M+H-H_2O]^+$ 322.8927, found 322.8928. HRMS-ESI calcd for $C_9H_9{}^{81}BrI$ $[M+H-H_2O]^+$ 324.8906, found 324.8907.

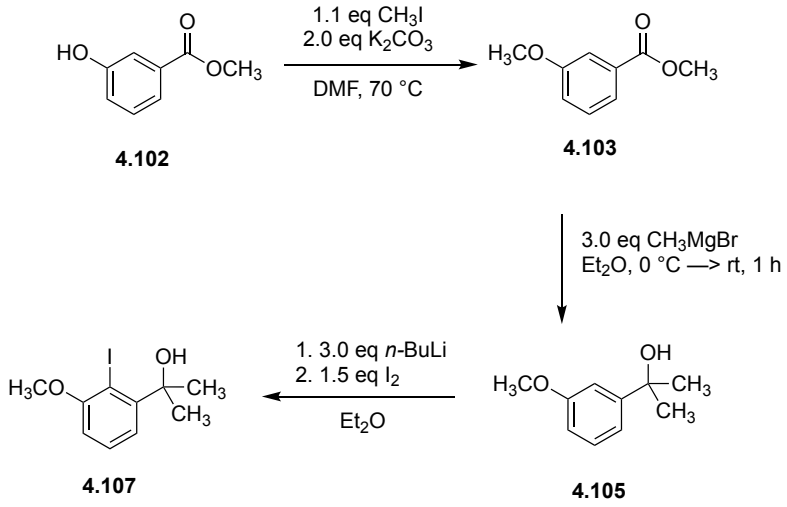
Methyl 3-hydroxybenzoate (4.102):



4.101 **4.102**

3-hydroxybenzoic acid (10 g, 72 mmol, 1.0 eq) was dissolved in methanol (100 mL, 0.72 M) at room temperature. Concentrated sulfuric acid (3 mL) was added slowly and the mixture was heated to reflux overnight. The reaction was cooled to room temperature and the methanol was removed under reduced pressure. The crude was dissolved in water and extracted with diethyl ether (3x), the organic layer was washed with water, brine and dried with $MgSO_4$, and isolated under reduced pressure to afford **4.102** as a white solid (10 g, 66 mmol, 92%). R_f = 0.26 (20% ethyl acetate in hexanes). ^{1}H-NMR (300 MHz; $CDCl_3$): δ 7.63-7.58 (m, 2H), 7.30 (t, *J* = 7.9 Hz, 1H), 7.09 (ddd, *J* = 8.1, 2.5, 0.8 Hz, 1H), 6.64 (br. s, 1H), 3.92 (s, 3H). ^{13}C-NMR (75 MHz, $CDCl_3$): δ 167.8, 156.2, 131.3, 129.9, 121.9, 120.6, 116.6, 52.6.[268]

Synthesis of 2-(2-iodo-3-methoxyphenyl)propan-2-ol (4.107):



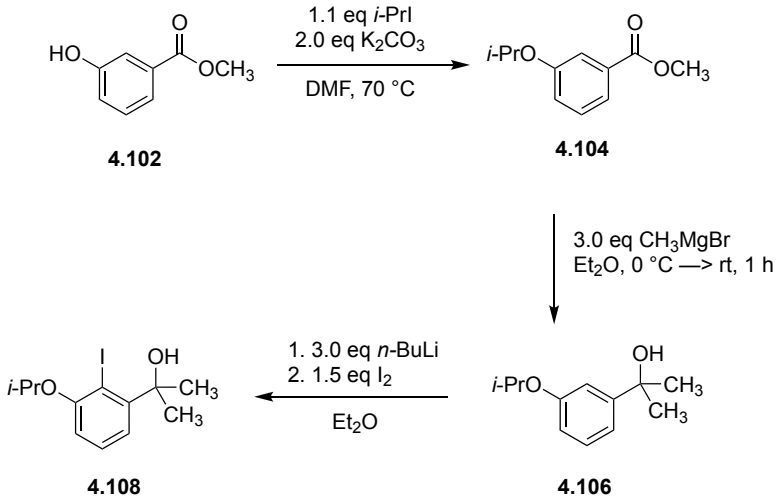
Methyl 3-methoxybenzoate (4.103): To a flame-dried round bottom flask under nitrogen was added methyl 3-hydroxybenzoate **4.102** (761 mg, 5.0 mmol, 1.0 eq), flame-dried K_2CO_3 (1.3 g, 10 mmol, 2.0 eq), anhydrous DMF (5.0 mL, 1.0 M) and methyl iodide (342 µL, 5.5 mmol, 1.1 eq) was added dropwise. The reaction was stirred at room temperature for 3 hours. The reaction was diluted with diethyl ether (30 mL) and water (20 mL). The layers were partitioned, and the organic layer was washed with water (20 mL, 4x), brine (20 mL), dried with $MgSO_4$, and concentrated to a clear oil **4.103** (802 mg, 4.8 mmol, 97%). ^{1}H-NMR (300 MHz; $CDCl_3$): δ 7.62 (ddd, *J* = 7.7, 1.4, 1.1 Hz, 1H), 7.55 (dd, *J* = 2.6, 1.5 Hz, 1H), 7.31 (dd, *J* = 8.9 Hz, 8.9 Hz, 1H), 7.09 (ddd, *J* = 8.3, 2.7, 1.0 Hz, 1H), 3.90 (s, 3H), 3.83 (s, 3H). ^{13}C-NMR (75 MHz; $CDCl_3$): δ 167.0, 159.6, 131.5, 129.5, 122.1, 119.6, 114.0, 55.5, 52.2.[269]

2-(3-methoxyphenyl)propan-2-ol (4.105): To a flame-dried round bottom flask under N_2 was added methyl 3-methoxybenzoate **4.103** (752 mg, 4.5 mmol, 1.0 eq) and anhydrous diethyl ether (9 mL, 0.5 M) and cooled to 0 °C. CH_3MgBr (4.5 mL, 13.6 mmol, 3.0 M in diethyl ether, 3.0 eq) was added dropwise, the reaction mixture was warmed to room temperature and stirred for 1 hour. The reaction was cooled to 0°C, quenched with sat. NH_4Cl and diluted with water. The aqueous layer was extracted with diethyl ether (3x). The organic layer was washed with water, brine, dried with $MgSO_4$ and isolated as a clear oil to afford **4.105** (629 mg, 3.8 mmol, 84%). ^{1}H-NMR (300 MHz; $CDCl_3$): δ 7.26 (ddd, *J* =

7.9, 7.9, 0.5 Hz, 1H), 7.08-7.03 (m, 2H), 6.79 (ddd, *J* = 8.2, 2.6, 1.0 Hz, 1H), 3.82 (s, 3H), 1.80 (br. s, 1H), 1.58 (s, 6H). ^{13}C-NMR (75 MHz; $CDCl_3$): δ 159.7, 151.1, 129.4, 116.9, 111.9, 110.7, 72.7, 55.4, 31.9.[270]

2-(2-iodo-3-methoxyphenyl)propan-2-ol (4.107): To a flame-dried round bottom flask with a stir bar was added 2-(3-methoxyphenyl)propan-2-ol **4.105** (629 mg, 3.77 mmol, 1.0 eq). The flask was evacuated and back-filled it nitrogen three times. Anhydrous diethyl ether (7.5 mL, 0.5 M) was added and the mixture was cooled to 0°C. *n*-BuLi (7.3 mL, 9.4 mmol, 1.3 M in hexanes, 2.5 eq) was added dropwise, the reaction was warmed to room temperature, and stirred for 3 hours. The solution was again cooled to 0 °C and iodine (2.9 g, 11.3 mmol, 3.0 eq) in diethyl ether (20 mL) was added dropwise. The reaction was stirred for 15 minutes at room temperature before being cooled to 0 °C and quenched with sat. NH_4Cl. The reaction mixture was diluted with water (20 mL). The layers were separated and the aqueous layer was extracted with diethyl ether (3x), the organic layer was washed with water, brine, dried with $MgSO_4$, and concentrated under reduced pressure. The crude material was plugged through silica gel to afford **4.107** (1.07 g, 3.66 mmol, 97%) as a clear oil. R_f = 0.35 (20% ethyl acetate in hexanes). ^{1}H-NMR (300 MHz; $CDCl_3$): δ 7.32-7.23 (m, 2H), 6.79 (dd, *J* = 7.3, 2.2 Hz, 1H), 3.91 (s, 3H), 3.10 (s, 1H), 1.82 (s, 6H). ^{13}C-NMR (75 MHz; $CDCl_3$): δ 158.2, 150.6, 129.3, 119.7, 109.9, 87.5, 74.4, 57.0, 30.1. HRMS-ESI calcd for $C_{10}H_{12}IO$ $[M+H-H_2O]^+$ 274.9927, found 274.9924. Calcd for $C_{10}H_{17}INO_2$ $[M+NH_4]^+$ 310.0299, found 310.0297. Calcd for $C_{10}H_{13}INaO_2$ $[M+Na]^+$ 314.9852, found 314.9850. Calcd for $C_{10}H_{13}IKO_2$ $[M+K]^+$ 330.9592, found 330.9591.

Synthesis of 2-(2-iodo-3-isopropoxyphenyl)propan-2-ol (4.108):



Methyl 3-isopropoxybenzoate (4.104): To a flame-dried round bottom flask under nitrogen was added methyl 3-hydroxybenzoate **4.102** (3.0 g, 20 mmol, 1.0 eq), flame-dried K_2CO_3 (5.53 g, 40 mmol, 2.0 eq), anhydrous DMF (10 mL, 1.0 M) and isopropyl iodide* (2.2 mL, 22 mmol, 1.1 eq) was added. The reaction was stirred at 70 °C. An additional 0.5 equivalents of both isopropyl iodide (0.5 mL, 5.0 mmol) and K_2CO_3 (691 mg, 5.0 mmol) were added after 3 hours and stirred for an additional 5 hours. The reaction was cooled to room temperature then diluted with water (50 mL) and diethyl ether (50 mL). The organic layer was washed with water (5x, 50 mL), brine, dried with $MgSO_4$, and concentrated under reduced pressure to afford a slightly yellow oil **4.104** (3.88 g, 20 mmol, quantitative). R_f = 0.38 (10% ethyl acetate in hexanes). ^{1}H-NMR (300 MHz; $CDCl_3$): δ 7.60 (ddd, *J* = 7.6, 1.5, 1.1 Hz, 1H), 7.55 (dd, *J* = 2.6, 1.5 Hz, 1H), 7.32 (ddd, *J* = 7.9, 7.9 , 0.4 Hz, 1H), 7.07 (ddd, *J* = 8.2, 2.6, 1.0 Hz, 1H), 4.61 (septet, *J* = 6.1 Hz, 1H), 3.90 (s, 3H), 1.34 (d, *J* = 6.1 Hz, 6H).[271] ^{13}C-NMR (75 MHz, $CDCl_3$): δ 167.2, 158.0, 131.5, 129.6, 121.9, 121.4, 116.2, 70.3, 52.3, 22.1.

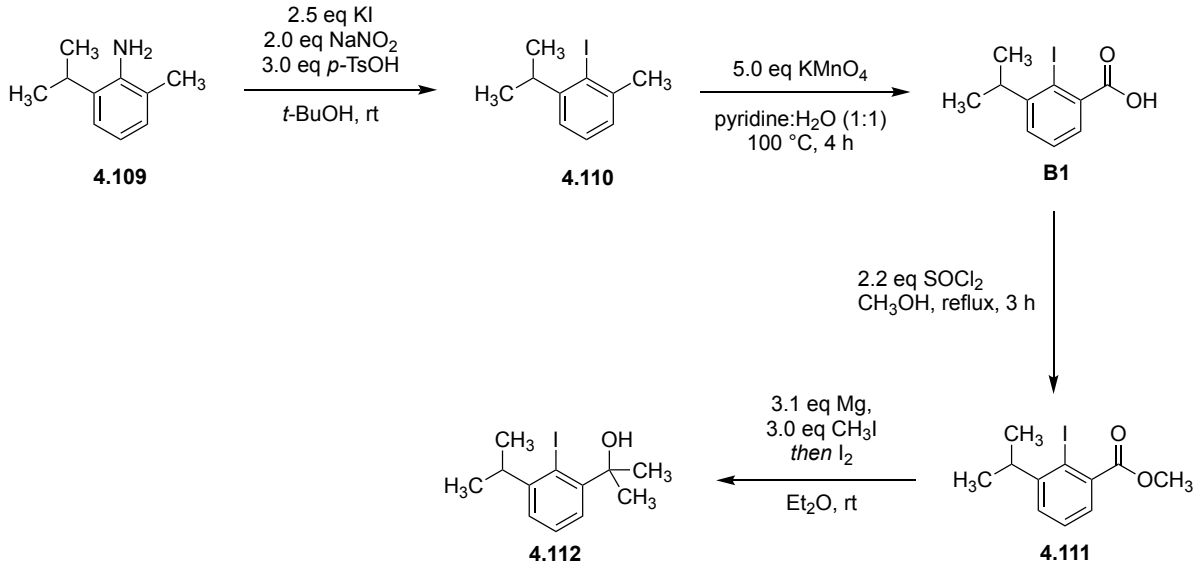
*Note: isopropyl iodide was freshly purified before use by passing it through a gravity column of basic alumina (Brockmann I).

2-(3-isopropoxyphenyl)propan-2-ol (4.106): To a flame-dried round bottom flask under N_2 was added methyl 3-isopropoxybenzoate **4.104** (1.75 g, 9.0 mmol, 1.0 eq) and anhydrous diethyl ether (18 mL, 0.5 M) and cooled to 0 °C. CH_3MgBr (9.0 mL, 27 mmol, 3.0 M in diethyl ether, 3.0 eq) was added

dropwise, the reaction mixture was warmed to room temperature and stirred for 1 hour. The reaction was cooled to 0 °C, quenched with sat. NH_4Cl and diluted with water. The aqueous layer was extracted with diethyl ether (3x). The organic layer was washed with water, brine, dried with $MgSO_4$ and isolated as a clear oil to afford **4.106** (quantitative). R_f = 0.27 (20% ethyl acetate in hexanes). ^{1}H-NMR (300 MHz; $CDCl_3$): δ 7.27-7.21 (m, 1H), 7.06-7.01 (m, 2H), 6.77 (ddd, *J* = 8.2, 2.4, 0.9 Hz, 1H), 4.57 (7, *J* = 6.1 Hz, 1H), 1.80 (s, 1H), 1.57 (s, 6H), 1.34 (d, *J* = 6.1 Hz, 6H). ^{13}C-NMR (75 MHz; $CDCl_3$): δ 157.8, 151.0, 129.2, 116.6, 113.5, 112.7, 72.5, 69.8, 31.7, 22. HRMS-ESI calcd for $C_{12}H_{17}O$ $[M+H-H_2O]^+$ 177.1274, found 177.1273.

2-(2-iodo-3-isopropoxyphenyl)propan-2-ol (4.108): To a flame-dried round bottom flask with a stir bar was added 2-(3-isopropoxyphenyl)propan-2-ol **4.106** (1.96 g, 10 mmol, 1.0 eq). The flask was evacuated and back-filled with nitrogen three times. Anhydrous diethyl ether (20 mL, 0.5 M) was added and the mixture was cooled to 0°C. *n*-BuLi (15 mL, 30 mmol, 2.0 M in hexanes, 3.0 eq) was added dropwise, the reaction was warmed to room temperature and stirred for 3 hours. The solution was again cooled to 0 °C and iodine (3.8 g, 15 mmol, 1.5 eq) in diethyl ether (20 mL) was added dropwise. The reaction was stirred for 15 minutes at room temperature before being cooled to 0 °C and quenched with sat. NH_4Cl. The reaction mixture was diluted with water (20 mL). The layers were separated and the aqueous layer was extracted with diethyl ether (3x), the organic layer was washed with water, brine, dried with $MgSO_4$, and concentrated under reduced pressure. The crude material was purified by column chromatography with 10% ethyl acetate in hexanes to afford **4.108** (765 mg, 2.4 mmol, 24%) as a clear oil. R_f = 0.38 (20% ethyl acetate in hexanes). ^{1}H-NMR (300 MHz; $CDCl_3$): δ 7.26-7.17 (m, 2H), 6.75 (ddd, *J* = 7.1, 2.4, 0.4 Hz, 1H), 4.57 (septet, *J* = 6.1 Hz, 1H), 3.22 (s, 1H), 1.79 (s, 6H), 1.41 (d, *J* = 6.1 Hz, 6H). ^{13}C-NMR (75 MHz, $CDCl_3$): δ 156.8, 150.7, 129.1, 119.6, 112.9, 90.1, 74.4, 72.7, 30.1, 22.3. Note: The larger scale reaction did not proceed according to the results obtained from the brief optimization (24 vs. 80% yield). A reaction at this scale was not repeated as 765 mg of material was enough to continue the study. HRMS-ESI calcd for $C_{12}H_{16}IO$ $[M+H-H_2O]^+$ 303.0240, found 303.0240.

Synthesis of 2-(2-iodo-3-isopropylphenyl)propan-2-ol (4.112):



2-Iodo-1-isopropyl-3-methylbenzene (4.110): At room temperature anhydrous *t*-BuOH* (128 mL, 0.25 M), 2-isopropyl-6-methylaniline **4.109** (5.0 mL, 32 mmol, 1.0 eq), and *p*-toluenesulfonic acid (18 g, 96 mmol, 3.0 eq) were added to a round bottom flask with a stir bar. The mixture was stirred until complete dissolution was observed. A solution of potassium iodide (13 g, 80 mmol, 2.5 eq) and sodium nitrite (4.4 g, 64 mmol, 2.0 eq) in water (19 mL) was added dropwise. After 3 hours the reaction was diluted with 500 mL of water, adjusted to pH = 9 with $NaHCO_3$, and reduced with 70 mL of sat. $Na_2S_2O_3$. The reaction mixture was extracted with hexanes (3x) and the combined organic layers were washed with water, brine, dried with $MgSO_4$, and concentrated under vacuum. Purification by flash column chromatography with hexanes afforded **4.110** (4.9 g, 19 mmol, 59%) as a clear oil. R_f = 0.58 (hexanes). ^{1}H-NMR (300 MHz; $CDCl_3$): δ 7.22 (dd, *J* = 7.5, 7.5 Hz, 1H), 7.13-7.05 (m, 2H), 3.41 (7, *J* = 6.8 Hz, 1H), 2.52 (s, 3H), 1.27 (d, *J* = 6.8 Hz, 6H). ^{13}C-NMR (75 MHz; $CDCl_3$): δ 151.2, 142.3, 128.1, 127.6, 123.1, 108.9, 38.9, 30.7, 23.4.[272] *Note: Although water is added to the reaction anhydrous *t*-BuOH was used to ensure an accurate ratio of *t*-BuOH:water was maintained in the reaction mixture.

Methyl 2-iodo-3-isopropylbenzoate (4.111):

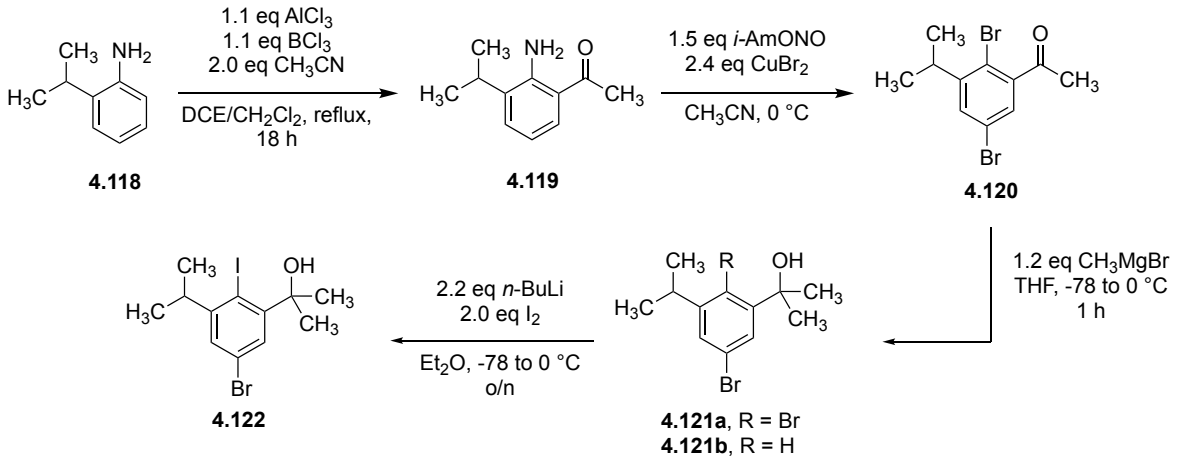
Step 1: 2-Iodo-1-isopropyl-3-methylbenzene **4.110** (1.9 g, 7.3 mmol, 1.0 eq), pyridine (7.3 mL) and water (7.3 mL) were added to a round bottom flask with a stir bar and fitted with a condenser. The reaction was heated in an oil bath to 100 °C and $KMnO_4$ (5.7 g, 36 mmol, 5.0 eq) was added portion wise. The reaction was stirred for 4 hours at this temperature and then cooled to room temperature. To the solution was added 3 M $NaOH_{(aq)}$ followed by dropwise addition of methanol until the remaining $KMnO_4$ was consumed. The resulting suspension was filtered through a short pad of celite. Volatiles were removed under vacuum. The solution was acidified with 3 M $HCl_{(aq)}$ and extracted with ethyl acetate (3x). The combined organic layers were washed with water, brine, dried with $MgSO_4$, and concentrated under vacuum. The crude white solid **B1** (1.1 g) was carried forward without further purification as a 7:1 mixture (prod:sm). ^{1}H-NMR (300 MHz; $CDCl_3$): δ 11.30 (br. s, 1H), 7.57 (dd, *J* = 6.1, 3.2 Hz, 1H), 7.41-7.35 (m, 2H), 3.48 (7, *J* = 6.8 Hz, 1H), 1.26 (d, *J* = 6.8 Hz, 6H). ^{13}C-NMR (75 MHz; $CDCl_3$): δ 174.1, 152.7, 137.3, 129.1, 128.42, 128.40, 100.1, 38.8, 23.3. HRMS-ESI calcd for $C_{10}H_{10}IO_2$ $[M-H]^-$ 288.9720, found 288.9732.

Step 2: Crude 2-iodo-3-isopropylbenzoic acid **B1** (1.1 g, 3.8 mmol, 1.0 eq) was dissolved in methanol (10 mL) and cooled to 0 °C. $SOCl_2$ (609 μL, 8.4 mmol, 2.2 eq) was added dropwise and the mixture was heated to reflux for 3 hours. The reaction was cooled to room temperature and the solvent was removed under reduced pressure. The crude was redissolved in 50 mL of diethyl ether and washed sequentially with water, sat. $NaHCO_3$, water, and brine; dried with magnesium sulfate, and isolated under reduced pressure. The crude oil was purified by flash column chromatography (hexanes to 5% ethyl acetate in hexanes) to afford the ester **4.111** (806 mg, 2.7 mmol, 36% over two steps) as a white solid. R_f = 0.53 (5% ethyl acetate in hexanes). ^{1}H-NMR (300 MHz; $CDCl_3$): δ 7.36-7.27 (m, 3H), 3.94 (s, 3H), 3.40 (septet, *J* = 6.8 Hz, 1H), 1.23 (d, *J* = 6.8 Hz, 6H). ^{13}C-NMR (75 MHz; $CDCl_3$): δ 169.5, 152.1, 139.7, 128.4, 128.0, 127.0, 99.5, 52.8, 38.7, 23.3. HRMS-ESI calcd for $C_{11}H_{14}IO_2$ $[M+H]^+$ 305.0033, found 305.0034.

2-(2-iodo-3-isopropylphenyl)propan-2-ol (4.112): A round bottom flask with magnesium turnings (149 mg, 6.2 mmol, 3.1 eq) was flame-dried under vacuum. After cooling to room temperature under N_2 a dry condenser fitted and purged under N_2. To the flask was added anhydrous diethyl ether (5.0

mL) and methyl iodide (374 µL, 6.0 mmol, 3.0 eq) dropwise. The solution was allowed to reflux then come to room temperature before transferring the methyl Grignard via cannula to a new dry round bottom flask with a stir bar. Additional anhydrous diethyl ether (2x, 2.0 mL) was used to rinse the flask. To this solution was added methyl 2-iodo-3-isopropylbenzoate **4.111** (608 mg, 2.0 mmol, 1.0 eq) in anhydrous diethyl ether (10 mL). The reaction was stirred for 3 hours at room temperature before iodine (1.5 g, 6.0 mmol, 3.0 eq, 30 mL diethyl ether) was added dropwise. If the solution does not remain a dark brown after the addition is complete addition iodine should be titrated into the reaction until a dark brown remains. After 10 minutes the reaction was poured into a solution of sat. Na_2SO_3, extracted with diethyl ether (3x), and the combined organic layers were washed with water, brine, dried with $MgSO_4$ and concentrated under vacuum. The crude oil was purified by flash column chromatography (7.5% to 10% ethyl acetate in hexanes) to afford the alcohol **4.112** (209 mg, 0.69 mmol, 34%) as an oil. R_f = 0.26 (10% ethyl acetate in hexanes). ^{1}H-NMR (300 MHz; $CDCl_3$): δ 7.44 (dd, *J* = 7.7, 1.8 Hz, 1H), 7.26 (dd, *J* = 7.7, 7.7 Hz, 1H), 7.16 (dd, *J* = 7.7, 1.8 Hz, 1H), 3.52 (septet, *J* = 6.8 Hz, 1H), 3.07 (s, 1H), 1.82 (s, 6H), 1.24 (d, *J* = 6.8 Hz, 6H). ^{13}C-NMR (75 MHz; $CDCl_3$): δ 152.3, 149.0, 128.4, 125.24, 125.15, 101.9, 74.8, 39.6, 30.5, 23.7. HRMS-ESI calcd for $C_{12}H_{16}I$ $[M+H-H_2O]^+$ 287.0291, found 287.0291. HRMS-ESI calcd for $C_{12}H_{17}INaO$ $[M+Na]^+$ 327.0216, found 327.0217. HRMS-ESI calcd for $C_{12}H_{17}IKO$ $[M+K]^+$ 342.9956, found 342.9955.

Exploratory synthesis of 2-(5-bromo-2-iodo-3-isopropylphenyl)propan-2-ol (4.122):



1-(2-amino-3-isopropylphenyl)ethan-1-one (4.119): A flame-dried 3-necked flask with a stir bar was fitted with a condenser and a connection to a drying tube packed with $CaCl_2$ leading into an $NaOH_{(aq)}$ trap. To this flask was added 2-isopropylaniline (4.2 mL, 30 mmol, 1.0 eq) and 1,2-DCE (21 mL, 1.4 M) then cooled to 0 °C. Boron trichloride (33 mL, 33 mmol, 1.1 eq, 1 M in CH_2Cl_2) was added dropwise. Aluminum chloride (4.4 g, 33 mmol, 1.1 eq) was added in portions, allowing the reaction to fully cool back to 0 °C between each addition. CH_3CN (3.1 mL, 60 mmol, 2.0 eq) was added dropwise and the reaction was warmed to room temperature. The reaction was heated slowly (over 1 hour) to 100 °C in an oil bath. After 40 hours the reaction was cooled to 0 °C and 1 M $HCl_{(aq)}$ (60 mL) was added very slowly. The reaction was again heated to reflux under an open atmosphere for 1 hour. The reaction was cooled and extracted with CH_2Cl_2 (3x). The combined organic layers were washed with 1 M $NaOH_{(aq)}$, water, brine, dried with $MgSO_4$ and concentrated under reduced pressure to afford **4.119** (3.6 g, 21 mmol, 68%) as an orange oil which was used without further purification. R_f = 0.47 (20% ethyl acetate in hexanes). ^{1}H-NMR (300 MHz; $CDCl_3$): δ 7.64 (dd, *J* = 8.1, 1.4 Hz, 1H), 7.29 (dd, *J* = 7.4, 1.2 Hz, 1H), 6.69-6.61 (m, 3H), 2.89 (septet, *J* = 6.8 Hz, 1H), 2.60 (s, 3H), 1.27 (d, *J* = 6.8 Hz, 6H). ^{13}C-NMR (75 MHz; $CDCl_3$): δ 201.4, 147.9, 133.4, 130.4, 130.0, 118.0, 115.4, 28.5, 27.1, 22.1.[273]

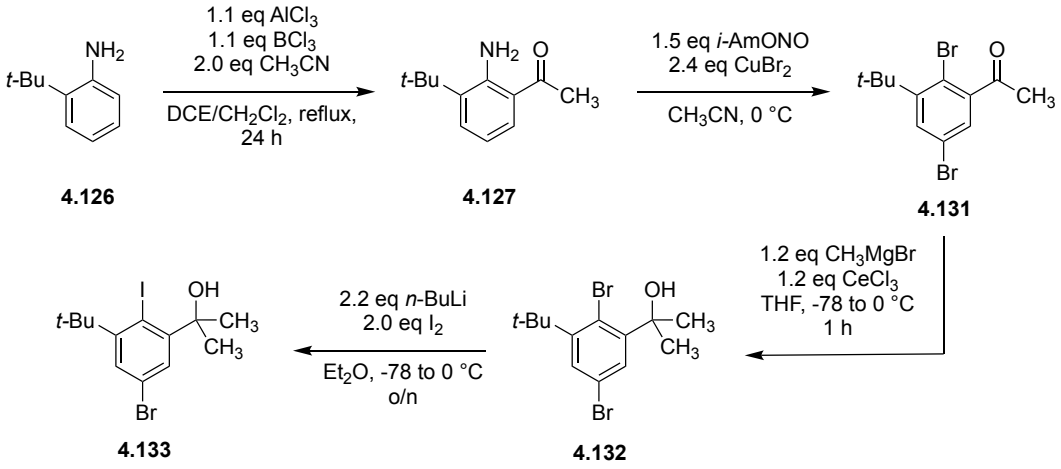
1-(2,5-dibromo-3-isopropylphenyl)ethan-1-one (4.120): To flame-dried round bottom flask with a stir bar was added 1-(2-amino-3-isopropylphenyl)ethan-1-one **4.119** (1.00 mg, 5.64 mmol, 1.0 eq), $CuBr_2$ (3.02 g, 13.5 mmol, 2.4 eq), and anhydrous CH_3CN (23 mL, 0.25 M). The solution was cooled to 0 °C and isoamyl nitrite (1.14 mL, 8.46 mmol, 1.5 eq) was added dropwise. The reaction was stirred at this temperature for 40 minutes. To the reaction was added ammonium hydroxide (~1 mL, 33%$_{(aq)}$), water (50 mL), and diethyl ether (25 mL). The layers were partitioned and the aqueous was extracted with diethyl ether (3x). The combined organic layers were washed with 3% $NH_{3(aq)}$, water, brine, dried with $MgSO_4$ and concentrated under reduced pressure to obtain an orange oil. The crude oil was plugged with silica gel (2.5% ethyl acetate in hexanes) to remove baseline impurities to afford **4.120** (1.42 g) as a solid. R_f = 0.35 (5% ethyl acetate in hexanes). ^{1}H-NMR (300 MHz; $CDCl_3$): δ 7.43 (d, *J* = 2.4 Hz, 1H), 7.23 (d, *J* = 2.4 Hz, 1H), 3.42 (septet, *J* = 6.8 Hz, 1H), 2.58 (s, 3H), 1.24 (d, *J* = 6.9 Hz, 6H).

2-(2,5-dibromo-3-isopropylphenyl)propan-2-ol (4.121a/b): To flame-dried round bottom flask with a stir bar and condenser was added Mg (130 mg, 5.33 mmol, 1.3 eq), iodine (one small crystal), and

anhydrous diethyl ether (3.0 mL). Methyl iodide (306 μL, 4.92 mmol, 1.2 eq) was added dropwise at room temperature. Additional diethyl ether (5.0 mL) was added as soon as the reaction began to reflux. In a separate flame-dried round bottom flask was added 1-(2,5-dibromo-3-isopropylphenyl)ethan-1-one **4.120** (1.32 g, 4.10 mmol, 1.0 eq), dissolved in anhydrous diethyl ether (16.3 mL, 0.25 M) and cooled to 0 °C. The freshly prepared Grignard was added dropwise. The reaction was stirred for 2 hours and then quenched with sat. NH_4Cl. The layers were partitioned and the aqueous was extracted with diethyl ether (3x). The combined organic layers were washed with water, brine, dried with $MgSO_4$ and concentrated under reduced pressure to obtain an oil. The crude oil was purified by flash column chromatography (10% ethyl acetate in hexanes) to afford **4.121a/b** (1.22 g, 11:1) as a solid. $R_f = 0.14$ (5% ethyl acetate in hexanes). ^{1}H-NMR (300 MHz; $CDCl_3$): δ 7.68 (d, $J = 2.5$ Hz, 1H), 7.31 (d, $J = 2.5$ Hz, 1H), 3.53 (septet, $J = 6.8$ Hz, 1H), 2.87 (s, 1H), 1.77 (s, 6H), 1.23 (d, $J = 6.8$ Hz, 6H).

2-(5-bromo-2-iodo-3-isopropylphenyl)propan-2-ol (4.122): To flame-dried round bottom flask with a stir bar was added 2-(2,5-dibromo-3-isopropylphenyl)propan-2-ol **4.121a/b** (1.22 g, 3.63 mmol, 1.0 eq), dissolved in anhydrous diethyl ether (13 mL, 0.28 M) and cooled to -78 °C. To this solution, *n*-BuLi (5.80 mL, 7.99 mmol, 2.2 eq, 1.39 M in hexanes) was added dropwise. The solution was stirred for 1 hour at -78 °C and resulted in a white suspension. After which iodine (1.84 g, 7.26 mmol, 2.0 eq) dissolved in anhydrous diethyl ether (26 mL, 0.28 M) was added dropwise and the reaction was warmed slowly to room temperature overnight (22 hours). Sat. Na_2SO_3 was added and the layers were partitioned. The aqueous layer was extracted with diethyl ether (3x). The organic layers were washed with water, brine, dried with $MgSO_4$ and concentrated under reduced pressure. The crude oil was purified by flash column chromatography (5% ethyl acetate in hexanes) to afford **4.122** (938 mg) as an impure thick clear oil which solidified into a waxy white solid on standing at 4 °C. $R_f = 0.12$ (5% ethyl acetate in hexanes). ^{1}H-NMR (300 MHz; $CDCl_3$): δ 7.64 (d, $J = 2.5$ Hz, 1H), 7.26 (d, $J = 1.9$ Hz, 1H), 3.49 (septet, $J = 6.8$ Hz, 1H), 2.80 (s, 1H), 1.81 (s, 6H), 1.23 (d, $J = 6.8$ Hz, 6H). ^{13}C-NMR (75 MHz; $CDCl_3$): δ 154.4, 151.3, 128.3, 128.1, 123.5, <u>99.8</u>, 74.6, 39.5, 30.3, 23.5. Note: the signal at 99.8 ppm is confirmation of C-I bond formation.

Synthesis of 2-(5-bromo-3-(*tert*-butyl)-2-iodophenyl)propan-2-ol (4.133):



1-(2-amino-3-(*tert*-butyl)phenyl)ethan-1-one (4.127): A flame-dried 3-necked flask with a stir bar was fitted with a condenser and a drying tube packed with $CaCl_2$ leading into an $NaOH_{(aq)}$ trap. To this flask was added 2-(*tert*-butyl)aniline (5.5 mL, 35 mmol, 1.0 eq) and 1,2-DCE (25 mL, 1.4 M) then cooled to 0 °C. Boron trichloride (38.5 mL, 38.5 mmol, 1.1 eq, 1 M in CH_2Cl_2) was added dropwise. Aluminum chloride (5.1 g, 38.5 mmol, 1.1 eq) was added in portions, allowing the reaction to fully cool back to 0 °C between each addition. CH_3CN (3.7 mL, 70 mmol, 2.0 eq) was added dropwise and the reaction was warmed to room temperature. The reaction was heated slowly (over 1 hour) to 100 °C in an oil bath. After 24 hours the reaction was cooled to 0 °C and 1 M $HCl_{(aq)}$ (70 mL) was added very slowly. The reaction was again heated to reflux under an open atmosphere for 1 hour. The reaction was cooled and extracted with CH_2Cl_2 (3x). The combined organic layers were washed with 1 M $NaOH_{(aq)}$, water, brine, dried with $MgSO_4$ and concentrated under reduced pressure to afford **4.127** (5.5 g, 28.8 mmol, 82%) as an orange solid. $R_f = 0.51$ (20% ethyl acetate in hexanes). ^{1}H-NMR (300 MHz; $CDCl_3$): δ 7.69 (dd, $J = 8.0$, 1.2 Hz, 1H), 7.40 (dd, $J = 7.6$, 1.1 Hz, 1H), 6.98 (br. s, 2H), 6.63 (t, $J = 7.8$ Hz, 1H), 2.63 (s, 3H), 1.46 (s, 10H). ^{13}C-NMR (75 MHz; $CDCl_3$): δ 201.6, 149.5, 134.3, 131.8, 130.7, 118.4, 114.9, 34.3, 29.7, 28.8. HRMS-ESI calcd for $C_{12}H_{18}NO$ $[M+H]^+$ 192.1383, found 192.1382.

1-(2,5-dibromo-3-(*tert*-butyl)phenyl)ethan-1-one (4.131): To flame-dried round bottom flask with a stir bar was added 1-(2-amino-3-(*tert*-butyl)phenyl)ethan-1-one **4.127** (622 mg, 3.0 mmol, 1.0 eq),

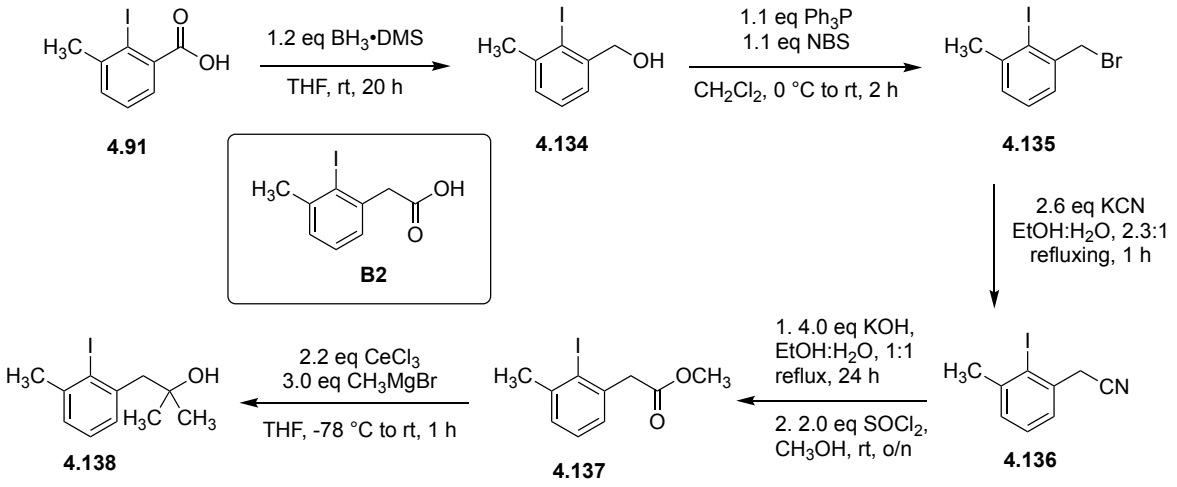
$CuBr_2$ (1.61 g, 7.2 mmol, 2.4 eq), and anhydrous CH_3CN (12 mL, 0.25 M). The solution was cooled to 0 °C and isoamyl nitrite (605 µL, 4.5 mmol, 1.5 eq) was added dropwise. The reaction was stirred at this temperature for 1 hour. The reaction was filtered through celite and concentrated under reduced pressure. The crude solid was purified by flash column chromatography (2.5% ethyl acetate in hexanes) to afford **4.131** (1.0 g, 3.0 mmol, quant.) as a solid. R_f = 0.5 (10% ethyl acetate in hexanes). ^{1}H-NMR (300 MHz; $CDCl_3$): δ 7.56 (d, *J* = 2.4 Hz, 1H), 7.14 (d, *J* = 2.3 Hz, 1H), 2.54 (s, 3H), 1.49 (s, 9H). ^{13}C-NMR (75 MHz; $CDCl_3$): δ 202.4, 151.0, 147.8, 132.0, 127.2, 121.8, 116.0, 37.4, 31.2, 29.8. HRMS-ESI calcd for $C_{12}H_{15}{}^{79}Br_2IO$ $[M+H]^+$ 332.9484, found 332.9485. HRMS-ESI calcd for $C_{12}H_{15}{}^{79}Br^{81}BrIO$ $[M+H]^+$ 334.9464, found 334.9464. HRMS-ESI calcd for $C_{12}H_{15}{}^{81}Br_2IO$ $[M+H]^+$ 336.9443, found 336.9442.

2-(2,5-dibromo-3-(*tert*-butyl)phenyl)propan-2-ol (4.132): To flame-dried round bottom flask with a stir bar was added anhydrous $CeCl_3$ (1.4 g, 5.8 mmol, 1.2 eq) and anhydrous THF (9.6 mL, 0.5 M). This suspension was cooled to -78 °C and CH_3MgBr (1.9 mL, 5.8 mmol, 1.2 eq, 3.0 M in diethyl ether) dropwise. After stirring for 1 hour, 1-(2,5-dibromo-3-(*tert*-butyl)phenyl)ethan-1-one **4.131** (1.6 g, 4.8 mmol, 1.0 eq) in anhydrous THF (5.0 mL) was added dropwise and warmed to 0 °C. After an additional hour, the reaction was quenched with acetic acid (10 mL, 2 M). The aqueous layer was extracted with diethyl ether (3x), and the combined extracts were washed with sat. $NaHCO_3$ (3x), water, brine, dried $MgSO_4$ and concentrate under reduced pressure. The crude oil was purified by flash column chromatography (5% ethyl acetate in hexanes) to afford **4.132** (1.22 g, 3.5 mmol, 73%) a yellow oil. R_f = 0.34 (10% ethyl acetate in hexanes). ^{1}H-NMR (300 MHz; $CDCl_3$): δ 7.76 (d, *J* = 2.5 Hz, 1H), 7.51 (d, *J* = 2.5 Hz, 1H), 3.24 (s, 1H), 1.78 (s, 6H), 1.54 (s, 9H). ^{13}C-NMR (75 MHz; $CDCl_3$): δ 151.5, 149.8, 130.5, 128.9, 121.9, 121.0, 74.8, 38.2, 30.6, 30.1. HRMS-ESI calcd for $C_{13}H_{17}{}^{79}Br_2I$ $[M+H-H_2O]^+$ 330.9692, found 330.9691. HRMS-ESI calcd for $C_{13}H_{17}{}^{79}Br^{81}BrI$ $[M+H-H_2O]^+$ 332.9671, found 332.9670. HRMS-ESI calcd for $C_{13}H_{17}{}^{81}Br_2I$ $[M+H-H_2O]^+$ 334.9651, found 334.9648.

2-(5-bromo-3-(*tert*-butyl)-2-iodophenyl)propan-2-ol (4.133): To flame-dried round bottom flask with a stir bar was added 2-(2,5-dibromo-3-(*tert*-butyl)phenyl)propan-2-ol **4.132** (1.22 g, 3.48 mmol, 1.0 eq), dissolved in anhydrous diethyl ether (12 mL, 0.28 M) and cooled to -78 °C. To this solution, *n*-BuLi (5.52 mL, 7.67 mmol, 2.2 eq, 1.39 M in hexanes) was added dropwise. The solution was stirred

for 1 hour at -78 °C and resulted in a white suspension. After which iodine (1.77 g, 6.97 mmol, 2.0 eq) dissolved in anhydrous diethyl ether (25 mL, 0.28 M) was added dropwise and the reaction was slowly warmed to room temperature overnight (20.5 hours). Sat. Na_2SO_3 was added and the layers were partitioned. The organic layer was washed with water, brine, dried with $MgSO_4$ and concentrated under reduced pressure. The crude oil was purified by flash column chromatography (5% ethyl acetate in hexanes) to afford **4.133** (1.17 g, 2.9 mmol, 85%) a thick clear oil which solidified into a waxy white solid on standing at 4 °C. $R_f = 0.13$ (5% ethyl acetate in hexanes). ^{1}H-NMR (300 MHz; $CDCl_3$): δ 7.67 (d, $J = 2.5$ Hz, 1H), 7.49 (d, $J = 2.5$ Hz, 1H), 3.12 (br. s, 1H), 1.84 (s, 6H), 1.62 (s, 9H). ^{13}C-NMR (75 MHz; $CDCl_3$): δ 154.2, 152.3, 130.2, 128.6, 123.2, 94.9, 75.7, 39.2, 31.3, 30.9. HRMS-ESI calcd for $C_{13}H_{17}{}^{79}BrI$ $[M+H-H_2O]^+$ 378.9553, found 378.9554. HRMS-ESI calcd for $C_{13}H_{17}{}^{81}BrI$ $[M+H-H_2O]^+$ 380.9532, found 380.9532. HRMS-ESI calcd for $C_{13}H_{22}{}^{79}BrINO$ $[M+NH_4]^+$ 413.9924, found 413.9924. HRMS-ESI calcd for $C_{13}H_{22}{}^{81}BrINO$ $[M+NH_4]^+$ 415.9904, found 415.9902.

Synthesis of 1-(2-iodo-3-methylphenyl)-2-methylpropan-2-ol (4.138):



(2-iodo-3-methylphenyl)methanol (4.134): Procedure based on the literature.[274] To a flame-dried round bottom flask was added 2-iodo-3-methylbenzoic acid **4.91** (16 g, 61 mmol, 1.0 eq) and anhydrous THF (61 mL, 1 M). The solution was cooled to 0 °C, BH_3•DMS (6.9 mL, 73 mmol, 1.2 eq) was added dropwise and stirred at room temperature for 20 hours. The reaction was quenched with methanol and Na_2CO_3 (slow addition), then diluted with water and diethyl ether. The layers were separated, and the

aqueous layer was extracted with diethyl ether (3x). The combined organic layers were washed with water, brine, dried with $MgSO_4$, and concentrated under vacuum to afford **4.134** (15 g, 60 mmol, 99%) as a white solid. ^{1}H-NMR (300 MHz; $CDCl_3$): δ 7.26-7.23 (m, 2H), 7.21-7.15 (m, 1H), 4.70 (s, 2H), 2.48 (s, 3H), 2.16 (br. s, 1H). ^{13}C-NMR (75 MHz; $CDCl_3$): δ 143.3, 142.2, 129.1, 128.2, 125.8, 104.8, 70.4, 29.2.[274]

1-(bromomethyl)-2-iodo-3-methylbenzene (4.135): Procedure base on the literature.[275] To a flame-dried round bottom flask with a stir bar under nitrogen was added (2-iodo-3-methylphenyl)methanol **4.134** (3.6 g, 15 mmol, 1.0 eq), triphenylphosphine (4.2 g, 16 mmol, 1.1 eq) and anhydrous CH_2Cl_2 (73 mL, 0.2 M). An ice-water bath was used to maintain the reaction at room temperature. NBS (2.9 g, 16 mmol, 1.1 eq) was added portion wise and the reaction was stirred at room temperature for 2 hours. Hexanes (150 mL) was added, the reaction was filtered through a pad of celite, and the volatiles were removed by vacuum. The crude white solid was purified by column chromatography (100% hexanes) to afford the bromide **4.135** (3.4 g, 11 mmol, 78%) a white solid. R_f = 0.35 (5% ethyl acetate in hexanes). ^{1}H-NMR (300 MHz; $CDCl_3$): δ 7.29 (dd, *J* = 7.3, 2.0 Hz, 1H), 7.21 (dd, *J* = 7.4, 7.4 Hz, 1H), 7.16 (dd, *J* = 7.5, 2.0 Hz, 1H), 4.69 (s, 2H), 2.50 (s, 3H).[275]

2-(2-iodo-3-methylphenyl)acetonitrile (4.136): In a round bottom flask with a stir bar was added KCN (1.85 g, 28 mmol, 2.6 eq), ethanol (35 mL) and water (35 mL). A reflux condenser was attached, and the solution was heated to reflux. 1-(bromomethyl)-2-iodo-3-methylbenzene **4.135** (3.4 g, 11 mmol, 1.0 eq) in ethanol (45 mL) was added dropwise to the refluxing solution. The reaction was stirred for 1 hour, before cooling to 0 °C. Water (100 mL) was added and the precipitate was filtered. The filter cake was washed with ice cold water (3x, 20 mL) and dried under vacuum to afford the nitrile **4.136** (2.6 g, 10 mmol, 92%) as a white solid. R_f = 0.22 (5% ethyl acetate in hexanes). ^{1}H-NMR (300 MHz; $CDCl_3$): δ 7.36-7.20 (m, 3H), 3.88 (s, 2H), 2.50 (s, 3H). ^{13}C-NMR (75 MHz; $CDCl_3$): δ 143.4, 133.9, 129.5, 128.6, 126.4, 117.5, 106.4, 31.4, 29.8.[276]

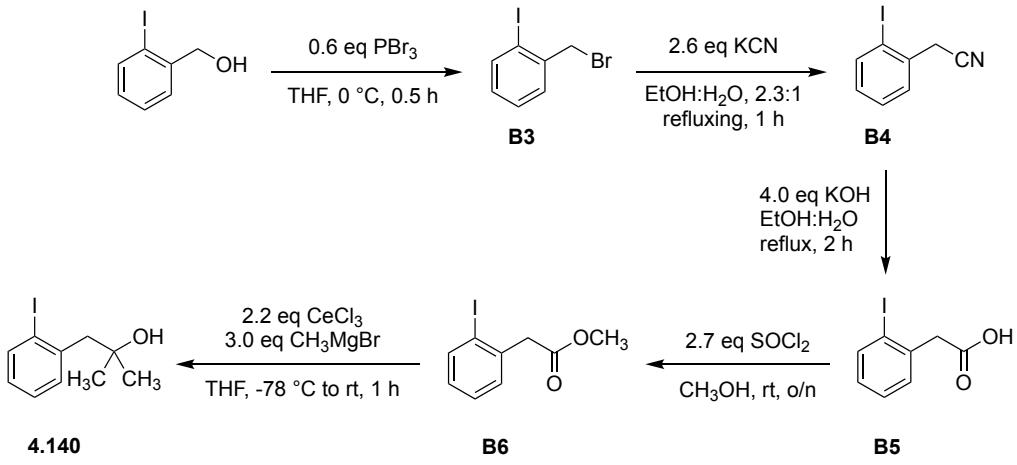
2-(2-iodo-3-methylphenyl)acetic acid (B2): 2-(2-iodo-3-methylphenyl)acetonitrile **4.136** (2.3 g, 8.9 mmol, 1.0 eq) was added to a round bottom flask with HCl (10 M, 50 mL). The solution was heated to 100 °C and stirred for 28 hours. The reaction was cooled to room temperature and extracted with ethyl acetate (3x). The combined extracts were washed with water, brine, dried with $MgSO_4$ and concentrated

by rotary evaporation to afford **B2** (2.4 g, 8.7 mmol, 98%) as a white solid. ^{1}H-NMR (300 MHz; $CDCl_3$): δ 7.23-7.14 (m, 2H), 7.09 (dd, *J* = 7.0, 2.0 Hz, 1H), 3.92 (s, 2H), 2.49 (s, 3H). ^{13}C-NMR (75 MHz; $CDCl_3$): δ 177.4, 142.9, 137.8, 128.9, 128.09, 128.06, 108.5, 47.4, 30.0. HRMS-ESI calcd for $C_9H_{10}IO_2$ $[M+H]^+$ 276.9720, found 276.9719. Note: On a larger scale (~40 mmol) the reaction did not proceed well, presumably due to the insolubility of **4.136** in the reaction solvent. Basic hydrolysis was achieved with **4.136** (1.0 eq), KOH (4.0 eq), and 1:1 H_2O:EtOH (0.4 M) at reflux for 24 hours.

Methyl 2-(2-iodo-3-methylphenyl)acetate (4.137): 2-(2-iodo-3-methylphenyl)acetic acid **B2** (2.3 g, 8.3 mmol, 1.0 eq) was dissolved in methanol (17 mL, 0.5 M) in a round bottom flask. The solution was cooled to 0 °C and thionyl chloride (1.2 mL, 16.7 mmol, 2.0 eq) was added dropwise and stirred overnight at room temperature. The volatiles were removed under vacuum, the residue dissolved in diethyl ether and washed with sat. $NaHCO_3$, water, brine, dried with $MgSO_4$, and concentrated to an oil (2.39 g, 8.2 mmol, 99%). R_f = 0.41 (15% ethyl acetate in hexanes). ^{1}H-NMR (300 MHz; $CDCl_3$): δ 7.25-7.15 (m, 2H), 7.10 (dd, *J* = 7.1, 2.0 Hz, 1H), 3.90 (s, 2H), 3.75 (s, 3H), 2.51 (s, 3H). ^{13}C-NMR (75 MHz; $CDCl_3$): δ 171.3, 142.8, 138.5, 128.6, 128.02, 127.99, 108.4, 52.3, 47.6, 30.0. HRMS-ESI calcd for $C_{10}H_{12}IO_2$ $[M+H]^+$ 290.9877, found 290.9873.

1-(2-iodo-3-methylphenyl)-2-methylpropan-2-ol (4.138): To flame-dried round bottom flask under N_2 was added anhydrous $CeCl_3$ (3.5 g, 14.4 mmol, 2.2 eq) and suspended in anhydrous THF (0.2 M, 33 mL). The solution was cooled to -78 °C and commercial CH_3MgBr (6.5 mL, 19.6 mmol, 3.0 eq) was added dropwise and stirred at this temperature for 1 hour. Methyl 2-(2-iodo-3-methylphenyl)acetate **4.137** (1.9 g, 6.5 mmol, 1.0 eq) dissolved in anhydrous THF (6.5 mL) was added dropwise and the reaction was warmed to room temperature for an additional hour. The reaction was quenched slowly with sat. NH_4Cl. The reaction was diluted with diethyl ether, the layers partitioned and the aqueous layer extracted with diethyl ether (2x). The combined organic layers were washed with water, brine, dried with $MgSO_4$ and concentrated under vacuum. The crude was purified by silica gel flash column chromatography with 15% ethyl acetate in hexanes to afford **4.138** (1.72 g, 5.9 mmol, 91%) as a clear oil. R_f = 0.26 (15% ethyl acetate in hexanes). ^{1}H-NMR (300 MHz; $CDCl_3$): δ 7.17-7.09 (m, 3H), 3.14 (s, 2H), 2.51 (s, 3H), 1.60 (s, 1H), 1.30 (s, 6H). ^{13}C-NMR (75 MHz; $CDCl_3$): δ 142.6, 141.9, 128.2, 128.0, 127.3, 110.5, 72.0, 53.2, 30.8, 29.7. HRMS-ESI calcd for $C_{11}H_{14}I$ $[M+H-H_2O]^+$ 273.0135, found 273.0127.

Synthesis of 1-(2-iodophenyl)-2-methylpropan-2-ol (4.140):



1-(bromomethyl)-2-iodobenzene (B3): To a flame-dried round bottom flask under N_2 was added (2-iodophenyl)methanol (1.2 g, 5.0 mmol, 1.0 eq) and anhydrous THF (0.86 M, 6.0 mL). The solution was cooled to 0°C and PBr_3 (285 µL, 3.0 mmol, 0.6 eq) was added dropwise. After 30 min at 0 °C the reaction was quenched with water. The aqueous layer was extracted with diethyl ether (3x). The organic layer was washed with sat. $NaHCO_3$, water, brine, dried with $MgSO_4$ and concentrated to an oil **B3** (1.44 g, 4.9 mmol, 97%). ^{1}H-NMR (300 MHz; $CDCl_3$): δ 7.86 (d, *J* = 7.9 Hz, 1H), 7.48 (dd, *J* = 7.6, 1.4 Hz, 1H), 7.34 (ddd, *J* = 7.5, 7.5, 1.1 Hz, 1H), 6.98 (ddd, *J* = 7.6, 7.6, 1.3 Hz, 1H), 4.60 (s, 2H).[277]

2-(2-iodophenyl)acetonitrile (B4): To a round bottom flask with a condenser was added ethanol (15 mL), water (15 mL) and potassium cyanide (796 mg, 12.2 mmol, 2.6 eq). The solution was heated to reflux and 1-(bromomethyl)-2-iodobenzene **B3** (1.4 g, 4.7 mmol, 1.0 eq) in ethanol (20 mL) was added dropwise. After refluxing the reaction for 4 hours it was cooled to room temperature and the volatiles were removed under reduced pressure. The aqueous layer was extracted with diethyl ether (3x). The organic layer was washed with water, brine, dried with $MgSO_4$ and concentrated to an oil **B4** (1.02 g, 4.2 mmol, 89%). ^{1}H-NMR (300 MHz; $CDCl_3$): δ 7.88 (dd, *J* = 7.9, 1.1 Hz, 1H), 7.54 (dd, *J* = 7.7, 1.4 Hz, 1H), 7.40 (ddd, *J* = 7.6, 7.6, 1.2 Hz, 1H), 7.05 (ddd, *J* = 7.7, 7.7, 1.4 Hz, 1H), 3.82 (s, 2H).[277]

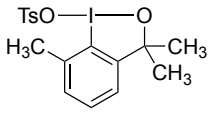
2-(2-iodophenyl)acetic acid (B5): In a round bottom flask KOH (943 mg, 16.8 mmol, 4.0 eq) was dissolved in water (2.1 mL, 2 M). To the solution was added 2-(2-iodophenyl)acetonitrile **B4** (1.01 g,

4.2 mmol, 1.0 eq) in ethanol (2.1 mL, 2 M) and the flask fitted with a reflux condenser. The solution was stirred at reflux for 2 hours. The volatiles were removed by rotary evaporation and the remaining aqueous layer was washed with diethyl ether (1x). The aqueous layer was acidified with 3 M HCl and extracted with diethyl ether (3x). The organic layer was washed with water, brine, dried with $MgSO_4$ and concentrated to a solid **B5** (950 mg, 3.6 mmol, 86%). ^{1}H-NMR (300 MHz; $CDCl_3$): δ 7.86 (dd, *J* = 7.9, 0.8 Hz, 1H), 7.36-7.28 (m, 2H), 6.98 (ddd, *J* = 7.9, 6.7, 2.4 Hz, 1H), 3.86 (s, 2H).[278]

Methyl 2-(2-iodophenyl)acetate (B6): 2-(2-iodophenyl)acetic acid **B5** (682 mg, 2.6 mmol, 1.0 eq) was dissolved in methanol (5.0 mL) and cooled to 0 °C. Thionyl chloride (500 µL, 6.9 mmol, 2.7 eq) and the reaction was stirred overnight at room temperature. The volatiles were removed by rotary evaporation and the crude was dissolved in diethyl ether. The diethyl ether was washed sequentially with sat. $NaHCO_3$, water, brine, dried with $MgSO_4$ and concentrated under vacuum. The crude oil was plugged through silica to afford **B6** (591 mg, 2.1 mmol, 82%) as a yellow oil. ^{1}H-NMR (300 MHz; $CDCl_3$): δ 7.85 (dd, *J* = 7.9, 0.9 Hz, 1H), 7.35-7.26 (m, 2H), 6.97 (ddd, *J* = 7.9, 6.7, 2.3 Hz, 1H), 3.81 (s, 2H), 3.72 (s, 3H).[279]

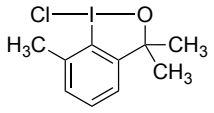
1-(2-iodophenyl)-2-methylpropan-2-ol (4.140): To flame-dried round bottom flask under N_2 was added anhydrous $CeCl_3$ (392 mg, 1.59 mmol, 2.2 eq) and suspended in anhydrous THF (0.2 M, 3.6 mL). The solution was cooled to -78 °C and commercial CH_3MgBr (0.723 mL, 3 M in Et_2O, 2.17 mmol, 3.0 eq) was added dropwise and stirred at this temperature for 1 hour. Methyl 2-(2-iodophenyl)acetate **B6** (200 mg, 0.72 mmol, 1.0 eq) dissolved in anhydrous THF (3.6 mL) was added dropwise and the reaction was warmed to room temperature for an additional hour. The reaction was quenched slowly with sat. NH_4Cl at 0 °C. The reaction was diluted with diethyl ether, the layers partitioned and the aqueous layer extracted with diethyl ether (2x). The combined organic layers were washed with sat. $NH_4Cl_{(aq)}$, water, brine, dried with $MgSO_4$ and concentrated under vacuum. The crude was purified by silica gel flash column chromatography with 20% ethyl acetate in hexanes to afford **4.140** (79 mg, 0.29 mmol, 40%) as a clear oil. R_f = 0.29 (30% ethyl acetate in hexanes). ^{1}H-NMR (300 MHz; $CDCl_3$): δ 7.88 (dd, *J* = 7.9, 1.2 Hz, 1H), 7.39 (dd, *J* = 7.7, 1.8 Hz, 1H), 7.31 (ddd, *J* = 7.5, 7.5, 1.2 Hz, 1H), 6.93 (ddd, *J* = 7.6, 7.6, 1.8 Hz, 1H), 3.04 (s, 2H), 1.61 (s, 1H), 1.31 (s, 6H). ^{13}C-NMR (75 MHz; $CDCl_3$): δ 141.3, 139.9, 131.3, 128.3, 128.1, 103.0, 72.1, 52.4, 29.7. HRMS-ESI calcd for $C_{10}H_{12}I$ $[M+H-H_2O]^+$ 258.9978, found 258.9978.

4.5.2 Preparation of Hypervalent Iodine Compounds



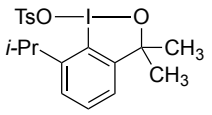
4.144

3,3,7-trimethyl-1λ^3-benzo[*d*][1,2]iodaoxol-1(3*H*)-yl 4-methylbenzenesulfonate (4.144): 2-(2-iodo-3-methylphenyl)propan-2-ol **4.93** (138 mg, 0.5 mmol, 1.0 eq) and Koser's reagent (196 mg, 0.5 mmol, 1.0 eq) were dissolved in CH_2Cl_2 (2.5 mL, 0.2 M) and stirred at room temperature for 24 hours. The yellow solution was concentrated under reduced pressure and the resulting oil was washed with hexanes (3x). The crude was precipitated from ethyl acetate with hexanes to afford **4.144** (189 mg, 0.42 mmol, 85%) as a yellow solid. ^{1}H-NMR (300 MHz; $CDCl_3$): δ 7.77 (d, *J* = 8.2 Hz, 2H), 7.40-7.30 (m, 2H), 7.23 (d, *J* = 8.2 Hz, 2H), 6.93 (dd, *J* = 7.1, 1.7 Hz, 1H), 2.56 (m, 4H), 2.38 (s, 3H), 1.60 (s, 6H). ^{13}C-NMR (75 MHz; $CDCl_3$): δ 150.3, 142.0, 141.0, 139.1, 133.5, 131.3, 129.3, 126.4, 124.1, 122.1, 91.4, 27.7, 24.0, 21.5. HRMS-ESI calcd for $C_{10}H_{12}IO$ $[M\text{-}OTs]^+$ 274.9927, found 274.9925. Following the same procedure **4.93** (1.45 g, 5.25 mmol, 1.0 eq), Koser's (2.06 g, 5.25 mmol, 1.0 eq), CH_2Cl_2 (0.2 M, 26 mL) gave **4.144** (2.09 g, 4.68 mmol, 89%).



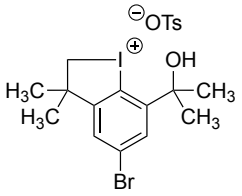
4.145

1-chloro-3,3,7-trimethyl-1,3-dihydro-1λ^3-benzo[*d*][1,2]iodaoxole (4.145): To a round bottom flask was added 2-(2-iodo-3-methylphenyl)propan-2-ol **4.93** (414 mg, 1.5 mmol, 1.0 eq) and chloroform (1.2 mL, 1.3 M). The solution was stirred at room temperature until **4.93** was fully dissolved before wrapping the flask in foil. Then *tert*-butyl hypochlorite (180 μL, 1.58 mmol, 1.05 eq) was added dropwise and the solution was stirred in the dark. The reaction progressed from yellow to orange over 25 minutes. After which all volatiles were removed under reduced pressure and the crude solid was recrystallized from acetonitrile. ^{1}H-NMR (300 MHz; $CDCl_3$): δ 7.35 (dd, *J* = 7.3, 7.3 Hz, 1H), 7.26 (ddd, *J* = 7.4, 1.7, 0.7 Hz, 1H), 6.95 (ddd, *J* = 7.1, 1.4, 0.5 Hz, 1H), 2.77 (s, 3H), 1.59 (s, 6H). ^{13}C-NMR (75 MHz; $CDCl_3$): δ 151.8, 141.1, 133.1, 130.8, 124.0, 120.1, 86.5, 28.3, 24.1. HRMS-ESI calcd for $C_{10}H_{12}IO$ $[M\text{-}Cl]^+$ 274.9927, found 274.9927.



4.150

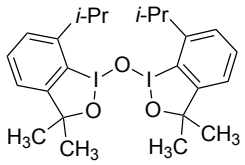
7-isopropyl-3,3-dimethyl-1λ^3-benzo[*d*][1,2]iodaoxol-1(3*H*)-yl 4-methylbenzenesulfonate (4.150): 2-(2-iodo-3-isopropylphenyl)propan-2-ol **4.112** (200 mg, 0.66 mmol, 1.0 eq) and Koser's reagent (258 mg, 0.66 mmol, 1.0 eq) were dissolved in CH_2Cl_2 (3.3 mL, 0.2 M) and stirred at room temperature for 24 hours. The yellow solution was concentrated under reduced pressure to afford an oil. The oil was dissolved in minimal CH_2Cl_2 and precipitated with hexanes. The solvent was pipetted off and the process was repeated twice more. The solid turns into an oil and expands rapidly under high vacuum. **4.150** (221 mg, 0.47 mmol, 71%). ^{1}H-NMR (300 MHz; $CDCl_3$): δ 7.78 (d, *J* = 8.2 Hz, 2H), 7.49-7.41 (m, 2H), 7.22 (d, *J* = 8.0 Hz, 2H), 6.92 (dd, *J* = 6.6, 2.4 Hz, 1H), 4.79 (br. s, 1H), 3.36 (septet, *J* = 6.7 Hz, 1H), 2.38 (s, 3H), 1.61 (s, 6H), 1.14 (d, *J* = 6.7 Hz, 6H). ^{13}C-NMR (75 MHz; $CDCl_3$): δ 151.2, 150.3, 141.9, 139.3, 131.8, 129.33, 129.28, 126.4, 124.6, 122.3, 92.4, 34.1, 27.7, 24.0, 21.6. HRMS-ESI calcd for $C_{12}H_{16}IO$ $[M\text{-}OTs]^+$ 303.0240, found 303.0240.



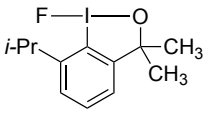
4.155

5-bromo-7-(2-hydroxypropan-2-yl)-3,3-dimethyl-2,3-dihydrobenzo[*b*]iodol-1-ium 4-methylbenzenesulfonate (4.155): 2-(5-bromo-3-(tert-butyl)-2-iodophenyl)propan-2-ol **4.133** (199 mg, 0.50 mmol, 1.0 eq) and Koser's reagent (196 mg, 0.50 mmol, 1.0 eq) were dissolved in CH_2Cl_2 (2.5 mL, 0.2 M) and stirred at room temperature for 24 hours. The clear orange solution was concentrated under reduced pressure to afford an oil. The oil was purified by flash column chromatography (15% ethyl acetate in hexanes to 30% ethyl acetate in hexanes to 5% methanol in dichloromethane to 10% methanol in dichloromethane) to obtain a thick oil which solidifies to a slightly yellow/white solid. The oil/solid was suspended in minimal ethyl acetate and precipitated with hexanes to yield **4.155** (189 mg, 0.34 mmol, 67%) as a white solid). ^{1}H-NMR (300 MHz; CD_3OD): δ 7.72-7.69 (m, 3H), 7.47 (d, *J* = 2.0 Hz, 1H), 7.23 (dd, *J* = 8.5, 0.6 Hz, 2H), 4.51 (s, 2H), 3.35 (s, 2H), 2.37 (s, 3H), 1.58 (s, 6H), 1.54 (s, 6H). ^{13}C-NMR (75 MHz; CD_3OD): δ 157.9, 150.7, 143.4, 141.7, 130.6, 130.5, 129.8, 127.3, 126.9,

105.9, 71.7, 49.9, 48.8, 30.2, 27.7, 21.3. HRMS-ESI calcd for $C_{13}H_{17}{}^{79}BrIO$ $[M\text{-}OTs]^+$ 394.9502, found 394.9502. HRMS-ESI calcd for $C_{13}H_{17}{}^{81}BrIO$ $[M\text{-}OTs]^+$ 396.9482, found 396.9482.



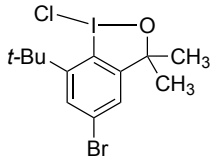
4.151



4.152

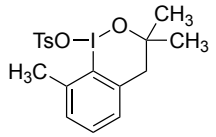
1,1'-oxybis(7-isopropyl-3,3-dimethyl-1,3-dihydro-1λ^3-benzo[*d*][1,2]iodaoxole) (4.151) and/or 1-fluoro-7-isopropyl-3,3-dimethyl-1,3-dihydro-1λ^3-benzo[*d*][1,2]iodaoxole (4.152): Procedure based on the literature.[182, 192] 7-isopropyl-3,3-dimethyl-1λ3-benzo[*d*][1,2]iodaoxol-1(3*H*)-yl 4-methylbenzenesulfonate **4.150** (50 mg, 0.11 mmol, 1.0 eq) was suspended in hexanes (550 µL, 0.2 M). To the vigorously stirring suspension was added TBAF (130 µL, 0.13 mmol, 1.2 eq, 1 M in THF). Almost immediately the solids are consumed, and an oil separates out of the hexanes. After stirring for 10 minutes at room temperature an additional 1 mL of hexanes was added and stirred for 2 min. The hexanes was removed by a glass Pasteur pipette. The addition of hexanes was repeated twice more. The combined hexanes extractions were concentrated under reduced pressure to afford a waxy solid.

Procedure 2: 7-isopropyl-3,3-dimethyl-1λ^3-benzo[*d*][1,2]iodaoxol-1(3*H*)-yl 4-methylbenzenesulfonate **4.150** (50 mg, 0.11 mmol, 1.0 eq) was dissolved in CH_2Cl_2 (1.0 mL, 0.11 M). To the solution was added triethylamine trihydrofluoride (10 drops) at room temperature. The yellow solution immediately goes clear and faintly yellow. The solution was stirred for 1 hour and then concentrated by rotary evaporation. Hexanes was added to the crude and washed with water (3x). The solution was again concentrated, and excess water was removed by azeotroping with toluene to afford a clear/yellow oil. Attempted recrystallization from dichloromethane and hexanes gave a crystal of **4.151**. ^{1}H-NMR (300 MHz; $CDCl_3$): δ 7.47-7.39 (m, 2H), 6.98 (dd, J = 6.7, 2.1 Hz, 1H), 3.85 (septet, J = 6.7 Hz, 1H), 1.54 (s, 6H), 1.27 (d, J = 6.8 Hz, 6H). ^{19}F-NMR (282 MHz; $CDCl_3$): δ -100.1. Note: the fluorine NMR signal is consistent with the presence of desired fluoroiodane **4.152**.



4.163

5-bromo-7-(*tert*-butyl)-1-chloro-3,3-dimethyl-1,3-dihydro-1λ^3-benzo[*d*][1,2]iodaoxole (4.163): To a flame-dried round bottom flask with a stir bar was added 2-(5-bromo-3-(*tert*-butyl)-2-iodophenyl)propan-2-ol **4.133** (14 mg, 0.035 mmol, 1.0 eq), anhydrous CH_2Cl_2 (1 mL, 0.035 M), and *t*-BuOCl (1 drop from a Pasteur pipette). The reaction was stirred in the dark at room temperature for 1 hour. The reaction was concentrated under reduced pressure and recrystallized from CH_2Cl_2 and hexanes. ^{1}H-NMR (300 MHz; $CDCl_3$): δ 7.70 (d, *J* = 2.2 Hz, 1H), 7.02 (d, *J* = 2.2 Hz, 1H), 1.62 (s, 6H), 1.56 (s, 9H). ^{13}C-NMR (75 MHz; $CDCl_3$): δ 155.3, 152.7, 133.4, 126.8, 125.7, 118.6, 87.6, 37.1, 31.5, 28.4.



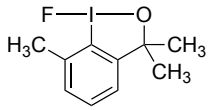
4.167

3,3,8-trimethyl-3,4-dihydro-1*H*-1λ^3-benzo[*e*][1,2]iodaoxin-1-yl 4-methylbenzenesulfonate (4.167):

Procedure 1: 1-(2-iodo-3-methylphenyl)-2-methylpropan-2-ol **4.138** (58 mg, 0.2 mmol, 1.0 eq) and Koser's reagent (78 mg, 0.2 mmol, 1.0 eq) were dissolved in CH_2Cl_2 (1.0 mL, 0.2 M) and stirred at room temperature for 65 hours. The yellow solution was concentrated under reduced pressure and the resulting oil was washed with hexanes (3x). The crude was precipitated from ethyl acetate with hexanes to afford **4.167** as a yellow solid. ^{1}H-NMR (300 MHz; $CDCl_3$): δ 7.61 (d, *J* = 8.2 Hz, 2H), 7.40 (dd, *J* = 7.4, 7.4 Hz, 1H), 7.27 (d, *J* = 7.0 Hz, 3H), 7.13 (d, *J* = 8.0 Hz, 2H), 2.99 (s, 2H), 2.57 (s, 3H), 2.35 (s, 3H), 1.21 (s, 6H). ^{13}C-NMR (75 MHz; $CDCl_3$): δ 141.6, 140.6, 139.1, 137.9, 134.8, 132.1, 130.0, 129.1, 128.8, 126.2, 79.6, 52.7, 27.7, 24.7, 21.5. HRMS-ESI calcd for $C_{11}H_{14}IO$ [M-OTs]$^+$ 289.0084, found 289.0081; calcd for C_8H_8I [M-OTs-$(CH_3)_2CO$]$^+$ 230.9665, found 230.9666. Note: for unknown reasons, this procedure was not always reproducible.

Procedure 2: Modified from the literature.[280] 1-(2-iodo-3-methylphenyl)-2-methylpropan-2-ol **4.138** (145 mg, 0.5 mmol, 1.0 eq) and *m*CPBA (123 mg, 0.55 mmol, 77%, 1.1 eq) were dissolved in $CHCl_3$ (0.75 mL, 0.67 M) and stirred at room temperature for 5 minutes. To this solution was added *p*TsOH•H_2O (105 mg, 0.55 mmol, 1.1 eq) and the reaction was stirred at room temperature for 19 hours. The reaction was concentrated under a stream of air to an oil. The oil was washed with ether (3x) and trace solvent was removed with high vacuum to yield **4.167** (69 mg, 0.13 mmol, 26%) as a white foam which solidifies. Analytical data matches that of Procedure 1.

General Procedure 1 – Preparation of fluoroiodanes with AgF_2 (GP1)[183]: A flame-dried round bottom flask with a stir bar was evacuated and back-filled with nitrogen (3x) then iodoalcohol (1.0 eq), anhydrous acetonitrile (0.1 M), and silver(II) difluoride (2.5 eq) were added. The reaction was stirred under nitrogen for 1 hour. The reaction was concentrated under reduced pressure and anhydrous diethyl ether was added (0.05 M). The mixture was filtered and concentrated to afford the desired fluoroiodanes. A solution of the crude in CH_2Cl_2 was layered with hexanes and allowed to slowly diffuse and evaporate at room temperature over a period of days to yield a colourless clear crystal from which an x-ray crystal structure was obtained.

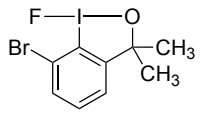


4.143

1-fluoro-3,3,7-trimethyl-1,3-dihydro-1λ^3-benzo[*d*][1,2]iodaoxole (4.143): 2-(2-iodo-3-methylphenyl)propan-2-ol **4.93** (100 mg, 0.36 mmol, 1.0 eq), AgF_2 (132 mg, 0.91 mmol, 2.5 eq) and acetonitrile (3.6 mL) were combined according to GP1. A dark solid was isolated (53 mg).

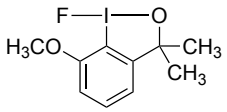
Preparation from tosylate **4.144** with TBAF: Procedure based on the literature.[182, 192] 3,3,7-trimethyl-1λ^3-benzo[*d*][1,2]iodaoxol-1(3*H*)-yl 4-methylbenzenesulfonate **4.144** (100 mg, 0.22 mmol, 1.0 eq) was suspended in hexanes (1.10 mL, 0.2 M). To the vigorously stirring suspension was added TBAF (264 µL, 0.264 mmol, 1.2 eq, 1 M in THF). Almost immediately the solids are consumed, and an oil separates out of the hexanes. After stirring for 10 minutes at room temperature an additional 1 mL of hexanes was added and stirred for 2 min. The hexanes was removed with a glass Pasteur pipette. The addition of hexanes was repeated twice more. The combined hexanes extractions were concentrated under

reduced pressure to afford **4.143** (45 mg, 0.15 mmol, 69%) as a white solid. Recrystallization: slow evaporation from CH_2Cl_2 layered with hexanes at room temperature. ^{1}H-NMR (300 MHz; $CDCl_3$): δ 7.35 (dd, *J* = 7.4, 7.4 Hz, 1H), 7.28-7.25 (m, 2H), 6.99 (ddd, *J* = 7.4, 1.6, 0.5 Hz, 1H), 2.64 (s, 3H), 1.53 (s, 6H). ^{13}C-NMR (75 MHz; $CDCl_3$): δ 150.1, 140.7, 133.2, 130.5, 123.5, 118.8, 85.6, 28.2, 22.9. ^{19}F-NMR (282 MHz, $CDCl_3$): δ -104.7.



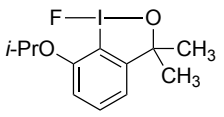
4.147

7-bromo-1-fluoro-3,3-dimethyl-1,3-dihydro-1λ^3-benzo[*d*][1,2]iodaoxole (4.147): 2-(3-bromo-2-iodophenyl)propan-2-ol **4.97** (61 mg, 0.18 mmol, 1.0 eq), AgF_2 (65 mg, 0.44 mmol, 2.5 eq), and acetonitrile (2 mL) were combined according to GP1. ^{1}H-NMR (300 MHz; $CDCl_3$): δ 7.66 (dd, *J* = 7.7, 1.3 Hz, 1H), 7.31 (dd, *J* = 7.6, 7.6 Hz, 1H), 7.12 (dd, *J* = 7.5, 1.3 Hz, 1H), 1.55 (s, 6H). ^{19}F-NMR (282 MHz; $CDCl_3$): δ -102.0 (br. s)



4.148

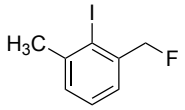
1-fluoro-7-methoxy-3,3-dimethyl-1,3-dihydro-1λ^3-benzo[*d*][1,2]iodaoxole (4.148): 2-(2-iodo-3-methoxyphenyl)propan-2-ol **4.107** (114 mg, 0.39 mmol, 1.0 eq), AgF_2 (142 mg, 0.98 mmol, 2.5 eq), and acetonitrile (3.9 mL) were combined according to GP1. ^{1}H-NMR (300 MHz; $CDCl_3$): δ 7.42 (dd, *J* = 7.8, 7.8 Hz, 1H), 6.98 (dd, *J* = 8.1, 0.9 Hz, 1H), 6.76 (dd, *J* = 7.5, 1.1 Hz, 1H), 3.94 (s, 3H), 1.52 (s, 6H). ^{19}F-NMR (282 MHz; $CDCl_3$): δ -108.2 (br. s).



4.149

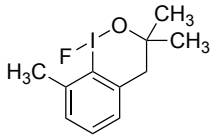
1-fluoro-7-isopropoxy-3,3-dimethyl-1,3-dihydro-1λ^3-benzo[*d*][1,2]iodaoxole (4.149): 2-(2-iodo-3-isopropoxyphenyl)propan-2-ol **4.108** (105 mg, 0.33 mmol, 1.0 eq), AgF_2 (120 mg, 0.82 mmol, 2.5 eq), and acetonitrile (1 mL) were combined according to GP1 and stirred for 2 hours. ^{1}H-NMR (300 MHz;

$CDCl_3$): δ 7.37 (dd, *J* = 8.1, 7.5 Hz, 1H), 6.97 (dd, *J* = 8.1, 0.7 Hz, 1H), 6.72 (dd, *J* = 7.5, 1.2 Hz, 1H), 4.65 (7, *J* = 6.1 Hz, 1H), 1.51 (s, 6H), 1.39 (d, *J* = 6.1 Hz, 6H). ^{19}F-NMR (282 MHz; $CDCl_3$): δ -105.8 (br. s).



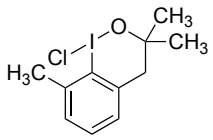
4.166

1-(fluoromethyl)-2-iodo-3-methylbenzene (4.166): 1-(2-iodo-3-methylphenyl)-2-methylpropan-2-ol **4.138** (172 mg, 0.59 mmol, 1.0 eq), AgF_2 (216 mg, 1.5 mmol, 2.5 eq), and acetonitrile (6 mL) were combined according to GP1. This sample was not recrystallized. After filtration a crude oil was obtained (68 mg, 0.27 mmol, 45%). The major product is consistent with compound **4.166.** ^{1}H-NMR (300 MHz; $CDCl_3$): δ 7.33-7.23 (m, 3H), 5.44 (d, *J* = 47.3 Hz, 2H), 2.50 (s, 3H). ^{19}F-NMR (282 MHz; $CDCl_3$): δ -212.6. Proton coupled ^{19}F-NMR (282 MHz; $CDCl_3$): δ -212.6 (t, 47.3 Hz).



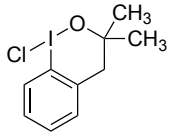
4.168

1-fluoro-3,3,8-trimethyl-3,4-dihydro-1*H*-1λ^3-benzo[*e*][1,2]iodaoxine (4.168): Procedure based on the literature.[182, 192] 3,3,8-trimethyl-3,4-dihydro-1*H*-1λ^3-benzo[*e*][1,2]iodaoxin-1-yl 4-methylbenzenesulfonate **4.167** (35 mg, 0.076 mmol, 1.0 eq) was suspended in hexanes (380 µL, 0.2 M). To the vigorously stirring suspension was added TBAF (91 µL, 0.091 mmol, 1.2 eq, 1 M in THF). Almost immediately the solids are consumed, and an oil separates out of the hexanes. After stirring for 10 minutes at room temperature an additional 1 mL of hexanes was added and stirred for 2 min. The hexanes was removed with a glass Pasteur pipette. The addition of hexanes was repeated twice more. The combined hexanes extractions were concentrated under reduced pressure to afford **4.168** as a white solid. Recrystallization: slow evaporation from CH_2Cl_2 layered with pentane at room temperature. Crystals were stored at -20 °C. ^{1}H-NMR (300 MHz; $CDCl_3$): δ 7.36 (dd, *J* = 7.3, 7.3 Hz, 1H), 7.30 (dd, *J* = 7.5, 1.6 Hz, 1H), 7.24 (dd, *J* = 7.2, 1.5 Hz, 1H), 2.94 (br. s, 2H), 2.72 (s, 3H), 1.15 (br. s, 6H). ^{19}F-NMR (282 MHz; $CDCl_3$): δ -100.1.



4.169

1-chloro-3,3,8-trimethyl-3,4-dihydro-1*H*-1λ^3-benzo[*e*][1,2]iodaoxine (4.169): In a flame-dried round bottom flask under N_2 1-(2-iodo-3-methylphenyl)-2-methylpropan-2-ol **4.138** (100 mg, 0.34 mmol, 1.0 eq) was dissolved in anhydrous $CHCl_3$ (2.0 mL). The flask was wrapped with aluminum foil and *t*-butylhypochlorite (40 μL, 0.36 mmol, 1.05 eq) was added. The reaction was stirred for 1 hour. The final solution should be a deep yellow. The volatiles were removed by vacuum to afford **4.169** as a yellow solid. Recrystallization from CH_2Cl_2 layered with hexanes gave crystals for x-ray. ^{1}H-NMR (300 MHz; $CDCl_3$): δ 7.40-7.24 (m, 3H), 3.17-2.95 (m, 2H), 2.89 (s, 3H), 1.20 (d, J = 148.7 Hz, 7H). ^{13}C-NMR (75 MHz; $CDCl_3$): δ 140.0, 138.3, 136.1, 131.5, 130.2, 128.3, 76.9, 53.3, 28.4, 25.4. Note: The written spectral data is a poor representation of the actual data. Please see the spectra.



4.170

1-chloro-3,3-dimethyl-3,4-dihydro-1*H*-1λ^3-benzo[*e*][1,2]iodaoxine (4.170): In a flame-dried round bottom flask under N_2 1-(2-iodophenyl)-2-methylpropan-2-ol **4.140** (20 mg, 0.072 mmol, 1.0 eq) was dissolved in anhydrous $CHCl_3$ (2.0 mL). The flask was wrapped with aluminum foil and *t*-butylhypochlorite (5 drops) was added. The reaction was stirred for 2 hours. The final solution should be a deep yellow. The volatiles were removed by vacuum to afford **4.170** as a yellow solid. ^{1}H-NMR (300 MHz; $CDCl_3$): δ 8.29-8.26 (m, 1H), 7.48-7.35 (m, 3H), 2.94 (s, 2H), 1.22 (s, 7H). ^{13}C-NMR (75 MHz; $CDCl_3$): δ 137.8, 132.1, 131.5, 131.3, 131.0, 129.1, 77.6, 51.5, 28.9. Note: See spectra for comparison with compound **4.169**.

References

(1) Mineral Commodity Summaries 2023. Interior, U. S. D. o. t., Ed. United States Geological Survey: Virginia, 2023; pp 90-91.

(2) Lauterbach, A., Iodine Production from Caliche. In *Iodine Chemistry and Applications*, 2014; pp 213-220.

(3) Krukowski, S. T., Iodine Production from Oilfield Brine. In *Iodine Chemistry and Applications*, 2014; pp 221-230.

(4) Kaneko, N.; Kaiho, T., Iodine Production from Natural Gas Brine. In *Iodine Chemistry and Applications*, 2014; pp 231-241.

(5) Krause, W., Iodinated X-Ray Contrast Agents. In *Iodine Chemistry and Applications*, 2014; pp 353-374.

(6) Kloo, L., Iodine in Dye-Sensitized Solar Cells. In *Iodine Chemistry and Applications*, 2014; pp 501-512.

(7) Musher, J. I., The Chemistry of Hypervalent Molecules. *Angew. Chem. Int. Ed.* **1969,** *8* (1), 54-68.

(8) Powell, W. H., Treatment of Variable Valence in Organic Nomenclature (Lambda Convention). *Pure Appl. Chem.* **1984,** *56* (6), 769-778.

(9) Pimentel, G. C., The Bonding of Trihalide and Bifluoride Ions by the Molecular Orbital Method. *J. Chem. Phys.* **1951,** *19* (4), 446-448.

(10) Hach, R. J.; Rundle, R. E., The Structure of Tetramethylammonium Pentaiodide1,1a. *J. Am. Chem. Soc.* **1951,** *73* (9), 4321-4324.

(11) Alcock, N. W.; Countryman, R. M.; Esperås, S.; Sawyer, J. F., Secondary bonding. Part 5. The crystal and molecular structures of phenyliodine(III) diacetate and bis(dichloroacetate). *J. Chem. Soc., Dalton Trans.* **1979,** (5), 854-860.

(12) Perkins, C. W.; Martin, J. C.; Arduengo, A. J.; Lau, W.; Alegria, A.; Kochi, J. K., An electrically neutral sigma-sulfuranyl radical from the homolysis of a perester with neighboring sulfenyl sulfur: 9-S-3 species. *J. Am. Chem. Soc.* **1980,** *102* (26), 7753-7759.

(13) Martin, J. C., "Frozen" Transition States: Pentavalent Carbon et al. *Science* **1983,** *221* (4610), 509-514.

(14) Zhdankin, V. V., *Hypervalent iodine chemistry: preparation, structure and synthetic applications of polyvalent iodine compounds*. John Wiley & Sons Ltd: United Kingdom, 2014; p 468.

(15) Ochiai, M.; Takaoka, Y.; Masaki, Y.; Nagao, Y.; Shiro, M., Synthesis of chiral hypervalent organoiodinanes, iodo(III)binaphthyls, and evidence for pseudorotation on iodine. *J. Am. Chem. Soc.* **1990,** *112* (14), 5677-5678.

(16) Edwards, A. J., Crystal structure of trichlorosulphonium(IV) tetrachloroiodate(III). *J. Chem. Soc., Dalton Trans.* **1978,** (12), 1723-1725.

(17) Okuyama, T.; Takino, T.; Sueda, T.; Ochiai, M., Solvolysis of Cyclohexenyliodonium Salt, a New Precursor for the Vinyl Cation: Remarkable Nucleofugality of the Phenyliodonio Group and Evidence for Internal Return from an Intimate Ion-Molecule Pair. *J. Am. Chem. Soc.* **1995,** *117* (12), 3360-3367.

(18) Schleyer, P. v. R.; Pfeifer, W. D.; Bahn, C. A.; Bocher, S.; Harding, C. E.; Hummel, K.; Hanack, M.; Stang, P. J., Behavior of bent vinyl cations generated by solvolysis of cyclic trifluoromethanesulfonates. *J. Am. Chem. Soc.* **1971,** *93* (6), 1513-1516.

(19) Kazmierczak, P.; Skulski, L.; Kraszkiewicz, L., Syntheses of (Diacetoxyiodo)arenes or Iodylarenes from Iodoarenes, with Sodium Periodate as the Oxidant. *Molecules* **2001,** *6* (11), 881-891.

(20) Iinuma, M.; Moriyama, K.; Togo, H., Simple and Practical Method for Preparation of [(Diacetoxy)iodo]arenes with Iodoarenes and m-Chloroperoxybenzoic Acid. *Synlett* **2012,** *23* (18), 2663-2666.

(21) Merritt, E. A.; Olofsson, B., Diaryliodonium Salts: A Journey from Obscurity to Fame. *Angew. Chem. Int. Ed.* **2009,** *48* (48), 9052-9070.

(22) Bielawski, M.; Olofsson, B., High-yielding one-pot synthesis of diaryliodonium triflates from arenes and iodine or aryl iodides. *Chem. Commun.* **2007,** (24), 2521-2523.

(23) Singhal, R.; Choudhary, S. P.; Malik, B.; Pilania, M., Cyclic diaryliodonium salts: applications and overview. *Org. Biomol. Chem.* **2023,** *21* (21), 4358-4378.

(24) Frigerio, M.; Santagostino, M.; Sputore, S., A User-Friendly Entry to 2-iodoxybenzoic Acid (IBX). *J. Org. Chem.* **1999,** *64* (12), 4537-4538.

(25) Meyer, S. D.; Schreiber, S. L., Acceleration of the Dess-Martin Oxidation by Water. *J. Org. Chem.* **1994,** *59* (24), 7549-7552.

(26) To, A. J.; Murphy, G. K., Iodolium salts as halogen-bond donor catalysts in the Nazarov cyclization: the molecular oxygen enigma. *New J. Chem.* **2022,** *46* (32), 15313-15320.

(27) Vaidya, T.; Eisenberg, R.; Frontier, A. J., Catalytic Nazarov Cyclization: The State of the Art. *ChemCatChem* **2011,** *3* (10), 1531-1548.

(28) Tius, M. A., Allene ether Nazarov cyclization. *Chem. Soc. Rev.* **2014,** *43* (9), 2979-3002.

(29) Wenz, D. R.; Read de Alaniz, J., The Nazarov Cyclization: A Valuable Method to Synthesize Fully Substituted Carbon Stereocenters. *Eur. J. Org. Chem.* **2015,** *2015* (1), 23-37.

(30) Yadykov, A. V.; Shirinian, V. Z., Recent Advances in the Interrupted Nazarov Reaction. *Adv. Synth. Catal.* **2020,** *362* (4), 702-723.

(31) Stephen, A.; Hashmi, K.; Bats, J. W.; Choi, J.-H.; Schwarz, L., Isomerizations on silica gel: Synthesis of allenyl ketones and the first Nazarov cyclizations of vinyl allenyl ketones. *Tetrahedron Lett.* **1998,** *39* (41), 7491-7494.

(32) Malona, J. A.; Cariou, K.; Frontier, A. J., Nazarov Cyclization Initiated by Peracid Oxidation: The Total Synthesis of (±)-Rocaglamide. *J. Am. Chem. Soc.* **2009,** *131* (22), 7560-7561.

(33) Bender, J. A.; Blize, A. E.; Browder, C. C.; Giese, S.; West, F. G., Highly Diastereoselective Cycloisomerization of Acyclic Trienones. The Interrupted Nazarov Reaction. *J. Org. Chem.* **1998,** *63* (8), 2430-2431.

(34) Rueping, M.; Ieawsuwan, W.; Antonchick, A. P.; Nachtsheim, B. J., Chiral Bronsted acids in the catalytic asymmetric Nazarov cyclization - The first enantioselective organocatalytic electrocyclic reaction. *Angew. Chem. Int. Ed.* **2007,** *46* (12), 2097-2100.

(35) Frontier, A. J.; Collison, C., The Nazarov cyclization in organic synthesis. Recent advances. *Tetrahedron* **2005,** *61* (32), 7577-7606.

(36) Liang, G. X.; Gradl, S. N.; Trauner, D., Efficient Nazarov cyclizations of 2-alkoxy-1,4-pentadien-3-ones. *Org. Lett.* **2003,** *5* (26), 4931-4934.

(37) Harrington, P. E.; Murai, T.; Chu, C.; Tius, M. A., Asymmetric Cyclopentannelation: Camphor-Derived Auxiliary. *J. Am. Chem. Soc.* **2002,** *124* (34), 10091-10100.

(38) Aggarwal, V. K.; Belfield, A. J., Catalytic asymmetric Nazarov reactions promoted by chiral Lewis acid complexes. *Org. Lett.* **2003,** *5* (26), 5075-5078.

(39) Denmark, S. E.; Jones, T. K., Silicon-directed Nazarov cyclization. *J. Am. Chem. Soc.* **1982,** *104* (9), 2642-2645.

(40) Grant, T. N.; Rieder, C. J.; West, F. G., Interrupting the Nazarov reaction: domino and cascade processes utilizing cyclopentenyl cations. *Chem. Commun.* **2009,** *N/A* (38), 5676-5688.

(41) Williams, D. R.; Robinson, L. A.; Nevill, C. R.; Reddy, J. P., Strategies for the Synthesis of Fusicoccanes by Nazarov Reactions of Dolabelladienones: Total Synthesis of (+)-Fusicoauritone. *Angew. Chem. Int. Ed.* **2007,** *46* (6), 915-918.

(42) He, W.; Huang, J.; Sun, X.; Frontier, A. J., Total Synthesis of (±)-Merrilactone A via Catalytic Nazarov Cyclization. *J. Am. Chem. Soc.* **2007,** *129* (3), 498-499.

(43) Malona, J. A.; Cariou, K.; Spencer, W. T., III; Frontier, A. J., Total Synthesis of (±)-Rocaglamide via Oxidation-Initiated Nazarov Cyclization. *J. Org. Chem.* **2012,** *77* (4), 1891-1908.

(44) Kong, L.; Su, F.; Yu, H.; Jiang, Z.; Lu, Y.; Luo, T., Total Synthesis of (−)-Oridonin: An Interrupted Nazarov Approach. *J. Am. Chem. Soc.* **2019,** *141* (51), 20048-20052.

(45) Que, Y.; Shao, H.; He, H.; Gao, S., Total Synthesis of Farnesin through an Excited-State Nazarov Reaction. *Angew. Chem. Int. Ed.* **2020,** *59* (19), 7444-7449.

(46) Beringer, F. M.; Brierley, A.; Drexler, M.; Gindler, E. M.; Lumpkin, C. C., Diaryliodonium Salts. II. The Phenylation of Organic and Inorganic Bases. *J. Am. Chem. Soc.* **1953,** *75* (11), 2708-2712.

(47) Carroll, M. A.; Wood, R. A., Arylation of anilines: formation of diarylamines using diaryliodonium salts. *Tetrahedron* **2007,** *63* (46), 11349-11354.

(48) Jalalian, N.; Ishikawa, E. E.; Silva, L. F.; Olofsson, B., Room Temperature, Metal-Free Synthesis of Diaryl Ethers with Use of Diaryliodonium Salts. *Org. Lett.* **2011,** *13* (6), 1552-1555.

(49) Aradi, K.; Tóth, B. L.; Tolnai, G. L.; Novák, Z., Diaryliodonium Salts in Organic Syntheses: A Useful Compound Class for Novel Arylation Strategies. *Synlett* **2016,** *27* (10), 1456-1485.

(50) Aggarwal, V. K.; Olofsson, B., Enantioselective α-Arylation of Cyclohexanones with Diaryl Iodonium Salts: Application to the Synthesis of (−)-Epibatidine. *Angew. Chem. Int. Ed.* **2005,** *44* (34), 5516-5519.

(51) Allen, A. E.; MacMillan, D. W. C., Enantioselective α-Arylation of Aldehydes via the Productive Merger of Iodonium Salts and Organocatalysis. *J. Am. Chem. Soc.* **2011,** *133* (12), 4260-4263.

(52) Harvey, J. S.; Simonovich, S. P.; Jamison, C. R.; MacMillan, D. W. C., Enantioselective α-Arylation of Carbonyls via Cu(I)-Bisoxazoline Catalysis. *J. Am. Chem. Soc.* **2011,** *133* (35), 13782-13785.

(53) Bigot, A.; Williamson, A. E.; Gaunt, M. J., Enantioselective α-Arylation of N-Acyloxazolidinones with Copper(II)-bisoxazoline Catalysts and Diaryliodonium Salts. *J. Am. Chem. Soc.* **2011,** *133* (35), 13778-13781.

(54) Kalyani, D.; Deprez, N. R.; Desai, L. V.; Sanford, M. S., Oxidative C−H Activation/C−C Bond Forming Reactions: Synthetic Scope and Mechanistic Insights. *J. Am. Chem. Soc.* **2005,** *127* (20), 7330-7331.

(55) Daugulis, O.; Zaitsev, V. G., Anilide ortho-Arylation by Using C-H Activation Methodology. *Angew. Chem. Int. Ed.* **2005,** *44* (26), 4046-4048.

(56) Phipps, R. J.; Gaunt, M. J., A Meta-Selective Copper-Catalyzed C–H Bond Arylation. *Science* **2009,** *323* (5921), 1593-1597.

(57) Pike, V. W.; Aigbirhio, F. I., Reactions of cyclotron-produced [18F]fluoride with diaryliodonium salts—a novel single-step route to no-carrier-added [18]fluoroarenes. *J. Chem. Soc., Chem. Commun.* **1995,** *N/A* (21), 2215-2216.

(58) Ross, T. L.; Ermert, J.; Hocke, C.; Coenen, H. H., Nucleophilic 18F-Fluorination of Heteroaromatic Iodonium Salts with No-Carrier-Added [18F]Fluoride. *J. Am. Chem. Soc.* **2007,** *129* (25), 8018-8025.

(59) Pike, V. W., Hypervalent aryliodine compounds as precursors for radiofluorination. *J. Labelled Compd. Radiopharm.* **2018,** *61* (3), 196-227.

(60) Kwon, Y.-D.; Son, J.; Chun, J.-H., Chemoselective Radiosyntheses of Electron-Rich [18F]Fluoroarenes from Aryl(2,4,6-trimethoxyphenyl)iodonium Tosylates. *J. Org. Chem.* **2019,** *84* (6), 3678-3686.

(61) Chen, K.; Koser, G. F., Direct and regiocontrolled synthesis of alpha-phenyl ketones from silyl enol ethers and diphenyliodonium fluoride. *J. Org. Chem.* **1991,** *56* (20), 5764-5767.

(62) Ackermann, L.; Dell'Acqua, M.; Fenner, S.; Vicente, R.; Sandmann, R., Metal-Free Direct Arylations of Indoles and Pyrroles with Diaryliodonium Salts. *Org. Lett.* **2011,** *13* (9), 2358-2360.

(63) Zhang, M.-R.; Kumata, K.; Suzuki, K., A practical route for synthesizing a PET ligand containing [18F]fluorobenzene using reaction of diphenyliodonium salt with [18F]F^-. *Tetrahedron Lett.* **2007,** *48* (49), 8632-8635.

(64) Zhao, K.; Duan, L.; Xu, S.; Jiang, J.; Fu, Y.; Gu, Z., Enhanced Reactivity by Torsional Strain of Cyclic Diaryliodonium in Cu-Catalyzed Enantioselective Ring-Opening Reaction. *Chem* **2018,** *4* (3), 599-612.

(65) Hou, M.; Deng, R.; Gu, Z., Cu-Catalyzed Enantioselective Atropisomer Synthesis via Thiolative Ring Opening of Five-Membered Cyclic Diaryliodoniums. *Org. Lett.* **2018,** *20* (18), 5779-5783.

(66) Zhu, D.; Liu, Q.; Luo, B.; Chen, M.; Pi, R.; Huang, P.; Wen, S., Synthesis of Carbazoles via One-Pot Copper-Catalyzed Amine Insertion into Cyclic Diphenyleneiodoniums as a Strategy to Generate a Drug-Like Chemical Library. *Adv. Synth. Catal.* **2013,** *355* (11-12), 2172-2178.

(67) Shimizu, M.; Ogawa, M.; Tamagawa, T.; Shigitani, R.; Nakatani, M.; Nakano, Y., Copper-Catalyzed Double S-Arylation of Potassium Thioacetate with Dibenziodolium Triflates: Facile Synthesis of Unsymmetrical Dibenzothiophenes. *Eur. J. Org. Chem.* **2016,** *2016* (16), 2785-2788.

(68) Chatterjee, N.; Goswami, A., Synthesis and Application of Cyclic Diaryliodonium Salts: A Platform for Bifunctionalization in a Single Step. *Eur. J. Org. Chem.* **2017,** *2017* (21), 3023-3032.

(69) Li, J.; Xu, Q.-N.; Wang, Z.-B.; Li, Y.; Liu, L., Synthesis of Dibenzofurans from Cyclic Diaryliodonium Triflates and Water via Oxygen–Iodine Exchange Approach. *ACS Omega* **2018,** *3* (10), 12923-12929.

(70) Wang, M.; Fan, Q.; Jiang, X., Nitrogen–Iodine Exchange of Diaryliodonium Salts: Access to Acridine and Carbazole. *Org. Lett.* **2018,** *20* (1), 216-219.

(71) Zhu, D.; Liu, Q.; Luo, B.; Chen, M.; Pi, R.; Huang, P.; Wen, S., Synthesis of Carbazoles via One-Pot Copper-Catalyzed Amine Insertion into Cyclic Diphenyleneiodoniums as a Strategy to Generate a Drug-Like Chemical Library. *Adv. Synth. Catal.* **2013,** *355* (11-12), 2172-2178.

(72) Zhu, D.; Wu, Z.; Luo, B.; Du, Y.; Liu, P.; Chen, Y.; Hu, Y.; Huang, P.; Wen, S., Heterocyclic Iodoniums for the Assembly of Oxygen-Bridged Polycyclic Heteroarenes with Water as the Oxygen Source. *Org. Lett.* **2018,** *20* (16), 4815-4818.

(73) Robidas, R.; Reinhard, D. L.; Legault, C. Y.; Huber, S. M., Iodine(III)-Based Halogen Bond Donors: Properties and Applications. *The Chemical Record* **2021,** *21* (8), 1912-1927.

(74) Labattut, A.; Tremblay, P. L.; Moutounet, O.; Legault, C. Y., Experimental and Theoretical Quantification of the Lewis Acidity of lodine(III) Species. *J. Org. Chem.* **2017,** *82* (22), 11891-11896.

(75) Mayer, R. J.; Ofial, A. R.; Mayr, H.; Legault, C. Y., Lewis Acidity Scale of Diaryliodonium Ions toward Oxygen, Nitrogen, and Halogen Lewis Bases. *J. Am. Chem. Soc.* **2020,** *142* (11), 5221-5233.

(76) Heinen, F.; Engelage, E.; Cramer, C. J.; Huber, S. M., Hypervalent Iodine(III) Compounds as Biaxial Halogen Bond Donors. *J. Am. Chem. Soc.* **2020,** *142* (19), 8633-8640.

(77) Heinen, F.; Engelage, E.; Dreger, A.; Weiss, R.; Huber, S. M., Iodine(III) Derivatives as Halogen Bonding Organocatalysts. *Angew. Chem. Int. Ed.* **2018,** *57* (14), 3830-3833.

(78) Wolf, J.; Huber, F.; Erochok, N.; Heinen, F.; Guérin, V.; Legault, C. Y.; Kirsch, S. F.; Huber, S. M., Activation of a Metal-Halogen Bond by Halogen Bonding. *Angew. Chem. Int. Ed.* **2020,** *59* (38), 16496-16500.

(79) Haraguchi, R.; Nishikawa, T.; Kanazawa, A.; Aoshima, S., Metal-Free Living Cationic Polymerization Using Diaryliodonium Salts as Organic Lewis Acid Catalysts. *Macromolecules* **2020,** *53* (11), 4185-4192.

(80) Zhang, Y.; Han, J.; Liu, Z.-J., Diaryliodonium salts as efficient Lewis acid catalysts for direct three component Mannich reactions. *RSC Adv.* **2015,** *5* (32), 25485-25488.

(81) Yunusova, S. N.; Novikov, A. S.; Soldatova, N. S.; Vovk, M. A.; Bolotin, D. S., Iodonium salts as efficient iodine(III)-based noncovalent organocatalysts for Knorr-type reactions. *RSC Adv.* **2021,** *11* (8), 4574-4583.

(82) Il'in, M. V.; Sysoeva, A. A.; Novikov, A. S.; Bolotin, D. S., Diaryliodoniums as Hybrid Hydrogen- and Halogen-Bond-Donating Organocatalysts for the Groebke–Blackburn–Bienaymé Reaction. *J. Org. Chem.* **2022,** *87* (7), 4569-4579.

(83) Boelke, A.; Kuczmera, T. J.; Caspers, L. D.; Lork, E.; Nachtsheim, B. J., Iodolopyrazolium Salts: Synthesis, Derivatizations, and Applications. *Org. Lett.* **2020,** *22* (18), 7261-7266.

(84) Reinhard, D. L.; Heinen, F.; Stoesser, J.; Engelage, E.; Huber, S. M., Tuning the Halogen Bonding Strength of Cyclic Diaryliodonium Salts. *Helv. Chim. Acta* **2021,** *104* (2), e2000221.

(85) Heinen, F.; Reinhard, D. L.; Engelage, E.; Huber, S. M., A Bidentate Iodine(III)-Based Halogen-Bond Donor as a Powerful Organocatalyst. *Angew. Chem. Int. Ed.* **2021,** *60* (10), 5069-5073.

(86) Yoshida, Y.; Fujimura, T.; Mino, T.; Sakamoto, M., Chiral Binaphthyl-Based Iodonium Salt (Hypervalent Iodine(III)) as Hydrogen- and Halogen-Bonding Bifunctional Catalyst: Insight into Abnormal Counteranion Effect and Asymmetric Synthesis of N,S-Acetals. *Adv. Synth. Catal.* **2022,** *364* (6), 1091-1098.

(87) Koenig, J. J.; Arndt, T.; Gildemeister, N.; Neudörfl, J.-M.; Breugst, M., Iodine-Catalyzed Nazarov Cyclizations. *J. Org. Chem.* **2019,** *84* (12), 7587-7605.

(88) Dreger, A.; Wonner, P.; Engelage, E.; Walter, S. M.; Stoll, R.; Huber, S. M., A halogen-bonding-catalysed Nazarov cyclisation reaction. *Chem. Commun.* **2019,** *55* (57), 8262-8265.

(89) Ochiai, M.; Suefuji, T.; Miyamoto, K.; Tada, N.; Goto, S.; Shiro, M.; Sakamoto, S.; Yamaguchi, K., Secondary Hypervalent I(III)···O Interactions: Synthesis and Structure of Hypervalent Complexes of Diphenyl-λ^3-iodanes with 18-Crown-6. *J. Am. Chem. Soc.* **2003,** *125* (3), 769-773.

(90) Gutmann, V., Empirical parameters for donor and acceptor properties of solvents. *Electrochim. Acta* **1976,** *21* (9), 661-670.

(91) Amere, M.; Blanchet, J.; Lasne, M.-C.; Rouden, J., 4-Toluenesulfonic acid: an environmentally benign catalyst for Nazarov cyclizations. *Tetrahedron Lett.* **2008,** *49* (16), 2541-2545.

(92) Murugan, K.; Srimurugan, S.; Chen, C., A mild, catalytic and efficient Nazarov cyclization mediated by phosphomolybdic acid. *Chem. Commun.* **2010,** *46* (7), 1127-1129.

(93) Sugimoto, K.; Oshiro, M.; Hada, R.; Matsuya, Y., 2,2′-Biphenol/$B(OH)_3$ Catalyst System for Nazarov Cyclization. *Chem. Pharm. Bull.* **2019,** *67* (9), 1019-1022.

(94) Nejrotti, S.; Iannicelli, M.; Jamil, S. S.; Arnodo, D.; Blangetti, M.; Prandi, C., Natural deep eutectic solvents as an efficient and reusable active system for the Nazarov cyclization. *Green Chem.* **2020,** *22* (1), 110-117.

(95) Dang, T. T.; Boeck, F.; Hintermann, L., Hidden Brønsted Acid Catalysis: Pathways of Accidental or Deliberate Generation of Triflic Acid from Metal Triflates. *J. Org. Chem.* **2011,** *76* (22), 9353-9361.

(96) Atmaca, U.; Usanmaz, H. K.; Çelik, M., Oxidations of alkenes with hypervalent iodine reagents: an alternative ozonolysis of phenyl substituted alkenes and allylic oxidation of unsubstituted cyclic alkenes. *Tetrahedron Lett.* **2014,** *55* (14), 2230-2232.

(97) Bee, C.; Leclerc, E.; Tius, M. A., The Palladium(II)-Catalyzed Nazarov Reaction. *Org. Lett.* **2003,** *5* (26), 4927-4930.

(98) Kokubo, M.; Kobayashi, S., Nazarov-type Reactions in Water. *Chem. Asian J.* **2009,** *4* (4), 526-528.

(99) Weinland, R. F.; Stille, W., Ueber Substitution von Sauerstoff durch Fluor in Jodo- und Jodosoverbindungen. *Justus Liebigs Ann. Chem.* **1903,** *328* (2), 132-139.

(100) Arrica, M. A.; Wirth, T., Fluorinations of α-Seleno Carboxylic Acid Derivatives with Hypervalent (Difluoroiodo)toluene. *Eur. J. Org. Chem.* **2005,** *2005* (2), 395-403.

(101) Emer, E.; Twilton, J.; Tredwell, M.; Calderwood, S.; Collier, T. L.; Liégault, B.; Taillefer, M.; Gouverneur, V., Diversity-Oriented Approach to CF_3CHF-, CF_3CFBr-, CF_3CF_2-, $(CF_3)_2CH$-, and $CF_3(SCF_3)CH$-Substituted Arenes from 1-(Diazo-2,2,2-trifluoroethyl)arenes. *Org. Lett.* **2014,** *16* (22), 6004-6007.

(102) Ye, C.; Twamley, B.; Shreeve, J. M., Straightforward Syntheses of Hypervalent Iodine(III) Reagents Mediated by Selectfluor. *Org. Lett.* **2005,** *7* (18), 3961-3964.

(103) Sarie, J. C.; Thiehoff, C.; Mudd, R. J.; Daniliuc, C. G.; Kehr, G.; Gilmour, R., Deconstructing the Catalytic, Vicinal Difluorination of Alkenes: HF-Free Synthesis and Structural Study of p-TolIF_2. *J. Org. Chem.* **2017,** *82* (22), 11792-11798.

(104) Ruppert, I., Arylioddifluoride durch direktfluorierung von iodaromaten. *J. Fluorine Chem.* **1980,** *15* (2), 173-178.

(105) Naumann, D.; Rüther, G., Synthesen von aryljod(III)-difluoriden durch direktfluorierung von aryljodiden. *J. Fluorine Chem.* **1980,** *15* (3), 213-222.

(106) Carpenter, W., Aryliodosodifluorides. *J. Org. Chem.* **1966,** *31* (8), 2688-2689.

(107) Lyalin, V. V.; Orda, V. V.; Alekseeva, L. A.; Yagupolskii, L. M., Difluoroiodine Derivatives of Organic Compounds. *Zh. Org. Khim.* **1970,** *6* (2), 329-332.

(108) Zupan, M.; Pollak, A., Preparation of a polymer-supported aryliodine(III) difluoride and its use to fluorinate olefins to difluorides. *J. Chem. Soc., Chem. Commun.* **1975,** *N/A* (17), 715-716.

(109) Zupan, M.; Pollak, A., Fluorination with xenon difluoride. Preparation of aryliodine/III/difluoride. *J. Fluorine Chem.* **1976,** *7* (4), 445-447.

(110) Sawaguchi, M.; Ayuba, S.; Hara, S., A Practical Synthetic Method of Iodoarene Difluorides without Fluorine Gas and Mercury Salts. *Synthesis* **2002,** *2002* (13), 1802-1803.

(111) Tao, J.; Murphy, G. K., A Practical, Large-Scale Synthesis of p-(Difluoroiodo)toluene (p-TolIF$_2$). *Synthesis* **2019,** *51* (16), 3055-3059.

(112) Lemal, D. M.; Tao, J.; Murphy, G. K., Difluoroiodotoluene. In *Encyclopedia of Reagents for Organic Synthesis (EROS)*, 2016; pp 1-6.

(113) Banik, S. M.; Medley, J. W.; Jacobsen, E. N., Catalytic, asymmetric difluorination of alkenes to generate difluoromethylated stereocenters. *Science* **2016,** *353* (6294), 51-54.

(114) Scheidt, F.; Schäfer, M.; Sarie, J. C.; Daniliuc, C. G.; Molloy, J. J.; Gilmour, R., Enantioselective, Catalytic Vicinal Difluorination of Alkenes. *Angew. Chem. Int. Ed.* **2018,** *57* (50), 16431-16435.

(115) Molnár, I. G.; Gilmour, R., Catalytic Difluorination of Olefins. *J. Am. Chem. Soc.* **2016,** *138* (15), 5004-5007.

(116) Fuchigami, T.; Fujita, T., Electrolytic Partial Fluorination of Organic Compounds. 14. The First Electrosynthesis of Hypervalent Iodobenzene Difluoride Derivatives and Its Application to Indirect Anodic gem-Difluorination. *J. Org. Chem.* **1994,** *59* (24), 7190-7192.

(117) Hara, S.; Hatakeyama, T.; Chen, S.-Q.; Ishi-i, K.; Yoshida, M.; Sawaguchi, M.; Fukuhara, T.; Yoneda, N., Electrochemical fluorination of β-dicarbonyl compounds using p-iodotoluene difluoride as a mediator. *J. Fluorine Chem.* **1998,** *87* (2), 189-192.

(118) Haupt, J. D.; Berger, M.; Waldvogel, S. R., Electrochemical Fluorocyclization of N-Allylcarboxamides to 2-Oxazolines by Hypervalent Iodine Mediator. *Org. Lett.* **2019,** *21* (1), 242-245.

(119) Doobary, S.; Sedikides, A. T.; Caldora, H. P.; Poole, D. L.; Lennox, A. J. J., Electrochemical Vicinal Difluorination of Alkenes: Scalable and Amenable to Electron-Rich Substrates. *Angew. Chem. Int. Ed.* **2020,** *59* (3), 1155-1160.

(120) Winterson, B.; Bhattacherjee, D.; Wirth, T., Hypervalent Halogen Compounds in Electrochemical Reactions: Advantages and Prospects. *Adv. Synth. Catal.* **2023,** *365* (16), 2676-2689.

(121) Motherwell, W. B.; Wilkinson, J. A., Observations on the Reaction of Dithioketals with para-Iodotoluene Difluoride: A Novel Route to gem-Difluoro Compounds. *Synlett* **1991,** *1991* (03), 191-192.

(122) Caddick, S.; Motherwell, W. B.; Wilkinson, J. A., A concise method for the preparation of glycosyl fluorides via displacement reactions of 1-arylthioglycosides with 4-methyl(difluoroiodo)benzene. *J. Chem. Soc., Chem. Commun.* **1991,** *N/A* (10), 674-675.

(123) Caddick, S.; Gazzard, L.; Motherwell, W. B.; Wilkinson, J. A., Preparation of 1-fluoroglycosides from 1-arylthio and 1-arylselenoglycosides using 4-methyl(difluoroiodo)benzene. *Tetrahedron* **1996,** *52* (1), 149-156.

(124) Koen, M. J.; Le Guyader, F.; Motherwell, W. B., Observations on the reaction of xanthate esters with 4-methyl(difluoroiodo)benzene: a new method for the conversion of alcohols to alkyl fluorides. *J. Chem. Soc., Chem. Commun.* **1995,** *N/A* (12), 1241-1242.

(125) Greaney, M. F.; Motherwell, W. B., Observations on the α-fluorination of α-phenylsulfanyl esters using difluoroiodotoluene. *Tetrahedron Lett.* **2000,** *41* (22), 4463-4466.

(126) Greaney, M. F.; Motherwell, W. B., Studies on the oxidation and fluorination of α-phenylsulfanylacetamides using difluoroiodotoluene. *Tetrahedron Lett.* **2000,** *41* (22), 4467-4470.

(127) Greaney, M. F.; Motherwell, W. B.; Tocher, D. A., Studies on the additive fluoro-Pummerer reaction of phenylsulfanylated lactams with difluoroiodotoluene. *Tetrahedron Lett.* **2001,** *42* (48), 8523-8526.

(128) Guyon, H.; Cahard, D., Selectfluor and Its Analogs Electrophilic Fluorination for Preparing Alkyl Fluorides. In *Fluorination*, Hu, J.; Umemoto, T., Eds. Springer Singapore: Singapore, 2017; pp 1-24.

(129) Hara, S.; Sekiguchi, M.; Ohmori, A.; Fukuhara, T.; Yoneda, N., Selective fluorination of β-ketoesters using iodotoluene difluoride and a HF–amine complex. *Chem. Commun.* **1996,** *N/A* (16), 1899-1900.

(130) Baur, M. A.; Riahi, A.; Hénin, F.; Muzart, J., Catalytic asymmetric protonation of fluoro-enolic species: access to optically active 2-fluoro-1-tetralone. *Tetrahedron: Asymmetry* **2003,** *14* (18), 2755-2761.

(131) Xiao, J.-C.; Shreeve, J. n. M., Microwave-assisted rapid electrophilic fluorination of 1,3-dicarbonyl derivatives with Selectfluor®. *J. Fluorine Chem.* **2005,** *126* (4), 473-476.

(132) Yoshida, M.; Fujikawa, K.; Sato, S.; Hara, S., α-Fluorination of β-dicarbonyl compounds using p-iodotoluene difluoride under neutral conditions. *Arkivoc* **2003,** *2003* (6), 36-42.

(133) Hara, S.; Yoshida, M.; Fukuhara, T.; Yoneda, N., Stereo- and regio-selective addition of iodotoluene difluoride to alk-1-ynes. Selective synthesis of 2-fluoro-1-iodoalk-1-enes. *Chem. Commun.* **1998,** *N/A* (9), 965-966.

(134) Tao, J.; Tran, R.; Murphy, G. K., Dihaloiodoarenes: alpha,alpha-Dihalogenation of Phenylacetate Derivatives. *J. Am. Chem. Soc.* **2013,** *135* (44), 16312-16315.

(135) Sinclair, G. S.; Tran, R.; Tao, J.; Hopkins, W. S.; Murphy, G. K., Borosilicate Activation of (Difluoroiodo)toluene in the gem-Difluorination of Phenyldiazoacetate Derivatives. *Eur. J. Org. Chem.* **2016,** *2016* (27), 4603-4606.

(136) Zhou, Y.; Zhang, Y.; Wang, J., Geminal difunctionalization of α-diazo arylmethylphosphonates: synthesis of fluorinated phosphonates. *Org. Biomol. Chem.* **2016,** *14* (44), 10444-10453.

(137) Leroy, J.; Wakselman, C., Electrophilic fluorination of diazoketones. *J. Chem. Soc., Perkin Trans. 1* **1978,** (10), 1224-1227.

(138) Patrick, T. B.; Scheibel, J. J.; Cantrell, G. L., Geminal fluorination of diazo compounds. *J. Org. Chem.* **1981,** *46* (19), 3917-3918.

(139) Tsushima, T.; Kawada, K.; Tsuji, T., α-fluorination of ketones by xenon and iodobenzene difluorides: A stereochemical evidence demonstrating their mechanistic differences. *Tetrahedron Lett.* **1982,** *23* (11), 1165-1168.

(140) Edmunds, J. J.; Motherwell, W. B., Observations on the reaction of some electron rich dienes with hypervalent iodoarene difluorides: a novel mechanism for fluorination. *J. Chem. Soc., Chem. Commun.* **1989,** *N/A* (13), 881-883.

(141) Joly, R.; Warnant, J., *Bull. Soc. Chim. Fr.* **1961,** *28*, 569-570.

(142) Hara, S.; Nakahigashi, J.; Ishi-i, K.; Sawaguchi, M.; Sakai, H.; Fukuhara, T.; Yoneda, N., Difluorination of Alkenes with Iodotoluene Difluoride. *Synlett* **1998,** *1998* (05), 495-496.

(143) Liu, G., Fluorination of Alkenes and Alkynes for Preparing Alkyl Fluorides. In *Fluorination*, Hu, J.; Umemoto, T., Eds. Springer Singapore: Singapore, 2017; pp 1-35.

(144) Sawaguchi, M.; Hara, S.; Fukuhara, T.; Yoneda, N., Fluorocyclization of unsaturated alcohols and carboxylic acids by iodotoluene difluoride and amine-HF complexes. *J. Fluorine Chem.* **2000,** *104* (2), 277-280.

(145) Patrick, T. B.; Scheibel, J. J.; Hall, W. E.; Lee, Y. H., Substituent effects in the fluorination-rearrangement of 1,1-diarylethenes with aryliodine(III) difluorides. *J. Org. Chem.* **1980,** *45* (22), 4492-4494.

(146) Middleton, W. J., New fluorinating reagents. Dialkylaminosulfur fluorides. *J. Org. Chem.* **1975,** *40* (5), 574-578.

(147) Grosse, A. V.; Linn, C. B., The Addition of Hydrogen Fluoride to the Triple Bond1. *J. Am. Chem. Soc.* **1942,** *64* (10), 2289-2292.

(148) Hara, S.; Nakahigashi, J.; Ishi-i, K.; Fukuhara, T.; Yoneda, N., Fluorinative ring-contraction of cyclic alkenes with p-iodotoluene difluoride. *Tetrahedron Lett.* **1998,** *39* (17), 2589-2592.

(149) Zhao, Z.; To, A. J.; Murphy, G. K., Difluorinative ring expansions of benzo-fused carbocycles and heterocycles are achieved with p-(difluoroiodo)toluene. *Chem. Commun.* **2019,** *55* (98), 14821-14824.

(150) Zhao, Z.; Racicot, L.; Murphy, G. K., Fluorinative Rearrangements of Substituted Phenylallenes Mediated by (Difluoroiodo)toluene: Synthesis of α-(Difluoromethyl)styrenes. *Angew. Chem. Int. Ed.* **2017,** *56* (38), 11620-11623.

(151) Kitamura, T.; Muta, K.; Oyamada, J., Hypervalent Iodine-Mediated Fluorination of Styrene Derivatives: Stoichiometric and Catalytic Transformation to 2,2-Difluoroethylarenes. *J. Org. Chem.* **2015,** *80* (21), 10431-10436.

(152) Scheidt, F.; Neufeld, J.; Schäfer, M.; Thiehoff, C.; Gilmour, R., Catalytic Geminal Difluorination of Styrenes for the Construction of Fluorine-rich Bioisosteres. *Org. Lett.* **2018,** *20* (24), 8073-8076.

(153) Banik, S. M.; Medley, J. W.; Jacobsen, E. N., Catalytic, Diastereoselective 1,2-Difluorination of Alkenes. *J. Am. Chem. Soc.* **2016,** *138* (15), 5000-5003.

(154) Lin, P.-P.; Huang, L.-L.; Feng, S.-X.; Yang, S.; Wang, H.; Huang, Z.-S.; Li, Q., gem-Difluorination of Methylenecyclopropanes (MCPs) Featuring a Wagner–Meerwein Rearrangement: Synthesis of 2-Arylsubstituted gem-Difluorocyclobutanes. *Org. Lett.* **2021,** *23* (8), 3088-3093.

(155) Sirotkina, E. V.; Efremova, M. M.; Novikov, A. S.; Zarubaev, V. V.; Orshanskaya, I. R.; Starova, G. L.; Kostikov, R. R.; Molchanov, A. P., Regio- and diastereoselectivity of the cycloaddition of aldonitrones with benzylidenecyclopropane: An experimental and theoretical study. *Tetrahedron* **2017,** *73* (21), 3025-3030.

(156) Leškovskis, K.; Gulbe, K.; Mishnev, A.; Turks, M., Ring opening of methylenecyclopropanes with halides in liquid sulfur dioxide. *Tetrahedron Lett.* **2020,** *61* (46), 152528.

(157) Zhu, Y.-Q.; Niu, Y.-X.; Hui, L.-W.; He, J.-L.; Zhu, K., Reaction of Isoquinolin-1(2H)-Ones with Methylenecyclopropanes via Rhodium(III)-Catalyzed C−H Activation. *Adv. Synth. Catal.* **2019,** *361* (12), 2897-2903.

(158) Yu, L.; Meng, J.; Xia, L.; Guo, R., Lewis Acid Catalyzed Reaction of Methylenecyclopropanes with 1,2-Diphenyldiselane or 1,2-Di-p-tolyldisulfane. *J. Org. Chem.* **2009,** *74* (14), 5087-5089.

(159) Yin, Q.; You, S.-L., Asymmetric Chlorination/Ring Expansion for the Synthesis of α-Quaternary Cycloalkanones. *Org. Lett.* **2014,** *16* (6), 1810-1813.

(160) Kim, Y.; Kim, D. Y., Synthesis of Fluoromethyl-Substituted Cyclopentanones via Radical Fluorination and 1,2-Alkyl Migration Cascade of Alkenyl Cyclobutanols. *Asian J. Org. Chem.* **2019,** *8* (5), 679-682.

(161) Zhang, E.; Tu, Y.-Q.; Fan, C.-A.; Zhao, X.; Jiang, Y.-J.; Zhang, S.-Y., Tandem Aziridination/Rearrangement Reaction of Allylic Alcohols: An Efficient Approach to 2-Quaternary Mannich Bases. *Org. Lett.* **2008,** *10* (21), 4943-4946.

(162) Wu, H.; Wang, Q.; Zhu, J., Copper-Catalyzed Enantioselective Domino Arylation/Semipinacol Rearrangement of Allylic Alcohols with Diaryliodonium Salts. *Chem. - Eur. J.* **2017,** *23* (53), 13037-13041.

(163) Alazet, S.; Preindl, J.; Simonet-Davin, R.; Nicolai, S.; Nanchen, A.; Meyer, T.; Waser, J., Cyclic Hypervalent Iodine Reagents for Azidation: Safer Reagents and Photoredox-Catalyzed Ring Expansion. *J. Org. Chem.* **2018,** *83* (19), 12334-12356.

(164) Yang, S.; Wu, J.-Y.; Lin, S.; Pu, M.; Huang, Z.-S.; Wang, H.; Li, Q., Divergent Fluorinations of Vinylcyclopropanes: Ring-Opening 1,5-Hydrofluorination and Ring-Retaining 1,2-Difluorination. *Chem. Asian J.* **2023,** *18* (16), e202300476.

(165) Zhang, Z.-Q.; Xu, Y.-H.; Dai, J.-C.; Li, Y.; Sheng, J.; Wang, X.-S., Copper-Catalyzed Trifluoromethylation/Cyclization of Alkynes for Synthesis of Dioxodibenzothiazepines. *Org. Lett.* **2021,** *23* (6), 2194-2198.

(166) Huang, W.; Xu, C.; Yu, J.; Wang, M., ZnI2-Catalyzed Aminotrifluoromethylation Cyclization of Alkenes Using PhICF3Cl. *J. Org. Chem.* **2021,** *86* (2), 1987-1999.

(167) Newcomb, M., Kinetics of Radical Reactions: Radical Clocks. In *Radicals in Organic Synthesis*, 2001; pp 316-336.

(168) Peng, H.; Yuan, Z.; Wang, H.-y.; Guo, Y.-l.; Liu, G., Palladium-catalyzed intermolecular fluoroesterification of styrenes: exploration and mechanistic insight. *Chem. Sci.* **2013,** *4* (8), 3172-3178.

(169) Justik, M. W.; Koser, G. F., Oxidative rearrangements of arylalkenes with [hydroxy(tosyloxy)iodo]benzene in 95% methanol: a general, regiospecific synthesis of α-aryl ketones. *Tetrahedron Lett.* **2004,** *45* (32), 6159-6163.

(170) Zhao, Z.; Kulkarni, K. G.; Murphy, G. K., Synthesis of Aryldihalomethanes by Denitrogenative Dihalogenation of Benzaldehyde Hydrazones. *Adv. Synth. Catal.* **2017,** *359* (13), 2222-2228.

(171) Chidley, T.; Jameel, I.; Rizwan, S.; Peixoto, P. A.; Pouységu, L.; Quideau, S.; Hopkins, W. S.; Murphy, G. K., Blue LED Irradiation of Iodonium Ylides Gives Diradical Intermediates for Efficient Metal-free Cyclopropanation with Alkenes. *Angew. Chem. Int. Ed.* **2019,** *58* (47), 16959-16965.

(172) Liu, C.; Yang, Y.-J.; Dong, J.-Y.; Zhou, M.-D.; Li, L.; Wang, H., Copper/B_2pin_2-Catalyzed Difluoroalkylation of Methylenecyclopropanes with Bromodifluorinated Acetates and Acetamides: One-Pot Synthesis of CF_2-Containing Dihydronaphthalene Derivatives. *J. Org. Chem.* **2019,** *84* (16), 9937-9945.

(173) Zhu, Z.-Z.; Chen, K.; Yu, L.-Z.; Tang, X.-Y.; Shi, M., Copper(I)-Catalyzed Intramolecular Trifluoromethylation of Methylenecyclopropanes. *Org. Lett.* **2015,** *17* (24), 5994-5997.

(174) Huang, L.-L.; Lin, P.-P.; Li, Y.-X.; Feng, S.-X.; Tu, F.-H.; Yang, S.; Zhao, G.-Y.; Huang, Z.-S.; Wang, H.; Li, Q., Oxidative Fluoroarylation of Benzylidenecyclopropanes with HF·Py and Aryl Iodides via Iodonio-[3,3]-Rearrangement. *Org. Lett.* **2022,** *24* (18), 3389-3394.

(175) Zhao, P.; Wang, W.; Gulder, T., Hypervalent Fluoro-iodane-Triggered Semipinacol Rearrangements: Synthesis of α-Fluoro Ketones. *Org. Lett.* **2023,** *25* (35), 6560-6565.

(176) Ilchenko, N. O.; Szabó, K. J., Geminal difluorination of α,α'- disubstituted styrenes using fluoro-benziodoxole reagent. Migration aptitude of the α-substituents. *J. Fluorine Chem.* **2017,** *203*, 104-109.

(177) Sreenithya, A.; Sunoj, R. B., On the activation of hypercoordinate iodine(iii) compounds for reactions of current interest. *Dalton Trans.* **2019,** *48* (13), 4086-4093.

(178) Liu, Y.-Z.; Zeng, Y.-F.; Wei, J.; Xiao, L.; Shu, B.; Song, J.-L.; Zou, W.-X.; Shen, D.-T.; Chen, S.-Y.; Zheng, Y.-C.; Zhang, S.-S., Rh(III)-Catalyzed Dienylation and Cyclopropylation of 1,2,3-Benzotriazinones with Alkylidenecyclopropanes. *Org. Lett.* **2023,** *25* (28), 5179-5184.

(179) Karimi, B.; Golshani, B., Mild and Highly Efficient Method for the Silylation of Alcohols Using Hexamethyldisilazane Catalyzed by Iodine under Nearly Neutral Reaction Conditions. *J. Org. Chem.* **2000,** *65* (21), 7228-7230.

(180) Högenauer, K.; Mulzer, J., A Novel Palladium-Catalyzed Intramolecular Redox Reaction. *Org. Lett.* **2001,** *3* (10), 1495-1497.

(181) Long, P.-W.; He, T.; Oestreich, M., $B(C_6F_5)_3$-Catalyzed Hydrosilylation of Vinylcyclopropanes. *Org. Lett.* **2020,** *22* (18), 7383-7386.

(182) Geary, G. C.; Hope, E. G.; Singh, K.; Stuart, A. M., Electrophilic fluorination using a hypervalent iodine reagent derived from fluoride. *Chem. Commun.* **2013,** *49* (81), 9263-9265.

(183) Ren, J.; Jia, M.-C.; Du, F.-H.; Zhang, C., A general method for one-step synthesis of monofluoroiodane(III) reagents using silver difluoride. *Chin. Chem. Lett.* **2022,** *33* (11), 4834-4837.

(184) Eisenberger, P.; Gischig, S.; Togni, A., Novel 10-I-3 Hypervalent Iodine-Based Compounds for Electrophilic Trifluoromethylation. *Chem. - Eur. J.* **2006,** *12* (9), 2579-2586.

(185) Niedermann, K.; Welch, J. M.; Koller, R.; Cvengroš, J.; Santschi, N.; Battaglia, P.; Togni, A., New hypervalent iodine reagents for electrophilic trifluoromethylation and their precursors: synthesis, structure, and reactivity. *Tetrahedron* **2010,** *66* (31), 5753-5761.

(186) Cortés González, M. A.; Nordeman, P.; Bermejo Gómez, A.; Meyer, D. N.; Antoni, G.; Schou, M.; Szabó, K. J., [18F]fluoro-benziodoxole: a no-carrier-added electrophilic fluorinating reagent. Rapid, simple radiosynthesis, purification and application for fluorine-18 labelling. *Chem. Commun.* **2018,** *54* (34), 4286-4289.

(187) Matoušek, V.; Václavík, J.; Hájek, P.; Charpentier, J.; Blastik, Z. E.; Pietrasiak, E.; Budinská, A.; Togni, A.; Beier, P., Expanding the Scope of Hypervalent Iodine Reagents for Perfluoroalkylation: From Trifluoromethyl to Functionalized Perfluoroethyl. *Chem. - Eur. J.* **2016,** *22* (1), 417-424.

(188) Abudken, A. M. H.; Hope, E. G.; Singh, K.; Stuart, A. M., Fluorinations of unsymmetrical diaryliodonium salts containing ortho-sidearms; influence of sidearm on selectivity. *Org. Biomol. Chem.* **2020,** *18* (31), 6140-6146.

(189) Legault, C. Y.; Prevost, J., 1-Fluoro-3,3-dimethyl-1,3-dihydro-1lambda(3)-benzo[d][1,2]iodoxole. *Acta Crystallogr Sect E Struct Rep Online* **2012,** *68* (Pt 4), o1238.

(190) Matoušek, V.; Pietrasiak, E.; Schwenk, R.; Togni, A., One-Pot Synthesis of Hypervalent Iodine Reagents for Electrophilic Trifluoromethylation. *J. Org. Chem.* **2013,** *78* (13), 6763-6768.

(191) Jacobson, O.; Kiesewetter, D. O.; Chen, X., Fluorine-18 Radiochemistry, Labeling Strategies and Synthetic Routes. *Bioconjugate Chem.* **2015,** *26* (1), 1-18.

(192) Racicot, L.; Valliant, J. F.; Murphy, G. K., Synthesis and Evaluation of Fluorous-Tagged and Polystyrene-Supported Precursors for Fluoro-benziodoxole. *Synthesis* **2023,** *55* (17), 2730-2736.

(193) Tang, L.; Yang, Z.; Jiao, J.; Cui, Y.; Zou, G.; Zhou, Q.; Zhou, Y.; Rao, W.; Ma, X., Chemoselective Mono- and Difluorination of 1,3-Dicarbonyl Compounds. *J. Org. Chem.* **2019,** *84* (16), 10449-10458.

(194) Ilchenko, N. O.; Tasch, B. O. A.; Szabó, K. J., Mild Silver-Mediated Geminal Difluorination of Styrenes Using an Air- and Moisture-Stable Fluoroiodane Reagent. *Angew. Chem. Int. Ed.* **2014,** *53* (47), 12897-12901.

(195) Ilchenko, N. O.; Cortés, M. A.; Szabó, K. J., Palladium-Catalyzed Iodofluorination of Alkenes Using Fluoro-Iodoxole Reagent. *ACS Catal.* **2016,** *6* (1), 447-450.

(196) Yuan, W.; Szabó, K. J., Catalytic Intramolecular Aminofluorination, Oxyfluorination, and Carbofluorination with a Stable and Versatile Hypervalent Fluoroiodine Reagent. *Angew. Chem. Int. Ed.* **2015,** *54* (29), 8533-8537.

(197) Geary, G. C.; Hope, E. G.; Stuart, A. M., Intramolecular Fluorocyclizations of Unsaturated Carboxylic Acids with a Stable Hypervalent Fluoroiodane Reagent. *Angew. Chem. Int. Ed.* **2015,** *54* (49), 14911-14914.

(198) Ulmer, A.; Brunner, C.; Arnold, A. M.; Pöthig, A.; Gulder, T., A Fluorination/Aryl Migration/Cyclization Cascade for the Metal-Free Synthesis of Fluoro-Benzoxazepines. *Chem. - Eur. J.* **2016,** *22* (11), 3660-3664.

(199) Minhas, H. K.; Riley, W.; Stuart, A. M.; Urbonaite, M., Activation of the hypervalent fluoroiodane reagent by hydrogen bonding to hexafluoroisopropanol. *Org. Biomol. Chem.* **2018,** *16* (39), 7170-7173.

(200) Andries-Ulmer, A.; Brunner, C.; Rehbein, J.; Gulder, T., Fluorine as a Traceless Directing Group for the Regiodivergent Synthesis of Indoles and Tryptophans. *J. Am. Chem. Soc.* **2018,** *140* (40), 13034-13041.

(201) Okada, M.; Nakamura, Y.; Horikawa, H.; Inoue, T.; Taguchi, T., Fluoro-lactonization of 4-alkenoic acid derivatives with N-fluoropentachloropyridinium triflate. *J. Fluorine Chem.* **1997,** *82* (2), 157-161.

(202) Zhao, J.-F.; Duan, X.-H.; Yang, H.; Guo, L.-N., Transition-Metal-Free Oxyfluorination of Olefinic Amides for the Synthesis of Fluorinated Heterocycles. *J. Org. Chem.* **2015,** *80* (21), 11149-11155.

(203) Yan, T.; Zhou, B.; Xue, X.-S.; Cheng, J.-P., Mechanism and Origin of the Unexpected Chemoselectivity in Fluorocyclization of o-Styryl Benzamides with a Hypervalent Fluoroiodane Reagent. *J. Org. Chem.* **2016,** *81* (19), 9006-9011.

(204) Zhou, B.; Yan, T.; Xue, X.-S.; Cheng, J.-P., Mechanism of Silver-Mediated Geminal Difluorination of Styrenes with a Fluoroiodane Reagent: Insights into Lewis-Acid-Activation Model. *Org. Lett.* **2016,** *18* (23), 6128-6131.

(205) Zhou, B.; Xue, X.-s.; Cheng, J.-p., Theoretical study of Lewis acid activation models for hypervalent fluoroiodane reagent: The generality of "F-coordination" activation model. *Tetrahedron Lett.* **2017,** *58* (13), 1287-1291.

(206) Charpentier, J.; Fruh, N.; Togni, A., Electrophilic Trifluoromethylation by Use of Hypervalent Iodine Reagents. *Chem. Rev.* **2015,** *115* (2), 650-682.

(207) Zhang, J.; Szabó, K. J.; Himo, F., Metathesis Mechanism of Zinc-Catalyzed Fluorination of Alkenes with Hypervalent Fluoroiodine. *ACS Catal.* **2017,** *7* (2), 1093-1100.

(208) Yang, B.; Chansaenpak, K.; Wu, H.; Zhu, L.; Wang, M.; Li, Z.; Lu, H., Silver-promoted (radio)fluorination of unsaturated carbamates via a radical process. *Chem. Commun.* **2017,** *53* (24), 3497-3500.

(209) Brunner, C.; Andries-Ulmer, A.; Kiefl, G. M.; Gulder, T., Hypervalent Fluoroiodane-Triggered Synthesis of Fluoro-Azabenzoxazepines and Azaindoles. *Eur. J. Org. Chem.* **2018,** *2018* (20-21), 2615-2621.

(210) Riley, W.; Jones, A. C.; Singh, K.; Browne, D. L.; Stuart, A. M., Accessing novel fluorinated heterocycles with the hypervalent fluoroiodane reagent by solution and mechanochemical synthesis. *Chem. Commun.* **2021,** *57* (60), 7406-7409.

(211) Yang, S.; Shi, S.; Chen, Y.; Ding, Z., Synthesis of Dihydroxazines and Fluorinated Oxazepanes Using a Hypervalent Fluoroiodine Reagent. *J. Org. Chem.* **2021,** *86* (20), 14004-14010.

(212) Cuzzucoli, F.; Racicot, L.; Valliant, J. F.; Murphy, G. K., Transition metal-free fluorocyclization of unsaturated N-methoxyamides gives cyclic N-methoxyimidates. *Tetrahedron* **2022,** *123*, 132982.

(213) Xu, K.; Yang, R.; Yang, S.; Jiang, C.; Ding, Z., Hypervalent iodane mediated reactions of N-acetyl enamines for the synthesis of oxazoles and imidazoles. *Org. Biomol. Chem.* **2019,** *17* (40), 8977-8981.

(214) Chen, Y.; Zhang, D.; Sun, M.; Ding, Z., Divergent synthesis of isoxazoles and 6H-1,2-oxazines via hypervalent iodine-mediated intramolecular oxygenation of alkenes. *New J. Chem.* **2022,** *46* (12), 5663-5667.

(215) Yuan, W.; Eriksson, L.; Szabó, K. J., Rhodium-Catalyzed Geminal Oxyfluorination and Oxytrifluoro-Methylation of Diazocarbonyl Compounds. *Angew. Chem. Int. Ed.* **2016,** *55* (29), 8410-8415.

(216) Mai, B. K.; Szabó, K. J.; Himo, F., Mechanisms of Rh-Catalyzed Oxyfluorination and Oxytrifluoromethylation of Diazocarbonyl Compounds with Hypervalent Fluoroiodine. *ACS Catal.* **2018,** *8* (5), 4483-4492.

(217) Kiefl, G. M.; Gulder, T., α-Functionalization of Ketones via a Nitrogen Directed Oxidative Umpolung. *J. Am. Chem. Soc.* **2020,** *142* (49), 20577-20582.

(218) Sanz-Marco, A.; Martinez-Erro, S.; Pauze, M.; Gómez-Bengoa, E.; Martín-Matute, B., An umpolung strategy to react catalytic enols with nucleophiles. *Nat. Commun.* **2019,** *10* (1), 5244.

(219) Václavík, J.; Zschoche, R.; Klimánková, I.; Matoušek, V.; Beier, P.; Hilvert, D.; Togni, A., Irreversible Cysteine-Selective Protein Labeling Employing Modular Electrophilic Tetrafluoroethylation Reagents. *Chem. - Eur. J.* **2017,** *23* (27), 6490-6494.

(220) Patrick Eisenberger, I. K., Raffael Koller, Kyrill Stanek, Antonio Togni, Preparation of a trifluoromethyl transfer agent: 1—trifluoromethyl-1,3-dihydro-3,3-dimethyl-1,2-benziodoxole. *Organic Synthesis* **2011,** *88*, 168-180.

(221) Wang, Y.; Tang, K.; Liu, Z.; Ning, Y., Disulfonation of terminal alkynes for 1,2-bisulfonylethenes. *Chem. Commun.* **2020,** *56* (86), 13141-13144.

(222) Sun, M.; Chen, J.; Ding, Z., Synthesis of Oxazolidines and Dihydroxazines via Cyclization of α-Aminated Ketones. *J. Org. Chem.* **2023,** *88* (15), 10647-10654.

(223) Akula, R.; Galligan, M.; Ibrahim, H., Umpolung of halide reactivity: efficient (diacetoxyiodo)benzene-mediated electrophilic α-halogenation of 1,3-dicarbonyl compounds. *Chem. Commun.* **2009,** (45), 6991-6993.

(224) Stockhammer, L.; Schörgenhumer, J.; Mairhofer, C.; Waser, M., Asymmetric α-Chlorination of β-Keto Esters Using Hypervalent Iodine-Based Cl-Transfer Reagents in Combination with Cinchona Alkaloid Catalysts. *Eur. J. Org. Chem.* **2021,** *2021* (1), 82-86.

(225) Andrews, L. J.; Keefer, R. M., The Unusual Effects of o-Carboxyl and Carbomethoxy Substituents on the Stability of Iodobenzene Dichloride. *J. Am. Chem. Soc.* **1959,** *81* (16), 4218-4223.

(226) Wang, M.; Zhang, Y.; Wang, T.; Wang, C.; Xue, D.; Xiao, J., Story of an Age-Old Reagent: An Electrophilic Chlorination of Arenes and Heterocycles by 1-Chloro-1,2-benziodoxol-3-one. *Org. Lett.* **2016,** *18* (9), 1976-1979.

(227) Parvathaneni, S. P.; Perumgani, P. C., Regioselective Chlorination of Aryl C−H bonds with Hypervalent Iodine(III) Reagent 1-Chloro-1,2-benziodoxol-3-one. *Asian J. Org. Chem.* **2018,** *7* (2), 324-327.

(228) Egami, H.; Yoneda, T.; Uku, M.; Ide, T.; Kawato, Y.; Hamashima, Y., Difunctionalization of Alkenes Using 1-Chloro-1,2-benziodoxol-3-(1H)-one. *J. Org. Chem.* **2016,** *81* (10), 4020-4030.

(229) Zhao, Z.; Murphy, G. K., Chlorination of phenylallene derivatives with 1-chloro-1,2-benziodoxol-3-one: synthesis of vicinal-dichlorides and chlorodienes. *Beilstein J. Org. Chem.* **2018,** *14*, 796-802.

(230) Binder, J.; Biswas, A.; Gulder, T., Biomimetic chlorine-induced polyene cyclizations harnessing hypervalent chloroiodane–HFIP assemblies. *Chem. Sci.* **2023,** *14* (14), 3907-3912.

(231) Lin, Q.-Y.; Xu, X.-H.; Qing, F.-L., Chemo-, Regio-, and Stereoselective Trifluoromethylation of Styrenes via Visible Light-Driven Single-Electron Transfer (SET) and Triplet–Triplet Energy Transfer (TTET) Processes. *J. Org. Chem.* **2014,** *79* (21), 10434-10446.

(232) Zhang, W.; Zhu, J.; Hu, J., Electrophilic (phenylsulfonyl)difluoromethylation of thiols with a hypervalent iodine(III)–CF_2SO_2Ph reagent. *Tetrahedron Lett.* **2008,** *49* (34), 5006-5008.

(233) Charpentier, J.; Früh, N.; Foser, S.; Togni, A., Tandem Radical Fluoroalkylation–Cyclization: Synthesis of Tetrafluoro Imidazopyridines. *Org. Lett.* **2016,** *18* (4), 756-759.

(234) Kiyokawa, K.; Kosaka, T.; Kojima, T.; Minakata, S., Synthesis and Structure of Hypervalent Iodine(III) Reagents Containing Phthalimidate and Application to Oxidative Amination Reactions. *Angew. Chem. Int. Ed.* **2015,** *54* (46), 13719-13723.

(235) Caramenti, P.; Nandi, R. K.; Waser, J., Metal-Free Oxidative Cross Coupling of Indoles with Electron-Rich (Hetero)arenes. *Chem. - Eur. J.* **2018,** *24* (40), 10049-10053.

(236) Wang, Y.-F.; Qiu, J.; Kong, D.; Gao, Y.; Lu, F.; Karmaker, P. G.; Chen, F.-X., The direct electrophilic cyanation of β-keto esters and amides with cyano benziodoxole. *Org. Biomol. Chem.* **2015,** *13* (2), 365-368.

(237) De Munari, S.; Frigerio, M.; Santagostino, M., Hypervalent Iodine Oxidants: Structure and Kinetics of the Reactive Intermediates in the Oxidation of Alcohols and 1,2-Diols by o-Iodoxybenzoic Acid (IBX) and Dess−Martin Periodinane. A Comparative ^{1}H-NMR Study. *J. Org. Chem.* **1996,** *61* (26), 9272-9279.

(238) Corey, E. J.; Palani, A., A mechanistic model for the selective oxidation of 1,4-diols to γ-lactols by o-iodoxybenzoic acid. *Tetrahedron Lett.* **1995,** *36* (44), 7945-7948.

(239) Moorthy, J. N.; Senapati, K.; Parida, K. N.; Jhulki, S.; Sooraj, K.; Nair, N. N., Twist Does a Twist to the Reactivity: Stoichiometric and Catalytic Oxidations with Twisted Tetramethyl-IBX. *J. Org. Chem.* **2011,** *76* (23), 9593-9601.

(240) Jiang, H.; Sun, T.-Y.; Wang, X.; Xie, Y.; Zhang, X.; Wu, Y.-D.; Schaefer, H. F., III, A Twist of the Twist Mechanism, 2-Iodoxybenzoic Acid (IBX)-Mediated Oxidation of Alcohol Revisited: Theory and Experiment. *Org. Lett.* **2017,** *19* (24), 6502-6505.

(241) Sun, T.-Y.; Chen, K.; Zhou, H.; You, T.; Yin, P.; Wang, X., Revisiting the effect of f-functions in predicting the right reaction mechanism for hypervalent iodine reagents. *J. Comput. Chem.* **2021,** *42* (7), 470-474.

(242) Chipman, A.; Farshadfar, K.; Smith, J. A.; Yates, B. F.; Ariafard, A., DFT-Based Comparison between Mechanistic Aspects of Amine and Alcohol Oxidation Mediated by IBX. *J. Org. Chem.* **2020,** *85* (2), 515-525.

(243) Parida, K. N.; Moorthy, J. N., Catalytic Oxidations with ortho-Substituted Modified IBXs. *Synlett* **2022,** *34* (06), 495-506.

(244) Altermann, S. M.; Richardson, R. D.; Page, T. K.; Schmidt, R. K.; Holland, E.; Mohammed, U.; Paradine, S. M.; French, A. N.; Richter, C.; Bahar, A. M.; Witulski, B.; Wirth, T., Catalytic Enantioselective α-Oxysulfonylation of Ketones Mediated by Iodoarenes. *Eur. J. Org. Chem.* **2008,** *2008* (31), 5315-5328.

(245) Guilbault, A.-A.; Legault, C. Y., Drastic Enhancement of Activity in Iodane-Based α-Tosyloxylation of Ketones: Iodine(III) Does the Hypervalent Twist. *ACS Catal.* **2012,** *2* (2), 219-222.

(246) Guilbault, A.-A.; Basdevant, B.; Wanie, V.; Legault, C. Y., Catalytic Enantioselective α-Tosyloxylation of Ketones Using Iodoaryloxazoline Catalysts: Insights on the Stereoinduction Process. *J. Org. Chem.* **2012,** *77* (24), 11283-11295.

(247) Abazid, A. H.; Nachtsheim, B. J., A Triazole-Substituted Aryl Iodide with Omnipotent Reactivity in Enantioselective Oxidations. *Angew. Chem. Int. Ed.* **2020,** *59* (4), 1479-1484.

(248) Golub, T. P.; Abazid, A. H.; Nachtsheim, B. J.; Merten, C., Structure Elucidation of In Situ Generated Chiral Hypervalent Iodine Complexes via Vibrational Circular Dichroism (VCD). *Angew. Chem. Int. Ed.* **2022,** *61* (50), e202204624.

(249) Abazid, A. H.; Hollwedel, T.-N.; Nachtsheim, B. J., Stereoselective Oxidative Cyclization of N-Allyl Benzamides to Oxaz(ol)ines. *Org. Lett.* **2021,** *23* (13), 5076-5080.

(250) Abazid, A. H.; Nachtsheim, B. J., Application of chiral triazole-substituted iodoarenes in the enantioselective construction of spirooxazolines. *Chem. Commun.* **2021,** *57* (70), 8822-8825.

(251) Brand, J. P.; Chevalley, C.; Scopelliti, R.; Waser, J., Ethynyl Benziodoxolones for the Direct Alkynylation of Heterocycles: Structural Requirement, Improved Procedure for Pyrroles, and Insights into the Mechanism. *Chem. - Eur. J.* **2012,** *18* (18), 5655-5666.

(252) Jiang, H.; Sun, T.-Y.; Chen, Y.; Zhang, X.; Wu, Y.-D.; Xie, Y.; Schaefer, H. F., Designing new Togni reagents by computation. *Chem. Commun.* **2019,** *55* (39), 5667-5670.

(253) Matsumoto, K.; Nakajima, M.; Nemoto, T., Determination of the best functional and basis sets for optimization of the structure of hypervalent iodines and calculation of their first and second bond dissociation enthalpies. *J. Phys. Org. Chem.* **2019,** *32* (8), e3961.

(254) Imamoto, T.; Kusumoto, T.; Tawarayama, Y.; Sugiura, Y.; Mita, T.; Hatanaka, Y.; Yokoyama, M., Carbon-carbon bond-forming reactions using cerium metal or organocerium(III) reagents. *J. Org. Chem.* **1984,** *49* (21), 3904-3912.

(255) Imamoto, T.; Takiyama, N.; Nakamura, K., Cerium chloride-promoted nucleophilic addition of grignard reagents to ketones an efficient method for the synthesis of tertiary alcohols. *Tetrahedron Lett.* **1985,** *26* (39), 4763-4766.

(256) Fier, P. S.; Roberts, R. A.; Larson, R. T., The Direct Conversion of Esters to Ketones Enabled by a Traceless Activating Group. *Org. Lett.* **2023,** *25* (17), 3131-3135.

(257) Cantillo, D.; de Frutos, O.; Rincon, J. A.; Mateos, C.; Kappe, C. O., A Scalable Procedure for Light-Induced Benzylic Brominations in Continuous Flow. *J. Org. Chem.* **2014,** *79* (1), 223-229.

(258) Fernández González, D.; Brand, J. P.; Mondière, R.; Waser, J., Ethynylbenziodoxolones (EBX) as Reagents for the Ethynylation of Stabilized Enolates. *Adv. Synth. Catal.* **2013,** *355* (8), 1631-1639.

(259) Yang, Z.; Sun, F.; Xu, J.; Li, Y.; Yang, K.; Du, Y., Preparation, Structural Identification and Reactivities of Two Benziodazole-type I(III) Reagents. *Adv. Synth. Catal.* **2023,** *365* (16), 2730-2736.

(260) Olah, G. A.; Melby, E. G., Onium ions. III. Alkylarylhalonium ions. *J. Am. Chem. Soc.* **1972,** *94* (17), 6220-6221.

(261) Béke, F.; Csenki, J. T.; Novák, Z., Fluoroalkylations and Fluoroalkenylations with Iodonium Salts. *The Chemical Record* **2023,** *23* (9), e202300083.

(262) Eliel, E. L.; Wilen, S. H.; Mander, L. N., *Stereochemistry of Organic Compounds*. John Wiley & Sons, Inc.: New York, NY, USA, 1994; p 696-697.

(263) Carey, F. A.; Sundberg, R. J., *Advanced Organic Chemistry, Part A: Structure and Mechanisms*. 5 ed.; Springer New York, NY, USA: 2007; p 153.

(264) Burchat, A. F.; Chong, J. M.; Nielsen, N., Titration of alkyllithiums with a simple reagent to a blue endpoint. *J. Organomet. Chem.* **1997,** *542* (2), 281-283.

(265) Krasovskiy, A.; Knochel, P., Convenient Titration Method for Organometallic Zinc, Magnesium, and Lanthanide- Reagents. *Synthesis* **2006,** *2006* (05), 0890-0891.

(266) Samadi, S.; Nazari, S.; Arvinnezhad, H.; Jadidi, K.; Notash, B., A significant improvement in enantioselectivity, yield, and reactivity for the copper-bi-o-tolyl bisoxazoline-catalyzed asymmetric allylic oxidation of cyclic olefins using recoverable SBA-15 mesoporous silica material. *Tetrahedron* **2013,** *69* (32), 6679-6686.

(267) Fukuda, H.; Karaki, F.; Dodo, K.; Noguchi-Yachide, T.; Ishikawa, M.; Hashimoto, Y.; Ohgane, K., Phenanthridin-6-one derivatives as the first class of non-steroidal pharmacological chaperones for Niemann-Pick disease type C1 protein. *Biorg. Med. Chem. Lett.* **2017,** *27* (12), 2781-2787.

(268) Yang, L.; Huang, Z.; Li, G.; Zhang, W.; Cao, R.; Wang, C.; Xiao, J.; Xue, D., Synthesis of Phenols: Organophotoredox/Nickel Dual Catalytic Hydroxylation of Aryl Halides with Water. *Angew. Chem. Int. Ed.* **2018,** *57* (7), 1968-1972.

(269) Yasukawa, T.; Yang, X.; Kobayashi, S., Development of N-Doped Carbon-Supported Cobalt/Copper Bimetallic Nanoparticle Catalysts for Aerobic Oxidative Esterifications Based on Polymer Incarceration Methods. *Org. Lett.* **2018,** *20* (17), 5172-5176.

(270) Xu, F.; Qian, X.-Y.; Li, Y.-J.; Xu, H.-C., Synthesis of 4H-1,3-Benzoxazines via Metal- and Oxidizing Reagent-Free Aromatic C–H Oxygenation. *Org. Lett.* **2017,** *19* (23), 6332-6335.

(271) WU, L.; Zhang, P.; Li, J.; Chen, S. S1P1 agonist and application thereof. CA 3034796 A1, 2018.

(272) Li, T.; Tsuda, Y.; Minoura, K.; In, Y.; Ishida, T.; Lazarus, L. H.; Okada, Y., Enantioselective Synthesis of a Phenylalanine Library Containing Alkyl Groups on the Aromatic Moiety: Confirmation of Stereostructure by X-Ray Analysis. *Chem. Pharm. Bull.* **2006,** *54* (6), 873-877.

(273) Zhai, F.; Jordan, R. F., Complexation of an indole-based α-aminoimine ligand to Pd(II). *Inorg. Chim. Acta* **2018,** *482*, 491-496.

(274) Boelke, A.; Nachtsheim, B. J., Evolution of N-Heterocycle-Substituted Iodoarenes (NHIAs) to Efficient Organocatalysts in Iodine(I/III)-Mediated Oxidative Transformations. *Adv. Synth. Catal.* **2020,** *362* (1), 184-191.

(275) Curran, D. P.; Fairweather, N., Quantitating the Effect of an Ortho Substituent on Cyclization and Intramolecular Hydrogen-Transfer Reactions of Aryl Radicals. *J. Org. Chem.* **2003,** *68* (7), 2972-2974.

(276) Zhao, W.; Huang, X.; Zhan, Y.; Zhang, Q.; Li, D.; Zhang, Y.; Kong, L.; Peng, B., Dearomative Dual Functionalization of Aryl Iodanes. *Angew. Chem. Int. Ed.* **2019,** *58* (48), 17210-17214.

(277) Landge, K. P.; Jang, K. S.; Lee, S. Y.; Chi, D. Y., Approach to the Synthesis of Indoline Derivatives from Diaryliodonium Salts. *J. Org. Chem.* **2012,** *77* (13), 5705-5713.

(278) Mei, T.-S.; Wang, D.-H.; Yu, J.-Q., Expedient Drug Synthesis and Diversification via ortho-C−H Iodination using Recyclable PdI2 as the Precatalyst. *Org. Lett.* **2010,** *12* (14), 3140-3143.

(279) Tummatorn, J.; Dudley, G. B., Generation of Medium-Ring Cycloalkynes by Ring Expansion of Vinylogous Acyl Triflates. *Org. Lett.* **2011,** *13* (6), 1572-1575.

(280) Merritt, E. A.; Carneiro, V. M. T.; Silva, L. F., Jr.; Olofsson, B., Facile Synthesis of Koser's Reagent and Derivatives from Iodine or Aryl Iodides. *J. Org. Chem.* **2010,** *75* (21), 7416-7419.

Appendices

Appendix A

Chapter 3: NMR Spectra

This appendix contains the ^{1}H-NMR, ^{13}C-NMR, and ^{19}F-NMR spectra of all new compounds which are unreported in the literature. Full chemical shift assignment of compound **3.71.**

Complete H and C chemical shift assignment of **3.71** based on the following NMR spectra:

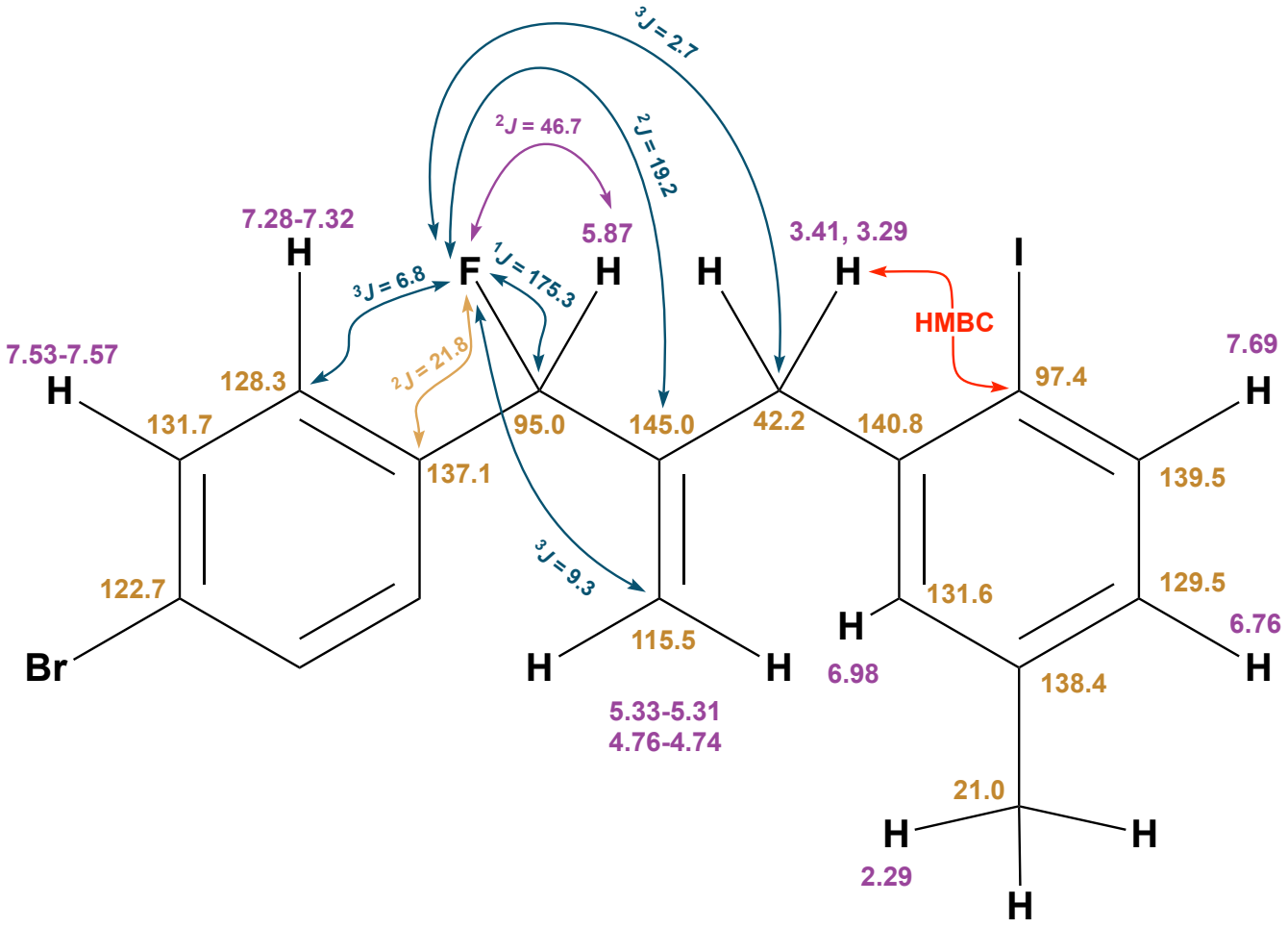


Figure A-1. ^{1}H-NMR (300 MHz, $CDCl_3$) of 2-(2-((4-bromophenyl)fluoromethyl)allyl)-1-iodo-4-methylbenzene (**3.71**):

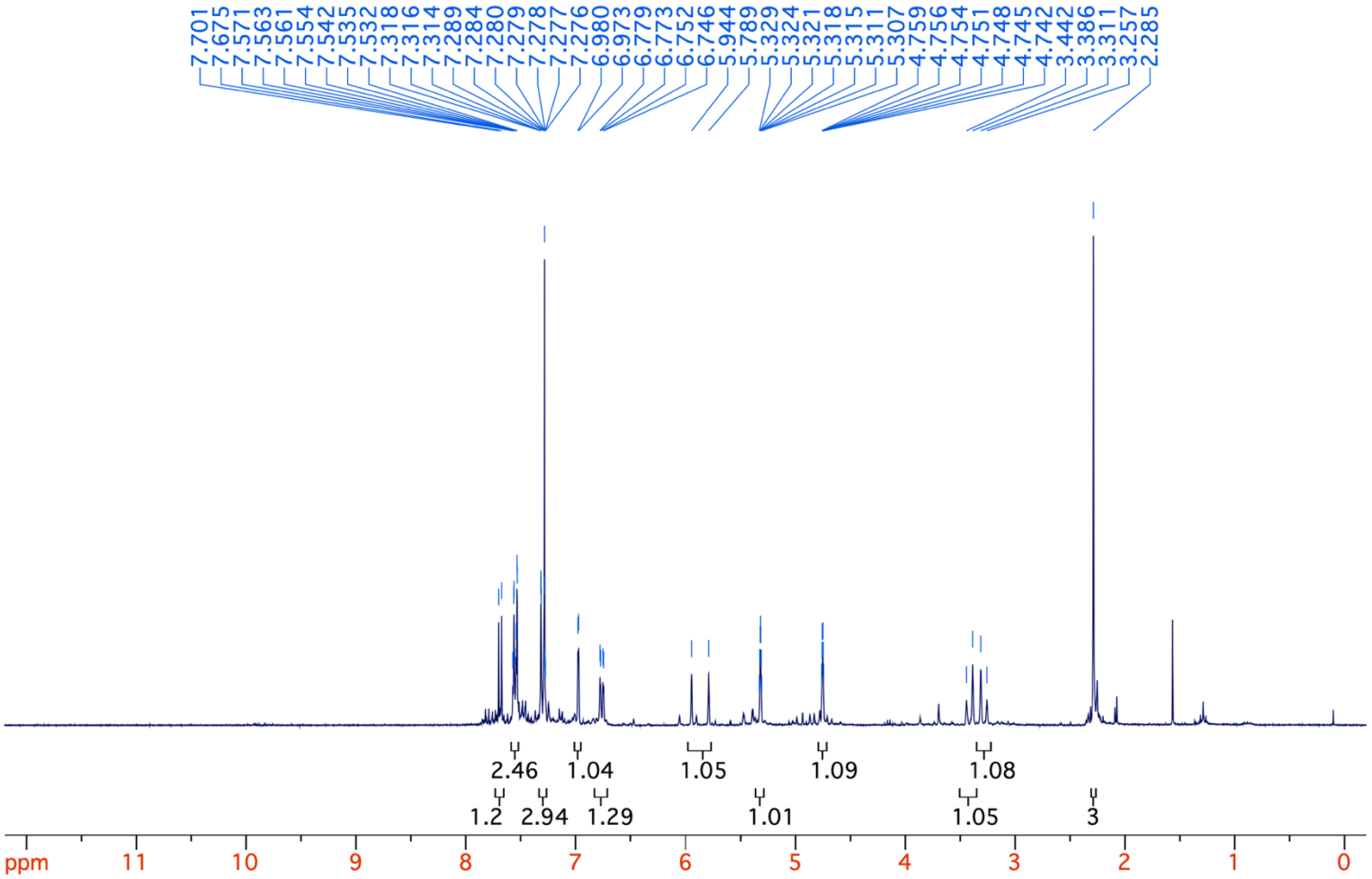


Figure A-2. ^{13}C-NMR (75 MHz, $CDCl_3$) of 2-(2-((4-bromophenyl)fluoromethyl)allyl)-1-iodo-4-methylbenzene (**3.71**):

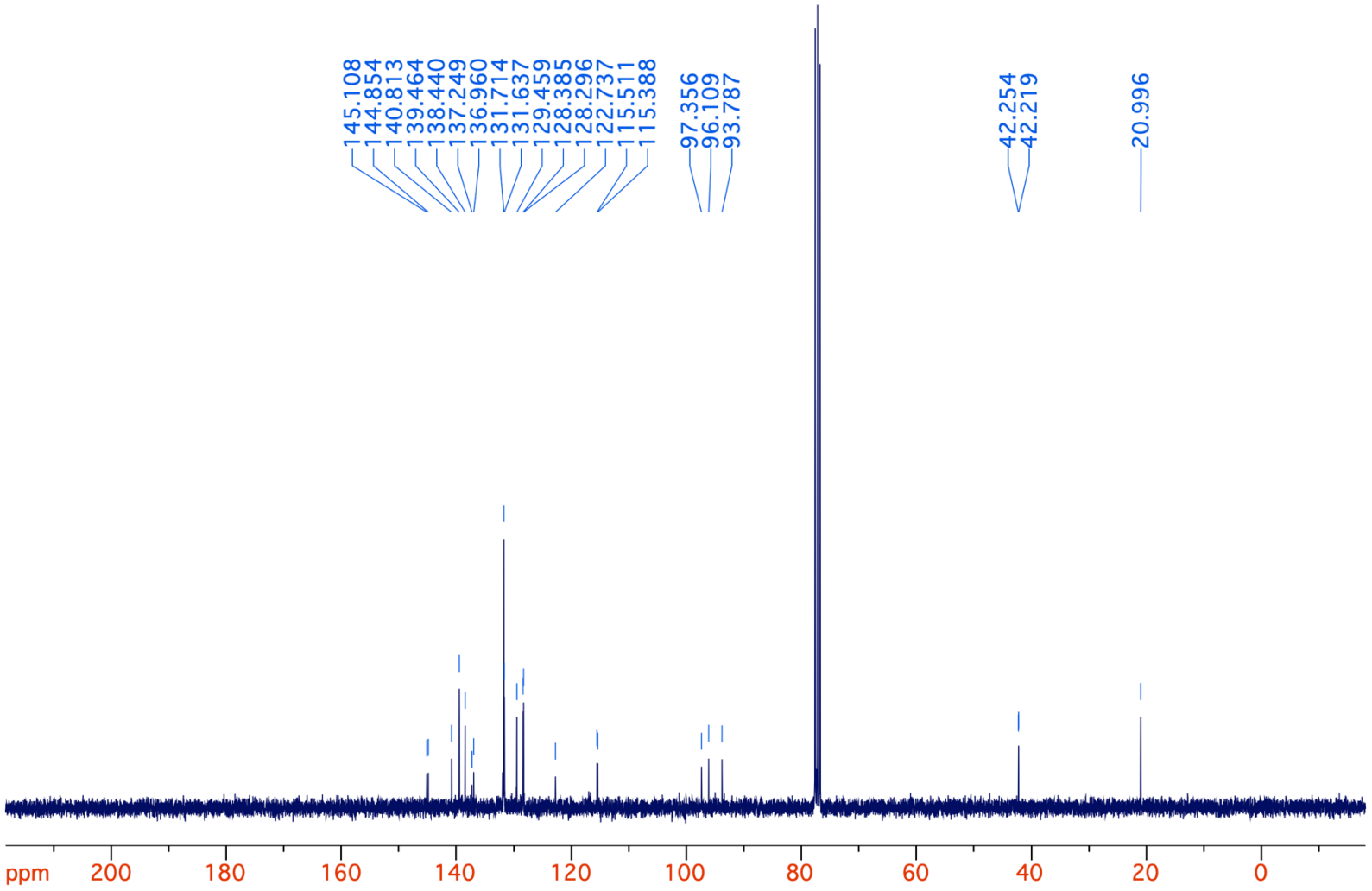


Figure A-3. ^{19}F-NMR (282 MHz, $CDCl_3$) of 2-(2-((4-bromophenyl)fluoromethyl)allyl)-1-iodo-4-methylbenzene (**3.71**):

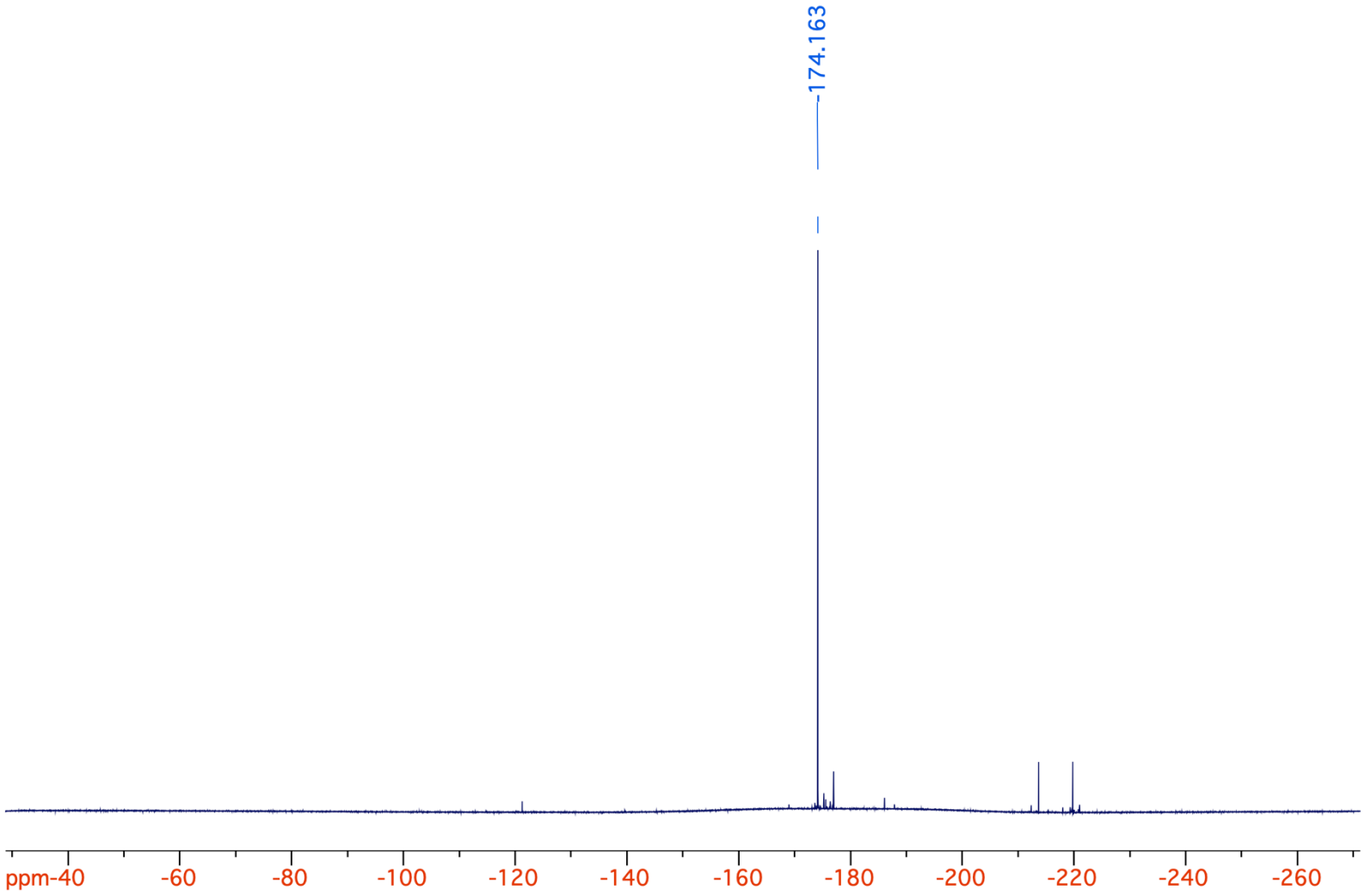


Figure A-4. ^{13}C-DEPT 135 (75 MHz, $CDCl_3$) of 2-(2-((4-bromophenyl)fluoromethyl)allyl)-1-iodo-4-methylbenzene (**3.71**):

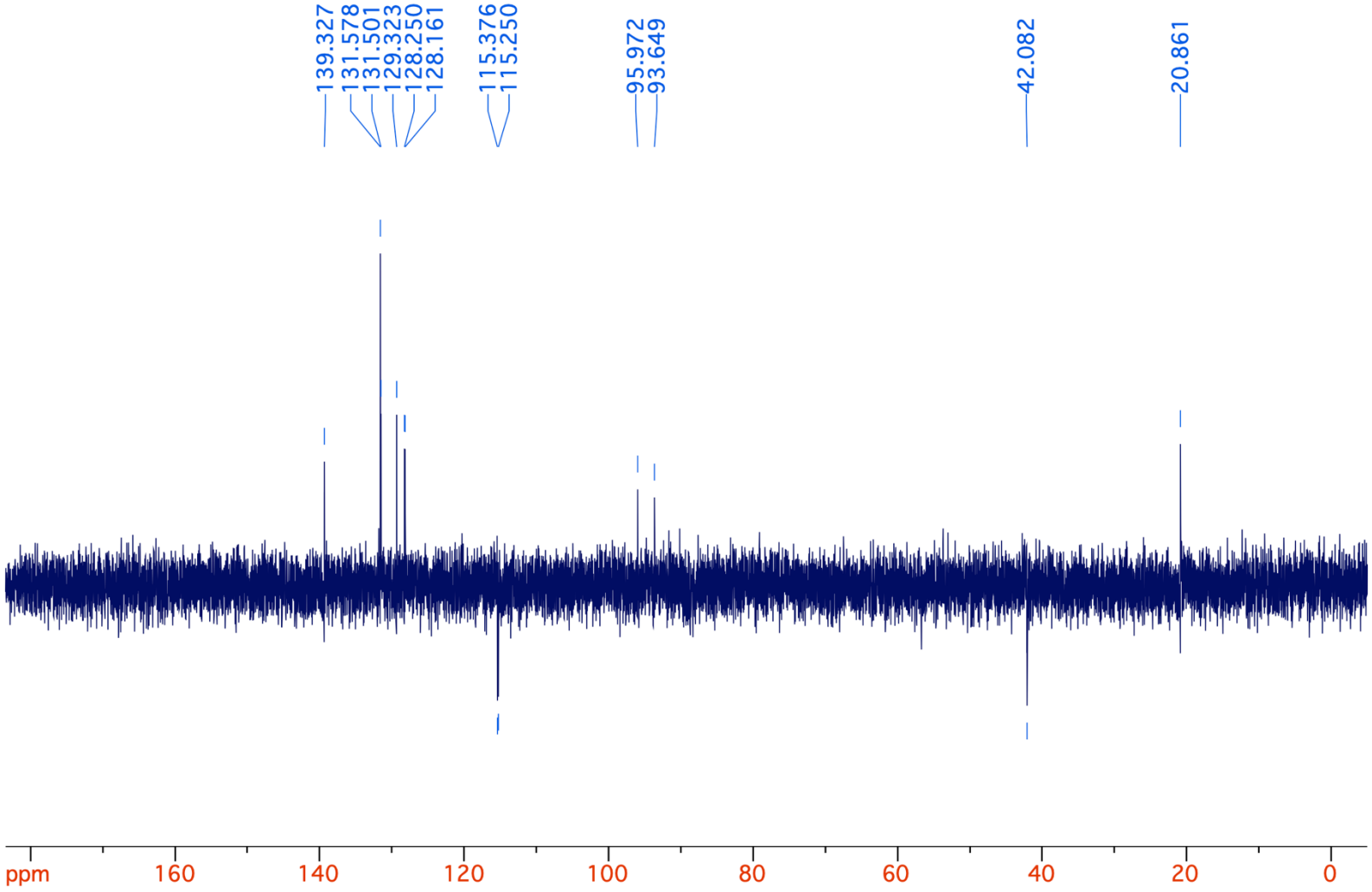


Figure A-5. ^{1}H, ^{13}C-HMQC (300 MHz, 75 MHz, $CDCl_3$) of 2-(2-((4-bromophenyl)fluoromethyl)allyl)-1-iodo-4-methylbenzene (**3.71**):

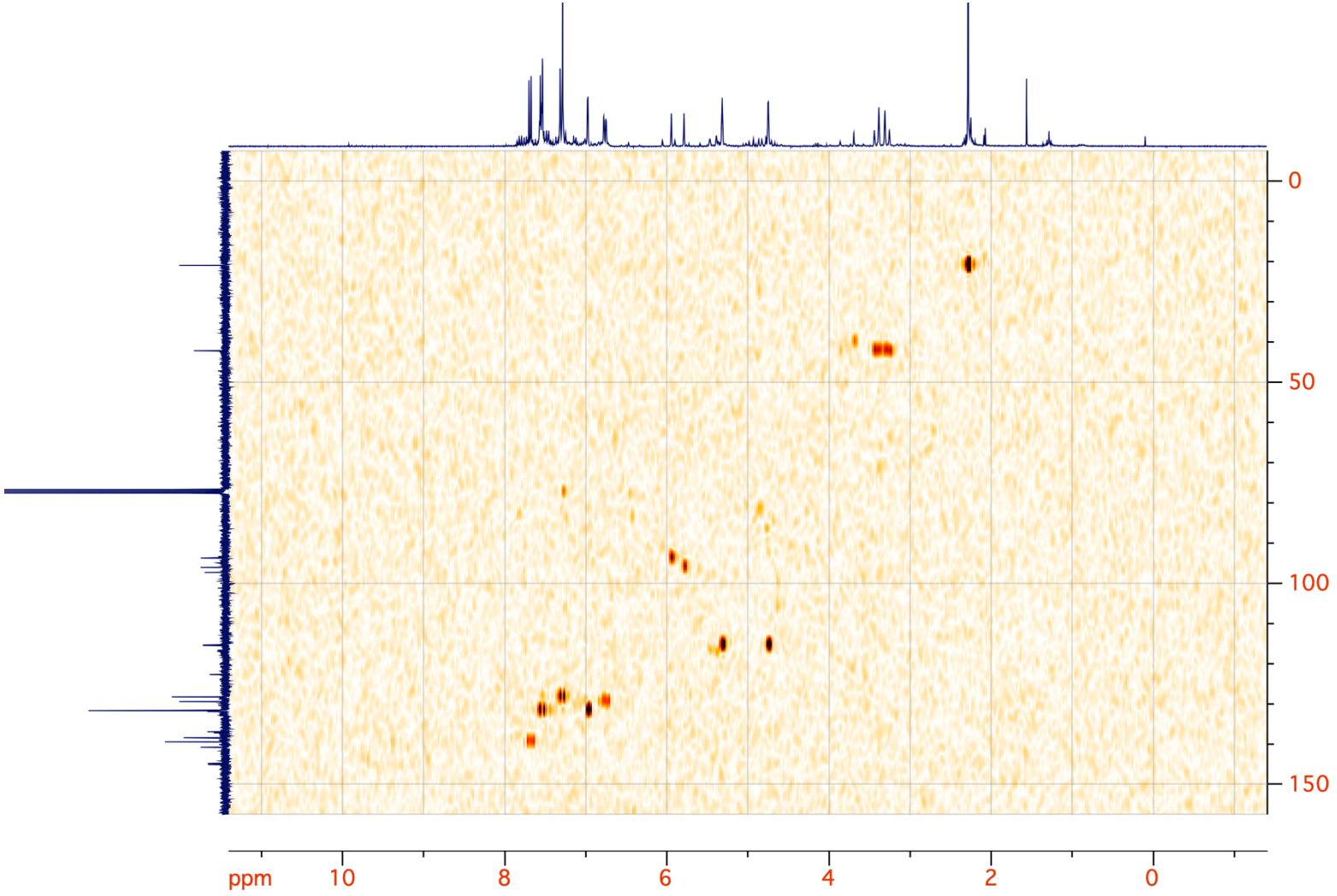
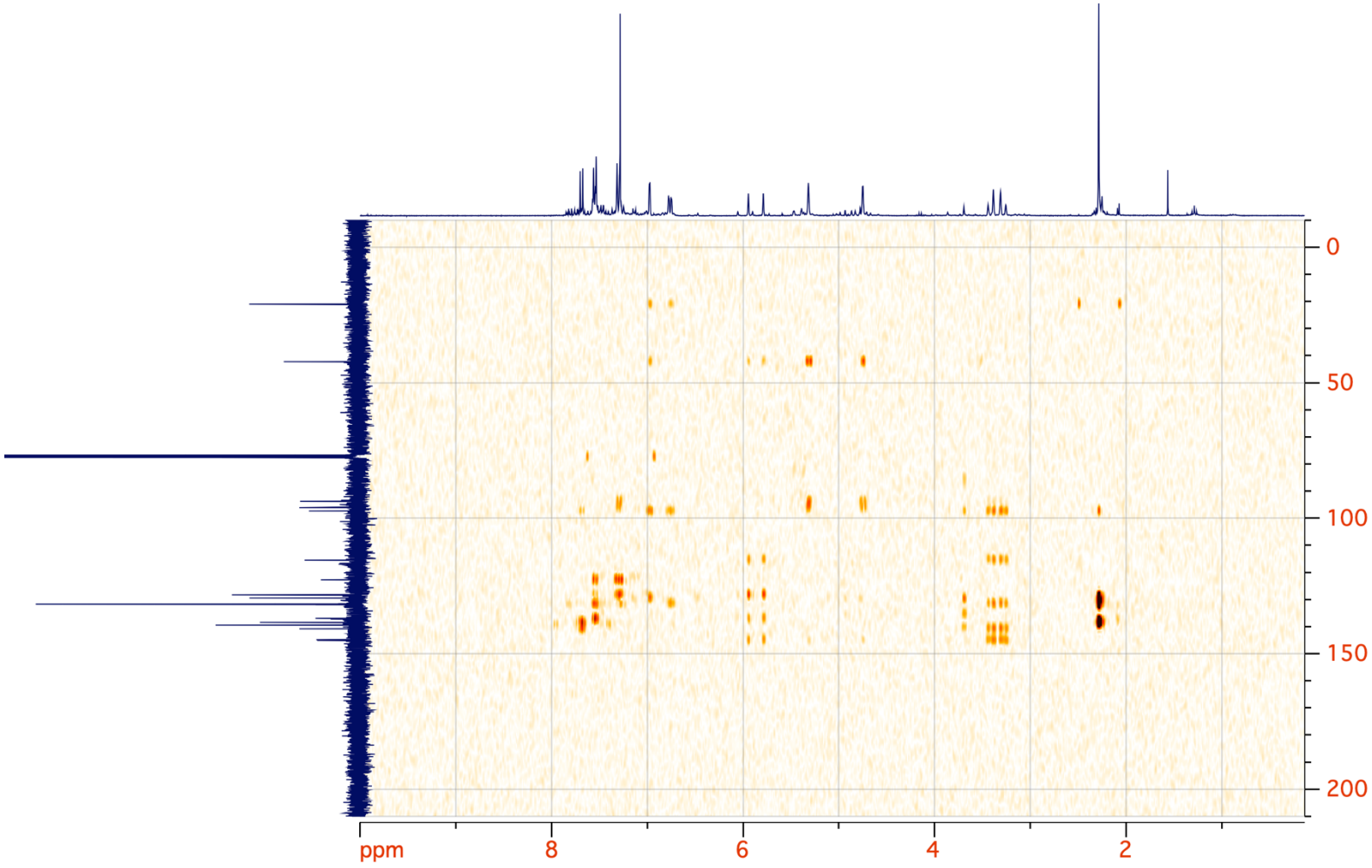


Figure A-6. ^{1}H, ^{13}C-HMBC (300 MHz, 75 MHz, $CDCl_3$) of 2-(2-((4-bromophenyl)fluoromethyl)allyl)-1-iodo-4-methylbenzene (**3.71**):



Appendix B

Chapter 4: NMR Spectra

This appendix contains the ^{1}H-NMR, ^{13}C-NMR, ^{19}F-NMR spectra of all new compounds which are unreported in the literature.

Figure B-1. ^{1}H-NMR (300 MHz, $CDCl_3$) of 2-(2-iodo-3-methylphenyl)propan-2-ol (**4.93**):

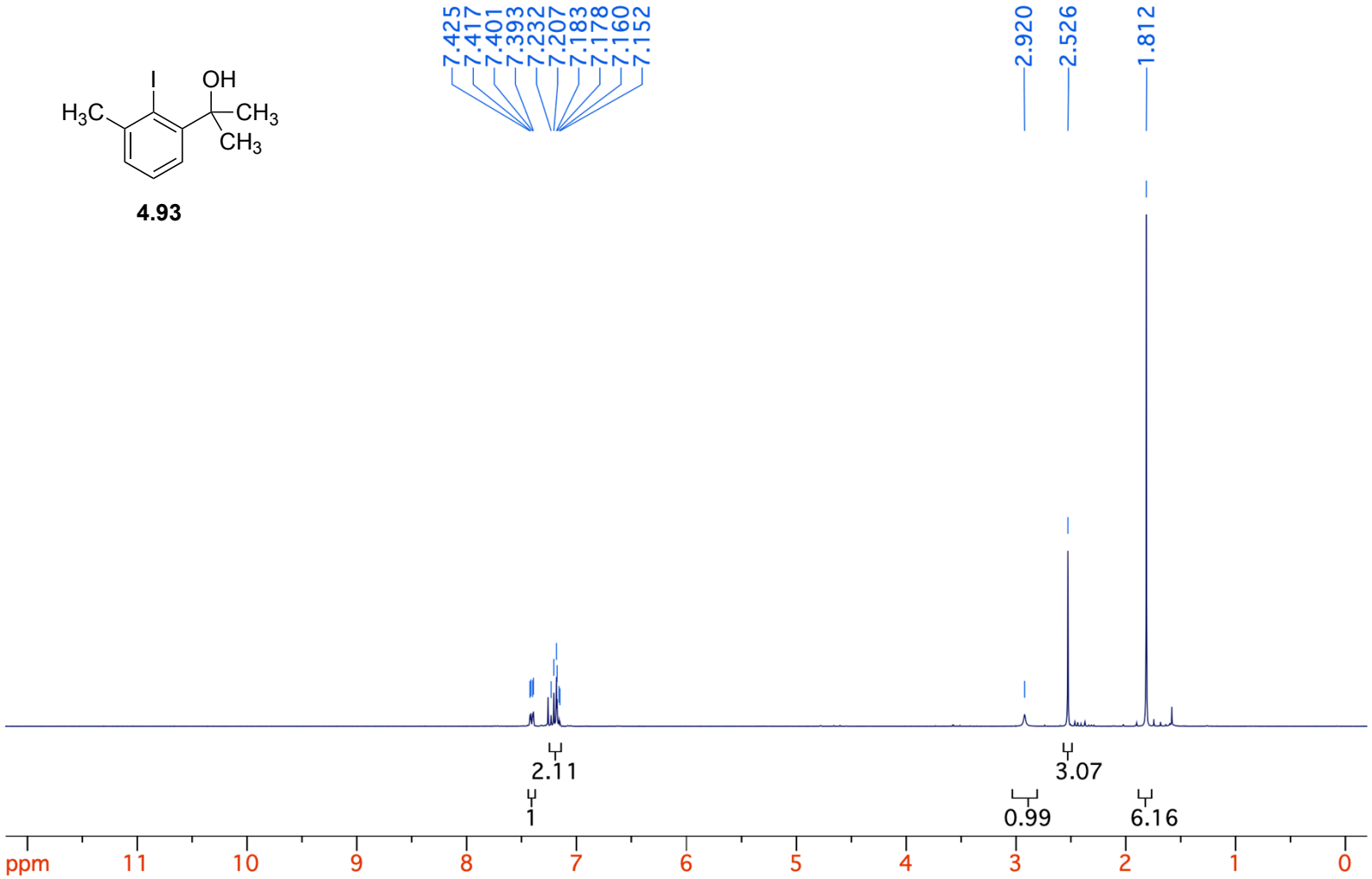


Figure B-2. ^{13}C-NMR (75 MHz, $CDCl_3$) of 2-(2-iodo-3-methylphenyl)propan-2-ol (**4.93**):

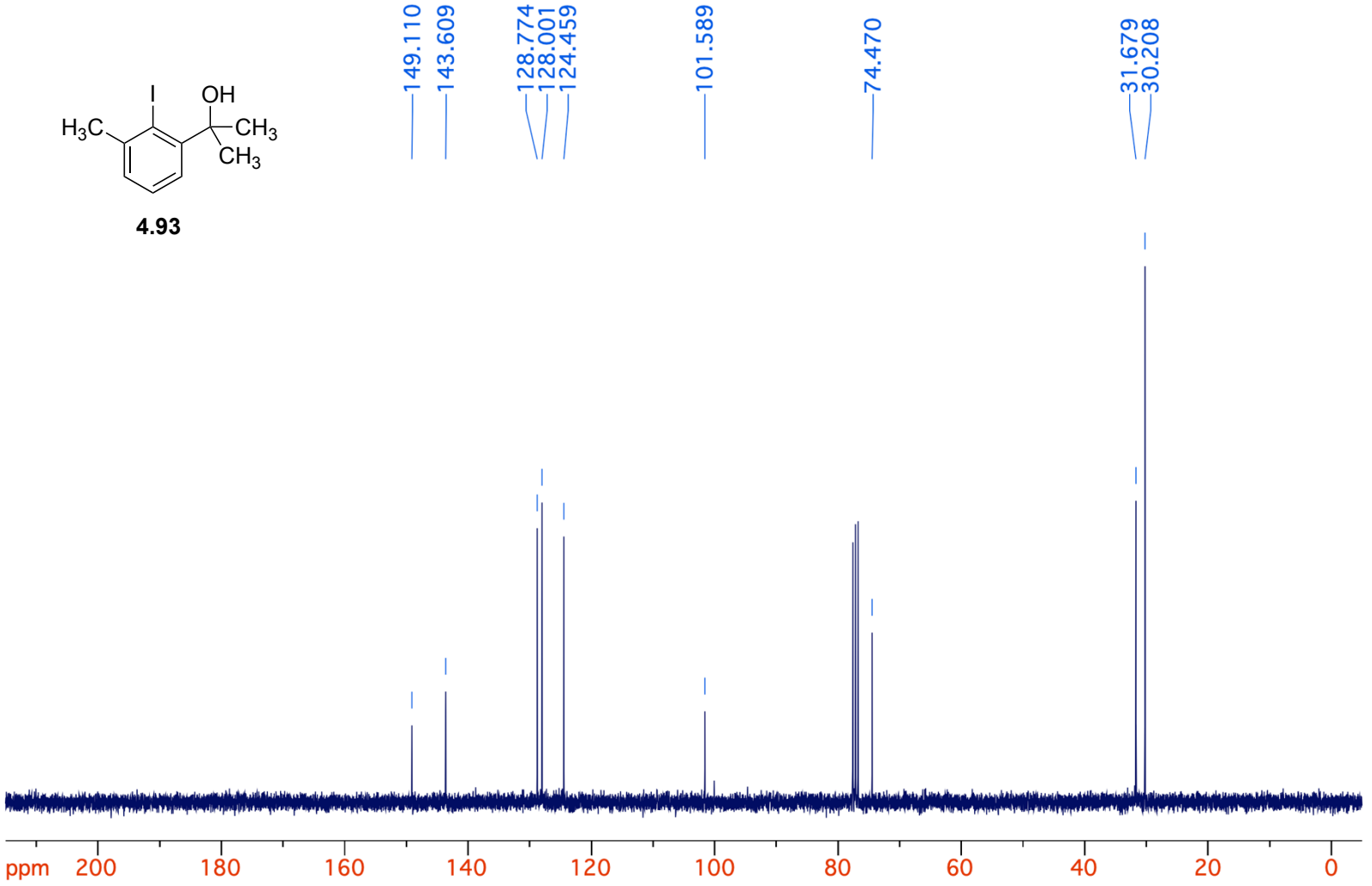


Figure B-3. ^{1}H-NMR (300 MHz, $CDCl_3$) of 2-amino-3-bromobenzoic acid (**4.94**):

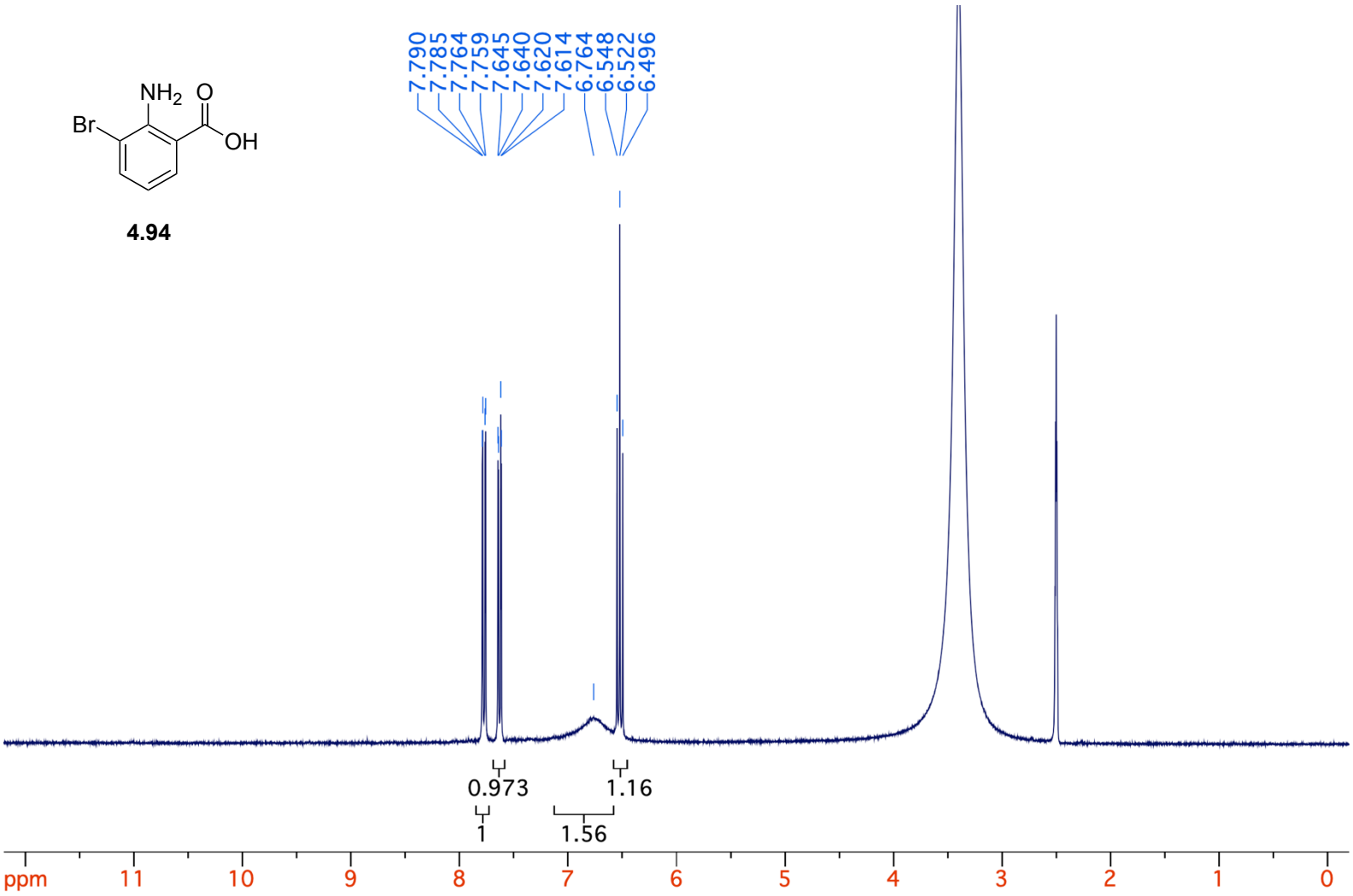


Figure B-4. ^{13}C-NMR (75 MHz, $CDCl_3$) of 2-amino-3-bromobenzoic acid (**4.94**):

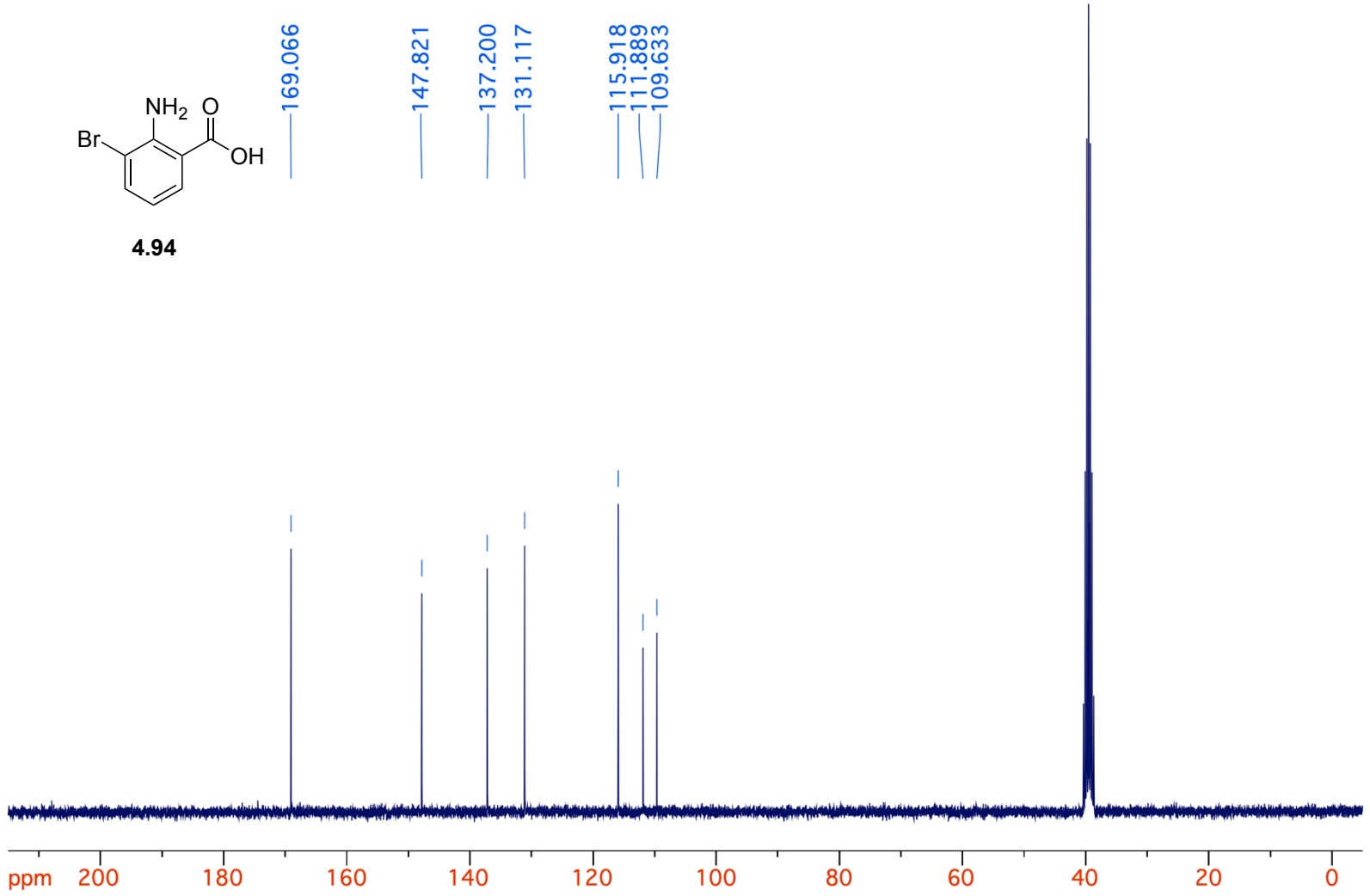


Figure B-5. ^{1}H-NMR (300 MHz, $CDCl_3$) of 2-(2-amino-3-bromophenyl)propan-2-ol (**4.96**):

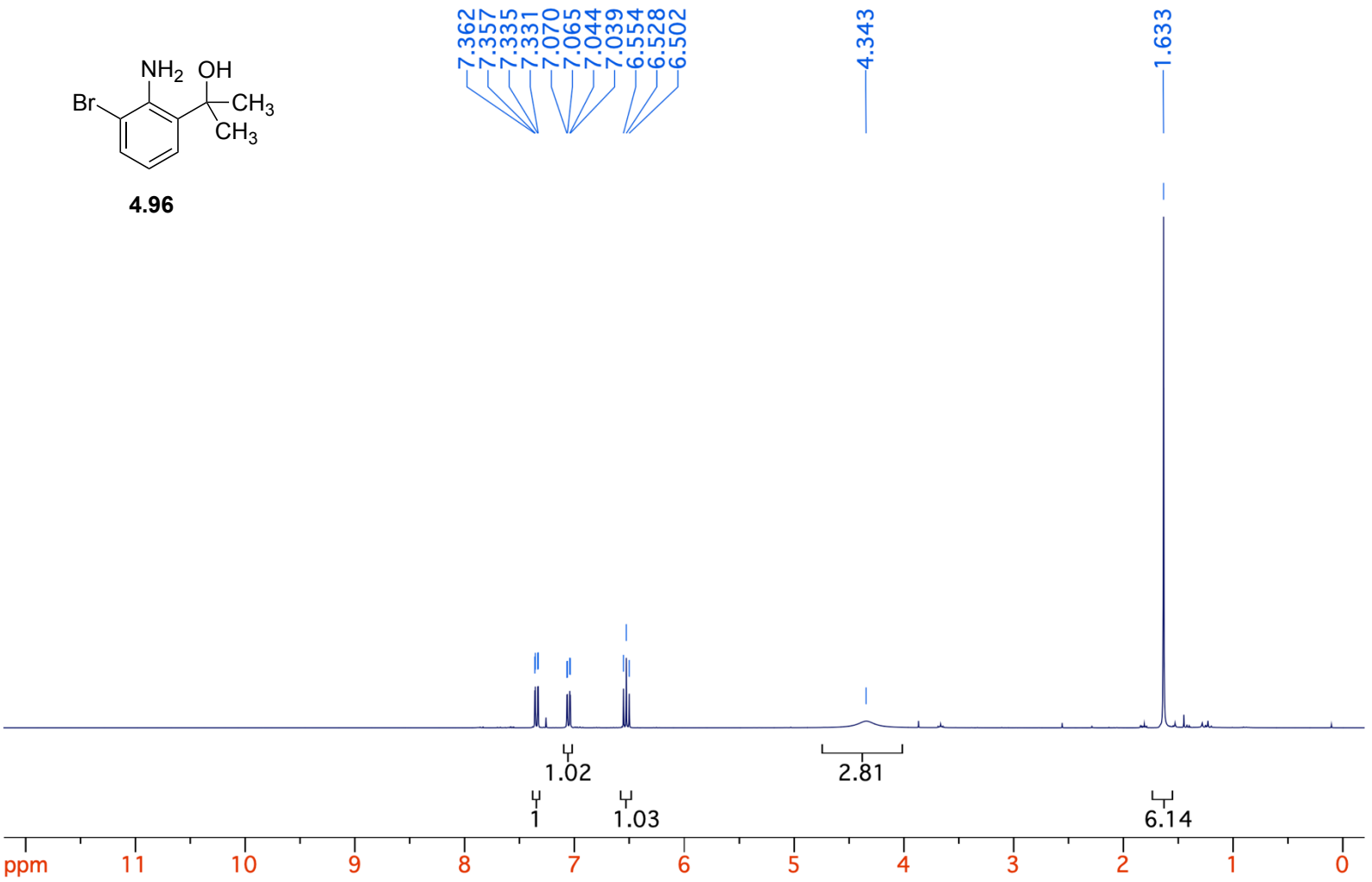


Figure B-6. ^{13}C-NMR (75 MHz, $CDCl_3$) of 2-(2-amino-3-bromophenyl)propan-2-ol (**4.96**):

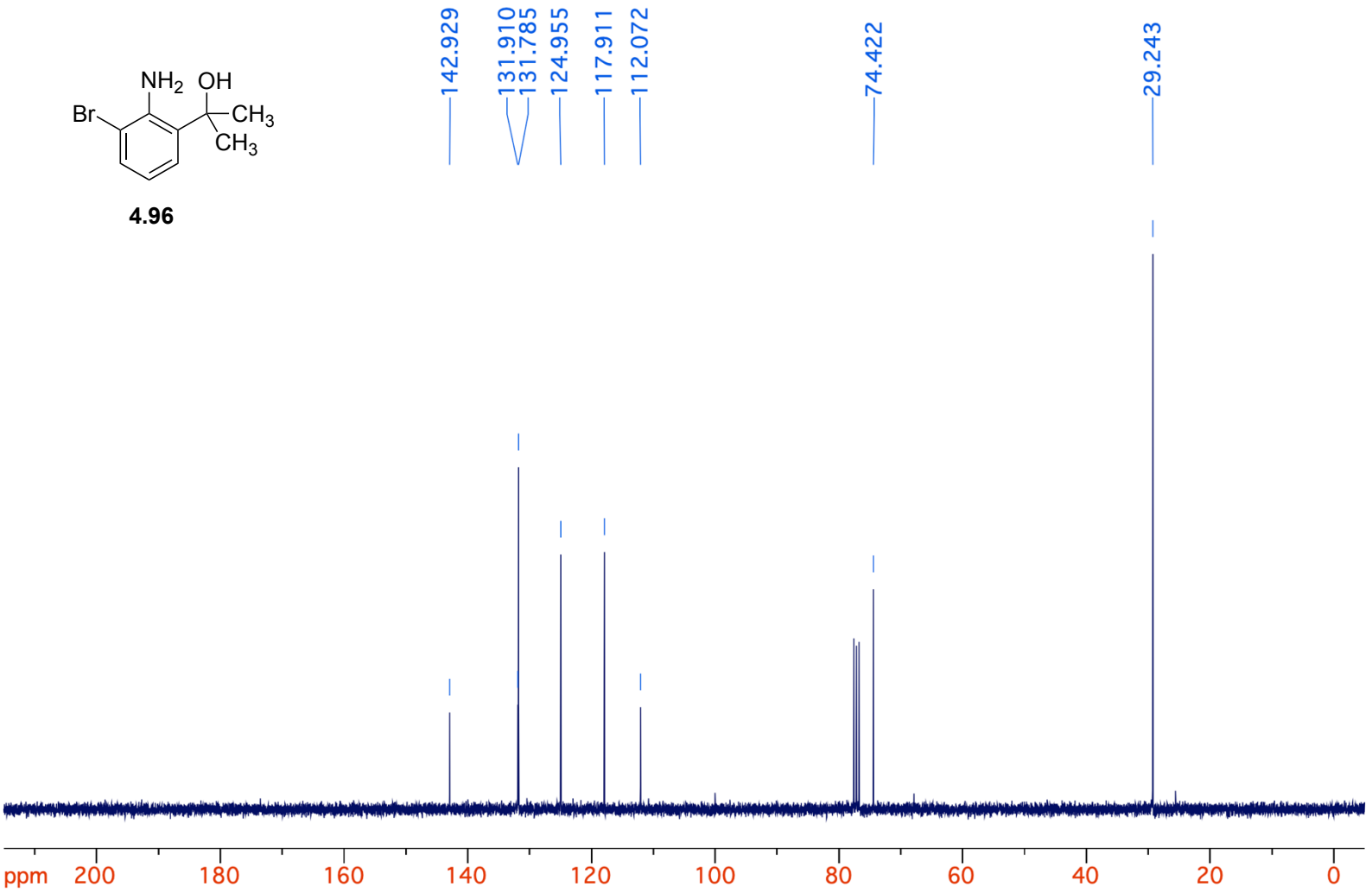


Figure B-7. ^{1}H-NMR (300 MHz, $CDCl_3$) of 2-(3-bromo-2-iodophenyl)propan-2-ol (**4.97**):

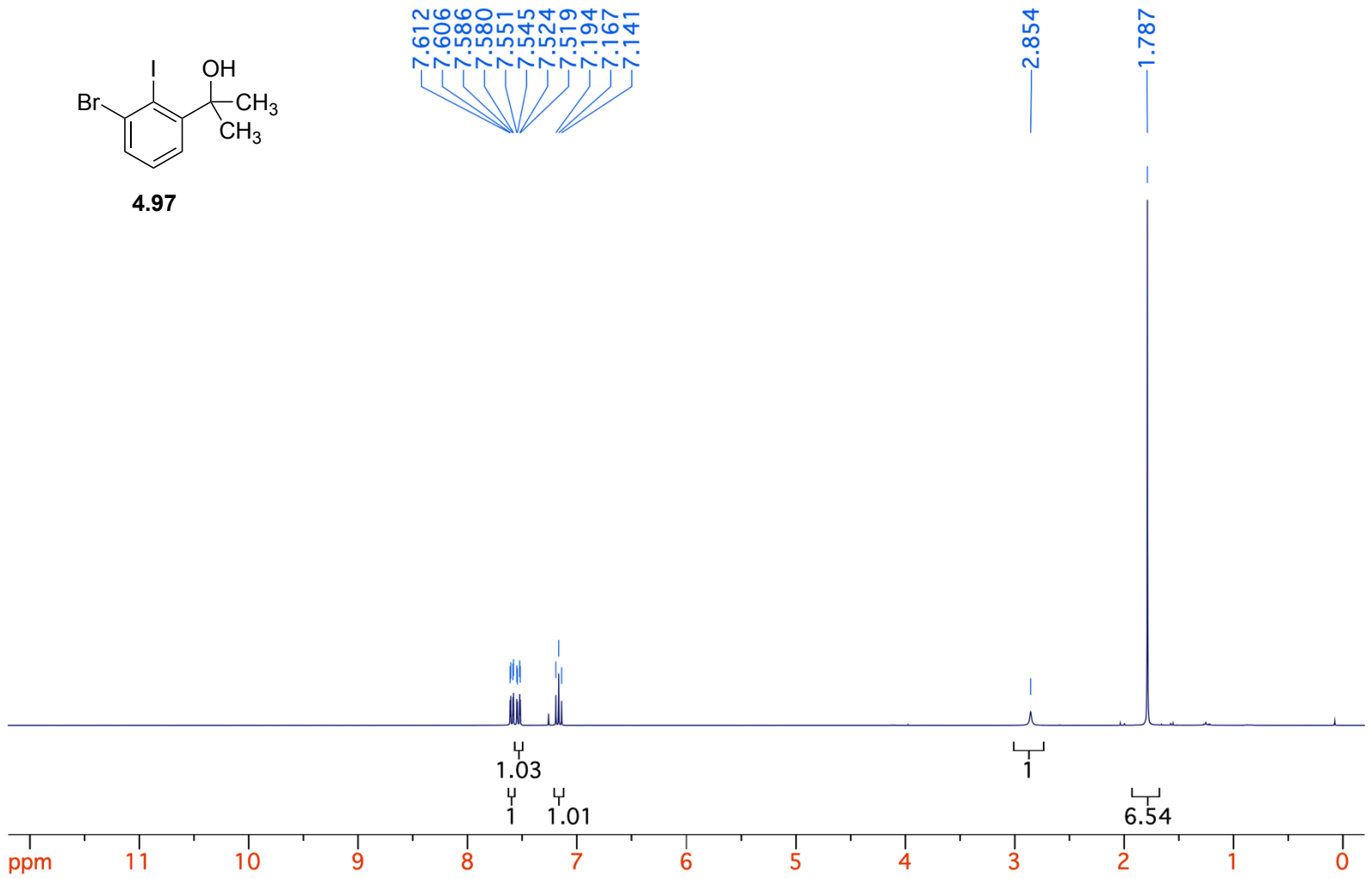


Figure B-8. ^{13}C-NMR (75 MHz, $CDCl_3$) of 2-(3-bromo-2-iodophenyl)propan-2-ol (**4.97**):

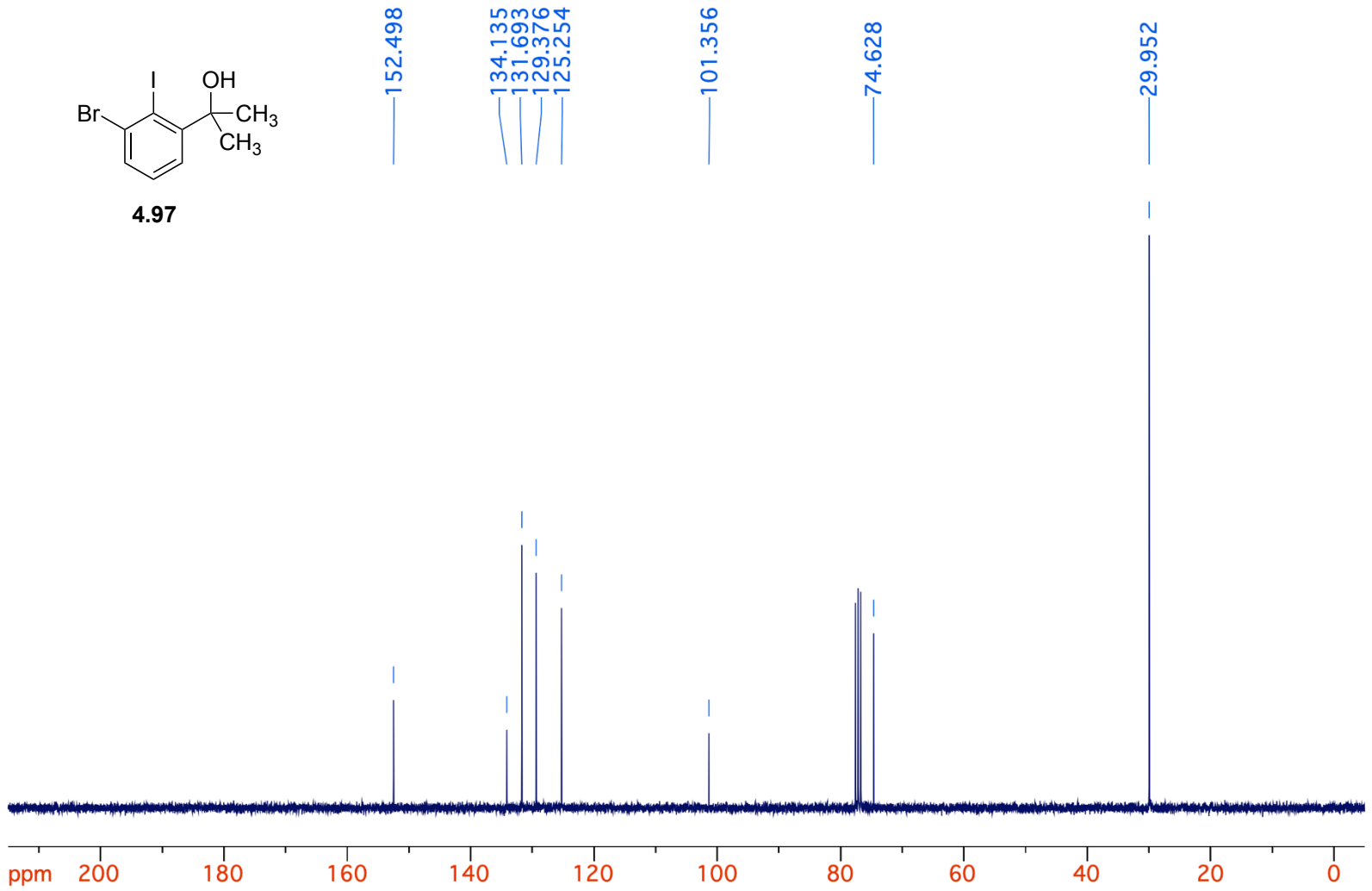


Figure B-9. ^{1}H-NMR (300 MHz, $CDCl_3$) of 2-(3-isopropoxyphenyl)propan-2-ol (**4.106**):

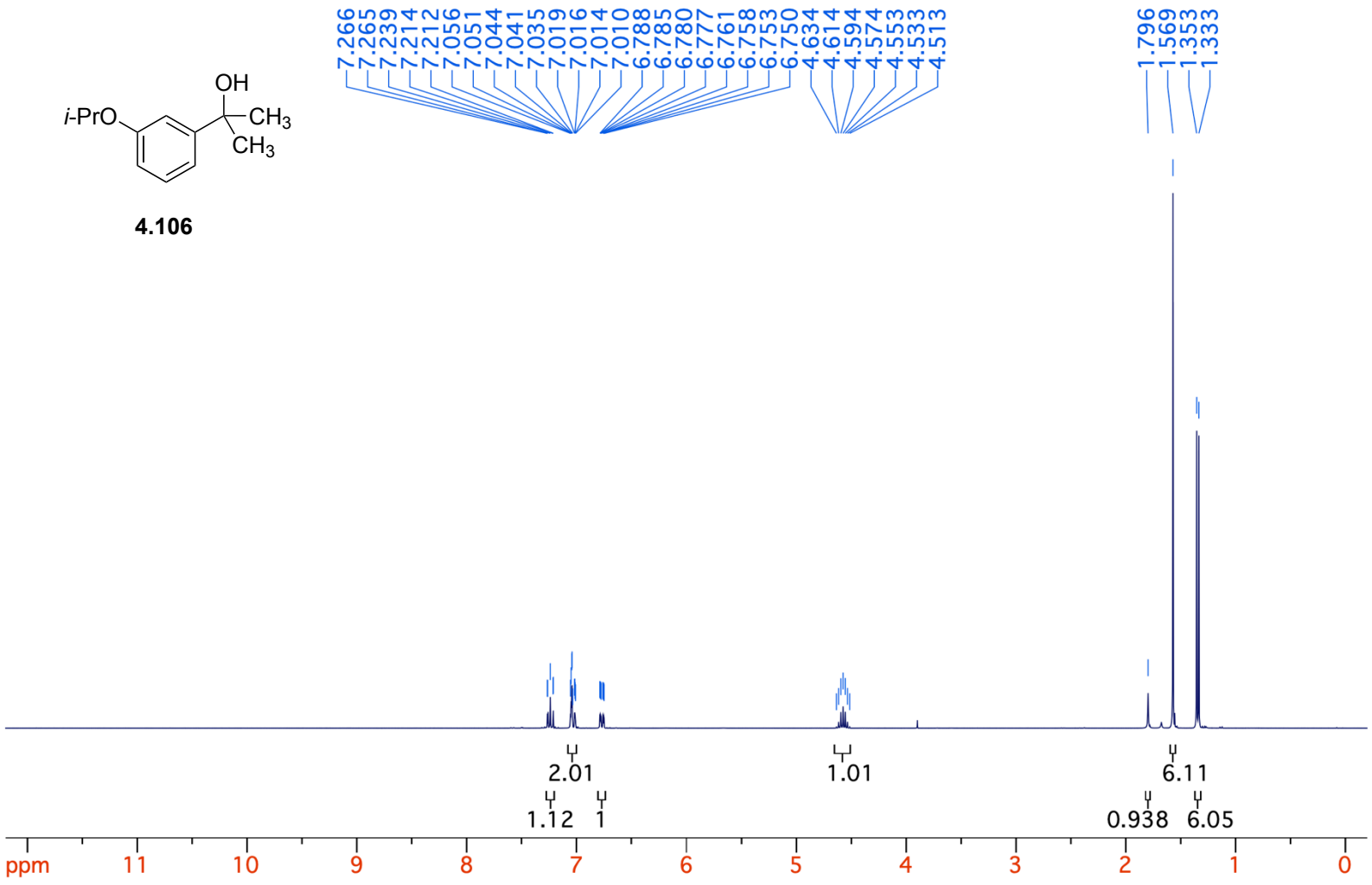


Figure B-10. ^{13}C-NMR (75 MHz, $CDCl_3$) of 2-(3-isopropoxyphenyl)propan-2-ol (**4.106**):

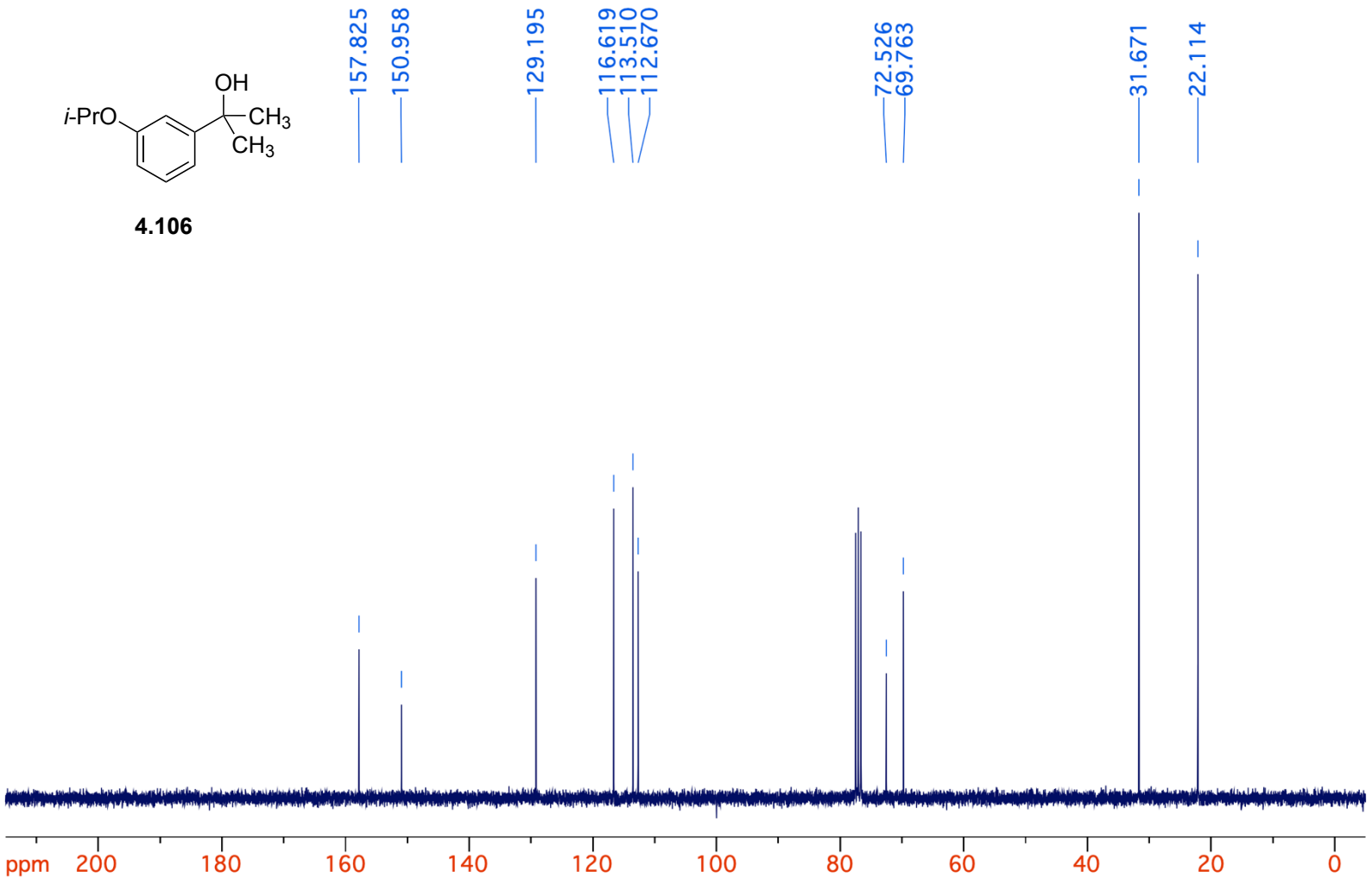


Figure B-11. ^{1}H-NMR (300 MHz, $CDCl_3$) of 2-(2-iodo-3-methoxyphenyl)propan-2-ol (**4.107**):

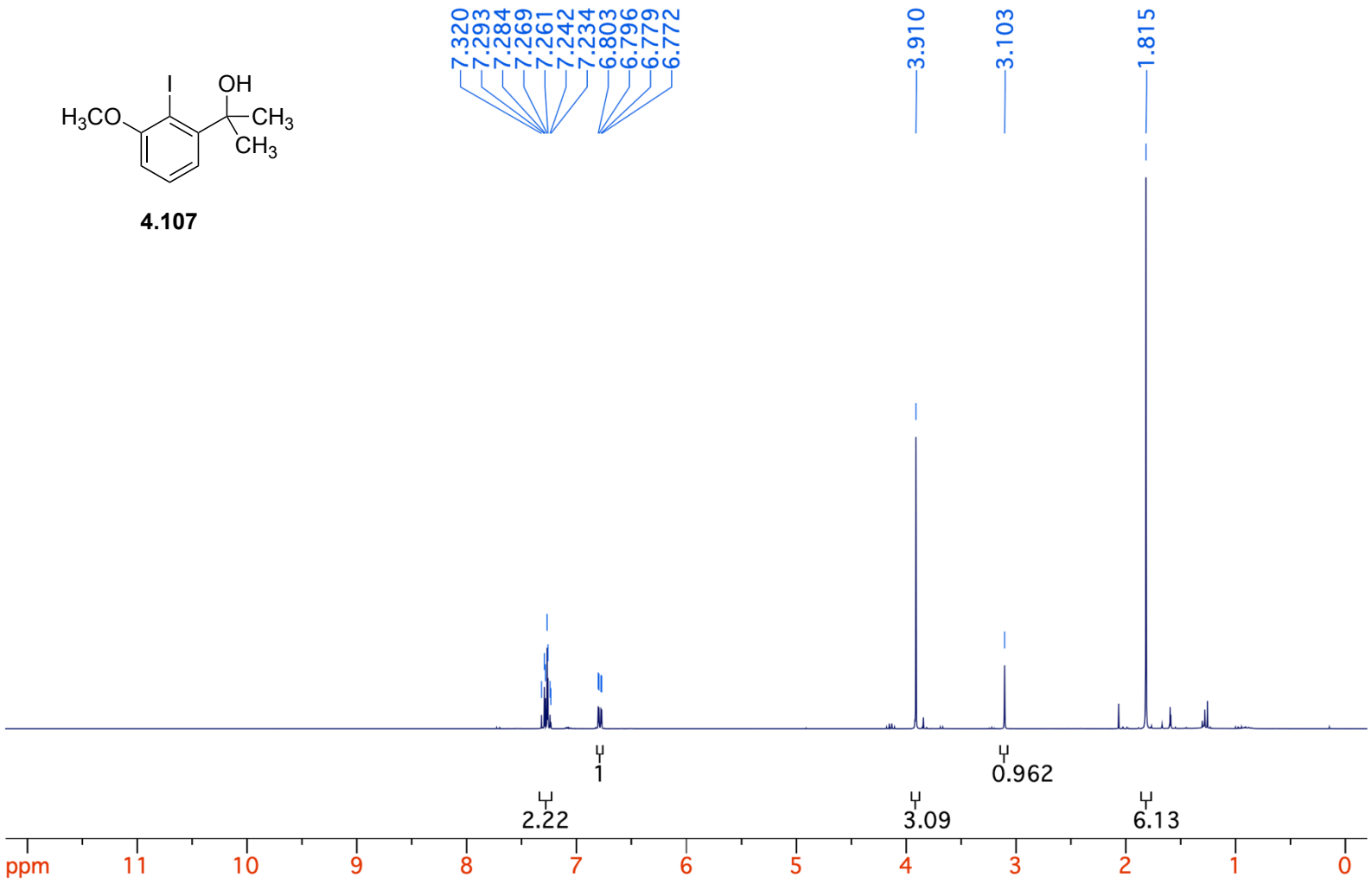


Figure B-12. ^{13}C-NMR (75 MHz, $CDCl_3$) of 2-(2-iodo-3-methoxyphenyl)propan-2-ol (**4.107**):

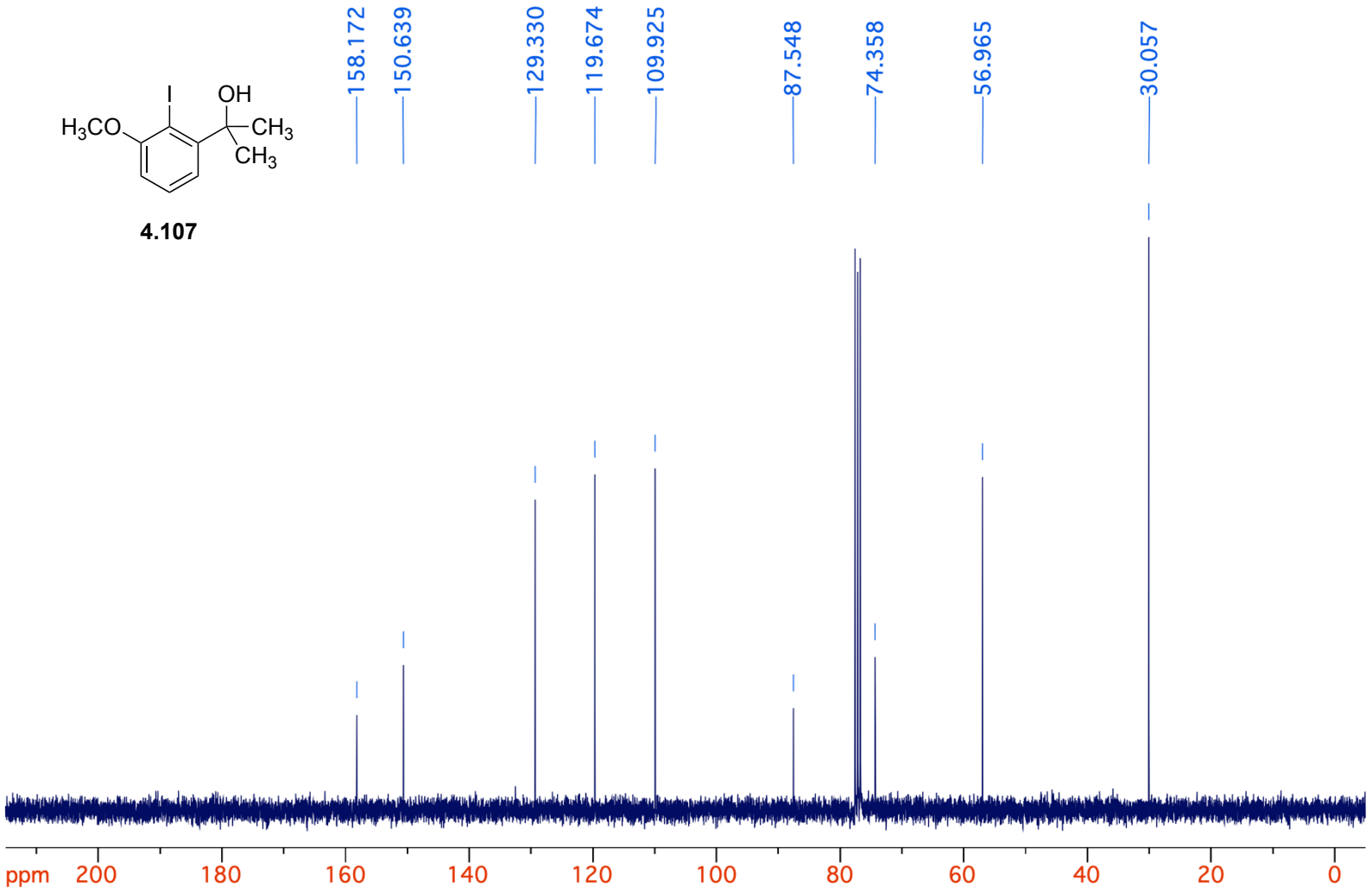


Figure B-13. ^{1}H-NMR (300 MHz, $CDCl_3$) of 2-(2-iodo-3-isopropoxyphenyl)propan-2-ol (**4.108**):

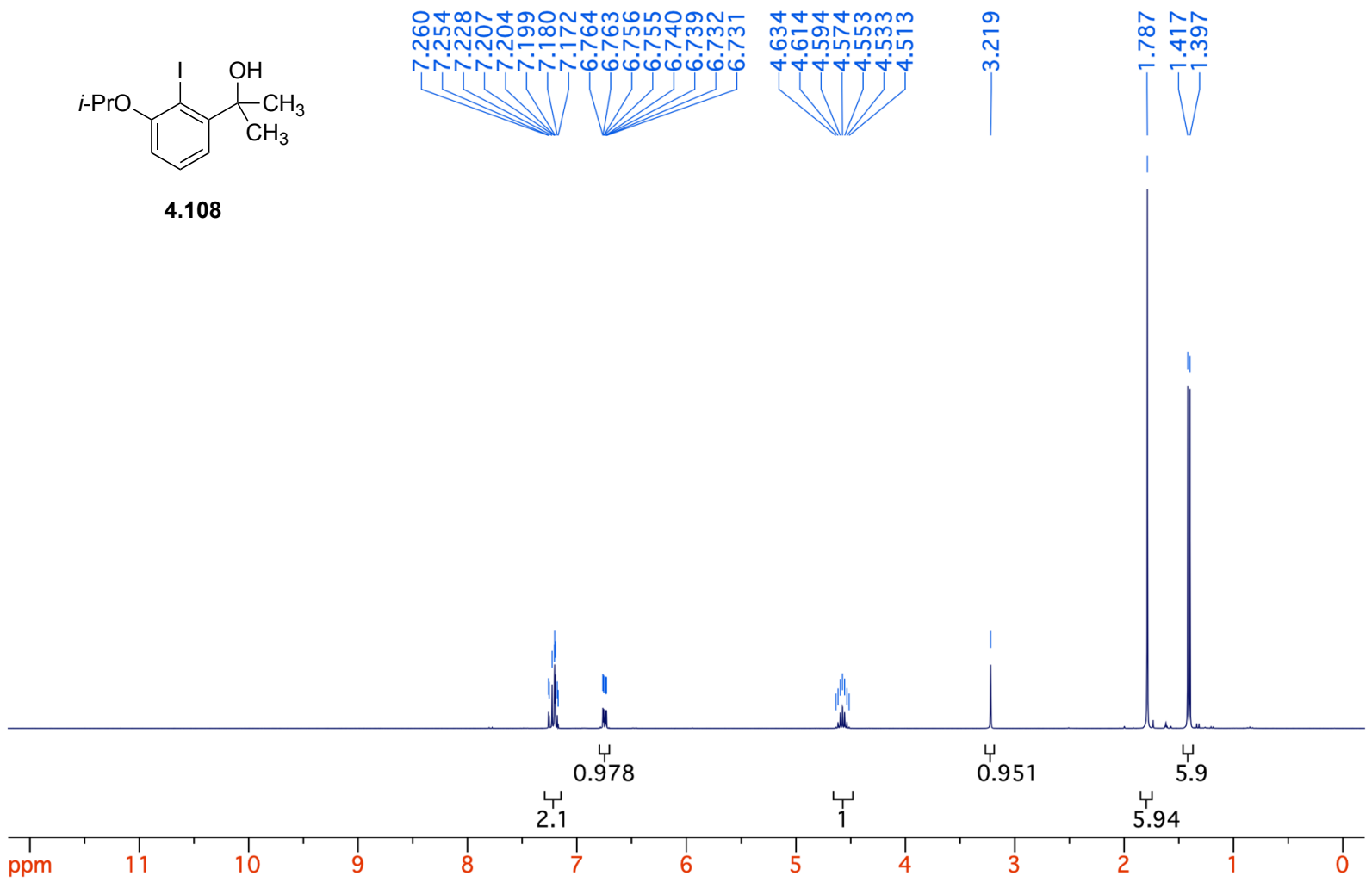


Figure B-14. ^{13}C-NMR (75 MHz, $CDCl_3$) of 2-(2-iodo-3-isopropoxyphenyl)propan-2-ol (**4.108**):

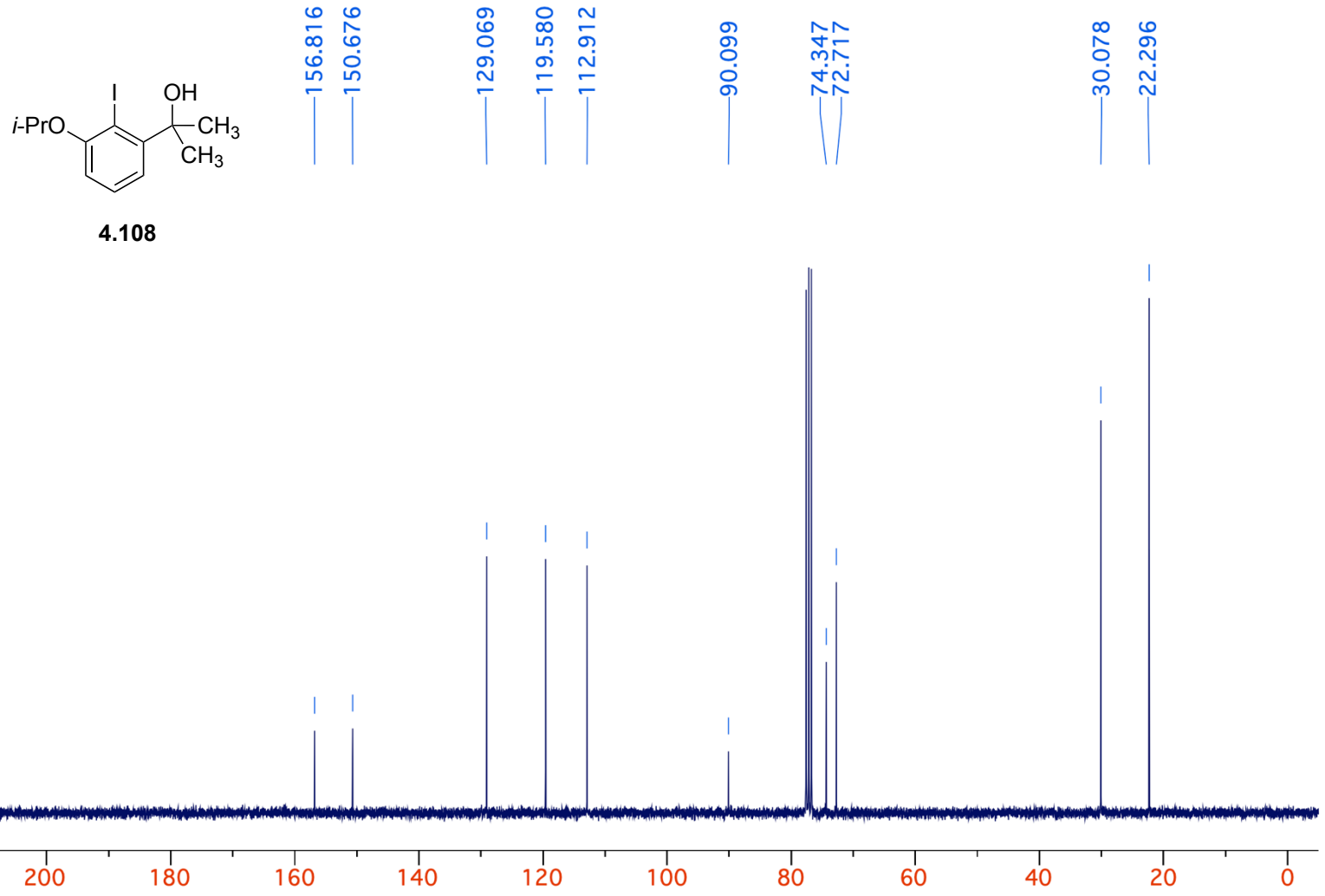


Figure B-15. ^{1}H-NMR (300 MHz, $CDCl_3$) of 2-iodo-3-isopropylbenzoic acid (**B1**):

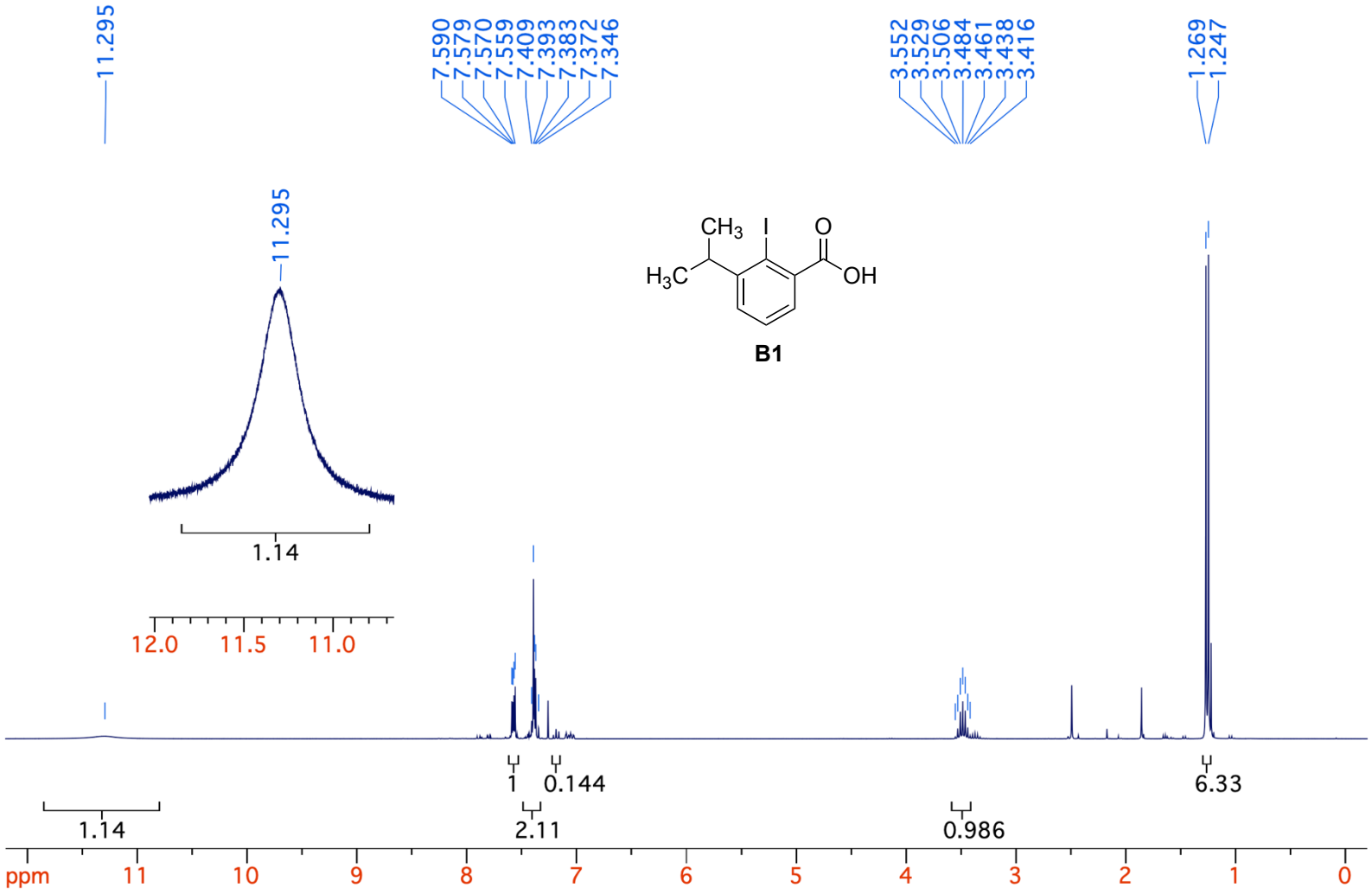


Figure B-16. ^{13}C-NMR (75 MHz, $CDCl_3$) of 2-iodo-3-isopropylbenzoic acid (**B1**):

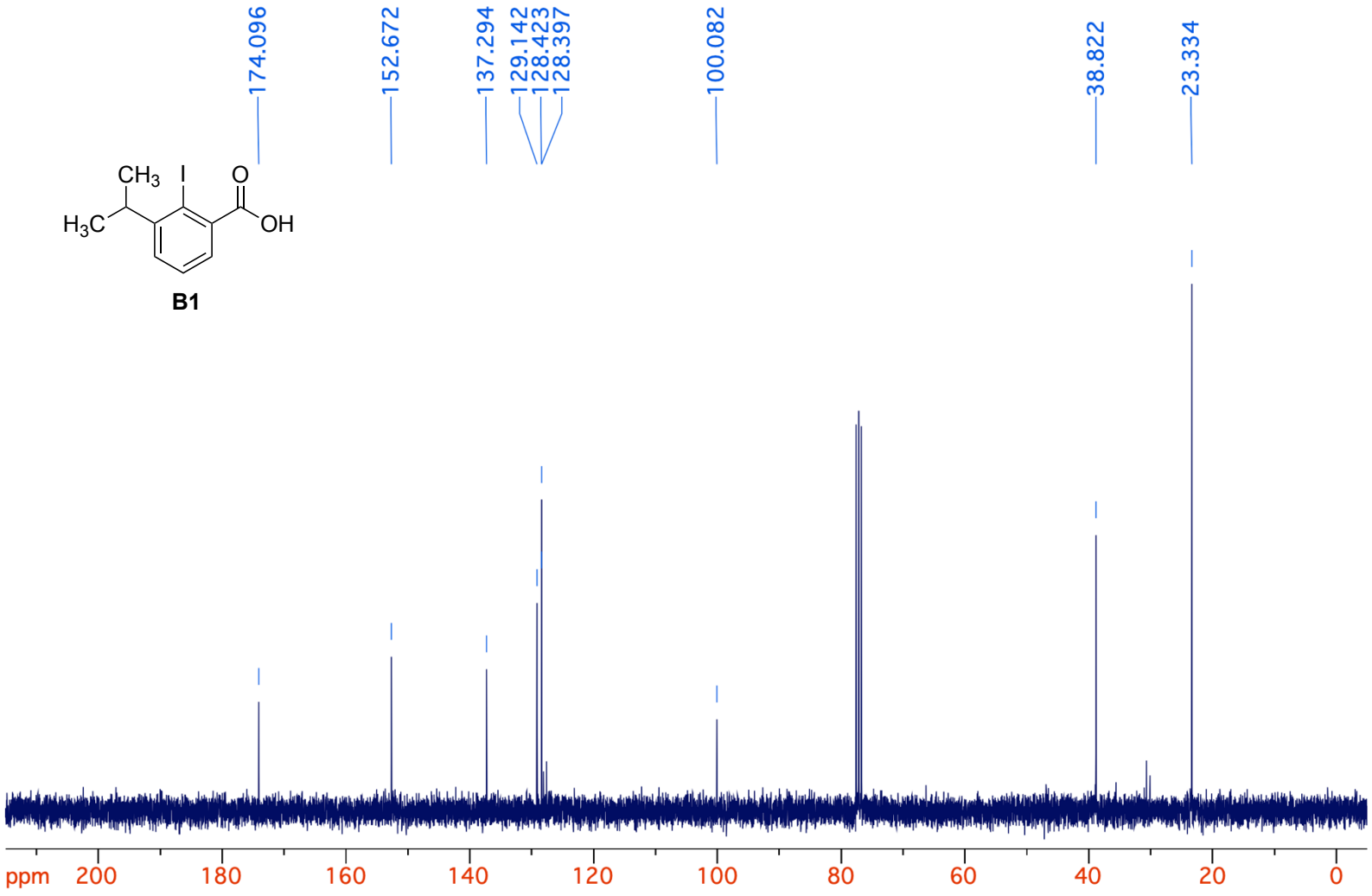


Figure B-17. ^{1}H-NMR (300 MHz, $CDCl_3$) of methyl 2-iodo-3-isopropylbenzoate (**4.111**):

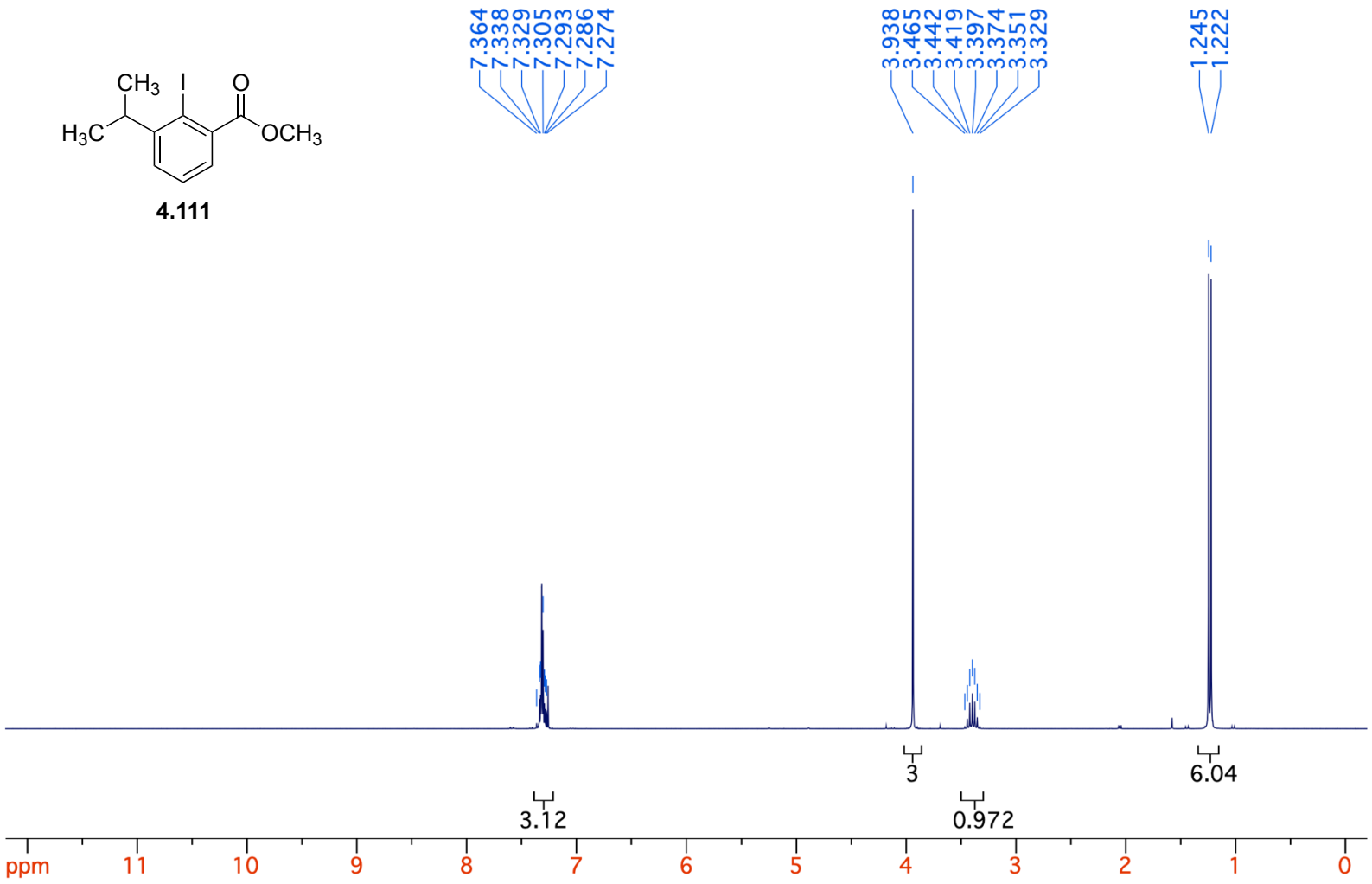


Figure B-18. ^{13}C-NMR (75 MHz, $CDCl_3$) of methyl 2-iodo-3-isopropylbenzoate (**4.111**):

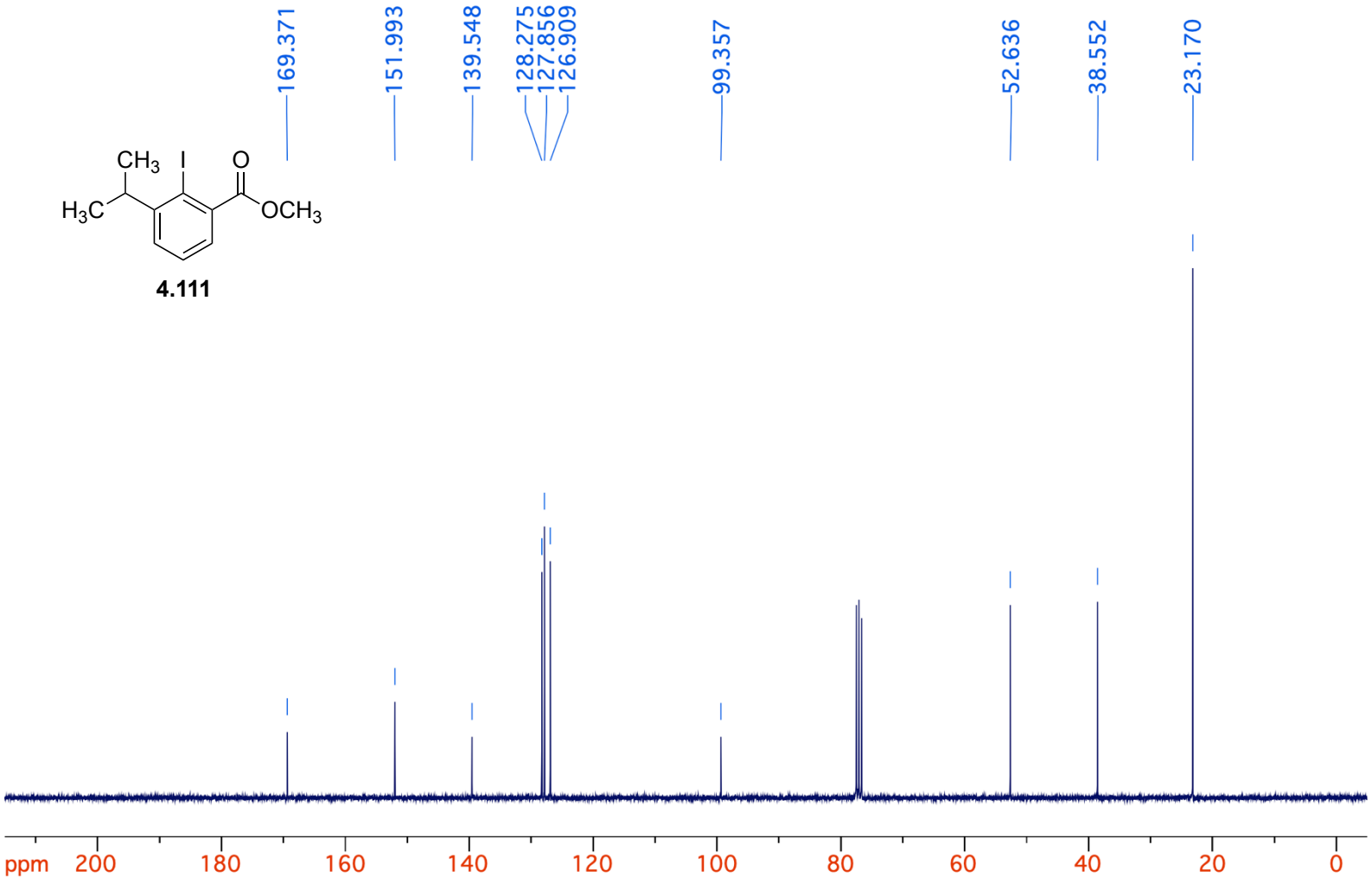


Figure B-19. ^{1}H-NMR (300 MHz, $CDCl_3$) of 2-(2-iodo-3-isopropylphenyl)propan-2-ol (**4.112**):

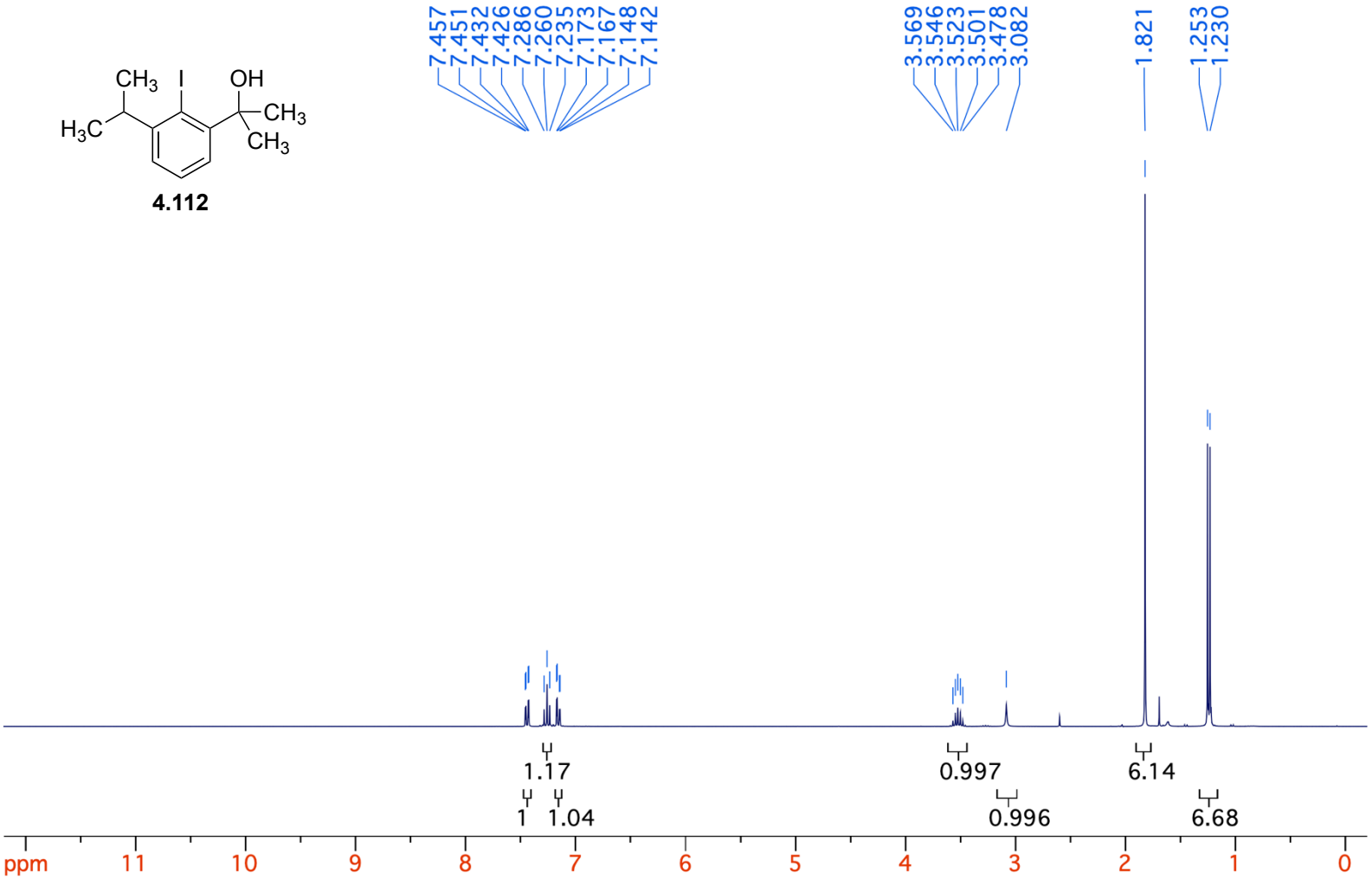


Figure B-20. ^{13}C-NMR (75 MHz, $CDCl_3$) of 2-(2-iodo-3-isopropylphenyl)propan-2-ol (**4.112**):

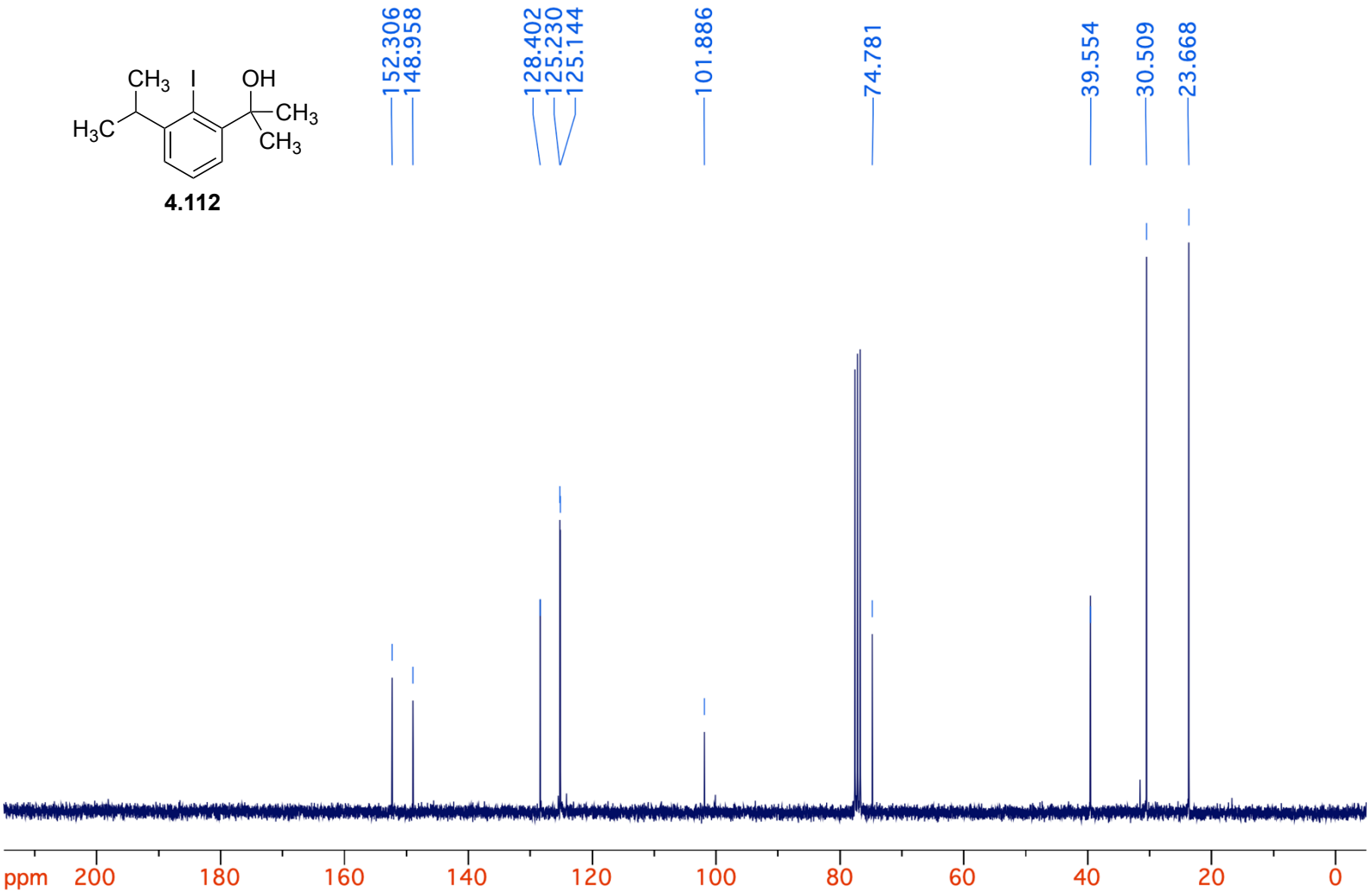


Figure B-21. ^{1}H-NMR (300 MHz, $CDCl_3$) of 1-(2-amino-3-(*tert*-butyl)phenyl)ethan-1-one (**4.127**):

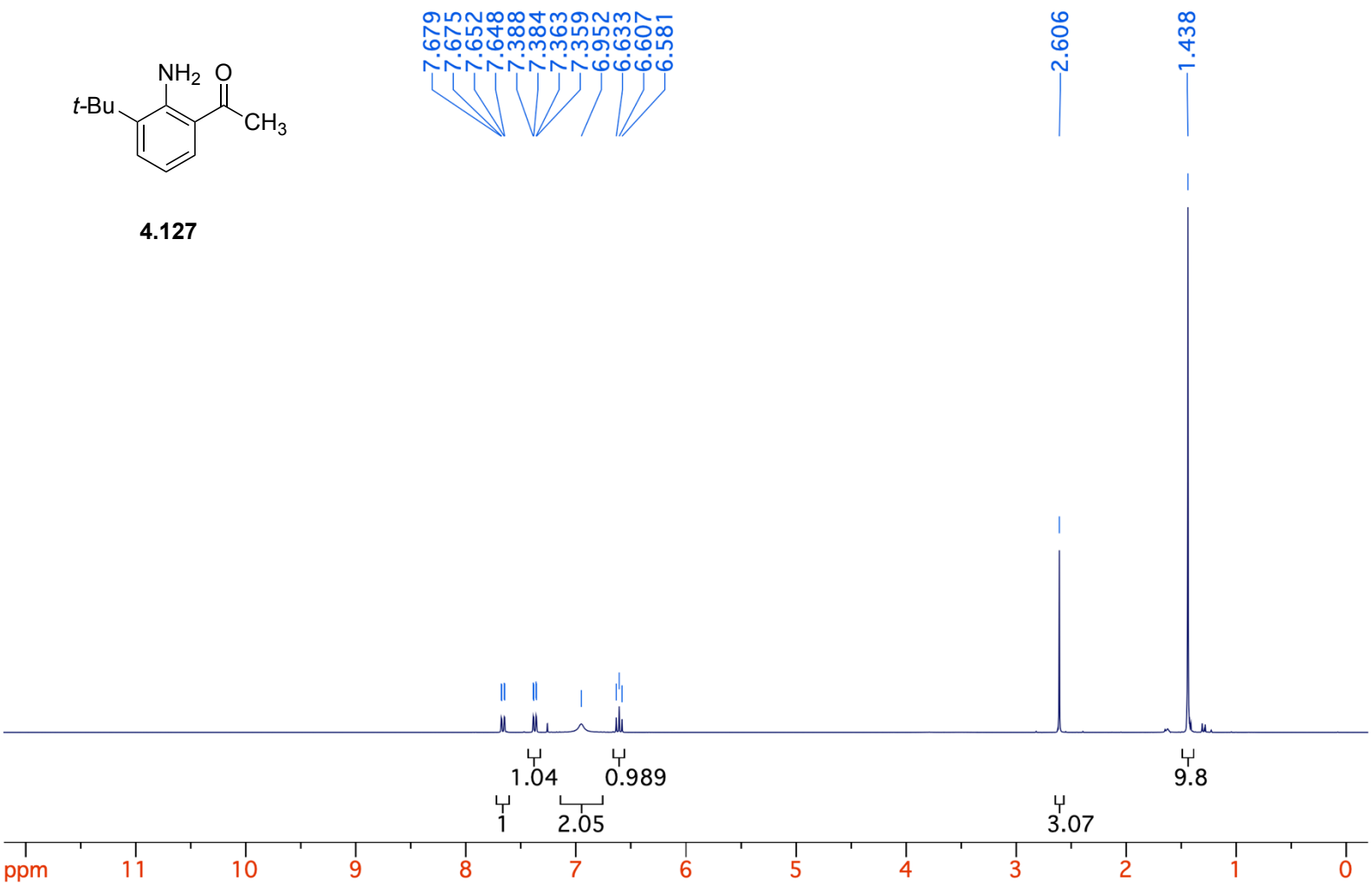


Figure B-22. ^{13}C-NMR (75 MHz, $CDCl_3$) of 1-(2-amino-3-(*tert*-butyl)phenyl)ethan-1-one (**4.127**):

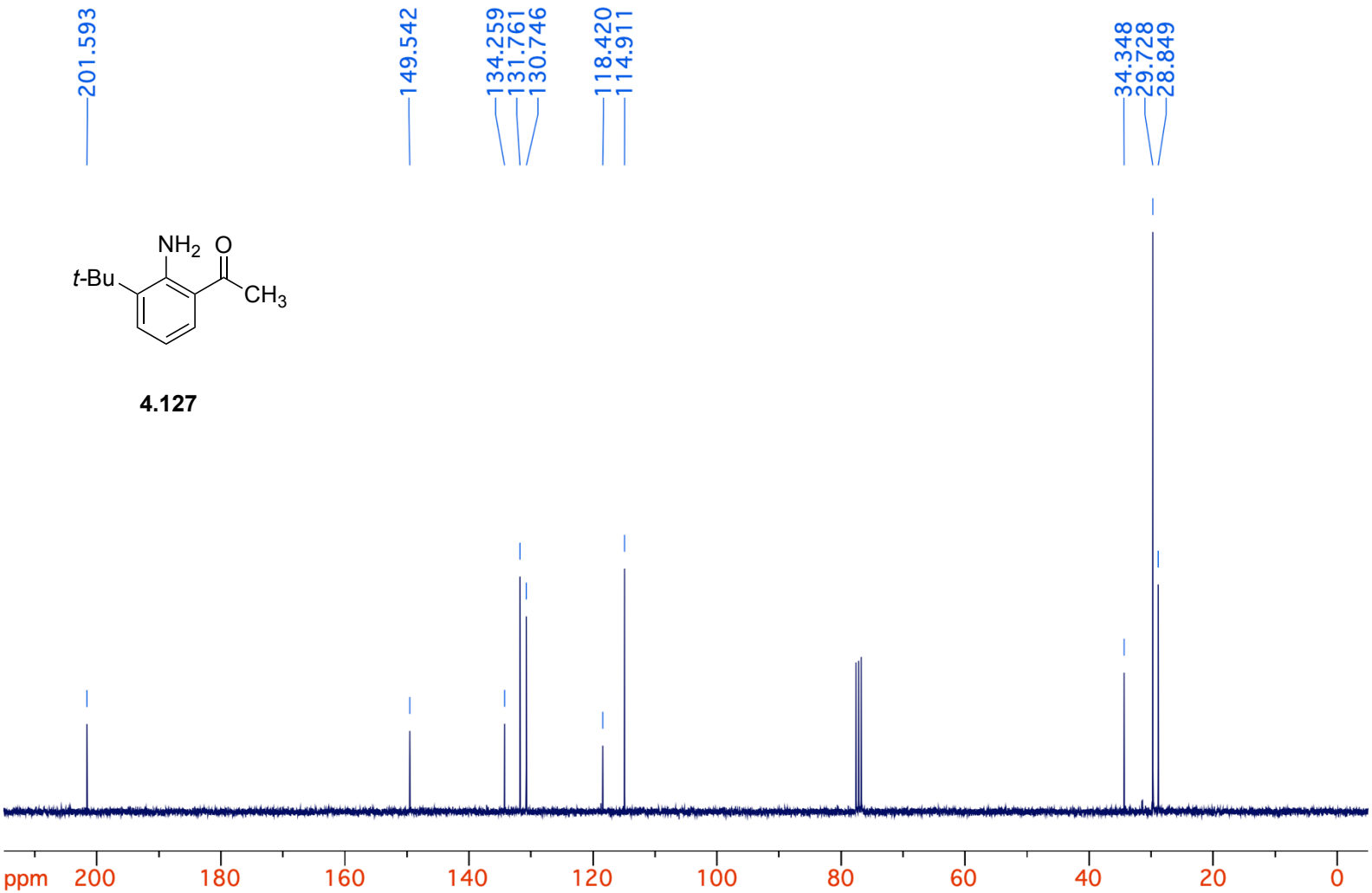


Figure B-23. ^{1}H-NMR (300 MHz, $CDCl_3$) of 1-(2,5-dibromo-3-(*tert*-butyl)phenyl)ethan-1-one (**4.131**):

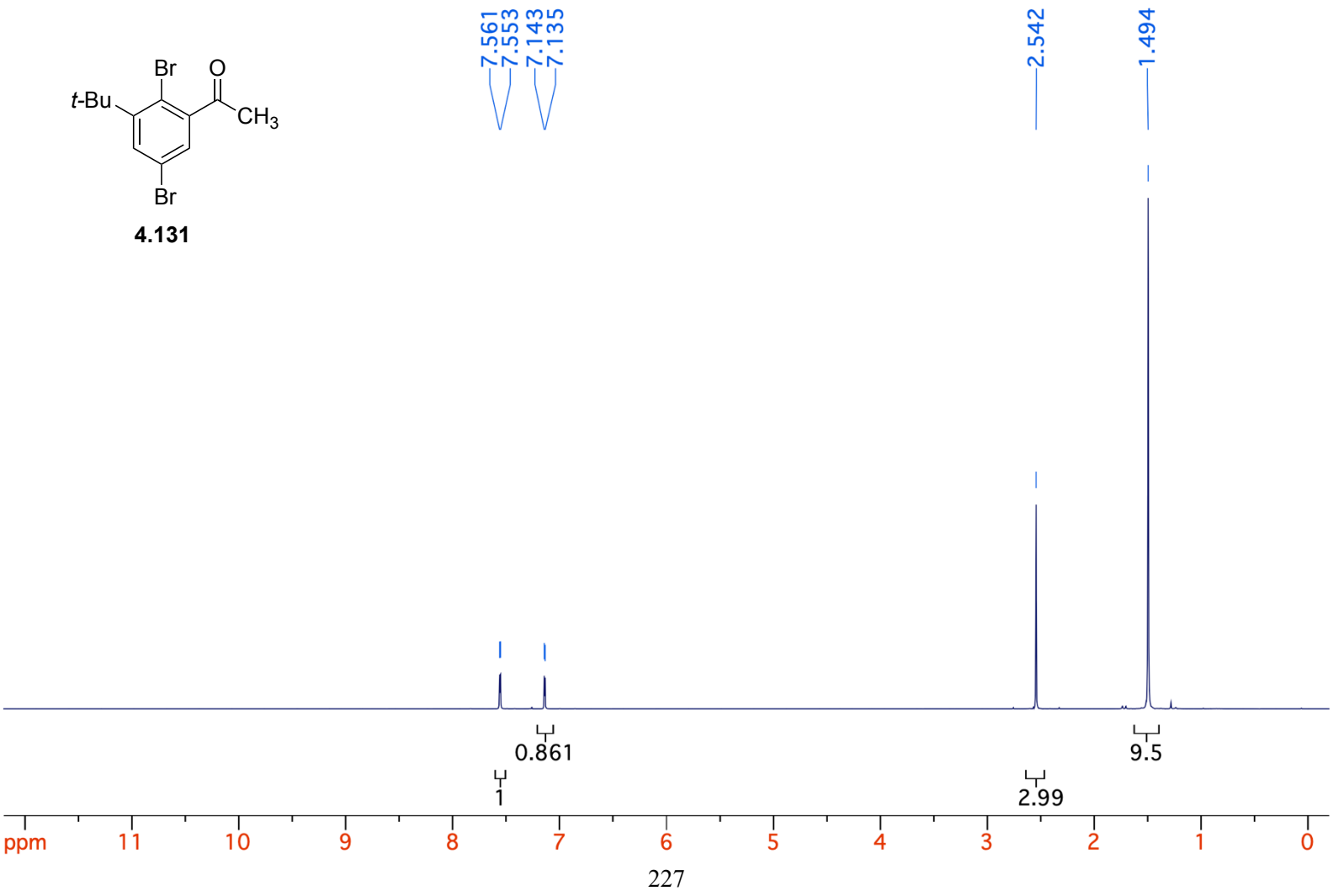


Figure B-24. ^{13}C-NMR (75 MHz, $CDCl_3$) of 1-(2,5-dibromo-3-(*tert*-butyl)phenyl)ethan-1-one (**4.131**):

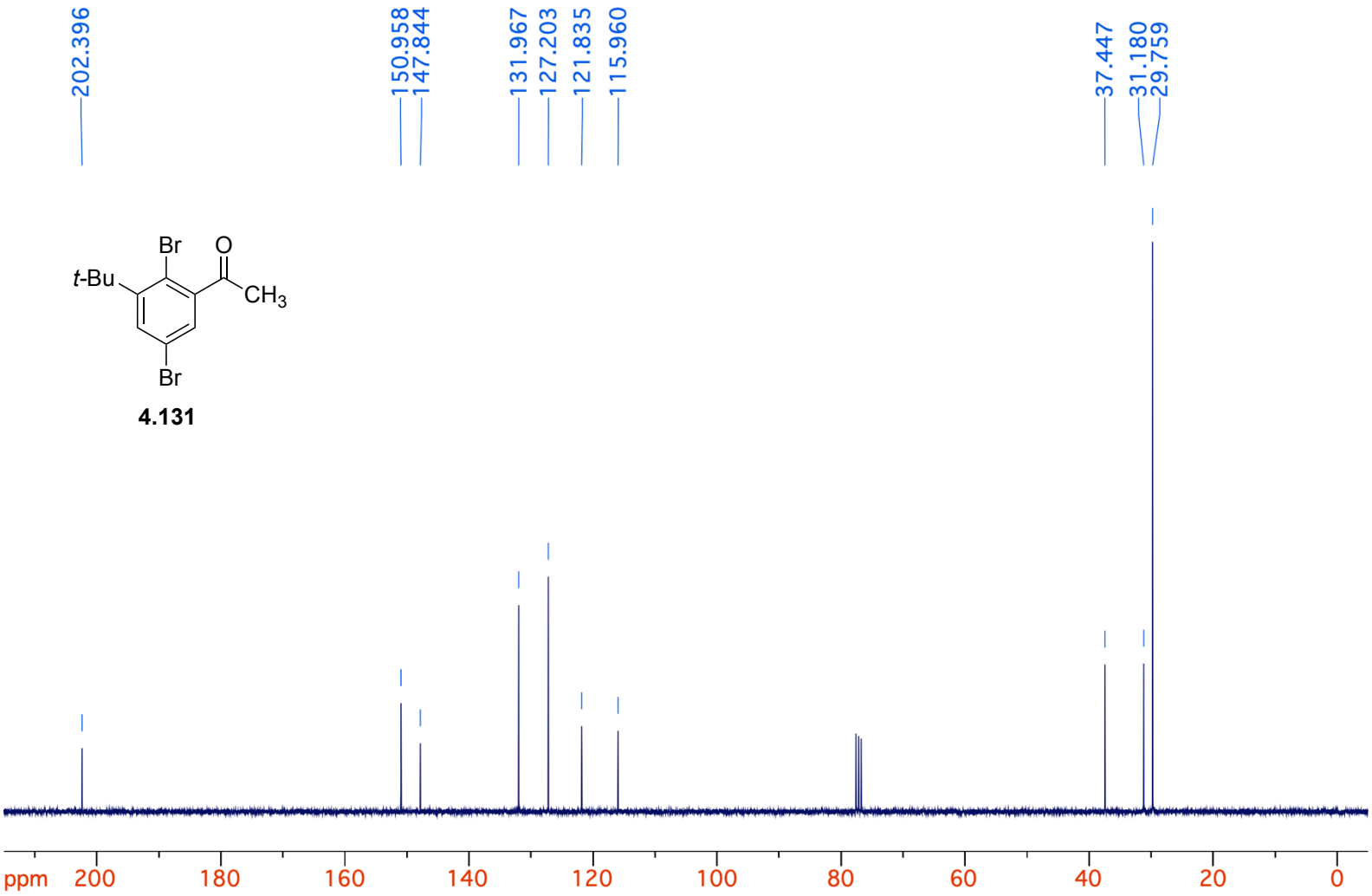


Figure B-25. ^{1}H-NMR (300 MHz, $CDCl_3$) of 2-(2,5-dibromo-3-(*tert*-butyl)phenyl)propan-2-ol (**4.132**):

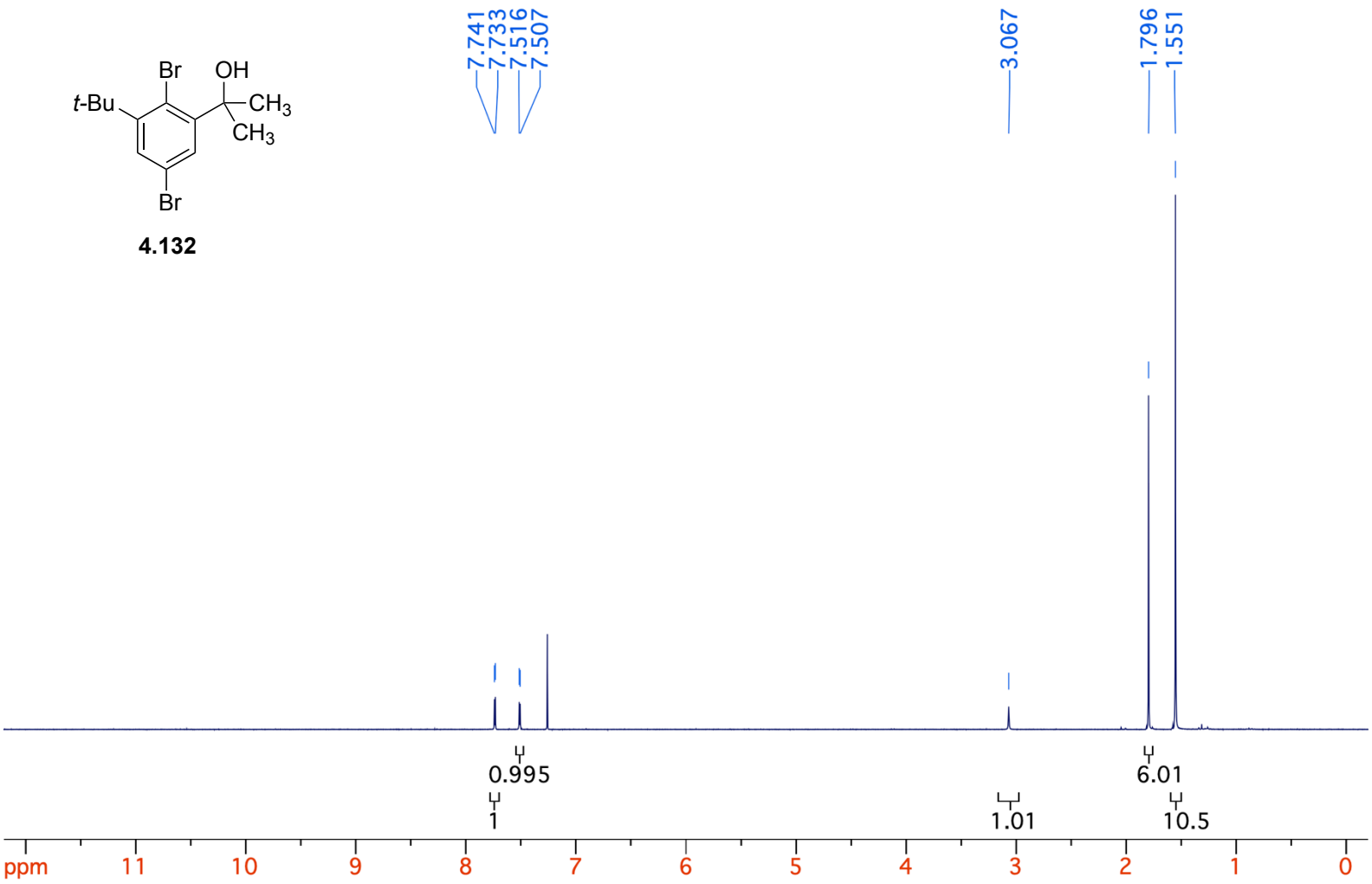


Figure B-26. ^{13}C-NMR (75 MHz, $CDCl_3$) of 2-(2,5-dibromo-3-(*tert*-butyl)phenyl)propan-2-ol (**4.132**):

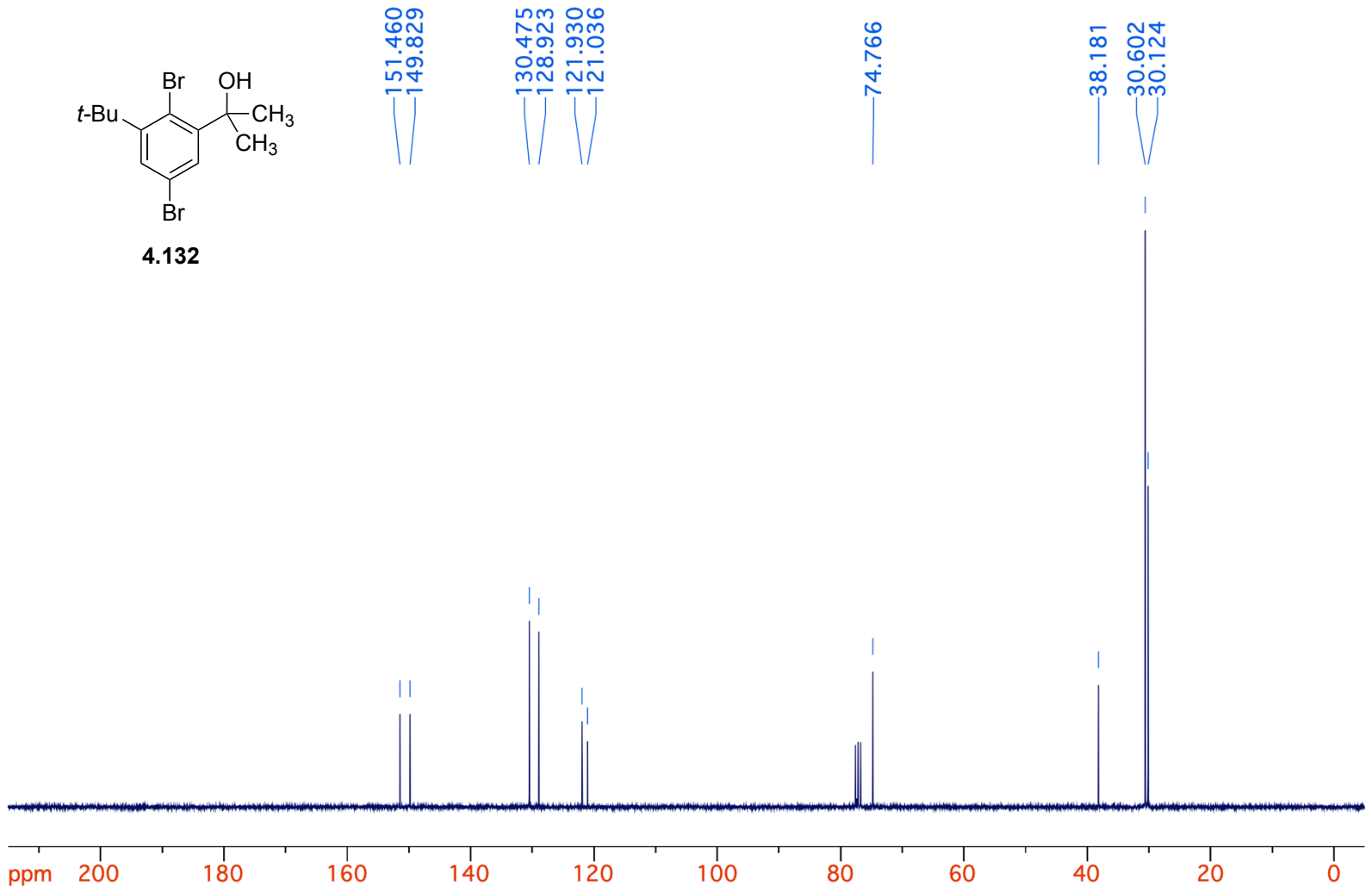


Figure B-27. ^{1}H-NMR (300 MHz, $CDCl_3$) of 2-(5-bromo-3-(*tert*-butyl)-2-iodophenyl)propan-2-ol (**4.133**):

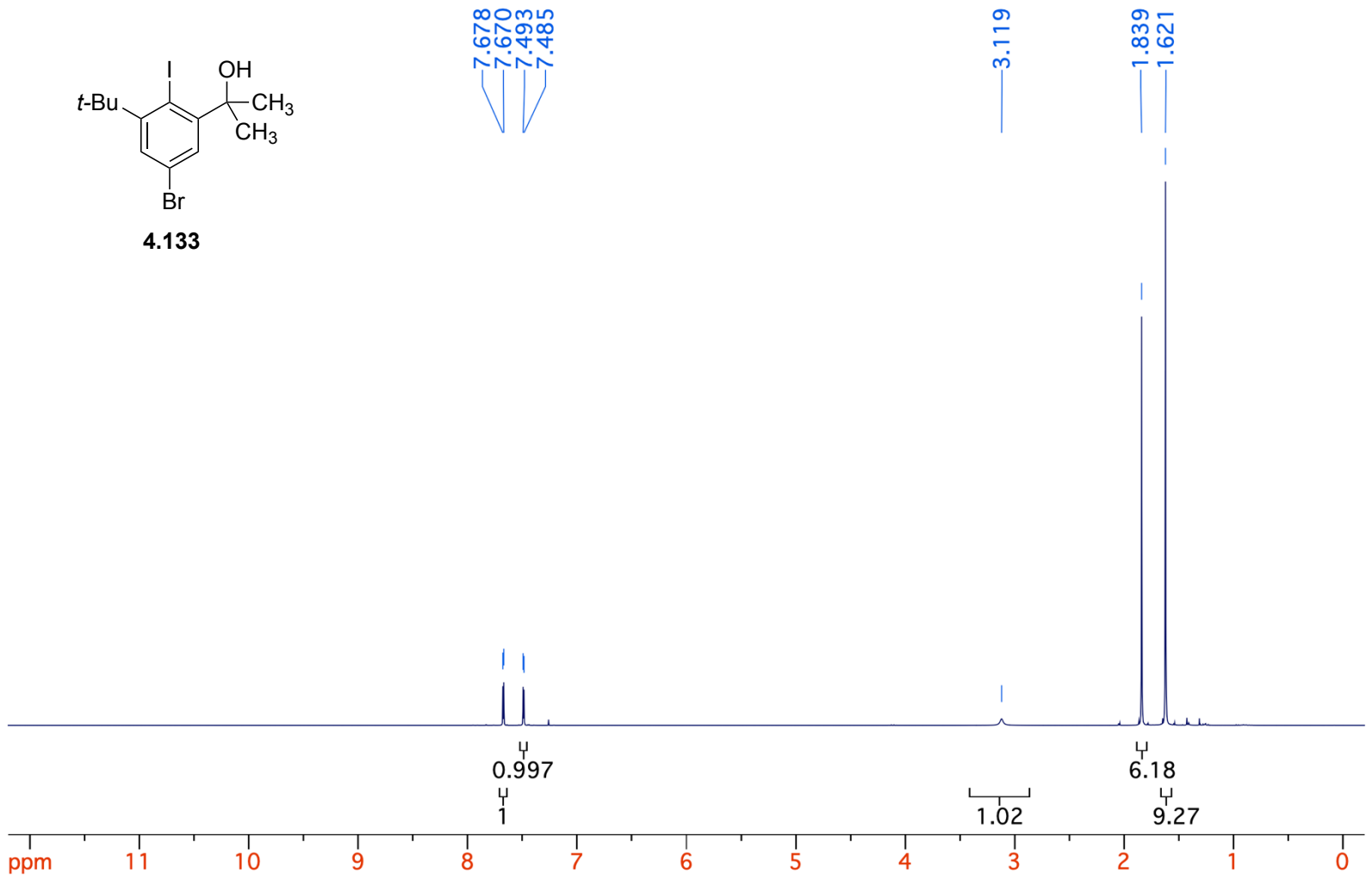


Figure B-28. ^{13}C-NMR (75 MHz, $CDCl_3$) of 2-(5-bromo-3-(*tert*-butyl)-2-iodophenyl)propan-2-ol (**4.133**):

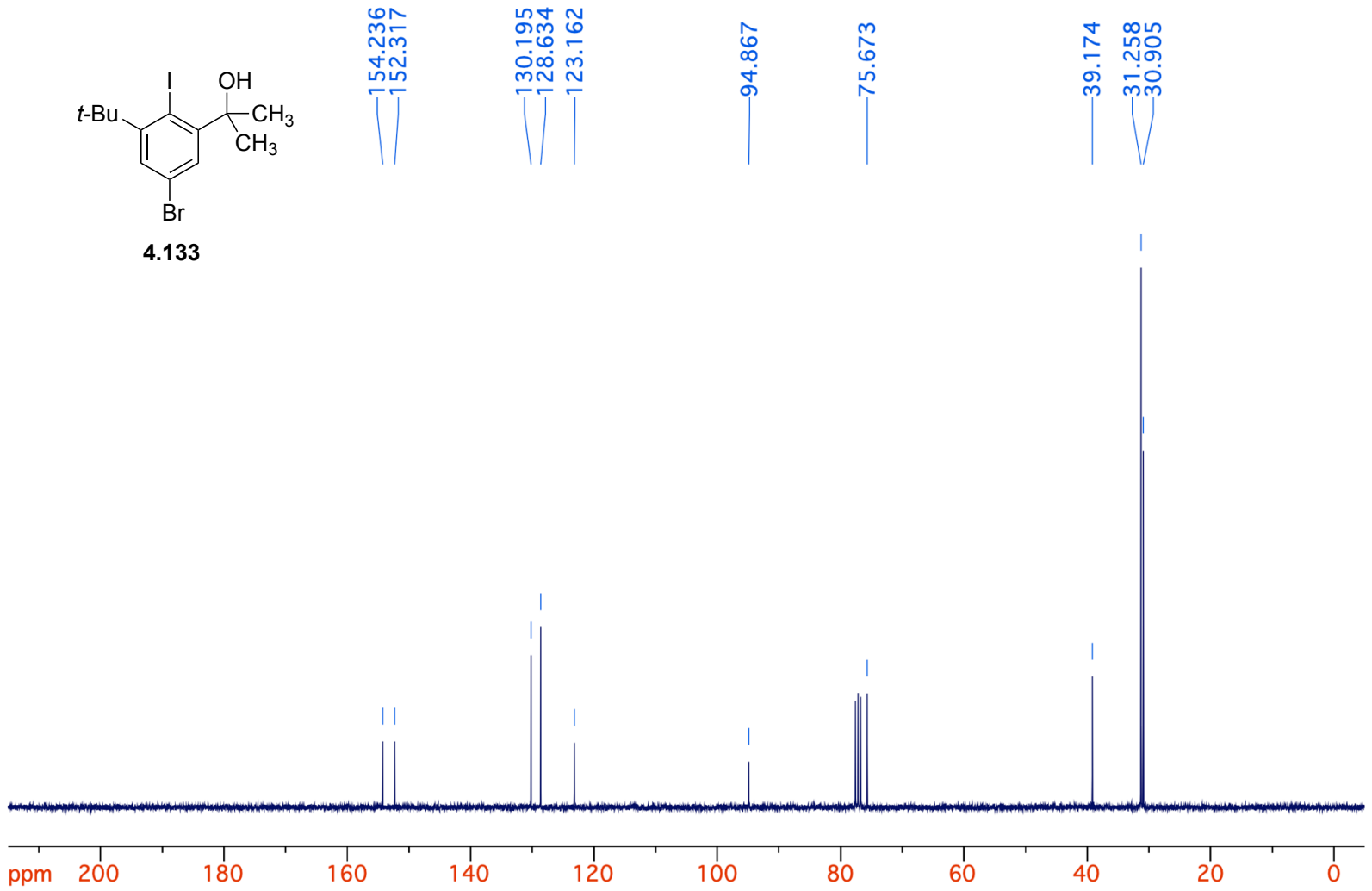


Figure B-29. ^{1}H-NMR (300 MHz, $CDCl_3$) of 2-(2-iodo-3-methylphenyl)acetic acid (**B2**):

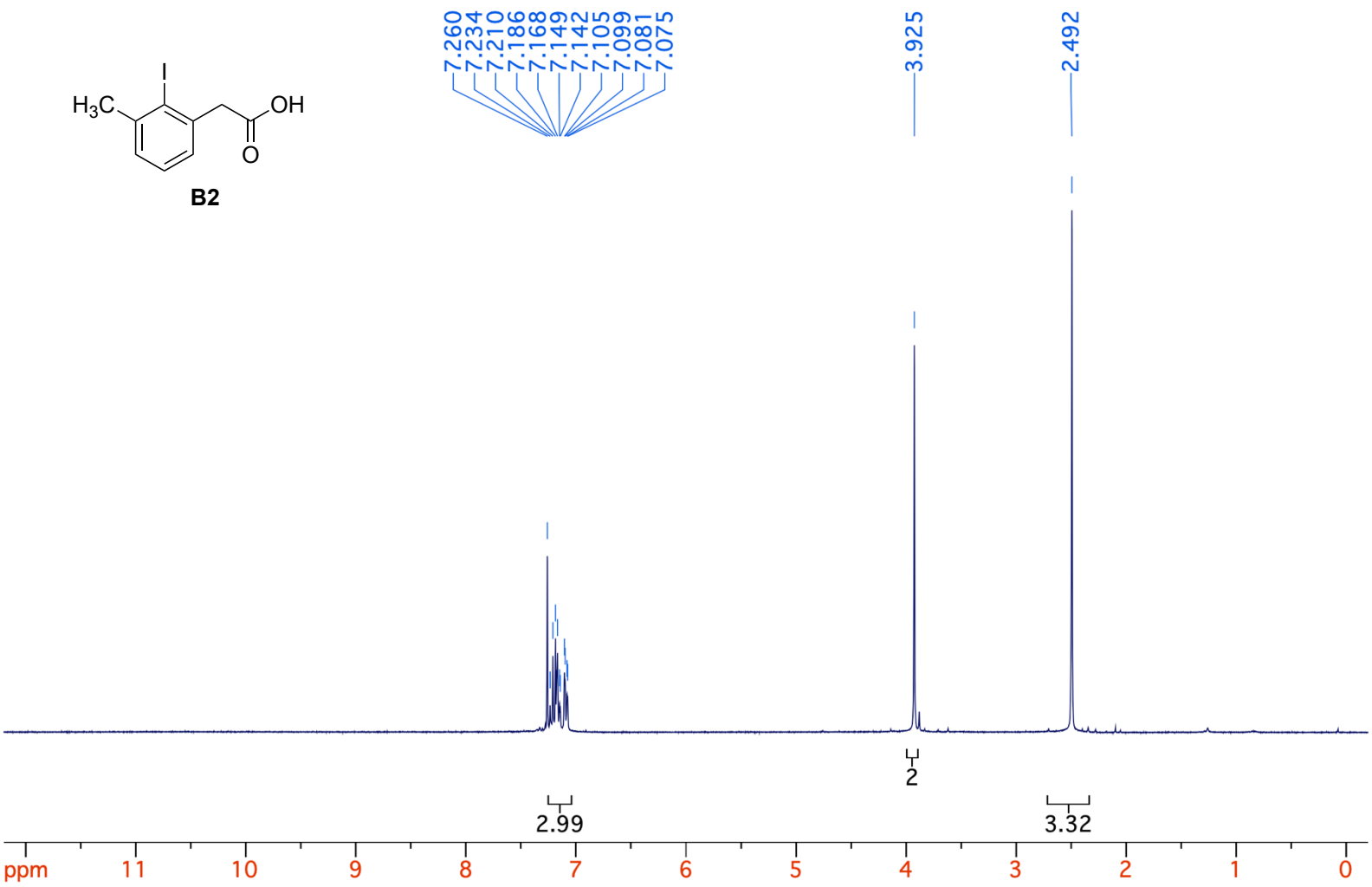


Figure B-30. ^{13}C-NMR (75 MHz, $CDCl_3$) of 2-(2-iodo-3-methylphenyl)acetic acid (**B2**):

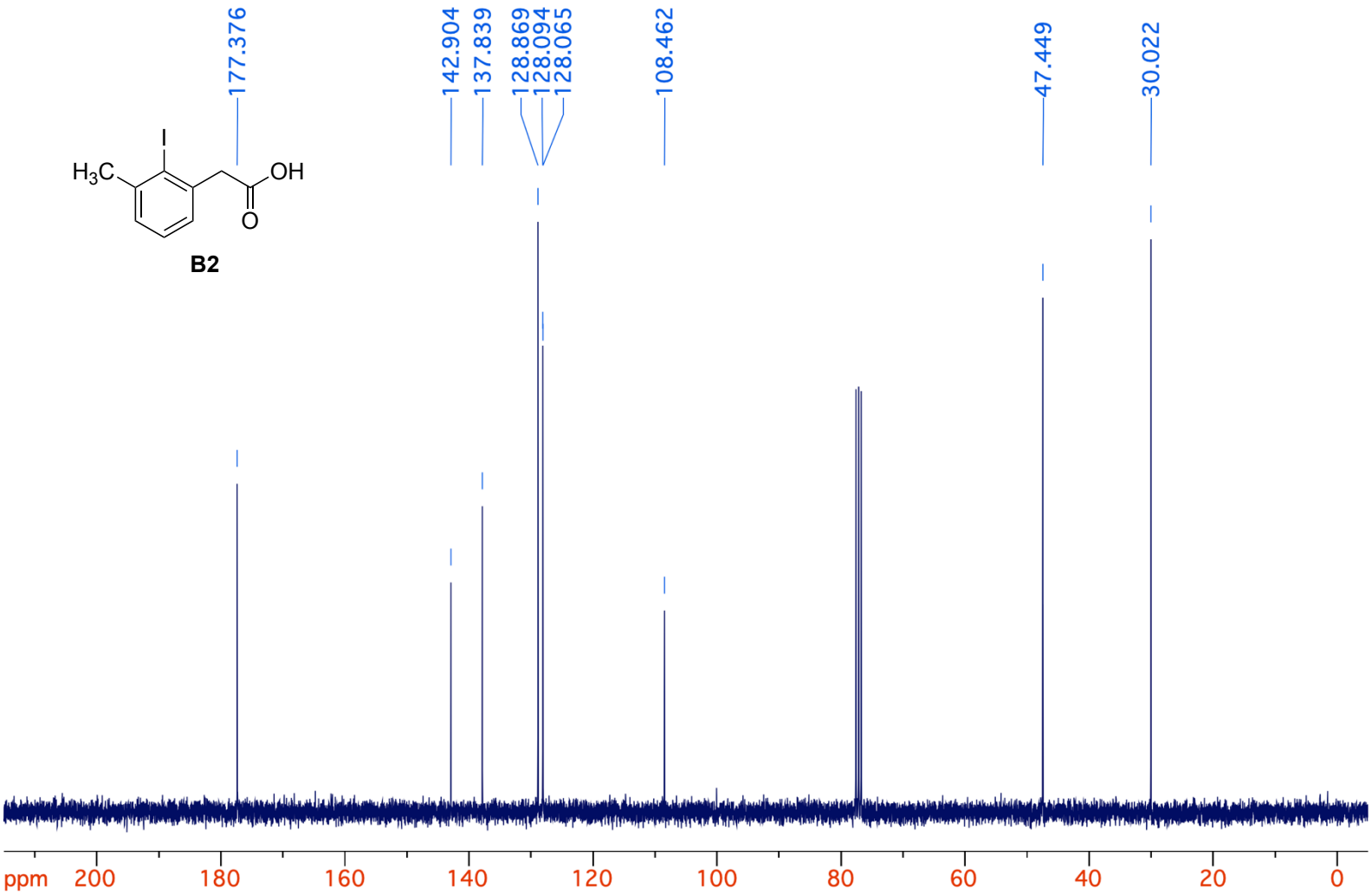


Figure B-31. ^{1}H-NMR (300 MHz, $CDCl_3$) of methyl 2-(2-iodo-3-methylphenyl)acetate (**4.137**):

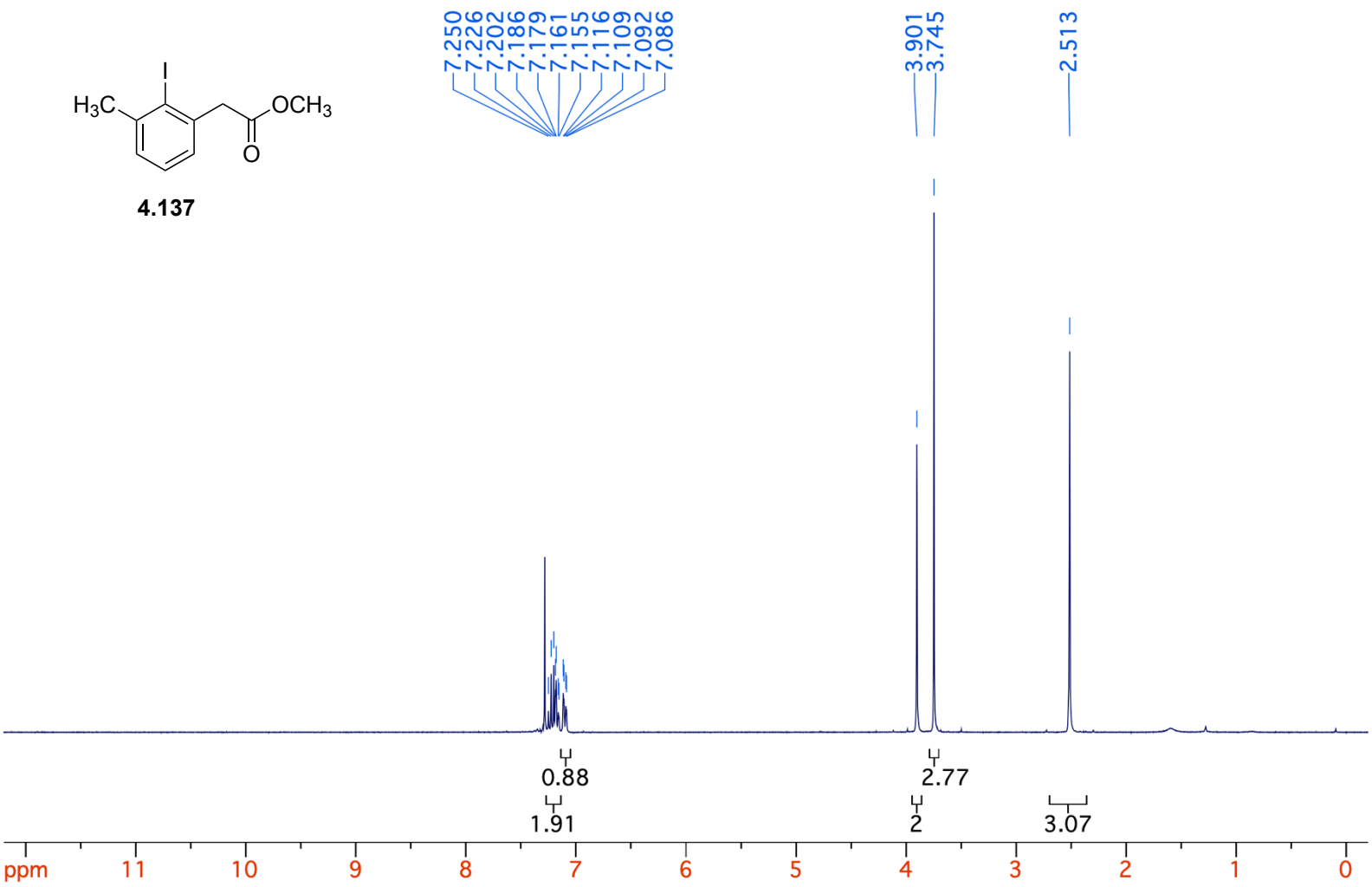


Figure B-32. ^{13}C-NMR (75 MHz, $CDCl_3$) of methyl 2-(2-iodo-3-methylphenyl)acetate (**4.137**):

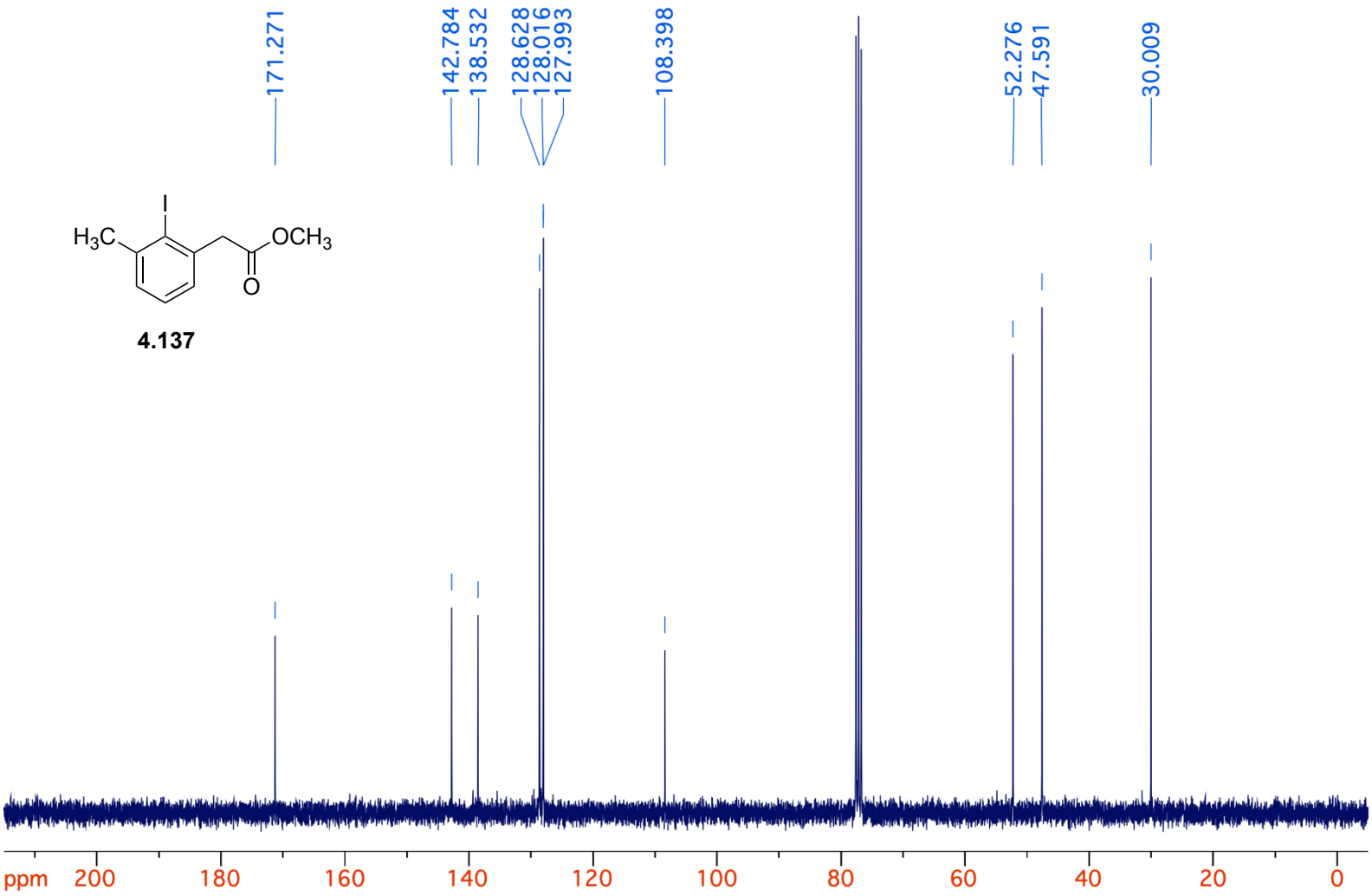


Figure B-33. ^{1}H-NMR (300 MHz, $CDCl_3$) of 1-(2-iodo-3-methylphenyl)-2-methylpropan-2-ol (**4.138**):

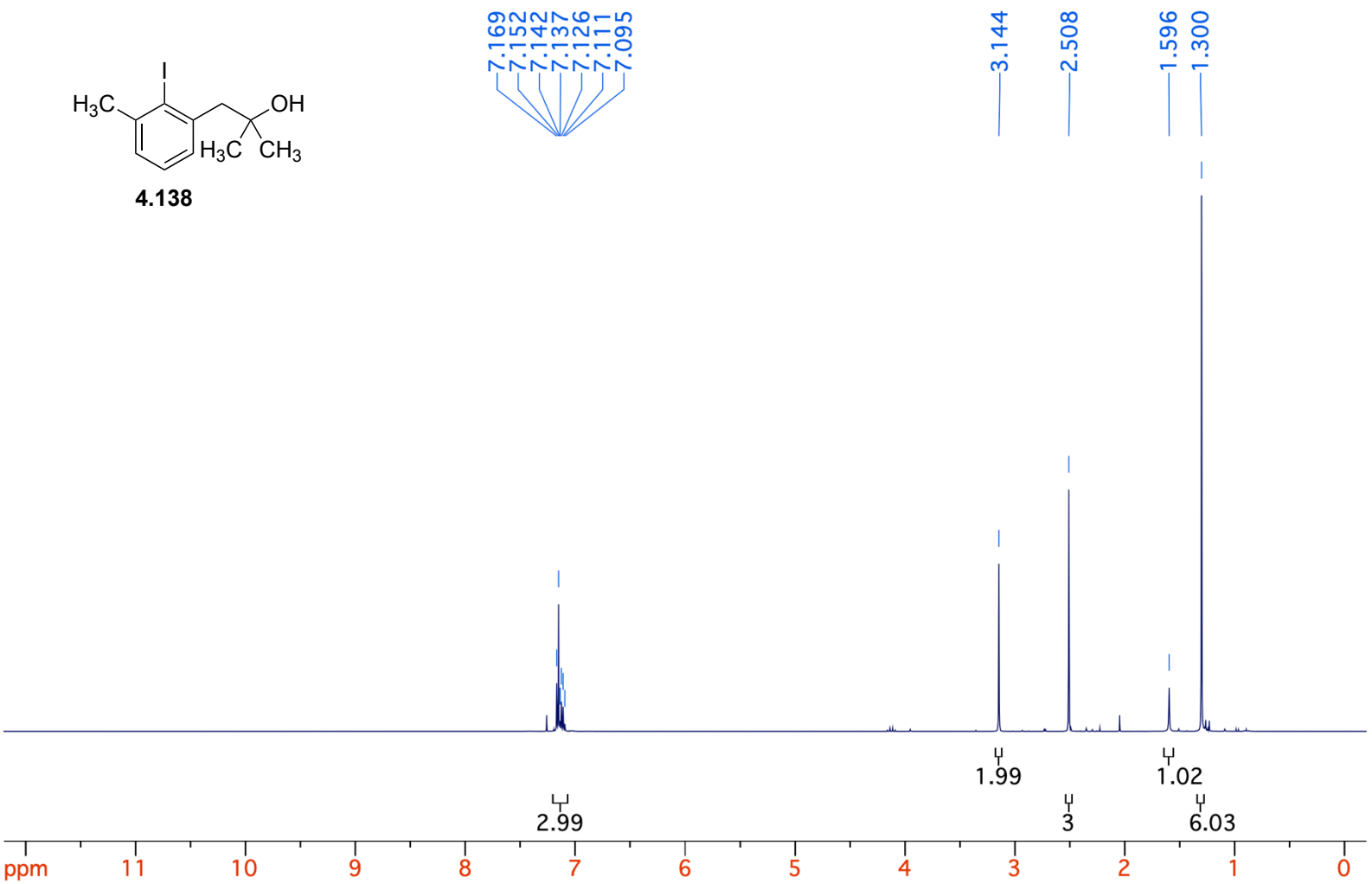


Figure B-34. ^{13}C-NMR (75 MHz, $CDCl_3$) of 1-(2-iodo-3-methylphenyl)-2-methylpropan-2-ol (**4.138**):

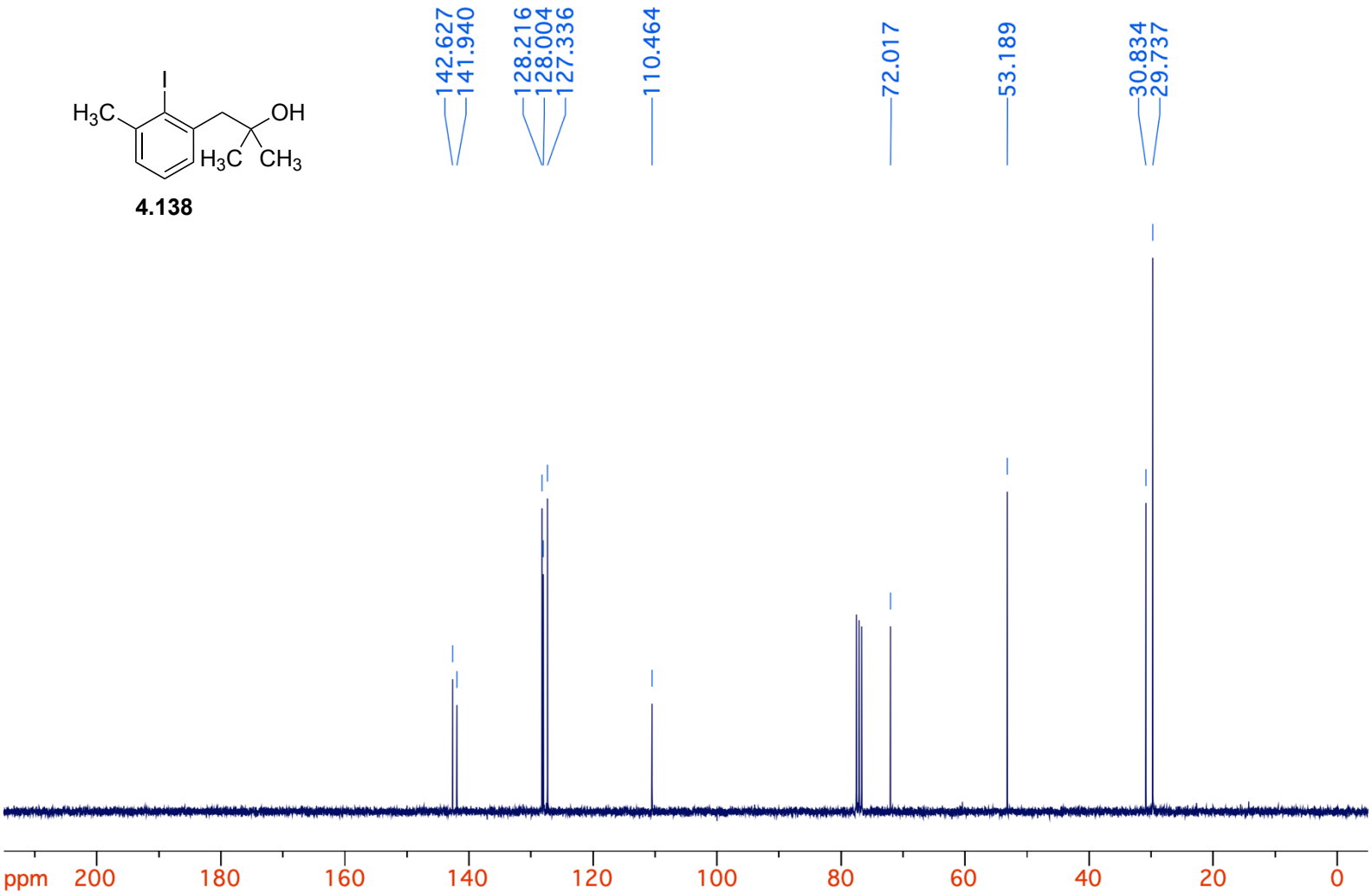


Figure B-35. ^{1}H-NMR (300 MHz, $CDCl_3$) of 1-(2-iodophenyl)-2-methylpropan-2-ol (**4.140**):

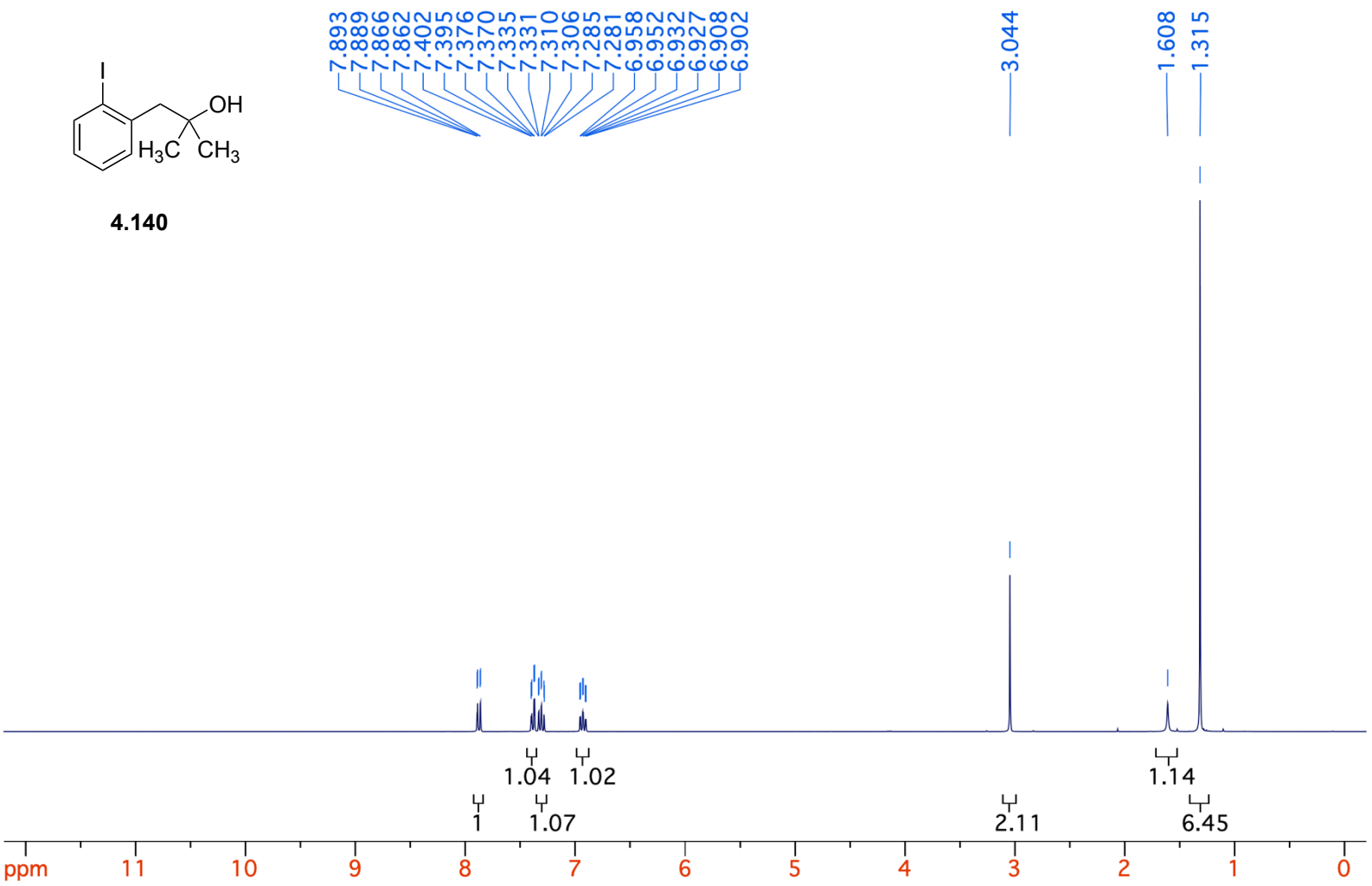


Figure B-36. ^{13}C-NMR (75 MHz, $CDCl_3$) of 1-(2-iodophenyl)-2-methylpropan-2-ol (**4.140**):

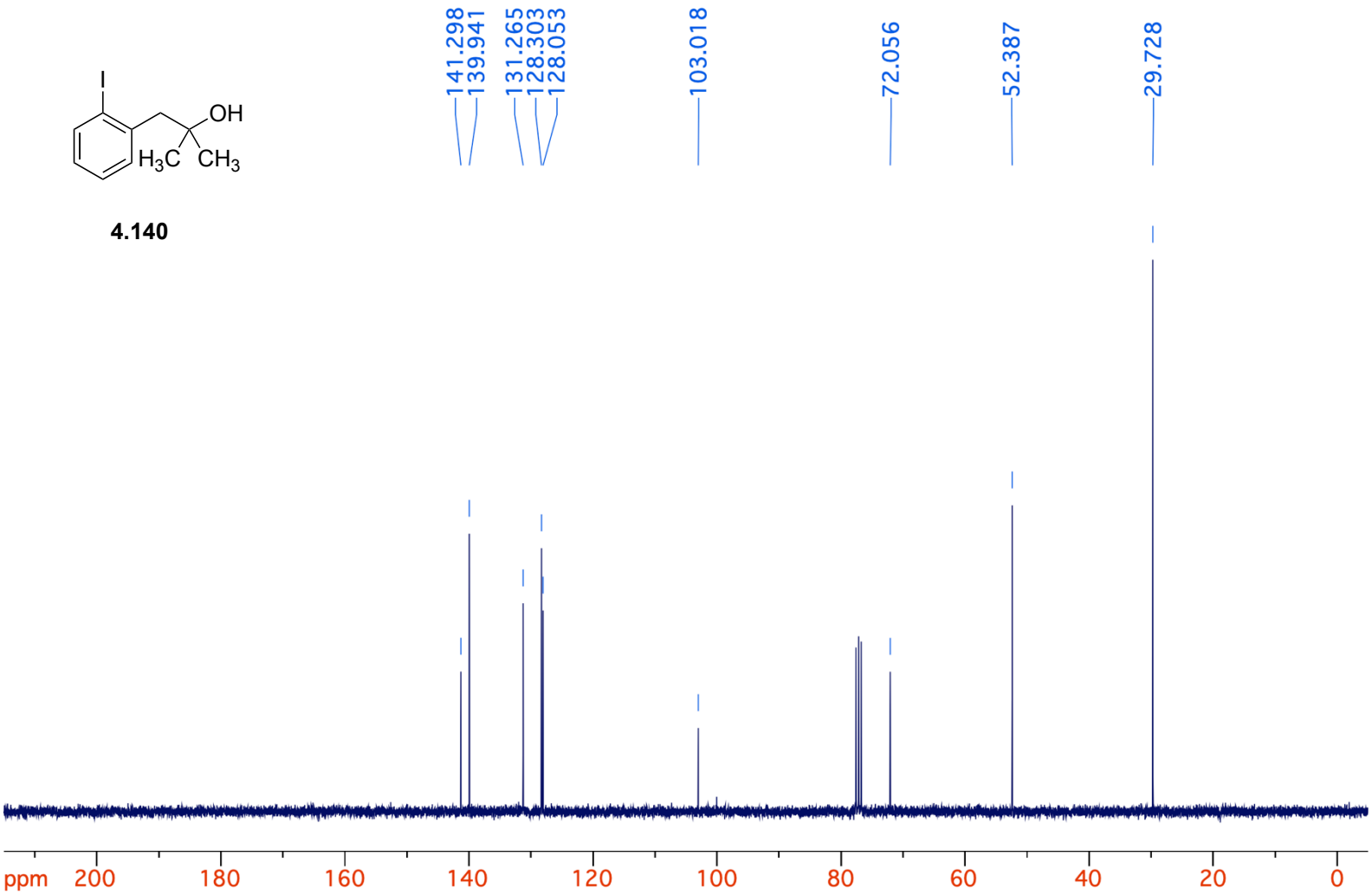


Figure B-37. ^{1}H-NMR (300 MHz, $CDCl_3$) of 1-fluoro-3,3,7-trimethyl-1,3-dihydro-1λ^3-benzo[*d*][1,2]iodaoxole (**4.143**):

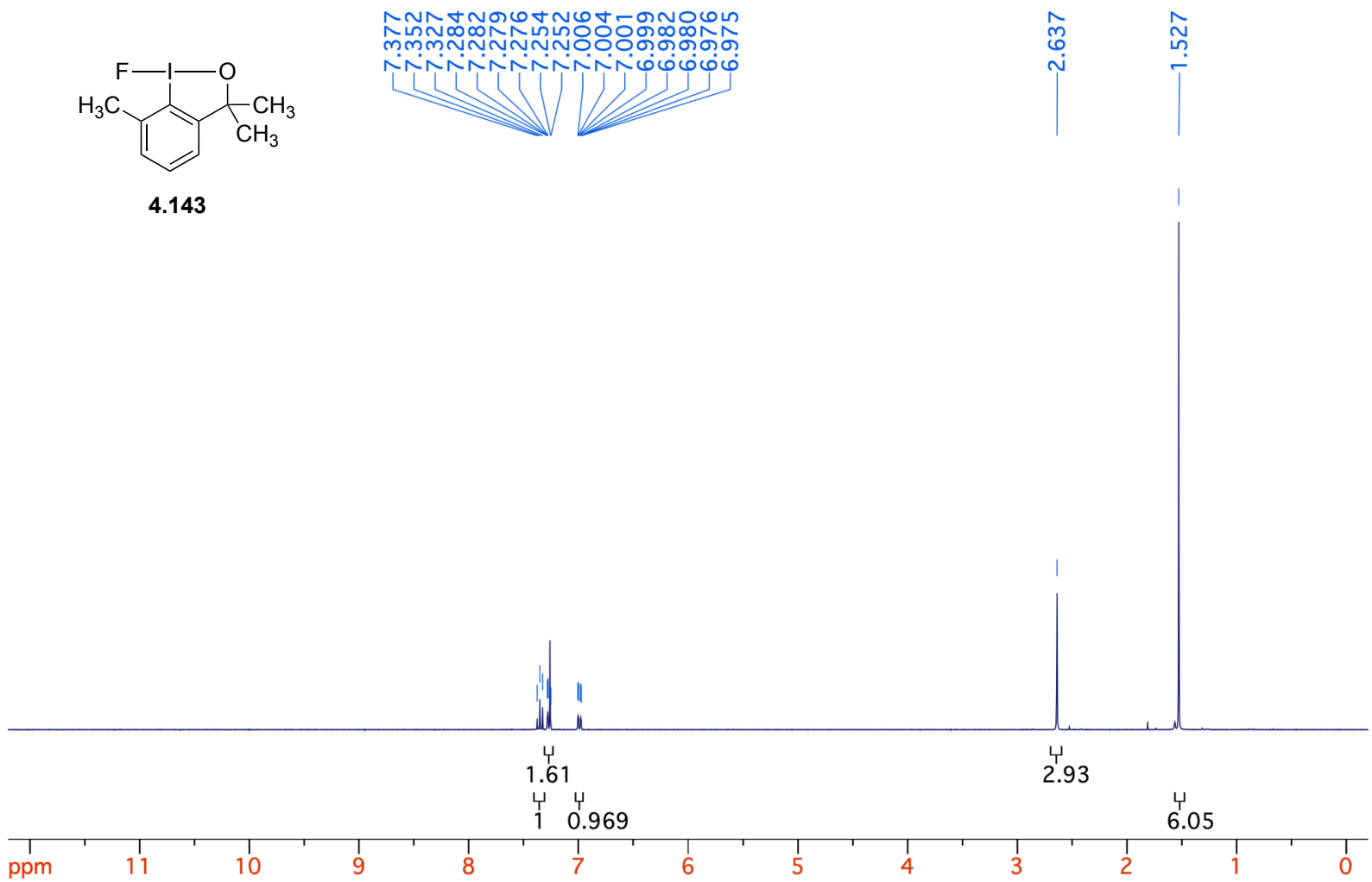


Figure B-38. ^{13}C-NMR (75 MHz, $CDCl_3$) of 1-fluoro-3,3,7-trimethyl-1,3-dihydro-1λ^3-benzo[*d*][1,2]iodaoxole (**4.143**):

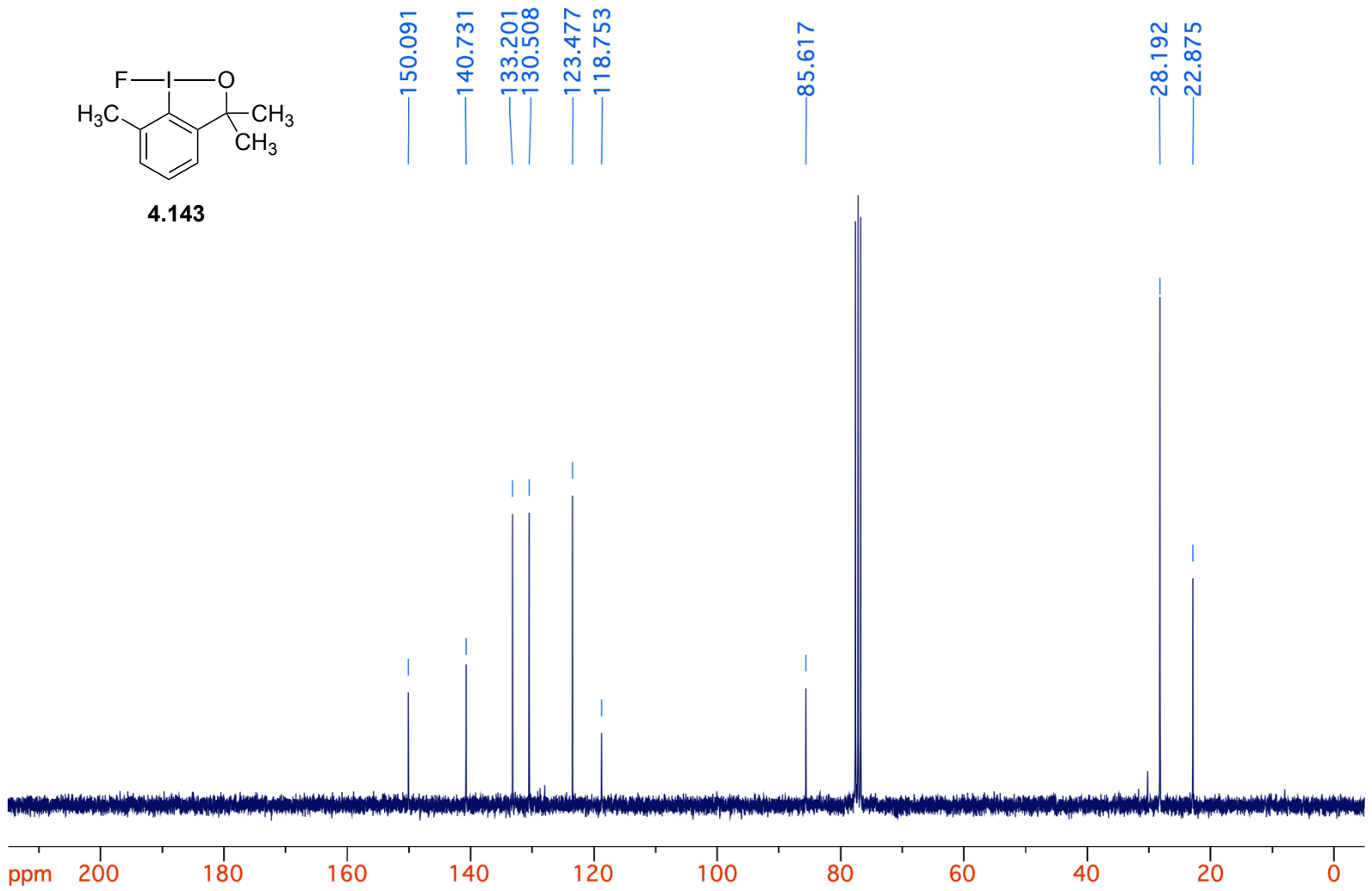
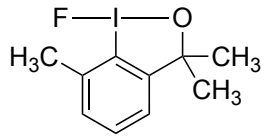


Figure B-39. ^{19}F-NMR (282 MHz, $CDCl_3$) of 1-fluoro-3,3,7-trimethyl-1,3-dihydro-1λ^3-benzo[*d*][1,2]iodaoxole (**4.143**):



4.143

Figure B-40. ^{1}H-NMR (300 MHz, $CDCl_3$) of 3,3,7-trimethyl-1λ^3-benzo[*d*][1,2]iodaoxol-1(3*H*)-yl 4-methylbenzenesulfonate (**4.144**):

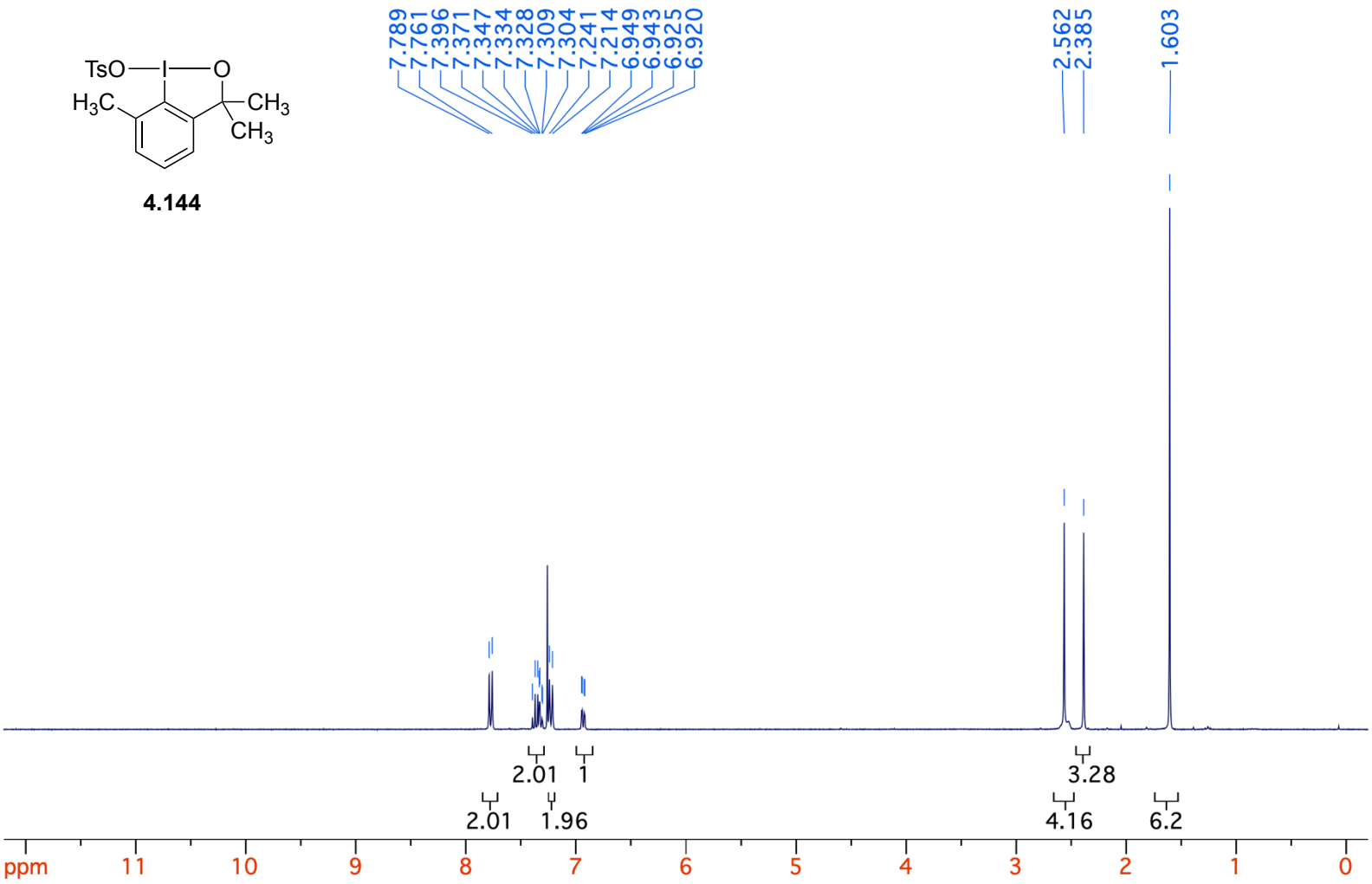


Figure B-41. ^{13}C-NMR (75 MHz, $CDCl_3$) of 3,3,7-trimethyl-1λ^3-benzo[*d*][1,2]iodaoxol-1(3*H*)-yl 4-methylbenzenesulfonate (**4.144**):

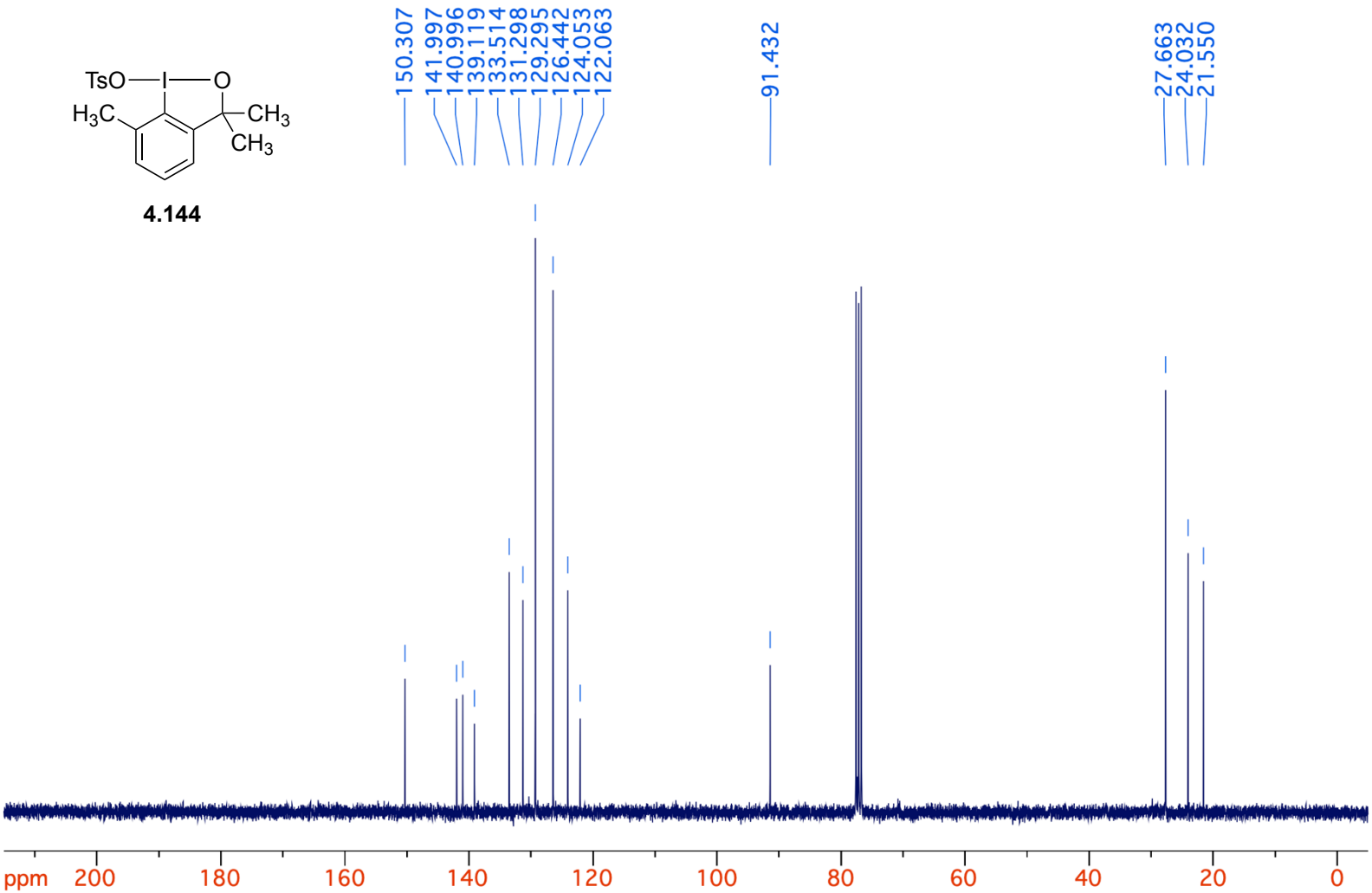


Figure B-42. ^{1}H-NMR (300 MHz, $CDCl_3$) of 1-chloro-3,3,7-trimethyl-1,3-dihydro-1λ^3-benzo[*d*][1,2]iodaoxole (**4.145**):

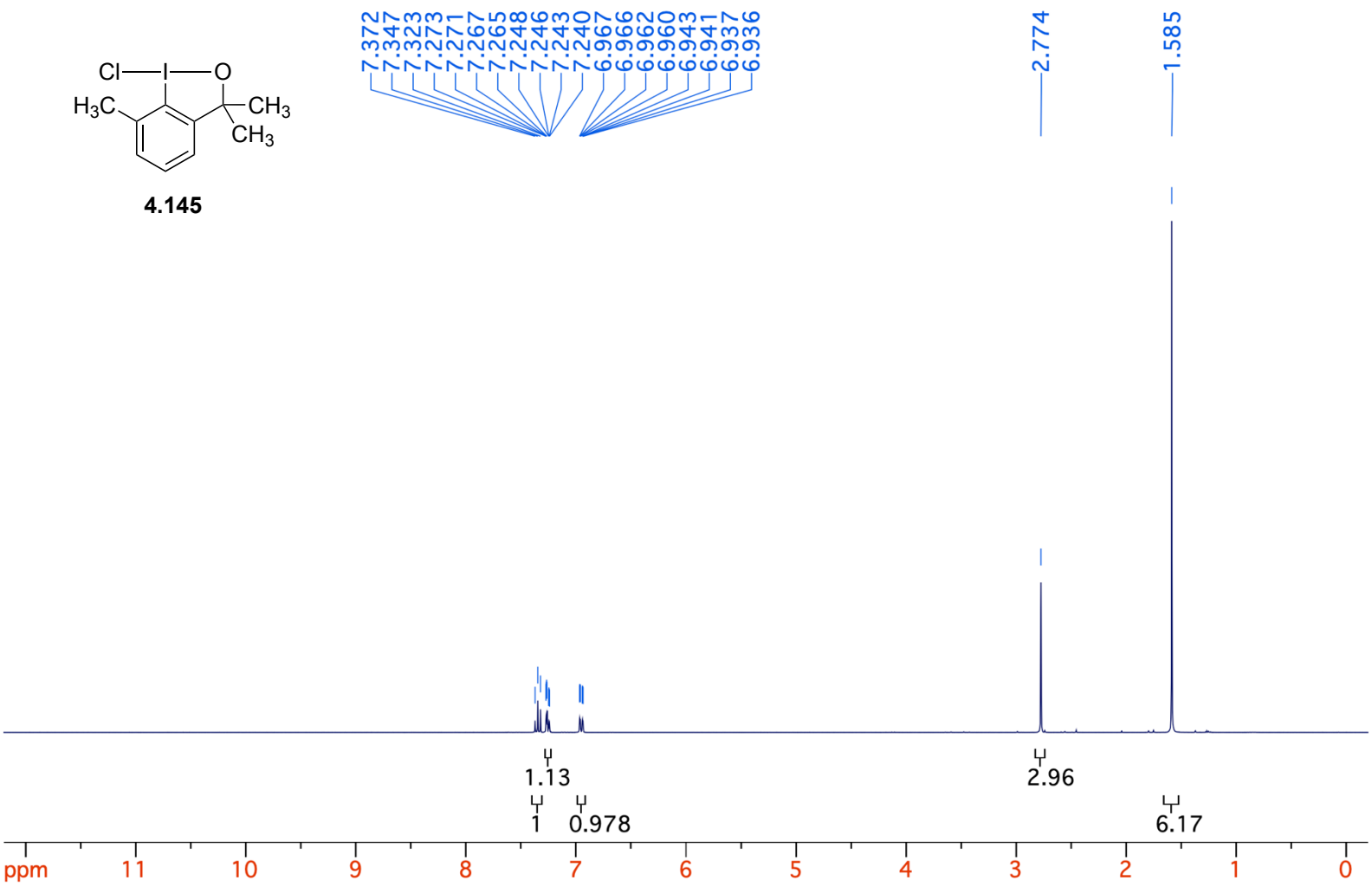


Figure B-43. ^{13}C-NMR (75 MHz, $CDCl_3$) of 1-chloro-3,3,7-trimethyl-1,3-dihydro-1λ^3-benzo[*d*][1,2]iodaoxole (**4.145**):

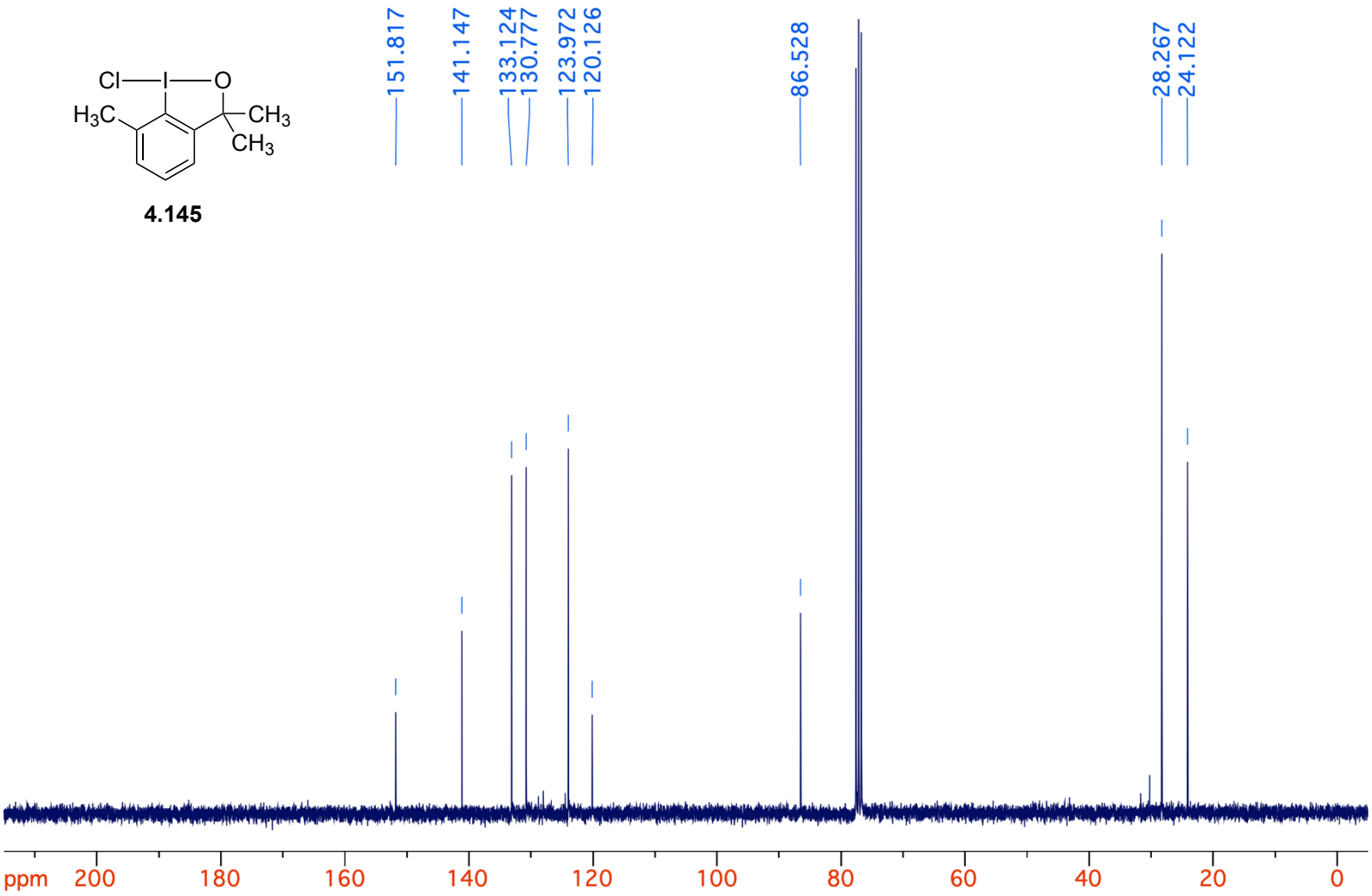


Figure B-44. ^{1}H-NMR (300 MHz, $CDCl_3$) of 7-bromo-1-fluoro-3,3-dimethyl-1,3-dihydro-1λ^3-benzo[*d*][1,2]iodaoxole (**4.147**):

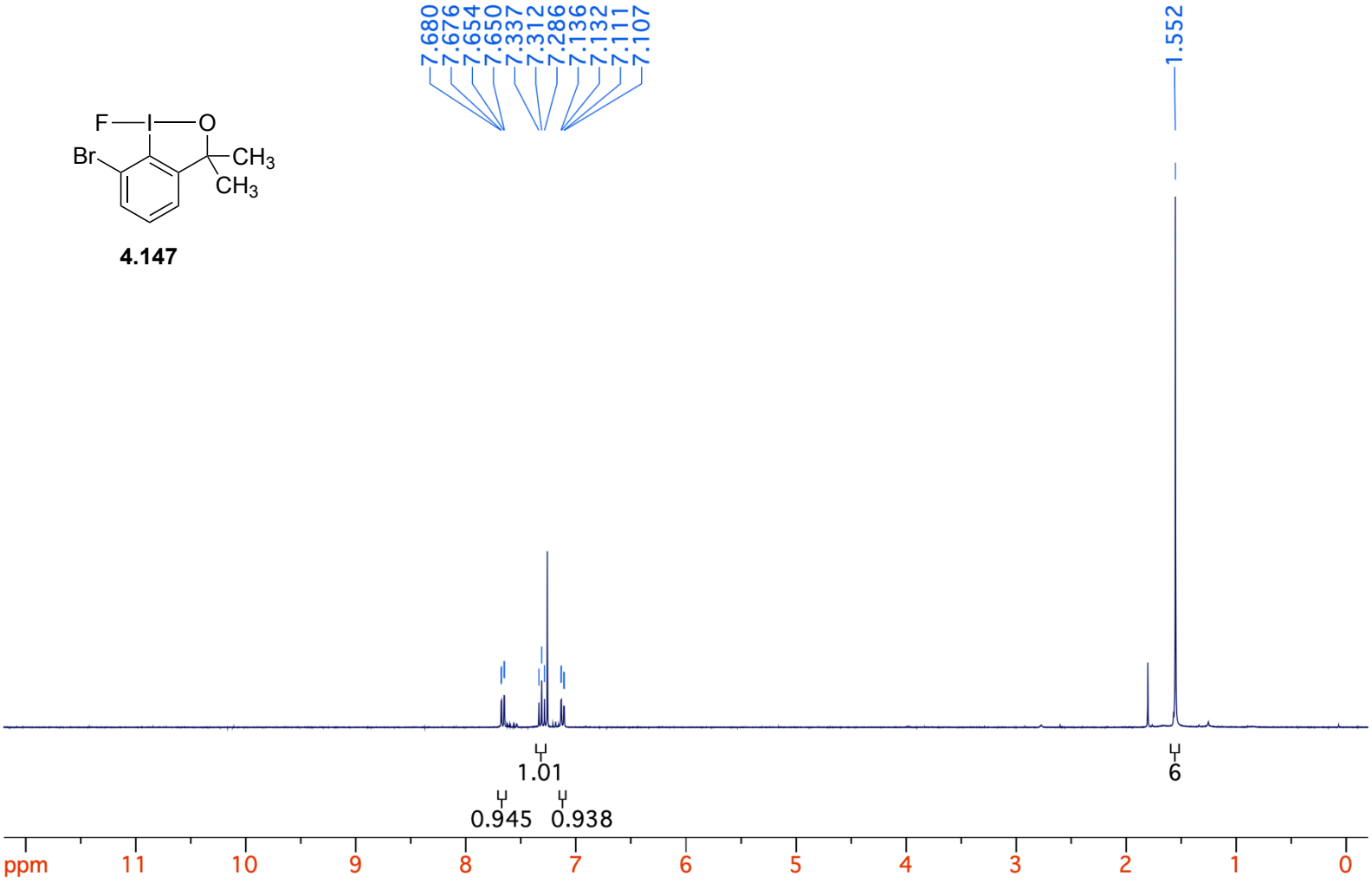
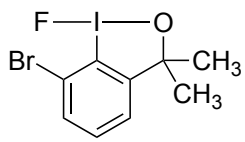


Figure B-45. ^{19}F-NMR (282 MHz, $CDCl_3$) of 7-bromo-1-fluoro-3,3-dimethyl-1,3-dihydro-1λ^3-benzo[*d*][1,2]iodaoxole (**4.147**):



4.147

Figure B-46. ^{1}H-NMR (300 MHz, $CDCl_3$) of 1-fluoro-7-methoxy-3,3-dimethyl-1,3-dihydro-1λ^3-benzo[*d*][1,2]iodaoxole (**4.148**):

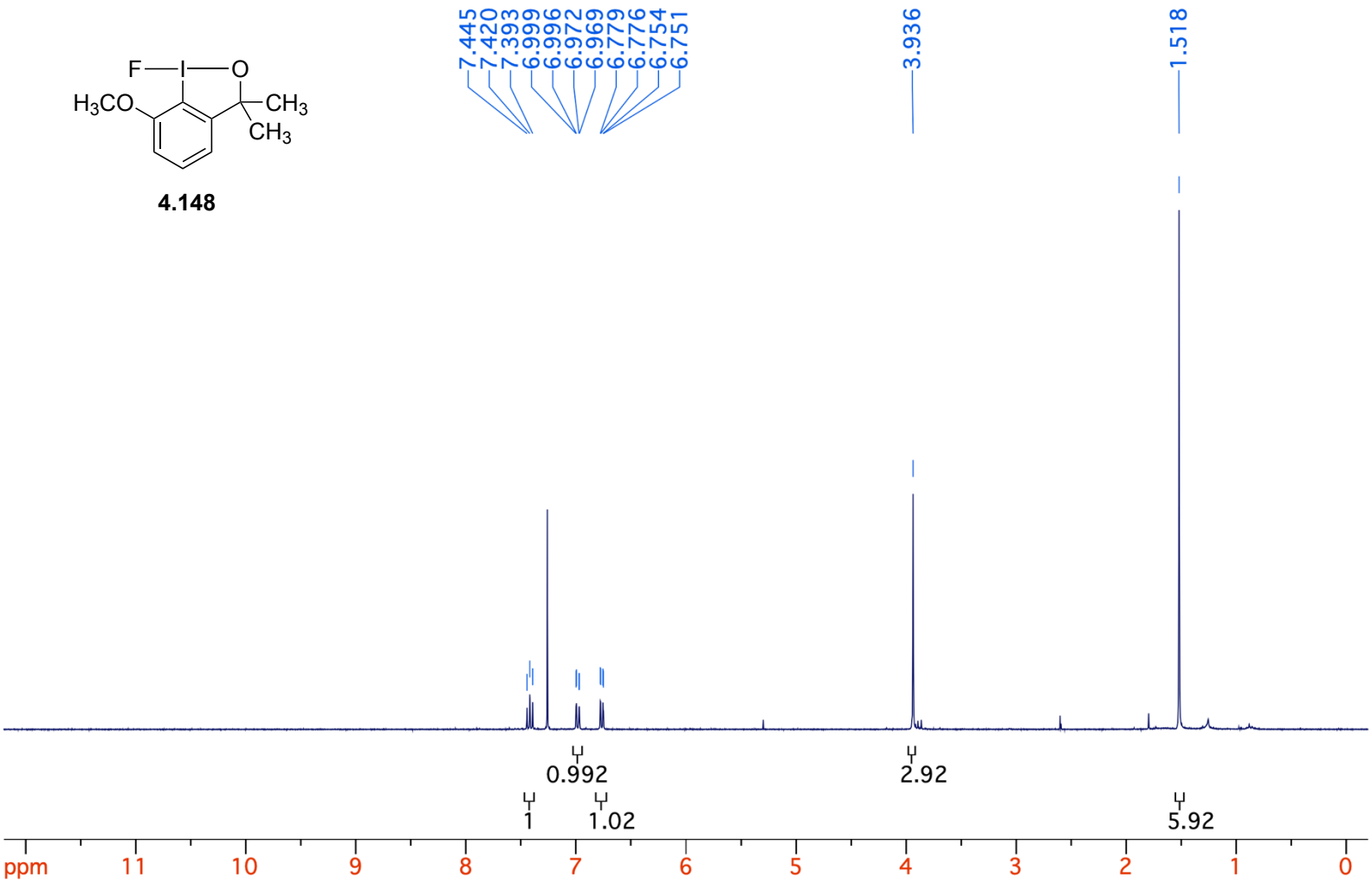
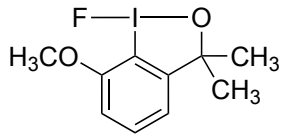


Figure B-47. ^{19}F-NMR (282 MHz, $CDCl_3$) of 1-fluoro-7-methoxy-3,3-dimethyl-1,3-dihydro-1λ^3-benzo[*d*][1,2]iodaoxole (**4.148**):



4.148

Figure B-48. ^{1}H-NMR (300 MHz, $CDCl_3$) of 1-fluoro-7-isopropoxy-3,3-dimethyl-1,3-dihydro-1λ^3-benzo[*d*][1,2]iodaoxole (**4.149**):

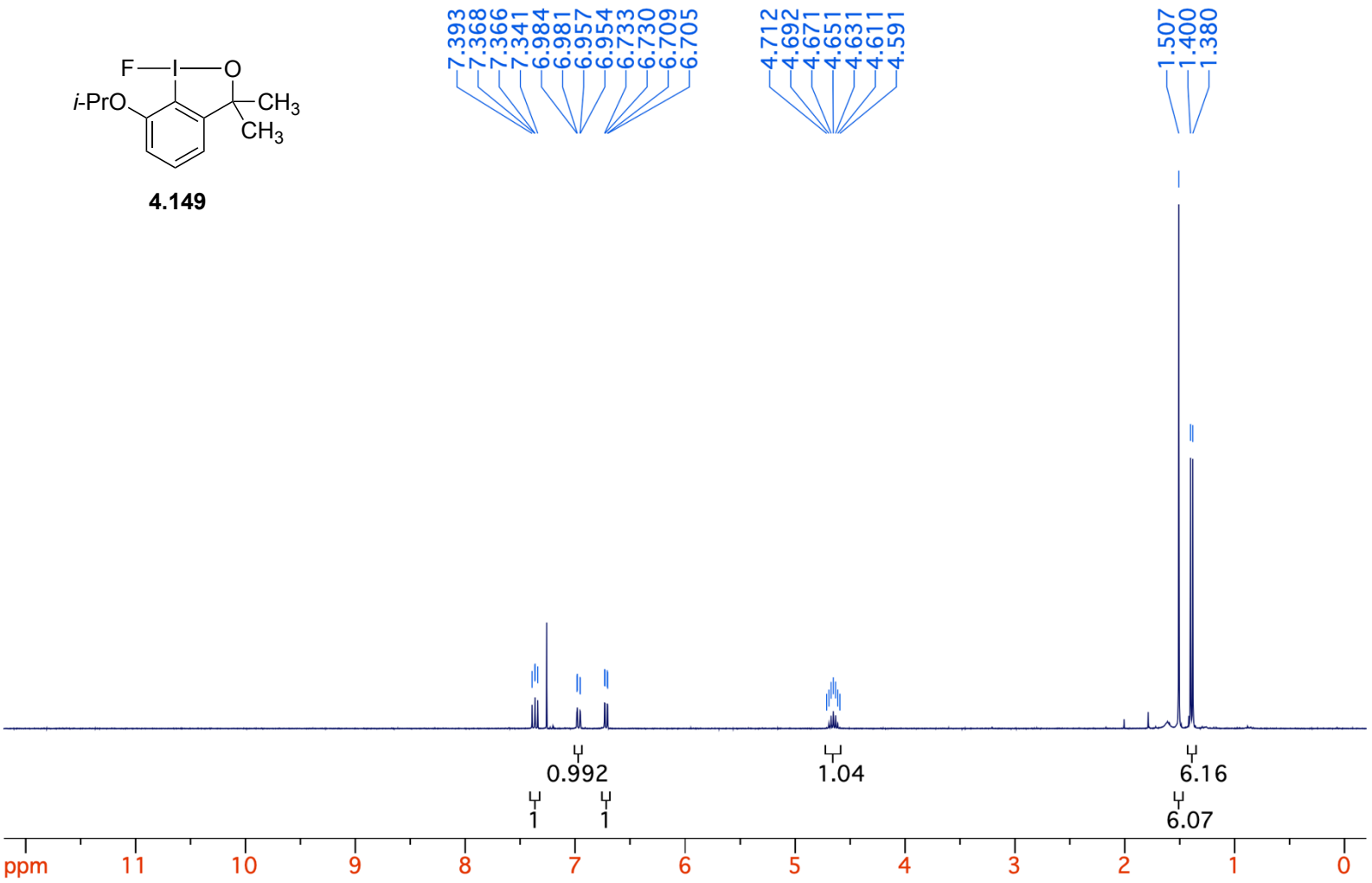
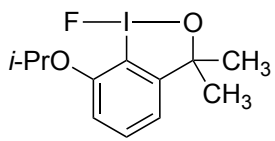


Figure B-49. ^{19}F-NMR (282 MHz, $CDCl_3$) of 1-fluoro-7-isopropoxy-3,3-dimethyl-1,3-dihydro-1λ^3-benzo[*d*][1,2]iodaoxole (**4.149**):



4.149

Figure B-50. ^{1}H-NMR (300 MHz, $CDCl_3$) of 7-isopropyl-3,3-dimethyl-1λ^3-benzo[*d*][1,2]iodaoxol-1(3*H*)-yl 4-methylbenzenesulfonate (**4.150**):

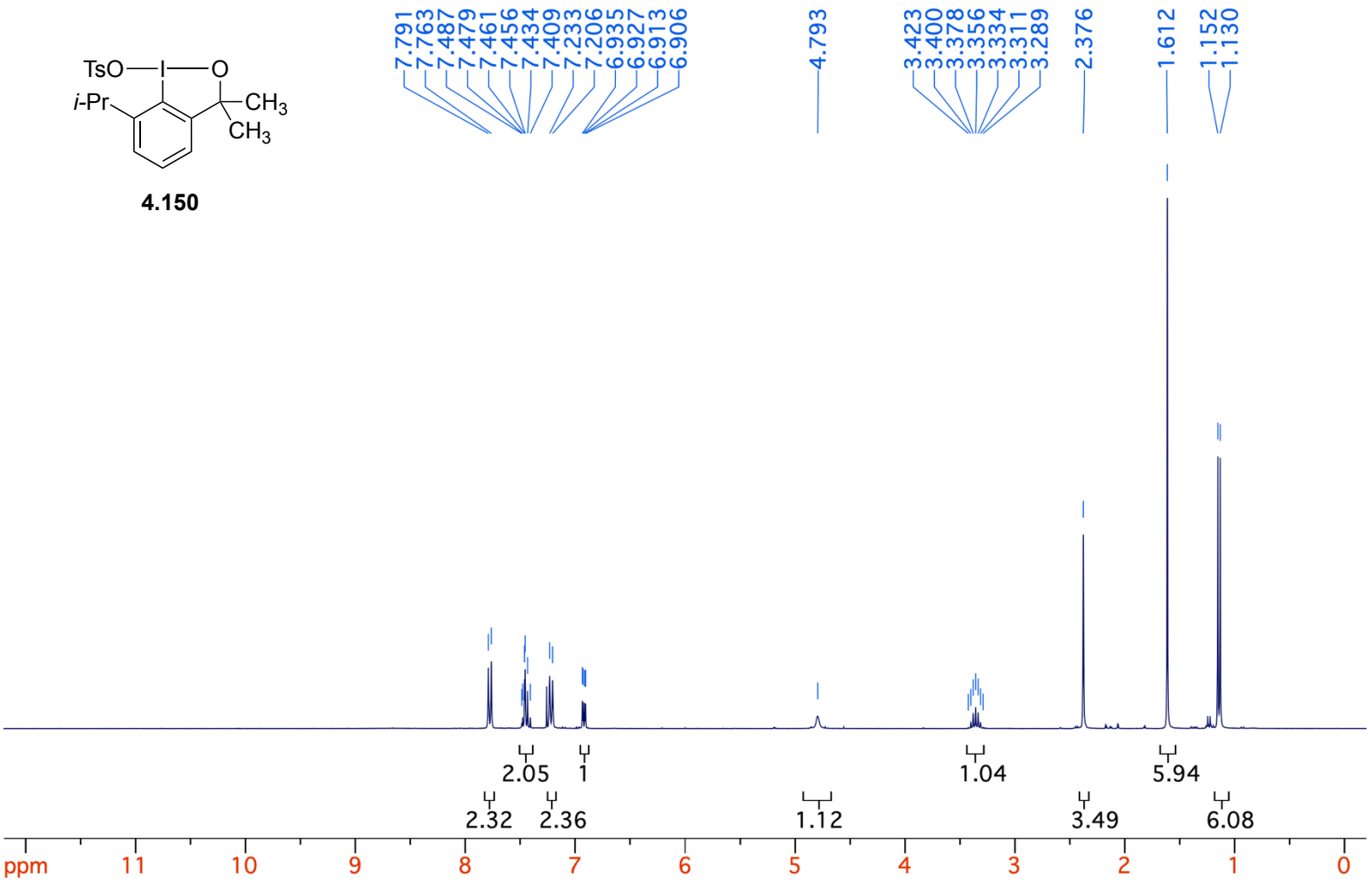


Figure B-51. ^{13}C-NMR (75 MHz, $CDCl_3$) of 7-isopropyl-3,3-dimethyl-1λ^3-benzo[*d*][1,2]iodaoxol-1(3*H*)-yl 4-methylbenzenesulfonate (**4.150**):

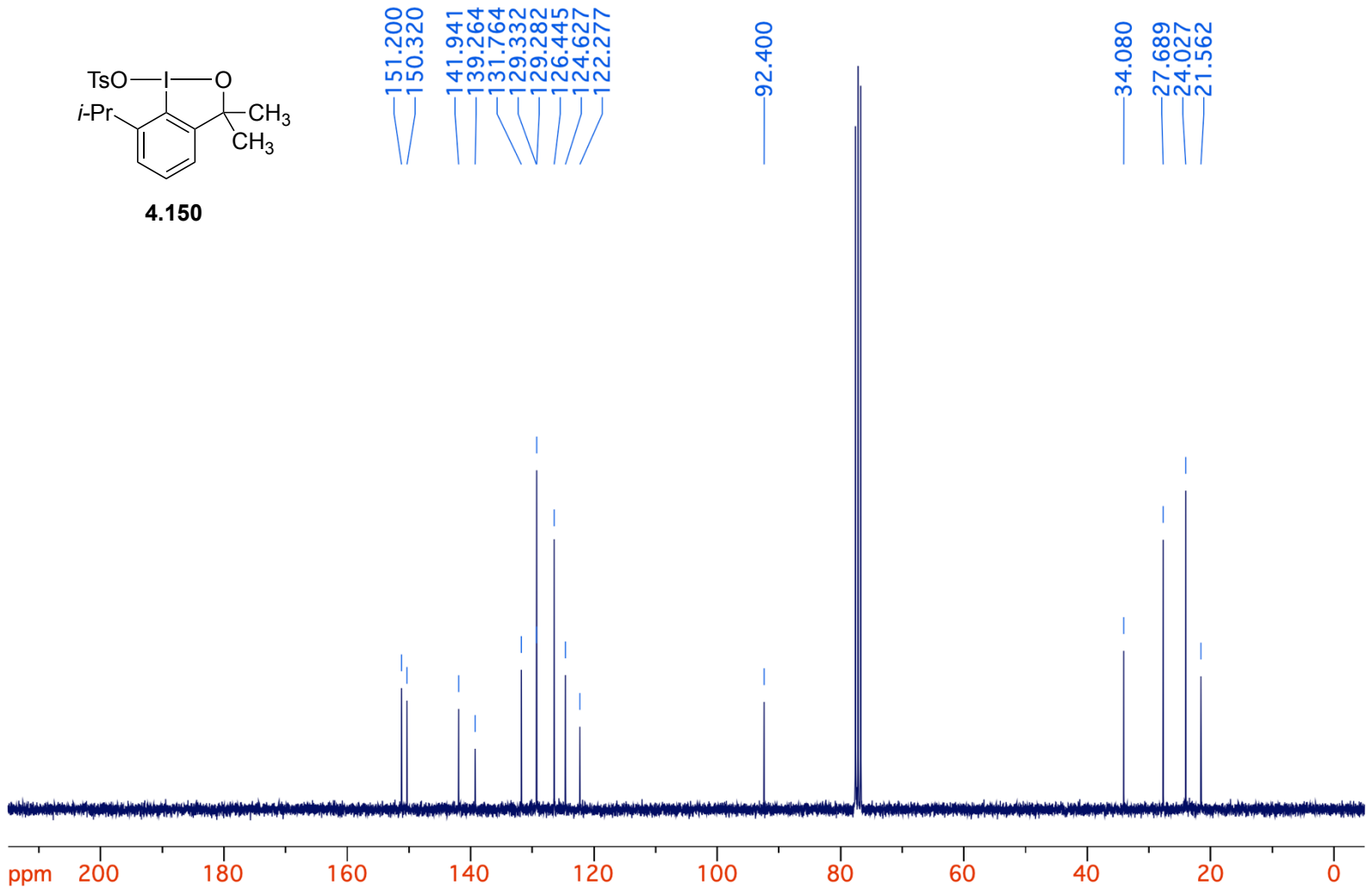
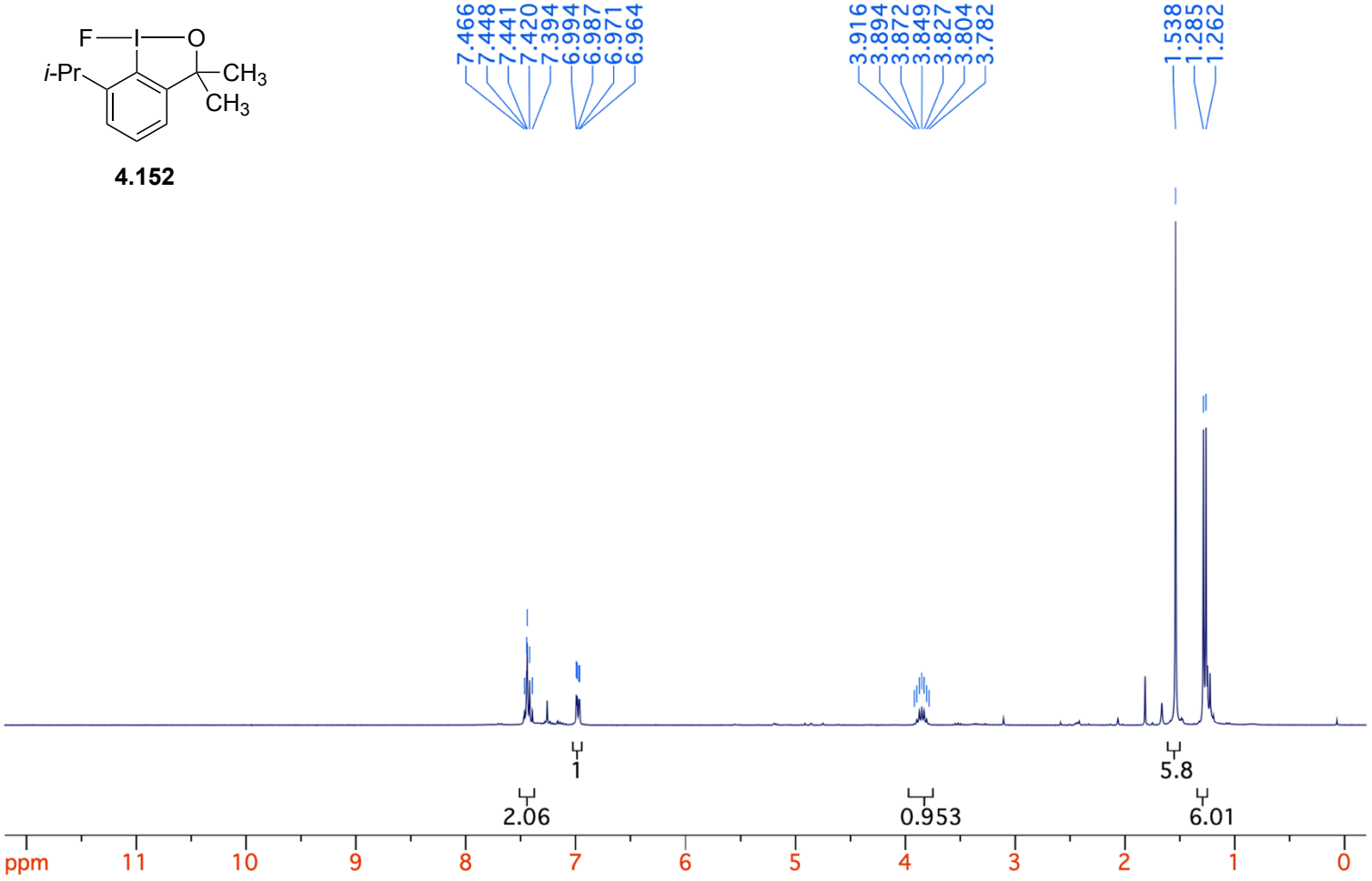
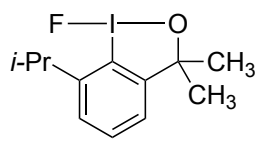


Figure B-52. ^{1}H-NMR (300 MHz, $CDCl_3$) of 1,1'-oxybis(7-isopropyl-3,3-dimethyl-1,3-dihydro-1λ^3-benzo[*d*][1,2]iodaoxole) (**4.151**) or 1-fluoro-7-isopropyl-3,3-dimethyl-1,3-dihydro-1λ^3-benzo[*d*][1,2]iodaoxole (**4.152**), likely **4.152** based on Figure B-53:



4.152

Figure B-53. Presumed ^{19}F-NMR (282 MHz, $CDCl_3$) of 1-fluoro-7-isopropyl-3,3-dimethyl-1,3-dihydro-1λ^3-benzo[*d*][1,2]iodaoxole (**4.152**):



4.152

Figure B-54. ^{1}H-NMR (300 MHz, $CDCl_3$) of 5-bromo-7-(2-hydroxypropan-2-yl)-3,3-dimethyl-2,3-dihydrobenzo[*b*]iodol-1-ium 4-methylbenzenesulfonate (**4.155**):

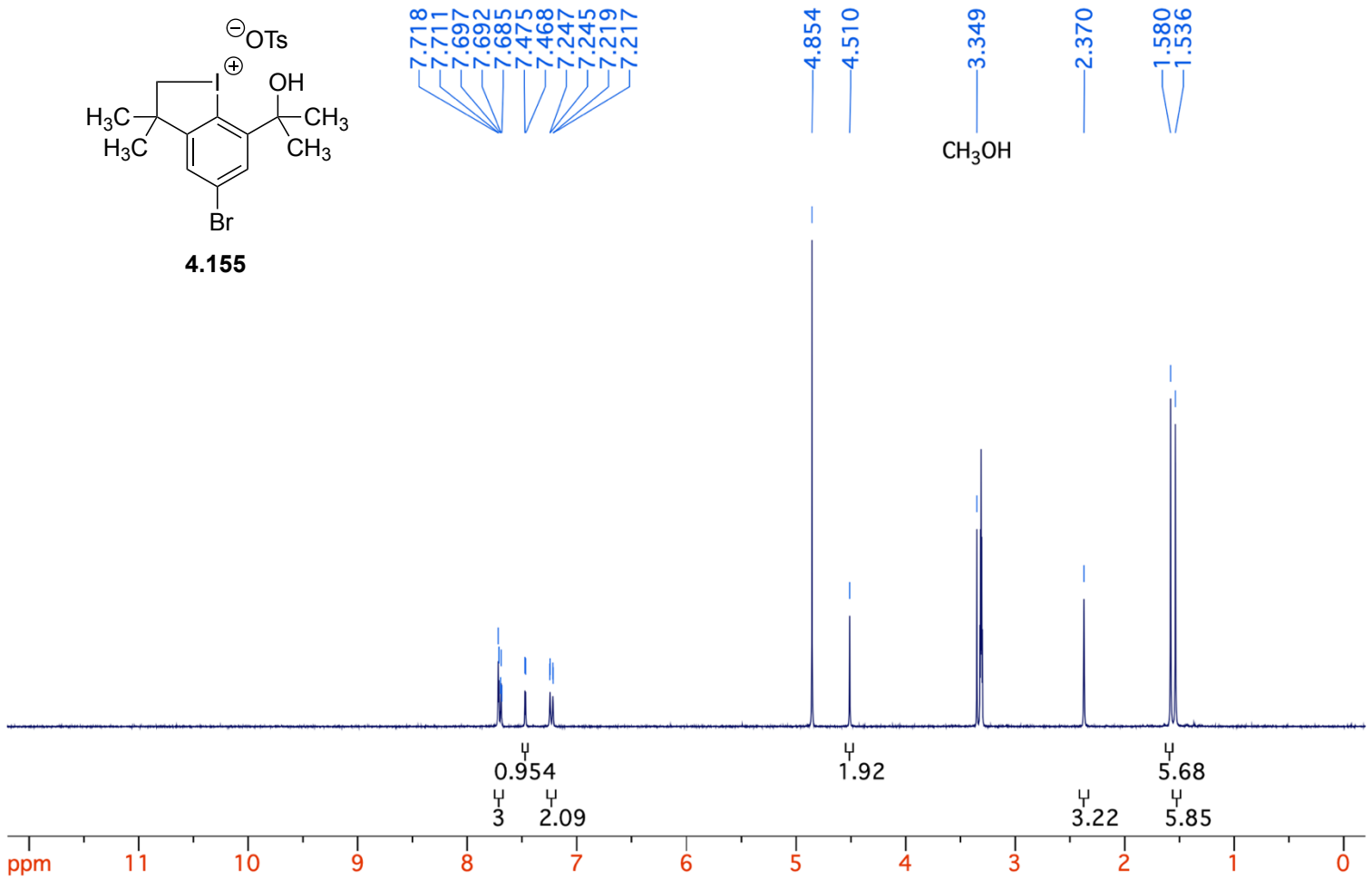


Figure B-55. ^{13}C-NMR (75 MHz, CD_3OD) of 5-bromo-7-(2-hydroxypropan-2-yl)-3,3-dimethyl-2,3-dihydrobenzo[*b*]iodol-1-ium 4-methylbenzenesulfonate (**4.155**):

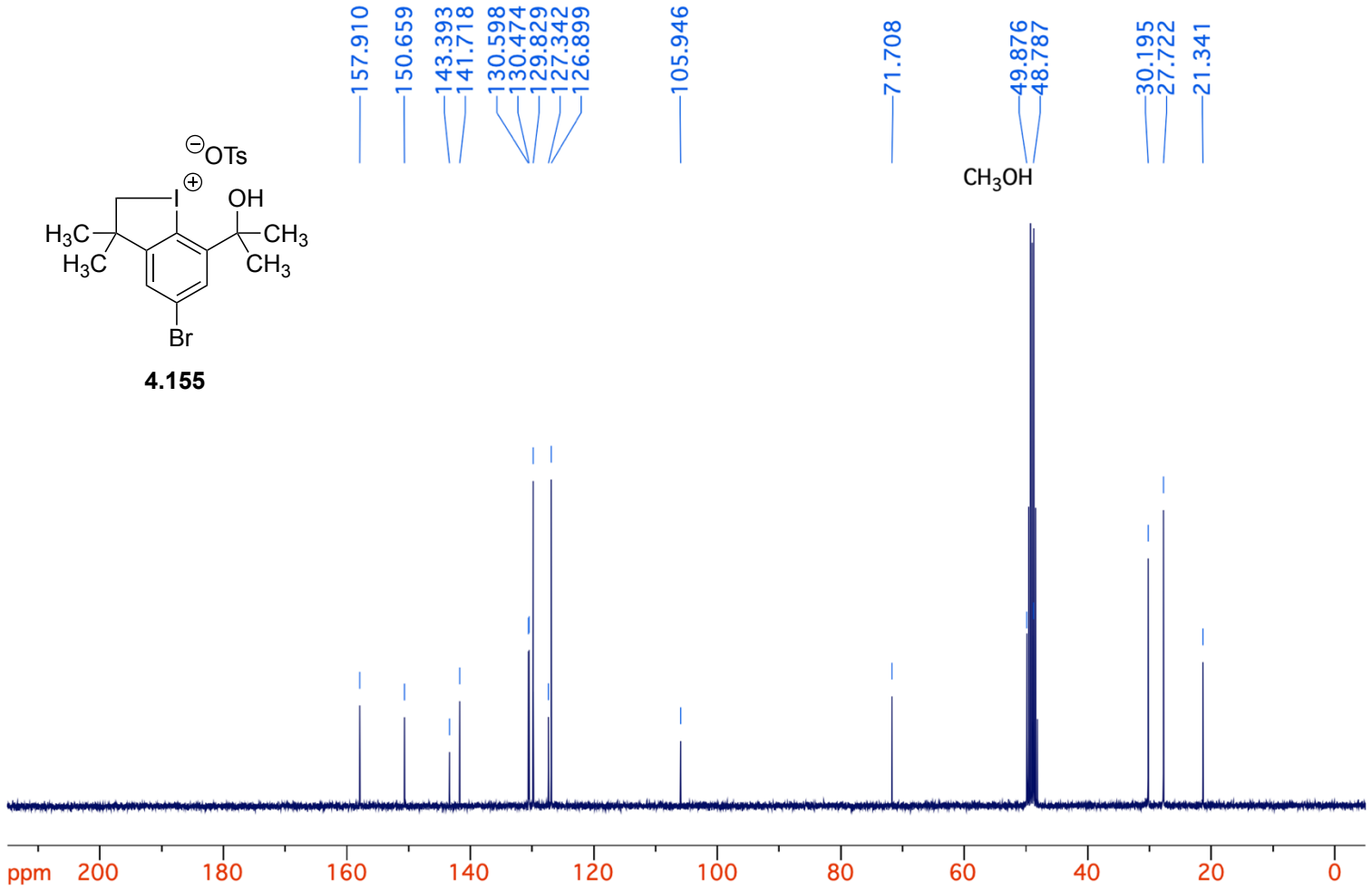


Figure B-56. ^{1}H, ^{13}C- HMQC (300 MHz, 75 MHz, CD_3OD) of 5-bromo-7-(2-hydroxypropan-2-yl)-3,3-dimethyl-2,3-dihydrobenzo[*b*]iodol-1-ium 4-methylbenzenesulfonate (**4.155**):

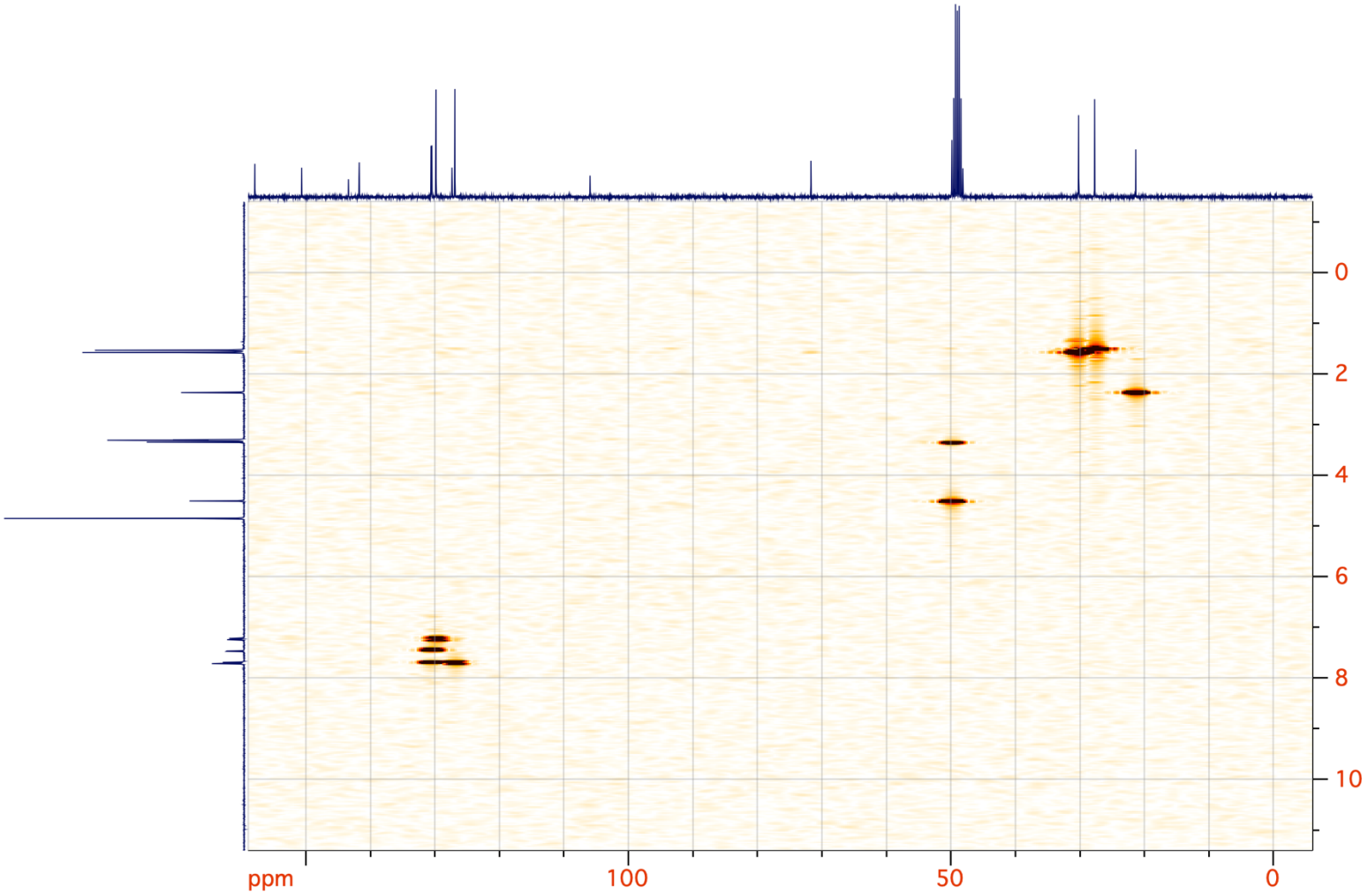


Figure B-57. ^{1}H, ^{13}C- HMBC (300 MHz, 75 MHz, CD_3OD) of 5-bromo-7-(2-hydroxypropan-2-yl)-3,3-dimethyl-2,3-dihydrobenzo[*b*]iodol-1-ium 4-methylbenzenesulfonate (**4.155**):

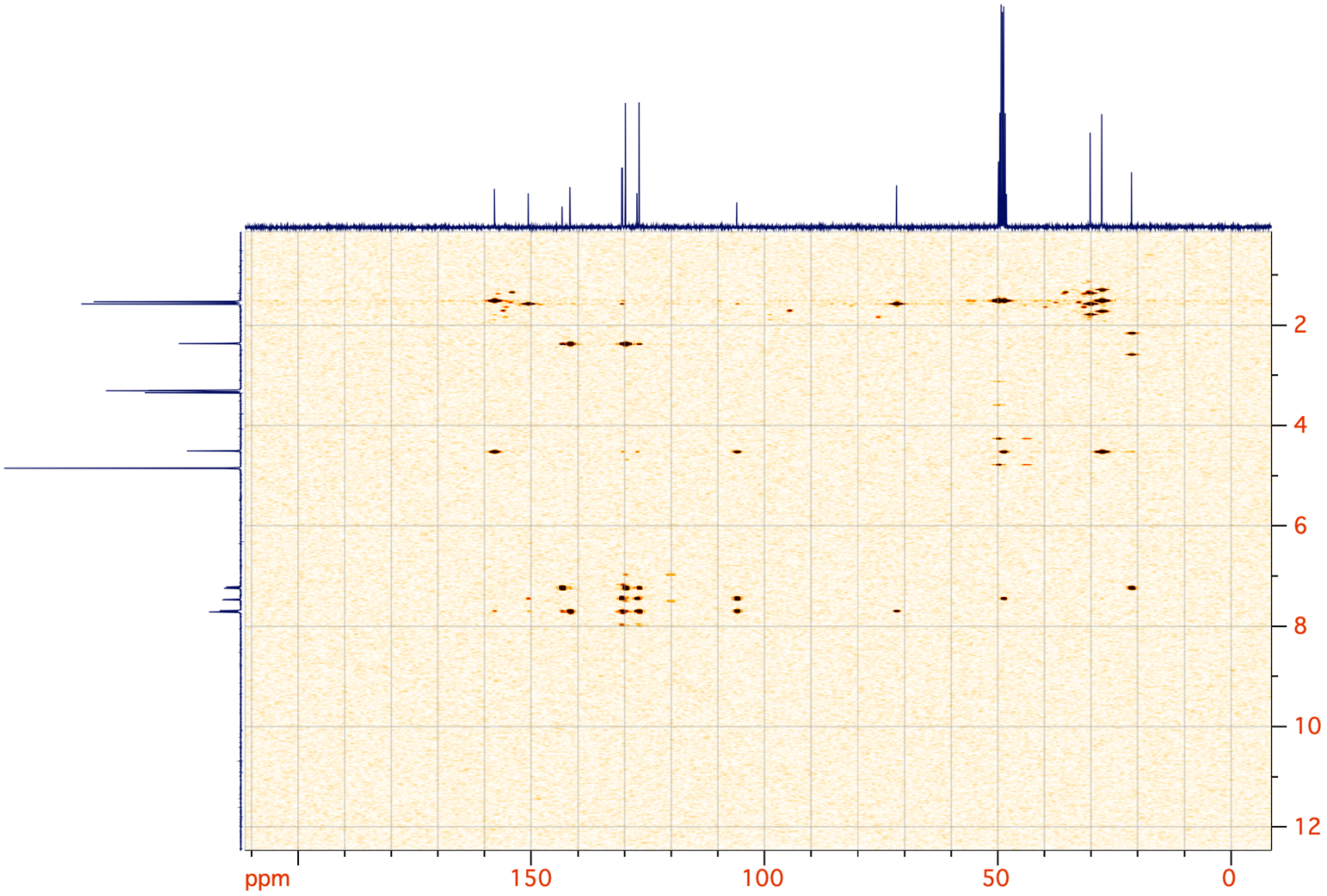


Figure B-58. ^{1}H-NMR (300 MHz, $CDCl_3$) of 5-bromo-7-(*tert*-butyl)-1-chloro-3,3-dimethyl-1,3-dihydro-1λ^3-benzo[*d*][1,2]iodaoxole (**4.163**):

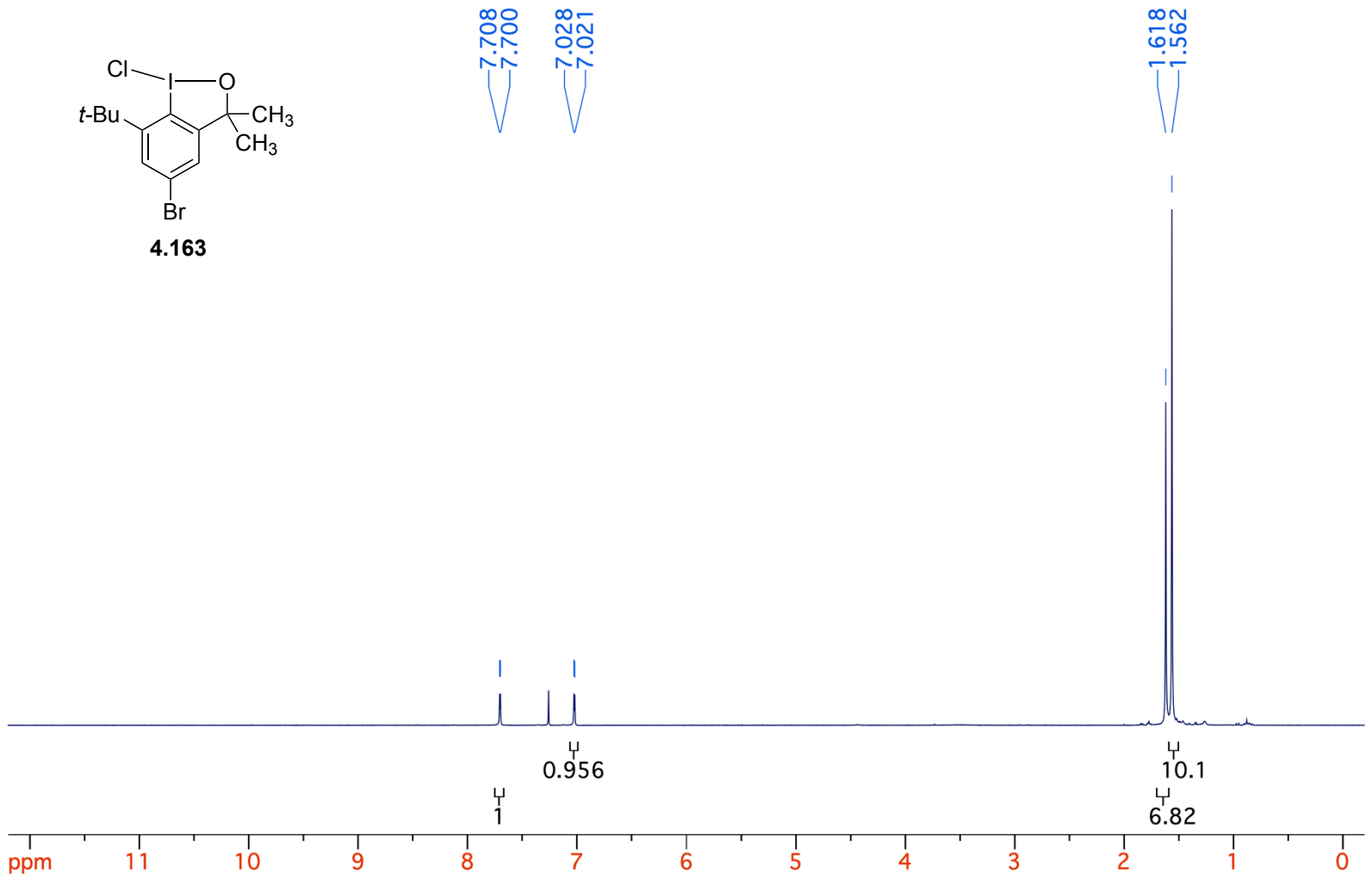


Figure B-59. ^{13}C-NMR (75 MHz, $CDCl_3$) of 5-bromo-7-(*tert*-butyl)-1-chloro-3,3-dimethyl-1,3-dihydro-1λ^3-benzo[*d*][1,2]iodaoxole (**4.163**):

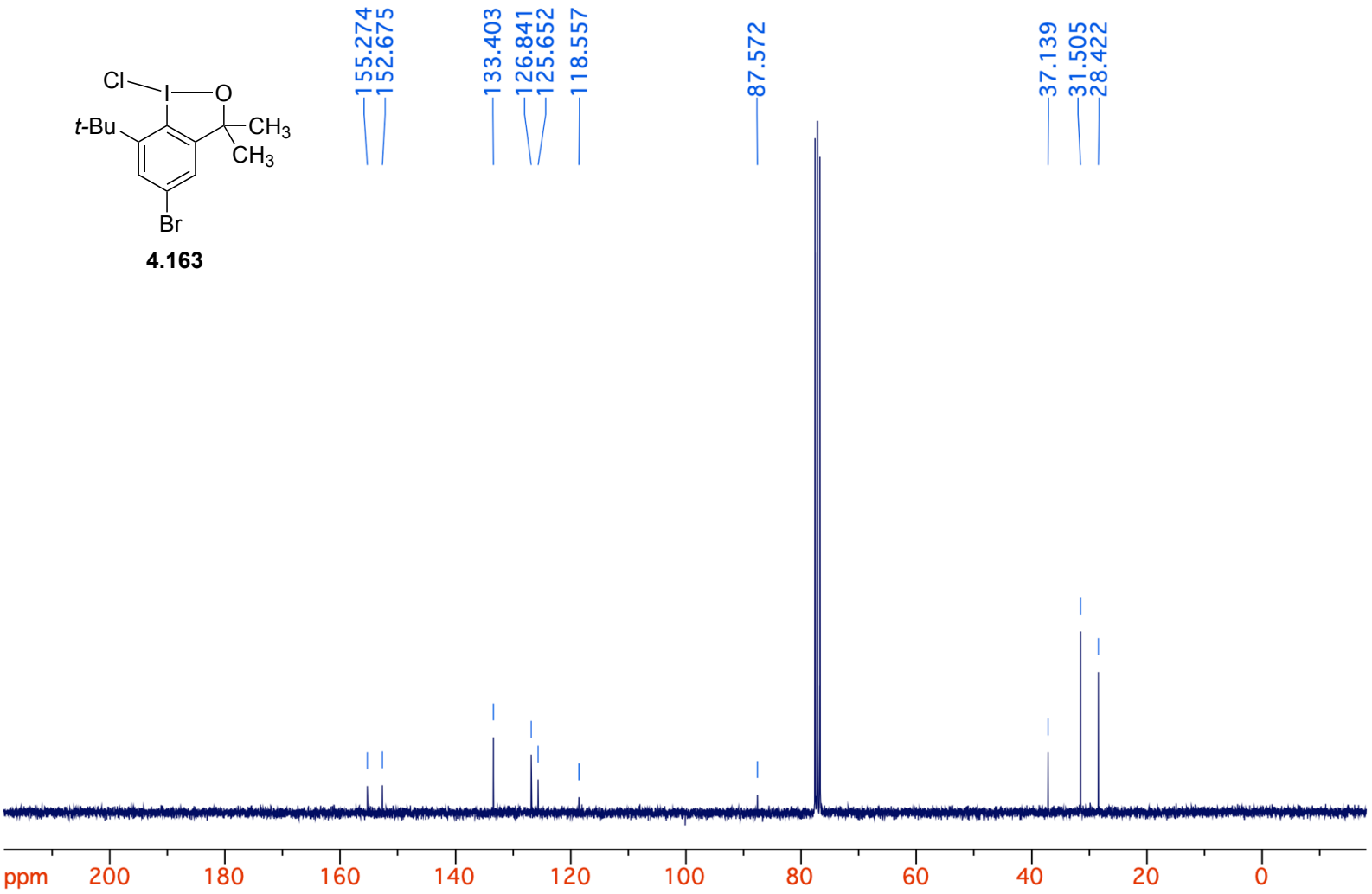


Figure B-60. ^{1}H-NMR (300 MHz, $CDCl_3$) of 1-(fluoromethyl)-2-iodo-3-methylbenzene (**4.166**):

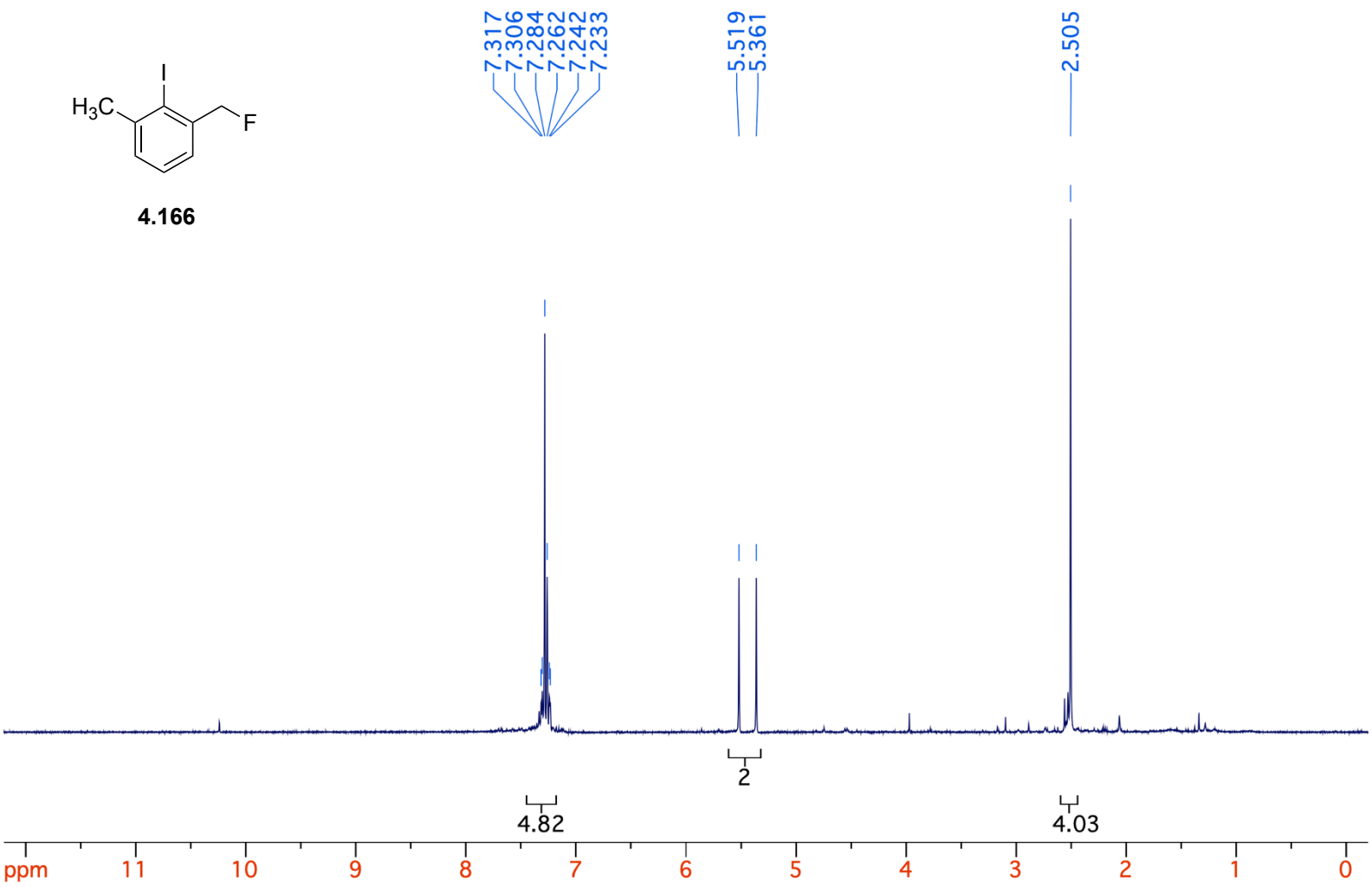
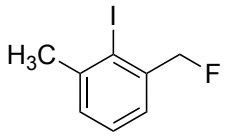


Figure B-61. ^{19}F-NMR (282 MHz, $CDCl_3$) of 1-(fluoromethyl)-2-iodo-3-methylbenzene (**4.166**):



4.166

Figure B-62. Proton coupled ^{19}F-NMR (282 MHz, $CDCl_3$) of 1-(fluoromethyl)-2-iodo-3-methylbenzene (**4.166**):

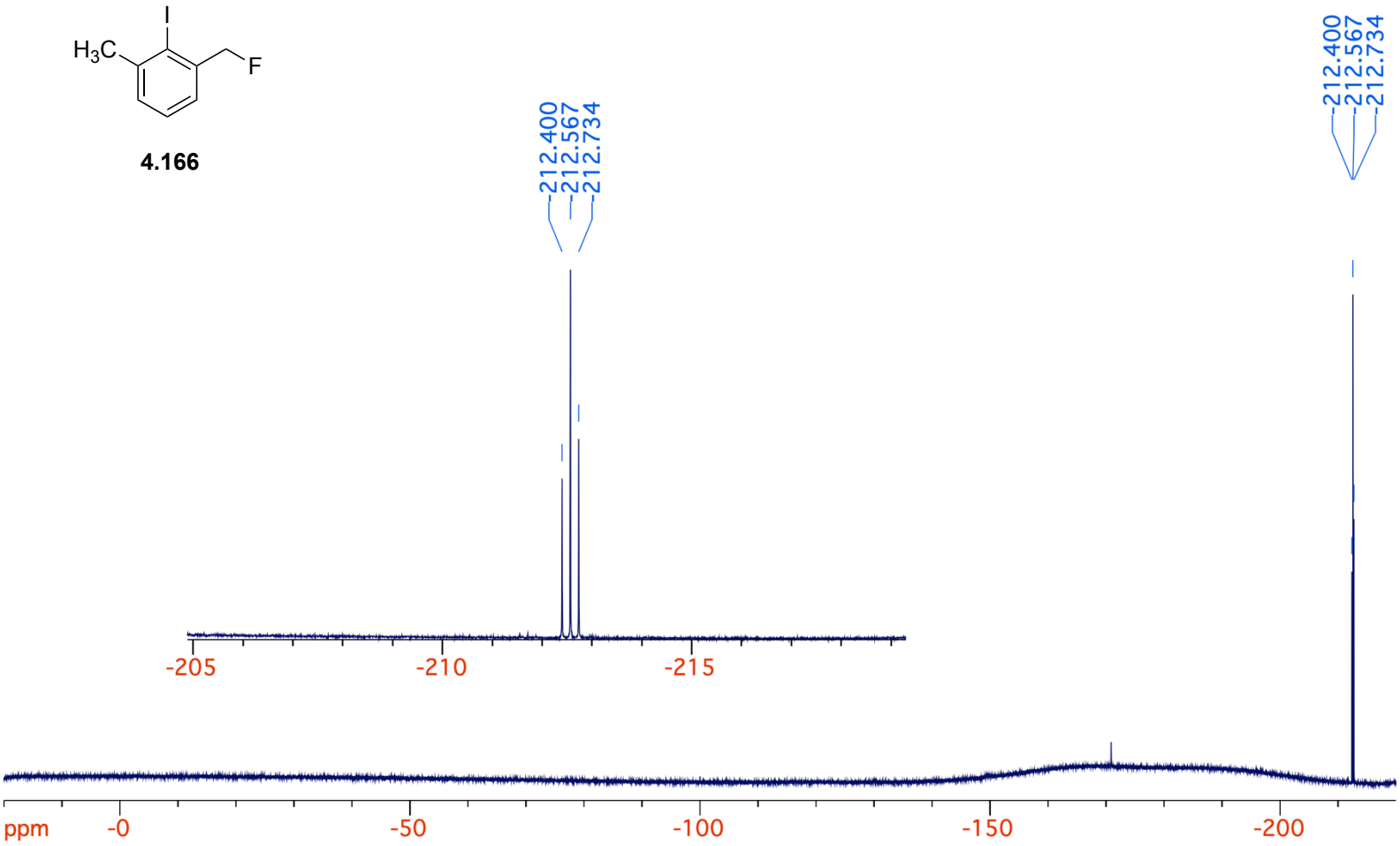


Figure B-63. ^{1}H-NMR (300 MHz, $CDCl_3$) of 3,3,8-trimethyl-3,4-dihydro-1*H*-1λ^3-benzo[*e*][1,2]iodaoxin-1-yl 4-methylbenzenesulfonate (**4.167**):

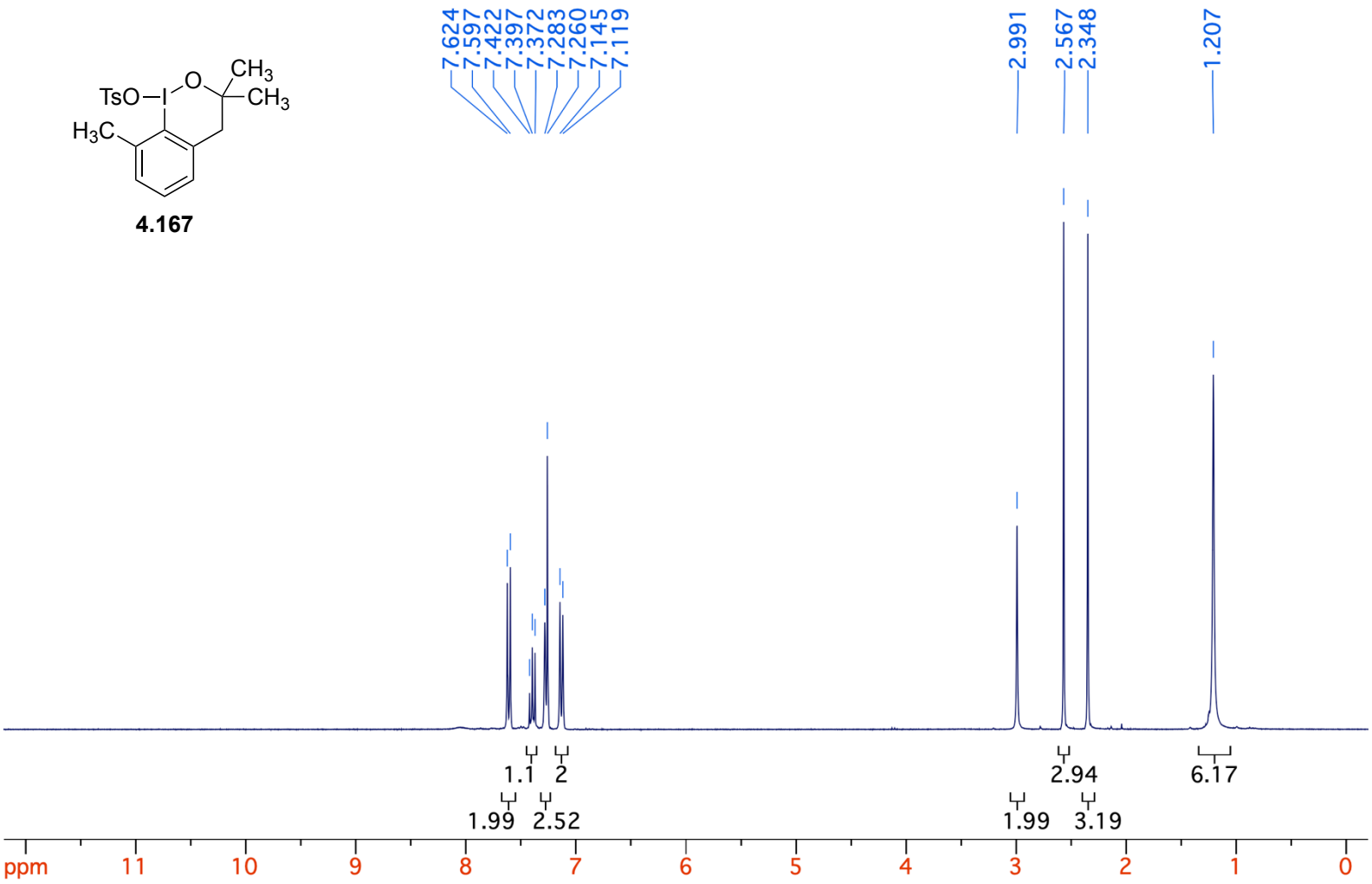


Figure B-64. ^{13}C-NMR (300 MHz, $CDCl_3$) of 3,3,8-trimethyl-3,4-dihydro-1*H*-1λ^3-benzo[*e*][1,2]iodaoxin-1-yl 4-methylbenzenesulfonate (**4.167**):

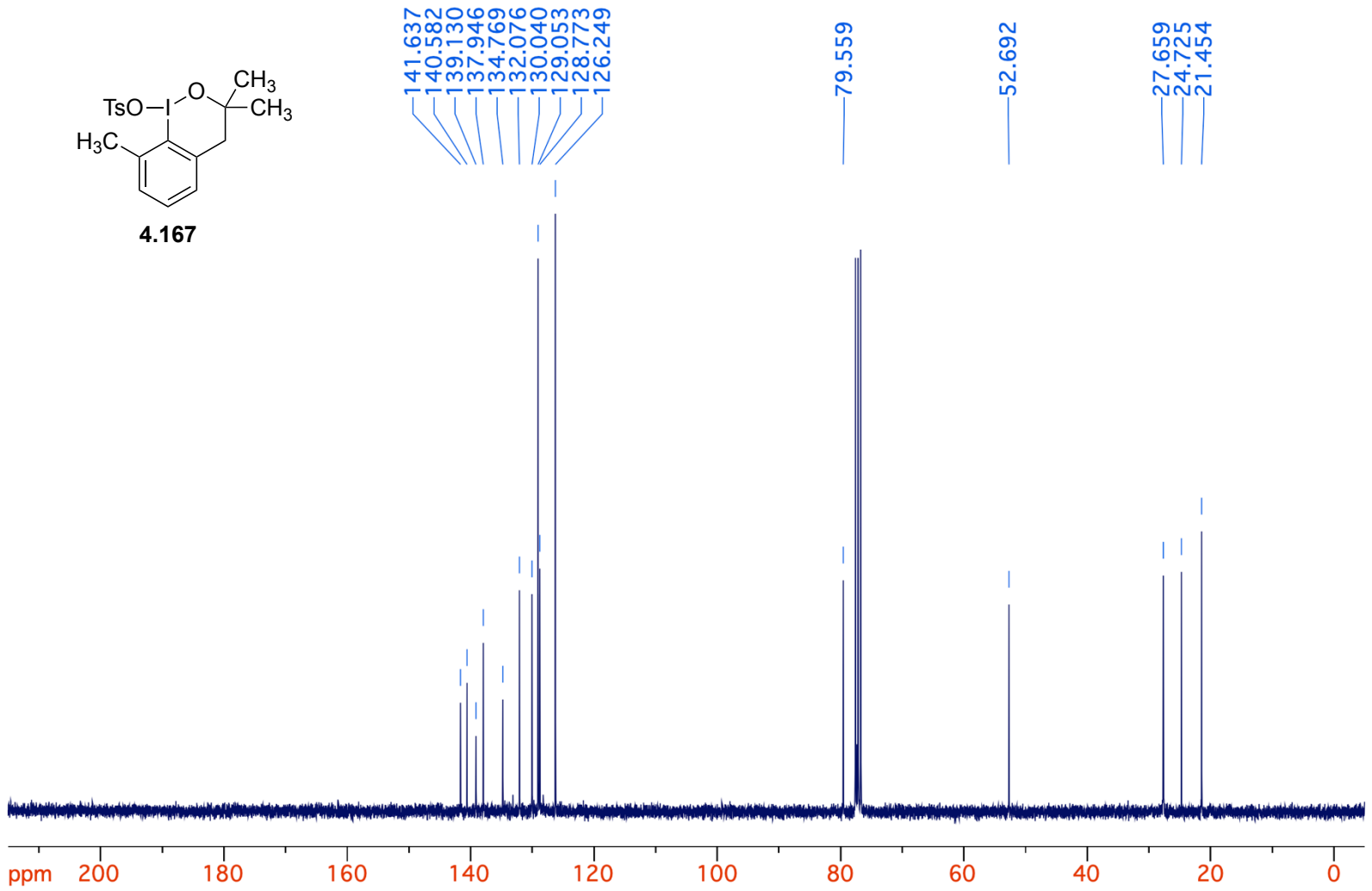


Figure B-65. ^{1}H-NMR (300 MHz, $CDCl_3$) of 1-fluoro-3,3,8-trimethyl-3,4-dihydro-1*H*-1λ^3-benzo[*e*][1,2]iodaoxine (**4.168**):

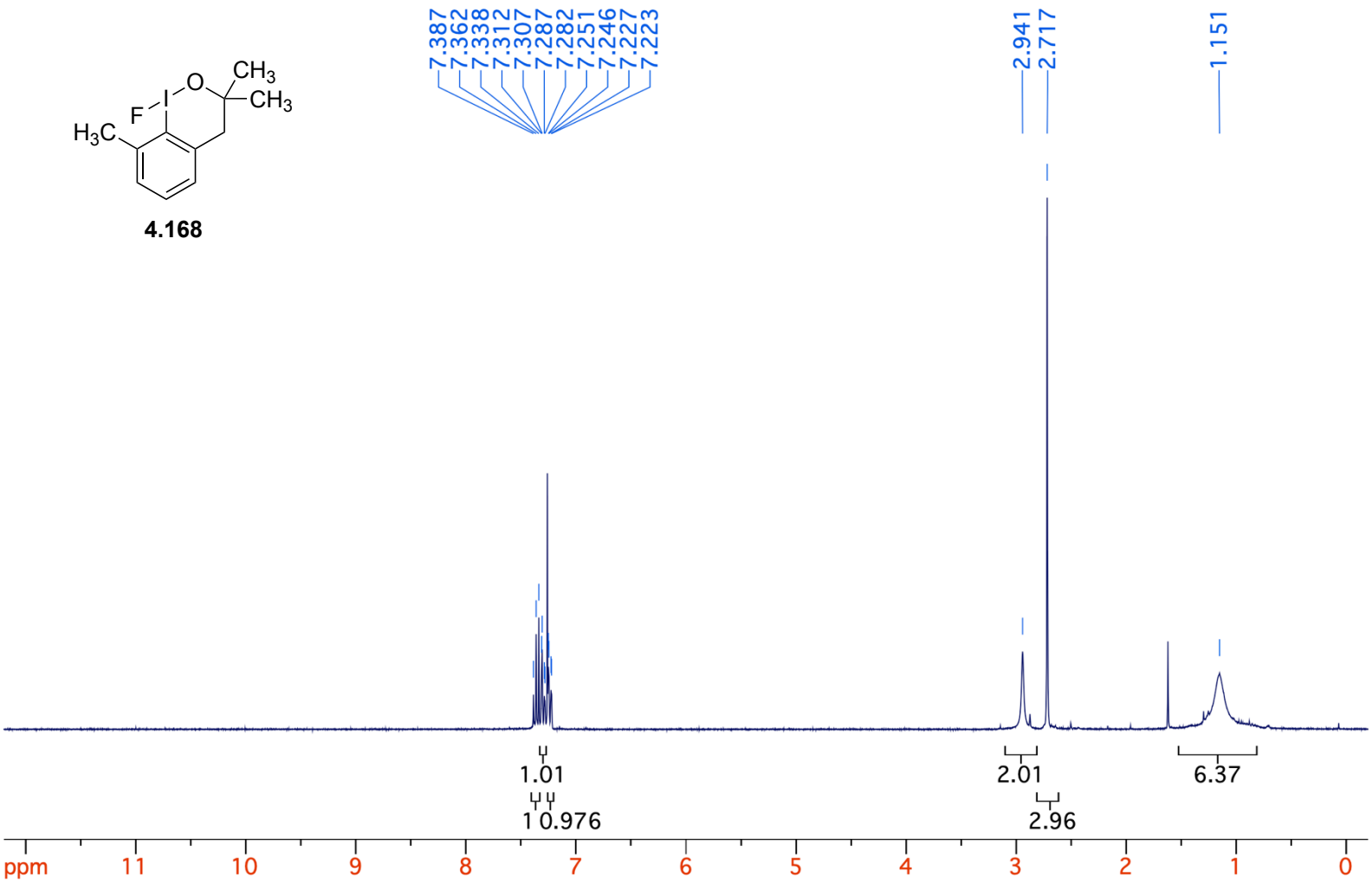


Figure B-66. ^{19}F-NMR (282 MHz, $CDCl_3$) of 1-fluoro-3,3,8-trimethyl-3,4-dihydro-1*H*-1λ^3-benzo[*e*][1,2]iodaoxine (**4.168**):

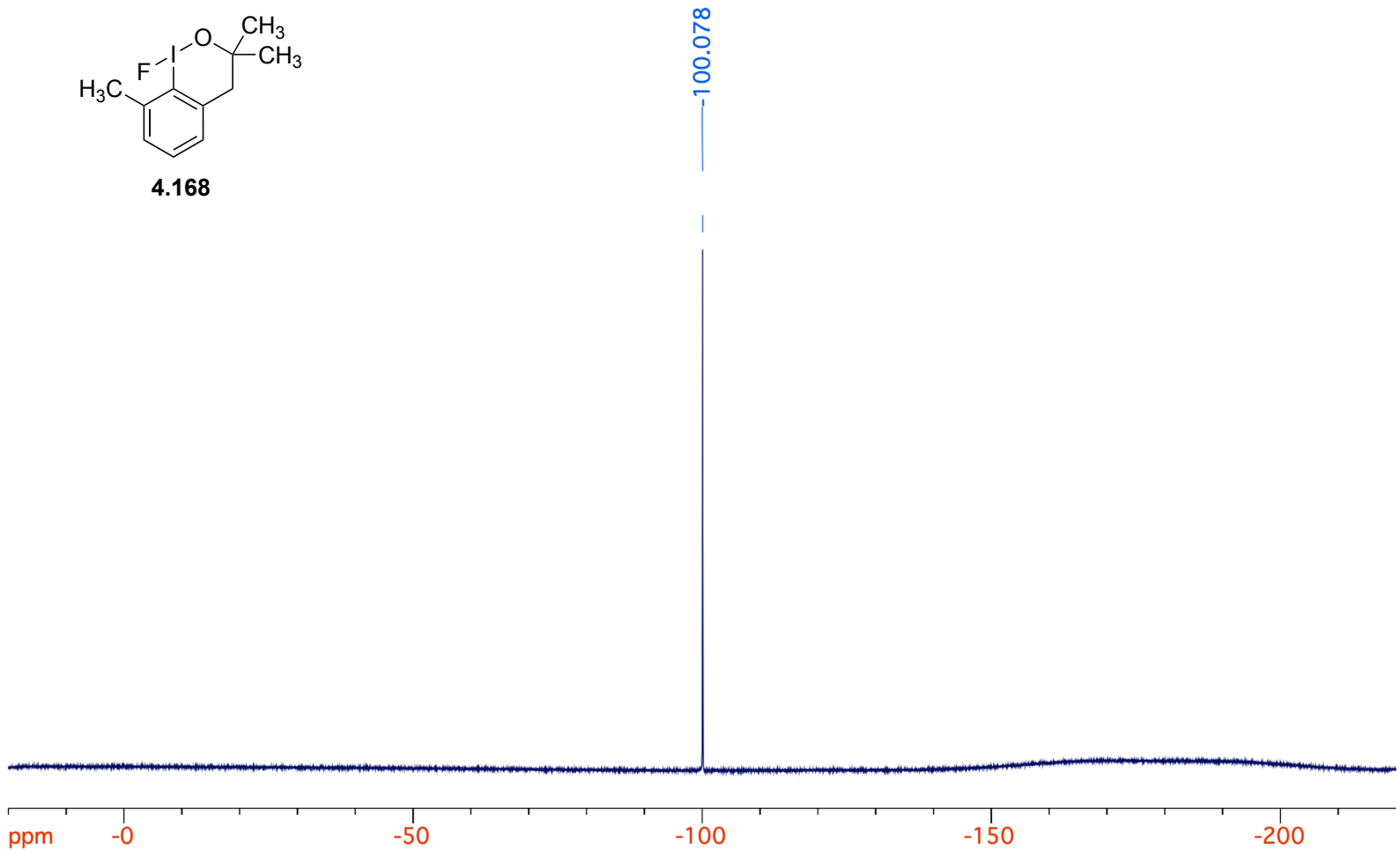


Figure B-67. ^{1}H-NMR (300 MHz, $CDCl_3$) of 1-chloro-3,3,8-trimethyl-3,4-dihydro-1*H*-1λ^3-benzo[*e*][1,2]iodaoxine (**4.169**):

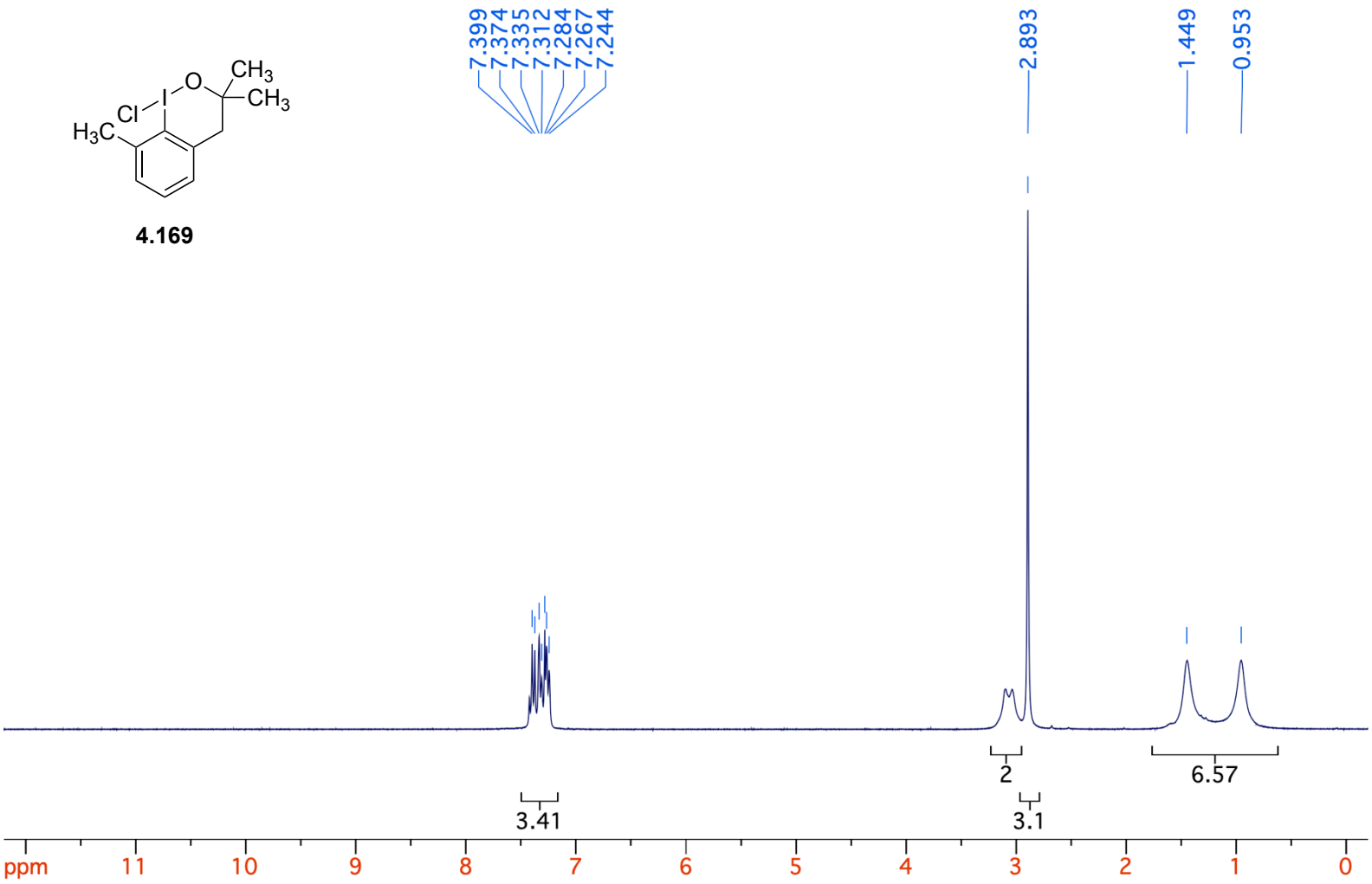
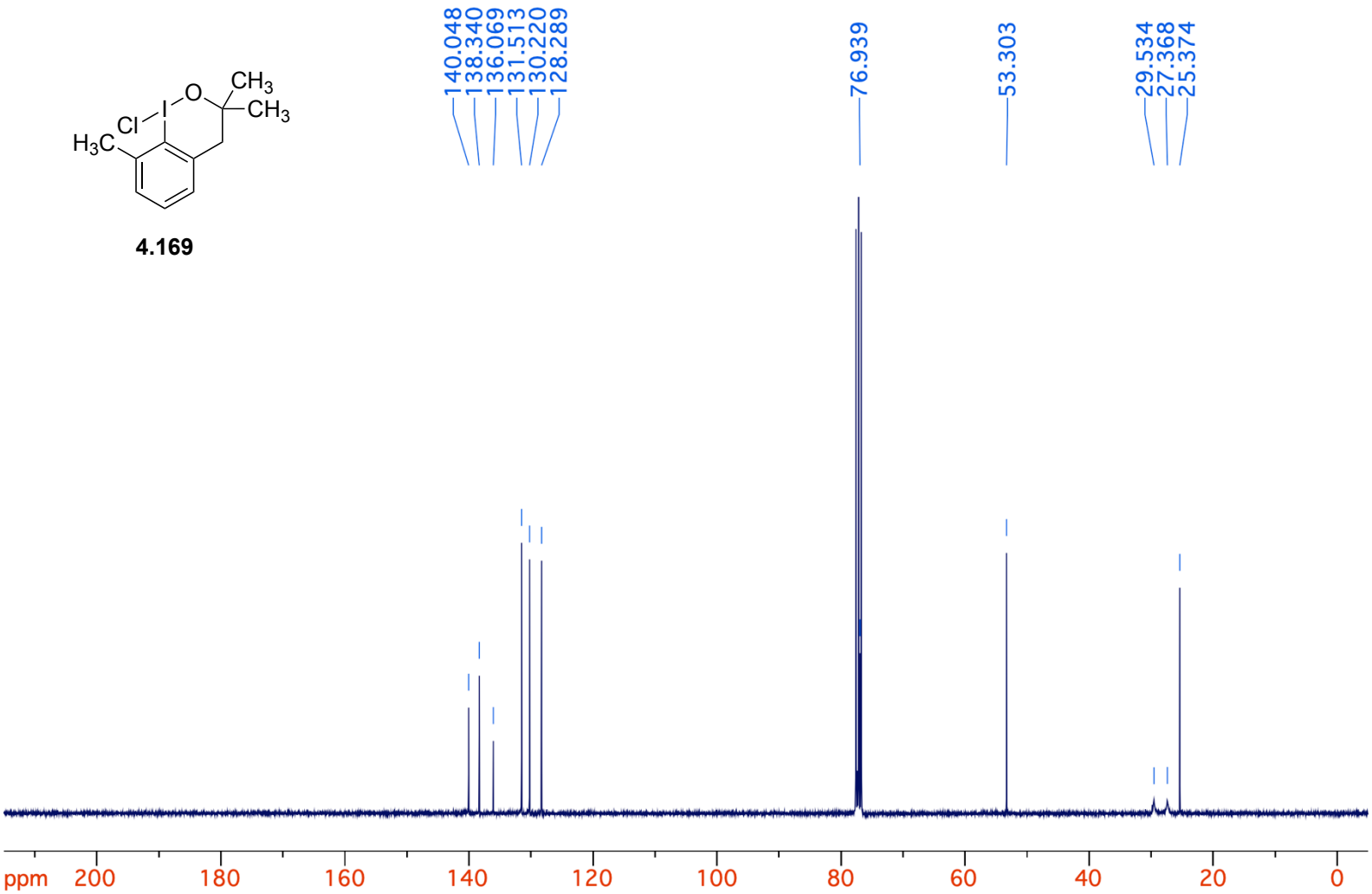


Figure B-68. ^{13}C-NMR (75 MHz, $CDCl_3$) of 1-chloro-3,3,8-trimethyl-3,4-dihydro-1*H*-1λ^3-benzo[*e*][1,2]iodaoxine (**4.169**):



4.169

Figure B-69. ^{1}H-NMR (300 MHz, $CDCl_3$) of 1-chloro-3,3-dimethyl-3,4-dihydro-1*H*-1λ^3-benzo[*e*][1,2]iodaoxine (**4.170**):

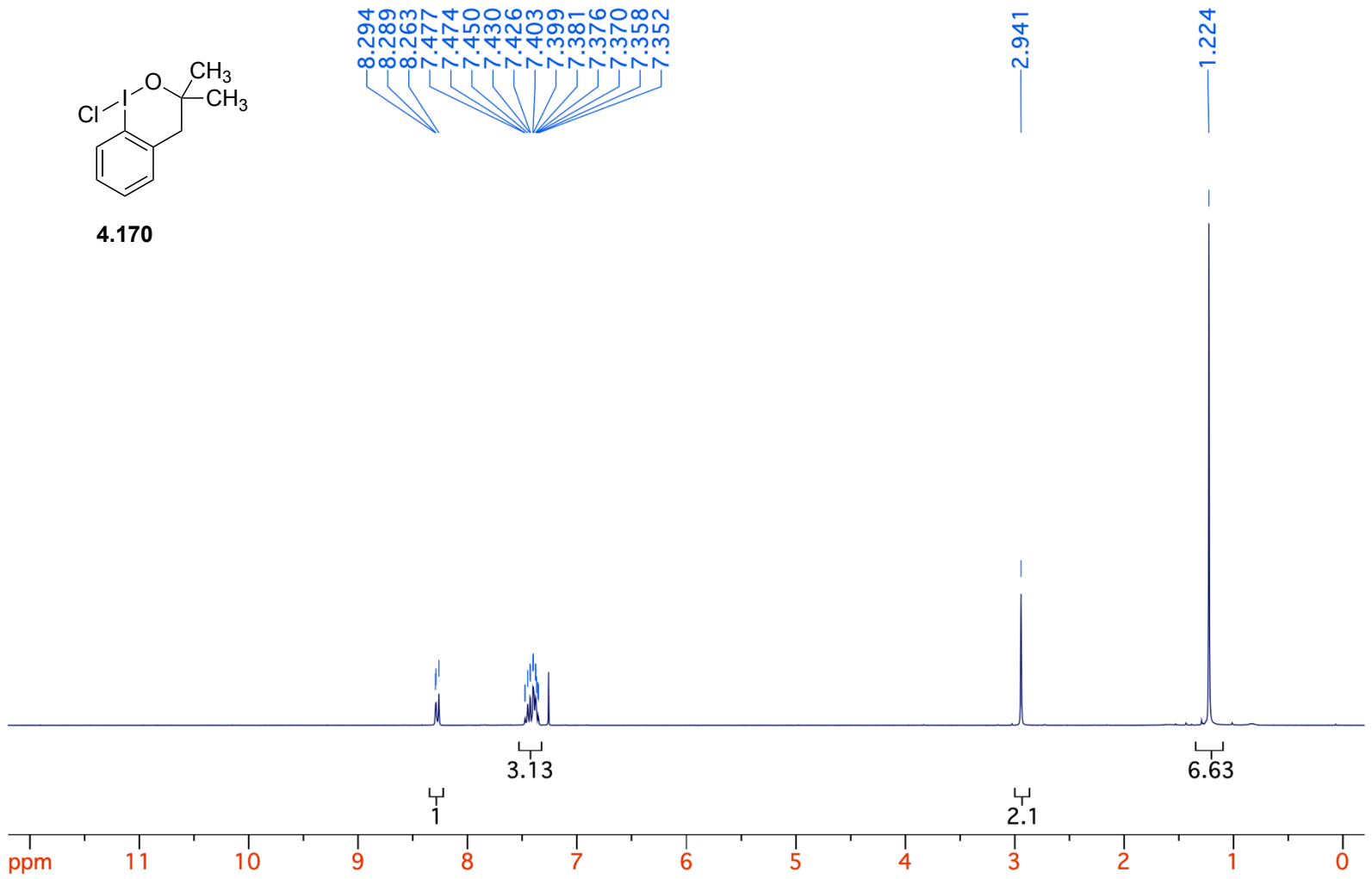
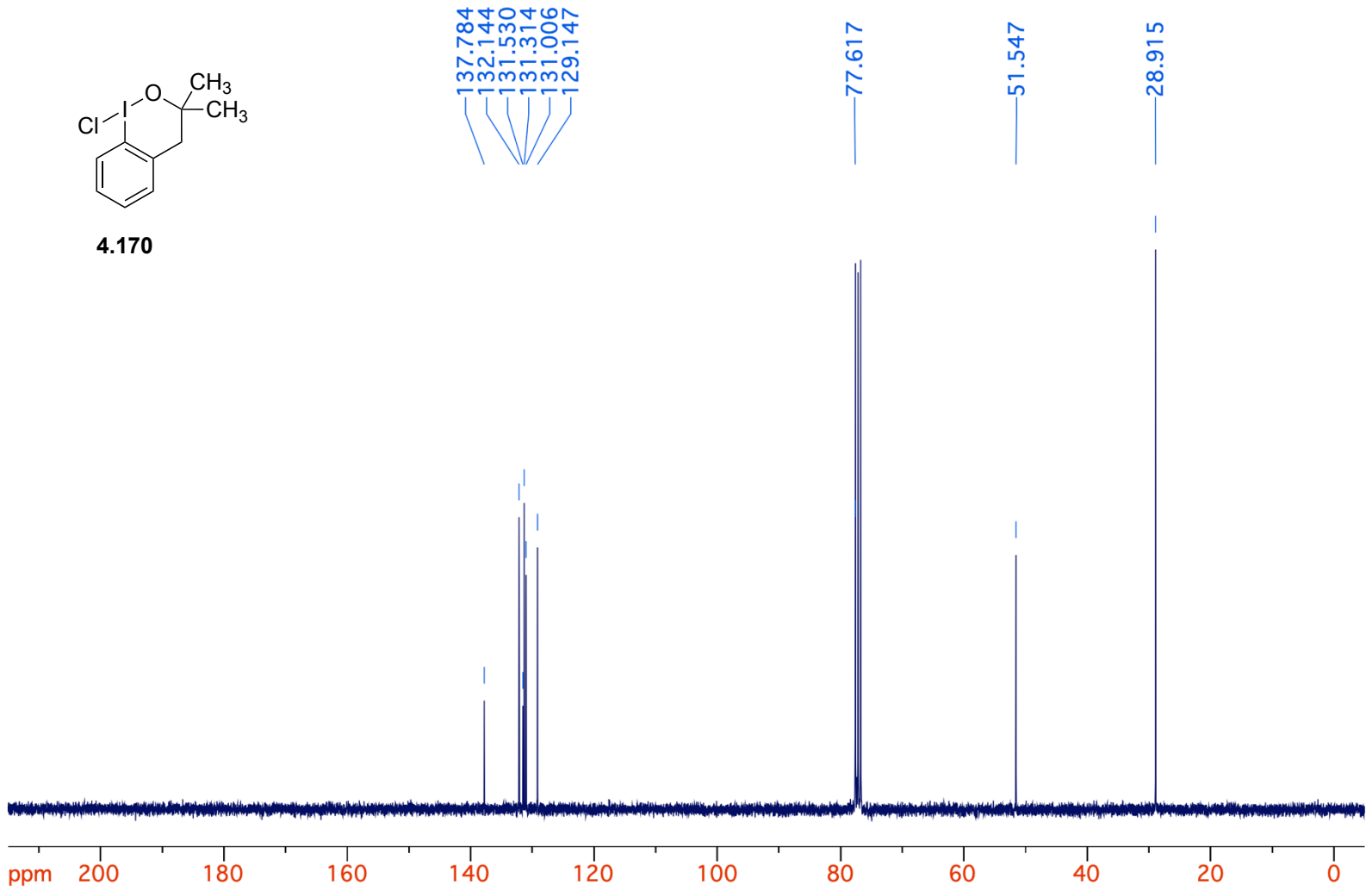


Figure B-70. ^{13}C-NMR (75 MHz, $CDCl_3$) of 1-chloro-3,3-dimethyl-3,4-dihydro-1*H*-1λ^3-benzo[*e*][1,2]iodaoxine (**4.170**):

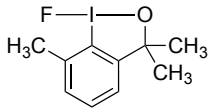


Appendix C

Chapter 4: X-ray Crystallography Data

This appendix contains the X-ray crystallography data collected for the structures in this thesis.

Crystallographic data for fluoroiodane 4.143 (R = CH_3):



4.143

Table 1. Crystal data and structure refinement for $C_{10}H_{12}FIO$

Empirical formula	$C_{10}H_{12}FIO$
Formula weight	294.10
Temperature	296(2) K
Wavelength	0.71073 Å
Crystal system	Triclinic
Space group	***P***-1
Unit cell dimensions	*a* = 7.901(4) Å, *b* = 8.298(4) Å, *c* = 8.819(5) Å *a*= 80.342(10)°, *b*= 69.934(10)°, *g* = 74.374(9)°.
Volume	521.1(5) $Å^3$
Z	2
Density (calculated)	1.874 g/cm^3
Absorption coefficient	3.046 mm^{-1}
F(000)	284
Crystal size	0.130 x 0.120 x 0.070 mm^3
Theta range for data collection	2.467 to 27.993°.
Index ranges	-10<=h<=10, -10<=k<=10, -11<=l<=11
Reflections collected	10625
Independent reflections	2510 [R(int) = 0.0140]
Completeness to theta = 25.242°	99.9 %
Absorption correction	Semi-empirical from equivalents
Max. and min. transmission	0.7460 and 0.6707
Refinement method	Full-matrix least-squares on F^2
Data / restraints / parameters	2510 / 0 / 166
Goodness-of-fit on F^2	1.057
Final R indices [I>2sigma(I)]	R1 = 0.0165, wR2 = 0.0409
R indices (all data)	R1 = 0.0180, wR2 = 0.0418
Extinction coefficient	n/a

Largest diff. peak and hole 0.683 and -0.230 e.Å^{-3}

Table 2. Atomic coordinates (x 10^4) and equivalent isotropic displacement parameters (Å^{2}x 10^3) for $C_{10}H_{12}FIO$

	x	y	z	U(eq)
I(1)	2340(1)	-493(1)	1083(1)	40(1)
F(1)	638(2)	-2022(2)	1185(2)	69(1)
O(1)	3765(2)	1172(2)	1184(2)	46(1)
C(1)	172(2)	1216(2)	2605(2)	37(1)
C(2)	-1524(3)	926(3)	3643(2)	46(1)
C(3)	-2719(3)	2300(4)	4473(3)	60(1)
C(4)	-2261(4)	3827(4)	4282(3)	63(1)
C(5)	-542(3)	4046(3)	3276(3)	53(1)
C(6)	714(3)	2724(2)	2426(2)	40(1)
C(7)	2637(3)	2855(2)	1300(2)	41(1)
C(8)	-2109(4)	-711(4)	3963(4)	66(1)
C(9)	3598(4)	3780(3)	1992(4)	58(1)
C(110)	2528(3)	3668(3)	-353(3)	51(1)
H(3)	-3820(40)	2130(40)	5210(40)	77(8)
H(4)	-3070(40)	4740(40)	4800(40)	74(8)
H(5)	-190(30)	5000(30)	3180(30)	51(6)
H(8A)	-2980(50)	-680(40)	4990(40)	90(10)
H(8B)	-1110(40)	-1550(40)	4110(40)	77(9)
H(8C)	-2380(40)	-910(40)	3010(40)	80(9)
H(9A)	2960(40)	4940(40)	2100(30)	64(8)
H(9B)	4830(40)	3630(30)	1320(30)	64(7)
H(9C)	3610(40)	3270(30)	3090(40)	73(8)
H(10A)	1800(40)	4830(40)	-250(30)	72(8)
H(10B)	1870(30)	3130(30)	-740(30)	54(6)
H(10C)	3710(40)	3620(30)	-1080(30)	57(6)

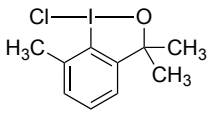
U(eq) is defined as one third of the trace of the orthogonalized U_{ij} tensor.

Table 3. Anisotropic displacement parameters ($Å^2 x\ 10^3$) for $C_{10}H_{12}FIO$

	U_{11}	U_{22}	U_{33}	U_{23}	U_{13}	U_{12}
I(1)	35(1)	31(1)	54(1)	-8(1)	-12(1)	-10(1)
F(1)	62(1)	57(1)	99(1)	-21(1)	-20(1)	-30(1)
O(1)	34(1)	36(1)	68(1)	-9(1)	-13(1)	-12(1)
C(1)	35(1)	37(1)	40(1)	-5(1)	-12(1)	-8(1)
C(2)	38(1)	56(1)	43(1)	-1(1)	-12(1)	-14(1)
C(3)	41(1)	81(2)	49(1)	-14(1)	-4(1)	-9(1)
C(4)	53(1)	67(2)	58(1)	-25(1)	-11(1)	5(1)
C(5)	58(1)	41(1)	62(1)	-15(1)	-20(1)	-5(1)
C(6)	41(1)	36(1)	44(1)	-5(1)	-15(1)	-7(1)
C(7)	41(1)	32(1)	54(1)	-6(1)	-16(1)	-13(1)
C(8)	57(1)	73(2)	67(2)	2(1)	-7(1)	-36(1)
C(9)	65(2)	48(1)	74(2)	-7(1)	-29(1)	-26(1)
C(110)	51(1)	51(1)	55(1)	1(1)	-16(1)	-21(1)

The anisotropic displacement factor exponent takes the form: $-2p^2[\ h^2\ a^{*2}U_{11} + ...\ + 2\ h\ k\ a^*\ b^*\ U_{12}\ ]$

Crystallographic data for chloroiodane 4.145 (R = CH_3):



4.145

Table 1. Crystal data and structure refinement for $C_{10}H_{12}ClIO$.

Empirical formula	$C_{10}H_{12}ClIO$
Formula weight	310.55
Temperature	296(2) K
Wavelength	0.71073 Å
Crystal system	Triclinic
Space group	*P*-1
Unit cell dimensions	*a* = 7.593(2) Å, *b* = 8.757(2) Å, *c* = 9.075(3) Å
	a = 86.375(6)°, *b* = 86.177(6)°, *g* = 68.396(6)°
Volume	559.2(3) $Å^3$
Z	2
Density (calculated)	1.844 g/cm^3
Absorption coefficient	3.063 mm^{-1}
F(000)	300
Crystal size	0.265 x 0.122 x 0.055 mm^3
Theta range for data collection	2.504 to 28.000°.
Index ranges	-10<=h<=10, -11<=k<=11, -11<=l<=11
Reflections collected	10187
Independent reflections	2682 [R(int) = 0.0128]
Completeness to theta = 25.242°	99.8 %
Absorption correction	Semi-empirical from equivalents
Max. and min. transmission	0.7460 and 0.6287
Refinement method	Full-matrix least-squares on F^2
Data / restraints / parameters	2682 / 0 / 121
Goodness-of-fit on F^2	1.176
Final R indices [I>2sigma(I)]	R1 = 0.0196, wR2 = 0.0491
R indices (all data)	R1 = 0.0213, wR2 = 0.0503
Extinction coefficient	n/a

Largest diff. peak and hole 1.136 and -0.333 e.Å^{-3}

Table 2. Atomic coordinates (x 10^4) and equivalent isotropic displacement parameters (Å^{2}x 10^3) for $C_{10}H_{12}ClIO$.

	x	y	z	U(eq)
I(1)	3204(1)	6251(1)	1712(1)	42(1)
Cl(1)	1052(1)	9148(1)	2418(1)	75(1)
O(1)	4730(3)	3883(2)	1156(2)	47(1)
C(1)	2789(3)	4930(3)	3674(2)	36(1)
C(2)	2383(3)	5513(3)	5104(2)	43(1)
C(3)	2156(3)	4382(4)	6179(3)	54(1)
C(4)	2338(4)	2814(4)	5861(3)	58(1)
C(5)	2831(3)	2272(3)	4445(3)	49(1)
C(6)	3096(3)	3331(2)	3323(2)	37(1)
C(7)	3779(3)	2805(2)	1749(2)	42(1)
C(8)	2264(4)	7164(4)	5544(3)	59(1)
C(9)	5300(4)	1088(3)	1711(3)	54(1)
C(10)	2118(4)	2945(3)	828(3)	58(1)
H(3)	1871	4700	7152	65
H(4)	2125	2115	6607	69
H(5)	2986	1201	4241	58
H(8A)	2398	7140	6590	89
H(8B)	1057	7971	5294	89
H(8C)	3259	7442	5030	89
H(9A)	4756	294	2061	82
H(9B)	6302	1024	2332	82
H(9C)	5801	864	715	82
H(10A)	1549	2182	1222	87
H(10B)	2562	2698	-176	87
H(10C)	1194	4043	859	87

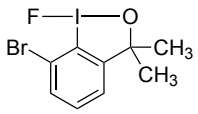
U(eq) is defined as one third of the trace of the orthogonalized U_{ij} tensor.

Table 3. Anisotropic displacement parameters ($Å^2 x\ 10^3$) for $C_{10}H_{12}ClIO$.

	U_{11}	U_{22}	U_{33}	U_{23}	U_{13}	U_{12}
I(1)	51(1)	29(1)	47(1)	-6(1)	9(1)	-16(1)
Cl(1)	82(1)	32(1)	100(1)	-10(1)	23(1)	-12(1)
O(1)	60(1)	33(1)	46(1)	-9(1)	14(1)	-17(1)
C(1)	33(1)	36(1)	39(1)	-3(1)	1(1)	-13(1)
C(2)	31(1)	52(1)	44(1)	-11(1)	0(1)	-12(1)
C(3)	41(1)	77(2)	39(1)	-2(1)	1(1)	-16(1)
C(4)	48(1)	70(2)	52(1)	18(1)	-3(1)	-22(1)
C(5)	46(1)	43(1)	57(1)	10(1)	-6(1)	-18(1)
C(6)	36(1)	35(1)	42(1)	0(1)	-4(1)	-13(1)
C(7)	53(1)	28(1)	44(1)	-4(1)	-2(1)	-14(1)
C(8)	53(1)	66(2)	60(2)	-30(1)	2(1)	-19(1)
C(9)	63(2)	31(1)	63(2)	-10(1)	-5(1)	-10(1)
C(10)	73(2)	45(1)	58(1)	-4(1)	-20(1)	-21(1)

The anisotropic displacement factor exponent takes the form: $-2p^2[\ h^2\ a^{*2}U_{11} + ...\ + 2\ h\ k\ a^*\ b^*\ U_{12}]$

Crystallographic data for fluoroiodane 4.147 (R = Br):



4.147

Table 1. Crystal data and structure refinement for C_9H_9BrFIO

Empirical formula	C_9H_9BrFIO
Formula weight	358.97
Temperature	296(2) K
Wavelength	0.71073 Å
Crystal system	Monoclinic
Space group	$P2_1/n$
Unit cell dimensions	a = 11.946(5) Å, b = 14.783(6) Å, c = 12.357(5) Å
	a= 90°, b= 106.113(8)°, g = 90°.
Volume	2096.6(14) $Å^3$
Z	8
Density (calculated)	2.275 g/cm^3
Absorption coefficient	6.839 mm^{-1}
F(000)	1344
Crystal size	0.130 x 0.120 x 0.040 mm^3
Theta range for data collection	2.200 to 27.997°.
Index ranges	-15<=h<=15, -19<=k<=19, -16<=l<=16
Reflections collected	32864
Independent reflections	5062 [R(int) = 0.0207]
Completeness to theta = 25.242°	99.9 %
Absorption correction	Semi-empirical from equivalents
Max. and min. transmission	0.7460 and 0.5930
Refinement method	Full-matrix least-squares on F^2
Data / restraints / parameters	5062 / 0 / 239
Goodness-of-fit on F^2	1.131
Final R indices [I>2sigma(I)]	R1 = 0.0232, wR2 = 0.0471
R indices (all data)	R1 = 0.0285, wR2 = 0.0486
Extinction coefficient	n/a

Largest diff. peak and hole 1.365 and -1.071 e.Å^{-3}

Table 2. Atomic coordinates (x 10^4) and equivalent isotropic displacement parameters (Å^{2}x 10^3) for C_9H_9BrFIO

	x	y	z	U(eq)
I(1A)	4430(1)	3938(1)	6453(1)	33(1)
Br(1A)	1189(1)	4448(1)	5844(1)	58(1)
F(1A)	3597(2)	5088(1)	6738(2)	51(1)
C(1A)	3025(2)	3112(2)	6575(2)	29(1)
C(2A)	1859(2)	3318(2)	6367(2)	35(1)
C(3A)	1094(3)	2647(2)	6488(3)	46(1)
C(4A)	1497(3)	1791(2)	6809(3)	47(1)
C(5A)	2655(3)	1584(2)	6991(3)	40(1)
C(6A)	3432(2)	2242(2)	6864(2)	31(1)
C(7A)	4725(3)	2070(2)	7042(3)	38(1)
O(8A)	5095(2)	2704(1)	6326(2)	41(1)
C(9A)	5381(3)	2210(3)	8279(3)	58(1)
C(10A)	4972(4)	1142(2)	6634(4)	63(1)
I(1B)	7259(1)	3343(1)	4930(1)	41(1)
Br(1B)	8220(1)	4057(1)	7989(1)	76(1)
F(1B)	6512(2)	4267(1)	5756(2)	58(1)
C(1B)	7915(2)	2572(2)	6414(2)	31(1)
C(2B)	8227(3)	2843(2)	7529(3)	38(1)
C(3B)	8640(3)	2210(2)	8368(3)	46(1)
C(4B)	8734(3)	1319(2)	8084(3)	48(1)
C(5B)	8484(3)	1064(2)	6976(3)	40(1)
C(6B)	8076(2)	1685(2)	6118(2)	32(1)
C(7B)	7817(3)	1465(2)	4869(3)	39(1)
O(8B)	7988(2)	2291(2)	4329(2)	46(1)
C(9B)	6563(3)	1131(3)	4408(3)	55(1)
C(10B)	8673(4)	794(3)	4625(3)	57(1)

H(3A)	305	2776	6351	56
H(4A)	981	1348	6905	57
H(5A)	2917	1000	7201	48
H(9AA)	6202	2143	8375	87
H(9AB)	5129	1768	8731	87
H(9AC)	5225	2806	8510	87
H(10A)	5789	1088	6700	95
H(10B)	4536	1066	5861	95
H(10C)	4748	684	7085	95
H(3B)	8852	2386	9120	55
H(4B)	8969	886	8648	58
H(5B)	8590	465	6797	48
H(9BA)	6402	1023	3613	82
H(9BB)	6037	1581	4540	82
H(9BC)	6464	580	4781	82
H(10D)	8510	711	3826	86
H(10E)	8600	225	4974	86
H(10F)	9452	1020	4920	86

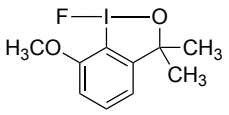
U(eq) is defined as one third of the trace of the orthogonalized U_{ij} tensor.

Table 3. Anisotropic displacement parameters ($Å^2 x\ 10^3$) for C_9H_9BrFIO

	U_{11}	U_{22}	U_{33}	U_{23}	U_{13}	U_{12}
I(1A)	36(1)	26(1)	39(1)	1(1)	14(1)	-2(1)
Br(1A)	46(1)	40(1)	76(1)	4(1)	-4(1)	13(1)
F(1A)	58(1)	28(1)	70(1)	-7(1)	19(1)	4(1)
C(1A)	32(1)	26(1)	28(1)	1(1)	9(1)	-2(1)
C(2A)	33(1)	33(1)	36(2)	0(1)	4(1)	3(1)
C(3A)	28(1)	54(2)	54(2)	1(2)	6(1)	-4(1)
C(4A)	43(2)	45(2)	52(2)	6(2)	11(2)	-16(1)
C(5A)	48(2)	30(2)	43(2)	6(1)	13(1)	-3(1)
C(6A)	36(1)	28(1)	30(1)	3(1)	12(1)	2(1)
C(7A)	40(2)	30(1)	49(2)	10(1)	21(1)	10(1)
O(8A)	46(1)	31(1)	56(1)	8(1)	30(1)	7(1)
C(9A)	39(2)	74(3)	58(2)	21(2)	10(2)	13(2)
C(10A)	73(3)	34(2)	99(3)	11(2)	51(2)	17(2)
I(1B)	38(1)	35(1)	53(1)	16(1)	17(1)	6(1)
Br(1B)	88(1)	41(1)	85(1)	-25(1)	1(1)	9(1)
F(1B)	58(1)	41(1)	81(2)	11(1)	30(1)	12(1)
C(1B)	26(1)	27(1)	42(2)	5(1)	11(1)	0(1)
C(2B)	34(1)	30(1)	50(2)	-6(1)	11(1)	1(1)
C(3B)	46(2)	50(2)	37(2)	-6(1)	6(1)	2(2)
C(4B)	60(2)	44(2)	40(2)	12(1)	12(2)	15(2)
C(5B)	44(2)	26(1)	49(2)	3(1)	14(1)	3(1)
C(6B)	29(1)	28(1)	39(2)	2(1)	11(1)	-1(1)
C(7B)	45(2)	35(2)	38(2)	2(1)	14(1)	0(1)
O(8B)	53(1)	44(1)	48(1)	11(1)	26(1)	6(1)
C(9B)	55(2)	59(2)	47(2)	-6(2)	9(2)	-15(2)
C(10B)	73(3)	49(2)	55(2)	-5(2)	28(2)	12(2)

The anisotropic displacement factor exponent takes the form: $-2p^2[\ h^2\ a^{*2}U_{11} + ...\ + 2\ h\ k\ a^*\ b^*\ U_{12}]$

Crystallographic data for fluoroiodane 4.148 (R = OCH_3):



4.148

Table 1. Crystal data and structure refinement for $C_{10}H_{12}FIO_2$

Empirical formula	$C_{10}H_{12}FIO_2$
Formula weight	310.10
Temperature	296(2) K
Wavelength	0.71073 Å
Crystal system	Monoclinic
Space group	$P2_1/n$
Unit cell dimensions	a = 11.391(4) Å, b = 7.188(3) Å, c = 13.288(5) Å
	a = 90°, b = 99.206(8)°, g = 90°
Volume	1074.1(7) $Å^3$
Z	4
Density (calculated)	1.918 g/cm^3
Absorption coefficient	2.968 mm^{-1}
F(000)	600
Crystal size	0.240 x 0.200 x 0.050 mm^3
Theta range for data collection	2.568 to 27.997°.
Index ranges	-15<=h<=14, -9<=k<=9, -17<=l<=17
Reflections collected	26268
Independent reflections	2600 [R(int) = 0.0169]
Completeness to theta = 25.242°	99.9 %
Absorption correction	Semi-empirical from equivalents
Max. and min. transmission	0.7460 and 0.6319
Refinement method	Full-matrix least-squares on F^2
Data / restraints / parameters	2600 / 0 / 130
Goodness-of-fit on F^2	1.025
Final R indices [I>2sigma(I)]	R1 = 0.0207, wR2 = 0.0564
R indices (all data)	R1 = 0.0220, wR2 = 0.0577
Largest diff. peak and hole	1.514 and -0.681 $e.Å^{-3}$

Table 2. Atomic coordinates (x 10^4) and equivalent isotropic displacement parameters ($Å^2$x 10^3) for $C_{10}H_{12}FIO_2$

	x	y	z	U(eq)
I(1)	3524(1)	1647(1)	60(1)	37(1)
F(1)	1718(2)	1797(2)	-373(2)	58(1)
O(1)	5284(2)	1703(2)	655(1)	42(1)
O(2)	1850(2)	5412(3)	237(1)	46(1)
C(1)	3566(2)	3899(3)	1085(2)	28(1)
C(2)	2718(2)	5321(3)	1064(2)	32(1)
C(3)	2842(2)	6540(3)	1891(2)	38(1)
C(4)	3791(2)	6349(3)	2685(2)	39(1)
C(5)	4670(2)	5017(3)	2654(2)	35(1)
C(6)	4562(2)	3786(3)	1832(2)	28(1)
C(7)	1096(3)	6996(4)	130(2)	51(1)
C(8)	5481(2)	2275(3)	1713(2)	32(1)
C(9)	6749(2)	3030(4)	1915(2)	45(1)
C(10)	5335(2)	624(4)	2402(2)	45(1)
H(3)	2288	7483	1912	45
H(4)	3838	7128	3249	47
H(5)	5322	4949	3173	42
H(7A)	621	6993	-535	77
H(7B)	1572	8105	214	77
H(7C)	586	6961	639	77
H(9A)	6950	3367	2621	68
H(9B)	6804	4107	1498	68
H(9C)	7289	2092	1754	68
H(10A)	5599	966	3100	67
H(10B)	5801	-403	2225	67
H(10C)	4513	268	2315	67

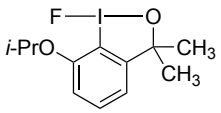
U(eq) is defined as one third of the trace of the orthogonalized U_{ij} tensor

Table 3. Anisotropic displacement parameters ($Å^2 x\ 10^3$) for $C_{10}H_{12}FIO_2$

	U_{11}	U_{22}	U_{33}	U_{23}	U_{13}	U_{12}
I(1)	33(1)	41(1)	34(1)	-12(1)	-5(1)	9(1)
F(1)	35(1)	62(1)	68(1)	-17(1)	-14(1)	7(1)
O(1)	31(1)	53(1)	39(1)	-12(1)	0(1)	11(1)
O(2)	43(1)	45(1)	46(1)	-6(1)	-10(1)	19(1)
C(1)	29(1)	27(1)	29(1)	-3(1)	2(1)	2(1)
C(2)	28(1)	31(1)	34(1)	0(1)	3(1)	4(1)
C(3)	37(1)	30(1)	47(1)	-5(1)	8(1)	6(1)
C(4)	43(1)	33(1)	41(1)	-11(1)	4(1)	-2(1)
C(5)	33(1)	34(1)	35(1)	-5(1)	-2(1)	-3(1)
C(6)	26(1)	28(1)	31(1)	0(1)	2(1)	0(1)
C(7)	49(1)	46(1)	55(2)	6(1)	-3(1)	22(1)
C(8)	25(1)	35(1)	33(1)	-3(1)	0(1)	3(1)
C(9)	27(1)	57(2)	51(1)	-4(1)	4(1)	-3(1)
C(10)	42(1)	38(1)	54(1)	8(1)	7(1)	9(1)

The anisotropic displacement factor exponent takes the form: $-2p^2[\ h^2\ a^{*2}U_{11} + ...\ + 2\ h\ k\ a^*\ b^*\ U_{12}\ ]$

Crystallographic data for fluoroiodane 4.149 (R = O*i*-Pr):



4.149

Table 1. Crystal data and structure refinement for $C_{12}H_{16}FIO_2$

Empirical formula	$C_{12}H_{16}FIO_2$
Formula weight	338.15
Temperature	296(2) K
Wavelength	0.71073 Å
Crystal system	Orthorhombic
Space group	*Pna*2$_1$
Unit cell dimensions	a = 8.3138(6) Å, b = 9.9189(6) Å, c = 15.1741(9) Å α= 90°, β= 90°, γ = 90°.
Volume	1251.31(14) Å^3
Z	4
Density (calculated)	1.795 g/cm^3
Absorption coefficient	2.556 mm^{-1}
F(000)	664
Crystal size	0.120 x 0.100 x 0.060 mm^3
Theta range for data collection	2.453 to 27.998°.
Index ranges	-10<=h<=10, -12<=k<=13, -20<=l<=20
Reflections collected	26303
Independent reflections	3009 [R(int) = 0.0283]
Completeness to theta = 25.242°	99.9 %
Absorption correction	Semi-empirical from equivalents
Max. and min. transmission	0.7460 and 0.6163
Refinement method	Full-matrix least-squares on F^2
Data / restraints / parameters	3009 / 1 / 149
Goodness-of-fit on F^2	1.032
Final R indices [I>2sigma(I)]	R1 = 0.0177, wR2 = 0.0397
R indices (all data)	R1 = 0.0236, wR2 = 0.0421
Absolute structure parameter	0.034(11)

Extinction coefficient	n/a
Largest diff. peak and hole	0.406 and -0.303 e.Å^{-3}

Table 2. Atomic coordinates (x 10^4) and equivalent isotropic displacement parameters (Å^{2}x 10^3) for $C_{12}H_{16}FIO_2$

	x	y	z	U(eq)
I(1)	4928(1)	6544(1)	6191(1)	34(1)
O(1)	3065(3)	6032(3)	5399(2)	42(1)
O(2)	8360(2)	4740(2)	6167(2)	45(1)
F(1)	6981(3)	6927(2)	6914(2)	51(1)
C(1)	6122(4)	5278(3)	5281(2)	30(1)
C(2)	7602(4)	4611(4)	5385(2)	34(1)
C(3)	8148(4)	3861(4)	4678(2)	40(1)
C(4)	7271(4)	3766(4)	3907(2)	43(1)
C(5)	5800(5)	4395(4)	3829(2)	41(1)
C(6)	5204(4)	5150(4)	4523(2)	33(1)
C(7)	3565(4)	5852(4)	4503(2)	34(1)
C(8)	9823(3)	3995(4)	6333(4)	41(1)
C(9)	3685(5)	7200(4)	4037(3)	52(1)
C(10)	2292(5)	4951(5)	4082(3)	52(1)
C(11)	10646(5)	4711(4)	7088(3)	44(1)
C(12)	9418(6)	2547(4)	6559(3)	55(1)
H(3)	9125	3411	4723	49
H(4)	7679	3274	3435	52
H(5)	5209	4312	3312	49
H(8)	10512	4020	5809	49
H(9A)	4445	7763	4339	77
H(9B)	2650	7629	4034	77
H(9C)	4037	7061	3441	77
H(10A)	1247	5339	4171	77
H(10B)	2329	4073	4348	77

H(10C)	2500	4873	3462	77
H(11A)	11589	4217	7258	66
H(11B)	9922	4770	7579	66
H(11C)	10950	5602	6905	66
H(12A)	8801	2524	7094	82
H(12B)	10394	2044	6638	82
H(12C)	8802	2156	6089	82

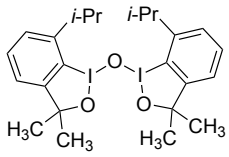
U(eq) is defined as one third of the trace of the orthogonalized U_{ij} tensor.

Table 3. Anisotropic displacement parameters ($Å^2 x\ 10^3$) for $C_{12}H_{16}FIO_2$

	U_{11}	U_{22}	U_{33}	U_{23}	U_{13}	U_{12}
I(1)	35(1)	39(1)	29(1)	-4(1)	0(1)	4(1)
O(1)	32(1)	59(2)	36(1)	-5(1)	2(1)	1(1)
O(2)	42(1)	53(1)	40(1)	-8(2)	-9(2)	19(1)
F(1)	48(1)	56(1)	48(1)	-14(1)	-14(1)	8(1)
C(1)	35(2)	28(2)	28(2)	0(1)	4(1)	0(1)
C(2)	34(2)	33(2)	35(2)	2(2)	1(1)	0(1)
C(3)	38(2)	40(2)	44(2)	-2(2)	6(2)	7(2)
C(4)	51(2)	44(2)	33(2)	-6(2)	11(2)	4(2)
C(5)	47(2)	48(2)	28(2)	-2(2)	-2(2)	4(2)
C(6)	35(2)	33(2)	31(2)	4(1)	2(1)	-1(1)
C(7)	33(2)	38(2)	32(2)	0(2)	-1(1)	2(1)
C(8)	30(1)	47(2)	46(4)	0(2)	1(2)	4(1)
C(9)	53(2)	47(2)	56(2)	13(2)	6(2)	8(2)
C(10)	39(2)	61(3)	55(2)	-8(2)	-6(2)	-2(2)
C(11)	38(2)	43(2)	52(2)	1(2)	-6(2)	2(2)
C(12)	56(2)	44(2)	65(3)	1(2)	-9(2)	-1(2)

The anisotropic displacement factor exponent takes the form: $-2\pi^2[\ h^2\ a^{*2}U_{11} + ...\ + 2\ h\ k\ a^*\ b^*\ U_{12}\ ]$

Crystallographic data for dimer 4.151 (R = *i*-Pr):



4.151

Table 1. Crystal data and structure refinement for $C_{24}H_{32}I_2O_3$

Empirical formula	$C_{24}H_{32}I_2O_3$
Formula weight	622.29
Temperature	200(2) K
Wavelength	0.71073 Å
Crystal system	Monoclinic
Space group	$P2_1/n$
Unit cell dimensions	a = 12.094(9) Å, b = 11.429(8) Å, c = 19.655(13) Å
	a = 90°, b = 107.64(2)°, g = 90°
Volume	2589(3) $Å^3$
Z	4
Density (calculated)	1.596 g/cm^3
Absorption coefficient	2.449 mm^{-1}
F(000)	1224
Crystal size	0.160 x 0.080 x 0.020 mm^3
Theta range for data collection	2.339 to 27.998°.
Index ranges	-15<=h<=14, -14<=k<=15, -24<=l<=25
Reflections collected	31880
Independent reflections	6205 [R(int) = 0.0368]
Completeness to theta = 25.242°	99.9 %
Absorption correction	Semi-empirical from equivalents
Max. and min. transmission	0.7460 and 0.5477
Refinement method	Full-matrix least-squares on F^2
Data / restraints / parameters	6205 / 0 / 270
Goodness-of-fit on F^2	1.106
Final R indices [I>2sigma(I)]	R1 = 0.0243, wR2 = 0.0537
R indices (all data)	R1 = 0.0333, wR2 = 0.0584

Extinction coefficient	n/a
Largest diff. peak and hole	1.141 and -1.215 e.Å^{-3}

Table 2. Atomic coordinates (x 10^4) and equivalent isotropic displacement parameters (Å^{2}x 10^3) for $C_{24}H_{32}I_2O_3$

	x	y	z	U(eq)
I(1A)	6236(1)	3745(1)	5512(1)	27(1)
O(1A)	6110(2)	5107(2)	4762(1)	31(1)
C(1A)	7887(2)	3631(2)	5314(1)	21(1)
C(2A)	7791(2)	4120(2)	4641(1)	22(1)
C(3A)	8755(2)	4023(3)	4385(2)	28(1)
C(4A)	9769(2)	3476(3)	4805(2)	32(1)
C(5A)	9856(2)	3077(3)	5490(2)	30(1)
C(6A)	8918(2)	3159(2)	5777(1)	24(1)
C(7A)	9110(2)	2813(3)	6558(2)	31(1)
C(8A)	10164(3)	3476(3)	7066(2)	40(1)
C(9A)	9250(3)	1475(3)	6659(2)	44(1)
C(10A)	6649(2)	4749(3)	4236(1)	28(1)
C(11A)	6878(3)	5877(3)	3872(2)	45(1)
C(12A)	5843(3)	3909(3)	3685(2)	40(1)
O(2)	6639(2)	2286(2)	6190(1)	40(1)
I(1B)	5492(1)	908(1)	5884(1)	31(1)
O(1B)	4135(2)	-364(2)	5678(1)	42(1)
C(1B)	4711(2)	1295(2)	6707(1)	25(1)
C(2B)	3552(2)	897(3)	6488(2)	29(1)
C(3B)	2856(3)	1203(3)	6916(2)	37(1)
C(4B)	3327(3)	1855(3)	7538(2)	40(1)
C(5B)	4497(3)	2155(3)	7763(2)	38(1)
C(6B)	5245(2)	1866(2)	7357(2)	28(1)
C(7B)	6551(3)	2121(3)	7674(2)	34(1)
C(8B)	6816(4)	3444(3)	7768(2)	61(1)

C(9B)	7061(3)	1463(4)	8390(2)	60(1)
C(10B)	3122(3)	141(3)	5801(2)	35(1)
C(11B)	2447(3)	911(3)	5162(2)	48(1)
C(12B)	2366(3)	-887(3)	5904(2)	55(1)
H(3A)	8718	4328	3929	33
H(4A)	10404	3375	4621	38
H(5A)	10565	2740	5772	36
H(7A)	8403	3049	6687	37
H(8AA)	10208	3313	7563	61
H(8AB)	10067	4319	6976	61
H(8AC)	10880	3214	6978	61
H(9AA)	9327	1275	7156	66
H(9AB)	9946	1220	6544	66
H(9AC)	8567	1082	6342	66
H(11A)	7257	5679	3512	68
H(11B)	7383	6396	4231	68
H(11C)	6140	6272	3642	68
H(12A)	6211	3698	3321	60
H(12B)	5101	4298	3456	60
H(12C)	5707	3200	3928	60
H(3B)	2065	969	6783	44
H(4B)	2841	2097	7812	48
H(5B)	4801	2565	8200	45
H(7B)	6946	1813	7331	41
H(8BA)	7656	3562	7959	91
H(8BB)	6437	3772	8101	91
H(8BC)	6522	3838	7305	91
H(9BA)	7899	1605	8572	91
H(9BB)	6918	622	8314	91
H(9BC)	6689	1746	8738	91
H(11D)	1767	1251	5260	71
H(11E)	2195	431	4730	71
H(11F)	2952	1541	5093	71

H(12D)	1642	-585	5962	83
H(12E)	2787	-1331	6330	83
H(12F)	2189	-1400	5485	83

U(eq) is defined as one third of the trace of the orthogonalized U^{ij} tensor.

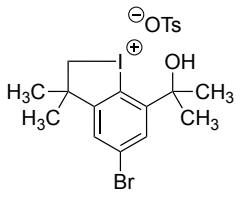
Table 3. Anisotropic displacement parameters ($Å^2 x\ 10^3$) for $C_{24}H_{32}I_2O_3$

	U^{11}	U^{22}	U^{33}	U^{23}	U^{13}	U^{12}
I(1A)	18(1)	41(1)	22(1)	2(1)	7(1)	3(1)
O(1A)	27(1)	38(1)	29(1)	4(1)	10(1)	11(1)
C(1A)	16(1)	26(1)	23(1)	-2(1)	6(1)	0(1)
C(2A)	20(1)	24(1)	21(1)	-2(1)	6(1)	0(1)
C(3A)	29(2)	33(2)	24(1)	-1(1)	12(1)	-4(1)
C(4A)	23(1)	38(2)	37(2)	-5(1)	14(1)	0(1)
C(5A)	17(1)	34(2)	36(2)	-1(1)	6(1)	3(1)
C(6A)	18(1)	28(1)	24(1)	0(1)	3(1)	-1(1)
C(7A)	22(1)	41(2)	25(1)	5(1)	2(1)	0(1)
C(8A)	32(2)	50(2)	31(2)	1(1)	-2(1)	-3(2)
C(9A)	40(2)	41(2)	41(2)	13(2)	-2(2)	-6(2)
C(10A)	24(1)	35(2)	23(1)	4(1)	6(1)	5(1)
C(11A)	41(2)	46(2)	50(2)	24(2)	15(2)	11(2)
C(12A)	29(2)	59(2)	27(2)	-5(1)	1(1)	4(2)
O(2)	25(1)	60(2)	31(1)	15(1)	5(1)	-9(1)
I(1B)	26(1)	41(1)	29(1)	-4(1)	13(1)	2(1)
O(1B)	34(1)	40(1)	55(1)	-15(1)	16(1)	0(1)
C(1B)	26(1)	26(1)	25(1)	4(1)	13(1)	4(1)
C(2B)	26(2)	29(2)	34(2)	6(1)	12(1)	4(1)
C(3B)	27(2)	45(2)	43(2)	12(2)	18(1)	7(1)
C(4B)	41(2)	56(2)	31(2)	12(2)	22(1)	19(2)
C(5B)	47(2)	44(2)	23(1)	4(1)	14(1)	12(2)
C(6B)	31(2)	28(2)	25(1)	6(1)	9(1)	4(1)
C(7B)	35(2)	39(2)	25(1)	1(1)	6(1)	-4(1)

C(8B)	66(3)	49(2)	61(3)	-10(2)	10(2)	-16(2)
C(9B)	38(2)	86(3)	48(2)	22(2)	0(2)	-1(2)
C(10B)	28(2)	34(2)	44(2)	-6(1)	11(1)	-1(1)
C(11B)	42(2)	53(2)	41(2)	-10(2)	3(2)	5(2)
C(12B)	42(2)	39(2)	86(3)	-9(2)	19(2)	-13(2)

The anisotropic displacement factor exponent takes the form: $-2p^2[h^2 a^{*2}U^{11} + ... + 2 h k a^* b^* U^{12}]$

Crystallographic data for alkyl aryl iodonium 4.155:



4.155

Table 1. Crystal data and structure refinement for $C_{20}H_{24}BrIO_4S$

Empirical formula	$C_{20}H_{24}BrIO_4S$
Formula weight	567.26
Temperature	296(2) K
Wavelength	0.71073 Å
Crystal system	Monoclinic
Space group	*C*2/*c*
Unit cell dimensions	*a* = 23.005(4) Å, *b* = 15.757(4) Å, *c* = 16.815(4) Å
	a = 90°, *b* = 130.652(10)°, *g* = 90°.
Volume	4624.5(17) $Å^3$
Z	8
Density (calculated)	1.630 g/cm^3
Absorption coefficient	3.224 mm^{-1}
F(000)	2240
Crystal size	0.100 x 0.085 x 0.030 mm^3
Theta range for data collection	2.334 to 25.992°.
Index ranges	-28<=h<=28, -19<=k<=17, -20<=l<=20
Reflections collected	29782
Independent reflections	4555 [R(int) = 0.0419]
Completeness to theta = 25.242°	100.0 %
Absorption correction	Semi-empirical from equivalents
Max. and min. transmission	0.7460 and 0.6882
Refinement method	Full-matrix least-squares on F^2
Data / restraints / parameters	4555 / 6 / 254
Goodness-of-fit on F^2	1.118
Final R indices [I>2sigma(I)]	R1 = 0.0340, wR2 = 0.0622

R indices (all data)	R1 = 0.0572, wR2 = 0.0692
Extinction coefficient	n/a
Largest diff. peak and hole	0.949 and -0.754 e.Å^{-3}

Table 2. Atomic coordinates (x 10^4) and equivalent isotropic displacement parameters (Å^{2}x 10^3) for $C_{20}H_{24}BrIO_4S$

	x	y	z	U(eq)
I(1)	6291(1)	2540(1)	4305(1)	48(1)
Br(1)	6139(1)	3723(1)	7977(1)	83(1)
C(1)	6263(2)	2823(2)	5501(3)	36(1)
C(2)	6247(2)	3686(2)	5620(3)	37(1)
C(3)	6221(2)	3961(3)	6384(3)	44(1)
C(6)	6259(2)	2206(3)	6084(3)	43(1)
C(5)	6228(2)	2505(3)	6829(3)	51(1)
C(4)	6207(2)	3361(3)	6965(3)	49(1)
C(7)	5957(3)	3843(3)	3934(3)	48(1)
C(8)	6300(2)	4288(3)	4961(3)	46(1)
C(9)	7144(3)	4489(4)	5557(4)	81(2)
C(10)	5836(4)	5096(3)	4683(4)	84(2)
C(11)	5438(3)	985(3)	4947(5)	80(2)
C(12)	6252(3)	1260(3)	5870(4)	58(1)
C(13)	6595(4)	717(3)	6836(5)	104(2)
O(14)	6680(2)	1133(2)	5535(2)	60(1)
C(15)	6266(2)	7467(3)	6242(3)	43(1)
C(16)	5756(2)	7274(3)	5190(3)	50(1)
C(17)	5765(3)	7738(3)	4499(4)	60(1)
C(18)	6266(3)	8397(3)	4834(4)	62(1)
C(19)	6764(3)	8587(3)	5878(4)	71(1)
C(120)	6768(3)	8129(3)	6585(4)	62(1)
C(121)	6268(4)	8903(4)	4065(5)	110(2)
S(1)	6253(1)	6879(1)	7125(1)	56(1)

O(1)	6892(3)	7078(5)	8120(3)	185(3)
O(2)	5645(3)	7190(4)	7041(4)	168(3)
O(3A)	5938(4)	6064(4)	6686(5)	100(2)
O(3B)	6773(8)	6177(7)	7418(9)	100(2)
H(3)	6213	4537	6498	53
H(5)	6221	2121	7243	62
H(7A)	6149	4095	3618	58
H(7B)	5403	3893	3445	58
H(9A)	7188	4820	5119	121
H(9B)	7425	3970	5746	121
H(9C)	7349	4804	6179	121
H(10A)	5839	5432	4209	125
H(10B)	6059	5415	5309	125
H(10C)	5318	4949	4355	125
H(11A)	5440	401	4786	120
H(11B)	5242	1331	4349	120
H(11C)	5120	1050	5125	120
H(13A)	6632	139	6693	157
H(13B)	6272	746	7011	157
H(13C)	7096	925	7414	157
H(14A)	7125	1283	6002	72
H(16)	5406	6834	4944	60
H(17)	5423	7599	3791	72
H(19)	7108	9032	6119	85
H(120)	7111	8271	7293	75
H(12A)	6357	9492	4260	165
H(12B)	5782	8842	3371	165
H(12C)	6667	8696	4078	165

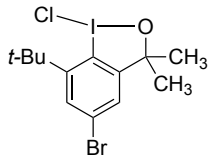
U(eq) is defined as one third of the trace of the orthogonalized U^{ij} tensor.

Table 3. Anisotropic displacement parameters ($Å^2 x\ 10^3$) for $C_{20}H_{24}BrIO_4S$

	U^{11}	U^{22}	U^{33}	U^{23}	U^{13}	U^{12}
I(1)	65(1)	48(1)	50(1)	-9(1)	46(1)	-7(1)
Br(1)	127(1)	93(1)	78(1)	-8(1)	89(1)	0(1)
C(1)	36(2)	45(2)	33(2)	-4(2)	25(2)	0(2)
C(2)	43(2)	39(2)	34(2)	-3(2)	27(2)	-4(2)
C(3)	53(3)	42(2)	44(2)	-3(2)	35(2)	0(2)
C(6)	46(2)	47(2)	42(2)	5(2)	31(2)	4(2)
C(5)	66(3)	56(3)	50(2)	12(2)	45(2)	7(3)
C(4)	58(3)	60(3)	43(2)	-1(2)	40(2)	1(2)
C(7)	60(3)	51(3)	43(2)	1(2)	37(2)	-4(2)
C(8)	61(3)	41(2)	45(2)	-3(2)	39(2)	-7(2)
C(9)	92(4)	87(4)	70(3)	-21(3)	56(3)	-46(3)
C(10)	152(6)	51(3)	89(4)	24(3)	97(4)	29(3)
C(11)	95(4)	51(3)	120(5)	-19(3)	82(4)	-24(3)
C(12)	80(4)	44(3)	72(3)	9(2)	59(3)	5(3)
C(13)	179(7)	56(3)	119(5)	36(3)	115(5)	38(4)
O(14)	66(2)	48(2)	72(2)	-5(2)	48(2)	3(2)
C(15)	46(2)	49(2)	42(2)	0(2)	32(2)	2(2)
C(16)	53(3)	54(3)	46(2)	-5(2)	33(2)	-6(2)
C(17)	76(3)	67(3)	47(3)	-4(2)	44(3)	1(3)
C(18)	74(3)	68(3)	64(3)	7(3)	53(3)	-2(3)
C(19)	75(4)	74(4)	73(3)	-5(3)	53(3)	-24(3)
C(120)	62(3)	74(3)	47(3)	-10(2)	34(3)	-15(3)
C(121)	151(6)	116(5)	105(5)	16(4)	102(5)	-15(5)
S(1)	62(1)	66(1)	47(1)	6(1)	39(1)	-1(1)
O(1)	144(4)	322(8)	54(3)	3(4)	48(3)	-120(5)
O(2)	118(4)	272(7)	170(5)	133(5)	118(4)	68(4)
O(3A)	176(6)	64(3)	78(4)	-17(3)	91(4)	-54(4)
O(3B)	176(6)	64(3)	78(4)	-17(3)	91(4)	-54(4)

The anisotropic displacement factor exponent takes the form: $-2p^2[\ h^2\ a^{*2}U^{11} + ...\ + 2\ h\ k\ a^*\ b^*\ U^{12}]$

Crystallographic data for chloroiodane 4.163 (R = *t*-Bu):



4.163

Table 1. Crystal data and structure refinement for $C_{13}H_{17}BrClIO$

Empirical formula	$C_{13}H_{17}BrClIO$
Formula weight	431.52
Temperature	290(2) K
Wavelength	0.71073 Å
Crystal system	Triclinic
Space group	*P*-1
Unit cell dimensions	*a* = 6.1112(15) Å, *b* = 9.883(2) Å, *c* = 12.806(3) Å
	a = 87.831(7)°, *b* = 89.468(7)°, *g* = 78.875(7)°.
Volume	758.4(3) $Å^3$
Z	2
Density (calculated)	1.890 g/cm^3
Absorption coefficient	4.906 mm^{-1}
F(000)	416
Crystal size	0.130 x 0.060 x 0.010 mm^3
Theta range for data collection	2.589 to 25.995°.
Index ranges	-7<=h<=7, -12<=k<=12, -15<=l<=15
Reflections collected	14858
Independent reflections	3002 [R(int) = 0.0417]
Completeness to theta = 25.242°	99.9 %
Absorption correction	Semi-empirical from equivalents
Max. and min. transmission	0.7460 and 0.6219
Refinement method	Full-matrix least-squares on F^2
Data / restraints / parameters	3002 / 0 / 159
Goodness-of-fit on F^2	1.148
Final R indices [I>2sigma(I)]	R1 = 0.0280, wR2 = 0.0525
R indices (all data)	R1 = 0.0367, wR2 = 0.0548

Largest diff. peak and hole 0.857 and -0.664 e.Å^{-3}

Table 2. Atomic coordinates (x 10^4) and equivalent isotropic displacement parameters (Å^{2}x 10^3) for $C_{13}H_{17}BrClIO$

	x	y	z	U(eq)
I(1)	8522(1)	3701(1)	6176(1)	33(1)
Br(1)	1738(1)	1287(1)	9683(1)	82(1)
Cl(1)	7940(2)	6605(1)	5312(1)	60(1)
O(1)	9759(4)	1721(2)	6418(2)	45(1)
C(1)	6217(6)	3231(3)	7376(3)	31(1)
C(2)	6437(6)	1800(4)	7432(3)	35(1)
C(3)	5069(7)	1215(4)	8123(3)	49(1)
C(4)	3602(7)	2066(4)	8725(3)	48(1)
C(5)	3403(6)	3481(4)	8669(3)	42(1)
C(6)	4717(6)	4114(4)	7993(3)	34(1)
C(7)	4467(6)	5696(4)	7942(3)	38(1)
C(8)	6729(7)	6093(4)	8128(3)	48(1)
C(9)	3490(7)	6234(4)	6874(3)	54(1)
C(10)	2888(7)	6385(4)	8788(4)	56(1)
C(008)	8031(6)	935(4)	6704(3)	38(1)
C(00E)	6839(7)	633(4)	5742(3)	54(1)
C(00H)	9373(8)	-364(4)	7223(4)	58(1)
H(3)	5159	265	8170	58
H(5)	2369	4021	9093	50
H(8A)	6530	7075	8184	73
H(8B)	7708	5809	7553	73
H(8C)	7368	5645	8762	73
H(9A)	3553	7194	6780	81
H(9B)	1967	6122	6841	81
H(9C)	4338	5724	6333	81
H(10A)	2827	7363	8747	84

H(10B)	3427	6024	9464	84
H(10C)	1423	6198	8683	84
H(00A)	5705	122	5940	82
H(00B)	7887	100	5282	82
H(00C)	6165	1485	5391	82
H(00D)	8402	-993	7405	88
H(00E)	10064	-130	7844	88
H(00F)	10502	-792	6749	88

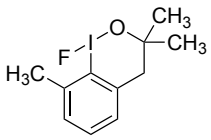
U(eq) is defined as one third of the trace of the orthogonalized U_{ij} tensor.

Table 3. Anisotropic displacement parameters ($Å^2 x\ 10^3$) for $C_{13}H_{17}BrClIO$

	U_{11}	U_{22}	U_{33}	U_{23}	U_{13}	U_{12}
I(1)	37(1)	25(1)	37(1)	3(1)	10(1)	-5(1)
Br(1)	114(1)	84(1)	66(1)	-15(1)	49(1)	-65(1)
Cl(1)	61(1)	41(1)	72(1)	3(1)	21(1)	6(1)
O(1)	45(2)	26(1)	61(2)	5(1)	14(1)	0(1)
C(1)	34(2)	32(2)	29(2)	-2(2)	9(2)	-12(2)
C(2)	44(2)	31(2)	33(2)	0(2)	2(2)	-11(2)
C(3)	70(3)	39(2)	42(2)	-2(2)	12(2)	-26(2)
C(4)	60(3)	55(3)	38(2)	-2(2)	15(2)	-33(2)
C(5)	45(2)	50(2)	36(2)	-10(2)	13(2)	-20(2)
C(6)	37(2)	38(2)	28(2)	-5(2)	3(2)	-12(2)
C(7)	37(2)	32(2)	43(2)	-3(2)	9(2)	-7(2)
C(8)	52(3)	39(2)	57(3)	-11(2)	8(2)	-18(2)
C(9)	46(3)	52(3)	58(3)	5(2)	3(2)	2(2)
C(10)	54(3)	46(2)	66(3)	-15(2)	20(2)	-6(2)
C(008)	49(2)	27(2)	39(2)	0(2)	4(2)	-9(2)
C(00E)	61(3)	51(3)	51(3)	-14(2)	4(2)	-9(2)
C(00H)	71(3)	34(2)	66(3)	12(2)	3(2)	-3(2)

The anisotropic displacement factor exponent takes the form: $-2p^2[\ h^2\ a^{*2}U_{11} + ...\ + 2\ h\ k\ a^*\ b^*\ U_{12}]$

Crystallographic data for fluoroiodane 4.168 (R = CH_3, six membered):



4.168

Table 1. Crystal data and structure refinement for $C_{11}H_{14}FIO$

Empirical formula	$C_{11}H_{14}FIO$
Formula weight	308.12
Temperature	200(2) K
Wavelength	0.71073 Å
Crystal system	Orthorhombic
Space group	*Pbca*
Unit cell dimensions	a = 8.004(2) Å, b = 14.602(4) Å, c = 18.970(6) Å
	a = 90°, b = 90°, g = 90°.
Volume	2217.1(11) $Å^3$
Z	8
Density (calculated)	1.846 g/cm^3
Absorption coefficient	2.868 mm^{-1}
F(000)	1200
Crystal size	0.200 x 0.100 x 0.040 mm^3
Theta range for data collection	2.790 to 27.997°.
Index ranges	-10<=h<=10, -19<=k<=19, -25<=l<=24
Reflections collected	41353
Independent reflections	2682 [R(int) = 0.0386]
Completeness to theta = 25.242°	99.9 %
Absorption correction	Semi-empirical from equivalents
Max. and min. transmission	0.7460 and 0.6652
Refinement method	Full-matrix least-squares on F^2
Data / restraints / parameters	2682 / 0 / 130
Goodness-of-fit on F^2	1.162
Final R indices [I>2sigma(I)]	R1 = 0.0264, wR2 = 0.0684
R indices (all data)	R1 = 0.0291, wR2 = 0.0710
Extinction coefficient	n/a

Largest diff. peak and hole 0.792 and -1.206 e.Å^{-3}

Table 2. Atomic coordinates (x 10^4) and equivalent isotropic displacement parameters (Å^{2}x 10^3) for $C_{11}H_{14}FIO$

	x	y	z	U(eq)
I(1A)	5047(1)	1232(1)	5564(1)	25(1)
F(1A)	3828(3)	-25(1)	5689(1)	48(1)
O(1A)	6121(2)	2485(1)	5576(1)	23(1)
C(1A)	4240(3)	1580(2)	6580(1)	23(1)
C(2A)	3561(3)	2458(2)	6619(1)	23(1)
C(3A)	3154(3)	2781(2)	7286(1)	30(1)
C(4A)	3446(4)	2255(2)	7881(1)	36(1)
C(5A)	4156(4)	1399(2)	7818(1)	36(1)
C(6A)	4574(3)	1033(2)	7164(1)	30(1)
C(7A)	5377(4)	103(2)	7125(2)	41(1)
C(8A)	3354(3)	3029(2)	5967(1)	25(1)
C(9A)	5034(3)	3274(2)	5611(1)	22(1)
C(10A)	4723(3)	3622(2)	4866(1)	31(1)
C(11A)	5978(3)	3978(2)	6045(1)	30(1)
H(3A)	2668	3371	7335	36
H(4A)	3157	2485	8333	43
H(5A)	4366	1050	8231	43
H(7AA)	5655	-107	7602	62
H(7AB)	6399	140	6842	62
H(7AC)	4600	-331	6906	62
H(8AA)	2763	3602	6092	30
H(8AB)	2649	2692	5626	30
H(10A)	3971	4151	4883	47
H(10B)	4212	3135	4583	47
H(10C)	5787	3804	4652	47
H(11A)	5362	4558	6043	45

H(11B)	7090	4073	5840	45
H(11C)	6092	3758	6530	45

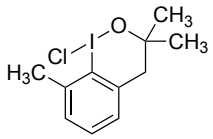
U(eq) is defined as one third of the trace of the orthogonalized U^{ij} tensor.

Table 3. Anisotropic displacement parameters ($Å^2 x\ 10^3$) for $C_{11}H_{14}FIO$

	U^{11}	U^{22}	U^{33}	U^{23}	U^{13}	U^{12}
I(1A)	33(1)	19(1)	24(1)	-6(1)	7(1)	-4(1)
F(1A)	64(1)	27(1)	53(1)	-15(1)	14(1)	-19(1)
O(1A)	25(1)	18(1)	24(1)	0(1)	3(1)	-1(1)
C(1A)	27(1)	21(1)	20(1)	-1(1)	6(1)	-1(1)
C(2A)	24(1)	22(1)	22(1)	1(1)	4(1)	0(1)
C(3A)	35(1)	26(1)	28(1)	-2(1)	10(1)	6(1)
C(4A)	47(2)	38(1)	23(1)	-1(1)	13(1)	4(1)
C(5A)	48(2)	34(1)	24(1)	9(1)	9(1)	2(1)
C(6A)	35(1)	23(1)	32(1)	5(1)	9(1)	1(1)
C(7A)	56(2)	24(1)	44(2)	12(1)	12(1)	11(1)
C(8A)	27(1)	24(1)	24(1)	2(1)	-1(1)	4(1)
C(9A)	28(1)	19(1)	18(1)	2(1)	-1(1)	1(1)
C(10A)	36(1)	35(1)	23(1)	8(1)	-3(1)	-2(1)
C(11A)	38(1)	21(1)	31(1)	-1(1)	-5(1)	-3(1)

The anisotropic displacement factor exponent takes the form: $-2p^2[\ h^2\ a^{*2}U^{11} + ...\ + 2\ h\ k\ a^*\ b^*\ U^{12}]$

Crystallographic data for chloroiodane 4.169 (R = CH_3, six membered):



4.169

Table 1. Crystal data and structure refinement for $C_{11}H_{14}ClIO$

Empirical formula	$C_{11}H_{14}ClIO$
Formula weight	324.57
Temperature	296(2) K
Wavelength	0.71073 Å
Crystal system	Orthorhombic
Space group	*Pbca*
Unit cell dimensions	*a* = 8.279(9) Å, *b* = 15.286(17) Å, *c* = 19.01(2) Å
	a = b = g = 90°
Volume	2406(5) $Å^3$
Z	8
Density (calculated)	1.792 g/cm^3
Absorption coefficient	2.851 mm^{-1}
F(000)	1264
Crystal size	0.204 x 0.110 x 0.020 mm^3
Theta range for data collection	2.665 to 30.157°.
Index ranges	-11<=h<=11, -21<=k<=21, -26<=l<=26
Reflections collected	26700
Independent reflections	3522 [R(int) = 0.1374]
Completeness to theta = 25.242°	99.9 %
Absorption correction	Semi-empirical from equivalents
Max. and min. transmission	0.7460 and 0.5678
Refinement method	Full-matrix least-squares on F^2
Data / restraints / parameters	3522 / 0 / 131
Goodness-of-fit on F^2	0.997
Final R indices [I>2sigma(I)]	R1 = 0.0444, wR2 = 0.0736
R indices (all data)	R1 = 0.1199, wR2 = 0.0956
Extinction coefficient	0.00054(13)

Largest diff. peak and hole 0.725 and -0.960 e.Å^{-3}

Table 2. Atomic coordinates (x 10^4) and equivalent isotropic displacement parameters (Å^{2}x 10^3) for $C_{11}H_{14}ClIO$

	x	y	z	U(eq)
I(1)	5418(1)	3698(1)	4325(1)	38(1)
Cl(1)	3871(2)	5156(1)	4124(1)	64(1)
O(1)	6477(4)	2501(2)	4406(2)	41(1)
C(1)	4881(6)	3297(3)	3289(2)	35(1)
C(2)	4182(6)	2480(3)	3282(2)	38(1)
C(3)	3879(8)	2135(3)	2612(3)	58(2)
C(4)	4286(8)	2587(4)	2017(3)	63(2)
C(5)	5018(8)	3381(4)	2063(3)	59(2)
C(6)	5364(7)	3777(3)	2709(2)	43(1)
C(7)	3851(7)	1981(3)	3940(3)	45(1)
C(8)	5403(7)	1753(3)	4352(3)	40(1)
C(9)	6203(8)	4638(3)	2731(3)	60(2)
C(10)	6383(8)	1057(3)	3976(3)	52(2)
C(11)	4954(8)	1453(4)	5092(3)	60(2)
H(3)	3391	1589	2572	69
H(4)	4061	2349	1577	76
H(5)	5297	3672	1651	71
H(7A)	3289	1444	3821	54
H(7B)	3145	2325	4239	54
H(9A)	6796	4722	2303	90
H(9B)	6933	4650	3123	90
H(9C)	5419	5096	2782	90
H(10A)	6593	1241	3502	79
H(10B)	5788	518	3970	79
H(10C)	7388	971	4218	79
H(11A)	4406	1918	5333	89

H(11B)	5916	1300	5345	89
H(11C)	4256	953	5063	89

U(eq) is defined as one third of the trace of the orthogonalized U_{ij} tensor.

Table 3. Anisotropic displacement parameters ($Å^2 x\ 10^3$) for $C_{11}H_{14}ClIO$

	U_{11}	U_{22}	U_{33}	U_{23}	U_{13}	U_{12}
I(1)	44(1)	32(1)	37(1)	-8(1)	-7(1)	5(1)
Cl(1)	82(1)	47(1)	63(1)	-15(1)	-15(1)	27(1)
O(1)	43(2)	31(2)	49(2)	-1(2)	-7(2)	2(2)
C(1)	49(4)	29(3)	29(2)	-4(2)	-11(2)	1(2)
C(2)	37(3)	33(3)	44(3)	-5(2)	-8(2)	-4(2)
C(3)	78(4)	32(3)	63(4)	-10(3)	-26(4)	-7(3)
C(4)	90(6)	56(4)	43(3)	-15(3)	-21(3)	5(4)
C(5)	87(5)	52(4)	38(3)	0(3)	-10(3)	15(3)
C(6)	56(3)	36(3)	37(2)	-2(2)	-4(3)	7(3)
C(7)	42(3)	31(3)	61(4)	0(3)	-2(3)	-7(3)
C(8)	44(3)	35(3)	40(3)	2(2)	0(3)	-3(3)
C(9)	75(4)	36(3)	69(4)	13(3)	10(4)	-5(3)
C(10)	66(4)	35(3)	56(3)	-2(3)	10(3)	9(3)
C(11)	73(5)	60(4)	47(3)	17(3)	15(3)	8(3)

The anisotropic displacement factor exponent takes the form: $-2p^2[h^2 a^{*2} U_{11} + ... + 2 h k a^* b^* U_{12}]$